2017 International Workshop on Micropiles
9th Lizzi Lecture

Loading Effects on Battered Micropiles Supporting Lateral and Compression Forces

John R. Wolosick, P.E., D.GE and Robert F. Scott, Jr., P.E.
Hayward Baker Inc., Atlanta, GA and Nashville, TN

Abstract

The use of battered pile foundations has gone from being 'in-vogue' to 'verboten,' in particular for seismic design, during the 20th century. This flip-flop in design and construction practice is examined in this paper. There are several reasons for these changes. In particular, popular pile types have changed significantly over the years. This paper examines the reasons for changes in practice affecting the use of battered piles and in particular looks at the effects of compression and lateral loads on micropiles. Micropiles have small cross-sectional areas. They also have limited resistance to lateral loads and bending moments when installed in vertical configurations due to their small diameters. Therefore, using micropiles at a batter can be particularly advantageous to carry lateral loads. However, using battered micropiles indiscriminately, without understanding the effects of soil loading on the piles and the impacts of increased foundation stiffness, can lead to unsatisfactory performance of the foundation system. Analysis methods for evaluating battered pile foundations vary and some common design methods may be incorrect. These errors could lead to yielded piles in service – particularly for uncased bar or hollow-bar micropiles. This serious concern is discussed and methods of correcting this common problem are presented. Moreover, this paper discusses the compression and lateral loading induced forces on battered micropiles used for foundation support.

A Bit of History

Battered piles have had a tough time lately. In 1998, ASCE's Technical Council on Lifeline Earthquake Engineering recommended that "The use of Batter piles at ports is typically not encouraged because of their poor seismic performance during past earthquakes" (Kavazanjian, 2006). This warning concerning battered pile use was generated primarily through the observed performance of pre-stressed concrete battered piles at port facilities in California during the 1989 Loma Prieta and 1994 Northridge earthquakes as well as the 1996 Manzanillo, Mexico earthquake. During these events, battered pile heads typically sheared off and tremendous damage was done to the port facilities (Kavazanjian, 2006).

The history of deep foundations carrying lateral loads is worth noting. The lateral foundation loads requiring deep foundation support discussed in this paper are typically generated from earth, wind, seismic, water currents, vehicle braking forces, impact, etc. The types of structures that are required to support these lateral loads include bridge piers and abutments, anchored bulkheads, retaining walls, docks and building foundations (Kavazanjian, 2006). It should also be noted that many of these loads are transient – of short duration. More severe lateral loads from seismic events are also discussed.

In the first half of the 20th century, battered piles were not often utilized in the United States to carry lateral loads due to the types of commonly available and economically viable deep

foundation types in use. Timber piles, Franki™ piles and Raymond Step-Taper™ piles (Kavazanjian, 2006) were very difficult to analyze under lateral loadings. Each of these deep foundation types contained varying cross-sections that, at a glance, would not perform well when loaded laterally while also carrying the required vertical loads. Features like knots in wood, cold joints in concrete and highly variable cross-sections do not lend themselves well to analysis or satisfactory lateral performance. However, towards the end of the 20th century, battered piles were the 'go-to' solution to carry lateral foundation loadings. Steel H Piles and Pipe piles as well as pre-cast concrete piles offered uniform geometric shapes and plenty of steel area to carry lateral loads. Throughout the 1960's, 12 and 14 inch H piles were commonly used to support lateral loads for bridge piers and abutments. Augercast/CFA piles appeared in the late 60's and early 70's, but were not accepted for use on most public works projects until recently. Then, in the 1970's and 1980's, vertical drilled shafts often replaced both vertical and battered piles as foundation support for many bridges, mainly due to a push from the Federal Highway Administration (Kavazanjian, 2006). This push was supported by the availability of new, accurate software for analysis of vertical deep foundations subjected to lateral loading and new construction procedures and equipment available to reliably install the drilled shafts. However, battered piles were still often used on many projects to carry lateral loads until the earthquakes in California and Mexico mentioned above.

Micropiles, conceived in Italy in the 1950's, have been in use in North America since 1973. Micropile use and technology grew rapidly in North America starting in the mid-1980s (Sabatini, 2005). Micropiles are used extensively for industrial, commercial and transportation structures to both underpin existing structures and to support new structures. Often, micropiles are required to carry both axial and lateral loads. Micropiles exhibit excellent axial load carrying capacity, however due to the relatively small diameters typically installed, they have little lateral load carrying capacity when compared with steel H or pipe piles or drilled piers. This small lateral load carrying capacity many times necessitates battering of micropiles to resist lateral loads. Of note is that the installation of micropiles on a batter does not add cost to most projects. The rigs that install micropiles can easily drill at a batter. The cost per linear foot for battered piles is the same as for vertical piles. Only the small additional footage to extend the pile to depth on the angle must be paid for. The design and analysis of vertical micropiles is well understood by the engineering community, however the design and analysis of battered micropiles is much less well understood.

Deep Foundation Comparisons

Battered piles are defined as deep foundations that are installed at an inclination from vertical. Typical batter angles are 5 to 10 degree or up to 30 degrees from vertical. However, greater batter angles have been used. The use of battered micropiles can be an important element in the design of an efficient arrangement for a deep foundation system. Due to their relatively small diameter compared to their relatively large axial capacity, micropiles are at a distinct disadvantage to resist lateral loads compared to many other larger foundation systems. As an example, the table below presents a standard sized micropile as compared to a standard sized H-pile and corresponding capacities as per the International Building Code (IBC). We have

presented the HP 14 (360 mm) since it has a similar allowable load capacity in compression compared to a 7 inch (178 mm) diameter micropile pipe.

Pile Size	**HP14 x 73 (Grade 50 ksi) HP360 x 109 (Gr. 345 MPa)**	**7" x 0.498" (N80) 178 x 12.5 (Gr. 550 MPa)**
Allowable Axial (K) (kN)	380 (1,700)	365 (1,625)
Allowable Moment (K*ft) (kN*m)	294 (400)	68 (92)
Moment of Inertia (in^4) (mm^4)	729 ($303x10^6$)	54 ($22.5x10^6$)
Area of Steel (in^2) (mm^2)	21.4 (13,806)	10.2 (6,581)
Axial Stiffness-EA (K) (kN)	620,600 (2,760,430)	295,800 (1,315,718)
Bending Stiffness EI ($K*ft^2$) ($kN*m^2$) Weak Axis	525,625 (217,083)	108,895 (44,974)
Bending Stiffness EI ($K*ft^2$) ($kN*m^2$) Strong Axis	1,468,125 (606,366)	108,895 (44,974)
Weight per Foot (lb) (kg/m)	73 (109)	35 (52)

Table 1. H Pile to Steel Pipe Comparison

Table 1 shows that there is a large lateral capacity versus axial capacity discrepancy for micropiles as compared similar axial capacity driven piles. The ability of the micropile to carry significant axial load is due to the higher working load stress level enabled by higher strength pipe (Fy = 80 ksi (550MPa)). While the driven H pile and the micropile exhibit similar axial capacities, the allowable bending stiffness and moment resistance of the H pile are much greater than the micropile, even in the weak axis of the H pile. Note that the micropile pipe has less than on-half of the weight per foot of the H pile. Further, the driven pile has a significantly larger effective diameter with which to transmit lateral load to the soil. The same holds true for drilled piers. Note that the micropile pipe has a substantial area of steel when compared to bars: the equivalent to 2.5 #18 (#57) bars, 4.5 #14 (#43) bars, 6.5 #11 (#36) bars, 13 #8 bars (#25), 23 #6 bars (#19) and 51 #4 bars (#13).

IBC 10.3.3.2 states that the lateral capacity of a pile is half of the load that produces 1 inch (25 mm) of lateral deflection. In practice this typically results in specifications that limit lateral deflection to ½ inch (13 mm). The use of battered micropiles is required many times to meet these specifications and to produce an efficient design.

Batter Angles

Batter angle nomenclature was developed early in pile driving technology. Pile Foreman were given ratios such as 1:12 etc. that could be easily translated to angles by making templates in the field. Tradition has retained these notations, rather than supplying driving angles on plans (J. Nicholson, 2017). For reference, typical batter angles are shown on Table 2.

Batter (H:V)	Angle from Vertical (Degrees)
1:12	4.8
1:10	5.7
1:8	7
1:6	9.5
1:4 3:12	14
1:3 4:12	18.4
1:2	26.5

Table 2: Batter Notation and Resultant Angles from Vertical

What Happened to Battered Piles in the Earthquakes?

Before the California and Mexican earthquakes, the heads of battered piles were typically designed considering the connection as 'pinned.' However, post-mortem on the failed port facility installations showed that design details employed for the heads of the pre-stressed piles hindered rotation and created large shear and moment forces acting on the pile heads. Since the design and the performance conditions did not match, big problems ensued. These unexpected shear and moment loadings resulted in failure of the pile heads and connections (Kavazanjian, 2006). See Figure 8 for an illustration of the difference in the deflected shapes between pinned and fixed piles under load. Table 3 shown below from the FHWA Micropile Manual (Sabatini, 2005) gives some guidance for understanding the level of fixity for micropile-pile cap connections.

The recognition of this problem and ensuing design changes have brought battered piles, when properly designed, back into the fold as an available tool to economically resist large lateral loads from seismic events. Pile heads of pre-stressed concrete piles have been strengthened and new ductile designs have been implemented to allow the pile heads to rotate without loss of capacity e.g. 'the structural fuse.' The use of battered piles to resist seismic loads is therefore no longer 'verboten!' Structural engineers are once again using battered pile to resist seismic forces. The new piers of the San Francisco Bay Bridge East Span incorporate 8 foot diameter driven steel battered piles, which are driven through the soft bay mud into firm to dense sands (Kavazanjian, 2006).

0 % Fixity (Pinned Head Condition)	50 % Fixity(1)	100 % Fixity (Fixed Head Condition)(1)
Casing embedment of 300 mm (12 in.) or less or Reinforcing bar embedment with or without bearing plate or Any detail where top of micropile embedment is at or below the level of the bottom reinforcement of the footing	Casing embedment of 450 mm (18 in.) or Shear connection between casing and existing footing with minimum casing embedment of 450 mm (18 in.)	Casing embedment of 600 mm (24 in.) or more

(1) Guidance provided assumes that footing itself is restrained. For example, if only one row of piles in direction of loading then 0% fixity should be assumed

Table 3: Guidance for Level of Fixity for Micropile-Pile Cap Connections (Sabatini, 2005)

Analysis Methods

The authors have seen many methods employed in the analysis of battered piles. Many of the available static equilibrium-based methods do not actually satisfy static equilibrium. A simple static equilibrium analysis can give good results when the line of action passes through a work point as shown on Figure 1. Some methods simply divide the total lateral load by the number of battered piles required to carry the load, then determine the axial force in the battered piles simply by dividing the lateral load by the sine of the batter angle. A simple free-body diagram will show that this analysis method does not satisfy equilibrium. Designs using these methods may have performed adequately, however, many of these cases have incorporated large pile elements such as big steel H or pipe piles or have been for lightly loaded structures, where small lateral loads and small bending moments are resisted. Potential performance issues have gone unnoticed since they did not result in noticeable deflections that would yield the piles in bending.

Another common misconception about battered piles is zero induced moment. Battered piles in compression will experience bending moments caused by the soil reaction resisting the foundation system deflection under load (Prakash, 1990, Richards, 2004)

The most efficient batter angle is measured as the inverse tangent of the lateral load divided by the axial load. Ideally, all load combinations would produce axial loads and lateral loads where the resultant angle is the same. However, very few structures exist where this happens. As discussed above, even when the forces are resolved into a resultant load applied at the resultant angle, moments still exist in the piles due to soil-structure interaction.

In most structures, there are numerous load combinations, prescribed by Code, that are considered in a design analysis. These load combinations represent the state of the practice to produce a safe and serviceable structure. For battered piles, the most efficient batter balances all of the load combinations to produce the desired serviceability requirements with the least number of piles. The ratio of lateral load and axial load varies for the different load combinations. For example, the axial loads may be very similar in a both wind and seismic conditions, but the lateral demand may vary significantly. If the designer balances the heavy seismic combination, the batter angle will be too great for the lighter wind combination. The art of selecting the batter angle is balancing the batter angle with all of the load combinations.

The authors approach this problem by first applying the various load combinations to determine the induced pile axial loads due to the applied axial loads and moments. After inspection of the axial loads, a determination is made as to what batter angle will roughly balance all the load combinations. The batter angle is then varied until the serviceability requirements are achieved. This analysis is carried out using a program such as Group by Ensoft, Inc.. The Group program allows three-dimensional, nonlinear soil P-Y response and pile interaction analysis.

In addition, the effects of combined loading must also be checked. Stress is induced into the piles both axially and from bending. These stresses must be calculated and checked, particularly at any threaded pipe joint locations (Sabatini, 2005).

Static Equilibrium vs. P-Y Soil Structure Interaction Analysis

In this paper, we compare the results of static equilibrium analyzes and p-y soil structure interaction analysis. In the example shown on Figure 1, the piles are battered at the location of the applied load, and are in-line with a work point at the base of the column. Using this method, the loads are resolved into axial loads in the piles with no net lateral load. The modeled end condition of the piles is pinned. Note that in this example there is no consideration of the effect of embedment in soil on the piles. Thus, no moment is induced into the pile by any vertical or lateral elastic deflection of the pile cap from load.

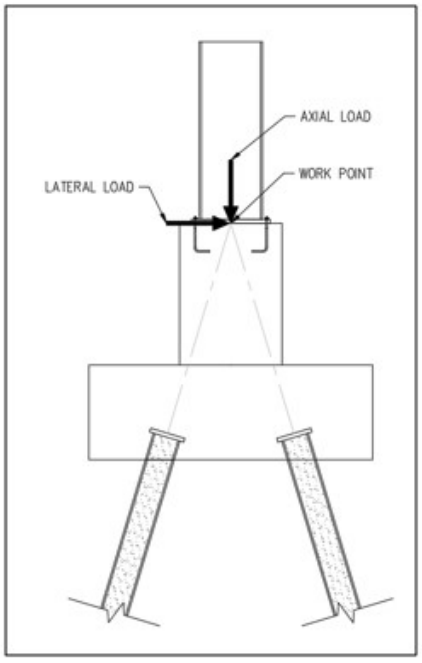


Figure 1

Figure 2 demonstrates the calculations to determine pile loads in battered piles in compression and lateral load using static analysis. In this case, the piles are aligned through the work point that is the center of the base of the column. As the basic static equilibrium calculations show, the forces resolve readily into axial loads only. The load magnitude is not important, so long as the geometry is maintained, static equilibrium is maintained. A similar analysis with a simple "A-Frame" in any structural software will yield the same results.

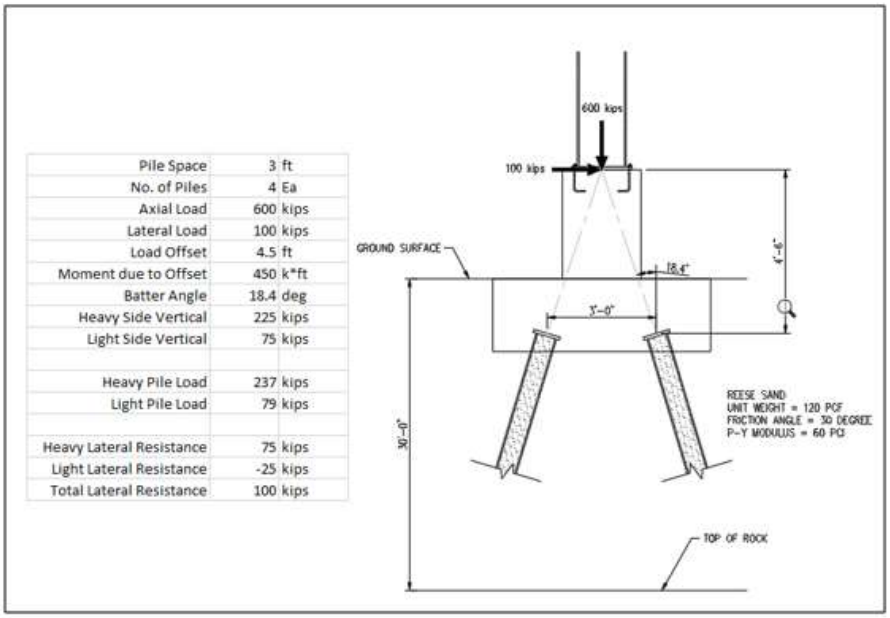


Figure 2

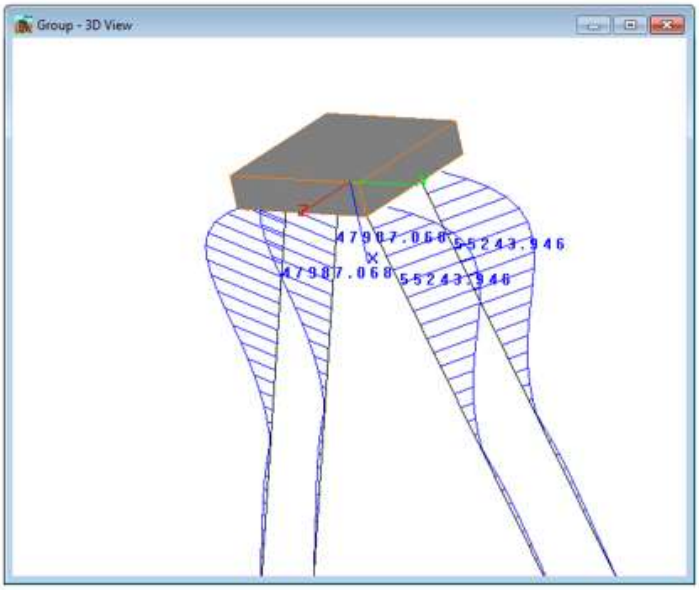


Figure 3

This same (pinned end condition) analysis was then performed in the program Group (2014), produced by Ensoft, Inc. As shown in Figure 3, a moment is induced on the piles. This moment is due to the soil structure interaction – the elasto-plastic 'springs' modeled by the program exert lateral loads on the pile as it deflects outward in response to the load. The pile spacing at the bottom of the cap is rigidly maintained, therefore when the piles elastically shorten the soil resists outward movement of the battered piles, and a shear load and corresponding moment are created. To better illustrate this concept, another analysis was performed where the

lateral load was removed, leaving only the 600 kips (2,669 kN) of vertical axial compression load on the pile cap. Figure 4 shows that there is again a moment induced on the piles, solely from the vertical compression load. Figure 5 shows the vertical displacement of the piles for this case.

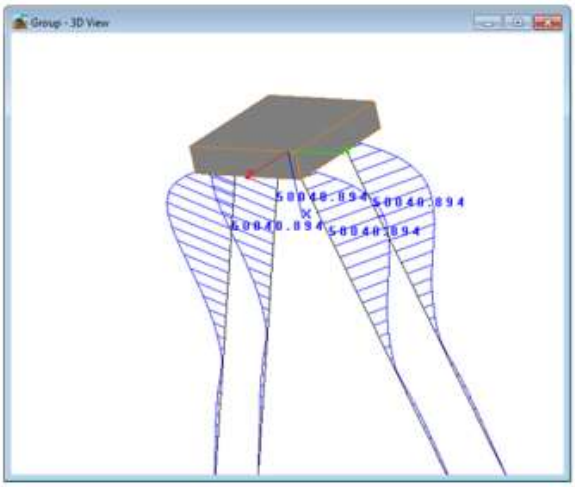


Figure 4

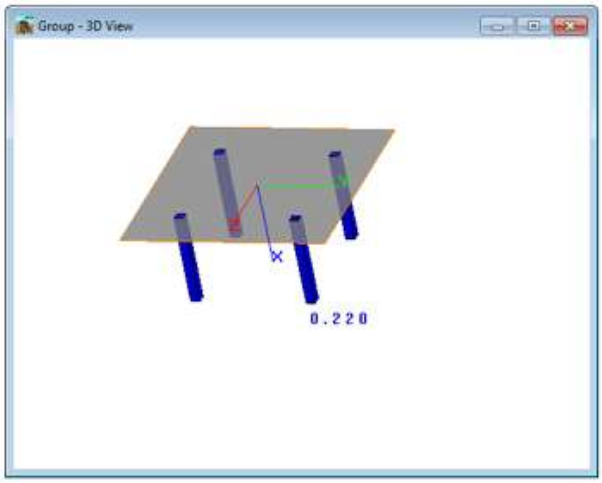


Figure 5

The vertical component of the piles elastic shortening in Figures 4 and 5 is 0.22 inch (5.6 mm). With the batter angle of 18.4 degrees (1H:3V) modeled, the horizontal component of the axial shortening is 0.073 inch (1.8 mm). To further analyze this problem, the axial load (600 kips (2,669 kN)) and the lateral deflection of 0.073 inch (1.8 mm) was input into L-Pile 2015 by Ensoft, Inc. As shown in Figures 6 and 7, the calculated net shear (2.35 K (10.5 kN)) per pile is the same in both the Group analysis (Figure 6) and the L-Pile analysis (Figure 7).

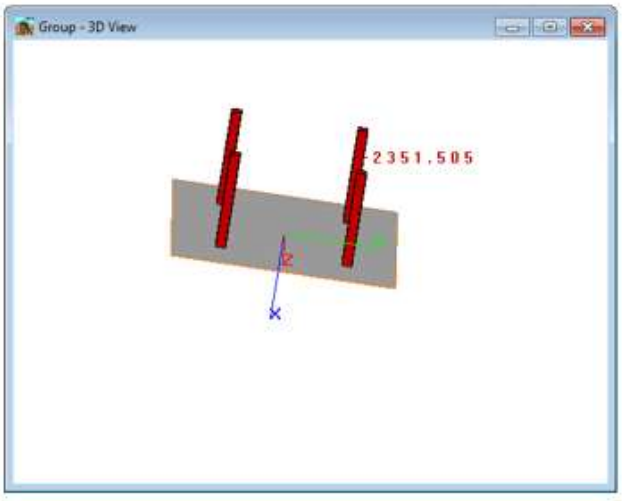


Figure 6

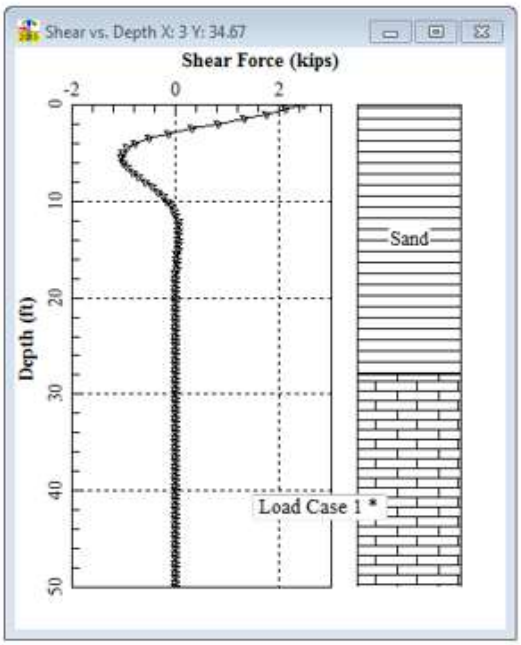


Figure 7

The other aspect that the proceeding analysis doesn't address is construction tolerances and constructability. In practice, piles typically have an installation tolerance of 3 inches (76 mm) in plan-view and an angular tolerance of 1-2 percent. These installation tolerances can also induce more pile bending moment than shown above. To illustrate the point, Figure 8 shows an exaggerated deflection of two conditions, free head and fixed head piles, under vertical load. The first diagram represents a free-head condition. As the piles elastically shorten, the soil around the piles, modeled as elasto-plastic springs, acts on the piles and produces the deformed shape shown, even though the pile heads are modeled as hinges (pinned). The second diagram represents a fixed-head condition. Again, as the piles shorten, the elasto-plastic springs act upon the piles and produce the deformed shape shown. The shapes differ since the fixed-head condition has a pile head that is fixed from rotation. The results are the deflected shapes shown on Figure 8.

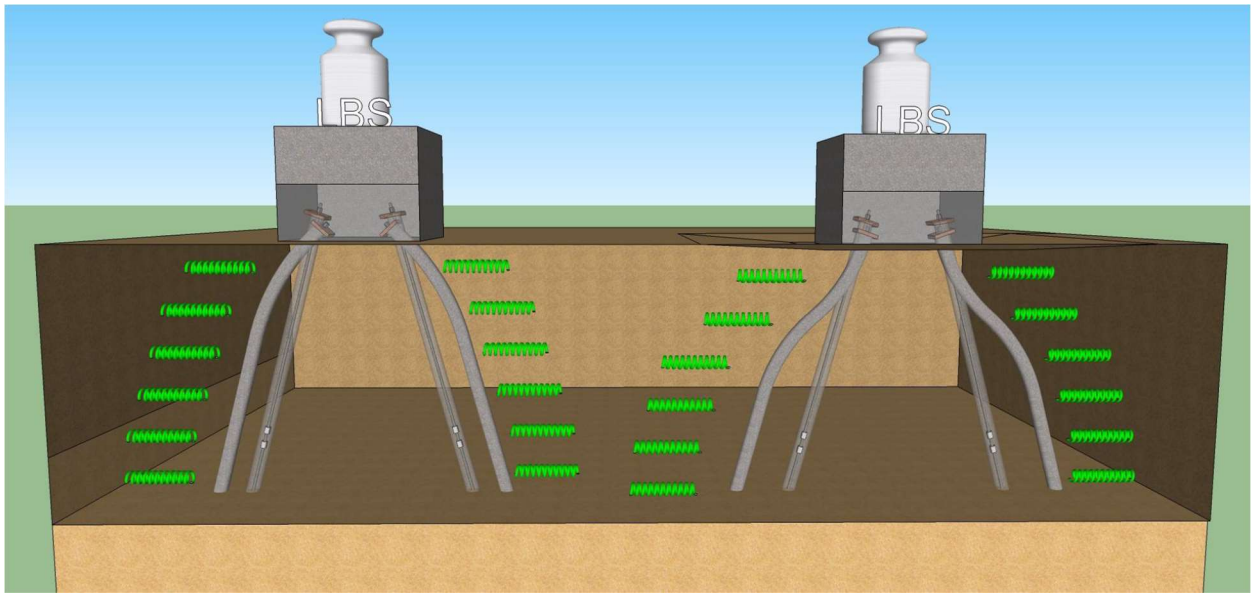


Figure 8: Model of the Exaggerated Deflected Shapes of Free-Head and Fixed Head Piles

Battering of All-Thread Bar and Hollow Bar Micropiles

The discussions in this paper so far have addressed mainly micropiles that include steel pipes. However, grouted all-thread bar micropiles have been used for decades. These types of micropiles consist simply of all-thread bars that are placed and grouted in drilled holes. This type of micropile has a successful track record. However, some designers will incorporate a steel pipe in the upper regions of these micropiles due to concerns over bending moments as shown on Figures 3 and 4. For battered bar piles, many designers consider the addition of these pipes as essential. This practice is highly recommended by the authors. For vertical bar piles, these bending moments can also exist due to location or angular installation tolerances as mentioned above. A very rough rule-of-thumb is to extend the pipe approximately 20-25 drill-hole diameters from the top of the micropile (Figure 9). The goal is to reinforce the pile to the point of contraflexure, where the bending moment goes to zero.

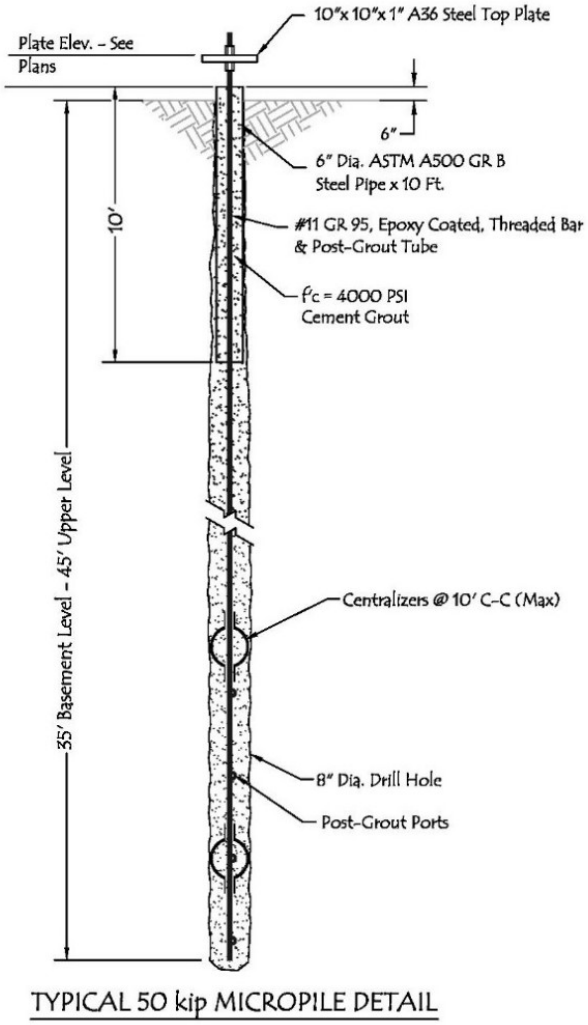


Figure 9: Bar Micropile with Steel Pipe at the Pile Head

As an example, Figure 10 shows a pile cap excavation for a 5 (vertical) pile foundation for a bar micropile project in Puerto Rico. The upper zone of the micropiles was reinforced with a 6 inch (150 mm) diameter steel pipe, 10 feet long. When excavating for the cap, the workers chipped off the grout that was bonded on the outside of the pipes. A plate was placed on the top of the pipe to transfer tension load into the pile. These micropiles were installed vertically and consisted of full-length, epoxy-coated #11 (#35) Grade 95 (655 MPa) bar piles set in grouted 8 inch (203 mm) diameter drill-holes. A 6 inch (152 mm) diameter thin-wall pipe was set at the top of each pile for the upper 10 feet (3 m) to resist any bending loads created by out of tolerance location of the micropiles. The design load was only 25 kips, as the piles were installed in a very soft silt, but the test load was specified to be 2.5 times the design load (Wolosick, 2009).



Figure 10: Micropile Pile Cap Excavation Showing Bar Piles with Top Pipe Reinforcement

Hollow-bar micropiles are often installed when caving and collapsing conditions are expected or encountered during drilling. These types of micropiles may vary significantly in diameter. The smaller diameter bars are of the most concern when using battered piles. These piles are flushed into the ground using disposable drill bits, using rotation from a drilling head and pumping grout through the hollow bar, which exits at the drill bit and flushes the soil up and out of the drill hole. When small diameter hollow bars are used for battered micropiles, bending stresses can be generated as discussed in this paper. Figure 11 shows a bending failure of a hollow-bar after unsatisfactory performance during a compression load test. The micropiles in this application were all battered, and did not include a section of steel pipe at the top of the micropile to help resist the bending stresses.



Figure 11: Hollow Bar Micropile Failure in Bending

Conclusions

As discussed, due to their small size, micropiles have disadvantages over some other foundation systems such as steel H or large pipe piles and drilled shafts when it comes to lateral capacity of vertical elements. In addition, micropiles consisting of grouted bars and hollow-bars have much reduced bending stiffness when compared to large steel pipes or H piles. Battered micropiles can be easily installed to provide an economical and effective design to carry lateral loads. The designer must understand that static equilibrium approaches can be used to determine pile axial loads when the geometry of the system is lined up with a work point, however the static equilibrium approach is simplified and will not determine the induced shears and corresponding bending moments when battered piles are employed.

On lightly loaded projects, the bending stresses may be small. However, they can be significant on heavily loaded structures, and severe in seismic events. The use of design programs such as Group by Ensoft, Inc. will accurately predict the bending moments generated from compression and lateral loads on pile foundations. This analysis is critical when considering heavily loaded uncased bar piles. Foundations using uncased bar piles have become very common, especially with the advent of self-drilling hollow all-thread bars. The use of battered or vertical small diameter all-thread bar or hollow-bar micropiles without steel pipe sections in the upper 20-25

drill-hole diameters (approximately) and under significant compression or lateral loads should be avoided. Some guidance for the design of micropiles is: "If there are lateral loads on your micropile foundation, you should always include a pipe at the pile head!"

References

1. Kavazanjian, Jr., Edward, "A Driven Pile Advantage: Batter Piles," Pile Driver, Q4, 2006, pp. 21-25.
2. Sabatini, Paul J., B. Tanyu, T. Armour, P. Groneck and J. Keeley, "Micropile Design and Construction," FHWA-NHI-05-039, U.S. Department of Transportation, 2005.
3. Richards, Thomas D. and M.J. Rothbauer, "Lateral Loads on Pin Piles (Micropiles)," GeoSupport 2004: Drilled Shafts, Micropiling, Deep Mixing, Remedial Methods, and Specialty Foundation Systems, J.P. Turner and P.W. Mayne eds., ASCE GSP 124, 2004, pp 158-174.
4. A. J. Nicholson, II, personal communication, 2017.
5. Prakash, Shamsher and Sharma, H.D., "Pile Foundations in Engineering Practice," John Wiley and Sons, 1990.
6. Wolosick, John R., "Ultimate Micropile Bond Stresses Observed in Sands and Clays," Proceedings, ASCE Contemporary Topics in Deep Foundations, ASCE GSP 185, Orlando, FL, 2009, pp. 12-22.

LATERAL PERFORMANCE OF HOLLOW BAR MICROPILE IN COHESIONLESS SOIL

Maged Abdlrahem[1], M. Hesham El Naggar, F. ASCE[2] and Wenbing Wu[3]

Hollow bar micropiles are increasingly used to support a variety of structures due to their fast installation and effective load transfer due to associated ground improvement. However, their lateral capacity is relatively small due to their small cross – sectional area. In this study, a full–scale micropile was installed in cohesionless soil and was subjected to monotonic lateral load test. The micropile was 115 mm in diameter and 6m in length. The soil at the test site was medium dense to dense sand. The test results are presented and discussed in terms of load – displacement curve. In addition, the micropile behavior during the test was analyzed numerically utilizing the program LPILE and the results are compared to the load-horizontal displacement curve obtained from the full-scale load test.

Keywords: Hollow bar micropile; Lateral loading; Cohesionless soil.

INTRODUCTION

Micropiles are increasingly used as a preferred foundation option in different civil projects to carry a considerable axial load but moderate lateral load. Federal Highway Administration (FHWA 2005) classifies micropiles into four main categories according to their grouting technique: Type A, the grout is placed under gravity; Type B, the grout is installed under pressure ranging from 0.5 to 1 MPa; Type C, initial grout is poured under gravity and then similar grout is pressurized before the hardening of the initial grout; and Type D, where initial grout is placed under gravity then before hardening of the initial grout, additional grout is pressurized at 2 to 9 MPa through sleeved pipe by using packers.

Recently, hollow bar micropiles were introduced as an efficient micropile construction technique where drilling and grouting are done in one step, eliminating the need for casing. The construction of hollow bar micropile starts with advancing a threaded hollow bar utilizing a drilling bit and drilling grout to the predetermine level and then the grout is pressurized through the nozzles of the drill bit.

Richards and Rothbauer (2004) compared the results of lateral load tests performed on micropiles installed as part of eight different projects to the predictions of the methods recommended by NAVFAC and CLM as well as that predicted from LPILE analysis. They concluded that the LPILE results compared well with the measured responses while the deflections obtained from CLM or NAVFAC methods were significantly less than the measured values. They indicated that the soil properties along the top 2 to 5 m controlled the response of the micropile.

[1] PhD Candidate, Dept. of Civil and Environmental Engineering, Western University, London, ON, Canada.

[2] Professor, Dept. of Civil and Environmental Engineering, Western University, London, ON, Canada.

[3] Associate Professor, Faculty of Engineering, China University of Geosciences, Wuhan City, Hubei Province, China

Long et al. (2005) reported the results of lateral load tests on micropiles installed in medium-strength clay overlying sand. The micropiles were installed to 15.2 m depth and reinforced with a high-strength threaded bar. The upper 9 m was stiffened by steel casing with 224 mm outer diameter and 13.8 mm thickness. The measured horizontal displacements were compared to the predicated values obtained from LPILE software. They concluded that the measured and predicated load-displacement curves agreed well with difference less than 10 percent. Abd Elaziz and El Naggar (2015) studied the performance of hollow bar micropiles under monotonic and cyclic lateral loads installed in stiff silty clay. The load test results were employed to calibrate a numerical model that was used to perform a parametric study. They concluded that the properties of soil along a depth of 10 times the pile diameter govern the load-displacement curve. They demonstrated the ability of hollow bar micropiles to carry moderate lateral loads with appropriate reinforcement configuration and pile head fixity.

SITE INVESTIGATION

An extensive site investigation was performed that included both in-situ and laboratory testing. Three mechanical boreholes were drilled to various depths using hollow stem auger of 130mm, followed by standard penetration test (SPT). Samples were extracted using split spoon sampling method and transported to the laboratory for further testing. Four CPT soundings were performed across the site. Figure 1 shows the SPT results for BH1 and BH2, including N values and water content for different soil layers. The first 400 mm consists of granular fill with some gravel and recycled asphalt overlaying a layer of very dense sand up to 11m below ground surface. Seams of silt and silty clay were observed at different levels. The ground water table was observed between 9.5 to 10.5m below ground surface. The average cone resistance corrected for pore water pressure (q_t) ranged from 10 to 30 MPa in the upper 6.5m and 30 to 45 MPa from 6.5m to 8m followed by a decrease in (q_t) with an average of 20 MPa.

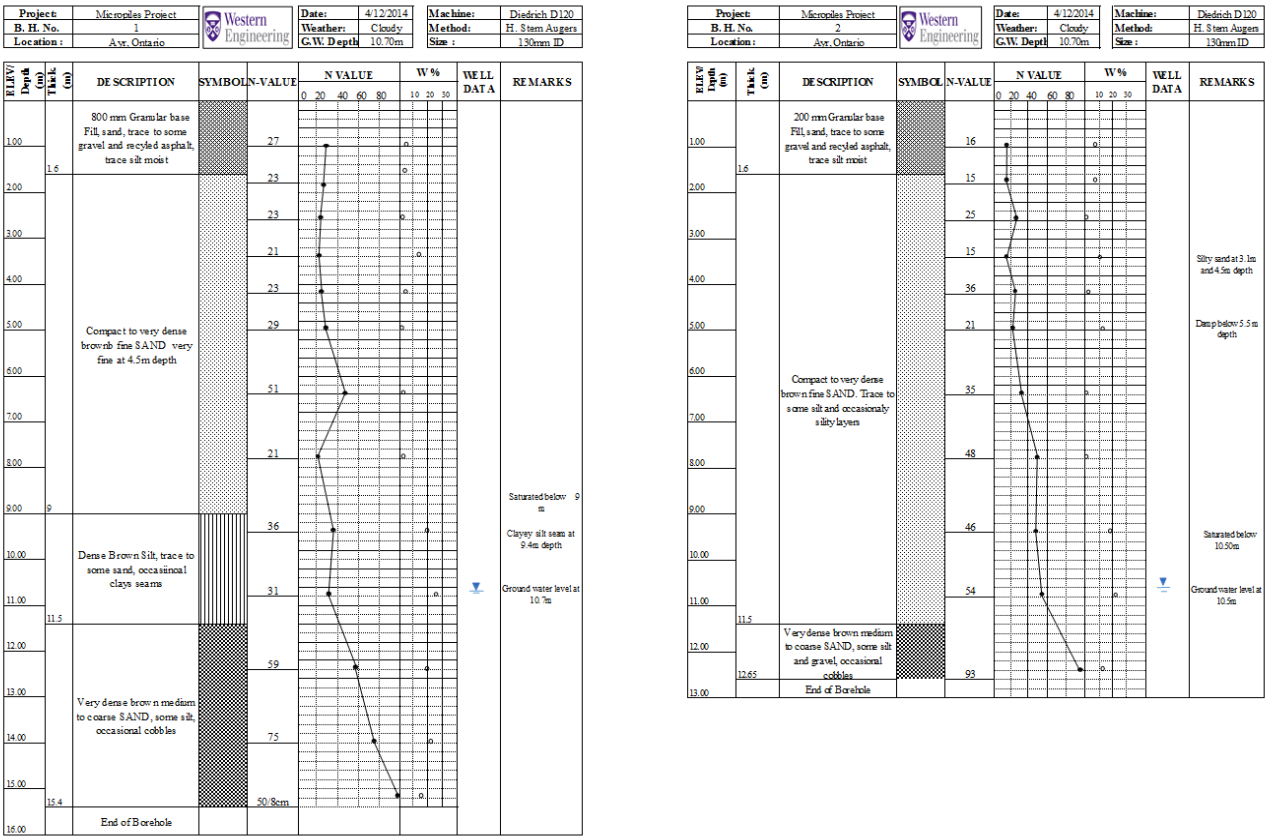


Fig 1. Boreholes 1 & 2, SPT N Value and water content.

MICROPILE MATERIALS AND INSTALLATION.

Six self-drilling hollow bar micropiles R51N were installed using an Ingersoll Rand ECM-350 drill rig. The outer diameter of the hollow bar was 51 mm and the inner diameter was 33 mm. A Tungsten carbide cross cut drill bit was used as an excellent choice for granular soils. Figure 2 presents a plan view of the micropiles locations in the test site. Six micropiles were constructed and tested. In this paper, the test results of only one micropile, denoted MP4 is presented. MP4 was installed using drill bit with 115 mm diameter. The diameter ratio of drill bit/ hollow bar (D_b/D_h) is 2.25. The total length of the micropiles is 6m with 5.75m embedded length.

The drill bit attached to the hollow bar was positioned in the predetermined location. The verticality of hollow bar was ensured by attaching a 1m-long magnetic water level to the hollow bar. Rotary percussive drilling was employed simultaneously with grout flushing technique. A Nonstructural grout with specific gravity between 1.4 and 1.5 was employed as drilling fluid to drill the hole to the required depth. Once the first segment of the hollow bar was installed, coupler was attached to allow the second segment to be installed. Upon completion the drilling, structural grout with specific gravity between 1.80 and 1.95 was injected at a pressure of 0.8 to 1 MPa. Grout cylinders were collected during the installation and were transported to a control room with a

relative humidity of 100% and constant temperature of 23ºC. The average compressive strength after 28 days of the grout cylinders was 40 MPa and the average spilt tensile strength was 3.97 MPa. The compressive strength was determined according to ASTM C39 and the tensile strength was obtained in according to ASTM C496. The compressive strength meets the minimum requirement (28 MPa) set by FHWA (2005).

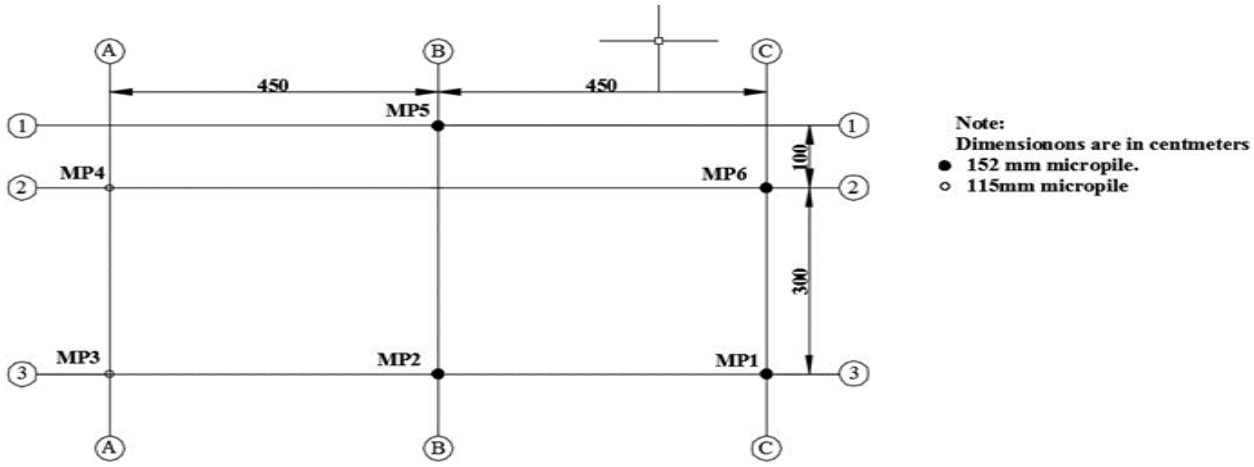


Fig 2. Plan view of micropiles locations.

TEST SETUP AND PROCEDURES.

A special loading system was designed and fabricated to apply the lateral loading to the micropile head. It consisted of a steel rod connecting the hydraulic jack to the micropile head; the steel rod was hinged to the pile head to ensure a free head condition. The load applied by the hydraulic jack was measured using a load cell that was connected to the loading system. Four HLP 190 linear potentiometers were employed to record the horizontal pile head movement and their average value was taken. The HLP 190 has 100 mm stroke and an accuracy of 0.01 mm. The potentiometers were attached to the loading steel plate in a square arrangement and clamped to an independent reference heavy steel beam.

The load was applied monotonically to the micropile head in increments of 3 kN. The load was maintained for 5 minutes for each loading increment. The load was increased until excessive settlement was observed.

TEST RESULTS AND ANALYSIS.

The load – displacement curve for MP4 is presented in Figure 3. The lateral response of the micropile exhibited two main regions: linear elastic response until about 3.5 mm displacement, which corresponds to about 3 % of the micropile diameter; and a non-linear behaviour extended to the test termination.

Two different mechanisms can define the pile failure: failure due to yielding of surrounding soil along the pile length, which is also called short pile behavior; or failure due to yielding of the pile materials when the maximum applied moment reaches the moment capacity of the pile, which is known as long pile behavior. Bierschwale et al (1981) used the slenderness ratio to define the pile rigidity and hence potential failure mechanism. The pile is short if its slenderness ratio is less than 6, while the long pile has slenderness ratio greater than 20. According to this criteria, MP4 is considered a long pile as it has a slenderness ratio of 44.

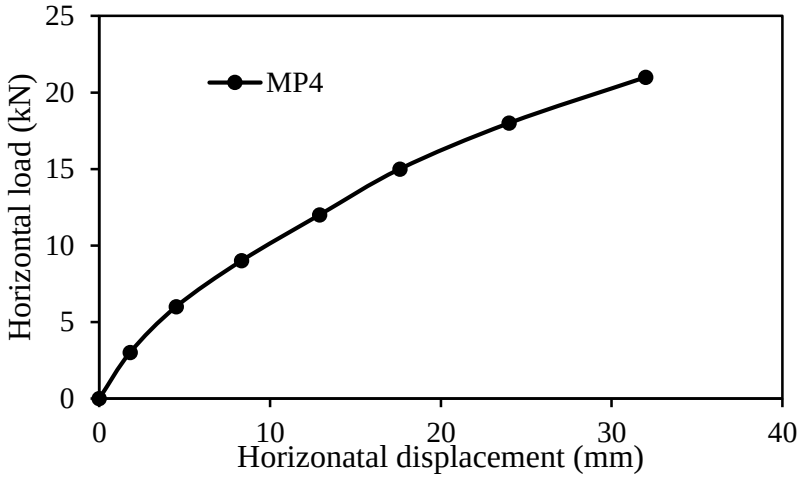


Fig. 3. Load – horizontal displacement curve for MP4.

Several interpretation criteria of ultimate lateral capacity of piles are presented in the literature. Five methods are compared in this paper: three are based on displacement limits, including McNulty (1956), Walker and Cox (1966), New York City (1981); and two are based on the displacement as function of pile diameter, i.e., Pyke (1984) and Briaud (1984). Table 1 summarizes the ultimate capacity according to these methods. It should be noted that the micropile diameter increased by 12.8 % over the drill bit diameter and is taken as 132 mm based on the real measurement of exhumed micropile diameter adjacent to MP4 and the top 2 m of MP3.

Table 1. Interpreted lateral failure loads for MP4

Method	Definition of failure load	Failure load (kN)
McNulty (1956)	Load at 6.25 mm head displacement	7.30
Walker and Cox (1966)	Load at 13.0 mm head displacement	12.10
New York City (1981)	Load at 25.0 mm head displacement	18.40
Pyke (1984)	Load at 5% the shaft diameter	7.50
Briaud (1984)	Load at 10 % the shaft diameter	12.10

Lpile computer software (Ensoft, 2006) was used to simulate the lateral response of hollow bar micropile installed in sand. Lpile utilizes the p-y curves approach assuming the pile acts as beam-column, representing the soil by nonlinear Winkler springs. The load-horizontal displacement curve obtained using Lpile software was calibrated using the load-horizontal displacement curve obtained from the field data. The hollow bar micropile was modeled in Lpile as round shaft with permanent casing and core. As the hollow bar micropile was installed without casing, the casing wall thickness in Lpile was set to zero. As the micropile was installed in cohesionless soil, sand model (Reese et al 1974) was utilized. The soil and pile properties were obtained from the results of the site investigation and the laboratory tests on grout cylinders. Figure 4 compares the results obtained from the calibrated Lpile model with the field test results. As it can be noticed from Fig. 4, there is a good agreement between the measured and calculated responses. Lpile results show a stiffer response for the first two load increments. However, the measured response was slightly stiffer than the calculated response at higher loads.

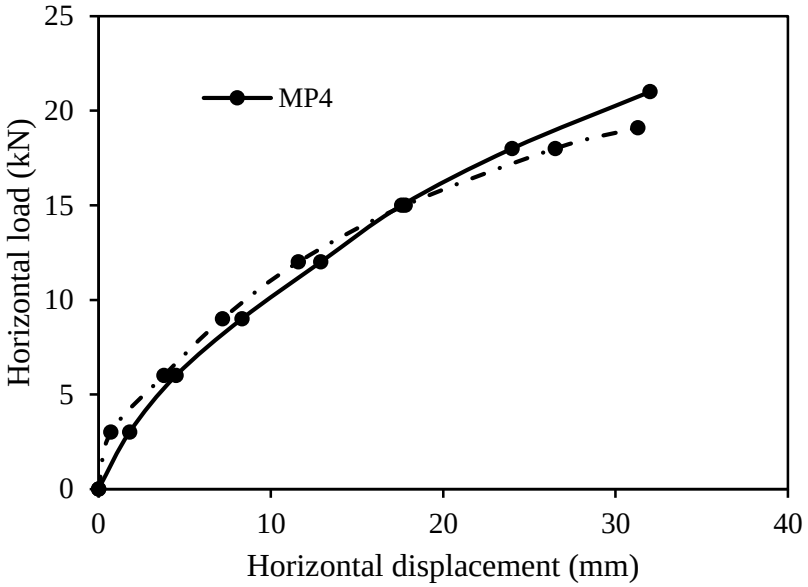


Fig. 4. Comparison between the field data and LPILE results.

Lpile can be utilized to calculate the deflection, bending moment and shear along the entire pile depth. Figure 5 (a and b) shows the micropile deflection and bending moment results obtained from Lpile model along the depth of the micropile. Figure 5 (a) indicates that the micropile behaves as long flexible pile and the top 1.0 m (about 8 micropile diameters) experienced lateral deflection, which indicated that the properties of the soil along the top 8 micropile diameter have an important influence on the lateral behavior of the hollow bar micropile installed in cohesionless soil. Lpile model was calibrated using the filed load test results and the maximum moment was about 8.9 kN.m. The analysis shows that the plastic hinge was developed at about 5 times the micropile diameter depth.

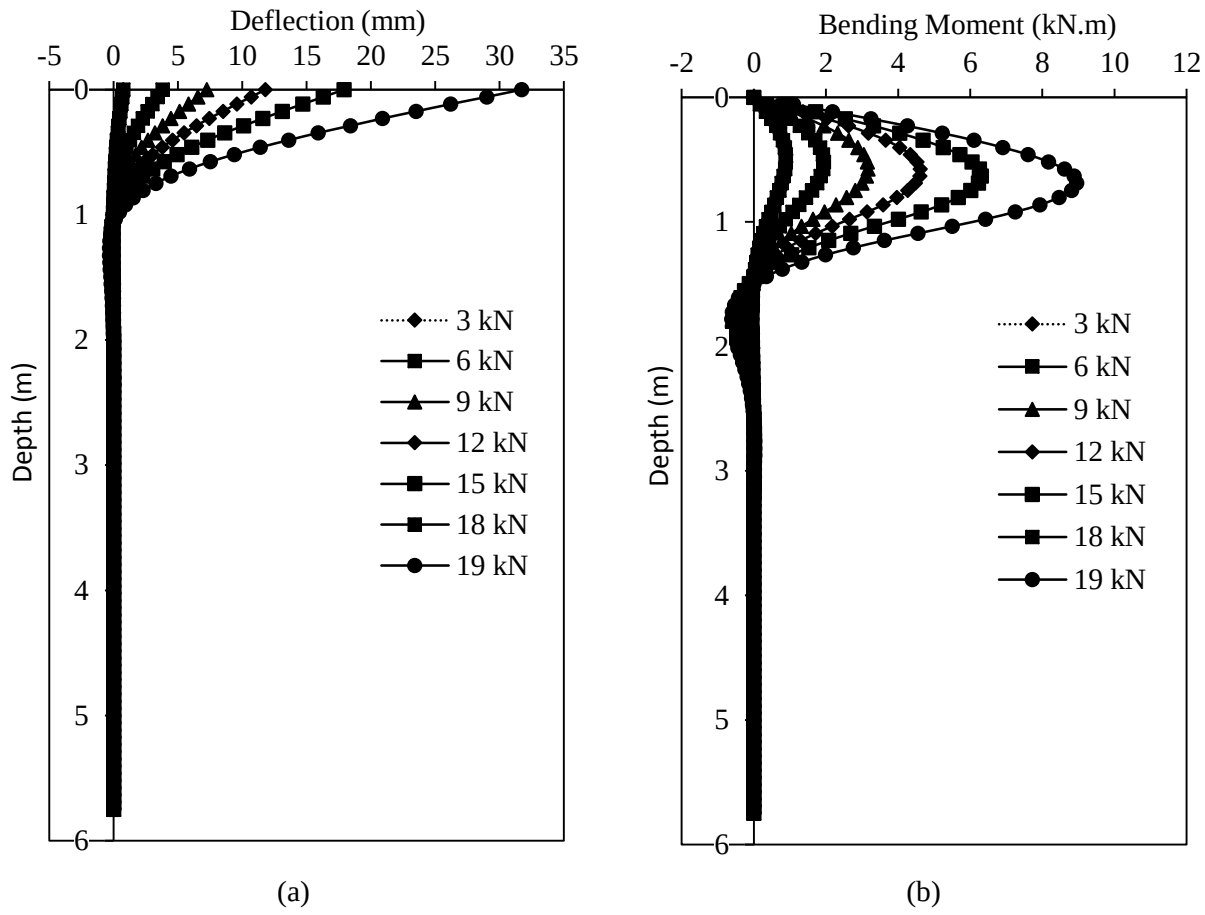


Fig. 8. Deflection and bending moment along the micropile depth.

SUMMARY AND CONCLUSIONS

A full-scale lateral test was conducted on a hollow bar micropile with D_b/D_h ratio of 2.25. The OD of the hollow bar was 51 mm and the ID was 33 mm. The drill bit diameter was 115 mm. The behavior of hollow bar micropile under lateral load was investigated and a numerical model using Lpile software was developed. The ultimate interpreted capacity was calculated using different methods and was compared with the predictions from LPILE analysis. The micropile did not show any sign of failure up to lateral deflection of 25 mm. Accordingly, the ultimate lateral capacity can be taken as the load corresponding to 25 mm lateral displacement with a factor of safety of 2 for the design purpose. Similar observations were made from testing the other micropiles

ACKNOWLEDGMENTS

The authors would like to acknowledge the support provided by HC MATCON for providing the materials, installing the micropiles and setting the reaction frames and NCERC for

partially funding the project. The authors would also like to thank the Libyan Ministry of Education for providing a scholarship to the first author.

REFERENCES

Abd Elaziz, A.Y., and El Naggar, M.H. (2015). *Performance of hollow bar micropiles under monotonic and cyclic lateral loads*. Journal Geotech. Geoenviron. Eng. 141 (5): 04015010.

Bierschwale, M.W., Coyle, H.M. and Bartoskewitz, R.E. (1981). *Field Tests and New Design Procedure for Laterally Loaded Drilled Shafts in Clay*. Research Report211- 3F, Texas transportation Institute, Texas A&M University, Collage Station, 116p.

Briaud, J. L. (1984). *Panel Discussion, Laterally Loaded Deep Foundation*. Philadelphia: American Society for Testing and Materials (ASTM).

FHWA NHI (Federal Highway Administration-National Highway Institute) (2005). *Micropile design and construction—Reference manual*. FHWA NHI-05-039, U.S. Dept. of Transportation, McLean, VA, 436.

Kulhawy, F.H., and Mayne, P.W. (1990). *Manual on estimating soil properties for foundation design*. Research project No. 1493-6, EL-6800, Electric Power Research Institute. Palo Alto, Calif.

Long, J., Maniaci, M., Menezes, G. (2004). *Results of lateral load tests on micropiles*. Geotechnical Special Publication, no. 124, Geosupport 2004 - Drilled Shafts, Micropiling, Deep Mixing, Remedial Methods, and Specialty Foundation Systems, Proceedings of Sessions of the GeoSupport Conference, p 122-133.

LPILE. (2006). A program for the analysis of piles and drilled shafts under lateral loads. Version 6.0.27 [computer program]. Austin, Tex: Ensoft Inc.

McNulty, J. F. (1956). *Thrust loading on piles*. Journal of Soil Mechanics and Foundations Division, 82(SM2), 1-25.

New York City. (1981). *Building code of the city of New York*. Binghamton.: Gould Publications.

Pyke, R. (1984). *Panel discussion, laterally loaded deep foundation*. Philadelphia: American Society for Testing and Materials (ASTM).

Reese, L. C., Cox, W.R., and Koop, F.D., (1974). *Analysis of laterally loaded piles in sand*. Proceedings of 6th Offshore Technology conference, Houston TX.

Richards, T. D., and Rothbauer, M. J. (2004). *Lateral loads on pin piles (micropiles)*. Drilled shafts, micropiling, deep mixing, remedial methods, and specialty foundation systems, Vol. 124, ASCE, Orlando, FL, 158–174.

Walker, J. N., & Cox, E. H. (1966). *Design of Pier Foundations for Lateral Loads*. Transactions of the ASABE, 9(3), 417-427.

RISK MITIGATION FOR MICROPILE FOUNDATIONS IN KARSTIC TERRAIN

Allen Cadden, PE, DGE[1], Philip Shull, PE[2]

ABSTRACT

Micropiles are typically recommended by the Geotechnical Engineer and designed by the Structural Engineer as they complete the foundation layout and pile cap designs. This leads to conservatism on both ends as neither the Geotechnical Engineer nor the Structural Engineer has a full understanding of both the ground conditions and building needs. This conservatism gets amplified when the site has difficult ground conditions, as a perception of greater risk drives more caution in the design expressed both as a higher design factor of safety and more redundancy through an increase in the number of piles.

The current practice for micropile foundations in karstic terrain is to install long, relatively lightly loaded micropiles extending through encountered and possible voids and fractured rock. Where voids and fractures are encountered, grout loss often occurs, which is resolved by the specialty contractor pumping dramatic volumes of high mobility micropile grout in an attempt to fill the hole. Additionally, fractures and soil seams throughout the rock strata are often disregarded and the bond zone started below the fractures and soil seams to get "good rock." These practices can lead to excessively long piles, an excessive number of piles, high quantities of cement use, larger than necessary pile caps, increased potential for pile conflicts, and unnecessary delays and cost to the owner.

It is time for these designs to be completed by the Foundation Engineer who understands the ground conditions, how micropiles are constructed, how they perform, and the demands of the structure. Only when the Foundation Engineer understands the entire project and has influence during construction, including quality control and treatment of anomalies encountered, are the risks of construction in difficult ground mitigated. This paper will demonstrate the value of such an approach and describe how real savings can be obtained.

CURRENT INDUSTRY PRACTICE

Current practice within the industry typically limits the involvement of the Geotechnical Engineer to the site exploratory phase, development of design recommendations, and inspection of earthwork and foundation element installation. After the exploratory phase, the Geotechnical Engineer issues a report recommending various foundation types that are applicable to the preliminary loading and building footprint.

[1] Principal, Schnabel Engineering, LLC, 1380 Wilmington Pike, Suite 100, West Chester, PA 19382, Phone: 610-696-6066, Fax: 610-696-7771, acadden@schnabel-eng.com
[2] Senior Engineer, Schnabel Engineering, LLC, 1380 Wilmington Pike, Suite 100, West Chester, PA 19382, Phone: 610-696-6066, Fax: 610-696-7771, pshull@schnabel-eng.com

Recommendations typically include allowable bearing pressures for footing, estimated total and differential settlement, or a recommended deep foundation system and capacity.

Typically, when micropiles are the recommended foundation, a geotechnical capacity and structural capacity for various sizes of micropiles are provided in the report. These recommendations are often conservative as they are meant to be a starting point for the design team to lay out the piles based on the loading and to estimate the cost of construction. Furthermore, they are often based on guidance manual design rules and have little site specific and constructability considerations factored in. This stage of the project warrants conservatism as there are many unknowns associated with the project during initial concept and pricing phases.

Unfortunately, once the Geotechnical Engineer provides the recommendations, they are often left out of the subsequent refinements and revisions. After the design footprint and loading are finalized, the Structural Engineer applies the conservative micropile recommendations to the project and lays out the piles. Micropiles are often new and unfamiliar to the design team and since the Structural Engineer did not develop the geotechnical capacity, this value is considered an absolute limit. Thus, most piles are usually under loaded. This practice leads to costly risk mitigation through the use of many lightly loaded piles.

Karstic Terrain

Karst is a highly irregular subsurface condition formed by the solutioning of carbonate rock strata. Additional complications arise during design and construction when such difficult ground conditions exist at the site. Karstic terrain is a particularly problematic formation and often an example of risk mitigation through ignorance and excess. During the investigation and design phases, the Geotechnical and Structural Engineers are even more conservative than usual as the site variability and perceived risk of unforeseen conditions are greater. The design bond zone is typically lengthened in an effort to reduce the impact of the rock formation unknowns. Additionally, more piles are often added to the footprint as the Structural Engineer is also wary of potential voids. This is similar to practices for driven piles where redundant piles are installed in case a pile refused on floating boulders or unstable pinnacles in the karst matrix.

A typical construction method is to define the bond zone as suitable continuous rock: “good rock.” Complications result from chasing this “good rock” when soils seams and small voids are found within the anticipated bonded zone. The result is that the top of the rock formation is disregarded and the final suitable bond zone is started well below the surface of the encountered rock. This problem gets compounded if the micropile designer does not observe the construction of the micropiles, which often happens as many owners choose to have the pile installation “inspected” by a low cost service provider instead of the specialized micropile designer with experienced micropile inspection personnel. When this happens (or is likely to happen), the designer will protect their interests and increase factors of safety and provide more restrictive specifications to assure an adequate micropile is constructed, thus negating the risk of variability from

voids and soil seams in the bond zone. This practice further leads to excessive pile lengths.

During construction, even the “good rock” will encounter some voids or seams that may result in a loss of grout. Unless carefully controlled, the standard practice is for the specialty contractors to pump more, high mobility micropile grout (often much more grout) in an attempt to fill the pile. This practice leads to excessive grout takes.

Consequences of Conservatism

Increased factors of safety, longer bond zones, and lightly loaded piles may seem like a reasonable approach when faced with difficult ground conditions, particularly to the engineers with whom the potential failure may weigh heavily. However, this conservatism comes at a price and more risk. More piles mean more holes drilled, which increase the potential for ground damage and conflicts with utilities, existing structures, and other micropiles. Additionally, more piles require larger pile caps, thus larger excavations exposed to the elements and possible standing water that could induce a sinkhole formation. Larger pile caps also increase the amount of concrete and reinforcing bars required, as well as more time required to install the piles. Longer piles mean more challenges during drilling, more flushing and greater risk of tooling failures in the hole.

Excessive grout takes from grouting voids and seams with high mobility grout and attempting to fill all cracks and crevices can lead to very high cement costs. Furthermore, injection of grout can cause ground heave, risk filling nearby utilities, or change groundwater flow patterns, increasing risk of subsurface erosion in other areas.

More piles, more time required to drill and install the foundation elements, high grout takes, and larger pile caps all increase the cost to the owner and do little to mitigate risk. Foundation base costs are a part of this, but the schedule costs and added risk of unforeseen problems also increase and may be much more significant.

PROPER RISK MITIGATION

The Foundation Engineer, the professional engineer who has the knowledge and skill set to address the specific geotechnical and structural aspects of the project, is the only one who has the ability to assimilate all of the information and knowledge to properly mitigate risk through an understanding of both the superstructure requirements and the ground conditions. This person must be involved as a key member of the project team from the initial design phase through the completion of foundation construction. A Foundation Engineer responsible for the design, layout, and quality assurance of the installation has a unique position to manage and mitigate risks and costs to the owner through a variety of techniques.

Design

The first step in mitigating risk and reducing costs is to reduce the required number and length of micropiles through efficient design and specifications. The Foundation Engineer, knowing they will have the opportunity to confirm assumptions and remediate difficult ground conditions, has the ability to manage risk and uncertainty and thus be less conservative in the foundation design. The bond length can be established based on site data and experience and less controlled by concern about unknowns that might be encountered during construction. With an efficient design, the piles can be loaded closer to their geotechnical and structural capacity, and configured in a manner to minimize the pile cap footprint. Furthermore, the guidance of the project documents can be more relevant for the project and less of a catch all that tends to create adversarial situations between the owner and contractor or specialty contractor.

An example of a more efficient design developed by an engineer integrating the challenges of complicated geotechnical and significant structural loading conditions is demonstrated in the following real world case history of a micropile foundation to support a multilevel structure in karstic limestone. Figure 1 shows the initial pile layout done the traditional way with a Geotechnical Engineer providing foundation recommendations (micropile capacity and bond length) and the Structural Engineer placing many lightly loaded piles to support the structural load.

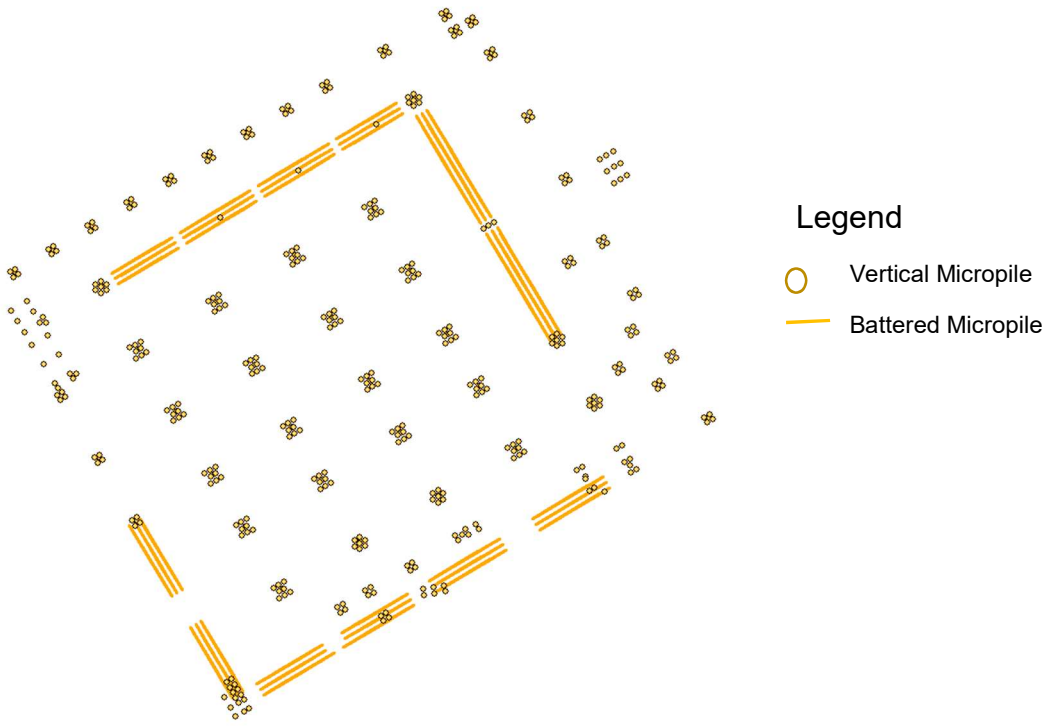


Figure 1. Initial pile layout with many lightly loaded piles.

The revised layout (Figure 2) shows the more efficient design achieved when a Foundation Engineer has a seat at the table during the design phase. Note that approximately 1 to 2 micropiles were removed from each pile cap supporting the vertical loads by utilizing the piles more efficiently. This represents about a 30% reduction in piles for the same loading conditions and, considering a cost of about $100 per foot, translated to an instant savings to the owner on the order of $500,000 in piles that were not constructed. The average pile length in this case was about 15m with the longest piles reaching upwards of 40m. This reduction in the number of required micropiles quickly reduces the overall foundation cost, but possibly more importantly, it reduced the construction schedule and risk exposure. Additional savings are realized due to the reduction in pile cap size, which reduces concrete and rebar costs, labor costs, and the time required to construct the pile caps.

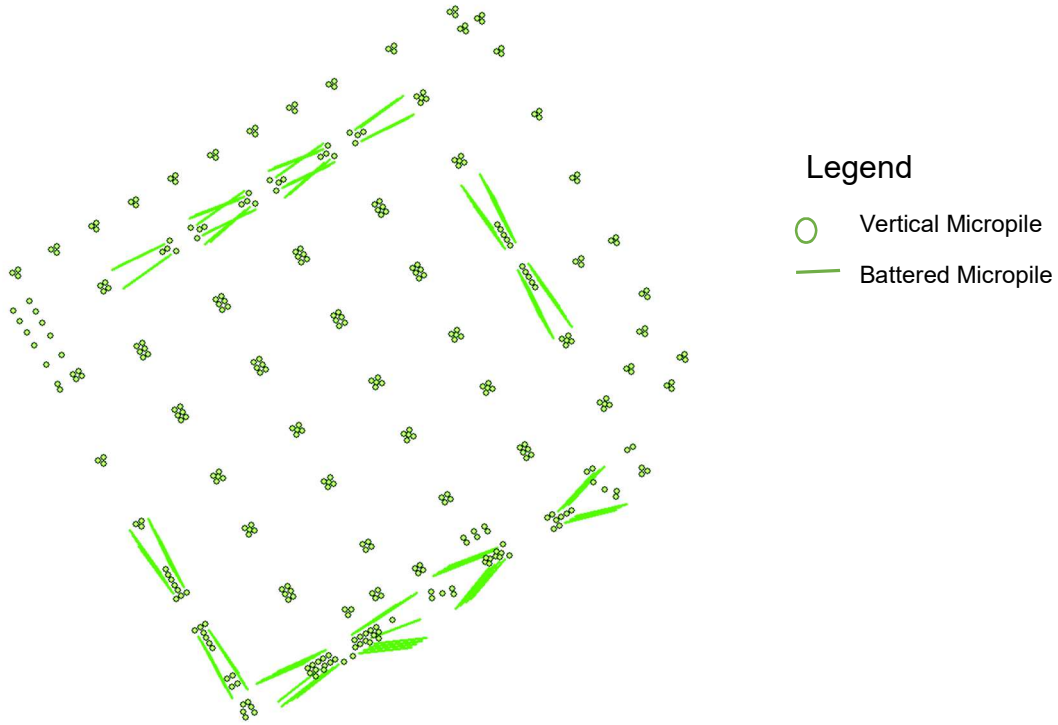


Figure 2. Revised pile layout with 1 to 2 piles removed per pile cap.

A further challenge posed by the initial design is depicted in Figure 3, which shows the potential conflicts of the battered piles in the original configuration. The initial pile layout would have risked striking previously installed piles as they attempted to reach “good rock.” The layout is reliant on rock being shallow and predictable, which was not the case at this site.

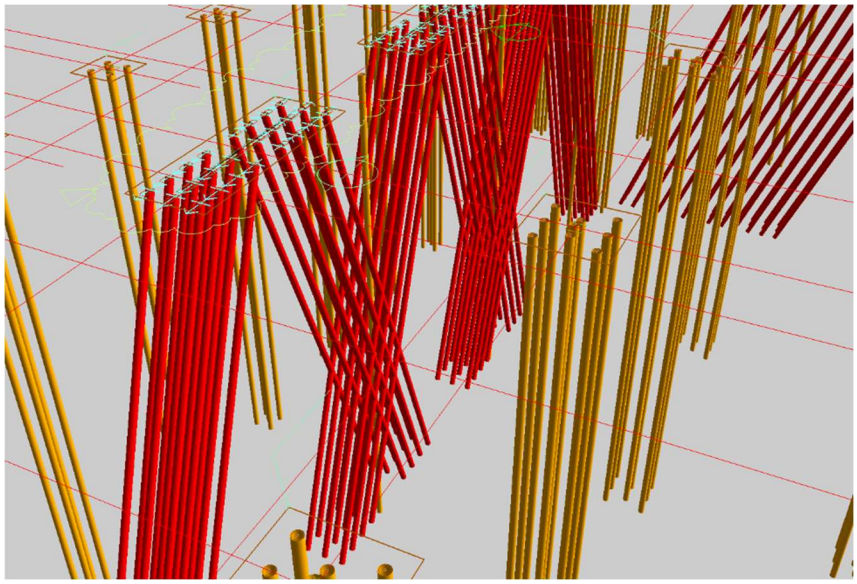


Figure 3. Original battered pile conflicts.

Figure 4 depicts the revised micropile layout for the shear walls utilizing a combination of vertical and battered piles to resist the lateral forces and minimize potential pile conflicts while drilling. This layout was able to accommodate varying depth to rock while not risking the striking of a previously drilled pile.

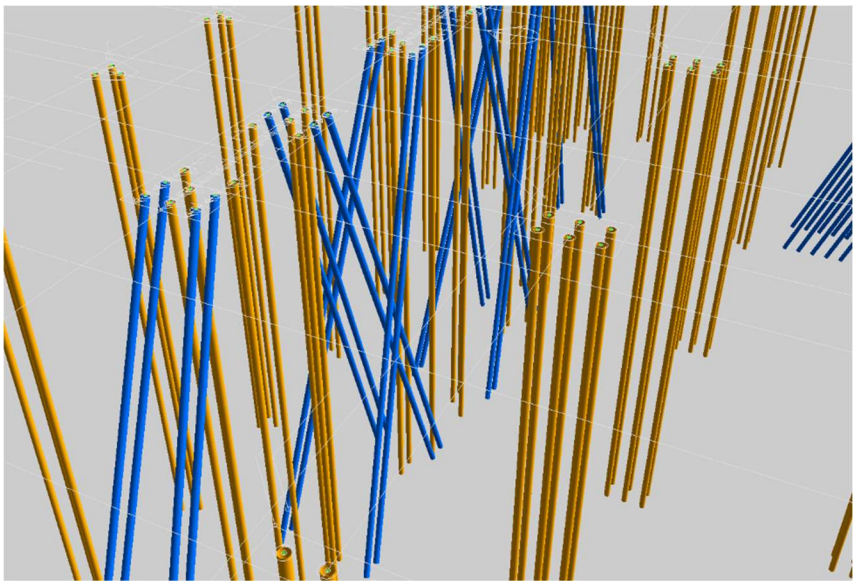


Figure 4. Revised battered and vertical shear key minimizing conflicts.

Specifications

Specifications are contract documents and must be specific to define expectations of the contractor to meet the client's needs. These documents help ensure qualifications of the construction personnel, expectations of the installation equipment and materials,

quality control and quality assurance, and may define measurement and payment methods. These are all key elements of good construction documents. However, they cannot become a crutch to replace sound engineering judgement and the ability to modify means and methods to accommodate variable site conditions.

In the world of micropile construction, it is imperative that the Foundation Engineer utilize the entire installation method as a tool to improve the design. Furthermore, ground conditions dictate the correct construction method to build the pile. Only by understanding and utilizing the tools available can the project be considered a success. The specification needs to allow the Foundation Engineer to collect information during drilling, determine the top and bottom of the bond zone based on that information, determine the best grouting process to ensure a stable hole, and ensure the reinforcement is placed correctly. It must be recognized that each pile record is not a stand-alone document; combined they provide significant insight into the subsurface condition that must be considered as a whole. Additionally, the specification must make the contractor aware of the role of the Foundation Engineer and the contractor's role to work together to build reliable piles.

Grouting of the holes is a critical element. Unfortunately, little flexibility is typically included in the specification so that the contractor is aware that the foundation engineer may require staged grouting, redrilling and regrouting, use of variable high mobility mixes, or even low mobility grouting to achieve a sound pile. Furthermore, little guidance is typically provided regarding how the specialty contractor will be compensated if such challenging grouting methods are deemed necessary.

Construction Observation

There are several advantages to the owner and project team to having the Foundation Engineer observe construction that may not be apparent at first glance. As noted above, the Foundation Engineering is a package deal from initial design through final construction. The goal is to reduce cost, schedule, and risk, which can only be accomplished through consistency in the foundation philosophy. That philosophy is realized during construction through confirmation. Once an efficient foundation system reaches construction, the savings (or losses) are not yet realized. Delivering on the efficiency requires coordinated delivery of the foundation construction.

Often (or typically) getting the project out of the ground is on the critical path. It is also the phase most often fraught with unforeseen conditions that can impact the schedule. As a result, the focus is how many piles can be drilled in a day and how many crews can be provided to accelerate this schedule. This message trumps all concerns discussed in the design team meetings with the owner. Unfortunately, this leads to short cuts. You see this in the form of drilling multiple piles too close together and connection between piles, leaving numerous pile ungrouted for extended periods of time, excessive grouting volumes rather than managed grout placement and possible redrilling. Furthermore, the tendency to drill to “good rock” actually provides relief to the specialty contractor since this gives them a basis for some schedule delays as it is an “unforeseen”

condition. Keeping the Foundation Engineer involved allows cooperative adaptation to site conditions while maintaining the design intent and allowing for quick responses by the design team.

Several decisions by the field personnel have the ability to significantly impact both cost and schedule. Some of these include:

- Establishing the bond zone. Rather than seeking "good rock," the entire borehole should be evaluated and considered for load transfer. There is a trade off in cost and time for drilling, casing, and grout for a long hole that must be compared to the benefit of shorter casing, easier reinforcement installation, yet possible grout loss and the need for additional regrouting or redrilling.
- Grouting of a hole. A defined volume of grout should be established for placement on initial grouting (within reason). This can be tied to a multiple of the theoretical volume of the bore hole and is typically 1.5 to 2 times; although actual site geology and designer experience should determine the specified volume. If this volume is exceeded, considerations of alternative grouting methods should be considered. These may include mix modification, waiting for grout set and regrouting, allowing grout to harden and redrilling, or electing to use other methods such as low mobility grouting.
- Allowing multiple holes to be drilled before grout placement. Many factors impact this including the ground conditions and quality of the bond zone material. Although attempted in many cases, and occasionally unavoidable, there are many down sides to this that go unnoticed and can be difficult to reliably correct.

The often overlooked benefit is the time factor involved when dealing with deep foundations in difficult terrain. Time is of the essence during micropile installation, and delays can not only increase the time and cost of the foundation, but can slow the progress of a typically critical path item, preventing the next phase of construction from beginning. A conflict between a proposed micropile and an existing utility or a problematic void, as examples, can take days to resolve if the Foundation Engineer does not have a presence on the site. The typical process is for the micropile contractor and/or inspector to notify the general contractor of the conflict. The general contractor will then submit an RFI to either the Structural Engineer or the Architect who forwards the RFI to the micropile designer. The designer must then review the information, which can be lacking and may not provide what the designer wants to see, and either request more information from the team (drill logs, record drawings, etc.) or issue an RFI response. This process will be repeated for each conflict, encountered void, broken casing in the hole, lost piece of drill string, etc.

The presence of the Foundation Engineer on site during construction means conflicts can be remediated more quickly as information is conveyed in real time, the Foundation Engineer has firsthand knowledge of the issues, and they can modify the micropile layout in a few minutes instead of days or weeks. This may be the biggest cost savings to the owner and it is often overlooked.

CONCLUSION

The profession is doing the owner a disservice by attempting to reduce risk by using excessive conservatism. It is time for us to make it clear to the owners that proper risk mitigation and cost savings can only be attained through involvement of the Foundation Engineer from the beginning to end of the project.

The entire project team wins when the Foundation Engineer is involved from design through construction. When the Foundation Engineer understands the entire project and has intimate involvement during construction, including quality control and treatment of anomalies encountered during construction, the risks of construction in difficult ground are mitigated and the owners save money (and time, which is money). We must communicate this message to owners and design teams so they recognize the benefits and cost savings of this approach.

Often an owner compares the cost of the Foundation Engineer to that of a typical construction inspector and does not see the need to pay a premium for what is seen as a commodity. With a little effort on our part, it will become clear that the owner will not only save on the cost of micropiles installed, but also on the cap size and associated rebar and concrete. More significantly, they will save time and schedule. We must be tireless in our efforts to educate the owners to show them what not involving the Foundation Engineer truly costs.

USE OF HIGH CAPACITY MICROPILES TO RESIST SEISMIC OVERTURNING OF COLUMNS

Peter Speier, P.E.

ABSTRACT

As a result of California State Law enacted in 1994, Sharp Memorial Hospital in San Diego, CA required an extensive seismic retrofit in order to remain in service past January 1, 2015. When built in 1972, the structure was founded on spread footings below the core columns. While these footings remain in service to support static dead loads and live loads, high capacity micropiles were needed to resist overturning moments that would occur at the base of the columns in a seismic event. Rather than tying the micropiles into the existing footings, the micropiles were anchored directly to the retrofitted column base plates. Complicating the installation was the fact that the hospital needed to remain fully operational throughout the entire construction. Not only were the micropiles to be installed in severely limited access conditions, complex management of phase construction, dust control, and spoils management were required to comply with the hospital's infection control policy.

This paper will discuss the complex nature of this project in further detail. Additionally, it will highlight the benefits of how partnering between Contractor, Owner, Engineers, and manufacturers resulted in an efficient, safe, and cost effective solution to an extremely difficult foundation problem.

PAPER

HISTORY

It is well known that the state of California has experienced major catastrophic earthquakes in the past and will certainly experience more in the future. Earthquake related deaths are relatively rare considering only 363 have been recorded in California within the last 100 years. While this may seem insignificant, it is more than all of the other 49 states combined. The low death rate is largely due to laws and regulations passed subsequent to major earthquakes that implement stricter seismic building codes to protect life and property. As a result of this action, the state of California is considered to be the worldwide leader in earthquake resistant design.

One such law was passed in 1973. The Alfred E. Alquist Seismic Safety Act established a seismic safety building standards program under the jurisdiction of The Office of Statewide Health Planning and Development (OSHPD). The act was a result of the loss of life incurred due to the collapse of a hospital during the Sylmar earthquake of 1971, and emphasized that essential facilities should remain operational after an earthquake.

After the Northridge earthquake in January 1994, it was found that hospitals built in accordance with the Act performed well structurally, while those built prior to the Act experienced major structural damage that required evacuation. This lead to the passage of Senate Bill 1953 later that same year. The Bill amended the 1973 Act to ensure that acute care hospitals are not only capable of remaining intact after a seismic event, but they can continue operation providing acute care after such an event. The Bill established requirements for hospitals to evaluate their seismic performance for placement into one of five specified Seismic Performance Categories (SPC), and required each acute care hospital facility to attain a specified SPC by specified timeframes.

THE PROBLEM

Sharp Memorial Hospital in San Diego, CA was first opened in 1955. Over the years, the hospital has undergone significant expansion. In 1972, a 9-story structure known as the Central Tower was completed. More recently, a major expansion project was completed in 2009. While the most recent expansion was done in accordance with the latest seismic requirements, the Central Tower was constructed just prior to the Alfred E. Alquist Seismic Safety Act, and was therefore severely deficient. Subsequent to analysis required by SB 1953, the Central Tower was categorized as having an SPC-1, the lowest rating and indicative of the greatest probability of collapse. To remain in service past January 1, 2015, the Central Tower would require significant seismic upgrades necessary for placement into SPC-2. Compliance with this provision would allow the Tower to remain in service until January of 2030.

The deficiency was that the tower would experience unacceptable story drift in a major earthquake. Interestingly, the lower floors of the tower were the problem, mainly due to the close proximity of the tower with adjacent structures. The original structure was founded on spread footings at each of the tower's 8 core columns. The spread footings were not able to resist the large overturning moments expected in a major seismic event. To remedy the problem would require establishing fixity to the columns at the foundation level.

The original design solution was to construct a mat foundation beneath the existing spread footings! When this solution was released for bid, it was difficult to even get a Contractor to agree to commit to pricing this high-risk solution, as it would require tunneling underneath the existing hospital lobby, presenting myriad problems with phasing, reinforcement placement, and safety, all of which would fall under heavy OSHPD Mining and Tunneling scrutiny.

It was clear that a solution utilizing micropiles would be much more feasible from a construction standpoint. Condon-Johnson & Associates, Inc. (CJA) was involved with the project very early in the process and proposed micropiles as a more economically feasible and significantly safer solution. After the General Contract was awarded to Swinerton Builders, the team agreed to explore the feasibility of the micropile solution under the premise that CJA would perform the work if the solution could be approved by OSHPD.

STRUCTURAL DESIGN

CJA and its Geotechnical Consultant, Leighton Consulting Group, worked closely with KPFF Consulting Engineers, the Structural Engineer for the Project, to advise and assist with the micropile design based on their installation and testing capabilities. The resulting preliminary concept design consisted of 76 high capacity micropiles with seismic compression and tension capacities of 2,738 kN (616 kips) and 1,507 kN (339 kips) respectively. The micropiles would support ten of the structure's core columns. Nine of the ten columns utilized 8 micropiles around the column, while the remaining column could only use 4 micropiles due to conflicts with existing utilities. The preliminary micropile section was an 8" diameter pile with casing in the upper 3 m (10 feet) of the pile, reinforced with 65mm (2-1/2") diameter 1034 MPa (150 ksi) all-thread bars.

One of the more unique aspects to the design was to anchor the micropiles directly to retrofitted column base plates rather than to the existing concrete footing or a new cast in place footing extension. The existing column base plates were too small and could not supply the required fixity to the base of the steel columns. The retrofitted base plates consisted of a 2-piece arrangement that allowed installation around the existing base plate after the micropiles were installed. One of the plates was "U" shaped, while the other was rectangular. To tie them into the existing column, gusset plates were welded to the base plates and the existing column. A sketch showing this arrangement can be seen in Figure 1, and a CAD rendering is shown in Figure 2. This solution resulted in very close spacing for the micropiles that were as little as 0.6 m (2 feet).

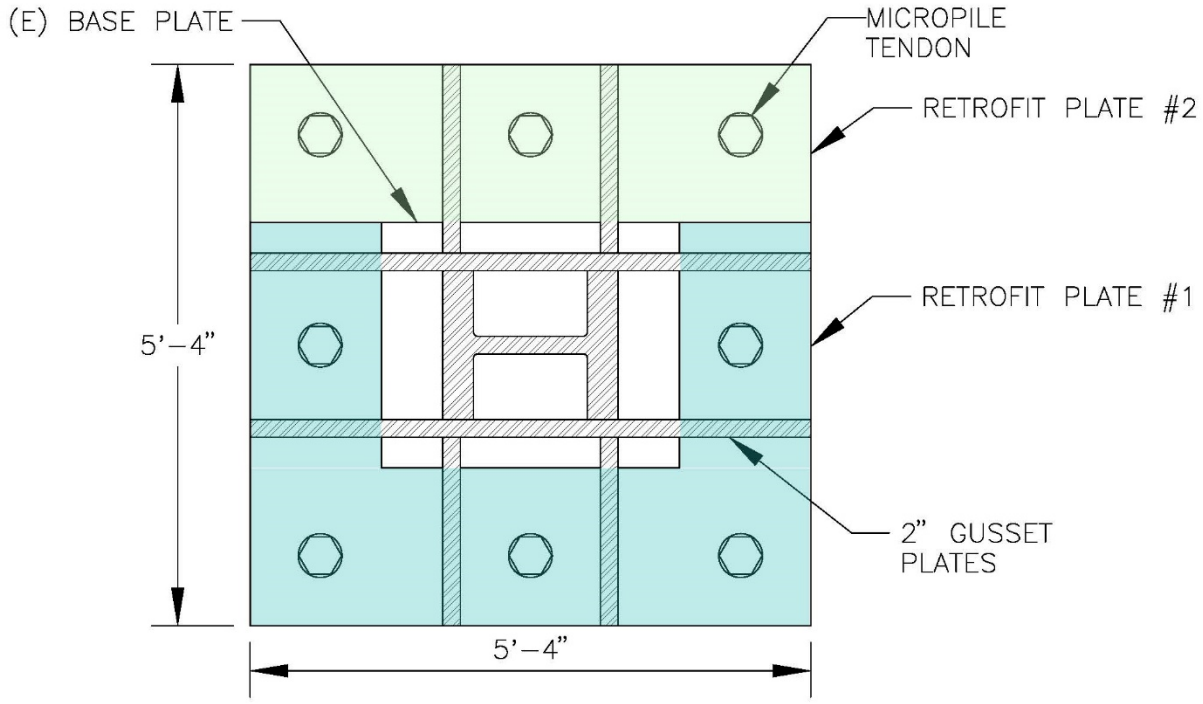


Figure 1: Typical Layout of Column and Retrofitted Base Plate

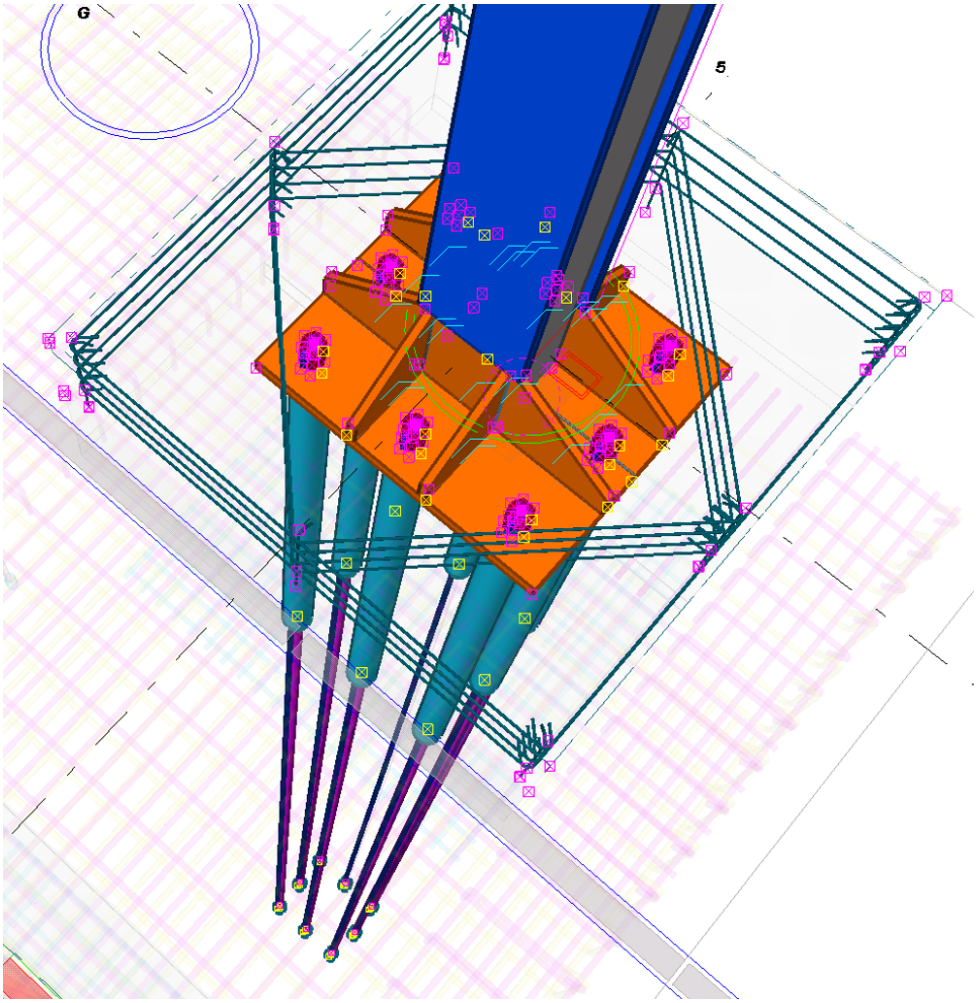


Figure 2: CAD rendering of retrofitted column

GEOTECHNICAL DESIGN AND PRE-PRODUCTION TESTING

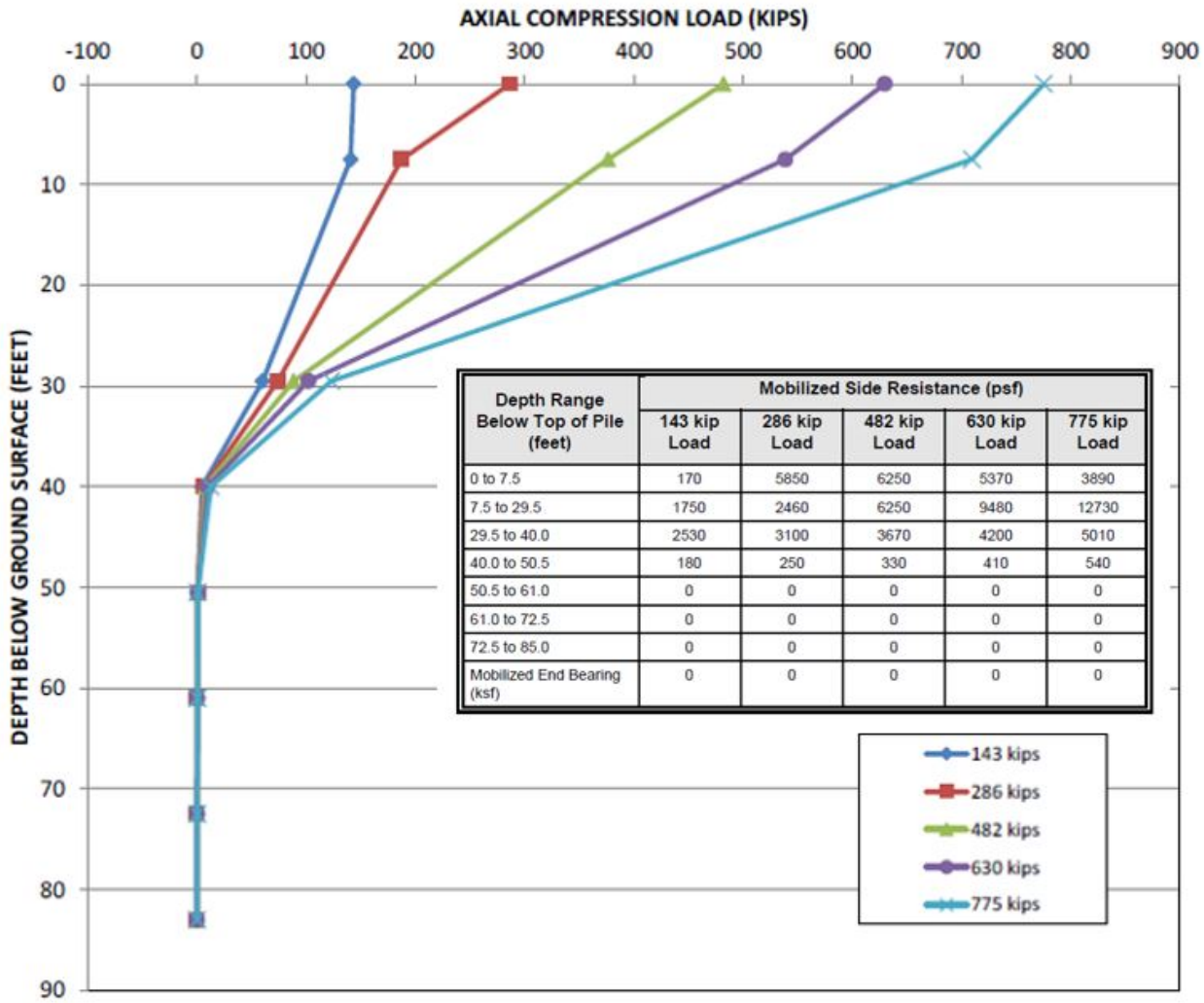
Once the concept design was accepted, OSHPD required that all design assumptions be verified by testing prior to granting final approval of the solution. The verification required formal analysis and a report providing design recommendations for the micropiles stamped by a Geotechnical Engineer. CJA contracted directly with Leighton Consulting Group to observe the test pile installation and load testing.

The Sharp Hospital site is immediately underlain by what is known as the Linda Vista Formation, which is a dense silty sandstone extending to a depth of approximately 6-7.6 m (20-25 feet) below ground surface (bgs). Below this is the Stadium Conglomerate, a dense locally cemented conglomerate of sands, gravels, and cobbles. Both formations provide exceptional bond strengths to transfer the high loads. Groundwater elevation was approximately 21.3 m (70 feet) bgs.

Working with Leighton and KPFF, a pre-production test program was developed to load a sacrificial test pile to 3,444 kN (775 kips) in both tension and compression.

Additionally, strain gauges were installed on the test pile tendon that were used to calculate the stress in the tendon at various depths of the pile throughout the test. Reaction piles on each side of the test pile were installed for the compression testing. All three piles were 200 mm (8 inch) diameter and drilled to a depth of 25.9 m (85 feet). The test pile was bored out to 225 mm (9 inches) in the top 4.25 m (14 feet), and an 220 mm (8-5/8 inch) OD casing was set in the top portion of the pile. The piles were reinforced with 75mm (3 inch) diameter 1034 MPa (150 ksi) Williams Threadbar, and grouted with Portland Cement and water grout.

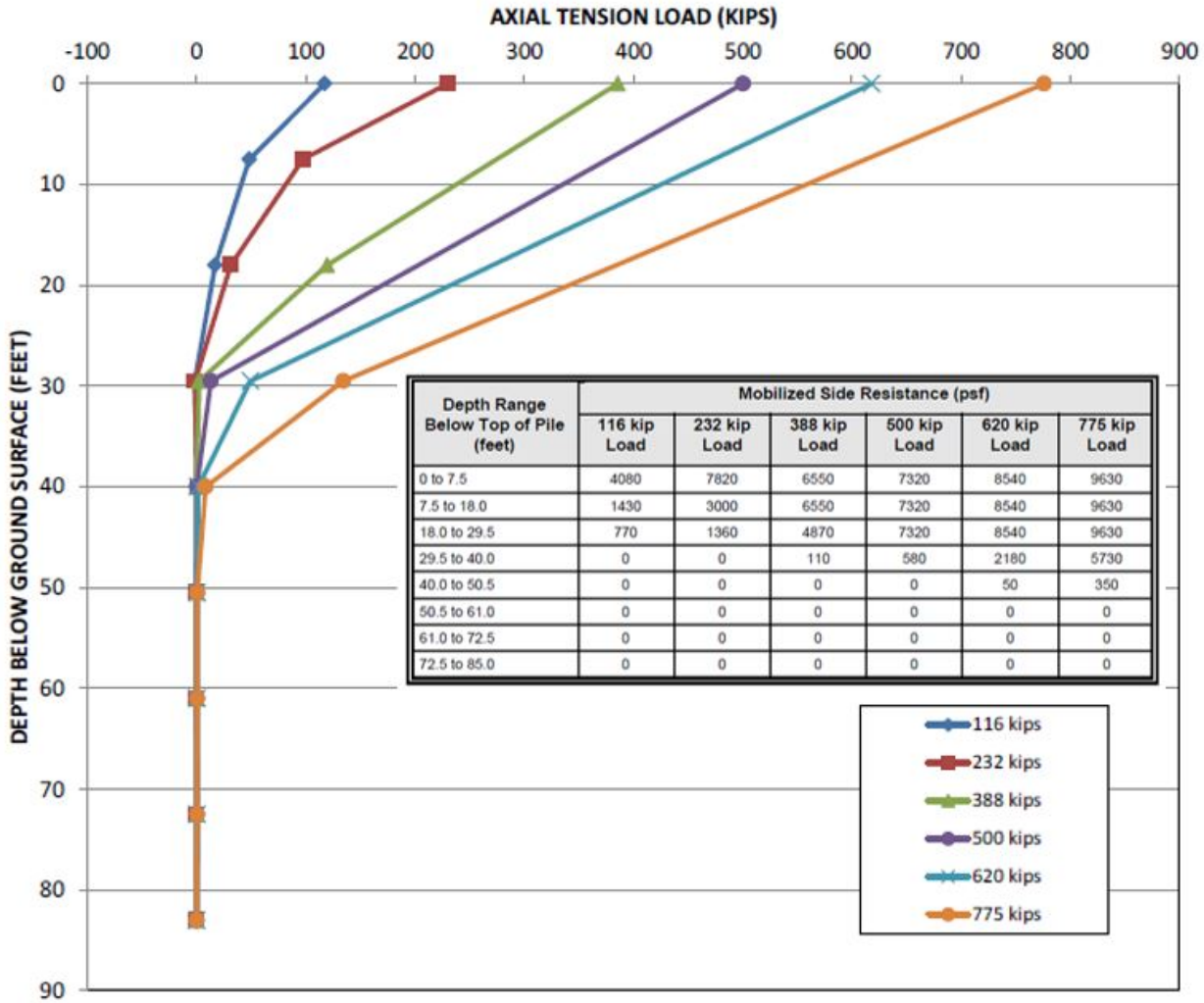
The test pile was loaded incrementally and deflection at the top of the pile were measured and recorded. Total Pile movements at the maximum test load were just over 25 mm (1 inch). The test pile easily met the acceptance criteria, which was consistent with recommendations in FHWA NHI-05-039 (2005), and required that the slope of the load deflection curve was less than 15 mm/kN (0.025 in/kip).



Depth Range Below Top of Pile (feet)	Mobilized Side Resistance (psf)				
	143 kip Load	286 kip Load	482 kip Load	630 kip Load	775 kip Load
0 to 7.5	170	5850	6250	5370	3890
7.5 to 29.5	1750	2460	6250	9480	12730
29.5 to 40.0	2530	3100	3670	4200	5010
40.0 to 50.5	180	250	330	410	540
50.5 to 61.0	0	0	0	0	0
61.0 to 72.5	0	0	0	0	0
72.5 to 85.0	0	0	0	0	0
Mobilized End Bearing (ksf)	0	0	0	0	0

Figure 3a: Graphical Results of Strain Gauge Readings for Compression Loads with inset showing average bond stress within various depth ranges for specific load increments

The data obtained from the strain gauges (Figure 3a and 3b) showed that nearly the entire compression and tension test loads of 3,444 kN (775 kips) were transferred through the top 12.2 m (40 feet) of the pile. This data was used to economize the design by establishing bond stresses much higher than would have been assumed without instrumentation of the testing. The increased bond stresses allowed the production micropiles to be reduced to 18.3 m (60 feet), which put the pile tip well above the groundwater elevation. This simplified installation tremendously since all drilling was done from inside the existing hospital lobby. The final micropile design utilized 65 mm (2-1/2 inch) diameter 1034 MPa (150 ksi) Williams Multiple Corrosion Protected (MCP) Threadbar tendons as reinforcement.



Depth Range Below Top of Pile (feet)	Mobilized Side Resistance (psf)					
	116 kip Load	232 kip Load	388 kip Load	500 kip Load	620 kip Load	775 kip Load
0 to 7.5	4080	7820	6550	7320	8540	9630
7.5 to 18.0	1430	3000	6550	7320	8540	9630
18.0 to 29.5	770	1360	4870	7320	8540	9630
29.5 to 40.0	0	0	110	580	2180	5730
40.0 to 50.5	0	0	0	0	50	350
50.5 to 61.0	0	0	0	0	0	0
61.0 to 72.5	0	0	0	0	0	0
72.5 to 85.0	0	0	0	0	0	0

Figure 3b: Graphical Results of Strain Gauge Readings for Tension Loads with inset showing average bond stress within various depth ranges for specific load increments

CONSTRUCTION

Installation of micropiles inside an operational hospital requires extensive planning and specialized equipment to maintain a nearly dust free work area. To minimize the impact to the lobby and maintain required access, the micropiles were installed in four separate phases. Equipment within the work areas was electrically powered, and any diesel fueled equipment was located outside the hospital within a dedicated staging area nearly 91 m (300 feet) away.

A TEI TD75 drill with a single rotary and duplex setup was used to drill the micropiles. This compact rig was able to drill up to a 250 mm (10 inch) diameter hole, and track into the work area through a standard size doorway (Fig 4). The holes were advanced inside the casing using a 125 mm (5 inch) down-the-hole hammer. While casing was not needed to stabilize the drill holes, it was used to facilitate containment of the drill spoils. By fabricating a spoil swivel attached to the casing flushing bell, drill spoils were transported through a vacuum duct to a sealed separation tank, and removed from the work area when full.



Figure 4: Micropile Drill entering hospital

The shortest route between the staging area and the work areas ran through a quiet meditation area known as “The Healing Garden”. This area is adjacent to the

Cancer Treatment Center, and is used by patients and family. Support lines for grout, water, and compressed air, as well as vacuum duct lines had to discreetly run through this area.

The ceiling height within the work area was as low as 2.4 m (8 feet), so the micropile reinforcement had be coupled with bar lengths of 2.25 m (7'-6"). Even with the short tendon length, each tendon still weighed 79 kg (175 lbs). CJA fabricated a steel tripod with an electric winch to hoist the tendons and suspend them over the hole while they were coupled together section by section.

To comply with infection control protocols, the work areas had to be completely contained to prevent dust and air within the work areas from entering the hospital. This was achieved by setting up temporary barriers and creating "negative air pressure". Negative air pressure is achieved by using vacuum pumps to keep the air pressure in the work area slightly below standard atmospheric air pressure. This way, any minor breaches in the temporary barriers will force air to flow from within the hospital into the work area rather than from the work area out.

Prior to pile installation, the slab was saw cut and the concrete from the area around the column was removed to the top of the footing. Then the existing footings were core drilled at each micropile location to facilitate the pile installation. After the holes were advanced to the correct elevation, the holes were grouted and the drill casing was withdrawn completely. Permanent casing was then set into the fluid grout and the tendon was lowered into the drill hole.

Because the micropiles were to be anchored to retrofitted base plates, location tolerance was extremely tight at only 1.6 mm (1/16 inch). To ensure proper placement of the tendon, template plates were used to hold the threadbar reinforcement in the correct position until the grout had set.

Four of the production micropiles were successfully load tested in both tension and compression to the seismic design capacity. To facilitate compression testing, adjacent production piles were used as reaction piles.

After all micropiles for a given column were complete, the retrofitted base plates were installed (See Fig 5). To facilitate transfer of both compression and tension loads, hex nuts were installed above and below the base plates. Finally, the slab cutout was poured back with concrete to cover the base plate, and micropile tendons to complete the work.



Figure 5: Completed retrofitted column

CONCLUSION

When Engineers are tasked with solving a difficult deep foundation solution, it is extremely beneficial to have the opportunity to consult with the Specialty Contractor that will be installing the work. Understanding the equipment capabilities and tooling to be used for the installation allows the Engineer the ability to optimize the design, resulting in the most cost effective solution possible.

The Owners of the Sharp Hospital Project not only facilitated collaboration, but encouraged further cost savings by approving additional costs to instrument the test pile; an investment that paid off by enabling shorter production pile lengths. The partnering between Owner, Contractor, Designer, and manufacturer on this project fostered excellent communication between the parties, and the final result was a difficult, yet very unique and highly successful Project allowing the hospital to remain open until at least 2030.

MICROPILE SOLUTIONS FOR CONSTRUCTION OF SAS SPAN OF THE NEW SAN FRANCISCO-OAKLAND BAY BRIDGE

Thuraisamy Thavaraj[1], Alex Sy[2], and David Dowdell[3]

ABSTRACT

The new east span of the San Francisco-Oakland Bay Bridge features a single tower self-anchored suspension (SAS) bridge that became the largest of its kind in the world when completed in 2013. During construction of the SAS bridge, micropiles were effectively used to solve three significant construction issues: (1) Construction of the SAS bridge required temporary towers and trusses to support the box girders until erection of the suspension cables is complete. Three of these towers were located on steep slopes of Yerba Buena Island bedrock outcrop. For these towers, vertical and sub-horizontal micropiles were used as a viable alternative to conventional piles, considering constructability, cost-effectiveness, schedule and environmental impact. All the micropiles were tested and performed well during construction of the bridge. (2) The installation method used for the main cable of the suspension bridge required the 160 m high main tower to be pulled 500 mm to the west, using 200 m long pull-back cables anchored to bedrock at Yerba Buena Island prior to the erection of the main cable. 18 m long micropiles were used as foundation for the tie-back cables inclined at 40 degrees. A reinforced concrete pile cap varying in thickness and width was used for testing the micropiles and for locking them off before the tiebacks were attached. (3) The bridge decks from the west approach connecting to the west pier of the SAS bridge needed to be pulled down 75 mm in order to make the hinge closure pour during construction. A tie-down system consisting of two pairs of steel beams with ten pull-down cables on each beam was used. Two rows of 20 m long vertical micropiles were used as foundation for the tie-down cables. The micropiles were tested using the adjacent micropiles as reaction piles, without a pile cap, and using the same steel beams. This paper describes the design and construction of the micropiles and the connection details between micropiles and the structure, focusing on some of the challenges faced during the design, installation and testing of the micropiles.

1. INTRODUCTION

The new east span of the San Francisco-Oakland Bay Bridge features a single tower self-anchored suspension (SAS) bridge and is the largest of its kind in the world since completion in 2013. The new east span replaced a double-deck steel bridge built in the mid-thirties.

The new SAS bridge with its unique design was built to withstand a much larger earthquake than the original structure. A span of the old steel bridge had collapsed during the 1989 Loma Prieta earthquake, subsequently repaired and was in service until the new

[1] Senior Geotechnical Engineer, Klohn Crippen Berger Ltd., Vancouver, BC, Canada, tthavaraj@klohn.com
[2] Vice President, Technical, Klohn Crippen Berger Ltd., Vancouver, BC, Canada, asy@klohn.com
[3] Senior Structural Engineer, Klohn Crippen Berger Ltd., Vancouver, BC, Canada, ddowdell@klohn.com

SAS bridge was completed in 2013. During construction of the SAS bridge, micropiles were effectively used to solve three significant construction issues. This paper presents details of the issues and how they were solved using micropiles.

2. SAS BRIDGE AND TEMPORARY TOWERS

Figure 1 shows a schematic of the new bridge with its 160 m high main tower T1 in the middle, and Piers W2 and E2 at the west and east ends, respectively. The west and east spans of the SAS bridge are 180 m and 385 m, respectively. Pier W2 is founded on the Yerba Buena Island (YBI) bedrock outcrop. Tower T1 and Pier E2 are founded in San Francisco Bay on piles installed through marine sediments into sedimentary bedrock.

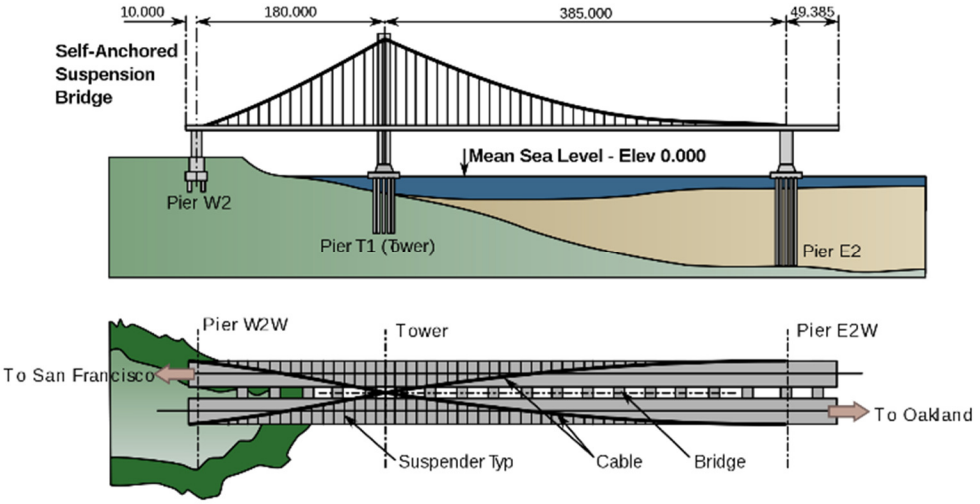


Figure 1. New east span of the San Francisco-Oakland Bay Bridge

During construction of the new bridge, a temporary bridge comprising towers and trusses was used to support the box girders of the new bridge until the loads from the box girders were transferred to the new suspension cables and the new permanent towers. Figure 2 (bottom part) is a schematic of the temporary bridge with the six pairs of temporary supporting towers along the eastbound and westbound lanes. Temporary Towers A, B and C were located on YBI between the permanent bridge Pier W2 and Tower T1. Temporary Tower D was located on either side of the permanent Tower T1 in the Bay, and Temporary Towers F and G were located between the permanent Tower T1 and Pier E2. The design loads on the temporary structures included construction loads, ship impact, wind and earthquake loads.

Along the bridge alignment, the general foundation conditions vary from sedimentary bedrock with interbedded sandstone, siltstone and claystone (Franciscan Formation) at the west end on YBI, to deep marine sediments with clay and sand overlying sloping bedrock at the east end in San Francisco Bay (Fugro-EMI, 2002). See Figure 3 for foundation conditions between Towers A and D.

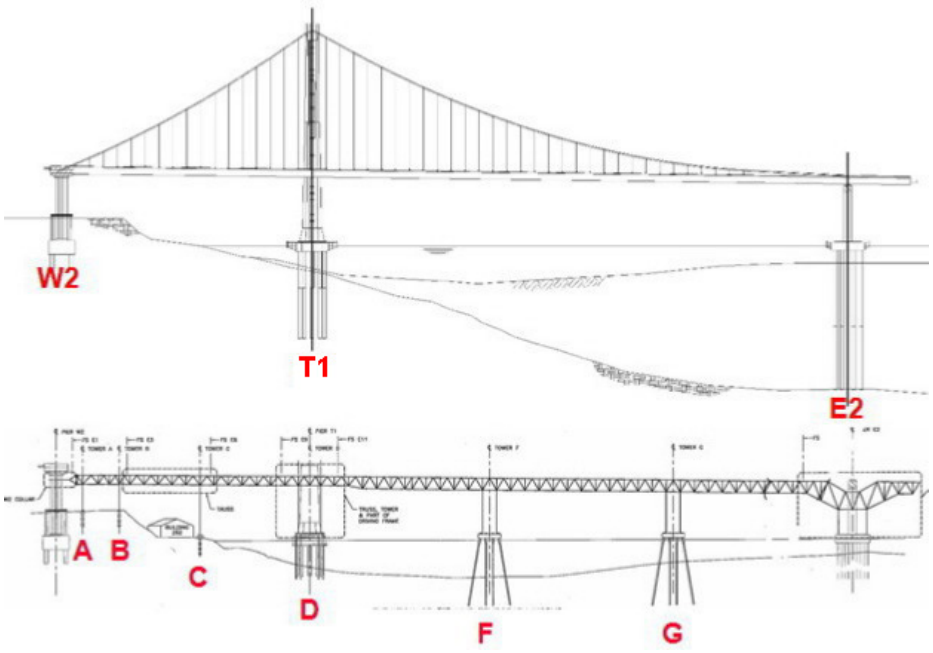


Figure 2. Permanent Tower T1, Piers W2 and E2 (above) and Temporary Towers A, B, C, D, F and G (below)

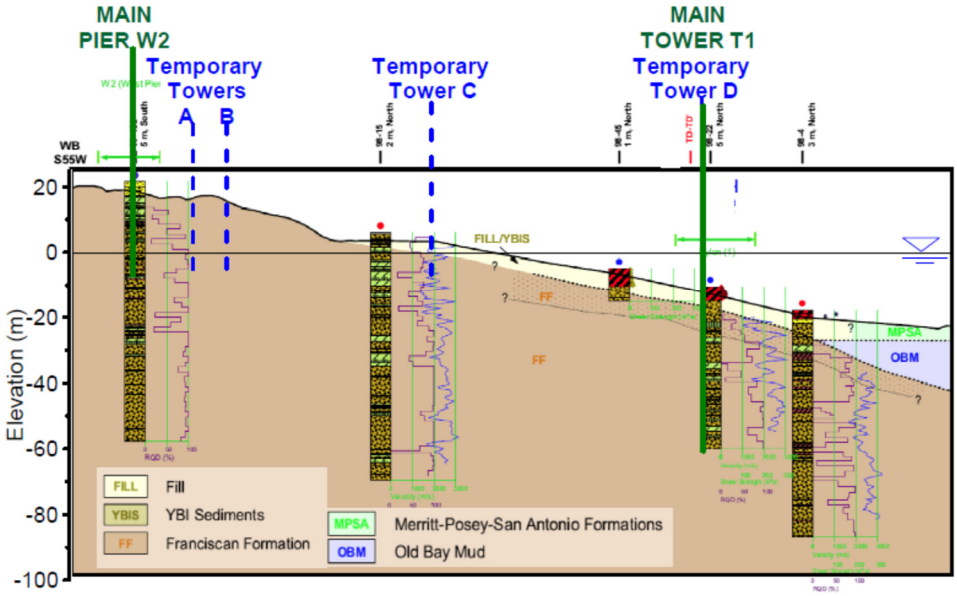


Figure 3. Geological profile along temporary Towers A to D (after Fugro-EMI, 2002)

Temporary Towers A and B, located on bedrock outcrop at YBI, were supported on micropiles on sloping ground and on drilled shafts on level ground. This paper focuses on the micropile foundations at A and B. Temporary Tower C, located near the shoreline, was supported on drilled shafts. The marine foundations for Towers D, F and G were supported on driven steel pipe piles. The design and construction of the drilled shaft and driven pipe pile foundations are described in Sy et al (2011) and Thavaraj et al (2013).

3. MICROPILE FOUNDATIONS FOR TEMPORARY TOWERS A AND B

As shown in Figure 4, on the north side or westbound lane, one footing (A1) for Tower A and two footings for Tower B (B1 and B2) were located on the north steep side slopes of the bedrock outcrop at YBI, and the remaining five footings were located on fairly flat ground. Some shallow fill covers the sedimentary bedrock sequence. The characteristics of the rock and thickness of the weathered zone vary spatially. Transition from intensely weathered to slightly weathered or fresh rock, however, occurs at relatively shallow depth.

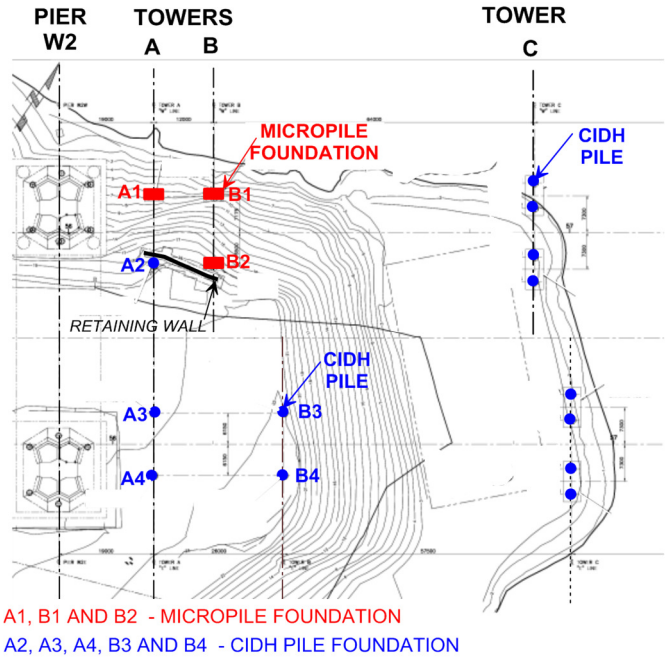


Figure 4. Temporary tower foundations A, B and C on Yerba Buena Island

Micropiles were selected as a viable alternative to drilled shafts at the steep rock slope for foundations at A1, B1 and B2. The micropile foundations could be constructed using lighter crane-supported equipment and adapted more easily to the actual site conditions. Utilising micropiles minimized the disturbance to the area surrounding an existing historical wall at foundation B2. At the completion of the bridge construction, foundations of the temporary works were removed and the original ground surface restored. Minimizing the foundation size reduced the effort required for site restoration.

Each micropile foundation consisted of 6 or 8 vertical and 2 subhorizontal (batter) piles designed to resist the vertical and lateral loads, respectively, from the tower columns. The batter piles were oriented at 10 degrees to the horizontal. The loads were transferred from the tower column to the piles through a cast-in-place 1.6 m thick concrete pile cap. 200 mm diameter micropiles were used with 65 mm diameter center bars (Williams' 1035 MPa all-thread bar). Two metre long casings were installed at the top within the intensely to moderately weathered bedrock; however, they were not designed to carry lateral loads. The micropiles were assumed to carry axial loads only, either in tension or compression. The bonded length of the micropile in contact with sound bedrock

was computed using an ultimate bond strength of 480 kPa, both in tension and compression. Maximum pile design load (including seismic) was 1800 kN. The static and seismic global stability of the slopes due to excavation and additional loads induced by the tower foundations was checked with rock wedge slope analysis (Swedge, 2005).

During construction, excavation of the rock faces and shoring support were required prior to the installation and testing of micropiles and construction of pile cap. Rock bolts, wire mesh and shotcrete were used for the temporary stabilization of rock faces. The 200 mm diameter holes for micropiles were drilled using a portable rotary percussion drill rig. The subhorizontal holes were drilled from a suspended platform held by a crane at the crest of the slope. The 65 mm diameter center bars were then inserted and grouted. Figures 5 to 7 show photos taken during micropile installation.



Figure 5. Typical micropile details and micropile installation at Tower A1



Figure 6. Drilling adjacent to historic retaining wall at B2



Figure 7. Micropile foundation construction at A1, B1 and B2

Tension proof tests were conducted on all vertical and batter micropiles. Custom test setup was used to test the batter piles. Twenty four piles were tested to the loads listed in Table 1 and the remaining four piles were tested to loads ranging between 56-75% of the target loads due to test setup problems that resulted in differential settlement and cracking of concrete bearing area and safety concern. The micropiles tested to the target loads showed consistent load-displacement behaviour that generally fell between the minimum and maximum elastic limits. The ten-minute creep displacements were also well within the allowable limit of 1 mm. Figure 8 shows typical tension proof test results on six vertical piles at micropile foundation A1.

Table 1. Maximum loads for tension proof tests

Micropile Foundation	Maximum Tension Load (kN)	
	Vertical Pile	Horizontal Batter Pile
A1	1100	500
B1	1800	500
B2	1800	1700

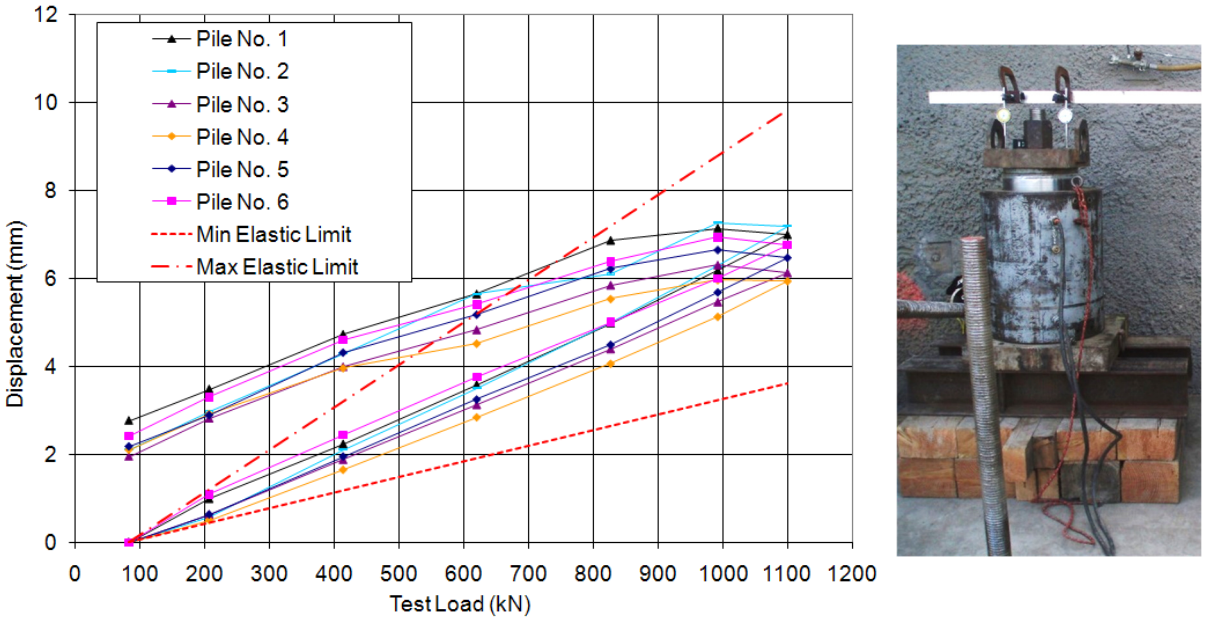


Figure 8. Tension proof test results for A1 piles and photo of test setup

An old retaining wall of historical importance, shown in Figures 4 and 6, was protected and monitored during construction but showed no movement due to adjacent micropile foundation construction at A1 and drilled shaft construction at A2. Figure 9 shows a photo of the temporary trusses and towers supported on micropile foundations A, B1 and B2 on the north rock slope of YBI, during construction of the SAS bridge.



Figure 9. Temporary towers and micropile foundations A1, B1 and B2 (right side)

4. MICROPILE FOUNDATION FOR MAIN TOWER PULL-BACK CABLES

Due to the asymmetrical spans, installation of the main cable of the suspension bridge required the 160 m high main tower, T1, be pulled 500 mm to the west, using 200 m long pull-back cables inclined 40 degrees to the horizontal, prior to the erection of main cables. The pull-back cables were supported by a group of ten 18 m long micropiles inclined at the same angle of 40 degrees to the horizontal. Figure 10 shows the Tower T1 tie-back cable arrangement.

The micropiles were founded on bedrock at YBI. Nine of these micropiles were spaced at 1.5 m and one pile at the north end was spaced at 2.4 m. As shown in Figure 11, 203 mm diameter micropiles were used with 65 mm diameter center bars with yield stress of 724 MPa. The minimum bond length was 15.6 m and the remaining unbonded length in the upper part was sleeved using a PVC pipe. The micropiles were nominally pressure grouted using a neat mix of concrete with water-cement ratio of 0.45 to obtain minimum 28-day compressive strength of 35 MPa. The tensile capacity of the micropile was computed assuming a bond strength 480 kPa for the pile in contact with the sound Franciscan Formation bedrock. The group effect of the single row of ten piles was checked using the method proposed by Littlejohn and Bruce (1977). The unbonded length was selected considering the condition of bedrock in the upper part, group effect and the stability of adjacent slope.

Tension proof tests were conducted on all micropiles to a maximum load of 2050 kN, in general accordance with the FHWA (2005) guidelines. Piles were then locked off at a tension load of 1200 kN.

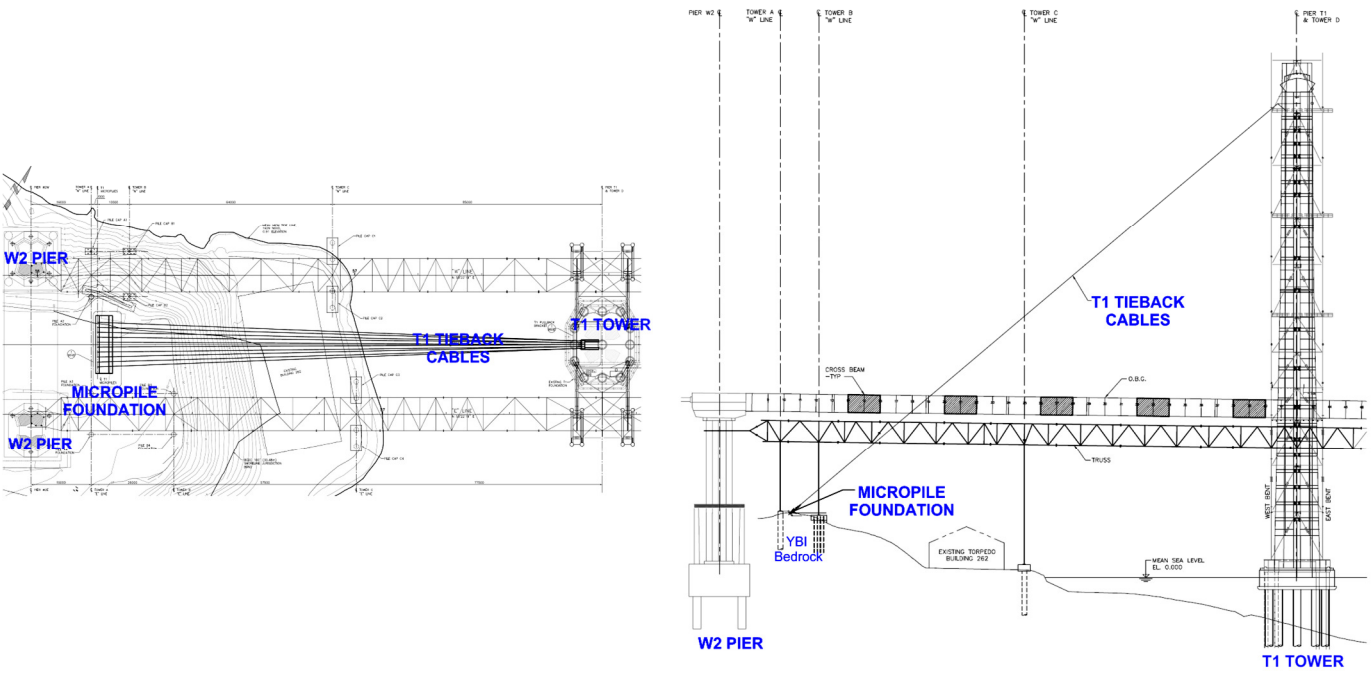


Figure 10. Plan (left) and elevation (right) views of Tower T1 tie-back cables

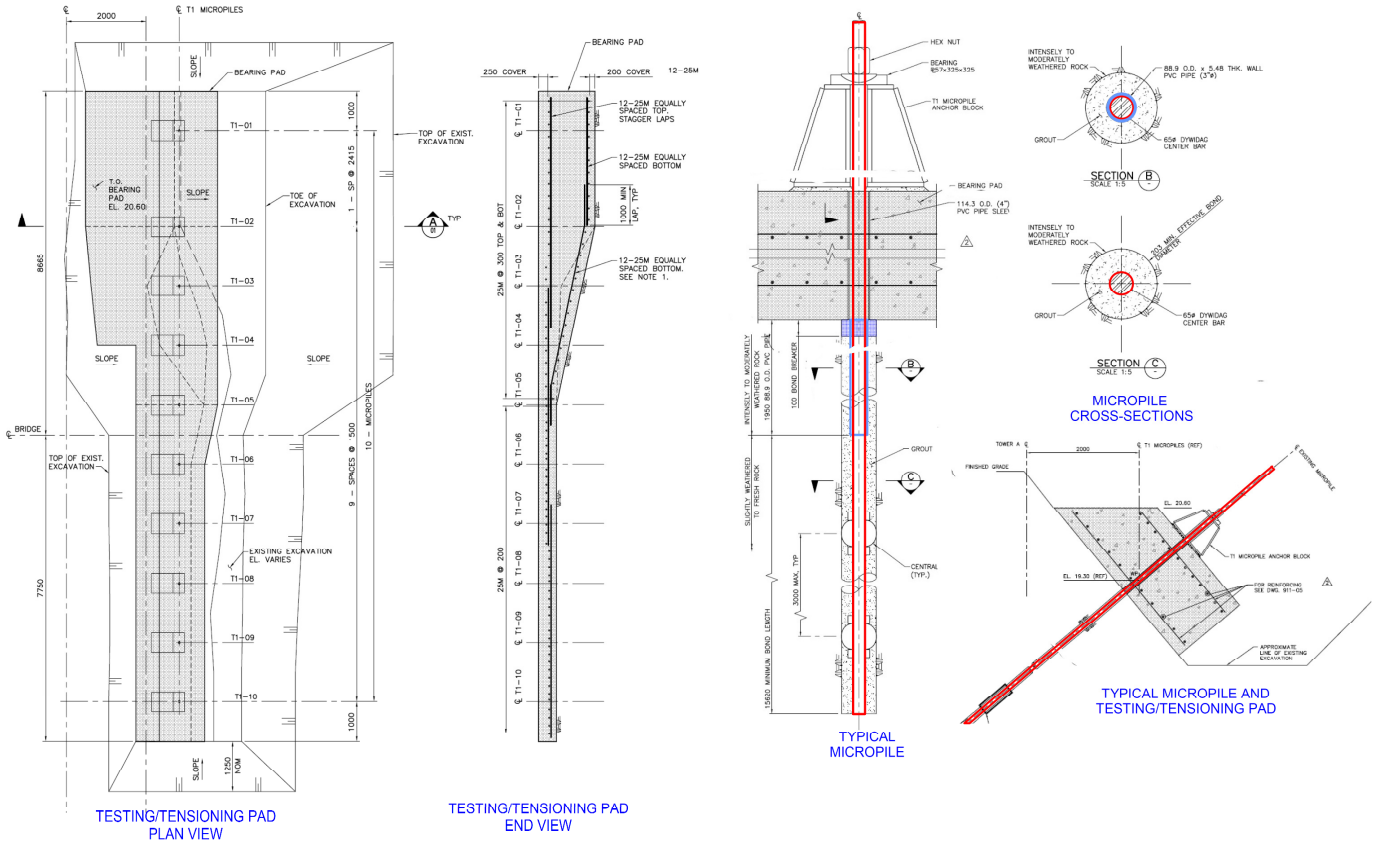


Figure 11. Testing/tensioning bearing pad and micropile foundation details

Prior to testing, there were concerns regarding the bearing capacity of overburden soils (fills) present above the bedrock due to lack of site-specific geotechnical information. Therefore, instead of testing all the micropiles to the full testing load, 1 m x 1 m square bearing pads were constructed at the locations of three selected micropiles, to assess the bearing capacity of the actual foundation material. The three micropiles chosen for testing were: Micropile 1 at the north end, Micropile 5 in the middle, and Micropile 10 at the south end. During application of tension test load on the micropile, both the elongation of micropile and the settlement of the 1m x 1m bearing pad were measured. The test results obtained for the foundation material indicated that the 1 m^2 pad at Micropile 10 was capable of sustaining the full test load of 2050 kN and the settlement of the pad was approximately 6 mm at full load. However, the 1 m^2 pad at Micropile 5 settled 25 mm at full test load and the 1 m^2 pad at Micropile 1 settled more than 25 mm at half of the full test load.

Based on these test results, it was decided to excavate the relatively weak fill material and use a continuous reinforced concrete pad (or pile cap) varying in thickness (from 0.45 m to 1.4 m) and width, as shown in Figure 11. The ground conditions at the south end were much stiffer than the conditions at the north end. Also, the northern most pile was located close to the slope. The thickness, width and stiffness of the pad were adjusted to suit the ground conditions, so that the pile cap would not undergo excessive displacements or failure during testing and in service.

Testing was subsequently conducted using the reinforced concrete pad as reaction base. During testing, both the elongation of the center bar and the settlement or deflection of the bearing pad were measured. The test results indicated that each of the micropiles sustained the test load with maximum displacement in the range of 19 mm to 28 mm and the corresponding settlement of bearing pad varied between 0.4 mm to 2.4 mm. All micropiles passed the ten-minute creep test (i.e. less than 1 mm) at the full test load of 2050 kN and the ten-minute creep varied between 0.3 mm and 0.6 mm.

Figure 12 shows photos of the micropile installation, the bearing pad used for testing and tensioning the micropiles, and a typical test arrangement. Figure 13 shows photos of the tie-back cables for tower T1 and the tie back cables supported on micropile foundation.



Figure 12. Micropile installation, testing/tensioning bearing pad and testing



Figure 13. Tower T1 tie-back cables and cable supported on micropiles

5. MICROPILES FOR WEST APPROACH DECK PULL-DOWN CABLES

The bridge decks of the west approach span on YBI needed to be pulled down approximately 75 mm during construction in order to make the hinge closure pour to complete the connection between the approach span and the west pier W2 of the SAS bridge. It was opted to use a tie-down system rather than adding weight to the approach span; the latter was initially attempted but subsequently abandoned. The weight required to deflect the bridge girder would have been quite large and would have introduced a seismic design issue; whereas a tie-down system would not.

The tie-down system consisted of two pairs of steel beams with ten tie-down cables on each beam. This arrangement was used for both the east line and west line bridge deck girders. Two rows of 20 m long vertical micropiles, unevenly spaced between 1.0 m and 1.8 m, were used as foundation for the tie-down cables. Hydraulic jacks were used to lower the bridge deck girder by pulling on the tie-down cable against the steel beam. One jack with capacity of 1780 kN was used at each cable. The cables were tensioned simultaneously until the deck was lowered by the required amount of 75 mm. Figure 14 shows the tie-down cable arrangement and the micropile foundation used for the east line bridge girders. The system used for west line girders was similar.

The micropiles were founded on bedrock at YBI. As shown in Figure 15, 165 mm diameter micropiles were used with 65 mm diameter center bars with yield stress of 1035 MPa. The minimum bond length in contact with the sound bedrock was 12 m, and the remaining 8 m unbonded length in the upper part was sleeved using a 76 mm Schedule 80 PVC pipe. The micropiles were nominally pressure grouted using a neat mix of concrete with water-cement ratio of 0.45 to obtain minimum 28-day compressive strength of 35 MPa. The tensile capacity of the micropile was computed using a bond strength of 480 kPa for the pile in contact with sound rock.

The group effect of the two rows of twenty piles (each row with ten piles at variable spacing and the rows separated by 1.22 m) was checked using the method proposed by Littlejohn and Bruce (1977). A factor of safety of two was used to calculate the required depth of the cone having friction angle of 55 degrees. To allow for group effect, the required unbonded length was taken as 8 m. The upper 3.5 m of the unbonded length of the micropile was cased using a 219 mm steel casing with 12.7 mm wall thickness and yield stress of 240 MPa. The cased part of the micropiles was predominantly in contact with surficial fill or intensely to moderately weathered bedrock.

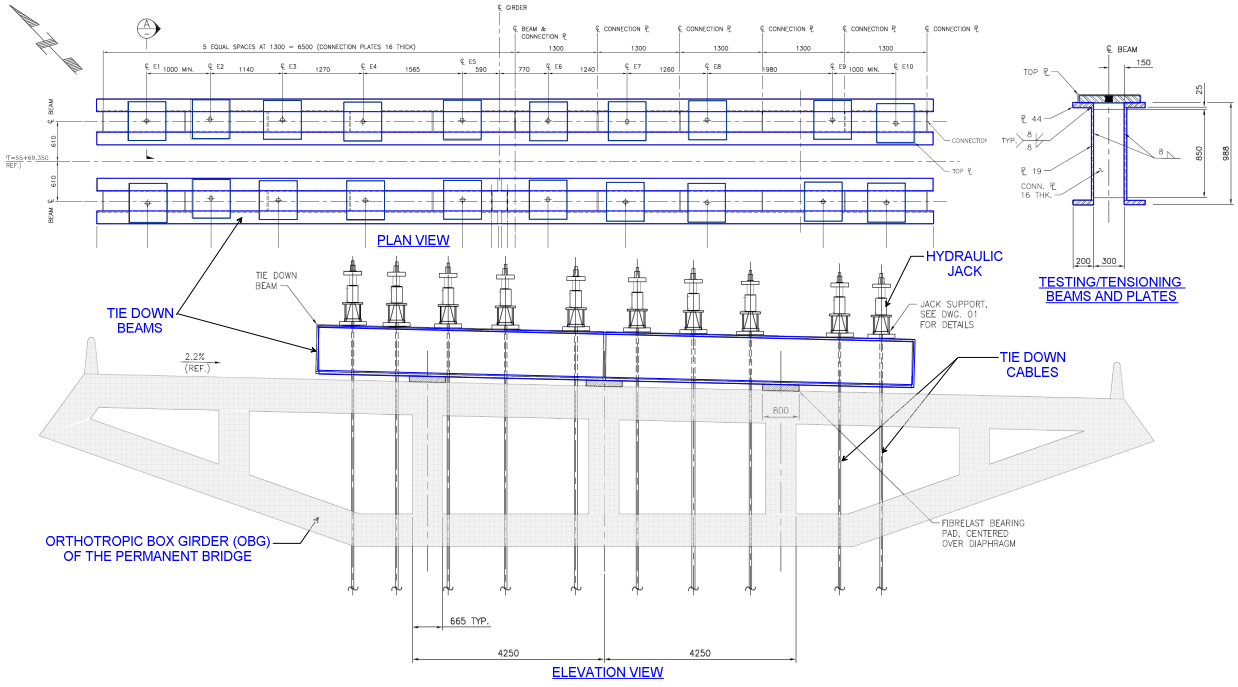


Figure 14. Tie-down cables and tie-down beam arrangement

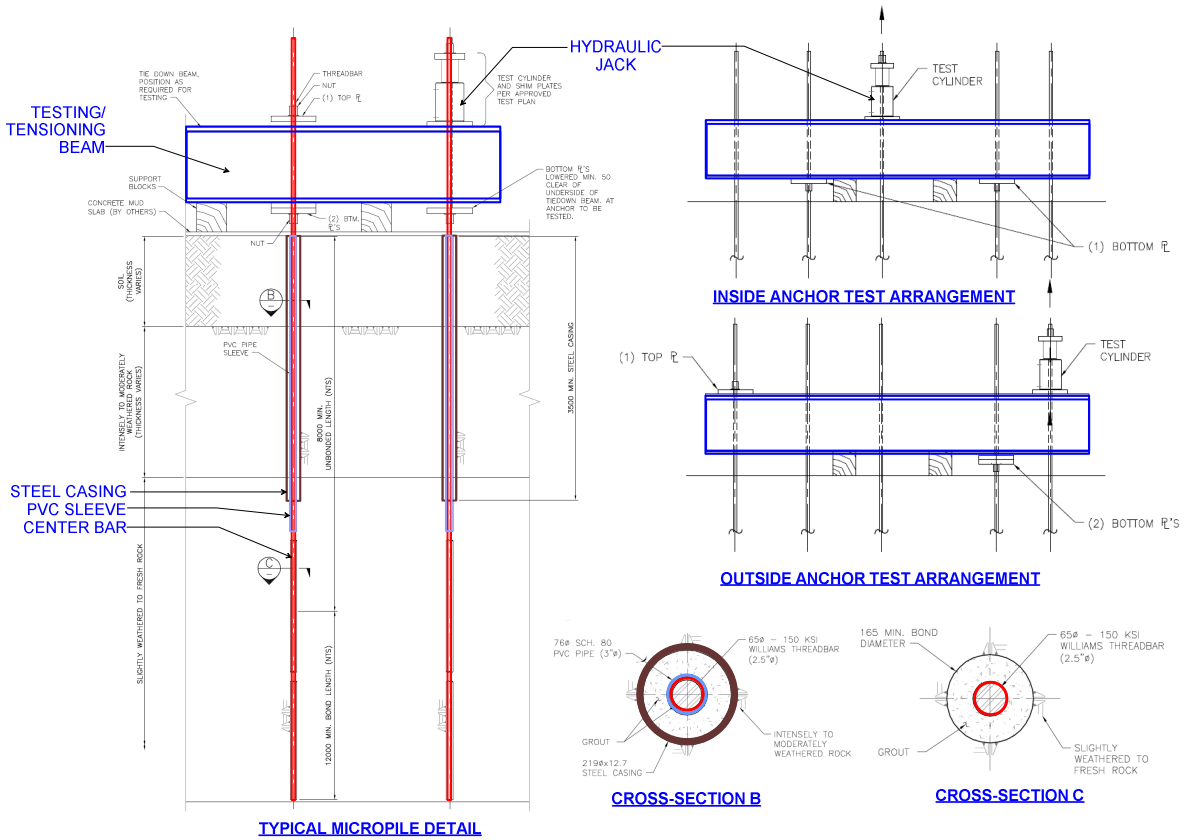


Figure 15. Typical micropile details and load test arrangements

Tension proof tests were conducted on all micropiles to a maximum load of 1650 kN in general accordance with the FHWA (2005) guidelines. The same steel beam and jack system was used to test the micropiles. Due to concern regarding the bearing capacity of the upper soils, each micropile was tested by using the adjacent micropiles as reaction piles, and the test arrangements used for testing inner and outer piles are shown in Figure 15. Utilizing the steel beam for testing eliminated the need to construct and later demolish a reinforced concrete beam for each set of tie-downs.

Each pile was loaded to maximum tension load of 1650 kN and followed by a ten-minute creep test. The maximum displacements ranged between 18 mm and 30 mm, and the corresponding residual displacements after unloading to alignment load ranged between 1 mm and 7 mm. The ten-minute creep varied between 0 and 0.97 mm. Figure 16 shows photos of the installed micropiles, and the test beam and typical load test arrangement.



Figure 16. Micropiles after installation, load test setup, and micropile testing

Following testing, the same steel beams were then moved to the top of the approach span deck and the tie-down cables were tensioned until the required movement of the bridge deck was obtained. Figure 17 shows photos of the tie-down cables tensioned using the same test beams as used for testing the micropile foundations.



Figure 17. Tie-down cables protruding above deck, tie-down cables through box girder, and tie beam set-up with hydraulic jacks at the top of the deck

6. SUMMARY

During construction of the SAS bridge, micropiles were effectively used to solve three significant construction issues. Firstly, three of the temporary towers were located on the steep side slopes of Yerba Buena Island bedrock outcrop. The foundations had to carry both vertical and horizontal loads. Vertical and subhorizontal micropiles were selected as viable alternative to conventional piles, considering constructability, cost-effectiveness, schedule and environmental impact. All the piles were tested and performed well during construction of the bridge.

Secondly, the installation method used for the main suspension cable required the 160 m high main tower to be pulled 500 mm to the west using 200 m long pull-back cables anchored to bedrock at Yerba Buena Island prior to the erection of the main cable. 18 m long micropiles were chosen as the foundation for the tie-back cables inclined at 40 degrees. A reinforced concrete pile cap varying in thickness and width was used for testing the micropiles to maximum of 2 MN load and for locking them off at 1.2 MN before the tie-backs were attached. The micropiles performed well until erection of the bridge cables was complete.

Thirdly, the bridge decks from the west approach connecting to the west pier of the SAS bridge needed to be pulled down 75 mm, in order to make the hinge closure pour during construction. A tie-down system consisting of two pairs of steel beams with ten tie-down cables on each beam was used. Two rows of 20 m long vertical micropiles were used as a viable foundation for the tie-down cables. All micropiles were tested to maximum load of 1.7 MN, using the adjacent micropiles as reaction piles, without a pile cap, and using the same steel beams that were subsequently used for tying down the cables.

7. REFERENCES

FHWA (2005). *Micropile Design and Construction.* Reference Manual. US Department of Transportation, Federal Highway Administration. Report No. FHWA NHI-05-039.

Fugro-EMI (2002). *Geotechnical Foundation Report for Yerba Buena Island Approach and Self-Anchored Suspension Bridge* - 100% Submittal, SFOBB East Span Seismic Safety Project, Fugro-Earth Mechanics Joint Venture, June 2002.

Littlejohn, G.S., and Bruce, D.A. (1977). *Rock Anchors – State of the Art*, Foundation Publications Ltd., Brentwood, Essex, England.

Sy, A., Thavaraj, T., Hamersley, B., Reyes, M., Dowdell, D. and Tudor, S. (2011). *Temporary Tower Foundations for the New San Francisco-Oakland Bay Bridge Self Anchored Suspension Span*. Proceedings of the 2011 PanAm-CGS Geotechnical Conference, Toronto, ON, Canada. Paper No. 359.

Swedge, 2005. *A Computer Program for 3D Surface Wedge Analysis of Slopes*, Rocscience Inc., Toronto, ON.

Thavaraj, T., Sy, A. and Reyes, M. (2013). *Driven Pipe Pile Solutions for the Temporary Foundations at the New San Francisco-Oakland Bay Bridge*. DFI 38th Annual Conference on Deep Foundations, Phoenix, AZ.

A POST-TENSIONED MICROPILE FOUNDATION SYSTEM

WITH GROUTABLE VOID FORMS (GVF)

Horst Aschenbroich, Dipl. Ing. [1]

ABSTRACT

This is a foundation solution for renewable energy sources such as wind turbine towers, solar collector panels, hydropower and towers for transmission lines. In all cases the focus is to provide the most cost effective, safe, and environmentally friendly solution. For that reason, micropile solutions can be considered as an alternative to mass concrete foundations. Micropile foundation systems are constructible in different ground conditions without the need for changing the equipment or the method of installation.

It is particularly desirable to have a deep foundation with a smaller footprint for wind turbine towers. To resist the imposed overturning moments, the concept of using post-tensioned micropiles (PTMP) in compression and/or tension with groutable void forms (GVFs), relies on the activation of the soil mass under the foundation (Figure 1). This allows for reducing the size and depth of the now pre-tested foundation, which results in savings in reinforcing steel and concrete.

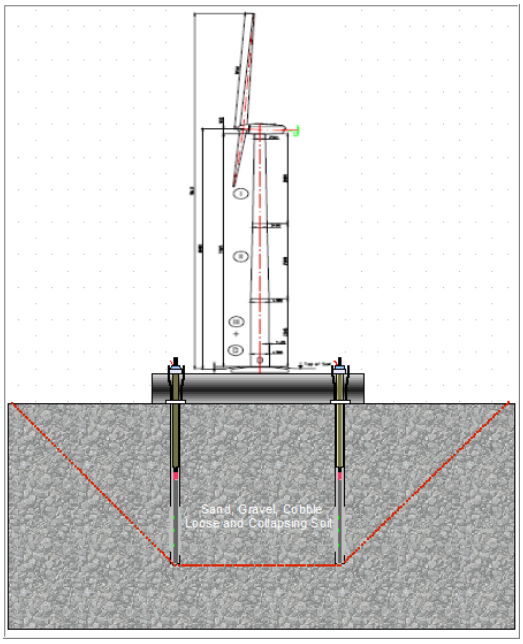


Figure 1. Activation of Soil Mass

[1] President / CEO of Con-Tech Systems Ltd.8150 River Road Delta BC Canada, E-mail; horst@contechsystems.com

Three possible post-tensioning scenarios for micropile foundations

Case I: No void.

Hard contact between micropile and foundation cap. There is no allowance for micropile movement to mobilize skin friction forces between the micropile grout and soil. The PT force in the pile becomes a compressive stress at the pile to cap interface. No actual pile testing is possible unless each pile is tested before the foundation is placed and locked off later on top of the finished foundation.

Case II: Unfilled compressible void.

Void between micropile and foundation cap for tensioning remains unfilled.
It permits unrestrained movement between the top of the pile and the bottom of the cap. Since the void remains unfilled, there is a possibility of long term consolidation and settlement if founded on soil. However; it can be used if founded on rock. In this case it is not a pile but an anchor in tension. The compression loads are supported by the rock.

Case III: Groutable void form (GVF) system.

As it is presented and described in this paper for foundations on soil.
The void between micropile and foundation cap is filled with cement grout after tensioning. It permits unrestrained pile movement between the top of the pile and the bottom of the cap during tensioning. After filling the void with cement grout, compressive forces as well as tension forces can be transmitted.

The technical benefits are:

No movements of the foundation and pile can occur unless externally applied forces are larger than the applied PT forces in tension or compression.

INTRODUCTION AND BACKGROUND

Standard Foundations

Foundations for wind turbines normally consist of large reinforced concrete spread footings. If founded on soils, the compression loads are only supported by the soil and the overturning loads are resisted by the counterweight provided by the concrete foundation (Figure 2). The changes in loading from compression to uplift can cause a fatigue problem, which is difficult to predetermine. Consequently, overturning of the wind turbine may result (Figure 3).



Figure 2. Large reinforced concrete spread footing, with 500 to 600 cy of concrete



Figure 3. Overturning failure caused by massive rainstorms

For foundations on soil, an alternative post-tensioned foundation system was developed using micropiles supporting a smaller foundation-pile cap. Not only will this micropile system minimize or eliminate the above mentioned fatigue problem, but it can also provide up to a 75% reduction in foundation area, a 40% reduction in concrete consumption, and a 70% reduction in reinforcing steel, resulting in a total foundation cost savings of about 25%.

Foundation Design Objectives

To provide a post-tensioned micro pile foundation system, such as for wind turbine foundations, the following design objectives should be achieved:

- Design and construct post-tensioned micropiles to achieve a design load in compression and/or tension with the required factor of safety.
- Provide a rigid foundation to resist extreme overturning moments while limiting the pile cap size.
- Improve rotational stiffness and reduce / eliminate movement of the foundation through post-tensioning.
- Reduce excavation and backfill required for the pile cap/tower foundation.
- Reduce consumption of concrete and steel reinforcing to optimize foundation efficiency and performance.
- Provide a cost effective post-tensioned deep foundation system on micropiles

In order to test and post-tension these foundations, a groutable void form (GVF) has been developed. The GVF temporarily separates the pile from the pile cap during stressing and testing, to a load higher than the design load in compression and tension, while also allowing for some range of pile movement. After post-tensioning the GVF is filled with cement grout in order to also transfer compression loads to the pile (Figure 4).

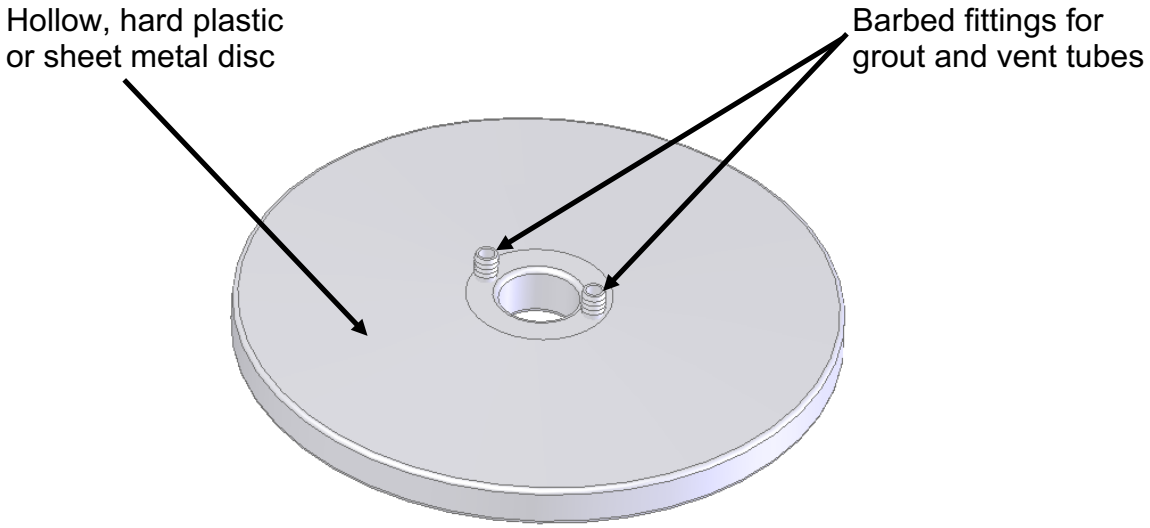


Figure 4. Groutable Void Form, (patented).

Prime Advantages

The post-tensioning procedure using GVFs with micropiles offers the following advantages:

1. Controls foundation settlement and prevents overloading the soil (bearing capacity failure) with a prescribed sequence of post-tensioning.
2. Post-tensioning in balanced anchor groups permits gradual load transfer into the piles without overstressing the soil.
3. Settlement of the foundation cap is minimized as the piles take over the compression load from the cap.
4. Fatigue failures can be eliminated since the post-tensioned tension and compression loads are higher than the design loads and as such minimize or eliminate movements during load changes (Figure 5).
5. With the reduction of concrete and steel, reduced environmental impact is also achieved.

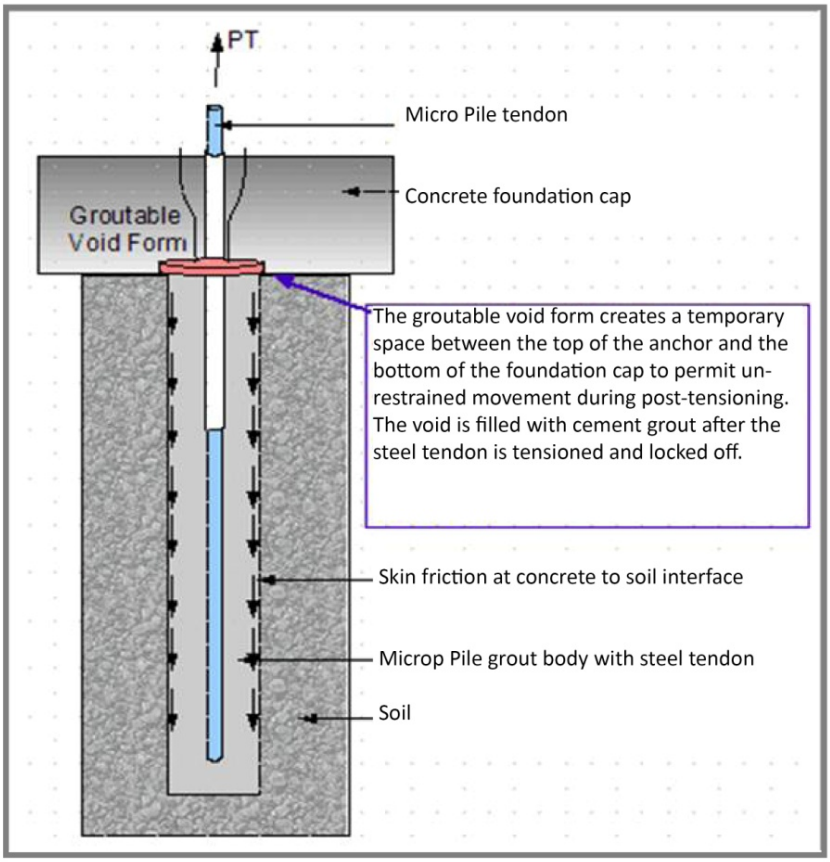


Figure 5. Load transfer diagram

Two CONSTRUCTION METHODS

1. Micropiles are installed prior to placing the concrete foundation cap.
2. Micropiles are installed after placing the concrete foundation cap. (i.e. Micropiles drilled through pre-installed sleeves inside the pile cap).

The advantage with the first method is that a larger drill hole diameter can be achieved using the open or cased hole drilling method and that the GVF can be wet set into the upper cement grout body of the pile (Figure 6). Three types of post-tensioning steel tendons may be used: (1) 7 wire, 270 ksi low relaxation strand, (2) solid, 150 ksi high strength bars, or (3) injection bored hollow bars. Strand and solid bars are used primarily for micropiles drilled through soil into rock, or for foundations on soil when a larger drill hole is required and the micropiles are pre-drilled.

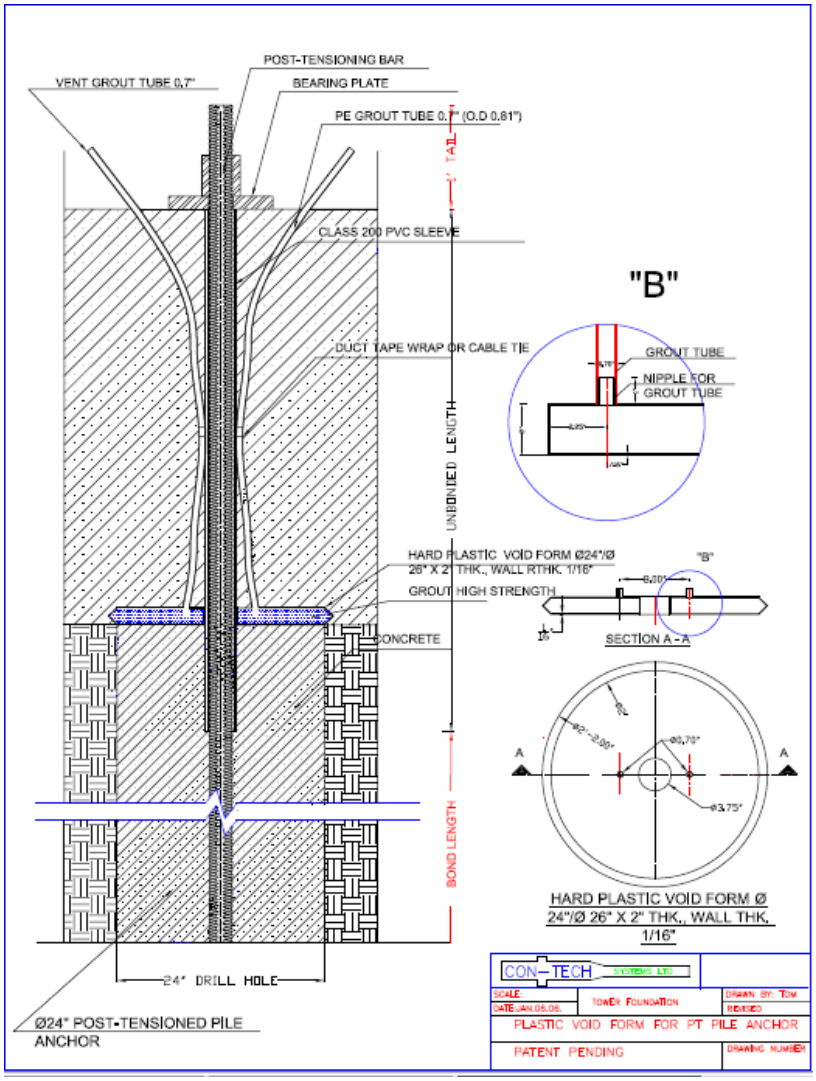
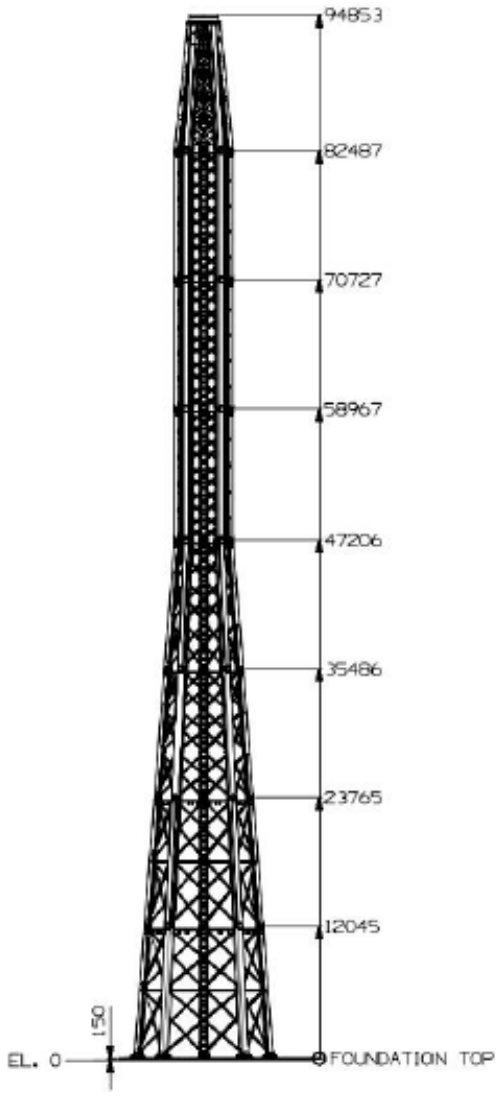


Figure 6. Location of the GVF with grout tubes

Method 1

A foundation for a 1.6 MW wind turbine was constructed in Tehachapi, California, using 300 mm diameter pre-drilled post-tensioned micropiles and GVFs. The 100 m tall lattice tower was founded on five individual pile caps, each supported by 4 micro piles.

The post-tensioned micropile/GVF system was load tested to provide assurance that the construction cost and long-term maintenance of the micropile system could be reduced.



Photographs of the drilling for the solid bar, double corrosion protected (DCP) micropiles are shown in Figures 7 and 8. These larger diameter holes were formed prior to the construction of the pile cap. The GVFs were wet set into the top of the micropile grout in the levelling pad with pipe sleeves and grout tubes (Figure 9) placing the rebar cages and forming pile caps (Figure 10). All pile caps are cast with a total of 20 micropiles (Figure 11). Micropiles are stressed in sequence after placing the bearing plates and nuts (Figures 12 and 13).

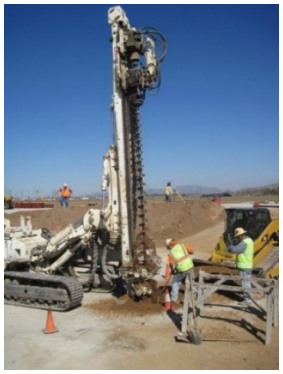


Figure 7. Drilling lager hole



Figure 8. Placing bar and grouting



Figure 9. Wet set GVF



Figure 10. Placing rebar and forms



Figure11. Ready for post-tensioning



Figure 12. Bearing plate with grout tubes



Figure 13. Stressing of solid bar tendon



Figure 14. Finished grouting the GVF

Grout is pumped through one tube and vented out of the other to ensure 100% filling of the GVF by the grout (Figure 14). Thereafter, the micropiles are able to transfer the applied loading into the ground.

METHOD 2

The advantage of the second method is that the micropiles are drilled through pre-formed sleeved holes in the foundation cap fitted with a pre-installed GVF under the foundation cap. (Figure 15).

The disadvantage is that the drill hole size is determined by the smaller sleeve, inside the foundation slab, which does not, therefore, provide sufficient cement grout body under the GVF. The smaller sleeve size is dictated by the size of the bearing plate for the micropile.

However, the issue with the grout under the GVF is not present when using the grout injection bored method with hollow bars (Figure 16). In this case the cement grout is injected simultaneously during the drilling operation. The drill bit has small diameter side holes through which the grout will exit under high pressure, similar to that during jet grouting. This will flush and create a larger size drill hole than the drill bit size under the GFV (Figure 17), as such creating a sufficient cement grout body underneath the GVF. This method also greatly improves the condition of the ground around the micro pile and, therefore, creates a very favourable higher skin friction capacity.



Figure 15. Pre-set sleeves in footing



Figure 16. Drilling of a hollow bar



Figure17.Grout injection

Stressing of the micropiles simultaneously in pairs, (Figure 18) will pre-stress the piles and post-tension the foundation before the GVF is filled with cement grout.

The amount of anchors stressed in pairs is dictated by the compression load capacity of the soil. When this load is reached, the GVFs are grouted. After the grout has reached sufficient strength, the stressing procedure can continue.



Figure 18. Stressing Arrangement

The typical stressing stages for a foundation system with 20 micropiles is shown in Figures 19 through 21.

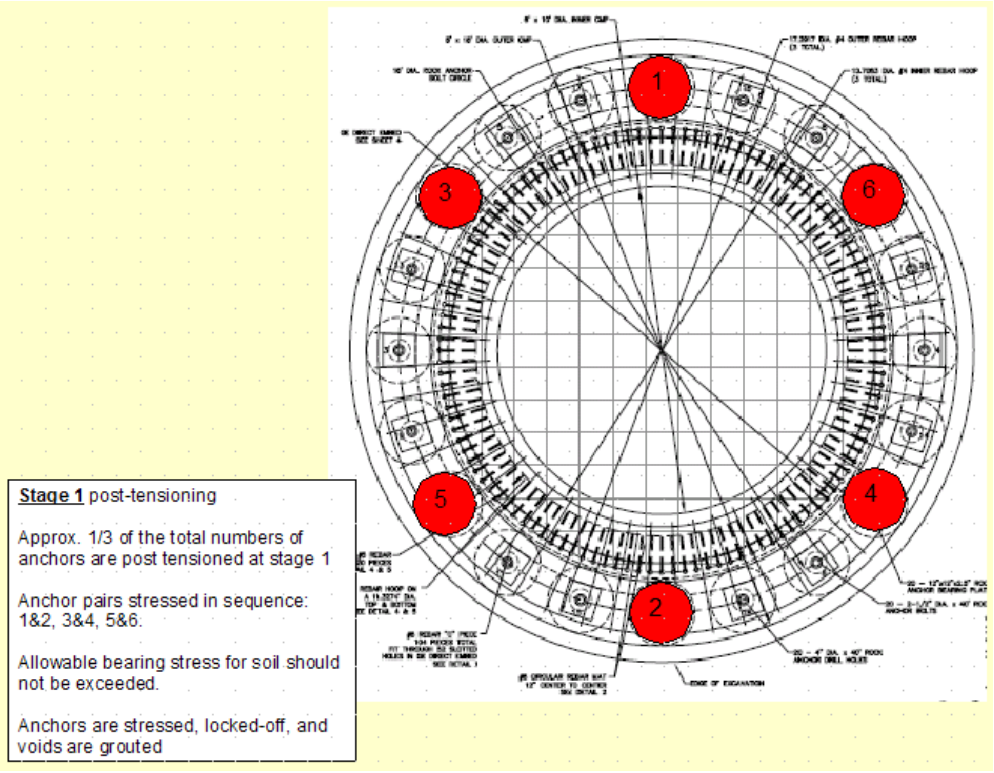
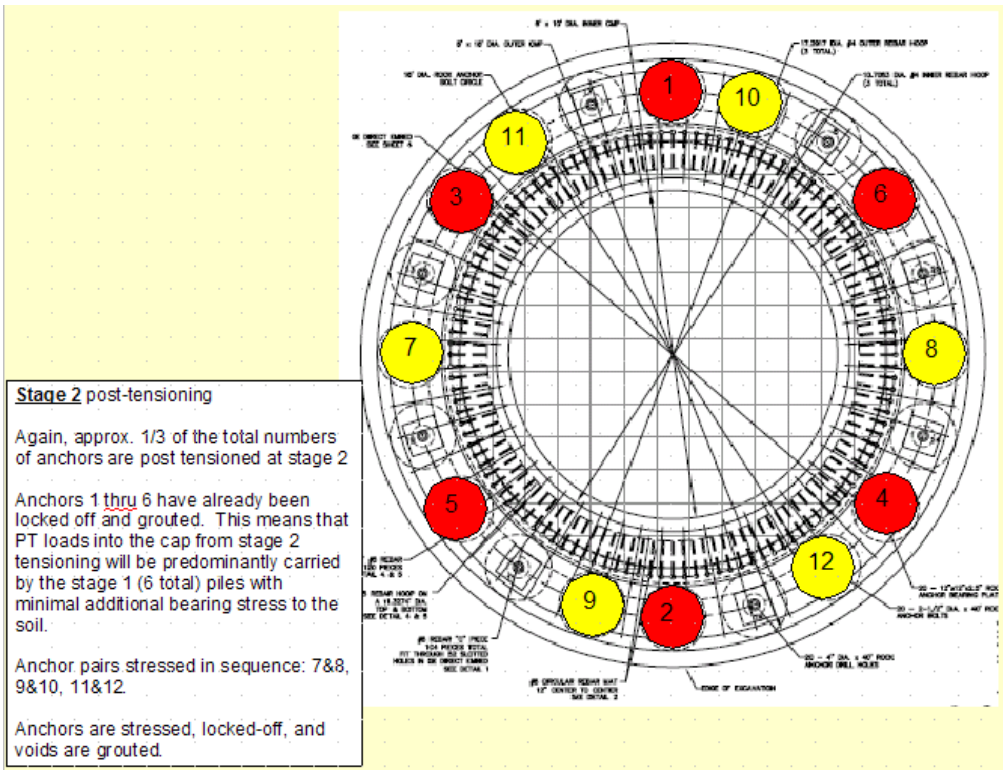


Figure 19. Stage 1 stressing



Stage 2 post-tensioning

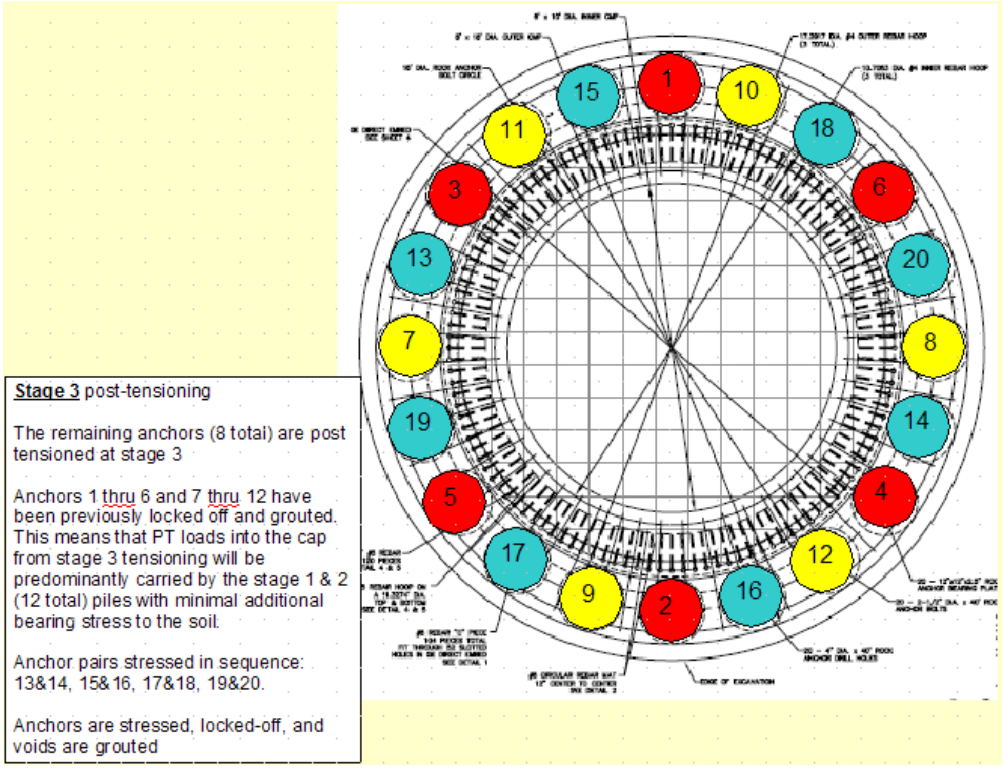
Again, approx. 1/3 of the total numbers of anchors are post tensioned at stage 2

Anchors 1 thru 6 have already been locked off and grouted. This means that PT loads into the cap from stage 2 tensioning will be predominantly carried by the stage 1 (6 total) piles with minimal additional bearing stress to the soil.

Anchor pairs stressed in sequence: 7&8, 9&10, 11&12.

Anchors are stressed, locked-off, and voids are grouted.

Figure 20. Stage 2 stressing



Stage 3 post-tensioning

The remaining anchors (8 total) are post tensioned at stage 3

Anchors 1 thru 6 and 7 thru 12 have been previously locked off and grouted. This means that PT loads into the cap from stage 3 tensioning will be predominantly carried by the stage 1 & 2 (12 total) piles with minimal additional bearing stress to the soil.

Anchor pairs stressed in sequence: 13&14, 15& 16, 17&18, 19&20.

Anchors are stressed, locked-off, and voids are grouted

Figure 21. Stage 3 stressing

Conclusions and Summary

Photographs of the completed post-tensioned micropile foundation are shown in (Figures 22 and 23).
Compared to a large diameter mass concrete foundation, the following observations were noted for the micropile/GVF foundation system:

- More than a 75% reduction in foundation area
- More than a 40% reduction in concrete consumption
- More than a 70% reduction in reinforcing steel consumption
- Preliminary estimated total foundation cost reduction of 20% to 30%



Figure 22. Typical post-tensioned micropile wind turbine foundation with hollow bars



Figure 23. Typical post-tensioned wind turbine foundation with strands

As a result of the findings in this paper, it can be stated that the safety of wind turbine foundations composed of post-tensioned micropiles with GVFs is improved and the cost greatly reduced. Therefore; the micropile/GVF system provides a competitive alternative to large diameter reinforced concrete spread foundations and to foundations on soil, if constructed with post-tensioned tie down anchors.

RENOVATION OF AN OLD SALES CENTER FOR ADDITIONAL UNDERGROUND PARKING

GUANGLEI LIU[1], PETER CHOI[2], QI WANG[3], JIA MA[4]

ABSTRACT

Due to the automotive vehicles increase, available parking lots become a new type of limited resources in central cities in China, especially in those old districts without visionary urban planning. Additional mechanical parking is an efficient solution to provide sufficient parking lots under the situation where the space is constrained. More severely, if there is no space on the ground, parking garage under an existing building may be the only way to fix the problem. One project is introduced in this paper about the renovation work of an old sales center in central Shijiazhuang urban area, China. The sales center was in a logistic park and no parking was designed for this building. The biggest challenge was to keep the upper level of building operating during the construction. The renovation work started from the beginning of 2016 and finished in May 2016, including the parking equipment installation and interior decoration. The new parking garage is currently in operation and satisfies the requirements by the client. The design work, details, construction consideration, load test and monitor results of this renovation work will be presented in this paper.

Keywords: building renovation, screw anchor pile, micro-pile, underground parking

1. Deputy Chief Engineer, Zhongyan Technology Co., Ltd., 12F, Tongjing Tower, No. 2, Pingguoyuan Road, Shijingshan District, Beijing, China, 100041, +86-10-57712508-609, +86-10-57712508-605, liuguanglei@zydd.com
2. R&D center director, SE EXT Co., Ltd., GBC 1402, 371-6 Gasan-dong, Geumchun-gu, Seoul, Korea +82-2-6326-5573, +82-2-6326-5570, choihk@extpile.co.kr
3. Engineer, Zhongyan Technology Co., Ltd., 12F, Tongjing Tower, No. 2, Pingguoyuan Road, Shijingshan District, Beijing, China, 100041, +86-10-57712508-609, +86-10-57712508-605, wangqi@zydd.com
4. Engineer, Zhongyan Technology Co., Ltd., 12F, Tongjing Tower, No. 2, Pingguoyuan Road, Shijingshan District, Beijing, China, 100041, +86-10-57712508-609, +86-10-57712508-605, majia@zydd.com

INTRODUCTION

Lack of parking is severe in many cities in China, especially for those old districts in central cities. Traffic condition gets worse when cars park on the street or move slowly to find parking spaces. Study shows that the normal ratio of available parking space to automotive vehicle number is about 1.2 in most major cities such as New York, Tokyo and Hong Kong. However this ratio is only 0.5 in Beijing. One possible solution is to move cars out of the central city. But still there are plenty of parking requirements for the residents in the central city.

Additional mechanical parking is an efficient solution to provide more parking lots where there is rare space. This paper presents one renovation project in Shijiazhuang city to add one basement to the existing old sales center for car parking consideration. SAP piles were used to support the super structure during the construction. The screw anchor piles were drilled into the ground and worked as permanent piles after grouting. The design work, details, construction considerations, load test and monitor results of the renovation work will be presented in this paper.

PROJECT DESCRIPTION

The logistic park is in Luquan district, Shijiazhuang city. The sales center is close to the entrance of this logistic park. It is a 2-storey steel structure building without basement. No car parking garages were planned for the building. There are many important persons every day and the owner found it inconvenient without exclusive parking places on site. After scheme study, the client decided to build an extra basement with mechanical parking equipment to solve this problem in September 2015. The design and construction work was conducted by Zhongyan Technology Co., Ltd. and SE EXT Co., Ltd. The GFA of the original building is about 1300m^2. The new basement was 8m x 10m in plan and 7.65m deep. Automatic mechanical car parking equipment with four parking lots were proposed. The demolishing work of partition structure was conducted in December 2015. The under-pinning work started from the beginning of 2016 and the main structure was accomplished in March 2016. All work finished in May 2016 including the installation and testing of the parking equipment. Before the excavation, each column was under-pinned by four SAP piles and the piles length were 24m or 25m. The sales center was kept open to public and the rooms at level two above the construction zone were also kept operational during the construction.

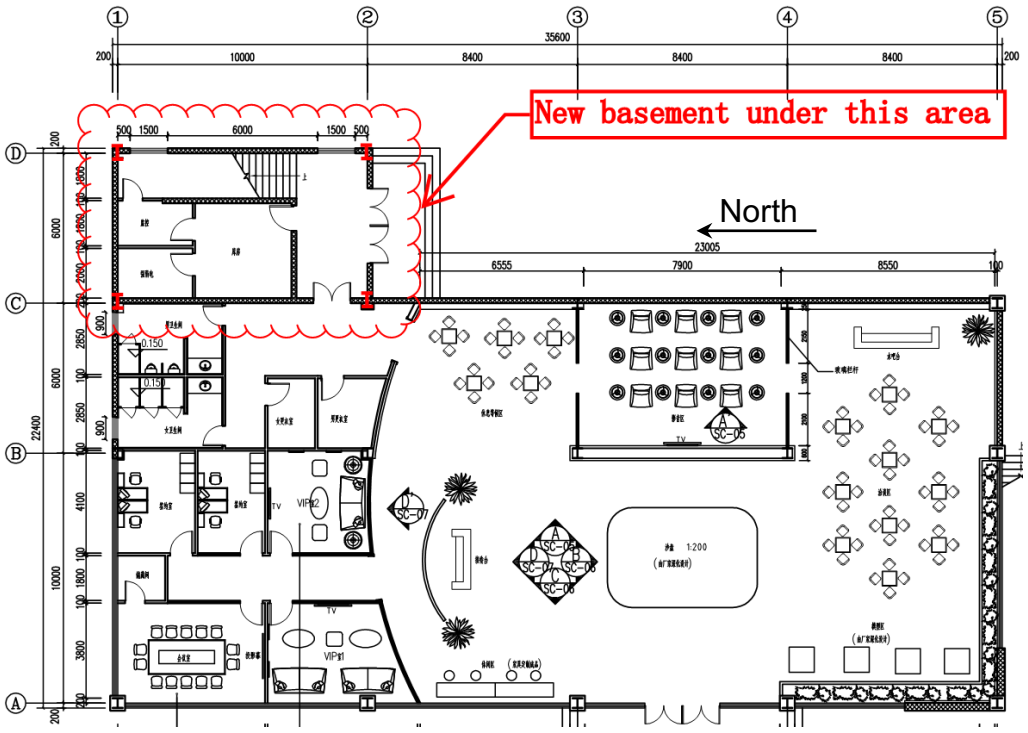


Figure 1. Plan of the sales center

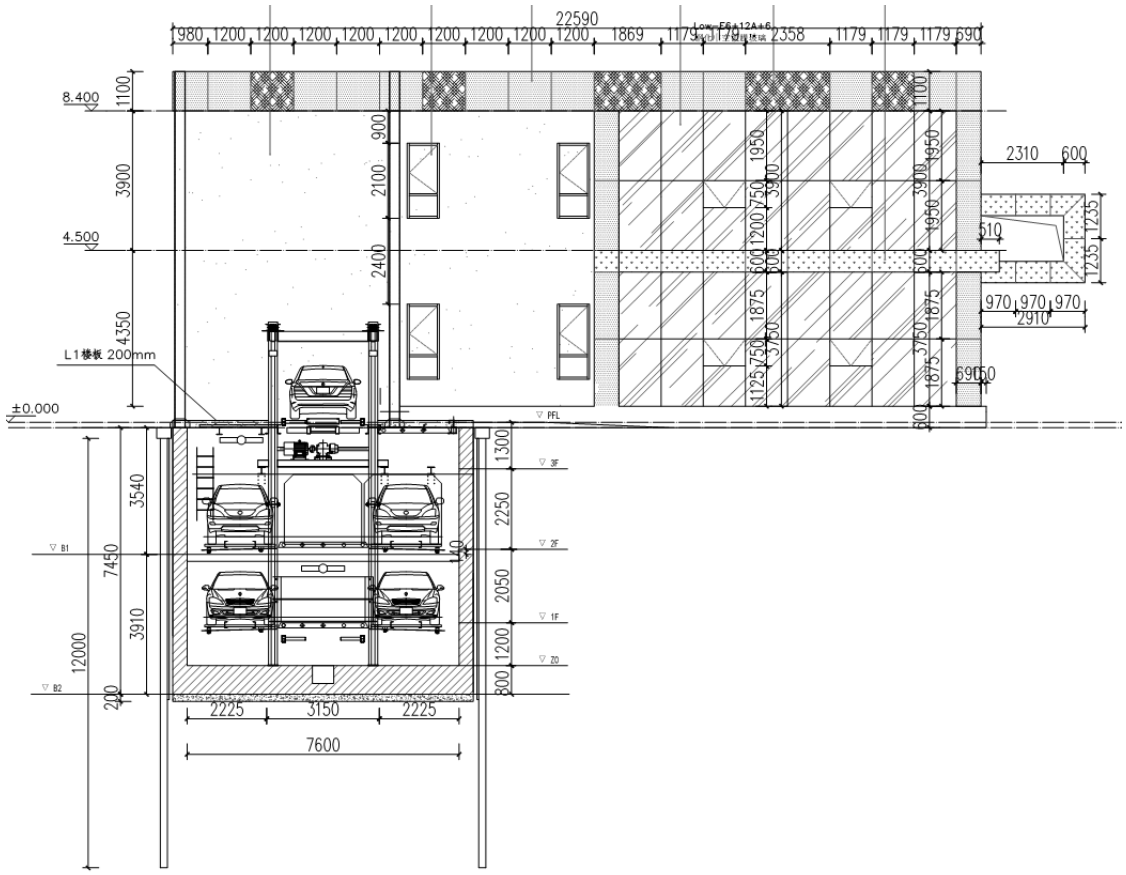


Figure 2. Section of the sales center

SITE CONDITIONS

The site is on a flat ground and the ground water level was lower than -40m, which means there was no ground water impact during the construction period. The site conditions are shown in Table 1 and Table 2 in accordance with the geotechnical investigations.

Table 1. Soil parameters

	f_{ak}（kPa）	Es（MPa）			
		100~200 (kPa)	200~400 (kPa)	400~600 (kPa)	600~800 (kPa)
loess like silt①	115	7.4	10.3		
loess like silt clay②	130	6.1	8.1	14.7	19.9
Silt③	150	8.0	10.3	18.0	22.8
silt clay④	170	8.3	10.3	16.7	21.5
Medium Sand④1	180	17			
silt clay⑤	190	9.3	11.8	17.2	21.6
Gravel⑥	220	20			
Round gravel⑦	210	22			
Gravel⑧	260	35			

Table 2. Soil parameters (Continue)

	q_{sik}（kPa）	q_{pk}（kPa）	γ (kN/m^3)	C_k (kPa)	φ_k °
loess like silt①	30		19.2	23.8	16.1
loess like silt clay②	40		19.1	25.2	14.5
Silt③	44		19.5	22.9	14.8
silt clay④	50				
Medium Sand④1	50				
silt clay⑤	60	1400			
Gravel⑥	80	2000			

STRUCTURAL AND FOUNDATION DESIGN CONSIDERATIONS

Structural and foundation scheme

The super structure is designed to be temporarily supported by 16 SAP piles. There are four steel columns to be under-pinned. Each one is supported by four SAP piles. The SAP piles under the east two columns are 24m long and the designed characteristic bearing capacity is 20T. The SAP piles under the two columns are 25m long and the designed characteristic bearing capacity is 35T. The new basement is 8m x 10m in plan and 7.65m deep. The retaining structure are micro steel piles with 12m length, 168mm@750. Top ring beams are concrete and the second ring beams are steel, supported by soil nails and horizontal bracing respectively. The retaining structures and under-pinned structure are shown in Figure 3 to Figure 5.

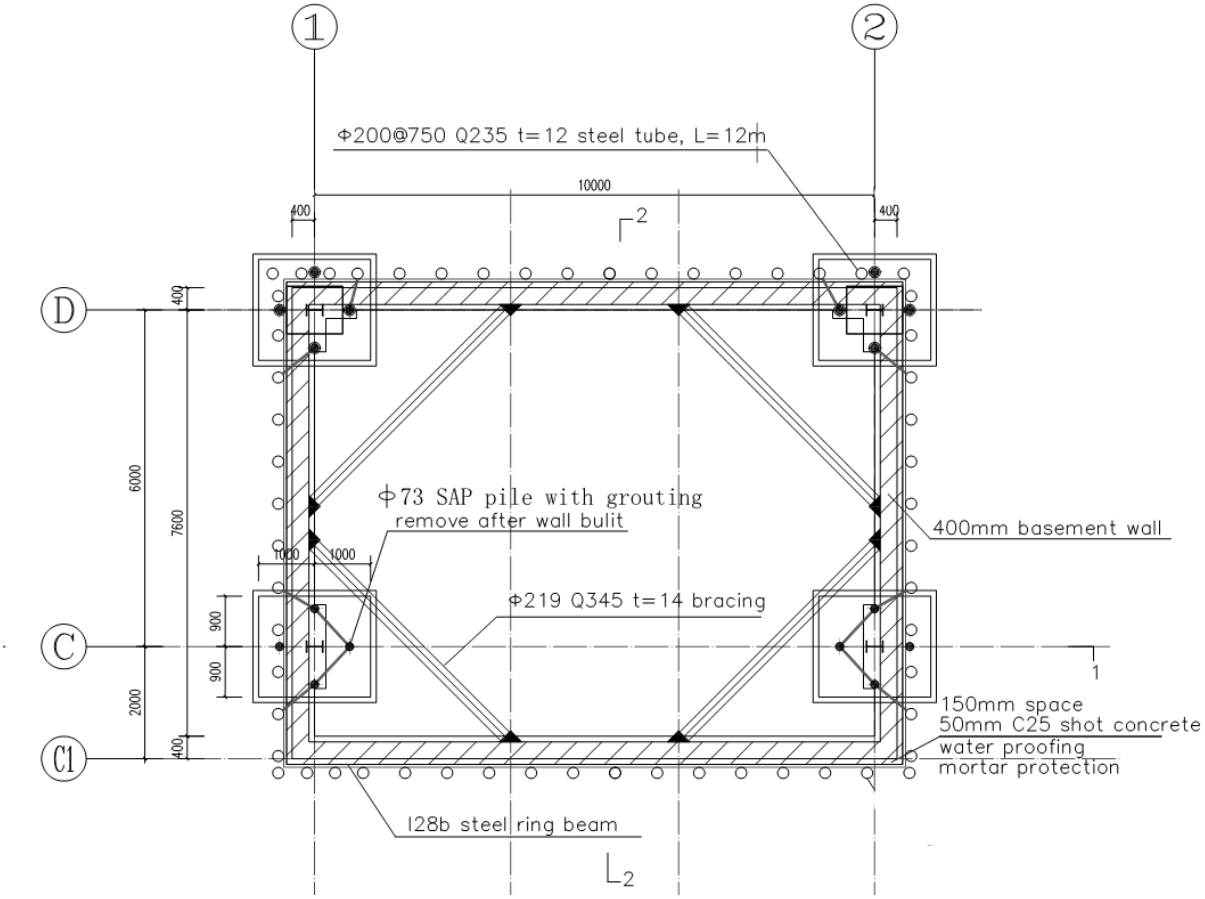


Figure 3. Plan of the excavation zone and temporary structures

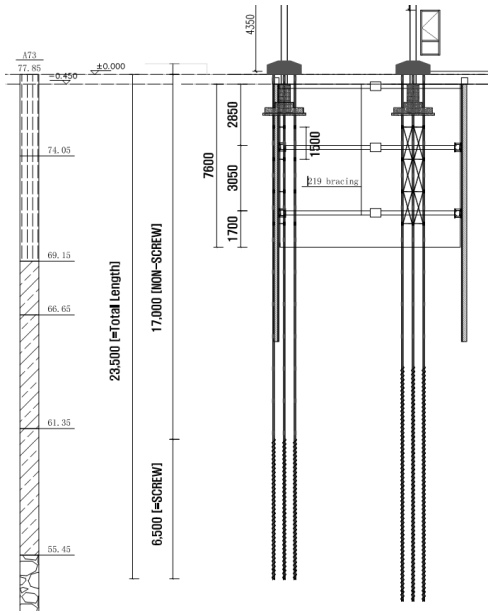


Figure 4. Section of the excavation zone and temporary structures

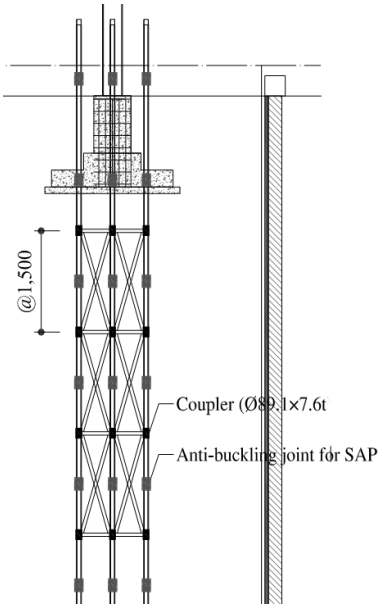


Figure 5. Under-pinned structures and Anti-buckling system

SAP pile design

The conception of SAP is to make the boring rod a permanent pile. That is, the boring rod excavates to the ground at the beginning, and then it will perform as a permanent pile with grouting.

After SAP is placed to desired depth using air or T4 drilling, grouting will be injected through both in and out of SAP. The attained frictional resistance between the grouting bulge and the ground should exceed design bearing capacity. Figure 6 illustrates the typical soil-pile interaction.

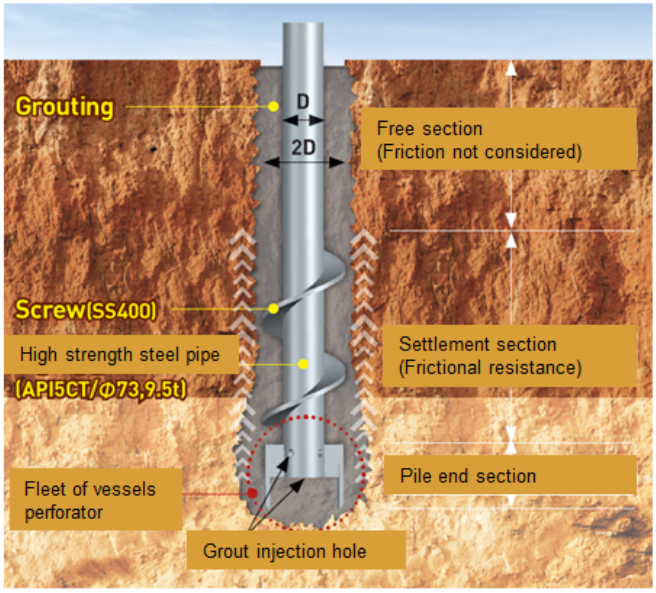


Figure 6. Soil-Pile Interaction

Vertical loads, material stress, buckling stress, buckling reinforcement, joint stress, etc. are considered in the SAP design.

(1) Calculate the compression loads applied at the top of the SAP and determine the screw length – which is equal to the bond zone. The SAP must be resisted by the grout to ground bond through the screw length.

Typical SAP piles transfer axial load through end bearing and pile-soil friction. In this case, however, end bearing capacity is not considered due to negligible toe area compared to surface area of the shaft. Only surface friction is considered in the design. To determine surface friction, it is assumed that soil/grout around the screw act as one body together with the pile.

Equation (1) is used to calculate allowable bearing capacity of pile under axial compression and tension loads according to FHWA NHI-05-039.

$$P_a = \frac{\pi \times D \times L}{F.S} \times \tau \quad (1)$$

$$D - Screw\ Diameter\ (mm)$$

$$L - \text{Length of Screw Section (mm)}$$

$$\tau - Frictional\ Resistance\ (N/mm^2)$$

$$F.S - Factor\ of\ Safety$$

Consider that current screw pile design methodologies use safety factor of 2 or less, as well as screw and grout interaction increases stability, safety factor of 2 is used in our design.

In addition, frictional resistance shall be based on *N* value for weathering soil. The length of screw section shall be determined by engineer's judgment.

(2) Evaluate the axial capacity of pile and calculate the compression loads applied at the top of the SAP. Even if the capacity of the ground is sufficient, the material failure may occur in conditions such as lack of material allowable strength. In this case, stability evaluation with calculating material allowable strength is necessary. The allowable compression loads for the cased length of the SAP is given by equation (2) according to German Standard.

$$P_a = \frac{f_{y-casing} \times A_{casing}}{F.S} \quad (2)$$

$$f_y - Yield\ strength\ of\ material\ (N/mm^2)$$

$$A - \text{Effective area of material } (mm^2)$$

$$F.S - Factor\ of\ Safety$$

Table 3. Axial Capacity of Pile Shaft by Material Rating

(Including couplers for steel splice)

Material	Rating	Yielding Load (MPa)	Tensile Load (MPa)	External Diameter (mm)	Thick ness (mm)	Weight (kg/m)	Cross Sectional Area (cm^2)	Allowable Load of material (tf/ea)	Section Modulus (cm^3)	Radius gyration of area (cm)	Moment of inertia (cm^4)
AP15CT	N80	552	689	73	11	16.7	21.42	70.53	29.0	2.22	106
AP15CT	P110	758	862	73	9.5	14.7	18.95	85.66	26.7	2.27	97.6
AP15CT	P110	758	862	73	11	16.7	21.42	96.85	29.0	2.22	106

(3) The center to center spacing between individual SAP Piles should be at least 750mm or more than 5 times of the SAP Pile diameter. This spacing criterion is for potential deviations in drilling and reducing group effects between SAP Piles.

(4) Evaluate the buckling of cased length of the SAP Piles and exposed length of the SAP Piles because of excavating to the ground. The cased length of the SAP Piles may be evaluated in very weak ground.

Considering the ground condition, if the lateral elastic modulus of specific ground is smaller than the limit value of E_s, buckling effect must be reviewed.

The buckling of cased length of the SAP Piles is given by Equation (3) according to Cadden and Gómez, 2002.

$$E_s \geq \frac{1}{\left(\frac{4I_{casing}}{A_{casing}^2}\right)\left(\frac{E_{steel}}{f_{y-casing}^2}\right)} = E_s^{Limit} \quad (3)$$

$$I - Moment\ of\ inertia\ (mm^4)$$
$$A - Effective\ area\ of\ material\ (mm^2)$$
$$E - Elastic\ modulus\ of\ material\ (N/mm^2)$$
$$f_y - Yield\ strength\ of\ material\ (N/mm^2)$$

Also, the exposed length of the SAP Piles requires the anti-buckling system for safety of the SAP Piles. The anti-buckling system and the center to center spacing of anti-buckling beam should be evaluated. X-bracing and horizontal bar are used in this project with 1m spacing.

Numerical Simulation

3D finite element software MIDAS/GTS was used to conduct the numerical simulation of the whole construction procedure and to be the reference of the design. Modified Mohr-Coulomb is used as the soil model in the analysis. The numerical simulation included 12 steps:

Step1: Free field simulation

Step2: Original steel structure construction

Step3: Excavate to -1m level to expose the original pad foundation of columns

Step4: Retaining steel piles, SAP piles installation

Step5: Top ring beam construction

Step6: Excavate to -3.35m, second ring beam and horizontal bracing construction

Step7: Excavate to -7.65 (bottom of the basement)

Step8: Base slab construction

Step9: Lower part basement wall construction

Step10: Remove second ring beam and horizontal bracing

Step11: Upper part basement wall construction

Step12: Remove SAP and finish the construction

The SAP axial forces, lateral displacements of the excavation zone, settlement of the columns and ground around the excavation zone were discussed basing on the simulation results.

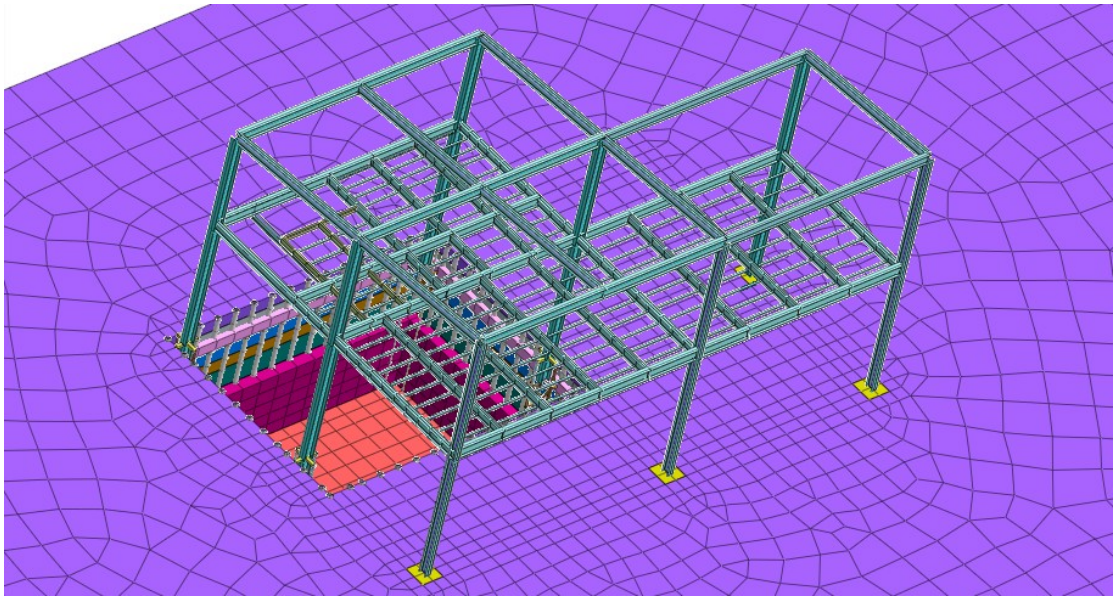


Figure 7. 3D soil-structure interaction modeling

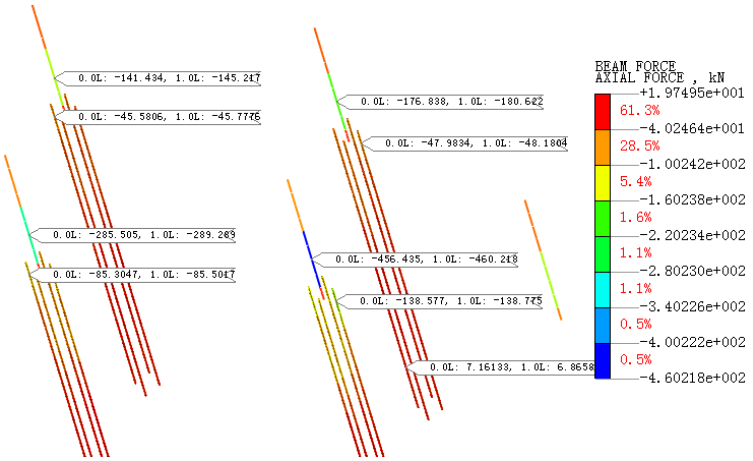


Figure 8. Axial force contour

The maximum column axial force is about 460kN, which is similar to the evaluation. The maximum axial force in the SAP piles is 138kN, which is smaller than the design pile capacity and all piles have enough capacity to resist upper structure loads.

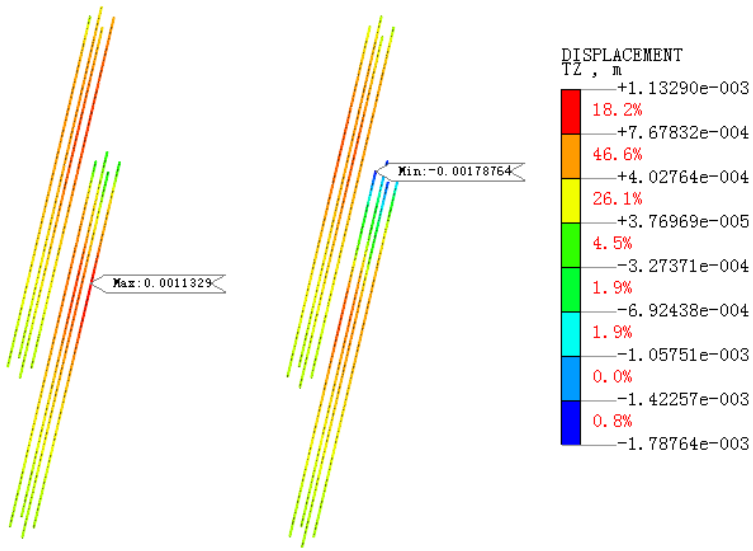


Figure 9. Settlement contour

The maximum settlement of the top of SAP piles is 1.79mm according to the simulation. The maximum settlement measured during the construction was 2.5mm. No wall crack was observed during the construction period.

CONSTRUCTION CONSIDERATIONS

Considering the constraints of the site, small equipment is required to do the drilling work. ‘SE-SAP-MR13 SAP’ is the dedicated equipment of SAP method and its size is 0.8x3.1x2.3m. The boring equipment consists of Main Machine as a role of drilling, Power Pack for Main Machine power supply, and Remote Controller such as attached component for Main Machine’s operation.

Besides those three components, Air-Compressor for boring, Mixer-Pump Plant for grouting, and Diesel-Engine Generator for electric power are needed as additional devices.

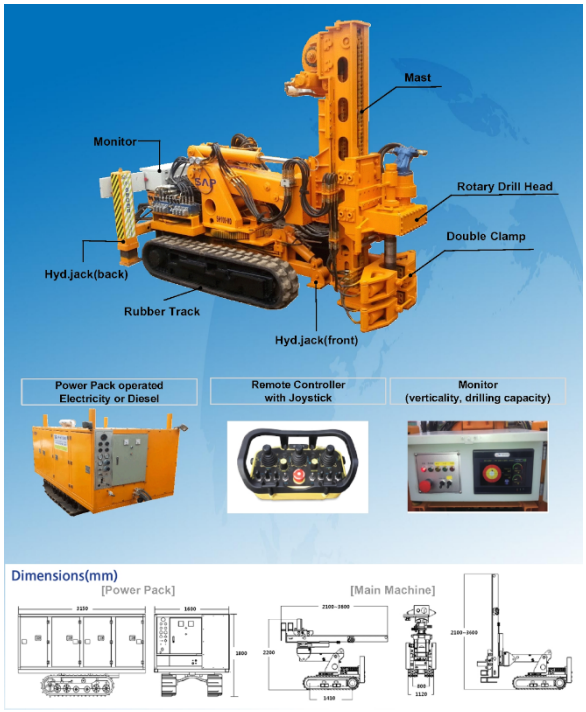


Figure 10. The components of SAP-drilling

The SAP is located in its place after mounting connection between the auger of the boring machine and the pile screw tab, and it is maintained verticality using a vertical measuring device. The rotary pressure is applied while putting high pressure air/water by operating compressor/hydraulic motor based on the ground and maintain proper penetration speed to prevent SAP from bending.

The piling work of the SAP pile using the screw tab continues until the design length. After boring, the air hose is prevented in order to pump the cement mortar into the SAP pile with grouting hose attached by SAP-drilling.

The cement mortar is pumped into the SAP pile through its top, and it is filled up to the ground level. After the Over-Flow of grout is checked at the ground surface, stop grouting and move the equipment to next construction location.

Once the grouting completes, SAP cutting work and joint work between column and SAP with wing plate should be followed at least 1 to 3 days after.

At this time, the amount of load transfer and increase of loads are checked by instruments in selective areas. After the installation of joint, boring work of lower ground is continued, and also connect SAP(partial) to SAP(partial) to minimize bucking while boring work.

If the boring depth is complete as scheduled, the joint is separated after pouring concrete at foundation and inside of the wall.

And then, set up new structures in extended area and proceed overground finishing work to complete the SAP construction.

It took one week to finish the SAP pile drilling work and the whole procedure of the construction please refer to Figure 11.

1. Move to the point	2. Set the equip.	3. Set the pile
		
4. Pile drilling	5. Grouting	6. Joint (column to pile)
		
7. Anti- buckling system	8. Excavation	9. Basement structure
		
10. Joint removing	11. Parking facility	12. Finish
		

Figure 11. Construction sequences

MONITORING AND LOAD TEST

The pile axial forces were monitored by four load cells and no axial forces exceeded the expected loads.

Three piles were tested after the basement construction. The super structure was supported by the new basement wall and the base slab formed a raft foundation. The SAP piles were no longer required supports and they were intentionally separated from the base slab to conduct the test. The test results show that all piles have sufficient bearing capacity comparing to the design.



Figure 12. Pile load cell



Figure 13. Load tests of SAP piles



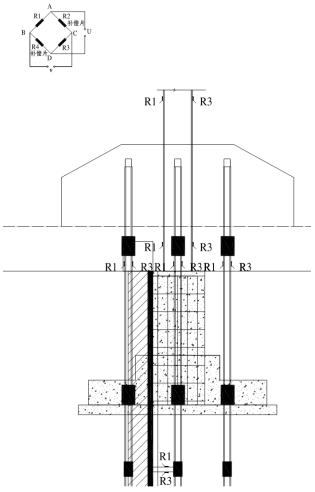


Figure 14. Strain gages

Strain gages were used to monitor the forces in the columns, piles and anti-buckling members. Settlements of the column bottom were also monitored periodically and the maximum value was 2.5mm, which was very small as the actual load was far away from the pile capacity.

CONCLUSIONS

This small project lasts about half year because of the limitation of the working space and working hours. However there were no safety problems during the construction and the client was satisfied with the result. The building was fully operational during the construction. The exterior of the renovated building is exactly the same except the additional entrance of the mechanical parking. More studies are required to confirm the performance of SAP technology to different site conditions. This project indicates that parking garage under an existing building may be one good solution to solve the problems in central cities.

ACKNOWLEDGEMENTS

We are grateful to Mr. Gary Koo, Mr. Un-Moo Lee, Mr. Myoung-Su Jo form SE EXT Co., Ltd.; Mr. Jianguo Liu, Mr. Siyu Wu, Mr. Wubao Li, Mr. Zengzhu Kang from Zhongyan Technology Co., Ltd. for their support during this project and in preparation of this paper.

REFERENCES

FHWA(2005), Micropile Design and Construction: Reference Manual, Sabatini P., Tanyu B., Amour T., Groneck P., and Keeley J., FHWA-NHI-05-039, Federal Highway Administration, December

NAFAC(1983), Department of the Naval Facilities Engineering Command, Naval Facilities Engineering Command, Soil Mechanics Design Manual 7.1

Cadden A. and Gómez J.(2002), “Buckling of Micropiles-A Review of Historic Research Experiences”, ADSC-IAF Micropile Committee

DIN 4128 (1983). “Small Diameter Injection Piles (Cast-in-place Concrete Piles and Composite Piles).

MICROPILES USED FOR DEEP FOUNDATION SUPPORT AT THE RITA LIDDY HOLLINGS SCIENCE CENTER AT THE COLLEGE OF CHARLESTON, CHARLESTON, SOUTH CAROLINA

William L. Snow, Sr.[1], William B. Wright, PE[2], & Will Snow, Jr., PE[3]

Charleston, South Carolina is one of the fastest growing metropolitan areas in the Southeastern part of the United States. Occupying the largest footprint in downtown Charleston, the College of Charleston is experiencing a similar growth, but in a confined area. In an effort to supply a growing student body with state of the art facilities, the College is continually renovating existing structures and occasionally, building new ones. The Rita Hollings Science Center Building combines both renovation and new construction. In order to review the final foundation design and construction, some basic facts and history unique to this area must be understood.

1. Charleston, South Carolina is located immediately adjacent to the Atlantic Ocean. The peninsula which represents downtown is located between the Ashley and Cooper rivers. Local custom holds that The Ashley and Cooper rivers merge together into Charleston harbor to form the Atlantic Ocean. From a geotechnical viewpoint, Charleston is in fact a unique location for a modern metropolis in that there is no bedrock to support the structures of the city. In addition, the city is in an active seismic zone which mandates the evaluation of lateral loads as well as liquefaction when considering foundation support systems. To accommodate the support of all structural design, the design professional must utilize deep foundations (piles) supported in the Cooper River Marl formation, which is not subject to liquefaction. Given the potential for seismic events as well as the frequency of hurricanes and resultant wind loads, for all practical purposes, all structures must be designed for axial as well as lateral support in the foundations as well as the buildings themselves.
2. The College of Charleston is basically landlocked in its historic footprint. All new physical facilities must be contained within that footprint, which is compact in nature. In 2010, a major construction project utilized driven piles as the primary foundation support. Although piles have been driven in the Charleston area for generations, this project took place during final exams at the College. The disruption from vibration as well as noise was more than a minor annoyance. In short, after much discussion, the Board of Directors of the College banned driven piles for all future projects, unless the designer could guarantee no disruptions from the process.
3. The Rita Hollings Science Center was designed as a renovation of the existing building attached to a newly constructed building as well as vertical expansion basically tripling the square footage of the facility. Since the original structure was built in the 1960's the entire foundation had to be upgraded and enhanced to support the vertical expansion as well as to meet current IBC codes.

[1]Palmetto Gunite Construction Co., Inc., PO Box 388, Ravenel, SC 29470, 843-889-2227, snowwl@aol.com
[2]Terracon Consultants, Inc., 1450 5th St. W., North Charleston, SC 29405, 843-514-0016, wbwright@terracon.com
[3]Terracon Consultants, Inc., 2201 Rowland Ave., Savannah, GA 31404, 912-200-9120, will.snow@terracon.com

4. Given the need for increased axial and lateral load requirements, coupled with the fact that driven piles were not practical for the facility; the designers looked to alternative deep foundation support systems.

In 2014, design was begun and a dual system of foundation support was included in the construction documents. Micropiles were indicated for the support of the renovation of the existing structure. Auger cast piles were specified for the adjacent new construction phase of the project. The project bid in early 2015, based on the project documents. When the bids were opened, the total price exceeded the engineer's estimate. Before the contract could be awarded, the owner entered intense discussions with the low bidder in an effort to find a way to reduce the overall cost of the project. Although the final negotiations did not bring the price down to the engineer's estimate, there was enough savings to prompt the owner to accept the general contractor's proposal and a contract was signed by both parties.

One area of significant savings was found when the designers accepted a proposal from the micropile contractor, Palmetto Gunite Construction Co., Inc., to substitute cased micropiles in lieu of the specified auger cast piles. Much of the savings were the result of the cost associated with the extremely tight working conditions that were much more favorable to micropiles when comparing the equipment needed and the storage required for the disposal of dirt resulting from the auger cast pile process.

The micropile contractor working with design professionals from Terracon Consultants, Inc. and Theodore Padgett, PE, PC – Consulting Engineer provided a design for the micropiles which provided support for the same loads as the auger cast piles with only minor changes to the pile caps with regard to spacing and connections to the micropiles. To fulfill the contract requirements for both the original micropiles as well as the micropiles offered as a substitute for the auger cast piles, test piles and reaction piles were installed at several locations on the project.

The test pile program consisted of seven (7) load tests for which, 5 piles were located at production locations and one pile was located at a non-production location, due to congestion constraints on the project site. The test piles and their corresponding tests were as follows:

- 3 axial compression piles designated TP-2, TP-3 and TP-4 (75 feet in length)
- 2 axial tension piles designated TP-5 and TP-6 (75 and 80 feet in length)
- 2 lateral tests on piles designated TP-1 and TP-5 (75 and 80 feet in length)

All axial load testing was conducted in general accordance with ASTM D1143-07. The results of the three static axial compressive tests were evaluated utilizing the Modified Davisson method, which was considered appropriate for cast-in-place piles such as the micropiles used on this project.

The chart listed below presents the results of the analysis for the load tests for this project:

Table 1. Results of the analysis for the load tests for this project.

Compression Load Tests Summary

Test Pile	Pile Depth (ft.)	Pile Design Diameter (in)	Maximum Loading (kips)	Ultimate Capacity (kips)[1]	Allowable Capacity (F.S=2.0)	Allowable Capacity (F.S=2.5)
TP-2	75	10	200	200	100	80
TP-3	75	10	200	200	100	80
TP-4	75	9	145	130	65	52

1. Based on IBC 2012-1810.3.3.2

Tensile Load Tests Summary

Test Pile	Pile Depth (ft.)	Pile Design Diameter (in)	Maximum Loading (kips)	Net Axial Deflection (in)	Ultimate Capacity (kips)[1]	Allowable Capacity (F.S=1.5)	Allowable Capacity (F.S=2.5)
TP-5	80	9	126 [2]	1	113	75	45
TP-6	75	10	98	0.8	98	65	39

1. Ultimate capacity analysis based on IBC 2012-1810.3.3.1.5
2. Net axial deflection of 1.3 inches at maximum loading

Lateral Load Tests Summary

Test Pile	Pile Depth (ft.)	Pile Design Diameter (in)	Maximum Loading (kips)	Net Lateral Deflection (in)	Ultimate Capacity (kips)[1]	Allowable Capacity (F.S=2.0)	Allowable Capacity (F.S=2.5)
TP-1	80	9	22	0.5	22	11	8.8
TP-5	75	10	15	1	15	7.5	6

1. Ultimate capacity analysis based on IBC 2012-1810.3.3.2

Source: Terracon Consultants, Inc.

Micropiles were chosen for this project for several reasons. First and foremost was the absence of noise and vibrations during the installation process. Most of the project was to take place while classes were in session. The project itself was located nearly in the center of campus so any noise and vibrations such as pile driving would produce, was unacceptable to the owner.

Another serious issue concerning vibrations, is that many of the buildings near the project are unreinforced masonry. This is an issue throughout the Charleston peninsula and surrounding historic areas. Many of the structures referred to survived the 1886 earthquake and have been under serious stress from that event for over 130 years. It is simply not possible to determine over a large area whether the structures can withstand extensive vibrations, given their overall condition. Alternate forms of foundation support such as micropiles and auger cast piles eliminate the concern for serious vibratory loads.

As stated above, the final structure will be a combination of new construction and upgrading the existing structure. The original project documents called for micropiles to be constructed beneath the original structure to bring that building up to modern codes

and to support the vertical expansion loads. Auger cast piles were originally shown on the contract drawings to support the new construction portion of the structure. The designer basically only considered the head room of the two phases of the project. Simply put, they felt the existing structure could not support the equipment required for auger cast, but outside the structure, there was unlimited headroom and they believed the auger cast could be installed cheaper than micropiles.

Before the final documents were completed, the micropile contractor offered a design-build option that utilized micropiles instead of auger cast for the new construction as well. This method was accepted for several reasons. The number one reason was that it was cheaper overall to use micropiles. The second consideration was the site was extremely small making it very difficult to move a crane around for the auger cast option. Storage and disposal of earthen spoils would also be problematic due to the small surrounding streets, especially when students were present. The last consideration was that the overall load requirements were easily within the capabilities of the cased micropiles proposed for all axial as well as lateral loads. Early load testing provided test results which made acceptance of the micropile option an easy decision for the structural engineer.

In the end, 149 micropiles were installed on the outside of the existing structure and 154 were installed on the inside. The piles installed on the outside of the building were 10-inch diameter piles extending into the marl to a depth of 75 feet below grade with a 10 inch casing installed to a depth of 5 feet from the top of the pile. The 148 micropiles installed on the inside of the structure were 9-inch diameter extending into the marl to a depth of 80 feet from the surface with no casing.

The micropile installation was considered a success for this project for several reasons. The micropile portion of the $45M project was the only sub-contract efforts that were completed on time with no additional change orders. This was an extremely confined workspace as well as a very complicated work sequence. Being on time and on budget was noticed by not only the professionals directly associated with the project, but also by the entire local Engineering/Construction community. The fact that there was no excessive noise, vibrations or significant traffic congestion associated with daily spoil removal, insured that micropiles will continue to be considered the standard deep foundation support system throughout this historic city when similar site conditions are present.

Stabilization of the Nyköping's riverbank with micropile-walls

Vazquez, A. [1], Aronsson, S.[1] and Marxmeier, N. [1]

[1]*ÅF Industry AB, Frösundaleden 2A, 169 99 Stockholm, Sweden*

E-mail:Alejandro.vazquez@zueblin.de, Stefan.aronsson@atkinsglobal.com, Natascha.marxmeier@afconsult.com,

ABSTRACT: Along the Nyköping River (100 km south of Stockholm), the slope of the northern riverbank indicated a potential sliding failure – especially around the area called "Åkroken" which is planned to become a new residential area. The cross section of "Åkroken" shows a steep slope (~ 20%) with heavy surcharge loads on top due to the building plans. The geology consists of approx. 1 m upper filling material "rich" on archaeological findings from medieval times (12th century). Beneath the filling there is approx. 7-9 m silty-clayey layer over the bedrock. This slope is supported with masonry gravity walls founded into the river bed. However, these walls showed clear signs of instability since the wall was tilting towards the river. As a prevention measure, the city council cordoned off the area. ÅF Consult was committed to assess the stability of the slope and design safety measures to both be able to renovate the masonry walls and increase the factor of safety for the entire fringe.

As a remediation measure a micropile-wall was recommended to prevent the effects of a landslide failure in the Nyköping River. The micro-pile wall's main functions was to avoid further displacements during the renovation of the old masonry walls, and later on to work as a permanent structure. The micropile-wall was designed for 100 years life-span according to Swedish Standards. Bored micropiles, Ruukki RD 170/12.5 mm, were installed c/c 1 m and filled with concrete. Tieback anchors, Ischebeck TITAN 73/53, were installed c/c 2.5 m with a 45 degrees inclination and embedded in rock. Numerical analysis (PLAXIS and Geostudio) were utilized to assess the slope stability and estimate the range of displacements during the construction of the micropile walls. Geotechnical investigations estimated the material properties for the calculations.

INTRODUCTION

This paper is prepared as part of the 13th International Workshop on Micropiles. The topic of this work focuses on the slope stabilization of a riverbank applying micropile-walls and tieback anchors.

The site was located along the Nyköping River (100 km south of Stockholm, Sweden) where the slope of the northern riverbank indicated a potential sliding failure – especially around the area called "Åkroken" which is planned to become a new residential area. The cross section of "Åkroken" shows a steep slope (~ 20%) with heavy surcharge loads on top due to the building plans. The geology consists of approx. 1 m upper filling material "rich" on archaeological findings from medieval times (12th century). Beneath the filling there is approx. 7-9 m of silt and silty-clayey layers over the bedrock. This slope is supported with masonry gravity walls founded into the river bed. However, these walls showed clear signs of instability since the wall was tilting towards the river. As a prevention measure, the city council cordoned off the area (See Figure 1). ÅF Consult was committed to assess the stability of the slope and design safety measures to both be able to renovate the masonry walls and increase the factor of safety on the entire fringe.

In general, methods to prevent slides on slopes can vary from case to case. Commonly known methods are: soil reinforcement, retaining structures, geometric improvements, re-vegetation, drainage or counterweight masses. In this particular case, apart from the common geotechnical uncertainties e.g., spatial variability [1] the design was limited by other factors, such as: archaeological findings, urban planning, existing buildings and the presence of a river regulated by a hydropower plant. Furthermore, it was necessary to repair the existing masonry wall and remove the trees that were slowly falling down. With these circumstances a soil reinforcement with micropile-walls seemed to fit the best to cope with these limitations. In this paper are described the analyses of the information for the instability failure mode, the design method for the retaining structure and the details of the final design of the remediation measures.



Figure 1 Slope instability signs on the masonry walls (Source: Nyköping City Council)

ANALYSIS OF THE INFORMATION FOR THE INSTABILITY FAILURE MODE

When ÅF Consult was committed to assess the slope stability the first task was to analyse the geotechnical conditions of the soils. Thus, based on the field test investigations (CPT, samples, piezometers, lab results) it was created a limit equilibrium model with the software Slope/W. The model showed critical safety factors slightly higher than 1, see Figure 2. Another aspect was the unfavorable inclination (~ 20%) of the soil layers to slide into the river, this was considered with the grid and radius method in Slope/W inclining also the radius lines of the slip surfaces [3]. Some of the characteristics of the methodology are included in Table 1.

Table 1 Characteristics of slope instability limit models

Limit equilibrium method	Soil failure mode	Pore-water pressure	Search slips method	Failure surface
Morgenstern-Price	Mohr-Coulomb Undrained andCombined	Manual piezometeric line with automatic correction	Grid and radius considering 20% slope	Circular slip

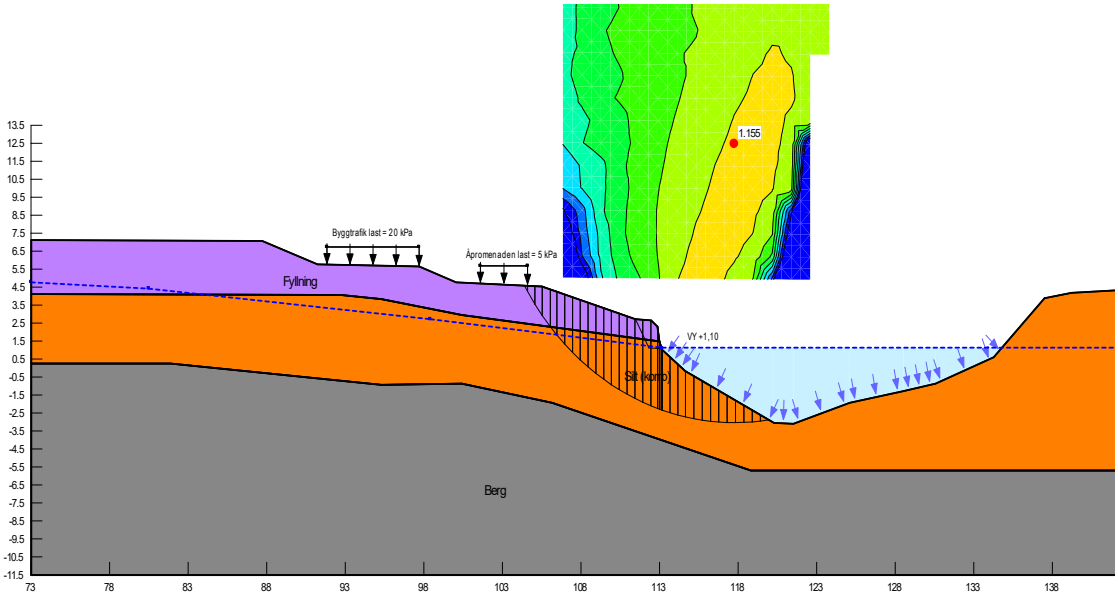


Figure 2 Critical slope stability 1.15. It was required a $SF_{combined}$>1.45

Introduction of remediation measures in the model

As a remediation measure for the unstable condition of the slope we recommended to build micropile-walls and tieback anchors embedded into the rock. These structural elements were included in the Slope/W model increasing the resisting forces of the anchors and micropile-wall until the required SF was fulfilled in each case.

DESIGN OF MICROPILE-WALLS AND TIEBACK ANCHORS

The retaining system was designed according to Swedish standards [8], [9], [10], [11] and [12] for a 100 years lifespan. The design considered two approaches. At first, an Ultimate Limit State (ULS) design was performed considering multiple variables, such as: construction plans, heavy spread loads, water and groundwater levels and reduction of effective steel sections due to oxidation. This approach was applied analytically including partial safety factors in the calculations. The other design approach consisted of a Serviceability Limit State (SLS) to analyse the stability and deformations during construction. There were considered 5 construction stages: 1) Installation of micropiles, 2) Excavation up to wale beam and tieback level, 3) Pre-stressing of the anchors at 220 kN, 4) Excavation and renovation of masonry walls, 5) Filling up the excavation to the original ground level. The soil and structural properties are included in Table 2 and Table 3 according to the soil investigations and [6] and [7].

Table 2 Soil properties, characteristic values

Material	Unit weight	Friction angle	Undrained Shear strength	Effectiv. cohesion	E-modulus	Poisson ratio
Symbol	ɣ	ϕ'	C_u	c'	E	*ν (nu)*
Units	[kN/m³]	[˚]	[kPa]	[kPa]	[MPa]	-
Filling	18	34	---	---	15	0.2
Silt/Silty Clay	16	27	30	3	10 (Undr 7.5)	0.2
Bedrock	26	-	-	-	50000	0.2

Table 3 Structural properties, micropiles and tieback anchors

Material	EA	EI	Unit weight	Diameter	c/c
Units	[kN/m]	[kN m²/m]	[kN/m³]	[m]	[m]
Micropile RD 170/12,5	912067 (1)	2672 (1)	78.4	0.16	1
Grouted rock anchor	55528	35	24	0.10	2.5
Soil anchor Titan 73/53	299000	143	51.2	0.073	2.5

(1) Reduction of 3 mm corrosion.

Ultimate and Serviceability Limit States

This design approach checked that the dimensions of the retaining system in the ULS calculations would not experience excessive deformations neither slope instability during the construction. The results of slope instability and displacements analyses for each construction stage are shown in Table 4. In the first stage, the results showed that the SF of the slope might be lower than 1 due to the heavy loading from the pile driving machines. However, the expected deformations were small. In the second stage, the slope stability raised to 1.14. The horizontal deformations remained small and towards the river until the anchors were pre-stressed in stage 3. At stage 5 the slope stability reached SF=1.3, and the maximum horizontal deformations were expected towards the backfill of the micropile-wall. Thus, the existing masonry walls could be repaired with minimum risk. Furthermore, it was possible to visualise other potential failure modes at each construction stage, e.g., heave at the bottom of the excavation due to unloading conditions, and therefore perform complementary calculations to avoid failure (See Figure 3).

Table 4 Compilation of safety factors and maximum displacements (mm)

Section BB SLS	Stage 1	Stage 2	Stage 3	Stage 4	Stage 5
Safety Factor	0.89	1.14	1.18	1.18	1.27
Horizontal Displacement: (+) To Nyköping river (-) To Kv. Åkroken	+3.6	+5.9	(-11.1)	(-11.1)	(-12.1)

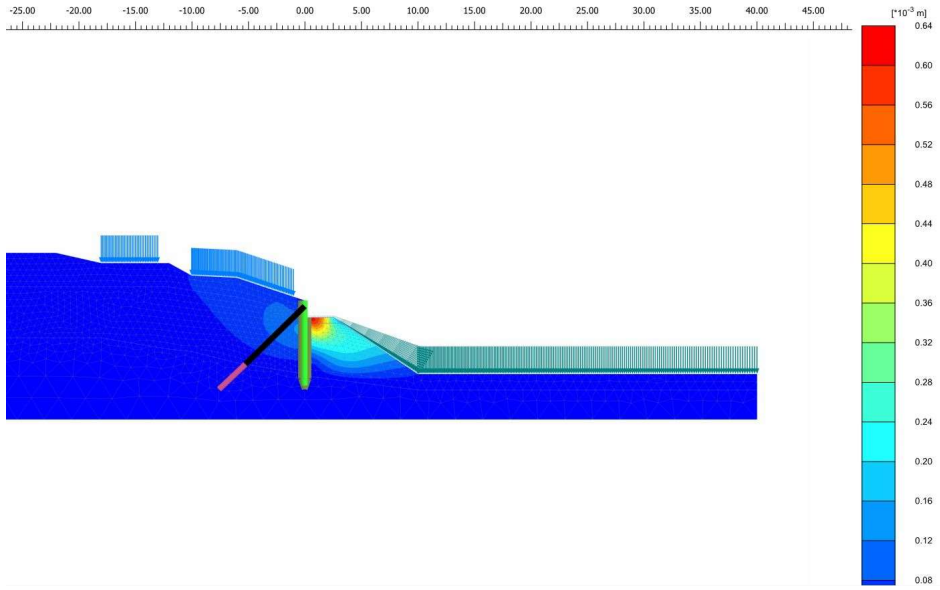


Figure 3 Potential failure mode due to heave at stage 4

FINAL DESIGN OF THE REMEDIATION MEASURES

The dimensioning process provided a retaining system consisting of bored micropiles, Ruukki RD 170/12.5 mm, installed c/c 1 m and filled with concrete and welding steel plates in between micropiles spacing. Tieback anchors, Ischebeck TITAN 73/53 shall be installed c/c 2.5 m with a 45 degrees inclination and embedded in rock. More details of the design can be seen in Figure 4.

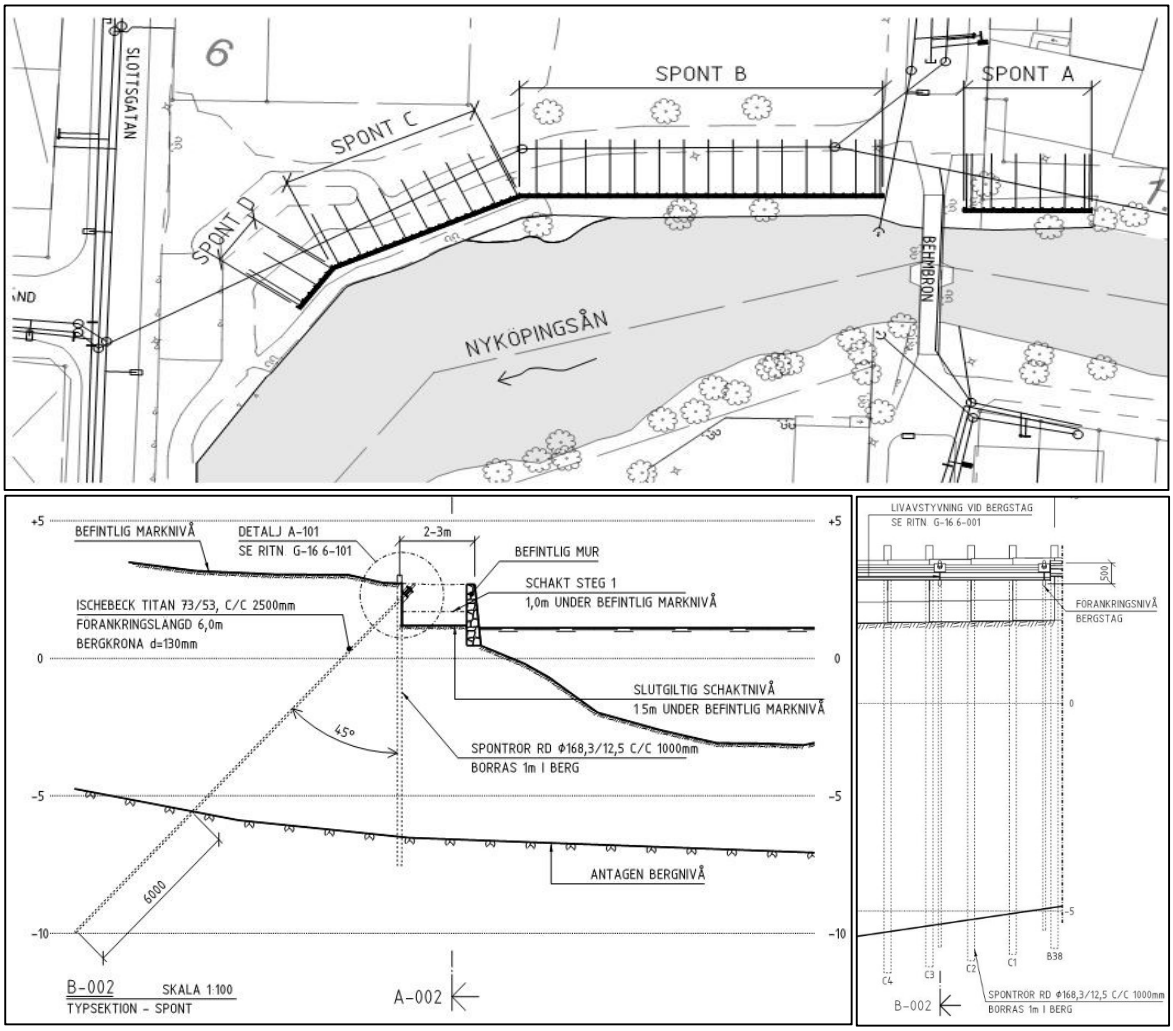


Figure 4 Plan view (top), cross section micropile-wall (bottom-left), profile (bottom-right)

DISCUSSION AND CONCLUSION

Regarding the analyses of the information for instability failure models, the results agreed with other studies performed in the same area. However, if unsaturated conditions were considered the results might have provided higher safety factors, perhaps more realistic [2], [3], [4] and [5]. Although, that assumption would have required further soil investigations [5] and still might overestimate the unsaturated shear strength [3].

The SLS approach using a FE-model provided an estimation of safety factors and deformations for each construction stage. This model assumed 10 kPa surcharge in a bigger extension than in practice. Thus, this 2D model was probably too conservative. However, this assumption remained on the safety side and it followed design standards. Therefore, it was recommended a restriction in surcharge loads adjacent to the masonry wall due to instability/low factor of safety against failure. In order to use the relatively light pile type and installation method, the Contractor could use light machinery or work from a safety distance to the wall. Furthermore, it was recommended to increase the resistance of the micropile-wall by filling each micropile with concrete.

The methodology presented here showed how micropile-walls with tieback anchors were designed to remediate a particular slope instability case. This remediation with micropile-walls fitted the best in "Åkroken" because it allowed access to renovate the masonry walls in safe and dry working conditions with minimum disturbance to the river and existing buildings.

REFERENCES

[1] Javankhoshdel, S., & Bathurst, R. J. (2014). Simplified probabilistic slope stability design charts for cohesive and cohesive-frictional (c-ϕ) soils. *Canadian Geotechnical Journal, 51(9), 1033-1045.*

[2] Fredlund, D. G., & Rahardjo, H. (1993). Soil mechanics for unsaturated soils. *John Wiley & Sons*

[3] Geo-Slope, International Ltd Manual, GeoStudio User's. (2012) *"Geo-Slope" Calgary, Alberta, Canada T2P 2Y5.*

[4] Westberg Wilde, M., & Vazquez, A. (2015). Theme B: System approach to probability of failure of an embankment dam. *13th ICOLD International Benchmark Workshop on the Numerical Analyses of Dams, pp. 217-225. Swiss Committee on Dams.* Lausanne (Switzerland).

[5] Nam, S., Gutierrez, M., Diplas, P., and Petrie, J. (2011). Determination of the shear strength of unsaturated soils using the multistage direct shear test, *Engineering Geology, Vol. 122, pp. 272-280.*

[6] SSAB (2015). RR and RD piles. Design and installation manual. Hämeenlinna, Finland.

[7] TITAN Ischebeck (2016). Titan Anchor Piles manual. Ennepetal, Germany.

[8] Ryner, A., Fredriksson, A., & Stille, H. (1996). Sponthandboken. *Handbok för konstruktion och utformning av sponter.*

[9] Swedish Standards. Eurocode 7: Geotechnical design. Part 1. General rules, 2005, SIS, Stockholm, *SS EN 1997-1, 2005*.

[10] Swedish Standards. Execution of special geotechnical works. Ground anchors, 2013, SIS, Stockholm, *SS EN 1537:2013*.

[11] Swedish Standards. Eurocode 3: Design of steel structures. Part 1-1. General rules and rules for buildings, 2009, SIS, Stockholm, *SS EN 1993-1-1:2005/AC: 2009*.

[12] Swedish Standards. Eurocode 3: Design of steel structures. Part 5. Piling, 2010, SIS, Stockholm, SS EN 1993-5:2007.

INVESTIGATION OF THE CONCENTRIC VERTICAL GROUND LOOP OF A HEAT PUMP IN AN ENERGY MICRO-PILE

Abdel Ramadan[1], Kamran Siddiqui[1], Hesham El Naggar[2]

ABSTRACT

The heat exchange process in a vertical ground-loop heat exchanger was numerically investigated. Among the three initial configurations (U-tube, concentric and spiral), the U-tube configuration yields the highest fluid temperature rise i.e. highest heat transfer rate while the concentric pipe configuration has the lowest fluid temperature rise. Despite lower performance, concentric pipe may be practically more feasible for integration into micropile foundation construction, especially when hollow bars are used as the reinforcing element. The performance of a concentric pipe in an energy pile was also simulated. Two distinct regions of temperature increase are observed. Higher temperature rise in the annular section than the inner pipe. Both regions showed semi-linear behavior of the temperature rise, which may be attributed to the varying ground temperature. The effect of variation of soil temperature in the vicinity of the pile should be further investigated.

1. INTRODUCTION

Heat pump is a device that transfers heat from a cold source to a heat source through the application of work. For an air-source heat pump, the performance of a heat pump decreases as the outdoor air temperature drops in the winter months and increases in the summer months. The performance of a heat pump can be increased substantially by using a ground-source heat pump. A ground-source heat pump system operates on the basis of using ground as a heat source for heating purposes in winter and as a heat sink for cooling purposes in summer. It has been reported that the temperature of the ground below a depth of 6 m remains almost constant throughout the year [Williams and Gold 1976]. This depth however may vary from region to region. The ground temperature at and below this depth is warmer than the ambient air in winter and is cooler than the ambient air in summer. This is the basis of operation for ground source heat pump systems (GSHP) where heat can be absorbed from the relatively warm ground in winter and rejected into the relatively cool ground in the summer through the use of GSHPs.

Although ground-source heat pump systems could be viewed as attractive and feasible from the energy cost point of view, the installation costs associated with the drilling of the boreholes containing the ground heat exchangers could be prohibitive and could act as a barrier for increasing the use and installation of beneficial GSHPs. Nonetheless, relatively novel methods have been explored in order to reduce this

[1] Department of Mechanical and Materials Engineering, University of Western Ontario
[2] Department of Civil and Environmental Engineering, University of Western Ontario

premium installation cost and one of these methods is the “Energy Pile” system where it utilizes the building structural foundation piles as ground heat exchangers [Suryatriyastuti et al, 2012]. Energy piles are basically foundation piles that incorporate a closed loop heat exchanger within it to act as a heat source in the heating season and a heat sink in the cooling season. The heat exchanger in the energy pile is ultimately connected to the GSHP system serving the building. The main advantage of an energy pile system over a conventional ground-source heat pump system is that the foundation structure that houses the ground heat exchanging system is already required for structural purposes and the ground-loop heat exchanger does not need to be drilled or constructed separately [Suryatriyastuti et al, 2012].

Relatively few studies have been conducted on the use of energy pile for ground-source heat pump systems (e.g. Ma & Grabe, Abdelaziz, 2010; 2009; Cervera, 2013; Gashti et al. 2014a & 2014b). Gashti et al. [2014a] performed a 3D numerical simulation for heating/cooling operations of a ground heat exchanger incorporated within a steel pile foundation (energy pile). Their results indicated that an increase in the number of piping loops inside the energy pile is more efficient than increasing the diameter of the pipes themselves (double U-tube systems performed better than single U-tube systems). They showed that this improved performance ranged from 10% to 60% depending of the fluid flow rate. Zarrella et al. [2014] used the equivalent thermal resistance and capacitance circuit approach to model heat transfer in an energy pile. Their results showed that helical-pipe energy piles performed better thermally than the conventional U-tube configuration. In addition, they compared the performance of a standard double U-tube borehole heat exchanger with the modelled two energy pile configurations. As expected, the thermal performance of the double U-tube heat exchanger was found to be lower than both energy pile configurations (30% lower than the helical-pipe energy pile and 13% lower than the triple U-tube one).

The present study numerically investigated the performance of various heat exchanger configurations for a ground-loop system and then studied the performance of the configuration that is practically suitable in an energy pile setup.

2. NUMERICAL MODEL

The first part of the investigation was focused on the configuration of the ground-loop heat exchanger. In a typical setup, the ground heat transfer process occurs within four main components, which are (i) surrounding soil, (ii) grout, (iii) piping and (iv) heat transfer fluid. Bourne-Webb et al. (2009) measured temperature variation around an energy pile in London and found that, at locations only 0.5 m from the test pile, the temperature change induced in the soil was halved, and was negligible at 2 m from the test pile. In the present study, however, the heat transfer process through the soil was not considered since the focus of this study is on the heat transfer process inside the ground-loop heat exchanger. Thus, a wall temperature boundary condition was set on the outer grout wall to simulate the temperature of the surrounding soil. In order to approximately account for change in soil

temperature on the efficiency of considered configurations, an average soil temperature distribution was applied at the boundary i.e. soil-grout interface.

ANSYS Fluent version 14.0 was used to simulate the process. The governing equations comprised of the conservation of mass (Continuity equation) and the conservation of momentum (Navier-Stokes equations) are numerically solved along with the conservation of energy (Energy equation). The turbulence was modelled using the realizable k-ϵ turbulence model, where k is the turbulent kinetic energy and ϵ is the rate of turbulent kinetic energy dissipation. This model has also been utilized for vertical ground loop simulations by other researchers [Cvetkovski 2014; Congedo et al. 2014] with accurate results. As the present modelling domain contains a fluid/solid interface involving heat transfer, the solver simulated it as a conjugate heat transfer problem. The FLUENT solver computes the conduction of heat through solids, coupled with convective heat transfer in the fluid.

A critical component of any CFD simulation is the setting up of appropriate thermal and physical parameters on the physical boundaries of the model. The boundary type at the pipe outlet in the model was selected to be a pressure outlet boundary condition with turbulent intensity factor and hydraulic diameter variables identical to those considered for the inlet boundary conditions. The fluid adjacent walls were set as stationary with no-slip conditions. The external grout walls were set with a constant temperature boundary condition representing the temperature of the soil.

The Fluent solver selected for this model was the pressure-based solver, which is intended for low-speed incompressible flows [FLUENT 2010]. The segregated pressure-based scheme SIMPLE, Semi-Implicit Method for Pressure-Linked Equations, was used which utilizes the relationship between velocity and pressure corrections to impose the mass conservation (continuity) and find the pressure field. The convergence criterion was set at 10^{-3} for the continuity equation, 10^{-4} for the axial velocity, 10^{-4} for k and ε, and 10^{-5} for the energy (temperature) equation. The “Second Order Upwind” spatial discretization scheme used to evaluate pressure, momentum, turbulent kinetic energy, turbulent dissipation rate, and energy quantities. See Ramadan [2016] for more details about the numerical model.

A mesh dependency test was performed for four different mesh sizes were generated for the same borehole geometry, ranging from very coarse to very fine. The comparison parameter considered in the mesh dependency test was the outlet temperature of the heat transfer fluid, The percentage difference in the outlet temperature was less than 2% between the finest and the next (second finest) mesh, indicating that the finest mesh was independent of the mesh size, which was thus selected for simulations.

In order to ensure that the developed model correctly simulates the physical process, it must be validated against experimental results. A published experimental work for a vertical ground-loop heat exchanger installation in Elazig, Turkey by Esen et al. [2009] was used for model validation. Seven cases reported in the experimental study

were numerically simulated for validation. Three cases were in the winter (heating) season and four cases were in the summer (cooling) season. The results from experimental study and present numerical model (under steady conditions) are tabulated in Table 1. The comparison of the results show that the percentage difference between the numerical and experimental results ranged from 0.61% to 4.14% in the summer season and from 10.5% to 18.5% in the winter season. The high percentage difference in winter could possibly be attributed to experimental uncertainties. These include the placement position of the temperature sensor within flow streams, the recording intervals of the outlet temperature, and the temperature difference between the inlet and the grout wall (ground temperature), which is higher in summer (up to 25 ^{o}C) than in winter (up to 11 ^{o}C). Considering these uncertainties associated with experimental measurements, it is concluded that the present model correctly simulates the thermo-fluid process inside the ground loop.

Table 1: Fluid outlet temperatures under steady conditions obtained from the numerical model compared with the experimental results of Esen et al. [2009].

Case Number	Summer Season		Winter Seasons	
	Current Model	Experimental	Current Model	Experimental
1	32.44 ^{o}C	31.15 ^{o}C	6.4 ^{o}C	7.15 ^{o}C
2	36.37 ^{o}C	36.15 ^{o}C	7.46 ^{o}C	9.15 ^{o}C
3	38.26 ^{o}C	38.65 ^{o}C	9.19 ^{o}C	11.65 ^{o}C
4	40.42 ^{o}C	41.15 ^{o}C		

3. RESULTS

In the first part of the study, simulations were conducted for three configurations of the vertical ground-loop heat exchanger, which were: U-tube piping; concentric piping and spiral (helical) piping. The materials selected for the simulations were the ones commonly used in the field i.e. HDPE for piping, bentonite mixture for grout and propylene glycol mixture as the working fluid. The total length of the pipe was also kept the same (60 m) for all three cases. The only difference was the total depth for the spiral piping configuration due to its geometry which was much shorter, 10.22 m, than the other two piping configurations which were 30 metres deep each.

The materials selected for the simulations in the present case arecommonly used in the field. The piping was selected as High Density Polyethylene (HDPE), the grout was a bentonite mixture and the heat transfer fluid was a propylene glycol mixture with a dynamic viscosity of 0.0016 $\frac{kg}{m \cdot s}$. Table 2 shows the thermophysical properties of the materials used.

Table 2: Thermophysical properties of material used in simulation

Material	Density (kg/m^3)	Thermal conductivity (W/mK)	Specific heat (J/kgK)
HT Fluid	1017	0.475	3947
HDPE Piping	960	0.4	2170
Grout (Bentonite)	1540	1.7	2030

A summary of the simulation results of the three piping configurations is shown in Table 3. As the table shows, U-tube configuration yielded the highest heat transfer rate, which is about 60% and 25% higher than concentric and spiral configurations, respectively. The analysis of the fluid temperature data along the pipe length was also conducted to investigate the local temperature change. It is observed that although the concentric pipe has low temperatures throughout the length compared to the other two configurations, the rise in temperature per unit length in the annular section of the concentric pipe configuration was 35% and 26% higher than U-tube and spiral configurations, respectively. The overall low outlet temperature in the concentric pipe configuration is due to the low temperature rise per unit length in the middle pipe, which was almost 13% of the temperature rise per unit length in the annulus section.

Although the concentric piping configuration had the least heat transfer and fluid outlet temperature, it would have the least cost of installation among the three piping configurations if it is integrated in the piling foundation of a structure (energy piles). With energy piles, the cost of drilling is already anticipated under the foundation work, and the concentric piping is mainly required to be inserted inside drilled piles. Furthermore, in the conventional boreholes, HDPE is used as the piping material which has the thermal conductivity of 0.4W/m.K (Ye et al., 2006). Such low thermal conductivity increases the thermal resistance of the circuit and hence reduces the rate of heat transfer. Energy Piles are made of steel with the thermal conductivity of 50 W/m.K. If a concentric pipe configuration is carved into the Energy Pile and hence eliminating the need of HDPE, it is expected to increase the heat conductance and hence the heat transfer rate.

Table 3: Summary of simulation results for three different piping configurations

Piping Configuration	Inlet Temp (^oC)	Outlet Temp (^oC)	ΔT (^oC)	Heat Transferred to Fluid (kW)
U-Tube	8.00	9.19	1.19	1.98
Concentric	8.00	8.75	0.75	1.25
Spiral	8.00	8.95	0.95	1.58

The performance of a concentric pipe in an energy micro-pile was also simulated. A hollow-bar configuration for micro-pile was considered. In order for this micro-pile system to be simulated as an energy micro-pile, the following modifications and assumptions are considered:

1- The inside of the hollow bar will be considered not to be filled with grout (i.e. inside is to be flushed so the grouting is only around the outside of the micro-pile)
2- A smaller inner HDPE pipe is considered to be inserted and concentrically fitted inside of the hollow bar micro-pile to act as the conduit for carrying the down-flow heat transfer fluid.
3- The annular region created between the inner HDPE pipe and the outer threaded steel hollow-bar is the space where the up-flow heat transfer fluid flows and ultimately leaves the micro-pile at the top.

Figure 1 shows the top and the side view of this configuration along with the dimensions used in the simulation.

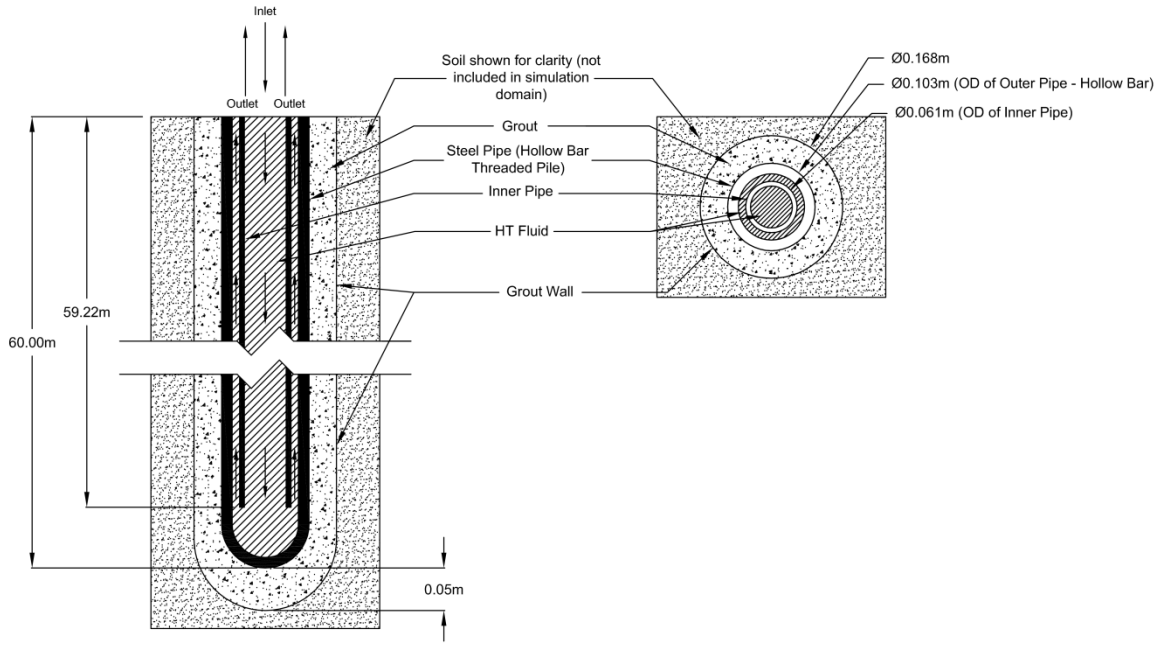


Figure 1: Top view and side view of energy micro-pile geometry domain used in simulation.

The threaded hollow bar dimensions and thicknesses were based on an actual product manufactured by Ischebeck (CTS/TITAN IBO Micropile). To further achieve a more realistic condition, the actual ground temperature profile was considered through the utilisation of a User Defined Function (UDF). Note that in the earlier cases, the ground temperature was considered to be constant over the entire depth. Available ground temperature data in South Western Ontario for depths of 60 m could only be obtained for the Goderich area from a previous Geophysical experimental study by Markle (2011).

This ground temperature profile was applied as the temperature boundary condition to the grouting wall in the simulation domain through a UDF. The same materials for heat transfer fluid and grout were used as described in Table 2.

Figure 2 shows the variation in the average fluid temperature under steady conditions at 10 m increments along the full length of the piping inside the energy micro-pile. The piping length was referenced from 0 m at the top of the inner pipe is considered at 0 m to 120 m at the top of the annular region (i.e. for a 60 m deep concentric geometry, the full length of the piping is 120 m).The temperature fluid shows two distinct regions of temperature increase. The first region, between 0 m and 60 m, represents the down-flow fluid temperature increase in the inner HDPE pipe while the second steeper region, between 60 m and 120 m, represents the up-flow fluid temperature increase in the annular region created between the threaded steel bar and the inner HDPE pipe. The temperature rise trend in both regions is semi-linear likely due to the varying ground temperature in the top 11 m (from 0 m to 11 m in for the fluid in the inner region and from 109 m to 120 m for the fluid in the annular region).

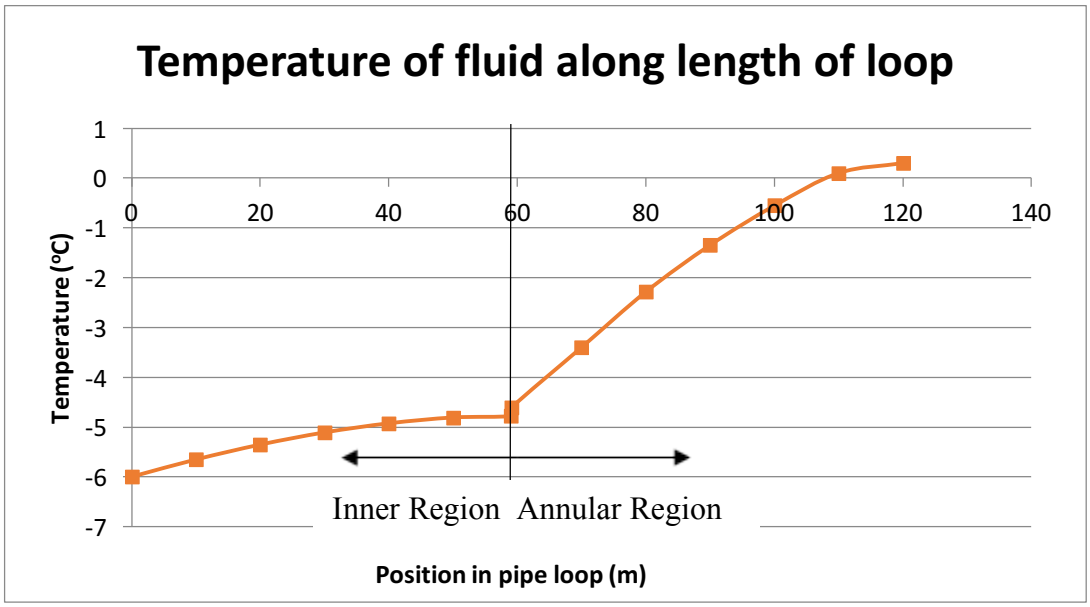


Figure 2: Temperature of fluid along full length of pipe

Table 4 shows the summary of the results for the energy micro-pile fitted with concentric piping. The total change in the temperature of the heat transfer fluid is 6.3°C and corresponding total heat gained by the fluid is 12.0 kW. The temperature increase and the heat transferred to the fluid inside the annular region were found to be 5.08°C and 9.68 kW, respectively, which is approximately 4.2 times more than the temperature increase and heat transferred to the inner HDPE pipe.

Table 4: Simulation results of energy micro-pile

Parameter	Value (Unit)
Inlet Temperature	-6.0^{o}C
Outlet Temperature	0.3^{o}C
Temperature Change in Fluid	6.3^{o}C
Total Heat Transferred	12.0 kW
Fluid Volume Flow Rate	0.000479 m^3/s (7.53 gpm)
Temperature Increase in inner region	1.22^{o}C
Heat Transferred in inner region	2.33 kW
Temperature Increase in annular region	5.08^{o}C
Heat Transferred in annular region	9.68 kW

4. CONCLUSIONS

A numerical study was conducted to simulate the heat exchange process in a vertical ground-loop heat exchanger. Three different configurations for the ground-loop heat exchanger were considered. The result show that the conventional U-tube configuration yields the highest fluid temperature rise i.e. highest heat transfer rate. Although the concentric tube configuration has overall low fluid temperature rise, it has the highest temperature rise per unit length in the annular section compared to U-tube and spiral configurations. Using the hollow bar as reinforcing element for micropiles can provide an element of the concentric tube configuration and hence can reduce cost. This should be considered in further investigation of employing the concentric tube configuration in energy piles applications. A second set of simulation was conducted by integrating a concentric pipe in an energy pile. The results show two distinct regions of temperature increase. In the inner pipe representing the down flow, the fluid temperature rise was lower than that in the annular region. The temperature rise trend in both regions is semi-linear likely due to the varying ground temperature. Further investigation should account for change in soil temperature.

5. REFERENCES

Abdelaziz, SL. (2010). Utilization of micropiles for heat exchangers. IWM International Workshop on Micropiles, September 22-25 2010. Washington D.C.

Bourne-Webb, P. J., Amataya, B., Soga, K., Amis, T., Davidson, C., and Payne, P. (2009). Geotechnique, 59, No. 3, 237–248 [doi: 10.1680/geot.2009.59.3.237]

Cervera, C.P. (2013). Ground thermal modelling and analysis of energy pile foundations. Master's Thesis. Espoo: Aalto University.

Rantamäki, M., Jääskeläinen, R., Tammirinne, M. (2009). *Geotekniikka* [Geotechnic]. 22. edition. Hakapaino Oy, Helsinki. Finland.

Congedo, P., Lorusso, C., Giorgi, M. D., & Laforgia, D. (2014). Computational Fluid Dynamic Modeling of Horizontal Air-Ground Heat Exchangers (HAGHE) for HVAC Systems. *Energies, 7*(12), 8465-8482.

Cvetkovski, C. (2014). Modelling of Flow and Heat Transport in Vertical Loop Ground Heat Exchangers. *ProQuest Dissertations Publishing.*

Esen, H., & Inalli, M. (2009). In-situ thermal response test for ground source heat pump system in elazığ, turkey. *Energy & Buildings, 41*(4), 395-401.

Fluent 13 Documentation (2010), Fluent Inc.

Gashti, E. H., Uotinen, V., & Kujala, K. (2014a). Numerical modelling of thermal regimes in steel energy pile foundations: A case study. *Energy and Buildings*, 69, 165-174.

Gashti, E.H.N., Malaska, M. & Kujala, K. (2014b). Structural Behaviour of Concrete Energy Piles in Thermal Loadings. World Academy of Science, Engineering and Technology, International Journal of Civil, Architectural, Structural and Construction Engineering Vol:8 No:12, 2014.

Markle, J. M. (2011). Thermal Plume Transport From Sand and Gravel Pits Potential Thermal Impacts on Cool-Water Streams. PhD thesis, University of Western Ontario.

Ma, X. & Grabe, J. (2009). Influence of Groundwater Flow on Efficiency of Energy Piles. Darmstadt Geotechnics No. 18. International Conference on Deep Foundations – CPRF and Energy Piles. 15.5.2009. Frankfurt am Main. Institute and Laboratory of Geotechnics, Darmstadt, Germany.

Ramadan, A. S. (2016). Parametric study of vertical ground loop heat exchangers for ground source heat pump systems. MESc thesis, University of Western Ontario

Suryatriyastuti, M. E., Mroueh, H., & Burlon, S. (2012). Understanding the temperature-induced mechanical behaviour of energy pile foundations. *Renewable and Sustainable Energy Reviews*, 16(5), 3344-3354. doi:10.1016/j.rser.2012.02.062

Williams, G. P.; Gold, L. W. (1976). CBD-180. Ground Temperatures. *Canadian Building Digest, National Research Council Canada*.

Ye, C-M, Shentu, B-Q. and Weng, Z-X. (2006). Thermal conductivity of high density polyethylene filled with graphite. Journal of Applied Polymer Science, Vol. 101, 3806–3810.

Zarrella, A., De Carli, M., & Galgaro, A. (2014). Thermal performance of two types of energy foundation pile: Helical pipe and triple U-tube. *Applied Thermal Engineering*, 61(2), 301-310. doi:10.1016/j.applthermaleng.2013.08.011

PERFORMANCE OF SOCKETED MICROPILES IN WEAK SOILS

Ahmed A. Al-Obaidi[1], Ansam A. Al-Karawi[2]

ABSTRACT

Micropiles are small diameter, cast-in-place replacement piles which are ideal for building foundations on sites with poor ground conditions and they are well suited for foundation underpinning, and increasing the capacity of existing foundations via transfer the loads from weaker strata to strong deeper strata.

Building No.12 – Internal Dormitories for Women at Tikrit University are two stories, constructed as bearing wall system. After a period of operation, several aggressive cracks had been found in the superstructure due to excessive foundation settlement. The borings for site investigation and geophysical exploration revealed that the building was constructed on weak gypseous Silty Sand layer extended more than 6m. This layer exhibited a large collapse when it exposed to water.

In this research, the performance of micropiles grouted by gravity Type (A) embedded in weak soils and socketed in the strong soil are investigated. The micropiles are simulated in ABAQUS/CAE program with different length and diameters ranged from 5m to 20m and 0.1m to 0.3m respectively, embedded in weak soil and penetrate the strong layer with proportions of their total length. The parameters that affect the ultimate capacity of the micropile foundation represented by the effect of socketed lengths in dense soil were investigated. The main results show that for long micropiles Type A socketed in dense layer, the load-settlement curve has no vertical tangent and there is no defend failure load and its ultimate capacity ratio increased with (1.029) to (1.487) as compare with these resting on dense soil. It has been found that micropiles with diameter 0.2m socketed 20% of their length in dense soil distance 2m c/c spacing is recommended for rehabilitation which can transfer the building load to the strong layer. Also, these micropiles can densify the surrounded soil.

INTRODUCTION

Numerous literature had been cited about the damage to structures in the world and are commonly related to soil characteristics, as a result of the circumstances of its composition or a change in environmental conditions causing the most problems

Many large land areas have been founded with transported soils which deposited primarily by one of the transportation methods and may be considered as weak soil. Also, the weak soil may be human-made soil, like bad filling or accumulated debris. Weak soil can initiate many geotechnical difficulties including inadequate bearing capacity, the potential for unacceptable settlements, (Slocombe, 2001).

The building No.12 is one of the building group at the internal dormitories for women in the campus of Tikrit University. Over time, several problems appear such as aggressive cracks in the superstructure and settlement. The cracks found in the southwest part of the building, the cracks were diagonal and horizontal (plate1), the settlement noted in the walkway around the building and the street behind the building, plate (2). Moreover, a cap of 10mm was found between the wall footing and the compacted sub-base as shown in Plate (3-a), besides several cracks in the footings also observed, (plate 3-b).

Assist. Prof. Civil Eng. Dept. Tikrit Univ. /Iraq +9647705357999 dr.obaidi.a.h@tu.edu.iq
M.Sc. Civil Eng. Dept. Cihan Univ. /Iraq +9647903869919 civileng88_2010@yahoo.com

From field and geophysical investigation, it seems that the building rests on the bad filling material, where there are a weak soil and cavities under the foundation of this building which leads to differential settlement.

Despite the availability of many methods for rehabilitation and restoration of buildings foundation, such as soil replacement, soil densification or reinforcement the soil with geosynthetic material or grouting. Comparison of these methods led to conclude that the use of micropiles is the best methods to underpinning this building for further use since this method reduced the demolitions and reconstruction.

In this paper micropiles Type (A) are simulated in ABAQUS/CAE program with different lengths and diameters embedded in weak soil and resting on and penetrate the strong soil. The results give an estimation of micropile capacity and the load distribution through the micropile length. Also, the connected method and distribution along the foundation are presented.



Plate 1. Cracks in building No.12



Plate 2. Settlement in Walkway and street around the building

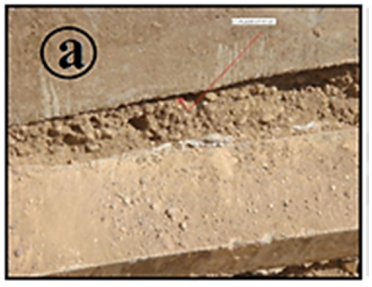




Plate 3. (a) A gap between compacted soil and foundation, b) Cracks in footings

BUILDING LOCATION AND SOIL DESCRIPTION

The building is located in Salah El Deen Province at the North of Iraq, inside the campus of Tikrit University. The general topography of the site is flat with waved elevation at the south sides of the property. The project consists of (17) buildings. These buildings are two stories and constructed as bearing wall system carried by 1.5m width wall footing reinforced with 16-ϕ16mm longitudinal reinforcement and ϕ12mm at 200mm c/c ties.

Two types of soil investigation were conducted, Geophysical and field exploration, (as shown in figure 1) Besides laboratory testing on extruded samples.

The geophysical investigation (cross-hole test) revealed an existing of a weak zone detected at depths from (2m) to (6m) under the building, this weak zone consists of fill material with bad compaction i.e. soil in relatively loose to medium state (SPT values in the range of (8 to 20) and the results obtained from the laboratory tests

indicated that the soil properties with cohesion c' = 0 and friction angle can be taken as ϕ' = 25°- 32° and the bulk density (γ_b) is in the range of (15-17) kN/m^3. The soil stratification and soil properties are shown in Figures (2) and (3) and Table (1) respectively.

GENERAL VIEW ON MICROPILES

Micropiles are small-diameter piles (typically less than 300 mm), constructed by drilling a borehole, placing a steel reinforcing element into the borehole and grouting the borehole. The grout is placed by gravity, under pressure methods or by a combination of both (post grouting). The drilling and grouting method used in micropile installation allow for high grout/ground bond value along the interface, FHWA (1997). Micropiles are ideal for building foundations on sites with poor ground conditions, sensitive surroundings, restricted vertical clearance, or difficult access. They are also well suited for foundation underpinning, arresting ground movements, and increasing the capacity of existing foundations, Richards, and Kartofilis (2006). Due to the small size of installation equipment, micropiles can be installed in very limited head room with access-restrictive environments

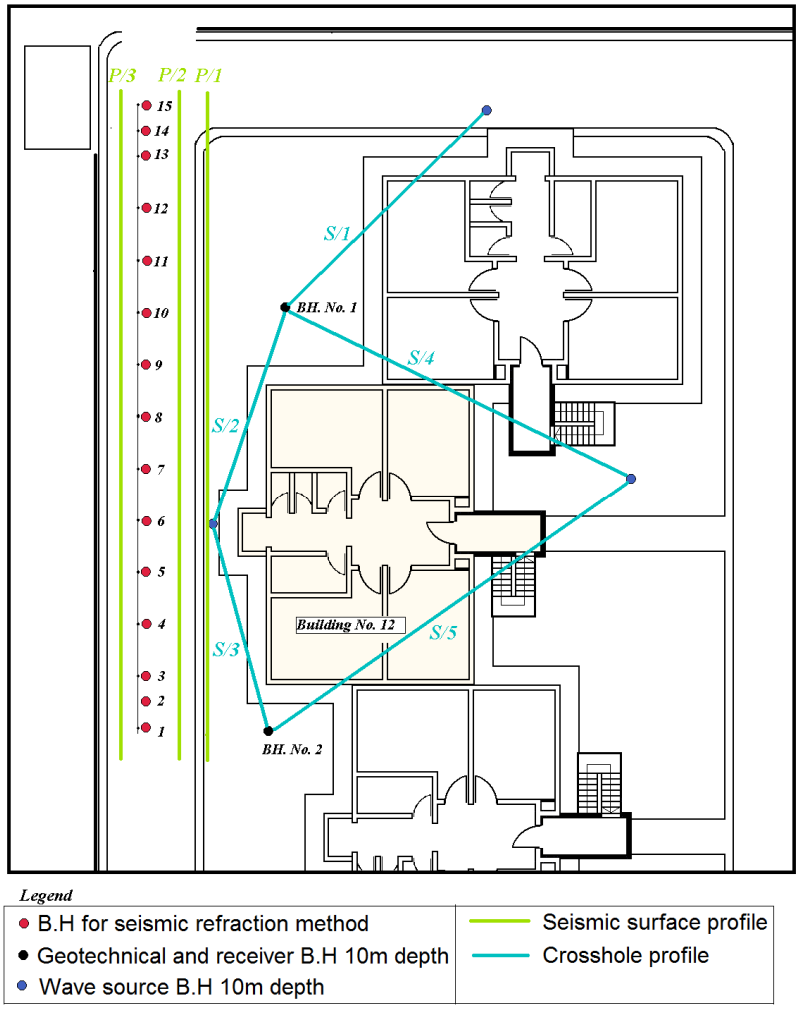


Figure 1. Site plan showing surface and cross-hole seismic profiles, and boreholes locations, (after Al-Obaidi, 2012)

These advantages combined make the micropiles, in some situations, not only the optimum deep foundation solution, but the only feasible one Tomlinson, and Woodward (2008). In the design application, there are two general types of application. The first type is CASE 1, where the micropile is directly loaded either axially or laterally, and the pile reinforcement resists the majority of the applied load. The second type of design application is CASE 2, where the micropile reinforces the soil to make a reinforced soil composite that resists the applied load and known as reticulated pile network. In the method of grouting, the micropiles classified as (Type A, Type B, Type C and Type D) is generally the most sensitive construction control over grout/ground bond capacity and varies directly with the grouting method, Shong, and Chung (2003).

Lizzi, (1985) providing the following simple empirical formula to quantify the ultimate load of micropiles P_{ult} (Kg):

$$P_{ult} = \pi * D * L * K * I$$

Where D; is the nominal diameter (in cm) of the pile, i.e. the drilling diameter, L; is the length of the pile (in cm), and K and I are coefficient depending on pile diameter and soil type.

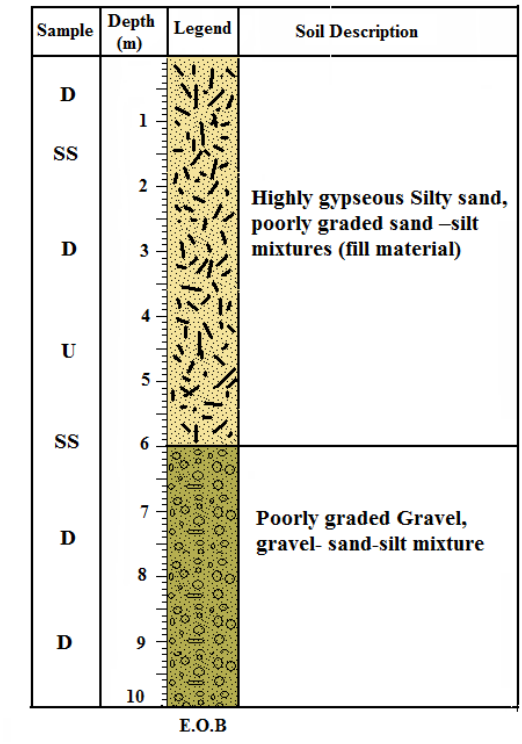


Figure 2. Soil stratification at BH. No. (1)

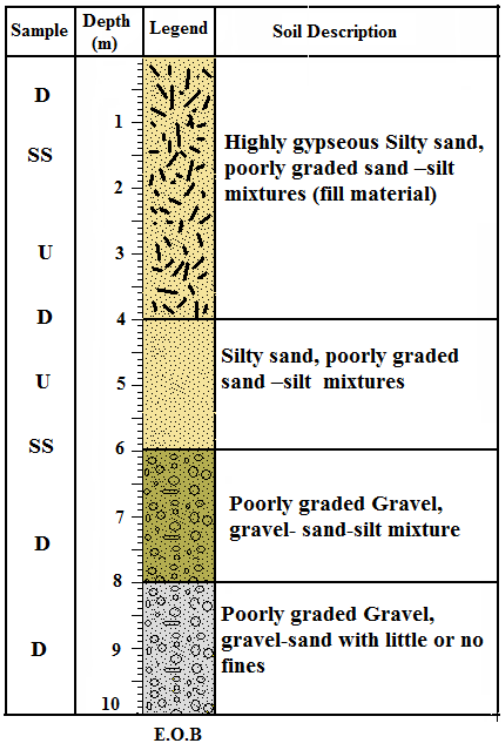


Figure 3. Soil stratification at BH. No. (2)

Table 1.soil properties at different depth

Angle of lateral friction, φº	Density Description	Unit Weight, γ, kN/m^3	Modulus Elasticity of soil, E, kN/m^2	Poisson's ratio, μ
25	Loose	15.4	25300	0.3
31	Medium	16.1	36500	0.3
35	Dense	17.0	48100	0.32
40	Very Dense	18.7	78000	0.35

(FHWA, 2005 and AASHTO LRFD, 2012) found that the nominal factor of safety on ultimate bond value varies typically from 2 to 2.5 and the allowable geotechnical bond capacity, PG-allowable is calculated as:

$$\text{PG-allowable} = \frac{\alpha\ bond}{FS}\ \pi * D * L_b$$

Where: $\alpha\ bond$ = grout to ground ultimate bond strength, FS = factor of safety applied to the ultimate bond strength, and L_b= bond length. Also general equations for calculation of ultimate bored piles can be used.

GEOMETRY MODEL AND NUMERICAL ANALYSIS

A Numerical model for micropiles Type (A) (gravity grouted) is adopted. A general finite element program (ABAQUS) was selected for the numerical analysis method to simulate the micropiles in weak soil and generate the solution.

The research focuses on micropile case one under axial loading with the following situations, (Figure 4):

1- Modeling of micropiles Type (A) embedded in weak soil and rest on strong soil
2- Modeling of micropiles Type (A) embedded in weak soil and socketed in the strong soil.

The micropiles Type (A) are simulated with different lengths (5, 10, 15, 20m) and diameters (0.1, 0.2, 0.3m) respectively, rest on strong soil and embedded in the weak soil. The socketed micropiles are penetrated the strong layer soil with different proportions of their total length. This portion defined as socketed lengths, (L_S). The socketed length equal to 5%, 10%, 15% and 20 % respectively from the total length.

In this work two parts used to simulate the soil-micropile system and the model is created with axisymmetric, deformable body with a shell, base feature. The soil layer extends in the lateral direction by a range equal (10.5 D), D, is the diameter of micropiles from the center of micropiles, and in the vertical direction arranged equal to (L+10D), L, the length of micropile.

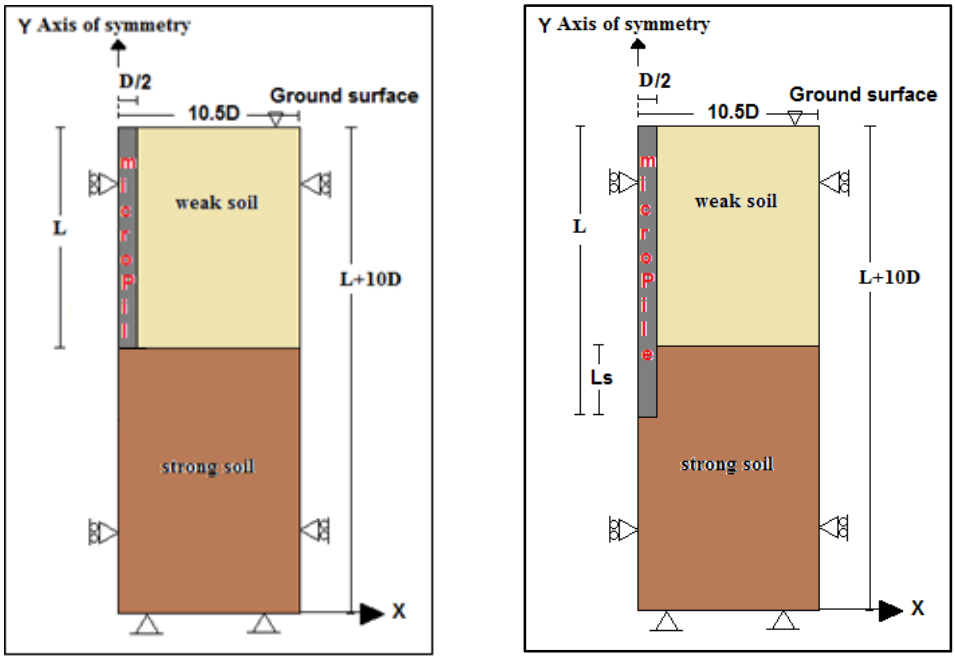


Figure 4. Micropile (a) on strong soil (Case 1), (b) socketed in strong soil (Case 2)

The boundary conditions assumed to be hinged at the end of the lower soil to prevent the horizontal and vertical movements, a roller inside of soils to allow a vertical movement and prevent horizontal movement, and symmetry/antisymmetry / ancastre for the micropile's side. Elasto-perfectly plastic model with Mohr- Coulomb failure criterion, usually named as Mohr-Coulomb model, is used in finite element analysis of geotechnical engineering, Salgado et al. (2007).

The weak soil properties are selected as cohesionless soil with parameters as shown in Table (1). The material of the micropile foundation supposed to be cement grouting, represented by the linear elastic model, Wang, and Sitar (2004). The value of the modulus of elasticity for the micropile is (14.2 GPa) according to Veludo et al. (2012), the Poisson's ratio is assumed to be 0.2, and unit weight is 24 kN/m^3.

The steps must be used to analyze the behavior of a single pile embedded in weak soil include initial, geostatic and loading steps. All the parts of the model are modeled using the Second-order continuum axisymmetric element (CAX4) with reduced order numerical integration available in ABAQUS (6.11). A relatively fine mesh was used near the micropile soil interface and the pile toe, and become coarser farther from the pile, a surface to surface contact formulation, where a second-order element CAX8 used to predict the capacity of pile foundation.

ULTIMATE CAPACITY OF MICROPILES TYPE (A) SOCKETED IN DENSE SOIL

Since this study focused on micropiles embedded in weak soil and hence the settlement must be controlled. Thus the method adopted by FHWA (2005) was selected to use for the load –settlement curve and to calculate the ultimate capacity

The effect of socketed lengths on the ultimate capacity of micropile is drowned and shown in Figures (5) and (6). These figures are chosen to be typical for all cases studied. The trend of curves in these figures revealed an increasing in the ultimate capacity of micropile with the increasing of the socketed length. Also, the ultimate capacity of micropiles embedded in different soil properties (different values of soil friction) appears to be drawn near and seems to be reached a limit value. This is true, where all soil around the micropile became dense. Thus, limiting the maximum socketed length not more 20% of the total micropile length will economically benefit.

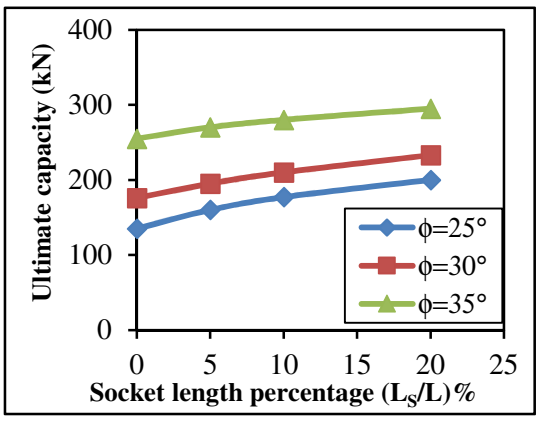


Figure (5). Ultimate micropile capacity versus Socket length % for different soil friction and constatnt diameter, D=0.1m and length,L =5m

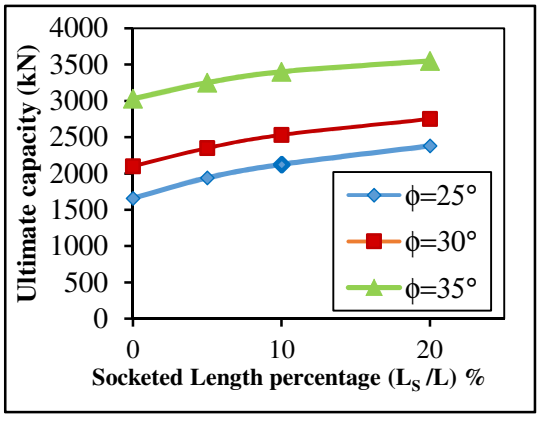


Figure (6). Ultimate micropile capacity versus Socket length % for different soil friction and constatnt diameter, D=0.3m and length,L=20m

ULTIMATE CAPACITY RATIO OF SOCKETED MICROPILES

To understand the effect of socketed length in dense soil on micropile ultimate capacity, it is preferable to use the term *Ultimate capacity ratio* $(U.C.R)_{Ls}$ which refer to the ultimate capacity of micropile socketed in the dense soil to an ultimate capacity of micropile rested on the dense soil. Figures (7) to (18) show the relationship between the $(U.C.R)_{Ls}$ and the socketed length percentage (L_S/L) % for different micropile lengths, diameter, and angle of soil friction.

The effect of angle of internal friction of soil is very clear on the ultimate capacity ratio $(U.C.R)_{Ls}$ with increasing of L_S/L% where increase the friction angle decreases the increment of ultimate capacity ratio $(U.C.R)_{Ls}$, this behavior take place because the properties of the soil around the micropile and the part that socketed became closed. Thus socketed the micropile embedded in medium soil into dense soil may be not recommended. The ultimate capacity ratio range from (1.029) to (1.487) for all micropile lengths, longest micropile give grater ultimate capacity ratio because of the socketed length larger as taken in percentage.

Review the results of socketed micropiles, indicated that the effect of micropile diameter is little on the ultimate capacity ratio $(U.C.R)_{Ls}$.

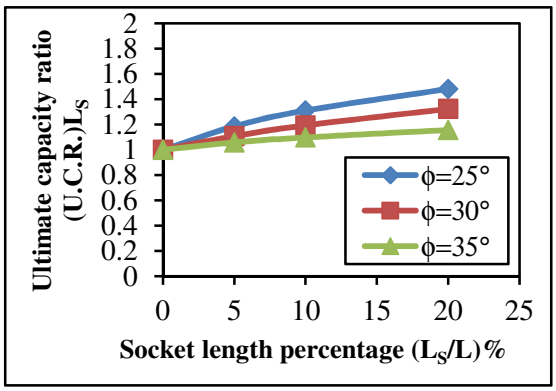


Figure 7.Ultimate capacity ratio versus Socket length % for different soil friction and constant diameter, D=0.1m and length, L =5m

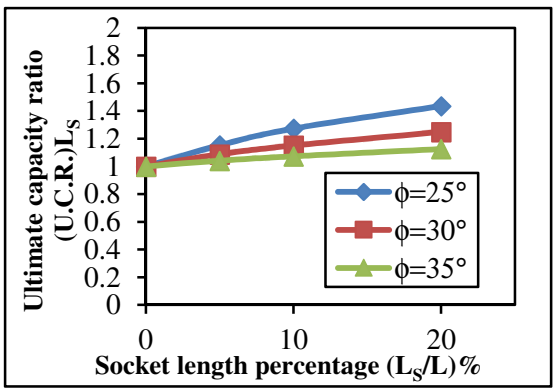


Figure 8. Ultimate capacity ratio versus Socket length % for different soil friction and constatnt diameter, D=0.1m and length,L =10m

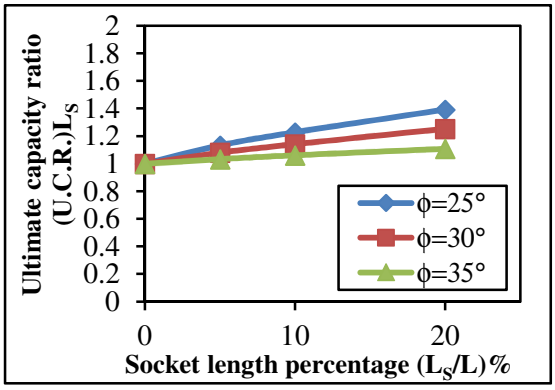


Figure 9. Ultimate capacity ratio versus Socket length % for different soil friction and constatnt diameter, D=0.1m and length,L =15m

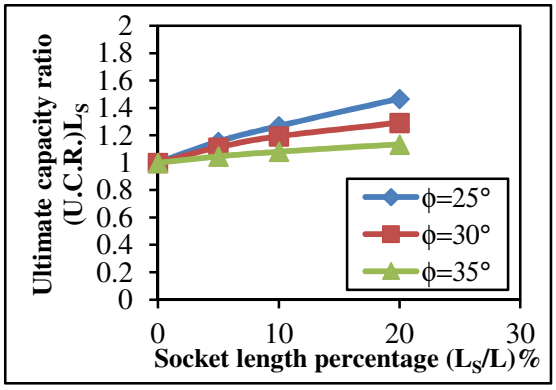


Figure 10.Ultimate capacity ratio versus Socket length % for different soil friction and constant diameter, D=0.1m and length, L =20m

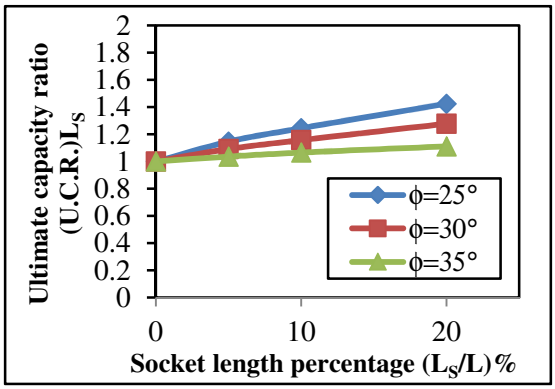


Figure 11. Ultimate capacity ratio versus Socket length % for different soil friction and constant diameter, D=0.2m and length, L =5m

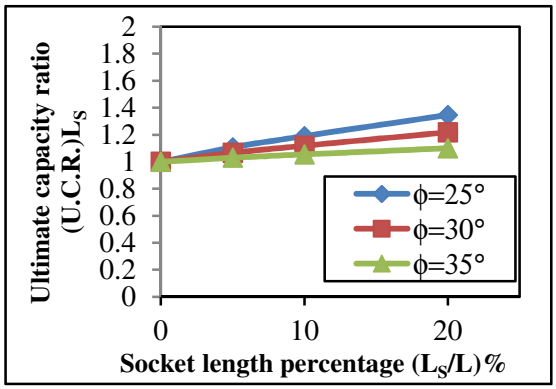


Figure 12. Ultimate capacity ratio versus Socket length % for different soil friction and constant diameter, D=0.2m and length, L =10m

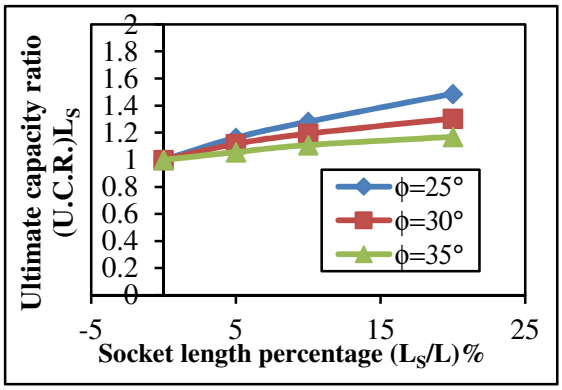


Figure 13. Ultimate capacity ratio versus Socket length % for different soil friction and constatnt diameter, D=0.2m and length,L =15m

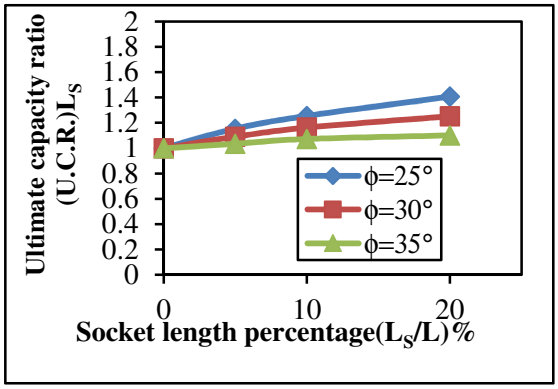


Figure 14. Ultimate capacity ratio versus Socket length % for different soil friction and constant diameter, D=0.2m and length, L =20m

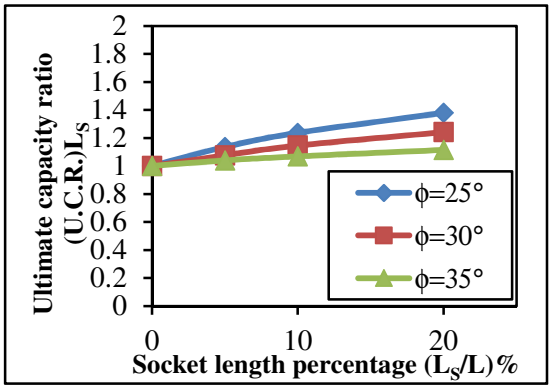


Figure 15. Ultimate capacity ratio versus Socket length % for different soil friction and constant diameter, D=0.3m and length, L =5m

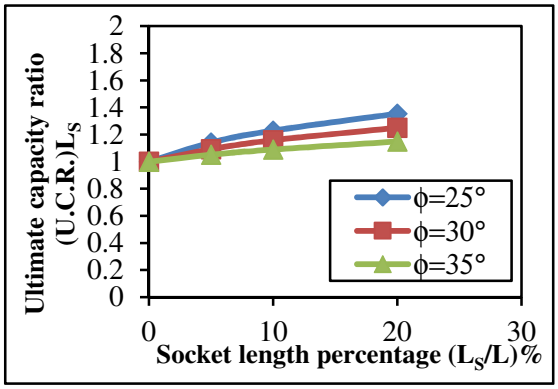


Figure 16. Ultimate capacity ratio versus Socket length % for different soil friction and constant diameter, D=0.3m and length, L =10m

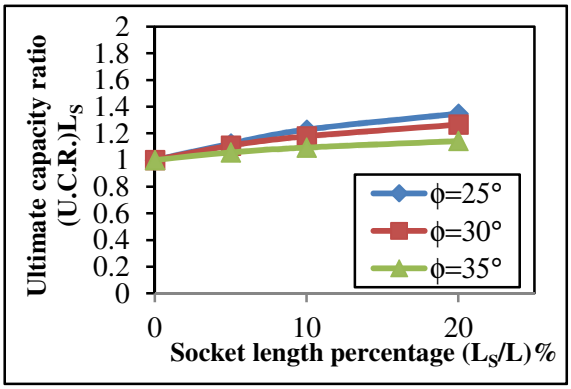


Figure 17. Ultimate capacity ratio versus Socket length % for different soil friction and constant diameter, D=0.3m and length, L =15m

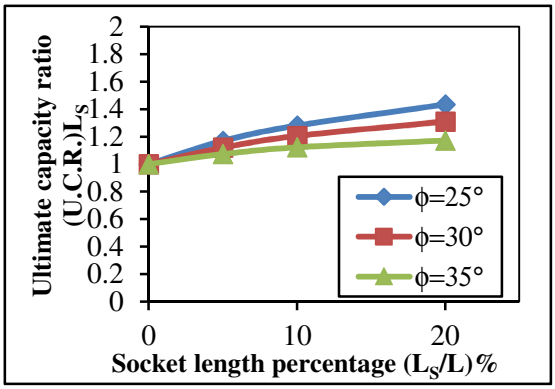


Figure 18. Ultimate capacity ratio versus Socket length % for different soil friction and constant diameter, D=0.3m and length, L =20m

LOAD TRANSFER THROUGH SOIL FOR MICROPILES TYPE (A) SOCKETED IN DENSE LAYER

Figure (19) shows the load transfer to the soil surrounded the micropiles in steps as obtained from the results of ABAQUS program. After loading the micropile, the loads transfer to the weak soil at the upper part and may be fully mobilized, then the load transfer to deeper layers and also transfer to the dense layer socketed the micropile in it. Before the failure, it seems that all the soil surrounded the micropile i.e. weak and dense soil are fully mobilized but the end bearing is not fully mobilized.

CONCLUSIONS

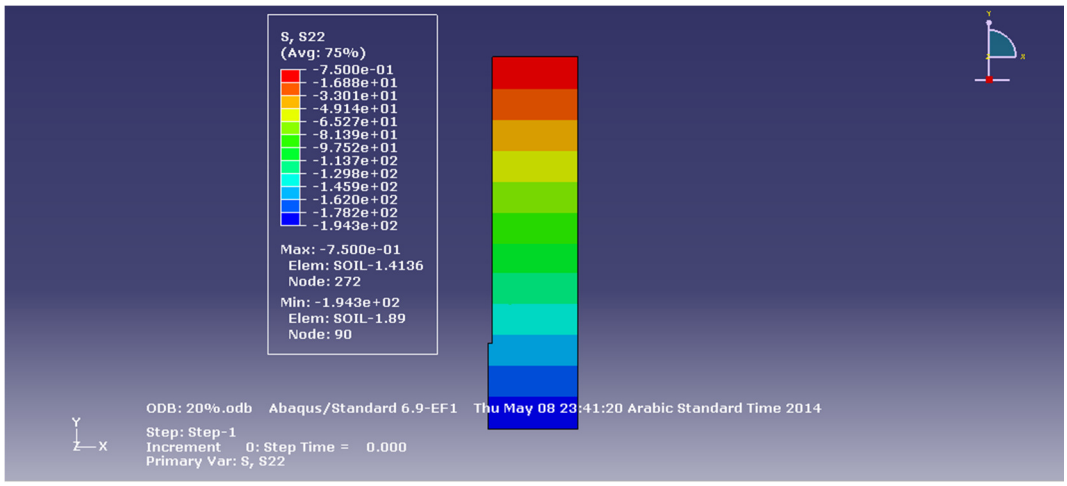
The present work provided a general review of the behavior of micropile foundation with a theoretical assessment of micropile design procedures and applications. A numerical model is developed to evaluate the ultimate capacity of micropiles embedded in the weak soil. The model is conducted using finite element method through the use of software program ABAQUS.

Based on the findings from the resulted, it can be concluded that the finite element model developed for micropile embedded in weak soil presented in this study provides to be a vital numerical model for the problem stated. Micropiles Type (A), Type (A) socketed in the dense layer can be simulated in ABAQUS program. As the micropile socketed into the dense soil, its ultimate capacity increased with percentage range between 10 to 15 as compared with these resting on dense soil.

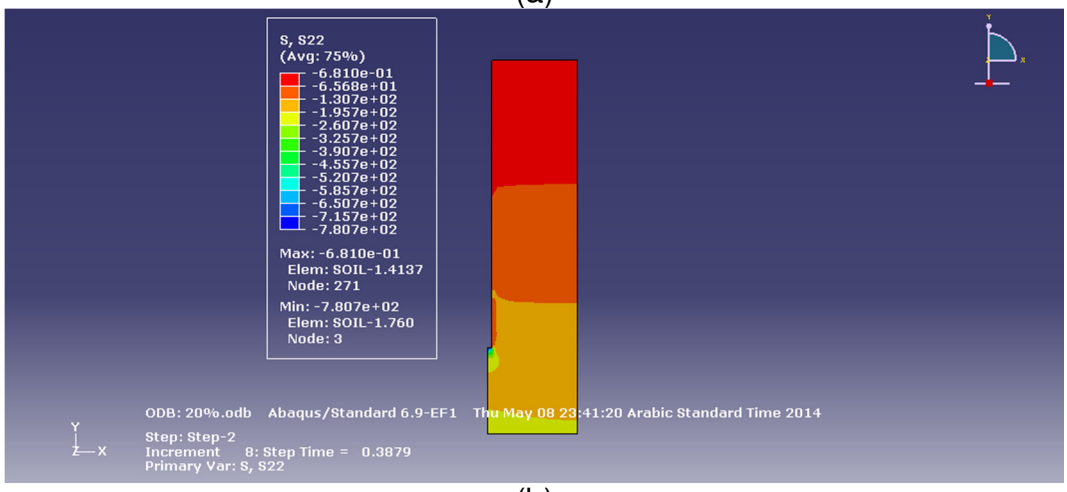
The end bearing for socketed micropiles is not fully mobilized since the most of the load carried by the skin friction. The end bearing, in this case, can be ignored, especially for small diameter and a short length. The angle of internal friction of soil has a great effect on the ultimate capacity ratio $(U.C.R)_{Ls}$, where increase the friction angle decreases the increment of the ultimate capacity ratio $(U.C.R)_{Ls}$. Thus socketed the micropile embedded in medium soil into dense soil may be not recommended.

The ultimate capacity ratio for micropiles socketed in dense layer range from (1.029) to (1.487) for all micropile lengths, longest micropile gives grater ultimate capacity ratio, in contrast; micropile diameter has a little effect on the ultimate capacity ratio $(U.C.R)_{Ls}$.

Finally, micropiles with diameter 0.2m socketed 20% of their length in dense soil distance 2m c/c spacing is recommended for rehabilitation which can transfer the building load to the strong layer, as shown in Figure (20). Also, these micropiles can densify the surrounded soil.



(a)



(b)

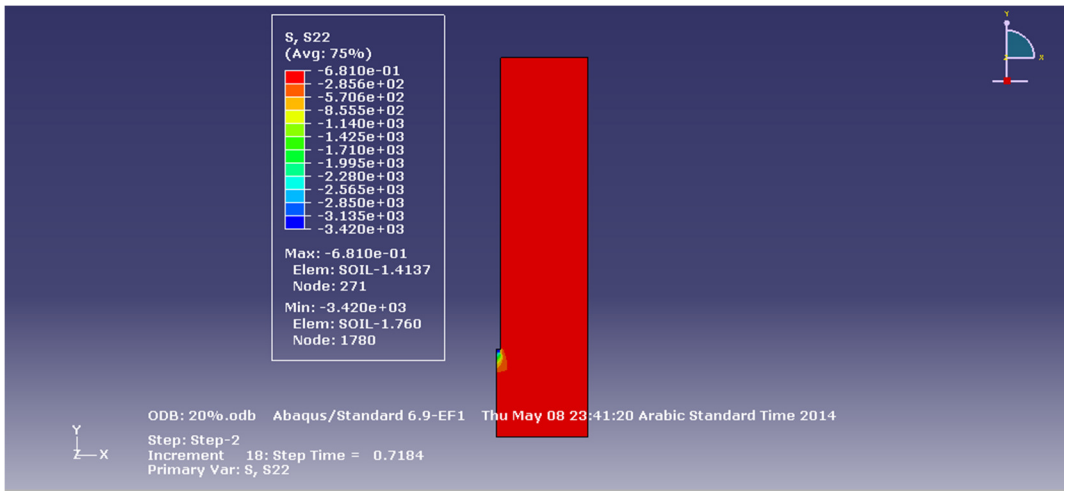
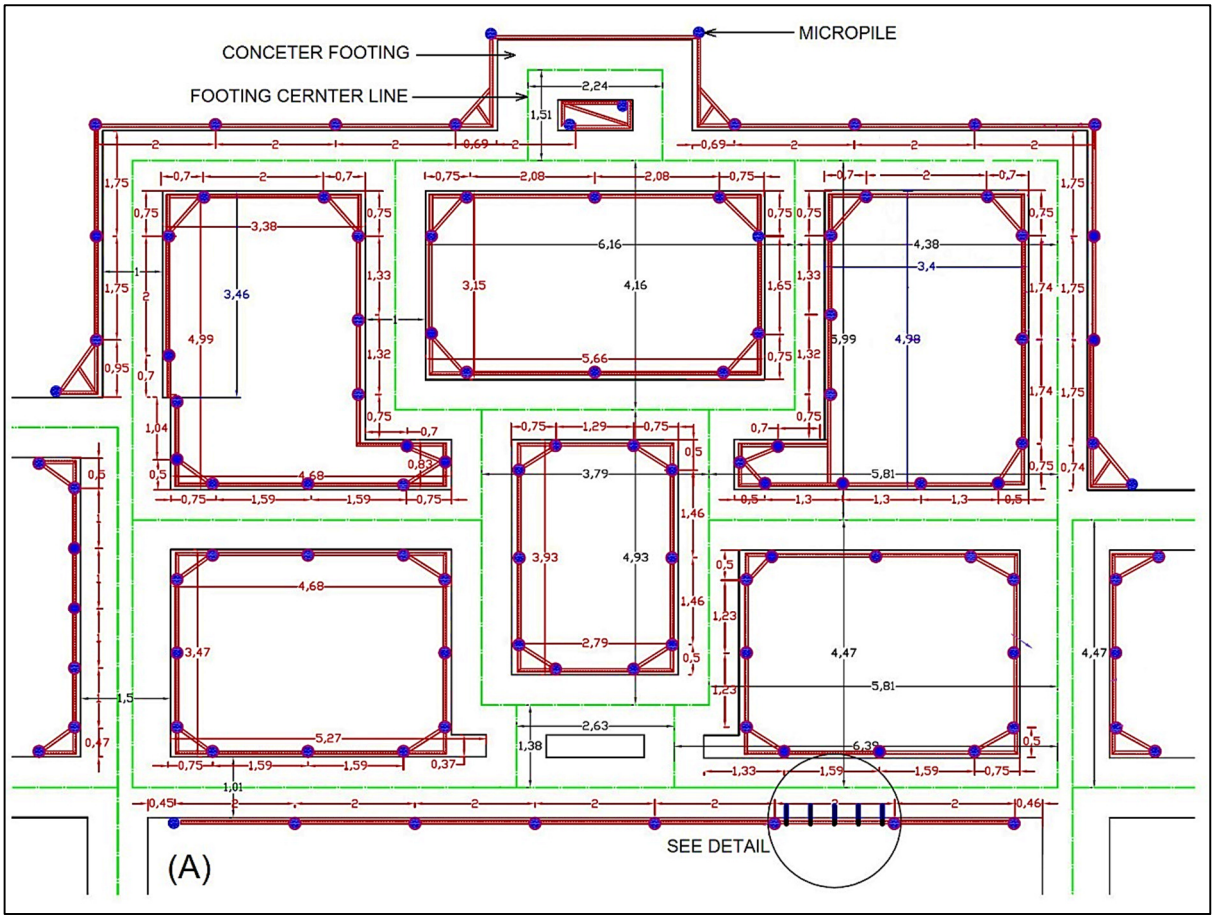


Figure 19. Load transfer for micropile socketed in dense soil, (a) geostatic condition, (b) part of load applied, (c) before failure



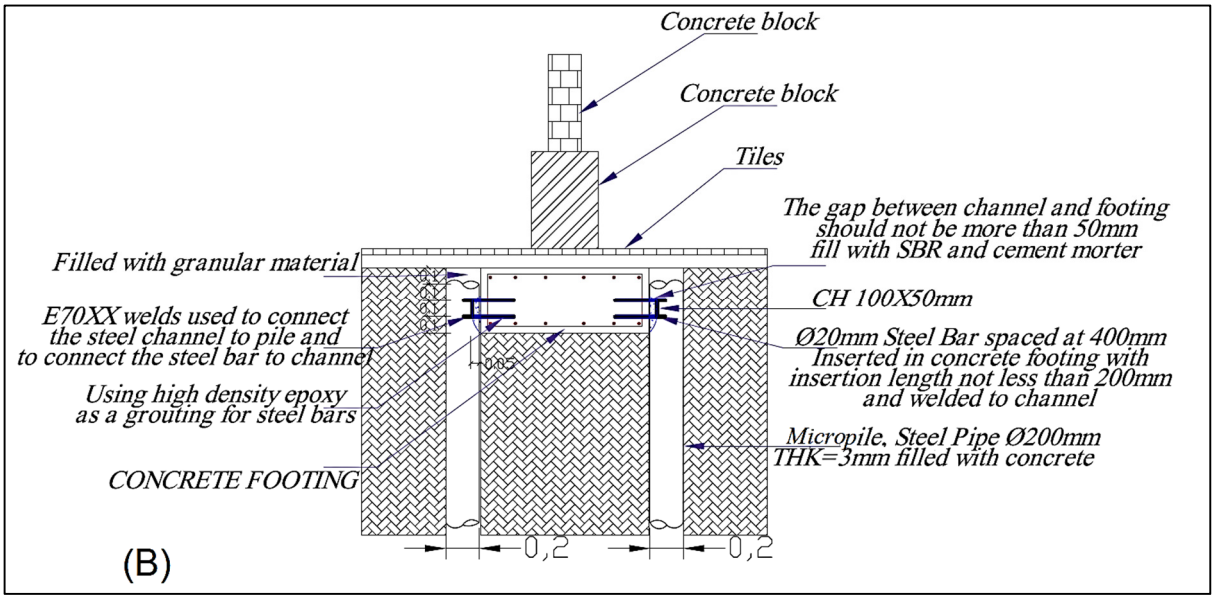


Figure 20: (A) Underpinning arrangement for building (B) Micropile-existing foundation connection

REFERENCES

- AASHTO LRFD (2012), *Bridge Design Specification*, American Association of State Highway and Transportation Officials, Washington, DC.
- ABAQUS Theory Manual (2011), Version 6.11, Hibbitt, Karlsson, and Sorenson, Inc.
- Al-Karawi, A. A, (2014), *Performance of Micropiles in Weak Soil*, MSc thesis, College of Engineering, Tikrit University.
- Al-Obaidi A.H. (2012), *Remedying of Building No. 12 Internal Dormitories for Women Tikrit University*. Report submitted to Engineering Consulting Bureau, Tikrit University, 68P
- FHWA (1997), *Drilled and Grouted Micropile*, *State-of-Practice Review*, Bruce, D.A. and Juran, I., Report No. FHWA-RD-96-016, 017,018 and 019.
- FHWA (2005), *Micropiles Design and Construction Reference Manual*, Sabatini, P.J., Tanya, B., Armour, T., Groneck, P. and Keely, J., Report No. FHWA-NHI-05-039.
- Lizzi, F. (1985), *Pali radice 'root piles' and 'Reticulated Pali Radice*, In Underpinning, Edited by Thorburn, S. and Hutchison, J.F., Surrey University Press, Blackie and Son, Ltd, London.
- Richards, T.D., and Kartofilis, D. (2006), *Micropiles Underpinning of the Mandalay Bay Hotel and Casino*, 45th Annual Geotechnical Engineering Conference, St. Paul, Minnesota, pp: 1-8
- Salgado, S., Prezzi, M. and Seo, H. (2007), *Advanced Modeling Tools for the Analysis of Axially Loaded Piles*, Advances in Deep Foundation, International Workshop on Recent Advanced of Deep Foundations (IWDPF07), Port and Airport Research Institute, Yokosuka, Japan.
- Shong, L.S., and Chung, F.C. (2003), *Design and Construction of Micropiles*, Geotechnical Course for Pile Foundation Design and Construction, pp: 1-49.
- Slocombe, B.C., (2001), *Deep Compaction of Problematic Soils*, Problematic Soils, Thomas Telford (London), pp: 163-181.
- Tomlinson, M. and Woodward, J. (2008), *Pile Design and Construction Practice*, Fifth Edition, Taylor and Francis, New York, 551p.
- Wang, G. and Sitar N. (2004), *Numerical Analysis of Piles in Elasto- Plastic Soils under Axial Loading*, 17th ASCE Engineering Mechanics Conference, University of Delaware, Newark, pp: 8-14.
- Veludo, J., Julio, E.N.B.S. and Dias-da-Costa, D. (2012), *Compressive Strength of Micropile-to-Grout Connection*, Construction and Building Material, vol.26, pp: 172-179.

MICROPILE FOUNDATIONS FOR RECONSTRUCTION OF HISTORIC LA LOMA BRIDGE IN PASADENA, CALIFORNIA

Casey Garneau[1]

ABSTRACT:

The historic La Loma Bridge, which crosses the Arroyo Seco in Pasadena, California, was built in 1914 to replace the 1898 California Street Bridge. The bridge is an open spandrel concrete arch bridge with a neoclassical design, which draws inspiration from Greek and Roman architectural design features with Renaissance interpretations of the classical forms. Inspired by the City Beautiful Movement, the bridge was built in response to the advent of the automobile and the increase in population in the surrounding areas.

Built just a year after, the La Loma Bridge, pictured in Figure 1, displays similarities of its “big sister”, Pasadena’s famous Colorado Street Bridge, nicknamed “Suicide Bridge”, which spans the Arroyo Seco less than a mile away. While the Colorado Street bridge connected Pasadena to Los Angeles, the La Loma Bridge played a substantial part in Pasadena’s development of the west side of the Arroyo, largely called San Rafael Heights, which was annexed by the City of Pasadena by the completion of this bridge. For several years, the two bridges were the only crossings over the Lower Arroyo and represent the city’s economic and physical need to facilitate automobile traffic over the Arroyo, while also providing impressive picturesque structures for the nearby communities.



Figure 1 – Original La Loma Bridge

[1] Project Manager, Malcolm Drilling Co., Inc., 4926 North Azusa Canyon Rd., Irwindale, CA 91706 USA, phone (626) 338-0035, fax (626) 338-7113, cgarneau@malcolmdrilling.com

On July 14, 2004, the bridge was added to the National Register for Historic Places under both Criterion A and C for its significance in transportation history and embodiment of distinguishing features of a Neoclassical bridge design and reflection of the City Beautiful movement in Pasadena. Besides its deck rehabilitation in 1962, the bridge remained unchanged from its original design and appearance. However, similar to when the Colorado Street Bridge was closed for a substantial seismic retrofit in 1989, the La Loma Bridge was in need of an extensive seismic retrofit and rehabilitation, made evident by its visual signs of distress through concrete spalling and exposure of reinforcing members.

At the end of 2014, the City of Pasadena advertised the La Loma Bridge Reconstruction project, which included the construction of new abutments and pier structures, shoring of existing spandrel columns and archways, and demolition of existing concrete slab-girder deck and replacement with new post-tensioned concrete box girder superstructure. Micropiles were the selected foundation type for the new pier structures largely due to the limited access at the bottom of the Arroyo Seco Canyon and between the existing bridge structures. The project was a collaborative effort between the City of Pasadena and California Department of Transportation with an estimated cost of approximately $16 million, funded by approximately $13.3 million in federal funds and the remaining in city funds. The City selected OHL USA, Inc. as the general contractor for the project, who listed Malcolm Drilling Co., Inc. as the micropile subcontractor. Construction began in June 2015 and is expected to be completed in early 2017.

PROJECT DESCRIPTION:

In an effort to preserve the historical value of the bridge, the project design consisted of constructing a completely new bridge superstructure supported on new abutments and pier columns built within the existing bridge structure. As such, the original bridge structure (spandrels and archways) would become the new bridge's stunning and historic façade. The project site is located at the bottom of the Arroyo Seco canyon, which consists of a concrete lined channel and a narrow access road surrounded by dense vegetation and popular pedestrian trails, with the west side of the project only accessible by a small pedestrian bridge. As such, access for any type of construction was challenging. Micropile foundations were selected for the structural support of the new bridge in part due to the limited access within the Arroyo Seco canyon and the minimal disturbance and versatility the micropile equipment and installation process provide. See Figure 2 for the profile of the existing and proposed bridge and Figure 3 for a typical cross-section of the proposed and existing bridge.

The micropile foundations were advertised as a design-build foundation element to be designed to increase the uplift and compression capacity of the four new pier footings. The project specifications also required four (4) preconstruction verification test micropiles, two (2) on each side of the bridge, to verify and demonstrate that the design-build micropiles meet the required

capacity. In addition, two (2) production micropiles per footing, for a total of eight (8) micropiles, were required to be proof tested.9

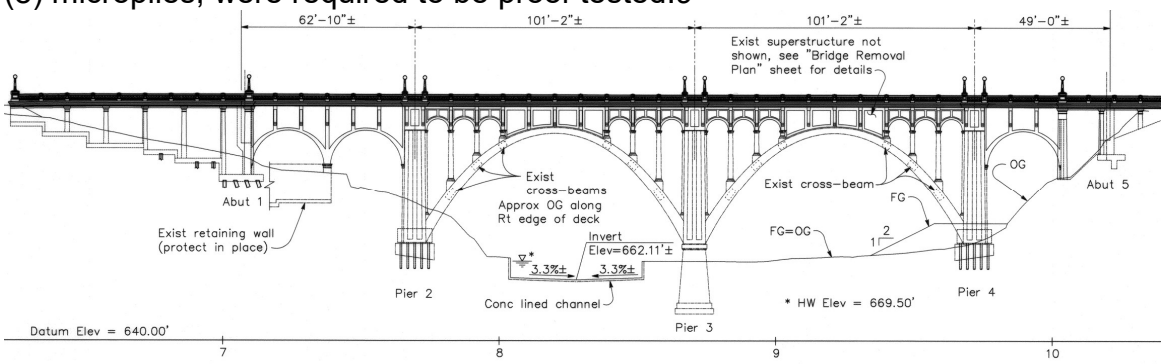


Figure 2 – Proposed Bridge Profile

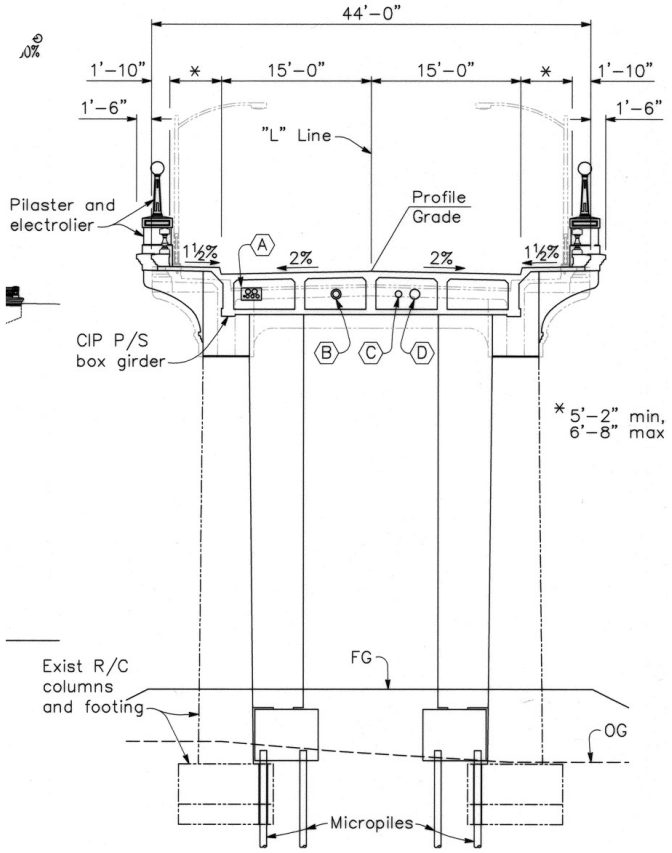


Figure 3 – Typical Cross-Section

SUBSURFACE CONDITIONS:

The existing bridge spans across the Eagle Rock Fault, which divides the underlying bedrock formations of which the bridge is founded on. On the east side of the fault (Pier 4), the site is underlain with highly weathered and oxidized intrusive quartz diorite rock, while the west side (Pier 2) is underlain with the Topanga Formation, a weathered sandstone conglomerate sedimentary rock.

Various depths of fill and recent alluvium were encountered at the surface at the bottom of the Arroyo Seco canyon consisting of interbedded layers of poorly graded to well graded sand with variable amounts of gravel and abundant cobbles and boulders within the fill layers. The geologic cross-section along the bridge profile is illustrated in Figure 4. All production micropiles were located at areas were the bedrock formations were exposed at the ground surface. Pre-construction photos of existing ground surface are shown in Figure 5 and 6 at Pier 4 (quartz diorite bedrock) and at Pier 2 (Topanga Formation), respectively.

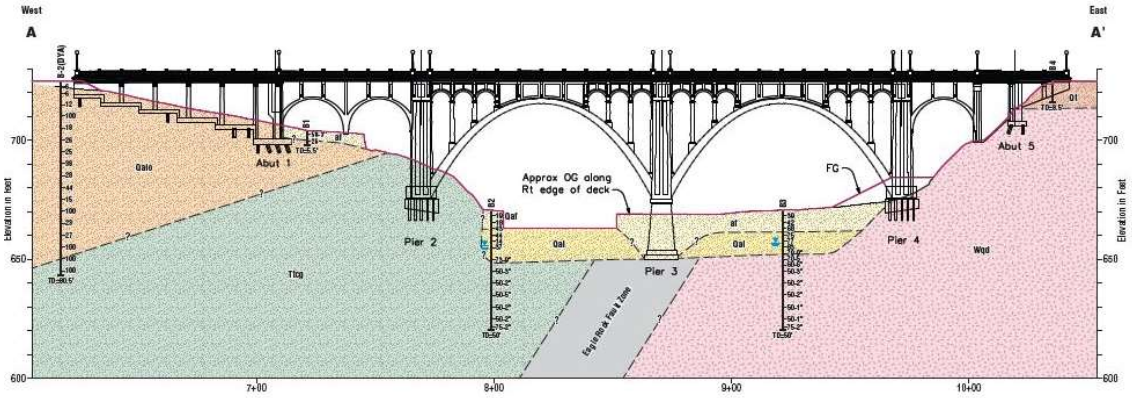


Figure 4 – Geological Cross-Section



Figure 5 – Pre-construction Conditions at Pier 4 (Quartz Diorite)



Figure 6 – Pre-construction Conditions at Pier 2 (Topanga Formation)

MICROPOILE DESIGN:

The proposed bridge foundations consist of forty (40) new micropile foundations with ten (10) micropiles per pier. Figure 7 illustrates the proposed foundation plan for the new bridge structure with the micropile foundations located at both Pier 2 and 4. At each pier location, the proposed pier footings are founded partially on the existing bridge foundation and partially on the exposed bedrock formation with the micropiles bridging through the existing footings with casing, which plunges into the underlying bedrock. Each micropile is designed to have a capacity of 270 kips in compression and 45 kips in tension.

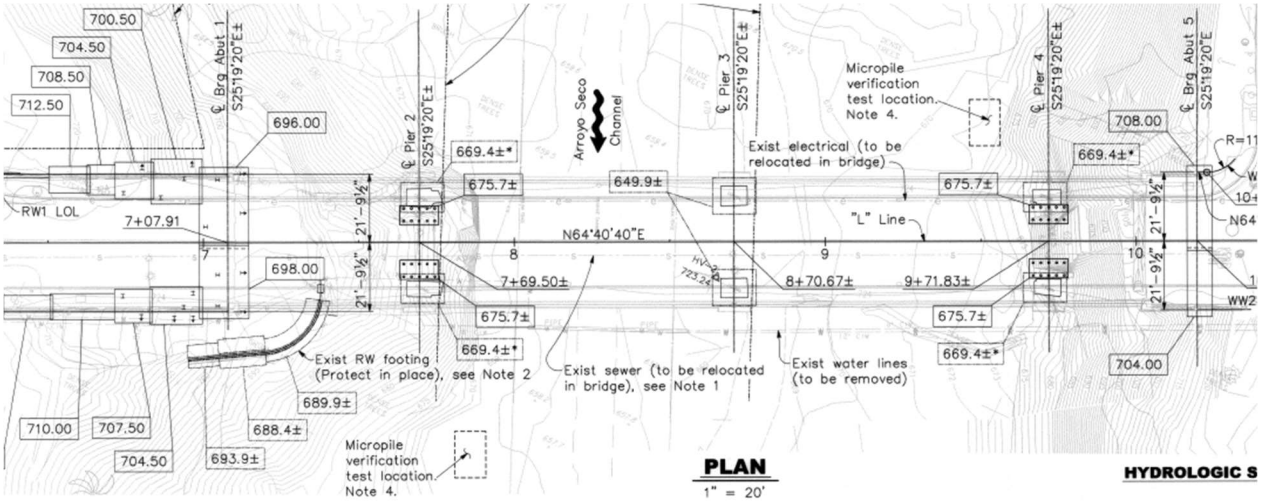


Figure 7 – Foundation Plan with New and Existing Structures

The micropiles are designed in accordance with the recommendations presented in FHWA NHI-05-039. An ultimate bond stress of 60 psi for gravity grouted micropiles (Type A) was selected for both the quartz diorite and sandstone bedrock formations based on recommendations in the geotechnical report, the PTI Manual “Recommendations for Prestressed Rock and Soil Anchors”, and past experience. For the design load of 270 kips, a bond length of 24 feet was determined based on utilizing a factor of safety of 2 and a micropile diameter of 10 inches. In order to meet the structural demand for the specified design load, a continuous #20 Grade 80 reinforcing bar was selected along with an 8.625” x 0.593” Sch. 100 steel pipe to plunge through the existing bridge footing, where applicable, and into the bedrock formation a minimum of 4 feet from bedrock surface or 3 feet below the bottom of footing. The length of pile spanning through the existing bridge footing was not counted as attributing to the frictional capacity of the micropile resulting in an overall micropile depth of approximately 30 feet. The micropile detail is shown in Figure 8.

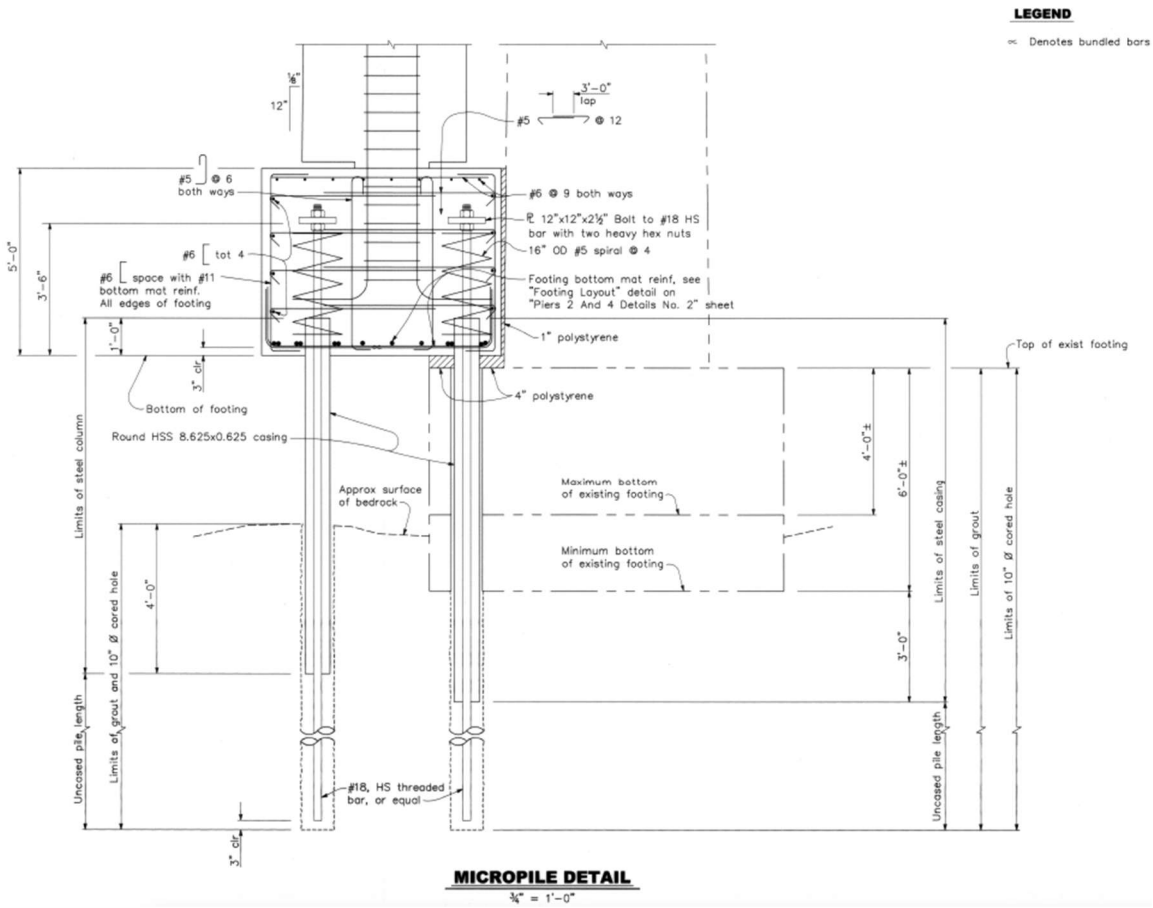


Figure 8 – Typical Micropile Detail

For verification and proof testing, the project specifications required the micropiles to be tested to 200% of the design load, which resulted in a maximum test load of 540 kips, which was tested in tension for both the preproduction

verification tests and proof tests of production micropiles. In order to facilitate testing of the grout-to-ground bond value to the required tension load, the reinforcing bar was upsized to a 2 ½" Grade 150 bar.

MICROPILE CONSTRUCTION:

Due to the limited access between the existing bridge pier columns and underneath the existing archways and crossbeams, a small Klemm 702-2 micropile drill rig was utilized to drill and install the micropiles. See Figure 9, which shows the drilling equipment being utilized. The presence of full depth competent bedrock at each pile location required the use of a down-the-hole hammer equipped with a 10" carbide-button hammer bit (see Figure 10). After the shaft was drilled to tip, the reinforcing bar was placed inside the open shaft with plastic centralizers and neat cement grout (water/cement ratio of 0.40 – 0.45) was placed by tremie method into the low end of the shaft. All micropiles were gravity grouted in a single stage for the entire depth of the hole. Post-grouting of the micropiles was not elected due to its limited effectiveness in bedrock type formations. Both the reinforcing center bar and the steel casing were placed at the proper elevation and tied off at the surface using timber and/or angle iron with wire. See Figure 11, which shows the completed micropiles for one of the proposed pier footings.



Figure 9 – Micropile Installation



Figure 10 – 10” Hammer Bit



Figure 11 – Completed Micropiles at Pier 2

MICROPILE TESTING:

The project specifications required four (4) total preconstruction verification test micropiles, two (2) near each pier location, and two (2) production proof test micropiles per footing, for a total of eight (8) micropiles. All verification and proof

micropiles were required to be tested 200% of the design load, for a total of 540 kips. The maximum factored test load was conservatively tested in tension only for both the verification and proof tests to avoid adding additional reaction piles. All micropiles were tested in accordance with ASTM D 3689 as shown in Figure 12, which details the test setup. The tension load was applied to the verification and proof test piles using a reaction system consisting of beams and cribbing. The applied load was measured using a calibrated jack and pressure gauge graduated in 100-psi increments. The micropile movement was measured with two dial displacement indicators capable of measuring to 0.001 inches. A minimum clear distance of 5 times the diameter of the micropile (4'-2") was maintained between the tested pile and the reaction cribbing bearing on competent bedrock material. The sacrificial verification test piles were located near each pier location such that they were installed in representative soil strata for the full depth of the micropile, which was challenging due to the topography of the site and varying layers of fill and recent alluvium located throughout the site. In addition, due to the site constraints and the proposed micropile layout, it was impractical to perform proof testing on many of the production micropiles due to the micropile spacing and proximity to existing bridge column. As such, the proof test locations were pre-selected and limited to only two locations per footing. See Figure 13 for the verification test setup at Pier 2 and Figure 14 for a typical proof test setup.

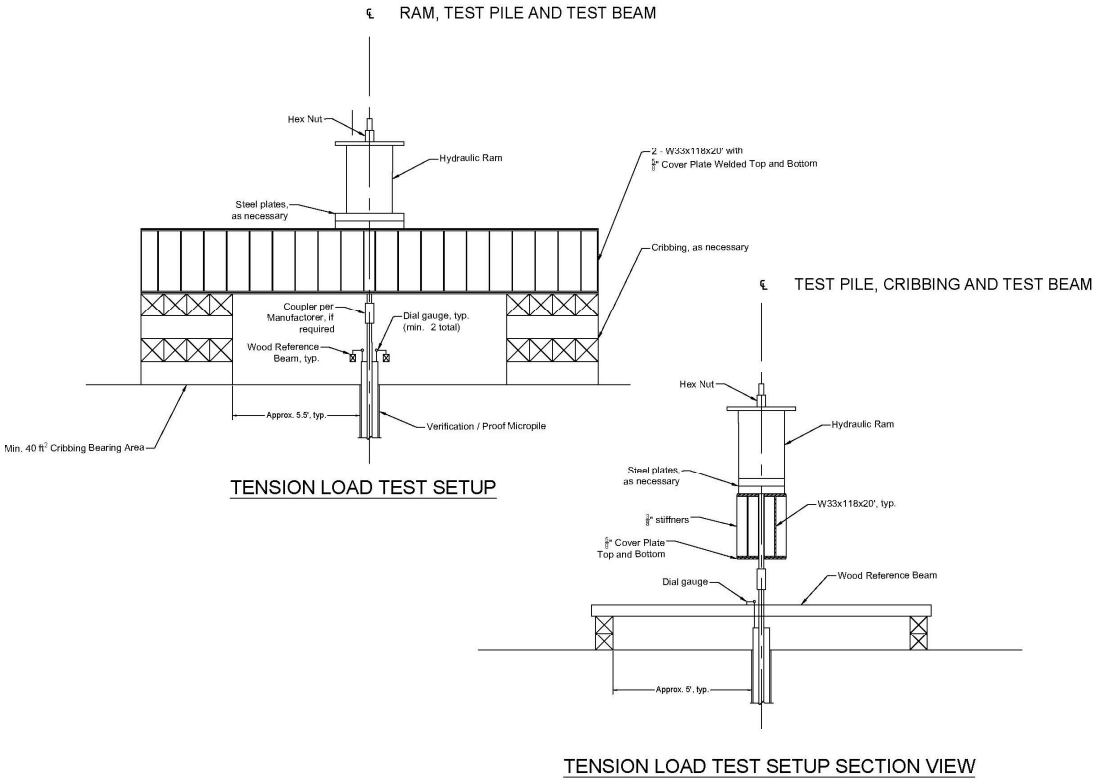


Figure 12 – Tension Load Test Setup Drawing



Figure 13 – Pier 2 Verification Test Set-up



Figure 14 – Proof Test Set-up

The tension test loads were incrementally loaded and unloaded according the test schedule shown in the project specifications. The project specifications also established three acceptance criteria for both the verification tests and proof tests. The first criterion was that axial movement at the top of the micropile measured

from the initial alignment load to the first application of 100% of the design load must not exceed 0.5 inch. The second criterion was that the slope of the applied test load versus the top of micropile movement must not exceed 0.025 inch per kip at the maximum test load. The last criterion was that the creep test movement must not exceed 0.04 inch measured from 1 to 10 minutes or 0.08 inch measured from 6 to 60 minutes with the rate of movement being linear of decreasing in time when graphed on a logarithmic scale. The applied load versus top of micropile movement was plotted for all verification and proof tests. Figure 15 shows the pile movement curve for one of the verification test. All verification and proof test micropiles were successfully tested to 200% of the design load and satisfied all acceptance criteria. Both bedrock formations, the intrusive quartz diorite and sandstone conglomerate bedrock, behaved fairly similarly. See Table 1 for a summary of all verification and proof test results.

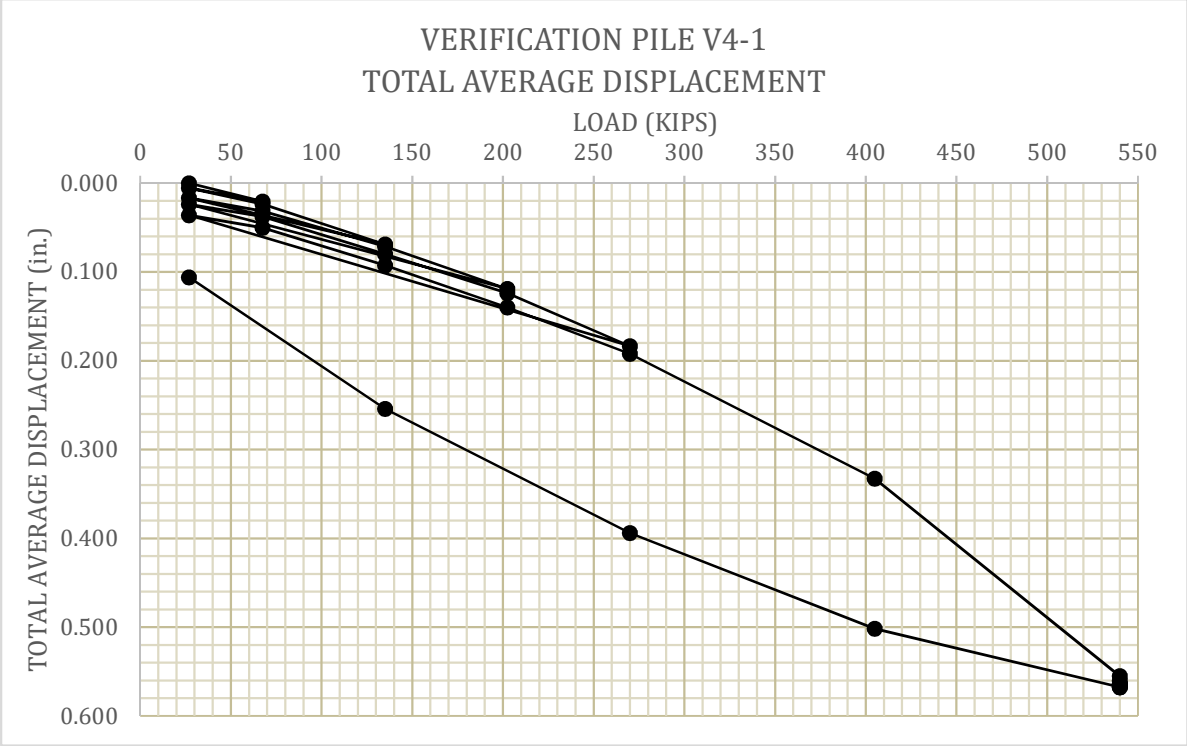


Figure 15 – Displacement Curve for Verification Test at Pier 4

Table 1 – Summary of Test Results

Test Pile Number	Test Type	Location	Bedrock Type	Axial Movement at 100% DL	Movement / Load @ Max Test Load	Creep Movement (1 to 10 minutes)
				(in.)	(in. / kip)	(in.)
V2-1	Verification	Pier 2	Topanga	0.135	0.00089	0.006
V2-2	Verification	Pier 2	Topanga	0.188	0.00173	0.016
V4-1	Verification	Pier 4	Quartz Diorite	0.184	0.00164	0.007
V4-2	Verification	Pier 4	Quartz Diorite	0.184	0.00139	0.008
R2-3	Proof	Pier 2	Topanga	0.177	0.00115	NR
R2-5	Proof	Pier 2	Topanga	0.104	0.00089	NR
L2-6	Proof	Pier 2	Topanga	0.145	0.00119	NR
L2-8	Proof	Pier 2	Topanga	0.130	0.00126	NR
R4-1	Proof	Pier 4	Quartz Diorite	0.136	0.00130	NR
R4-3	Proof	Pier 4	Quartz Diorite	0.122	0.00144	NR
L4-6	Proof	Pier 4	Quartz Diorite	0.237	0.00163	NR
L4-8	Proof	Pier 4	Quartz Diorite	0.204	0.00152	NR

CONCLUSION:

The micropiles were completed and successfully tested in October 2015. In order to preserve the historic value of the original La Loma Bridge and perform the necessary retrofitting and reconstruction of the bridge, the project design included the construction of a new bridge structure within the original bridge column and archway structures. As a result, micropiles provided the ideal foundation for the support of the new pier columns due to the limited access in the Arroyo Seco canyon and between the existing bridge structures as well as the installation process's minimal disturbance to the existing structure. Micropiles allowed for the new pier columns to be constructed immediately adjacent to the existing bridge columns so the new structure could be seamlessly integrated into the original bridge design.

ACKNOWLEDGEMENTS:

Owner – City of Pasadena - Department of Public Works, California, USA
Structural Engineer – Dokken Engineering - Folsom, CA
Geotechnical Engineer – Geocon Consultants, Inc. - Rancho Cordova, CA
General Contractor – OHL USA – Irvine, CA
Foundation Contractor – Malcolm Drilling Co., Inc. – Irwindale, CA

REFERENCES:

Dokken Engineering, *Project Plans for Construction of Seismic Retrofit & Reconstruction of La Loma Road Bridge*. November 18, 2014.

Geocon Consultants, *Foundation Report for the La Loma Bridge Reconstruction Pasadena, CA* (Project No. S9733-06-01). July 16, 2013.

Post-Tensioning Institute, *Recommendations for Prestressed Rock and Soil Anchors* (PTI DC35.1-14). 2014

United States Department of Interior National Park Service, *Nation Register of Historic Places Registration Form for La Loma Bridge.* November 6, 2008.

A Review of Micropiles Beneficial Aspects through a Case History near False Creek, Canada

M. Deriszadeh, M.Sc., Ph.D.[1] and M. J. Kokan, M.A.Sc., P.Eng.[2]

Micropiles, also known as minipiles are a type of deep foundations composed of placed or injected grout and steel reinforcement with diameters of typically smaller than 300 mm. Micropiles have recently gained higher acceptance in geotechnical engineering practice and have been utilized as a foundation solution in numerous applications such as seismic retrofitting, resisting uplift loads, control of settlements and underpinning of existing foundations. This paper presents a case history where micropiles were used as supporting elements for underpinning and controlling settlements of an existing foundation system adjacent to a 15 m shored cut for a residential tower development, located in close proximity to False Creek, in Vancouver, Canada. The existing foundation system, supporting each pier of an elevated viaduct, included a pilecap and a group of cast-in-place reinforced concrete piles with pile tips located significantly above the final excavation grades. The 15 m shored excavation was proposed to be completed directly adjacent to the existing pilecaps. The advantages of using micropiles in controlling the movements of the existing foundations of a sensitive structure (bridge viaduct) will be demonstrated. Laser displacement meters (LDM's) and tilt meters (TM's) were used to monitor the 3-dimensional displacements and rotation of the existing pilecaps during the excavation and shoring. In addition, traditional precision surveys were carried out to verify the data of the automated monitoring system. Monitoring results showed excellent performance for the micropile supported piers in a congested construction area to control the displacement/rotation of the existing viaduct structure adjacent to the shoring walls.

1. GeoPacific Consultants Ltd., Vancouver Office, Canada (Presenter). Email: deriszadeh@geopacific.ca
2. GeoPacific Consultants Ltd., Vancouver Office, Canada. Email: kokan@geopacific.ca
Phone: (604) 439-0922 – Fax: (604) 439-9189

INTRODUCTION

Micropiles were first introduced to the geotechnical engineering practice in early 1950's in Italy and mainly used for underpinning the historic structures with settling foundations (Shong and Chung, 2003). Micropiles have recently gained increased acceptance in geotechnical engineering practice and have been utilized for seismic retrofitting, resisting uplift loads, control of settlements and underpinning of existing foundations. This paper presents a construction case history of the application of micropiles in controlling settlement of an existing highly sensitive foundation system supporting a viaduct. The project included a residential tower (South Tower) with five levels of underground parking, located about 150 m to the north of False Creek, in Vancouver, Canada. Figure 1 shows the construction site area in relation to the surrounding structures and features.

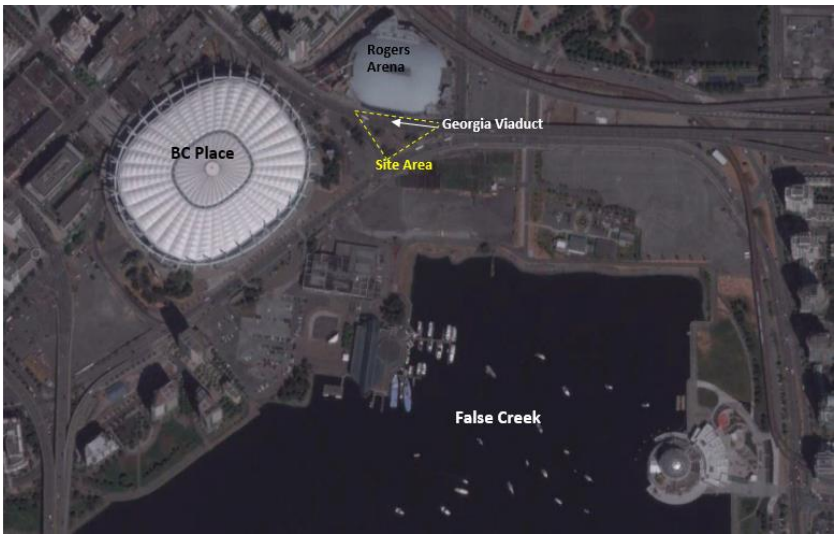


Figure 1. Site area in relation to surrounding developments/features (Google Image, 2014)

The high significance of this project was mainly due to the presence of sensitive structures such as the Georgia Viaduct and the Rogers Arena building (Vancouver's Ice Hockey Stadium) in the vicinity of the 15 m deep shored cut. The north side of the shoring line was located immediately adjacent to the Rogers Arena building and two pilecaps supporting the existing Georgia viaduct. The performance of both of the noted public structures are of high importance for the City of Vancouver and the safety of its residents that utilize the viaduct as a major commute to downtown Vancouver. Figure 2 displays a partial site plan showing the excavation area with respect to the adjacent sensitive structures.

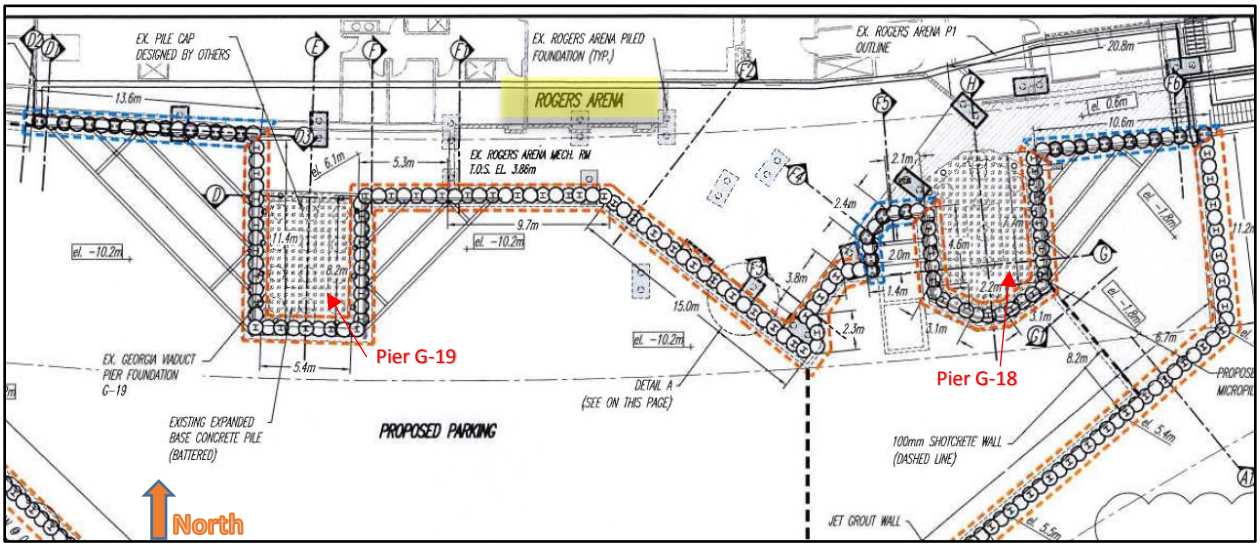


Figure 2. Partial site plan showing the viaduct pilecaps and Roger Arena in the vicinity of shoring area (GeoPacific's Drawing)

SITE CONDITIONS

The approximately 2,000 m^2 site area is bounded by the Rogers Arena building and the Georgia Viaduct piers to the north and City roads to the south, west and east. Prior to the construction, the site was generally level with an average geodetic elevation of about 4.5 metres. Based on the results of a geotechnical investigation program, completed by GeoPacific Consultants Ltd., the subsurface soils onsite were identified as 7 to 9 m of fills, overlying 2 to 3 m of a native deposit of firm to stiff silty clay with sand, underlain by dense to very dense silty sand with some gravel (glacial till). The dense glacial till was noted to be encountered at about 9 to 12 m depth.

Historically, the shoreline of False Creek was located northwest of the subject site and subsequently large amounts of fill materials were used to reclaim portions of False Creek. The fills can be separated into two different units due to differences in consistency and relative density of soils, observed during the geotechnical investigation. 'Recent fill' can generally be classified as compact and was noted to contain a smaller fraction of refuse materials and/or organics s compared to the originally deposited fills. The underlying historic fill is a heterogeneous unit, placed during the original reclamation of False Creek. The static groundwater level was identified at about 5 m depth over the site area. Each of the two viaduct piers, present within the construction area were supported on a group

of cast-in-place piles. These piers are shown as G-18 and G-19 on the site plan (Figure 2).

SHORING AND UNDERPINNING DESIGN

The foundation system of the two viaduct piers that were adjacent to the construction area included concrete pilecaps, supported on reinforced cast-in-place concrete piles. A review of as-built drawings showed that a total of twelve and thirteen cast-in-place concrete piles supported the pilecaps of piers G-19 and G-18, respectively. Pile tips were located at about 7 to 8 m below original site grades. Figure 3 shows a plan view of the pilecaps with the arrangement of the original concrete piles. The width and length of the pilecaps were in the range of 4 to 5 m and 6.5 to 8 m, and as shown in Figure 3, the 15-m deep shoring line was proposed to be adjacent to the pilecaps (within less than 1 m distance from the edge of pilecaps).

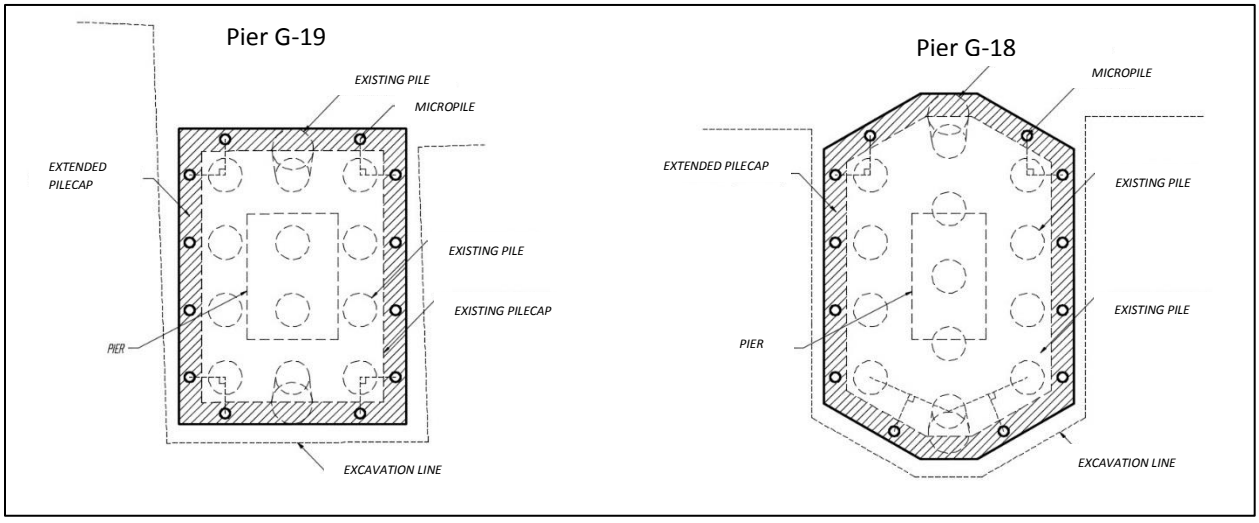


Figure 3. Plan view of the pilecaps supporting Georgia viaduct piers in the subject site area (GeoPacific's Drawing)

The shoring system, designed by GeoPacific Consultants for this project included a combination of anchored jet-grout walls, within the upper portions, and conventional anchored shotcrete walls, for the lower portion of shoring (below the level of glacial till layer). Details of the jet-grout shoring system is not included in the scope of this paper and was presented in a separate paper (Gazzarrini et al. 2016). A typical section view, showing the designed shoring system, and the position of the shoring walls in relation to the foundation system of the viaduct piers is presented in Figure 4.

Given the final grades of excavation and the line of shoring in relation to the existing piles and pilecaps, as schematically illustrated in Figure 5, the interaction between the existing

concrete piles and surrounding soils was anticipated to be influenced due to the expected movements of the underlying soils (re-arrangement of soil particles) under the effect of excavation and ground relaxation. This could result in excessive settlements of the entire foundation system, including the pilecaps, piles and their surrounding soils within the shoring walls around the pilecaps.

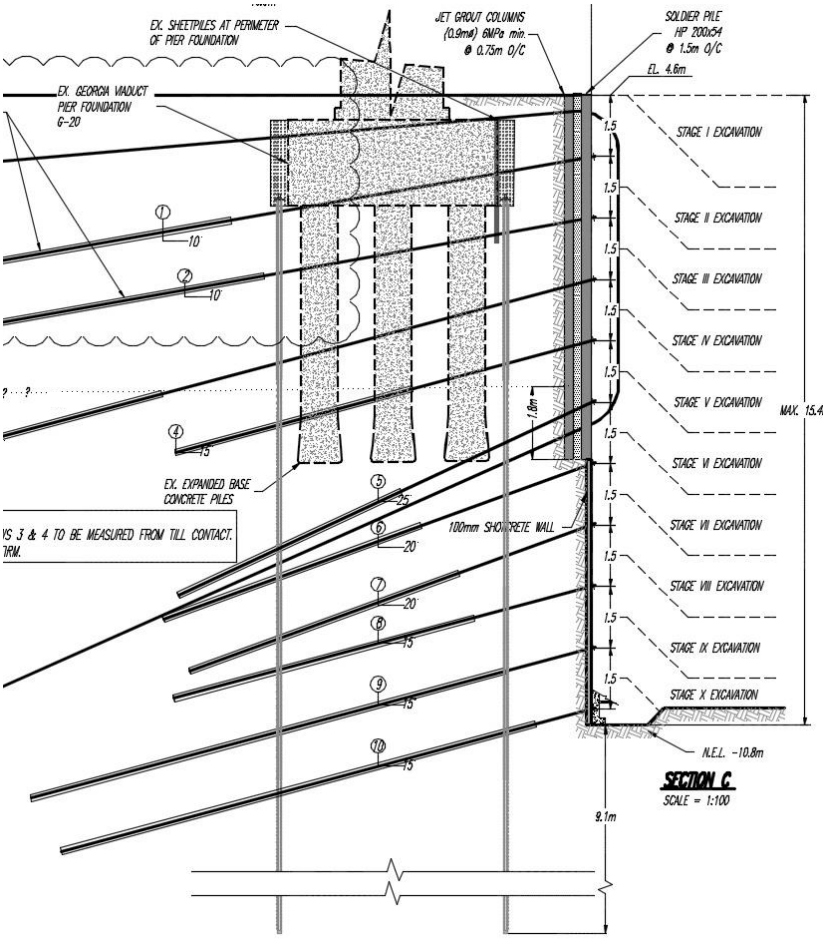


Figure 4. A typical section view of the shoring and underpinning system at the location of pier G-19 (GeoPacific's Drawing)

The anticipated settlements are proportional to the elevation difference between the pile tips and the final excavation grades such that the significant elevation difference between the toe of original piles and the final excavation depth would result in larger settlements in the foundation system, since the viaduct is well above the foundation level.

One of the key aspects of the excavation work in this project was controlling the possible movements in the foundation system of the Georgia Viaduct which was of extreme importance to the City of Vancouver.

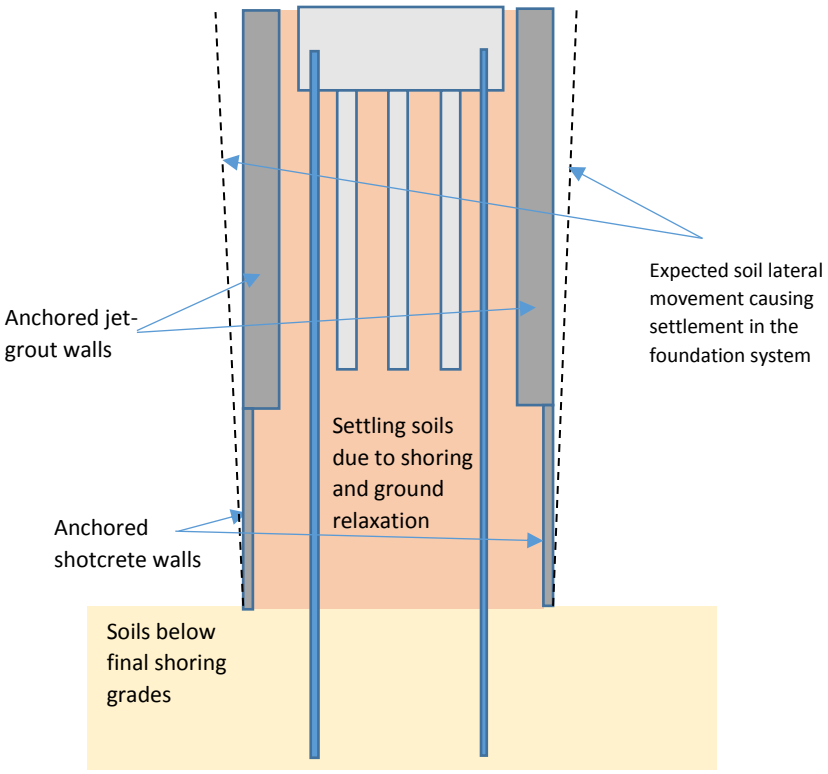


Figure 5: Schematic representation of underpinning micropiles, shoring system and the existing foundation system of viaduct piers

Based on the analysis of the existing viaduct structure by the bridge engineer of the project, threshold values for the 3-dimensional displacement and rotation of the viaduct foundations (G-18 and G-19), for the safe performance of the structure, were determined. Based on the results of the structural analysis of the bridge, the following thresholds of displacements and rotation were prescribed:

1) Threshold for rotation: 0.04^{o}
2) Threshold for longitudinal (horizontal) displacement: 10 mm
3) Threshold for transversal (horizontal) displacement: 5 mm
4) Threshold for vertical displacement (settlement): 10 mm

Level A and Level B of thresholds were accordingly defined as 50% and 80% of the prescribed limits. Horizontal displacements of the pilescaps were successfully maintained within the prescribed threshold limits by means of internal steel bracing, as a part of shoring system, installed at the corners of shoring walls (see Figure 2 and 6). Details of controlling the horizontal displacements of the pilecaps are not included in the scope of this paper.



(a) (b)

Figure 6. Internal bracing to control lateral movements (a) pilecap of pier G-19 and (b) pilecap of pier G-18

In order to control the settlements of the pilecaps, an underpinning system, using drilled micropiles was designed to directly transfer the pilecap loads to the deep glacial till layer, considerably below the excavation depth. Since the construction space under the viaduct structure was congested and a distance of less than 1 m between the proposed excavation lines and the edge of existing pilecaps was available (see Figure 3), mciropiles were suggested to provide an underpinning system to transfer the pilecap loads directly to the deep competent glacial till stratum which allowed for substantial elimination of the original concrete piles and their surrounding soils such that the possible soil/CIP pile settlement could not influence the pilecaps. A group of twelve micropiles were designed around each existing pilecap to underpin the viaduct pier foundations (Figure 3). These micropiles were then structurally engaged to the existing pilecaps by expanding the existing concrete pilecaps.

A typical section view of the micropiles, designed for underpinning the viaduct pier foundations is shown in Figure 7 and a view of an installed micropile in the field (prior to pilecap expansion) is shown in Figure 8. Each micropile was designed for a service load of 850 kN. The bonded length of the micropile, in contact with glacial till, was computed using a bond strength of 150 kPa, in both tension and compression. Given the maximum service load of 850 kN and the micropile diameter of 200 mm, a minimum bonded length of 9.1 m was considered in the design. Each micropile included a high-grade steel thread

bar with a bar nominal diameter of 66 mm and a steel casing, HSS 168 x 6.4 mm, ASTM 500 (in the upper portion), as shown in Figure 7. The bearing capacity of the micropiles was achieved using 35 MPa grout, injected into the 200 mm drilled holes as shown in Figure 7.

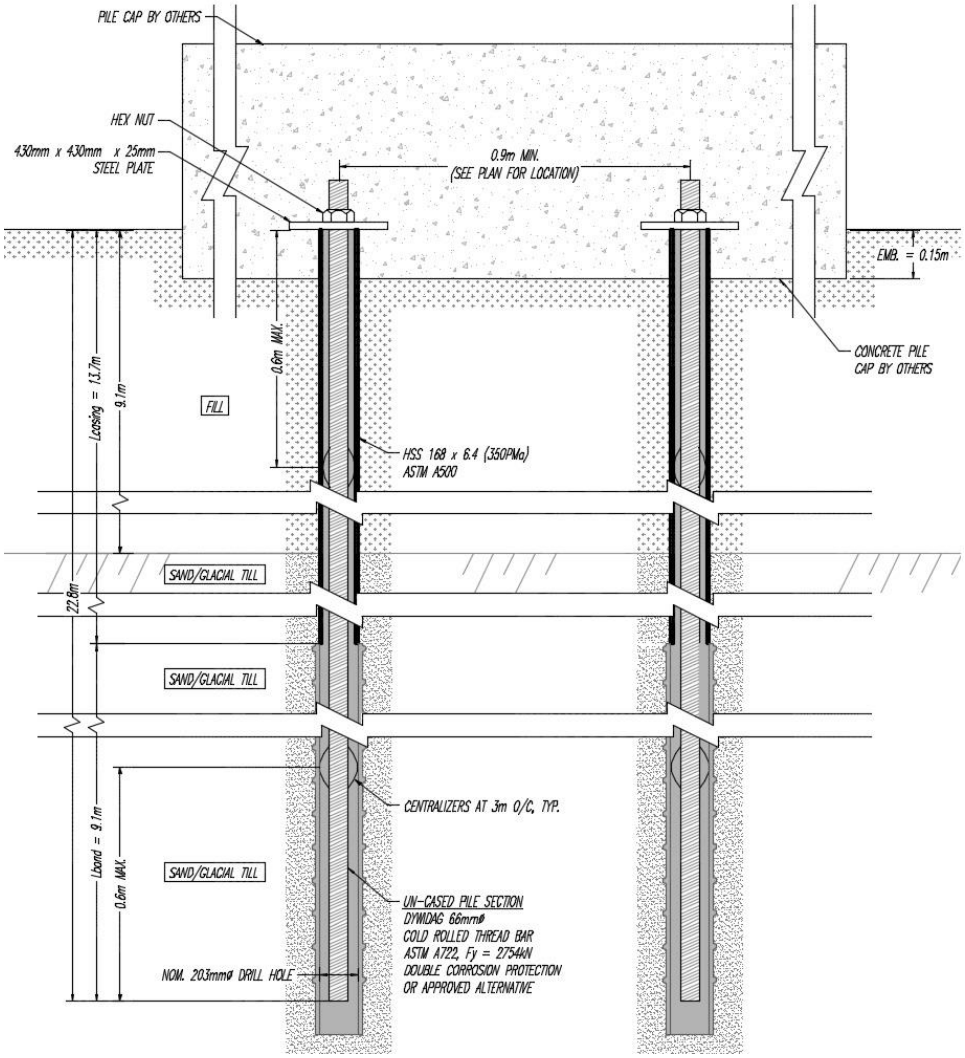


Figure 7. A typical profile of the micopiles designed for underpining the viaduct pier foundations

Despite the cast-in-place piles that may provide a relatively small tensile capacity, the designed micropile system worked in both compression and tension with a relatively similar capacity which is one of the advantages of these types of foundation/underpinning systems in controlling the rotations of the pilecaps as the group of micropiles can work in compression-tension mechanism and provide a coupled force system to control the pilecap rotations.



Figure 8. A view of an installed underpinning micropile on the north side of pier G-18 prior to pilecap expansion

The performance of the designed micropiles in controlling the settlements and rotation of the viaduct pier foundations was thoroughly monitored using an automated monitoring system as well as conventional survey. The results of the conventional survey and the automated monitoring system are presented and discussed in the following section. It should be noted that prior to excavation and shoring construction, all of the installed micropiles were successfully tested in general accordance with FHWA (2005) guidelines, which is typically used in the standard geotechnical engineering practice. All tested piles satisfied the referenced guideline criteria for performance testing.

MONITORING RESULTS AND DISCUSSION

In order to verify that the displacements and rotation of the subject pilecaps would be maintained within the referenced acceptable ranges, prescribed by the bridge engineer, an automated monitoring system was designed to continuously record the 3-dimensional displacements and rotation of the pilecaps for the full duration of excavation and shoring construction. The monitoring system for viaduct pilecap G-19 included two tilt meters (TM's), with the accuracy of 0.001º, and a Laser Displacement Meter (LDM), capable of measuring 3-dimensional displacements with the accuracy of 0.01 mm. For viaduct pilecap G-18 one TM and one LDM were used to measure the movements continuously. In order to validate the performance of the automated monitoring system, and also to investigate the influence of temperature variations and traffic noise on the monitoring

data, a 2-week trial monitoring period was conducted prior to the commencement of the shoring construction and bulk excavation. Upon the completion of the trial period, the effects of temperature variations and also direct sunlight on the results of the automated monitoring data were investigated and the sources of possible errors were either removed (e.g., direct sunlight) or quantified (e.g., temperature effects) and a baseline was established for all sets of the monitoring data.

In addition to the automated monitoring system, a conventional monitoring program via manual survey was conducted and a baseline for the coordinates of the selected monitoring points was established. The intent of considering a conventional survey in the monitoring program was to periodically validate the recorded data of the automated monitoring system.

The shoring and excavation operations and construction of the permanent structure to the level of the original ground were completed in about 12 months. During this period the automated monitoring system continuously recorded the displacement and rotation data of the pilecaps. The recorded monitoring results were available online to the design and construction team for the duration of the project. In addition, conventional survey was conducted on a bi-weekly basis (monthly at later stages of the project) to validate the automated data. It should be noted that the threshold limits were adjusted over the 12-month period of temporary shoring to account for the influence of seasonal temperature variations on the electronic output, generated by the automated instrumentation, installed on the viaduct pier foundations. These adjustments were carried out based on the correlations between the recorded movement data of the pier foundations and temperature variations during the trial period of the automated monitoring system. These correlations were established by the structural (bridge) and geotechnical teams of the project. Typical sample results of the automated monitoring data, at different time intervals during this project, are presented in the graphs of Figure 9. The prescribed threshold limits with their variations based on seasonal temperature levels are also included in these graphs. Comparison of the displacement and rotation data against the prescribed threshold limits is indicative of the excellent performance of the micropile underpinning system to control the movements of a highly sensitive structure in close proximity of the shored cuts.

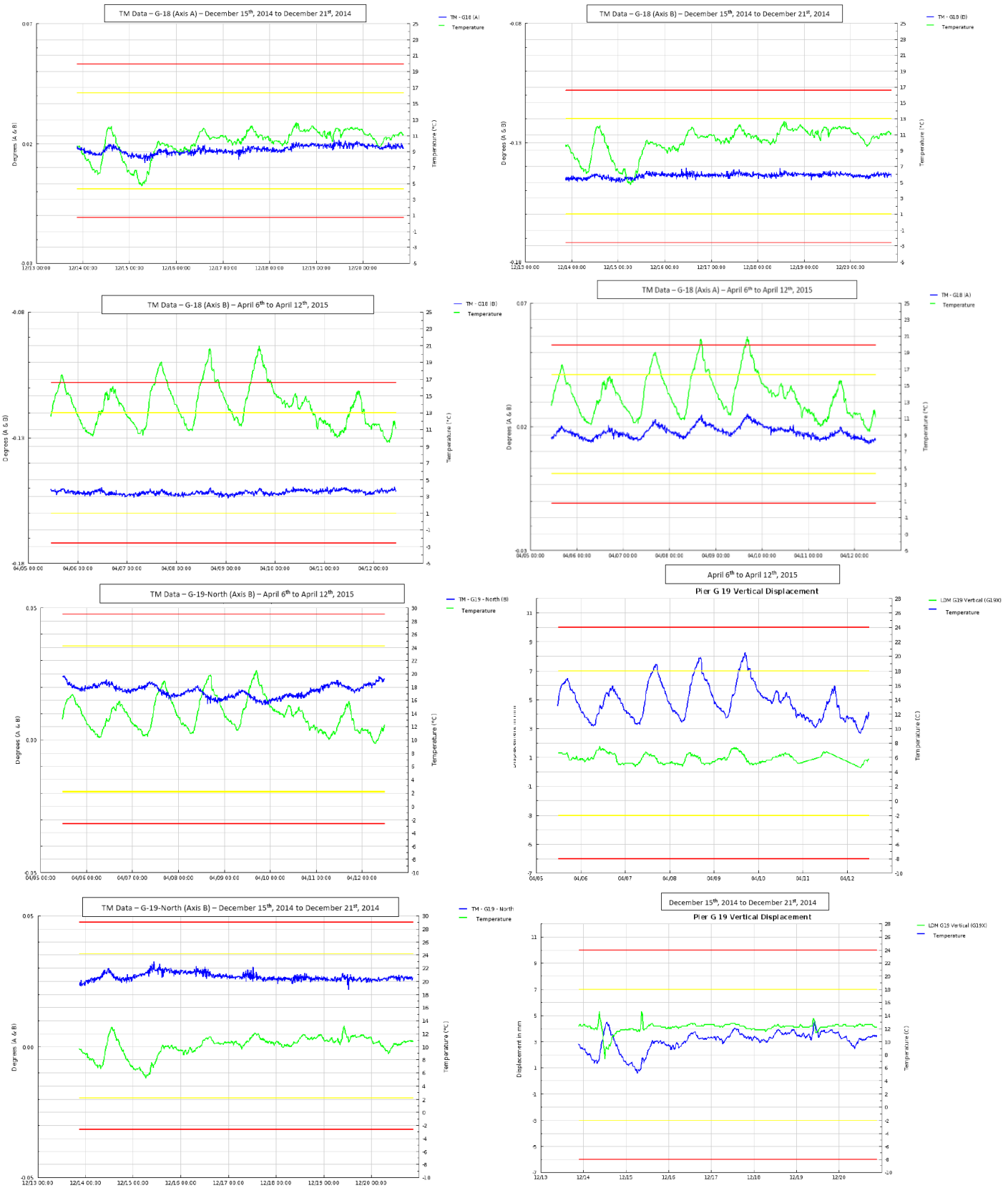


Figure 9. Typical graphs of the automated monitoring system for piers G-18 and G-19 at different time frames

Based on our experience in a number of shoring projects in downtown Vancouver for relatively similar subsurface conditions, excessive foundation settlements and rotation would be anticipated for the shoring system without the micropile underpinning system, indicating that properly designed micropiles can be considered as an excellent solution for controlling movements in the vicinity of deep excavations.

CONCLUSIONS

The South Tower project, demonstrated excellent performance of micropiles for underpinning and controlling foundation movements of a highly sensitive structure (Georgia Viaduct) in the vicinity of a deep shoring wall. Monitoring results confirmed that all foundation displacements and rotation were maintained within the prescribed limits for the safe performance of the viaduct structure. In spite of a limited construction space around the subject pilecaps, micropiles showed to be an excellent option for underpinning, particularly in congested construction areas, to control settlements and rotation of the existing footings. The capability of micropile systems in providing resistance against foundation rotations based on developing a coupled compressive-tensile force system is another advantage of micropiles which can safely secure the control of both vertical and rotational movements of pilecaps.

REFERENCES

FHWA (2005). "*Micropile Design and Construction. Reference Manual. US Department of Transportation, Federal Highway Administrcation"*. Report No. FHWA NHI-05-039

Gazarrini, P., Kokan M. J. and Hunt D., "*Jet Grouting For Structural Underpinning of the Existing Georgia Viaduct Foundations and Temporary Excavation Support: Rogers Arena, South Tower, Vancouver, BC, Canada*", *Geotechnical and Structural Engineering Congress*, Phoenix, Arizona, February 14 to 17, 2016.

Shong I. L. S. and Chung F. C., "*Geotechnical Course for Pile Foundation Design & Construction*", Ipoh, Malaysia, September 29 and 30, 2003.

HERITAGE FAÇADE SUPPORT AND EXCAVATION SHORING – A MICROPILE CASE HISTORY

Amanda Gordon, B.Eng.[1], Michael Sousa, P.Eng.[2]
Brian Isherwood, MICE FCSCE P.Eng.[3]

ABSTRACT

Originally built in 1927, the distinctive terracotta trim and red brick façade of the Canadian Westinghouse Building in Toronto's entertainment district is preserved in-situ on a temporary frame supported by Case 1 micropiles also employed as vertical members in a temporary excavation shoring system. Two street facing façades of this 6 storey heritage building were supported while the remainder was demolished to make way for development, including two towers and five underground parking levels.

A large diameter soldier pile excavation support system was originally planned around the site, however, proximity of a gas main and the preclusion of street closures due to traffic congestion and light rail tracks, required a hybrid solution with small diameter piles. The façade support frame was founded on two rows of vertical 356 mm diameter piles, designed to act in tension and compression to suit wind loading on the facade. The row of micropiles closest to site were also designed to withstand lateral earth pressures and allow for potential bedrock expansion that is known to develop in Toronto shales following excavation.

[1] Isherwood Geostructural Engineers, Unit 300, 1901 Rosser Avenue, Burnaby, BC, CANADA, 604.428.7080, amanda@isherwood.to

[2] Deep Foundations Contractors Inc. 145 Ram Forest Rd. Stouffville, ON CANADA, 905.750.5900, msousa@deep.ca

[3] Isherwood Geostructural Engineers, Unit 3, 3100 Ridgeway Drive, Mississauga, ON, CANADA, 905.820.3480, brian@isherwood.to

1. PROJECT BACKGROUND

Toronto has seen intensive construction over recent decades driven particularly by subway expansion and hundreds of high-rise condominium developments, most of which involve deep excavations for underground structures and basements. The expanding foundation construction industry has been kept very busy. Isherwood Geostructural Engineers (Isherwood) and Deep Foundations Contractors (Deep) have collaborated for more than forty years in executing many excavation shoring projects, including several of Toronto's iconic landmarks.

Driven by the strong natural soils underlying downtown Toronto (glacial tills and shale bedrock) as well as contractor investment in large specialist equipment, shoring practice in Toronto concentrates on drilled soldier pile and lagging and drilled secant caisson walls, typically with rock or soil anchor bracing.

Developers benefit from the City practice of allowing temporary shoring to be located on City Property, thus allowing building of underground structures to the limits of the developer's property.

2. EXISITING HERITAGE STRUCTURE

355 King Street West, at the intersection of Blue Jays Way (then called Peter Street) was redeveloped in 1927 for the Canadian Westinghouse Company as a show room, warehouse and district office. The structure was designed in two phases such that the first three levels were built first; then in 1935 three more levels were added to complete the building as shown in figure 1.

The building is designated by the City of Toronto (1992) under the Ontario Heritage Act for architectural reasons citing "its two-part design, restrained Classical detailing and the application of terra cotta trim on brick, a combination rarely used in the City of Toronto".



Figure 1. Canadian Westinghouse Building ***Source: KingBlueCondos.com***

3. PROPOSED NEW DEVELOPMENT

The Canadian Westinghouse Building Toronto forms part of the site of a condominium development by Greenland Group including two residential towers of 48 and 44 storeys. In order to maintain the streetscape, the two street facing façades of the heritage warehouse are being preserved in situ and will be incorporated into a podium of the same height – see figure 2.

In order to achieve this, a temporary steel frame located on the two sidewalks was required. Once installed, and the facades secured, the remainder of the building could be demolished to clear space for the new construction. Foundations for the façade support frame would have to allow for (the then proposed) seven underground basement levels immediately adjacent.



Figure 2. Proposed Development ***Source: KingBlueCondos.com***

4. LOCATION

The site, highlighted in blue in figure 3, is three blocks north from Toronto's Roger's Stadium and CN tower (both Isherwood/Deep projects). The building faces King Street West, a major commercial thoroughfare with Toronto's busiest street car line carrying 64,000 passengers daily (TTC, 2014).

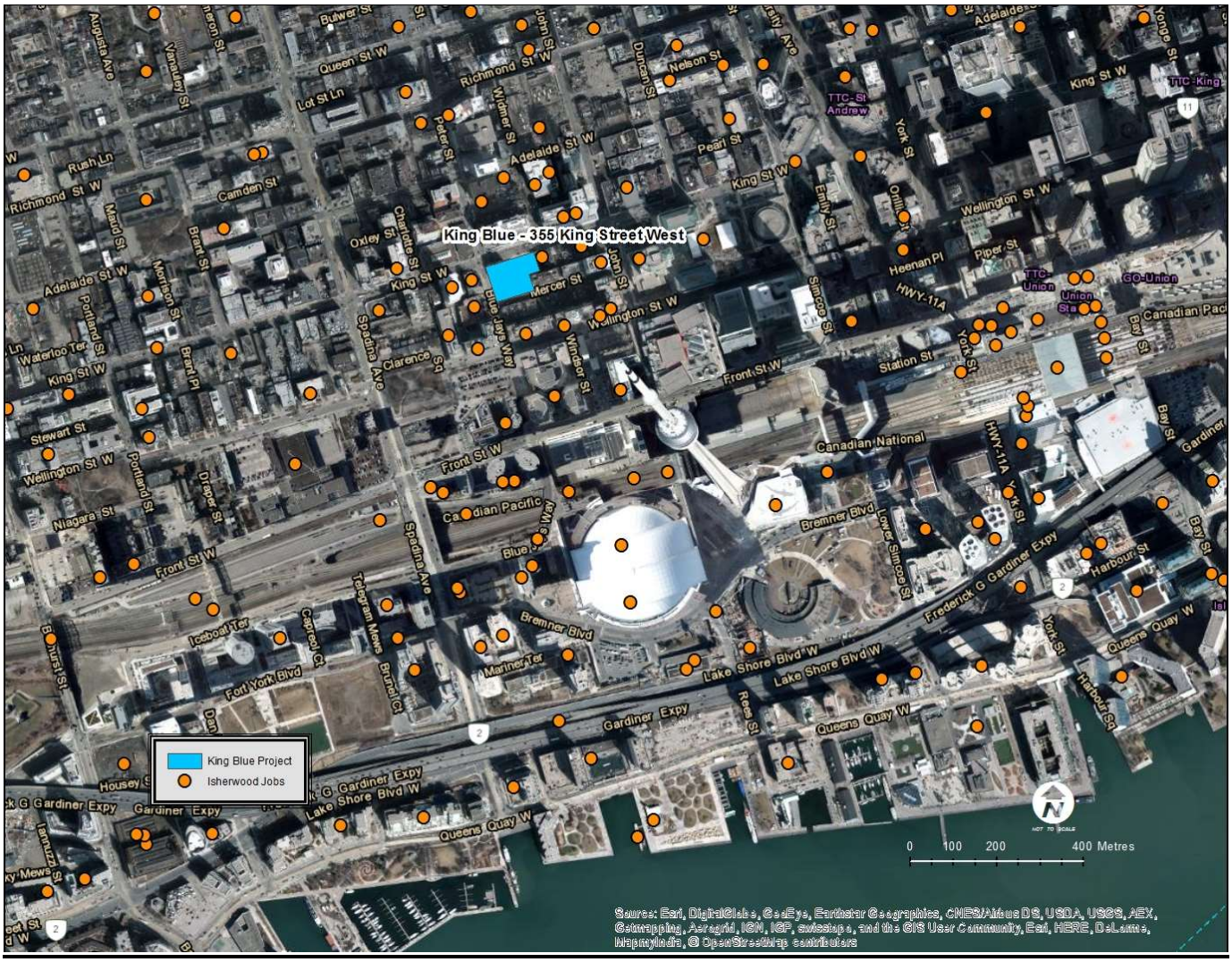


Figure 3. Location Map

5. STRUCTURAL STEEL FRAME

A temporary external frame, shown in figure 4, was designed by Structural Engineers Jablonsky, Ast and Partners to support the two historic facades.

Diligent coordination between Isherwood and Jablonsky was required throughout to ensure the geometry and foundation design could properly accommodate the loads.

It is worth noting, the authors understand that this is Toronto's tallest façade support project to date.



Figure 4. Facade Support Frame

6. GROUND CONDITIONS

a. Geology

The bedrock underlying downtown Toronto is Georgian Bay Shale; which was deposited in an ancient sea 450 million years ago and is interbedded with limestone and siltstone (Sharpe, 1980). This deposit was compressed for over a millennium under an average one kilometer of ice, consolidating it into shale. As this ice melted the vertical stresses in the rock were relieved, but high locked-in horizontal stresses remain and must be considered in any deep rock excavation.

Current overburden (laid down in the last 2.5 million years) consists mainly of glacio-lacustrine till, and is about 6 m thick at the site. The native overburden is overlain by up to 3 m of man-made fill.

b. Geotechnical Properties of Soil and Rock

The silty clay till has excellent stand up time well suited to wood lagging (see figure 10). High clay content in this soil reduces the effectiveness of grout/soil bond in post grouted tieback anchors. Tieback performance tests with single grout anchors indicated a working soil adhesion of 50 kPa.

Georgian Bay shale encountered at around 9 m below street grade is generally sound rock (5000 kPa SLS foundation bearing capacity) with 600 kPa working adhesion for tiebacks. It provides an excellent foundation for the CN Tower and many other tall buildings in downtown Toronto.

c. Seasonal Effects

Toronto's winter lasts from November to March and temperatures dip as low as -25 ºC (-13 ºF). Freezing water in unprotected soil can cause forces several times greater than the shoring system is designed to withstand. Isherwood has seen frost movements of up to 40 mm in one week and 90mm over a winter.

7. RESTRICTED SPACE CHALLENGES

Incorporation of heritage facades into new developments has become increasingly popular in many world cities. In Toronto, it is usual to employ a drilled soldier pile or secant caisson shoring wall immediately outside the façade with cantilevered brackets to support its weight, and an external steel frame to resist lateral and eccentric loads. A previous Isherwood/Deep project supported a four-storey façade on St. Joseph Street in this way, where we could occupy the sidewalk and curb lane for the duration of construction.

At King Blue a similar approach was contemplated. However, a study of existing utility records revealed a large electrical transformer vault occupying 7m of the sidewalk

on Blue Jays Way prohibiting drilling and construction traffic access. Of more consequence were existing gas lines along both streets encroaching into the planned space for the caisson wall. The long delay and cost of relocating these services was prohibitive to the developer.

The distance between the King façade and gas line appeared to be about 800 mm. The gas line company required 300mm minimum clearance between the gas line and any drilled holes, leaving a 500mm strip in which to fit a smaller shoring system. With this consideration, the idea of using micropiles was born. Moreover, the City would not allow occupancy of a traffic lane on King Street for drill operation, because of the streetcar tracks and heavy traffic, small drills that could work within the limits of the sidewalk would be required.

8. MICROPILE DESIGN

Micropiles were needed to provide foundations for the steel frame and act as soldier piles for the shoring system. Based on the narrow strip available a standard HSS 356 dia x 13 section pipe was selected for all micropiles. Replacing the planned W610 soldier piles with these smaller sections required that the pile spacing be reduced from 2400 to 1500.

To convert the micropiles to act as soldier piles supporting lagging, structural steel tees were welded to their near edge as shown in figure 5. These were installed during excavation in stages to suit each lift of lagging.

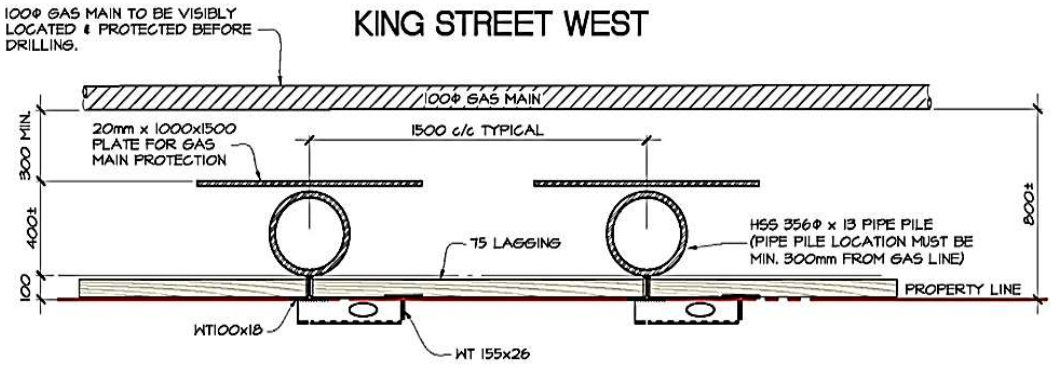


Figure 5. Micropile/Lagging Detail

For the outside frame support, near the curb, each leg generally required a pair of micropiles to resist wind load as illustrated on the Partial Plan (figure 6).

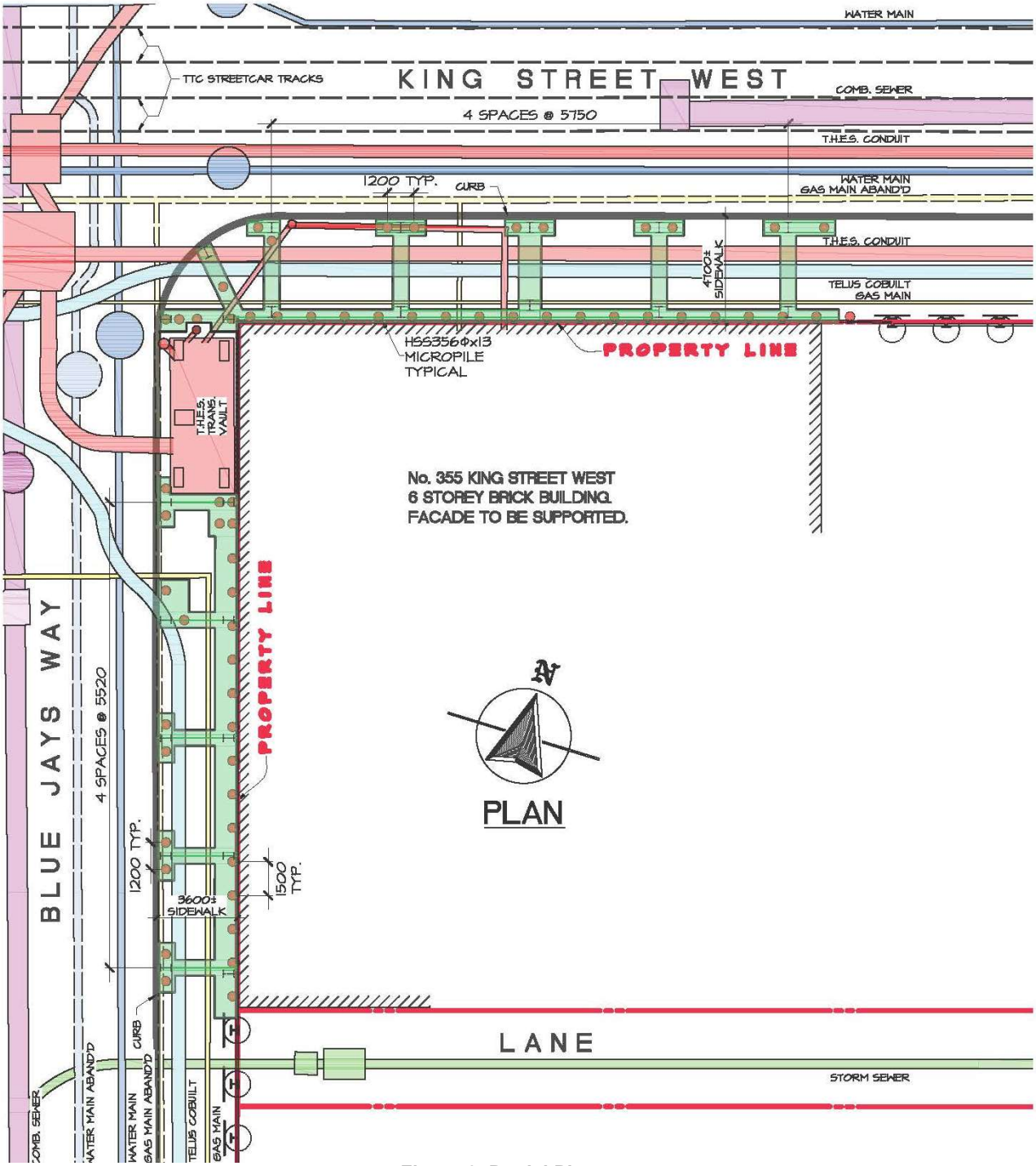


Figure 6: Partial Plan

In a case 1 micropile system, as used on this project, each pile is loaded directly and this load is resisted using the steel members and geotechnical resistance of each separate micropile (FHWA, 2005). Due to the site's high clay content, the micropile grout was gravity fed with no post grout, i.e. Type A micropiles.

The inner row of piles supporting the façade were designed for up to 390 kN of compression load due to the weight of the façade and wind loading, plus the vertical component of the soil and rock anchors. This vertical load was resisted by the 350 MPa steel casings (micropile type A2), and adhesion over the 8.5 m minimum length of the rock socket toe.

The outer row of piles at the curb were designed for up to 250 kN of compression and tension, due to wind loading on the façade, employing the same casing in a 3 m deep socket in sound rock, and then a #18 DYWIDAG Threadbar (517 MPa) advanced down another 3 m to resist tension through rock/grout adhesion. These are type A3 micropiles per FHWA (2005) and were fully encased in the ground, supporting the street side of the façade support frame.

The micropiles were capped by a grid of buried reinforced concrete grade beams set flush with the sidewalk as shown in plan on figure 6 and in section on figure 7. Those grade beams adjacent to the facades were poured directly against the exposed existing foundation walls, and connected by shear pins and pre-stressed tie rods to provide the bonding load transfer mechanism.

9. MICROPILE INSTALLATION

Utilities near each of the pile locations were exposed in advance by hydrovac for accurate location. Steel plates were inserted to protect the gas main, and all the holes backfilled with unshrinkable fill.

Deep Foundations chose suitable hydraulic drill rigs using a Hutte HBR 504FTW and Casagrande C7NG, both of which are capable of swiveling the drill head to work outside the tracks (see figure 8), allowing just a 100mm offset from the façade to outside of micropile holes.

Each rig worked on a separate street, with access to King via the east and Blue Jays via the south, since the large hydro vault near the corner blocked access. A Klemm KR 806-2D short-mast hydraulic drill rig was also brought in to drill underneath TTC overhead wires (4.5m headroom) at the corner of King Street and Blue Jays Way. All three drills used duplex drilling (advancing casing and drill rods simultaneously).

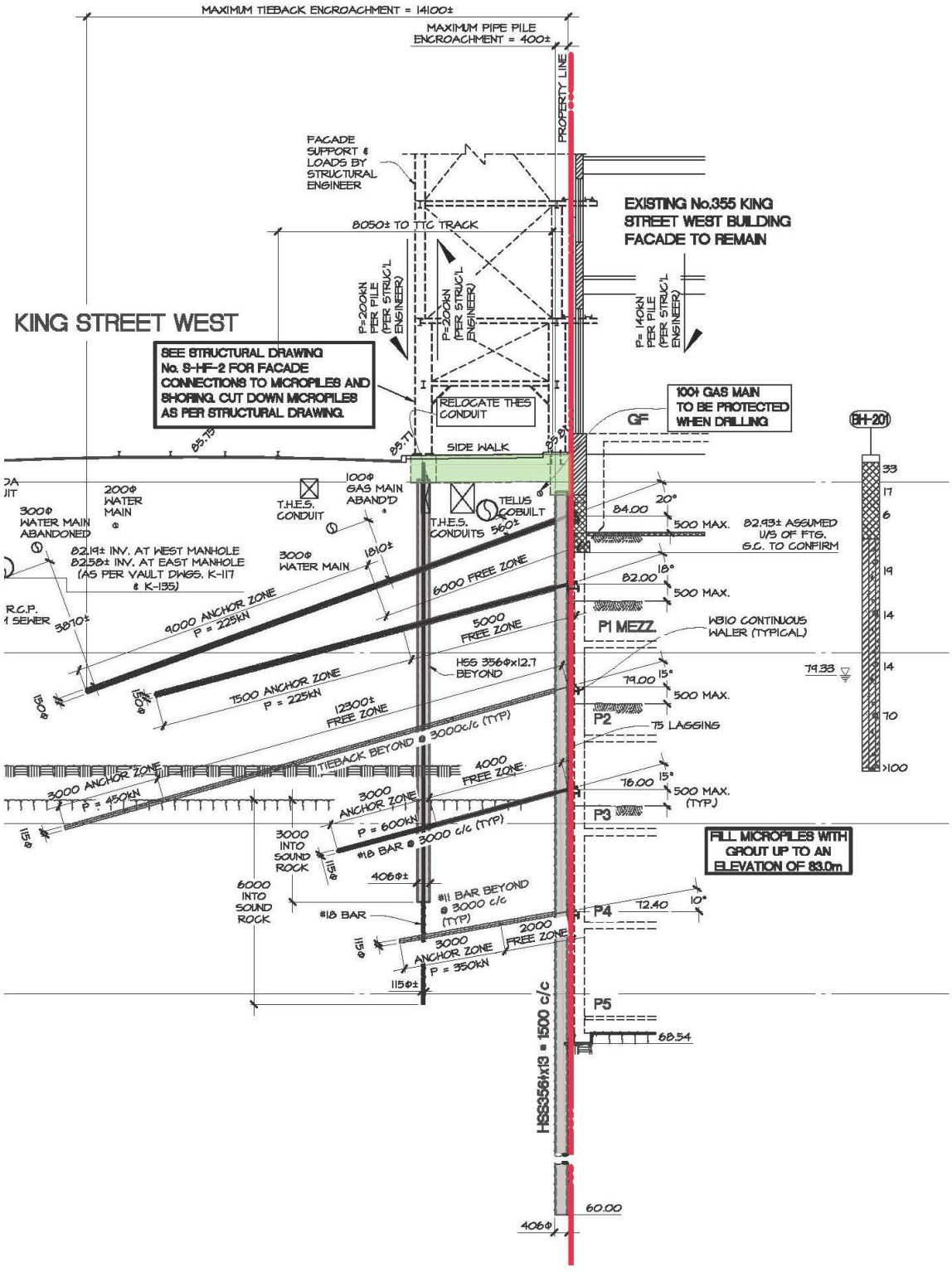


Figure 7. Section through North Façade

A wing bit and/or button bit (depending if the casing was to be advanced into the rock) was attached to a down the hole hammer (DTH) with a shock absorber. This tool measured over 3m in length. The Hutte and Casagrande rigs utilized 3m stainless steel single use HSS 356 dia x 13 starter casing with RH male and female threads, and 2m similar casing thereafter to the specified depths. Drill rods, HSS 219 dia (8 5/8”), were used to advance the DTH.

The Klemm utilized 1m long casing similar to above, and similar drill rods, but only 1m long, to advance the DTH. Casings were threaded together using the dual jaws of the rigs.

The tension threadbar in the curbside micropiles was installed in 3m lengths and connected by coupler.

A platform was constructed with timber mats to protect the utilities and accommodate the mobility of the rigs. Tarping of both the façade and the curbside hoarding provided protection from drilling fluids, which were collected and disposed off-site by means of hydrovac (see figure 9). Concrete was pumped to the drillhole locations due to tight site constraints.

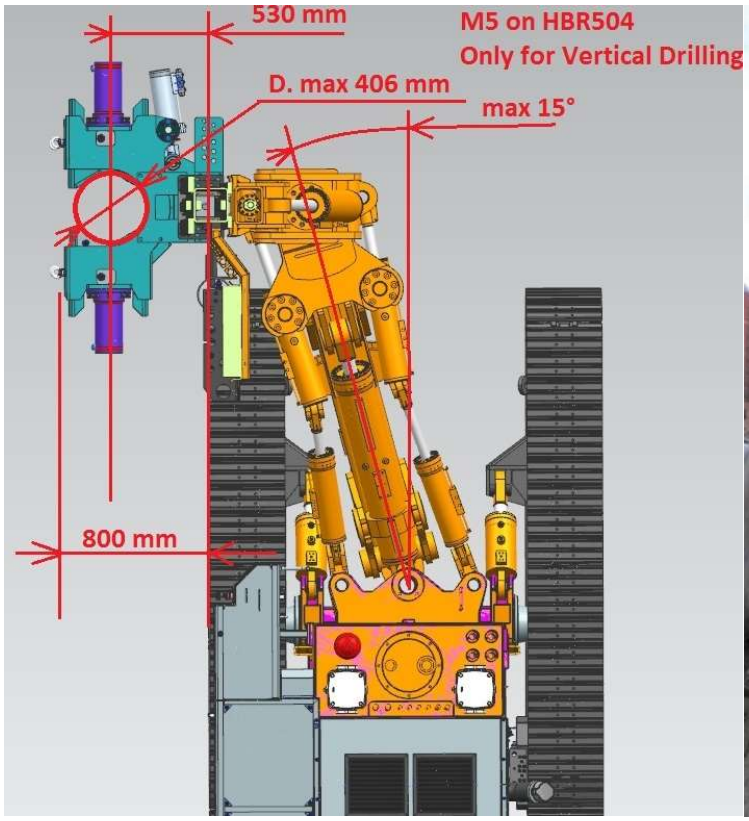


Figure 8. Hutte Swivel



Figure 9. Drilling against the Façade

10. EXCAVATION

Concurrent vertical drilling with conventional large diameter rigs operating from within the remainder of the site (beyond the Westinghouse building) was started for soldier pile and lagging shoring at the streets, and secant caisson walls for additional stiffness at existing neighbouring buildings.

Vertical drilling of micropiles and 1 metre diameter shoring piles began in September 2015 and were completed in January 2016, ready for the façade support frame to be installed and demolition to commence.

Originally seven underground parking levels were planned for the site. This was reduced to five levels during further design developments after most of the vertical drilling was complete.

Excavation and anchor installation began in May 2016. Tees welded to the micropiles allowed use of lagging in a shored face indistinguishable in appearance from standard piles and lagging (see figure 10). The narrow bays and stable clay soils permitted deeper than normal lifts for lagging installation.

Lateral bracing was provided by soil and rock anchors at shallow angles to reduce the additional vertical load added to the compression micropiles (see figure 7). The interaction between compression and bending was checked for each unbraced length of pile at each excavation stage.

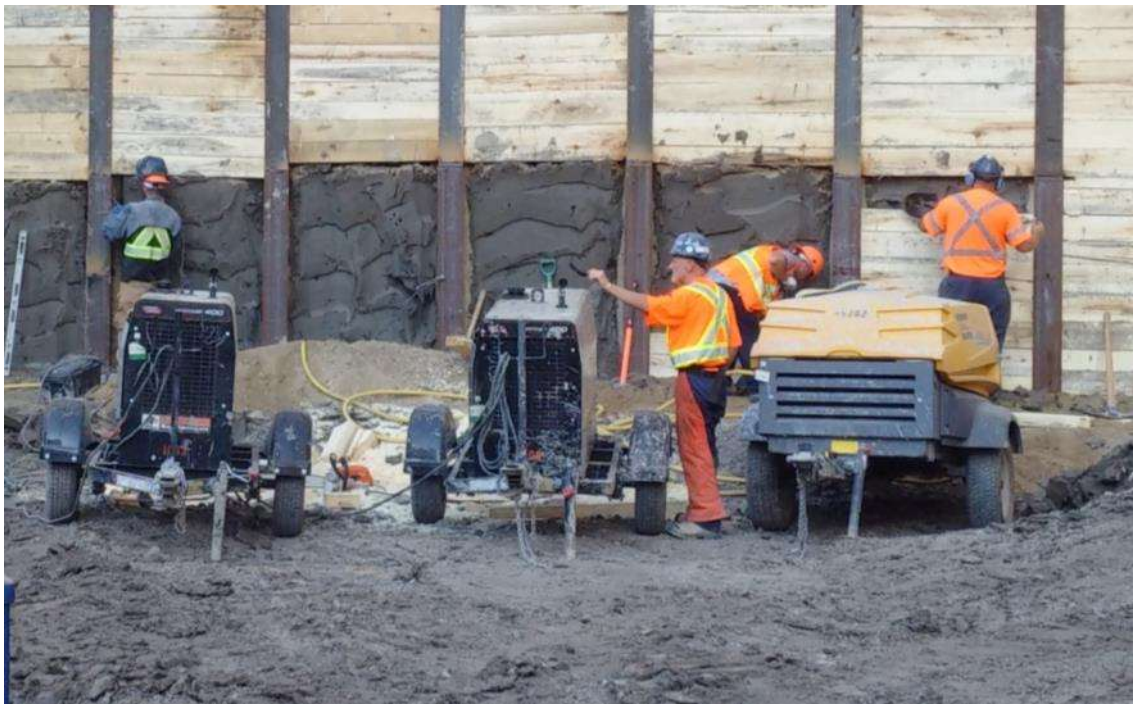


Figure 10. Silty Clay Till Bays ready for lagging

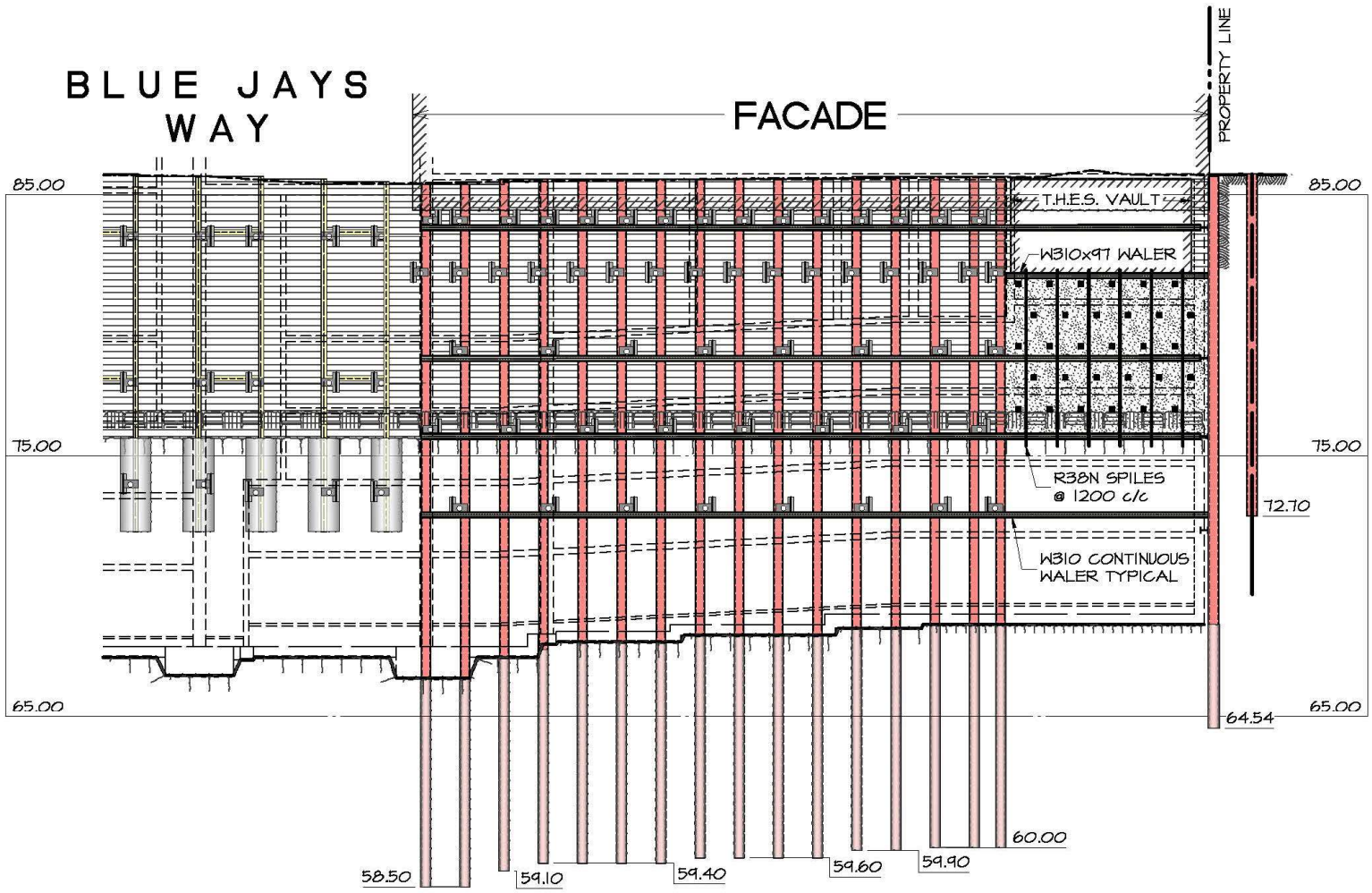


Figure 11. West Elevation

11. ELECTRICAL VAULT

As micropiles could not be installed at the 7 m long electrical transformer vault this area was bridged by the steel frame. The ground below it was supported with sprayed shotcrete, braced by soil nails at 1200 mm centres horizontal and vertical, and reinforced with inclined spiles, also at 1200 mm spacing, and drilled into sound rock (see figure 11).

The photo below (figure 12), taken when excavation reached the rock surface, shows the final lift of shotcrete being sprayed below the vault and the anchor system used. At the north wall a welder is installing the next section of structural tees, preparatory to lagging installation.

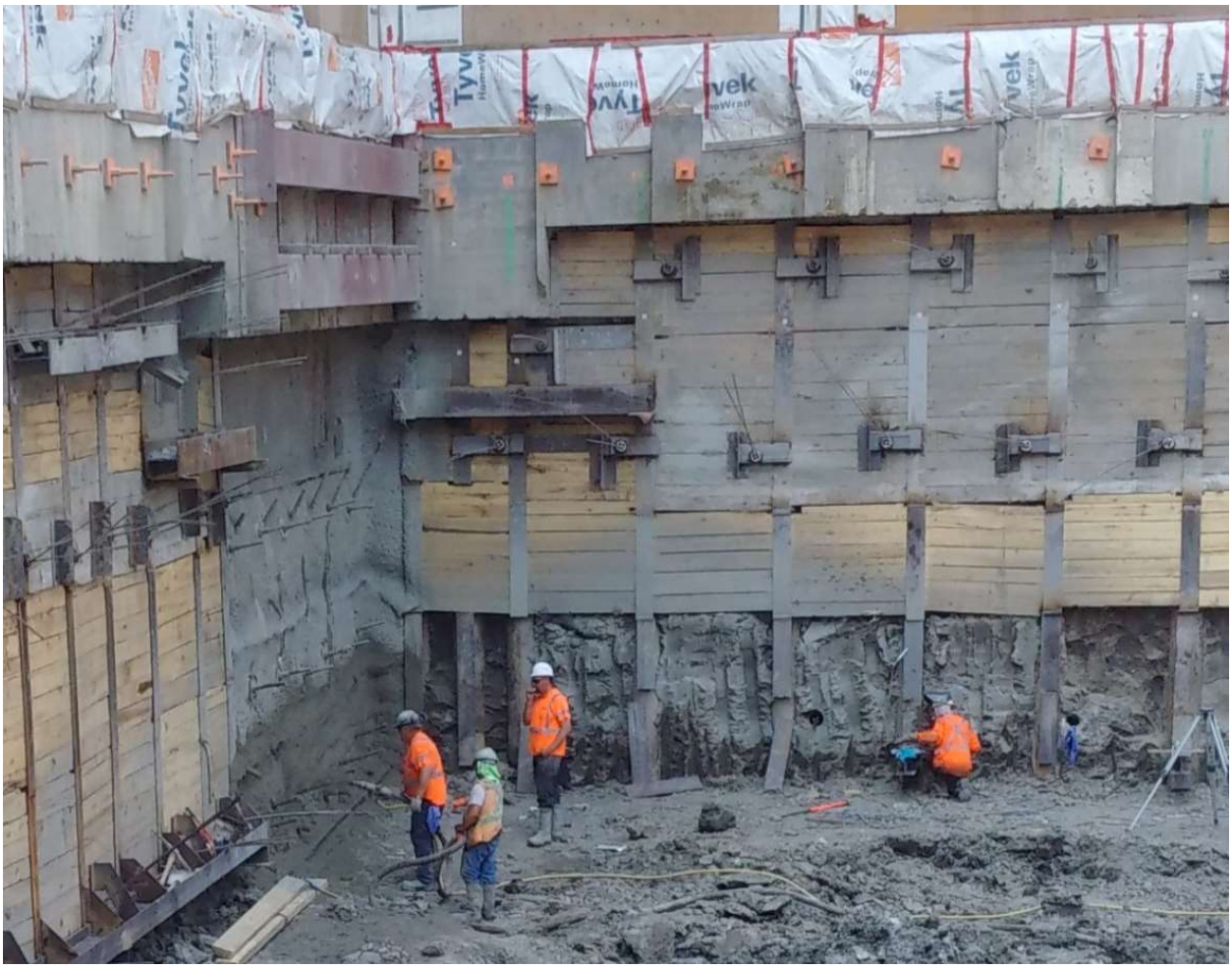


Figure 12. Welding Structural Tees to Exposed Micropile Casings

12. COMPLETED FAÇADE SUPPORT

Final excavation grade was reached in November 2016. Figure 13 shows the supported facade from inside the site. It also shows the frost protection blankets installed below the façade in early November. Construction of the new basements back to road grade is scheduled for completion in June 2017.

The new basement walls will directly underpin the heritage walls, transferring weight to the new structure. The steel frame will remain in place until construction reaches matching height.



Figure 13. Frost Protection under the Façade

13. MONITORING

A detailed monitoring plan was developed to verify the shoring and façade support performance including a combination of monitoring types. Inclinometer and Precision Survey Target locations are marked in the Monitoring Plan in figure 14.

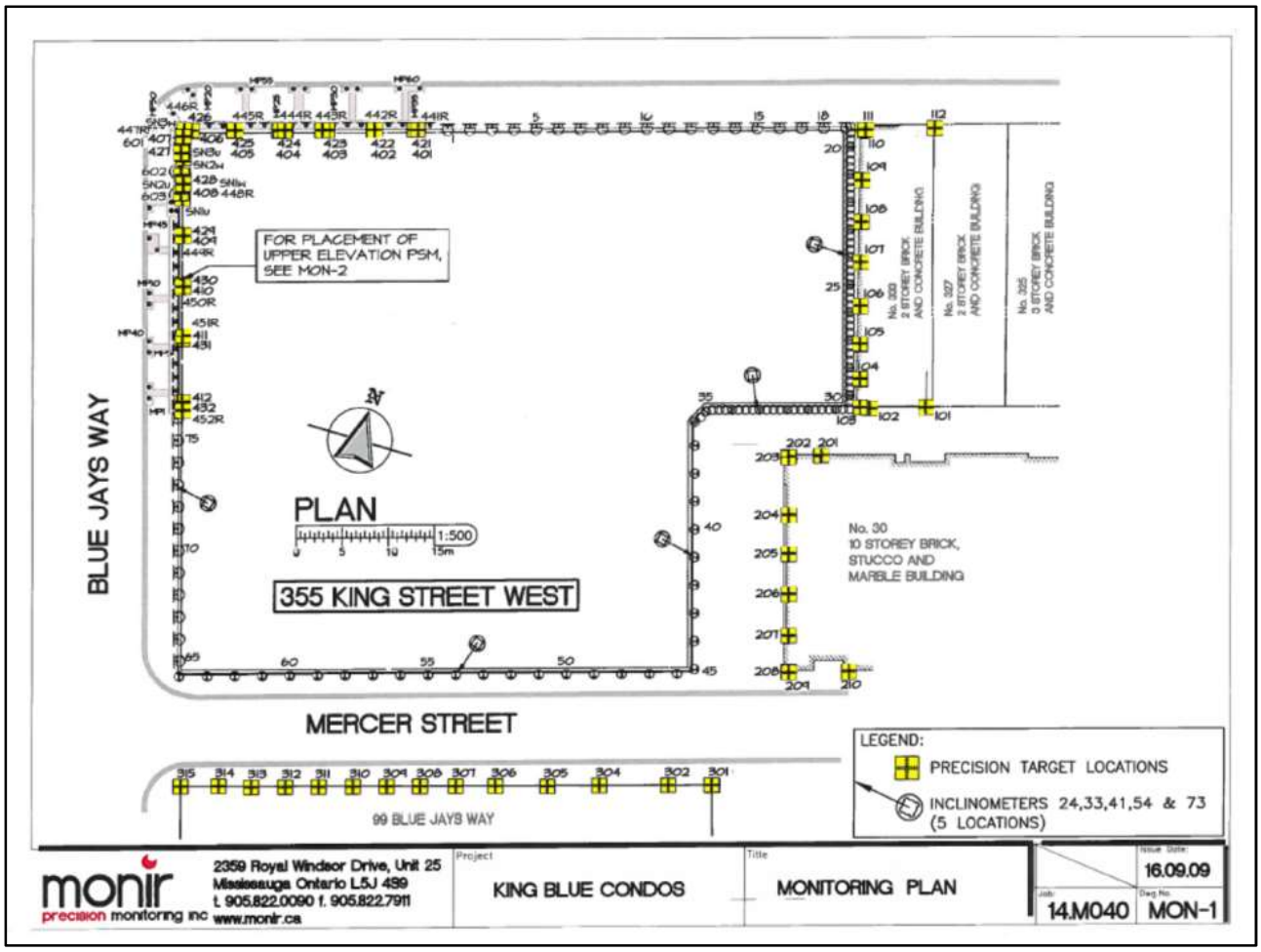


Figure 14. Monitoring Plan

a. Monitoring Types

Precision Survey Monitoring (PSM) targets were placed on the Westinghouse façade at 5 to 6 m spacing to measure horizontal and vertical movements. Targets were located in two rows along the bottom and mid height of the façade. PSM targets were also installed on the transformer vault shotcrete wall and neighbouring structures within the zone of influence.

Pile Target Monitoring (PTM) targets were installed at the top of every shoring pile during the first lift of excavation.

Five Pile Inclinometers were installed on conventional steel soldier piles at various locations around the site but could not be used at the façade support.

b. Monitoring Performance

At the time of preparing this paper the site had been dug to final excavation grade and build out had reached the third basement level. Figure 15 shows current PTM and PSM readings along the façade. Pile target monitoring indicates acceptable shoring performance with movements within the anticipated range. The façade wall shows the least movement at the site corner where it is naturally stiffest. Into site façade movement increases with distance from the corner, reaching a maximum of 38mm, and appears to be independent of micropile movement. Such movement was not predicted, but was deemed to be acceptable by the Structural Engineer.

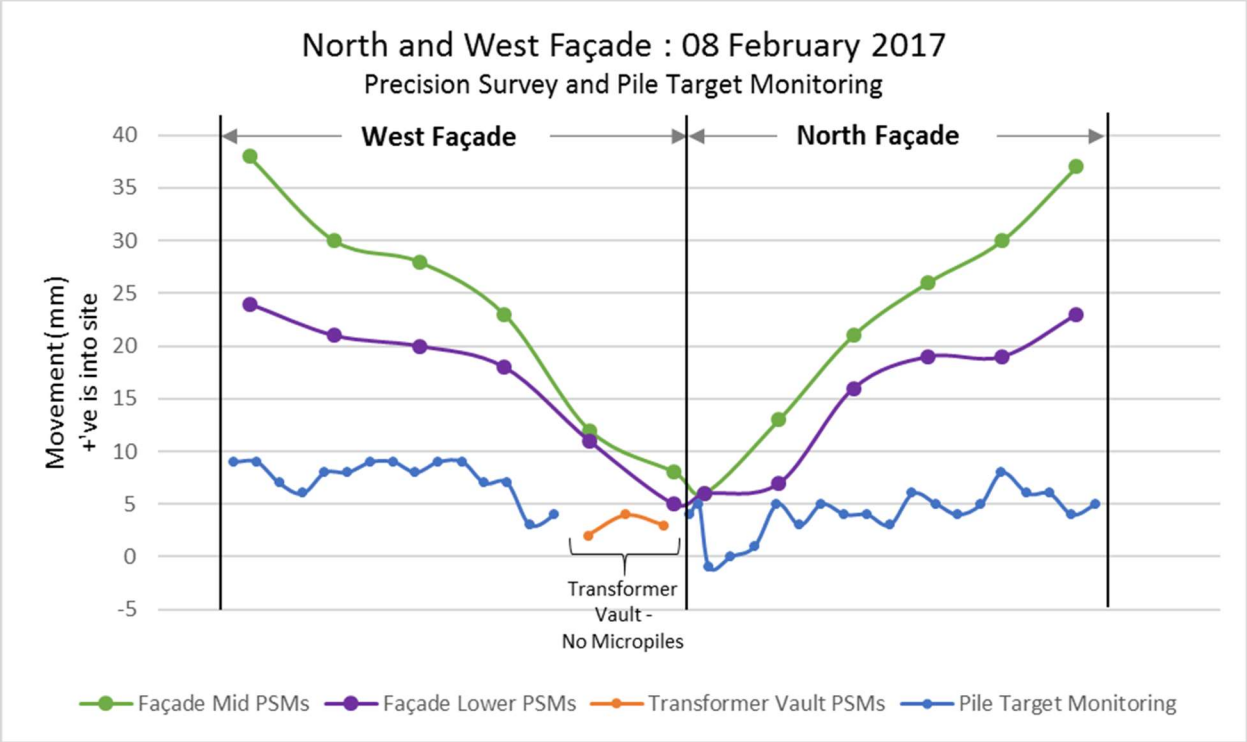


Figure 15. Monitoring Results

14. SUMMARY

Case 1 micropiles were successfully used to replace traditional shoring when inner city congestion precluded large diameter drilling.

In a hybrid system, these piles were to resist tension and compression loads as a foundation for a temporary steel frame façade support, along with bending moment from lateral earth pressure.

REFERENCES

City of Toronto (1992). *Designation By-Law, 355 King Street West,* Toronto, 5 p.

Hütte Bohrtechnik GmbH (no date). *HBR 504 Hydraulic Drill Rig* Brochure, Casagrande Group, Olpe, 12 p.

Sharpe, D.R. (1980). *Quaternary Geology Toronto and Surrounding Area; Ontario Geological Survey Preliminary Map P. 2204, Geological Series.* Scale 1:100 000. Compiled 1980

Toronto Transit Commission, TTC (2014). *All-Typical Business Day Ridership for Surface Routes*, available at http://www1.toronto.ca/wps/portal/contentonly?vgnextoid=34b6c316f16e8410VgnVCM10000071d60f89RCRD

U.S. Department of Transportation, Federal Highway Administration (FHWA) (2005). *Micropile Design and Construction Reference Manual.* Publication No. FHWA NHI-05-039. National Highway Institute, 452 p.

EDIFICIO PIEDRA REAL – CONCEPCION, CHILE
CASE STUDY OF AN UPLIFT REINFORCEMENT PROJECT

Freddy Lopez,

Geotechnical Engineer Friedr. Ischebeck GmbH, Ennepetal, GERMANY

lopez@ischebeck.de

Juan Manuel Fernandez,

Regional Technical Manager Pilotes Terratest S.A. CHILE

jmfernandez@terratest.cl

ABSTRACT

The rapid urban development that Chile has experienced since the early 2000s, has motivated real estate developers to conceive higher buildings and deeper excavation pits, in order to use the available spaces more efficiently.

Chile is among the countries with the highest seismicity in the world, therefore both the structural and the geotechnical design are confronted with complex and challenging conditions, and have to fulfill the safety requirements stablished by the national construction regulations, seeking the best technical and economical solutions.

The implementation of worldwide well known technologies and construction methods, such as micropiling, has enabled designers to come up with optimal solutions in order to satisfy the requirements of the urban development.

The following article presents the case study of the project "Piedra Real", located in Concepcion, the 2nd largest city of Chile. The border conditions of the project, as well as it´s specific geological and geotechnical parameters will be briefly described.

This paper will focus mainly on the geotechnical design of the permanent uplift reinforcement of the building, materialized by self-drilling grouted Ischebeck TITAN micropiles. The design considerations regarding the structural capacity and durability of the reinforcement system will be presented.

Furthermore, the direct interaction of the uplift reinforcement system with other relevant items of the project, such as the temporary shoring of the excavation pit and the temporary ground water lowering, will be discussed.

Finally, an overview of other potential application fields for the case study solution, such as road and railway infrastructure, will be presented.

KEYWORDS

Micropiling, geotechnical design, seismicity, uplift reinforcement, excavation shoring, urban development, infrastructure

1. INTRODUCTION

The project *Piedra Real (Las Heras)* is located in the downtown area of Concepcion (Bio-Bio Region), the second largest city in Chile (Figure 1).

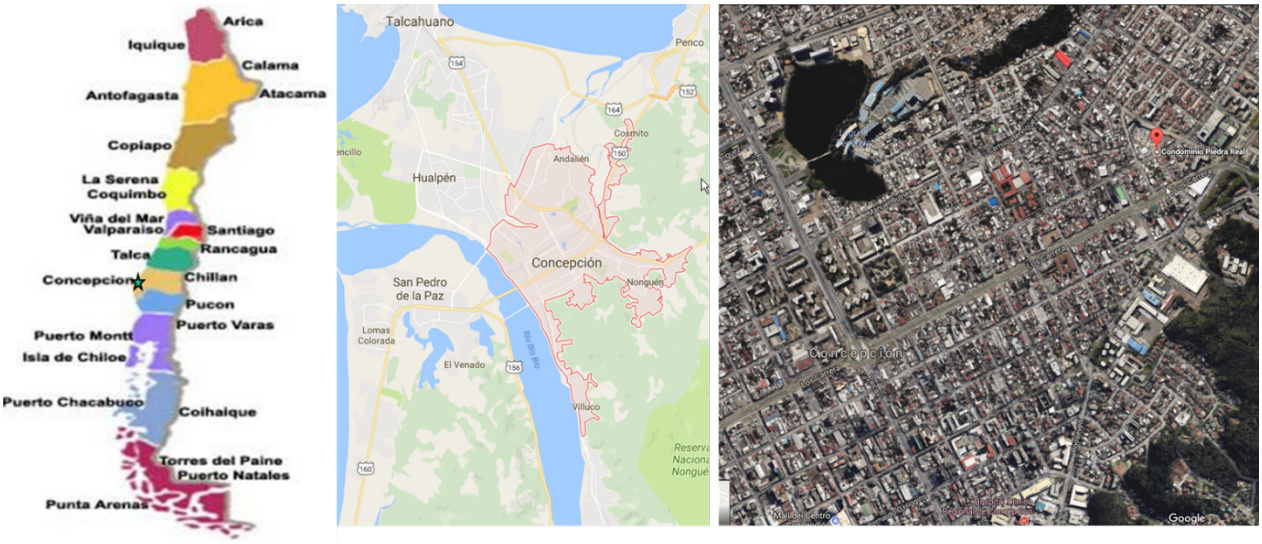


Figure 1 – Location of the Condo Piedra Real (Concepcion, Chile)

The condo consists in four 18-storey buildings, with two underground parking levels. The foundation of the complex was materialized by a reinforced concrete slab, with a surface of about 5680m^2. The projection of the towers occupies about 40% of the total building area (Figure 2).



Figure 2 – Overview Condo Piedra Real (Concepcion, Chile)

The architectural project required a free height of 7.0m for the underground parking levels (measured from the top of the foundation slab).

Due to the local groundwater conditions, the foundation slab is subjected to hydrostatic uplift, which – together with seismic actions – makes necessary a permanent reinforcement of the foundations to absorb the tension forces. The reinforcement was materialized by self-drilling grouted Ischebeck TITAN micropiles.

2. GEOLOGICAL DESCRIPTION

The city of Concepción is built on Tertiary sediments in a valley created by a graben, with metamorphic and granitic formations to the north, east, south, and beneath these Tertiary sediments. The sedimentary valley is depicted along with the 3 major faults that run through the area (Figure 3, [9]).

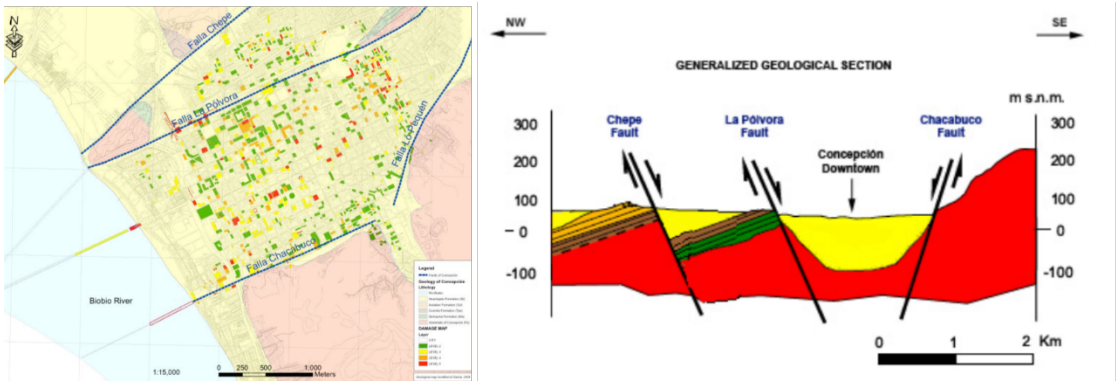


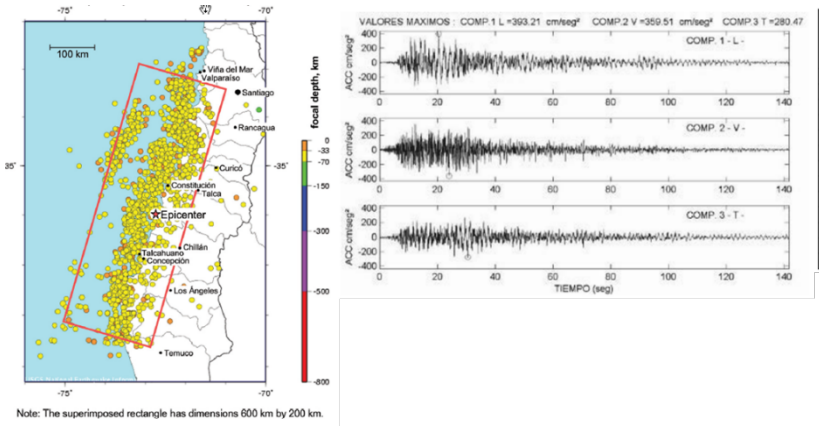
Figure 3 – Geology map and cross-section (NW-SE) of Concepcion [9]

3. CHILEAN SEISMICITY – THE MAULE EARTHQUAKE

Chile is one of the countries with the highest seismic activity in the world. According to the USGS [19], 3 out of the 20 largest earthquakes, recorded worldwide since 1900, have occurred in Chile.

On Saturday 27 February 2010 (03:34 local time) an earthquake with a magnitude (M_w) 8.8 struck the central-south region of Chile, with a following tsunami that hit the coastal areas. This event had a deep impact in the public perception of the high vulnerability of the infrastructure to seismicity, since about 75% of the Chilean population was affected, and an estimated loss of about US$ 30 Billion was caused [4].

The earthquake-induced ground shaking had a total duration of about 140 s, with the strongest part lasting 40 -50 s [1]. In the region of strongest ground shaking, ground accelerations exceeded 0.05g for over 60 s in most of the records, and more than 120 s in the records corresponding to the Concepcion area [6].



Station	Maximum Horizontal Acceleration (g)	Maximum Vertical Acceleration (g)
Santiago Universidad de Chile	0.17	0.14
Santiago Elevated Train Station Mirador	0.24	0.13
Santiago CRS MAIPU	0.56	0.24
Santiago Hosp. Tisne	0.30	0.28
Santiago Hosp. Sotero de Río	0.27	0.13
Santiago Cerro Calán	0.23	0.11
Santiago Campus Antumapu	0.27	0.17
El Roble Hill	0.19	0.11
Viña del Mar (Marga Marga)	0.35	0.26
Viña del Mar (Downtown)	0.33	0.19
Curico Hospital	0.47	0.20
Concepción Colegio San Pedro	0.65	0.58
Valdivia Hospital	0.14	0.05

Figure 4 – Left: Main shocks and aftershocks of Mw ≥ 4 between 2/27/10 and 3/26/10 [1], Middle: Strong motion record of Downtown Concepcion [13], Right: Preliminary Processed Records Maximum Accelerations [6]

Despite the intensity of the earthquake, the majority of the engineered buildings behaved very well and the damages were mostly restricted to non-structural elements, mainly due to the use of appropriate design codes and construction´s practice regulations. However, according to official estimations, about 2.5% of the

engineered buildings suffered severe damage, causing not only their structural failure (total or partial), but also human casualties [18].

Examples of severe damage were observed in Concepcion, mostly in its downtown area, where one building fully collapsed (Alto Rio Tower) and several others had to be demolished due to partial failure at localized floors (Figure 5).



Figure 5 – Alto Rio Tower (fully collapsed, left) and O´Higgins Tower (partially collapsed, right) [2]

Based on field observations of severe damage on mid-to-high rising buildings, it seems that vertical irregularities - due to set-backs in the upper floors or due to stiffness differences of vertical elements (reduced cross-sections of vertical shear walls at the parking levels) - might have triggered the failure of vertical elements, as a result of an induced concentration of stresses (compression and tension), compounded with flexural solicitations experienced during the earthquake [1]. The observed damage has been also associated with site and/or basin effects, ground failure (displacements caused by liquefaction) as well as with the soil classification, that led to define both the design spectra and the foundation type [9].

4. INFLUENCE ON THE DESIGN AND BUILDING REGULATIONS

Chile has experienced a high number of large magnitude earthquakes, and as a result, the relevant Chilean Design Codes: *NCh430.Of 2008* and *NCh433.Of96* have been subsequently updated, based on the lessons learned from past damaging events. The Maule Earthquake wasn´t an exception, and as a result of its occurrence, up to two amendments – in form of decree-laws - have been implemented to update and improve the building practice:

DS N° 60 (December 13, 2011): sets the new requirements for design of reinforced concrete structures, replacing the NCh430-Standard

DS N° 61 (December 13, 2011): sets the new requirements for seismic building design, modifying and/or complementing the NCh433-Standard, regarding the soil classification and the design spectra.

Also other national standards have been implemented, to set the requirements of special geotechnical works, such as excavations: *NCh3206.Of2010*

5. UPLIFT REINFORCEMENT – DESIGN AND IMPLEMENTATION

5.1 Geotechnical parameters of the subsoil

The geotechnical parameters for the construction site were defined by the geotechnical prospection as presented in Table 1.

The groundwater table is located near to the surface, at depths between 1.5m and 3.5m (Average ground water table -2.0m). Due to seasonal fluctuation, it was recommended to consider a design groundwater table at a depth of 0.5m below ground level [8].

Layer	Thickness (m)	γ / γ' (ton/m^3)	ϕ' (°)	c' (ton/m^2)	N_{SPT}
H1: sandy artificial fillings	1.9 - 3.0	-	-	-	-
H2: SM / SP-SM loosen to medium dense	2.7 – 4.5	1.7 / 9.5	28	0.0	10-30
H3: SP-SM / SM dense	Undefined (below 6.0m under ground level)	1.8 / 10.5	40	0.0	40-60

Table 1 – 20 Geotechnical Parameters [8]

The competent soil for the foundation of the structures corresponds to the layer H3, which was classified under category C according to the DS N°61.

5.2 Structural design

The structures were designed in accordance with the above mentioned Chilean Standards NCh433 and the decree-laws DS N°60 and DS N°61.

The towers were conceived with seismic dissipaters installed at the sides (Figure 6), in order to reduce the seismic effects both in the structural and non-structural elements [12].

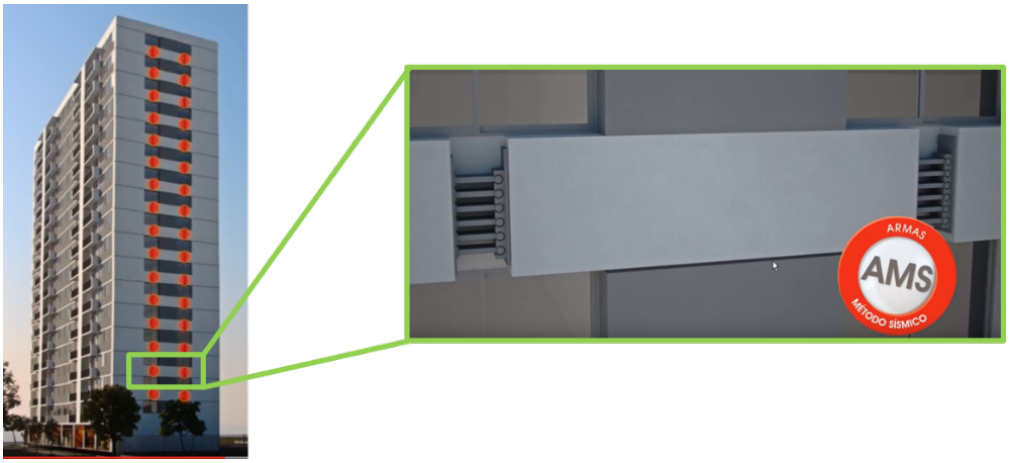


Figure 6 – Seismic dissipaters installed at the sides of the towers [12]

Focusing on the foundation design, the structural analysis resulted in the reinforcement requirement to absorb the following:

a) **Tension loads**, mainly caused by uplift in the areas outside the projection zones of the towers.
b) **Compression loads**, at certain locations under the towers, where the admissible load bearing capacity of the subsoil were exceeded. The reinforcement was materialized by 108 CFA-bored piles (Φ0.6m), however their design is outside of the scope of the present document and will not be further discussed.

The distribution of the required reinforcement is presented in Figure 7 (for half of the structure), and summarized Table 2 (for tension loads)

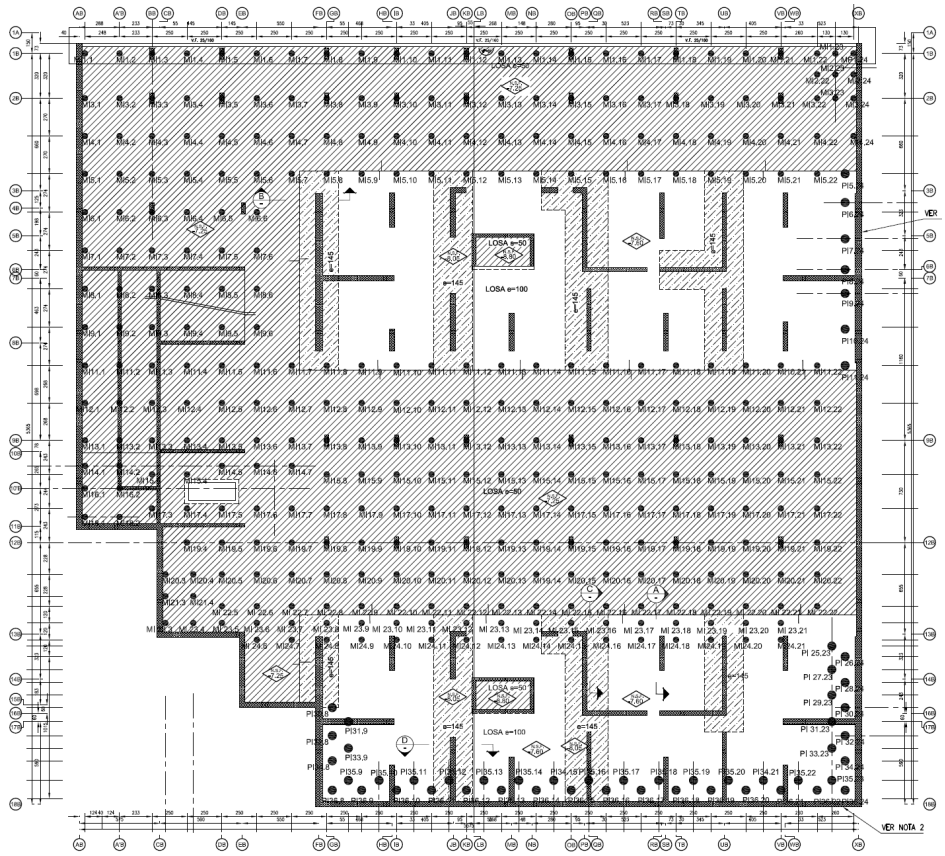


Figure 7 – Distribution of the required foundation reinforcement [16]

Total Quantity	Design (ultimate) load [ton]
516	40
104	53
32	71

Table 2 – Summary of the required reinforcement for tension loads [16]

5.3 Geotechnical design of the uplift reinforcement

There is no official Chilean norm for the design of special geotechnical works, thus the geotechnical design of the reinforcement elements was carried out in compliance with the German Standard DIN 1054:2010-12 and the EAP2007, considering the safety concept based on the *Partial Safety Factor Approach*, where the relationship:

design **E**ffect of actions ≤ **d**esign **R**esistance

$$E_d \leq R_d$$

has to be verified for all limit states (ultimate and serviceability). Figure 8 displays the geotechnical verifications required for the design of the uplift reinforcement and the results are summarized in Table 3.

The reinforcement was materialized with self-drilling Ischebeck TITAN grouted micropiles. Micropiles transfer the loads (tension and/or compression) coming from the structures to the foundation ground over skin friction.

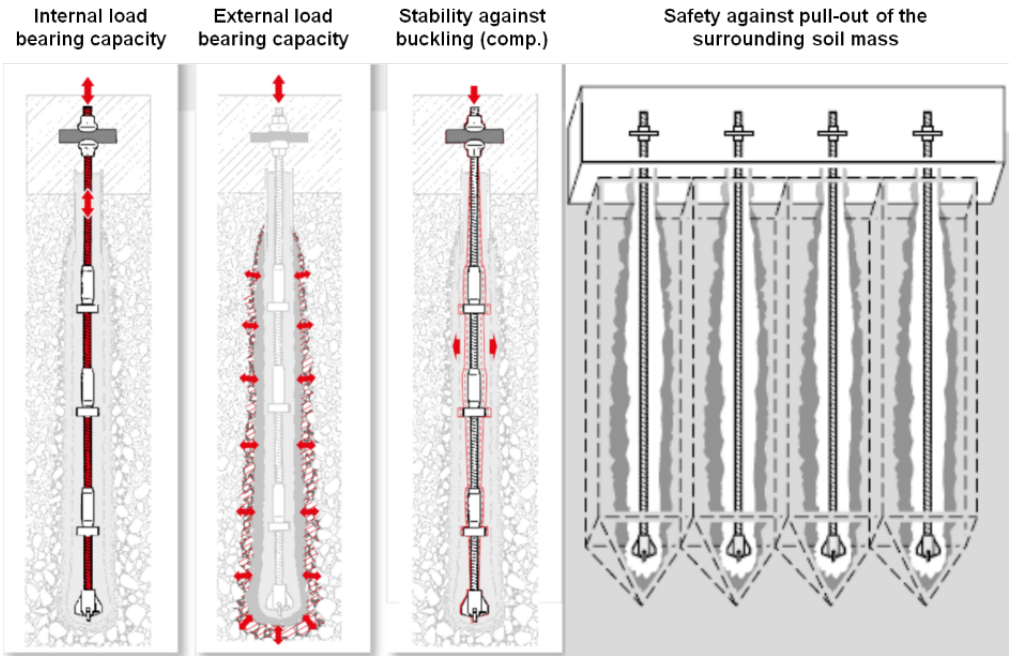


Figure 8 – Geotechnical verifications for the design of micropiles [7]

The TITAN micropiles consist of continuously threaded hollow bars, made out of seamless fine-grained steel pipes (S460 NH), installed via rotary percussive drilling. During the drilling process, the micropiles are continuously grouted (dynamic injection), building a rough interlocking at the interface grout-soil, increasing the skin friction. According to [10], the characteristic skin friction value of $\mathbf{q_{s,k} = 215kN/m^2}$ was adopted for the layer H3.

The components, the installation process and a typical cross-section of the grouted body are presented in Figure 9.

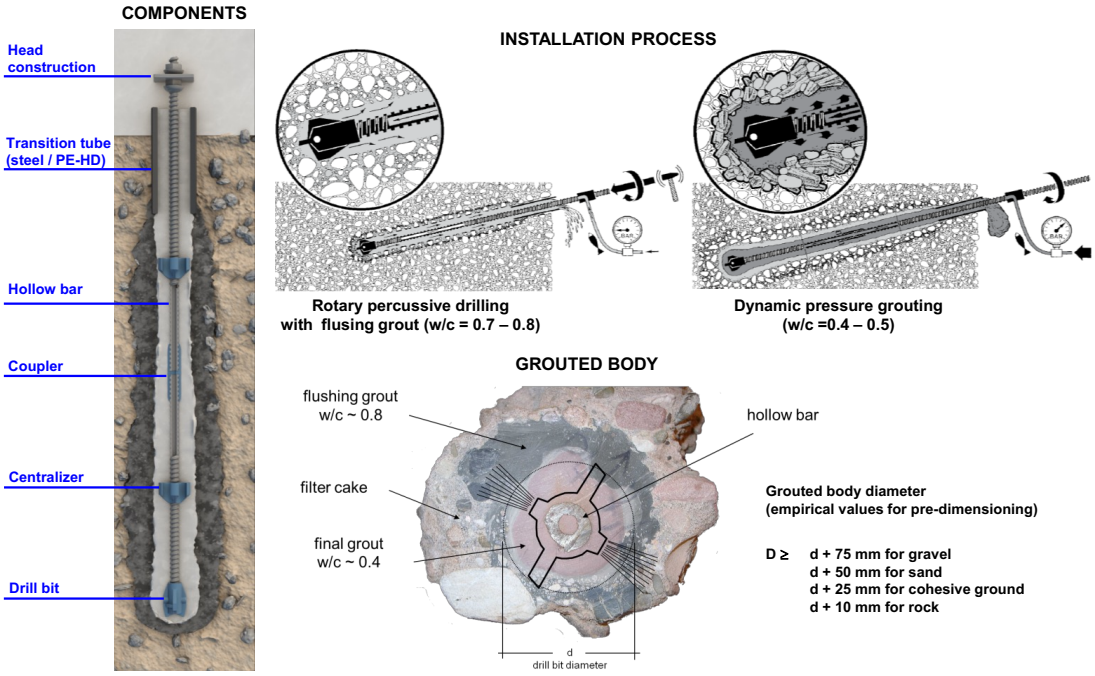


Figure 9 – TITAN System: components, installation process and grouted body [7]

Quantity	TITAN micropile	Design tension load (ultimate)	Load bearing capacity					Pull-out cone
			Internal	External				
		E_d [ton]	$R_{M,d}$ (1) [ton]	d [mm]	D (2) [mm]	L_{min} [m]	R_d (3) [ton]	L (4) [m]
516	40/16	40	41.5	90	140	7.0	44	7.0 – 14.0
104	52/26	53	56.5	130	180	10.0	57	10.0 – 21.0
32	73/53	71	77.3	130	180	10.0	80	10.0 – 13.0

(1) $R_{M,d} = R_{M,k} / \gamma_M$: $R_{M,k}$ according to [11] for a minimal grout covering c = 40mm. γ_M = 1.15 according to [5]

(2) Diameter of the grouted body, with an extension of 50mm (sandy soils,

(3) Figure **9**)

(4) $R_d = \pi * D * q_{s,k} * L / \gamma_p$: $q_{s,k}$ = 215 kN/m^2 according to [10]. γ_p = 1.5 according to [5]. Resistances associated to displacements ≤15mm

(5) Required length depending on the micropiles separation (s_x, s_y)

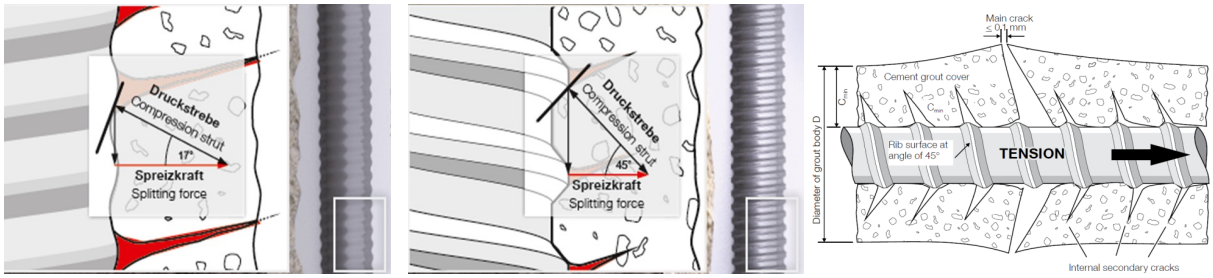
Table 3 – Uplift reinforcement – Design summary [16]

5.4 Durability

For permanent reinforcement systems, the design loadbearing capacity needs to be guaranteed during the serviceability of the planed structures. In the case of micropiles, it must be ensured that the steel load bearing elements are effectively protected against corrosion.

The permanent corrosion protection of 100 years of the TITAN micropiles is provided only by meanings of sufficient grout cover, as highlighted in the National Technical Approval Z.34.14-209, granted by the German Institute of Building Technology (DIBt) [11].

The steel quality and thread geometry of the TITAN hollow bars induce a regular cracking pattern in the grouted body, with crack widths smaller than 0.1mm, considered to be self-healing (Figure 10).



R-thread (acc. To ISO 10208) **TITAN-thread (acc. To EN 10080)** **TITAN-thread (crack width)**

Figure 10 – Cracking pattern and splitting forces on R-threaded hollow bars (left), on TITAN hollow bars (middle) and crack width limitation in the grouted body (right) [7]

5.5 Installation of the micropiles and load tests

The micropiles were installed from the bottom of the excavation pit (Figure 11). Up to three drilling machines were used for the installation: two Tamrock rigs and one Morath drifter (HB70), attached to a telescopic jib (Manitou). The achieved drilling performance was approx. 100m/day/equipment.

After installation, load tests were carried out in order to verify the adopted design considerations, especially regarding the skin friction of the layer H3. Three test micropiles were executed: 1x73/53, 1x 52/26 and 1x40/16. The micropiles were subjected to maximum test loads, equal to 90% of the yield force (at 0.2% elongation) for the correspondent micropile type, without reaching the ultimate limit state of the pull-out resistance (Figure 12). The required safety level and the adopted design considerations were validated. The registered displacements for the design loads were between 9 and 13mm.



Figure 11 – Installation of the micropiles (left) and load tests (right)

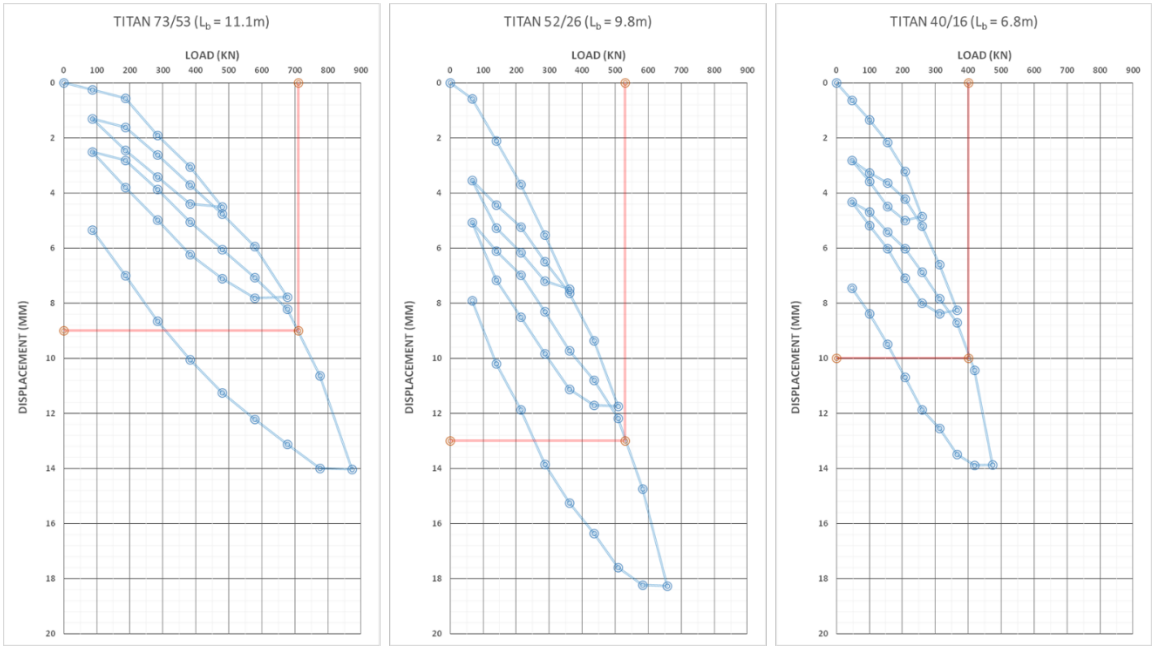


Figure 12 – Results of the executed load tests

According to [11] the required grout cover for the micropiles considered in the design was 40mm, in order to guarantee the permanent corrosion protection. The measurements at the micropiles necks showed grout covers of at least 45mm, fulfilling the requirements for the durability.

6. INTERACTION WITH OTHER RELEVANT PROJECT ITEMS

During the preliminary engineering approach, a 2.5m-thick bottom slab was considered to resist the uplift forces, taking into account the average ground water level. For the planned two underground parking levels, the project required an excavation pit with a free height of 9.5m, and a temporary excavation shoring consisting of an anchored soldier pile wall and a network of well-points to lower the groundwater had to be implemented. The corresponding requirement is schematically presented in Figure 13.

The implementation of the presented uplift reinforcement solution had also a positive effect in the temporary shoring and groundwater lowering, since the excavation depth was considerably reduced to 7.6m, making possible to optimize the design of the above mentioned items (Figure 14).

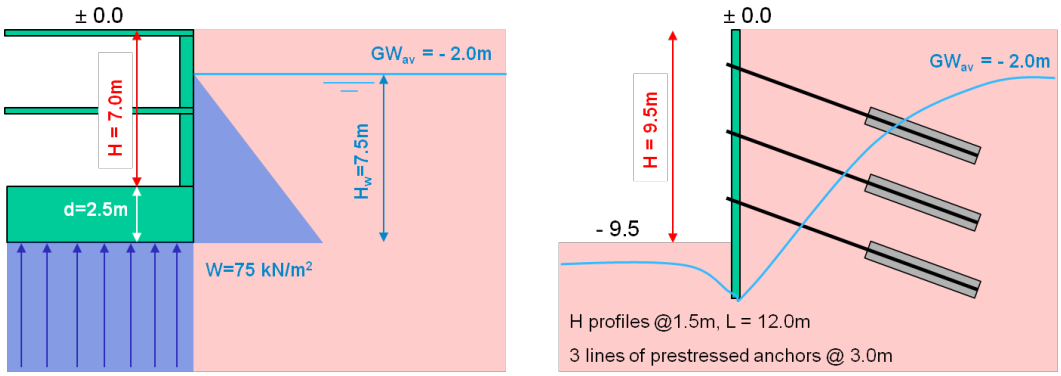


Figure 13 – Preliminary design approach (left) and constructive measures for the temporary excavation shoring (right)

The lateral support for the soldier pile wall was also materialized with TITAN tension piles (passive anchors). This solution was also proven to be more convenient than the originally considered use of strand anchors, since the higher installation speed of self-drilling anchors (>100meter/day) enabled to finish the excavation shoring faster. Furthermore, the installation of anchors and micropiles was carried out using the same equipment, simplifying the logistic at the construction site and reducing its costs (i.e. mobilization).

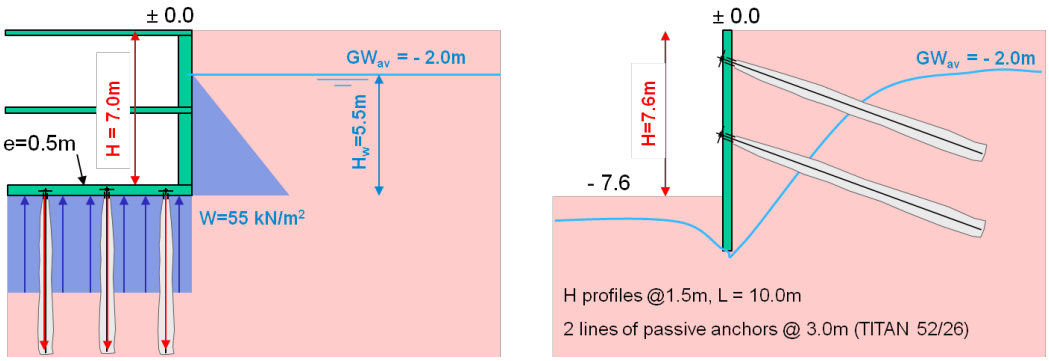


Figure 14 – Adopted design approach (left) and constructive measures for the temporary excavation shoring (right)

7. SUMMARY AND CONCLUSIONS

The present document described the implementation of an uplift reinforcement system for an 18-storey building located in the city of Concepcion-Chile, consisting of self-drilling grouted micropiles.

The difficult board conditions of the project, mainly related to the seismic activity of the region as well as the local geology, imply a high complexity for the design, in order to provide optimal solutions that fulfill the safety requirements stablished by the national construction regulations.

The presented solution highlights the technical benefits of micropiling, showing that its implementation can represent significant reductions on relevant items, such as the requirement of large amounts of reinforced concrete with the associated logistic involved in its time-consuming preparation and installation. Other relevant project items, such as the temporary shoring and groundwater lowering, necessary to materialize underground levels can also be optimized, having a favorable impact in the project as a whole, in terms of structural requirements, execution time and costs reduction.

The opportune interaction between structural and geotechnical designers is required, from the early stages of the planning process on, in order to facilitate and optimize the processes involved in the design.

It is evident that the use of micropiles as uplift reinforcement systems can be applied to other types of infrastructure, such as road and rail underpasses, caissons, tunnels, etc.

8. REFERENCES

[1] Alarcon J. E. and Guillermo Franco, AIR Worldwide. *The 8.8 magnitude Maule, Chile, earthquake - Seismological review and field survey observations* (2010)

[2] Almazan J.L. *Performance of seismic structures during the Maule's Earthquake and its possible effect on the seismic codes in Chile* (2010)

[3] Boroschek R., Soto P., Leon L., Comte D. *Central-South Chile Earthquake February 27, 2010. 4th Preliminary Report. Univ. of Chile* (2010)

[4] Chilean State Secretary for the Presidency. *Reconstruction Assessment, one year after 27/F* (2011)

[5] DIN 1054:2010 -12. *Verification of the safety of earthworks and foundations – Supplementary rules to DIN EN 1997-1* (2010)

[6] Earthquake Engineering Research Institute (EERI). *The Mw 8.8 Chile Earthquake of February 27, 2010 – Special Earthquake Report* (2010)

[7] Friedr. Ischebeck GmbH. *Technical Brochures TITAN Micropiles* (2012)

[8] GEOCAV Ltda. *Soil Mechanics Report Rev. 1, Project Las Heras-Concepcion* (2012)

[9] Geo-Engineering Extreme Events Reconnaissance (GEER) Association. *Geo-engineering Reconnaissance of the 2010 Maule, Chile Earthquake* (2010)

[10] German Geotechnical Society (DGGT). *EAP2007 – Recommendations on Piling* (2007)

[11] German Institute for Building Technology (DIBt). *National Technical Approval Z-34.14-209 TITAN Injection Piles* (2010)

[12] Inmobiliaria ARMAS. *Project exposé (http://www.iarmas.cl/proyectos/piedra-real).*

[13] Midorikawa S., Miura H. *Strong Motion Record Observed at Concepcion During the 2010 Chile Earthquake - 8th International Conference on Urban Earthquake Engineering* (2011)

[14] NCh430.Of 2008. *Requirements for the design of reinforced concrete structures* (2008)

[15] NCh433.Of96. *Earthquake resistant design of buildings* (1996)

[16] Pilotes Terratest S.A. *Design Report for the Foundation Reinforcement Rev. A, Project Las Heras-Concepcion* (2013)

[17] SIRVE S.A. *Design tension and compression loads acting on the foundation slab, Las Heras* (2013)

[18] Technological Development Corporation (CDT-CChC). *Seismic Protection of Structures – Technical Document Nr. 29* (2011)

[19] United States Geological Survey (USGS). *Earthquake Lists, Maps & Statistics (https://earthquake.usgs.gov).*

Micropiles Counter Unbalanced Loading During Partial Building Demolition

Helen Robinson, P.E. and Nate Dumas, P.E., Schnabel Engineering, Donna Adams, P.E., Dunbar Milby Williams Pittman and Vaughan

ABSTRACT

A new facility was constructed to replace the existing VCU Children's Hospital of Richmond Pavilion. The existing building consisted of two full floors below grade with one floor above grade on the south side and four floors above grade on the north side. As part of the proposed construction of the new Pavilion, the southern portion of the existing Pavilion was demolished and replaced with a new structure with four below-grade levels. This demolition and excavation resulted in unbalanced lateral earth pressures on the remaining portions of the building, and affected the structure's wind and seismic resistance. In addition, the portion of remaining structure adjacent to the new excavation would need to be underpinned to prevent instability to the 2 additional below grade floors. To remedy this condition, a system of concrete shear walls and buttresses were constructed inside the existing building to provide the required building bracing for lateral loads. A network of tiebacks and micropiles was conceived to provide the necessary lateral and vertical support during demolition and excavation. This paper discusses the rationale for selection of this system and describes the general design procedure followed, which involved tight collaboration between the structural and geotechnical engineer. Construction and quality control are also discussed.

INTRODUCTION

The 59,500 sq m (640,000 sq ft) VCU Health Children's Hospital of Richmond Pavilion is the largest, most advanced outpatient facility dedicated to children in the region and serves as a gateway to the VCU Medical Campus in Downtown Richmond, Virginia (Figure 1). The Children's Pavilion was redesigned from its existing four stories above grade and two below (Figure 2), to 11 stories above grade and 4 stories below grade, and encompasses more than two-thirds of a city block. The new construction extended 16.8 m (55 ft) below Broad Street, or 10.7 m (35 ft) deeper than the lowest grade of the existing Pavilion. The design needed to include potential future expansion of up to seven more floors above grade and expansion of the below-grade levels to the north. Additionally, the existing pavilion had to be kept operational throughout construction. Dunbar Milby Williams Pittman & Vaughan (DMWPV) provided structural engineering and Schnabel Engineering provided geotechnical and geostructural engineering for this significant project. The two firms collaborated on the design of the structural support and underpinning of the existing adjacent pavilion building. Nicholson Construction was the specialty subcontractor for the installation of micropiles and tiebacks.

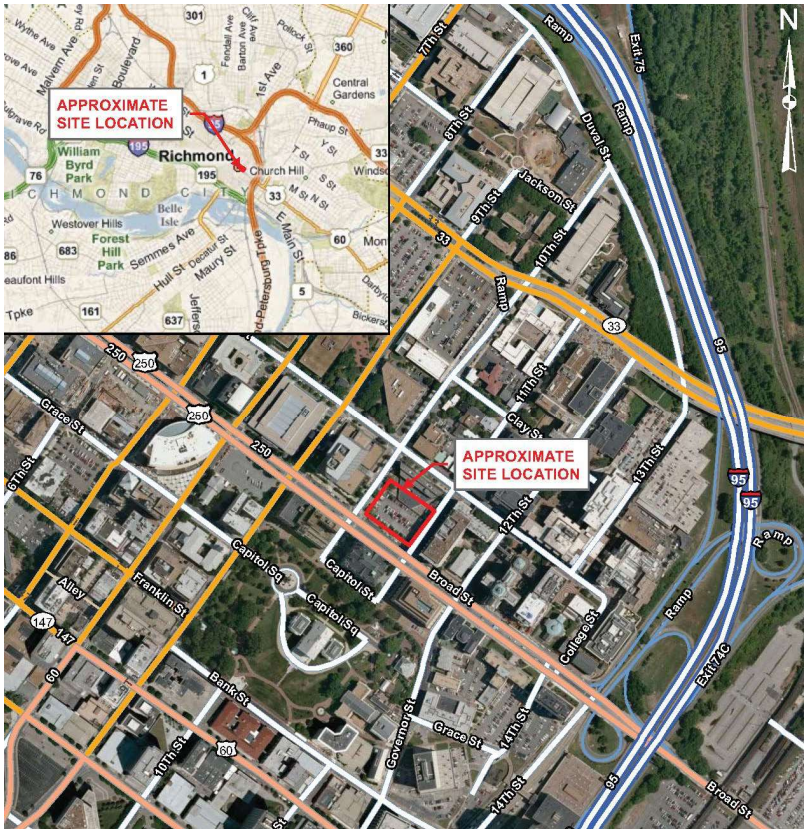


Figure 1. Site vicinity



Figure 2. Existing Building Prior to Demolition (credit Elmquist)

The first phase of construction for the Pavilion included demolishing the southern half of the existing Children's Pavilion (cut along Column Line D), see Figure 3, and installing the new Support of Excavation (SOE) pit south the existing building cut plane. The urban environment, deep excavation and necessity of keeping the Pavilion in service throughout construction created many structural, geostructural and geotechnical design challenges, chiefly: working space was limited and cluttered with utilities; deflection of nearby structures had to be limited to a very small magnitude; the foundation design had to account for future vertical expansion; and the time that the excavation was open had to be kept to a minimum.

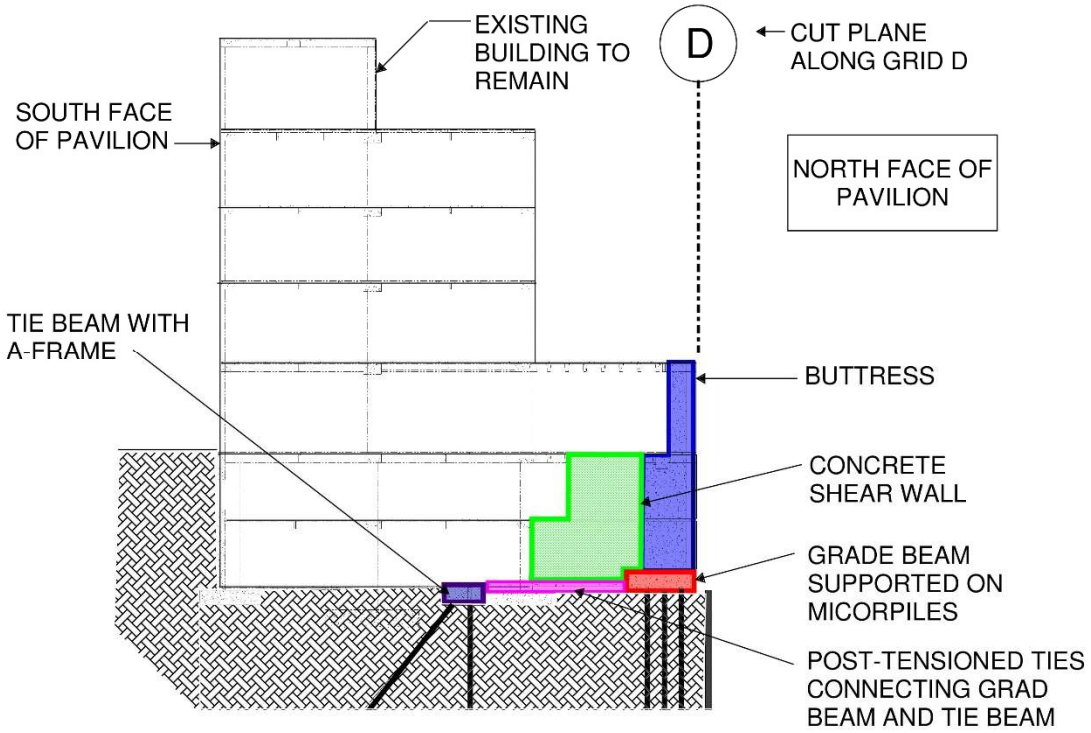


Figure 3. Elevation View of System

GEOLOGY

The geologic stratigraphy in downtown Richmond typically consists of Pleistocene Age terrace deposits, Miocene Age Calvert Formation, Eocene Age sands, Cretaceous Age sand and gravel, and residual soils and rock of the Petersburg granite formation. The terrace deposits are alluvial soils that typically consist of a mixture of clay, silt, sand and gravel exhibiting moderate strength and compressibility. The Calvert Formation consists of marine-deposited sediment. These soils exhibit moderate to high strength and low to moderate compressibility. The Eocene and Cretaceous Age soils are also marine sediments that typically exhibit high strength and low compressibility. Residual soils are derived from the chemical and physical weathering of the underlying parent material, the Petersburg granite rock.

Figure 4 shows the stratigraphy on site. The existing parking lot portion of the site has several feet of existing fill below the ground surface. Samples of the fill contained debris suggesting one or more structures were, at one time, located within this area of the site. This observation is supported by the Environmental Impact Report for this project prepared by others which references multiple buildings previously occupying the site including the Broad Street Methodist Church. Several borings encountered concrete obstructions at the bottom of the existing fill. These obstructions may indicate that the now-demolished structures had basements. Table 1 shows the properties considered for each soil layer.

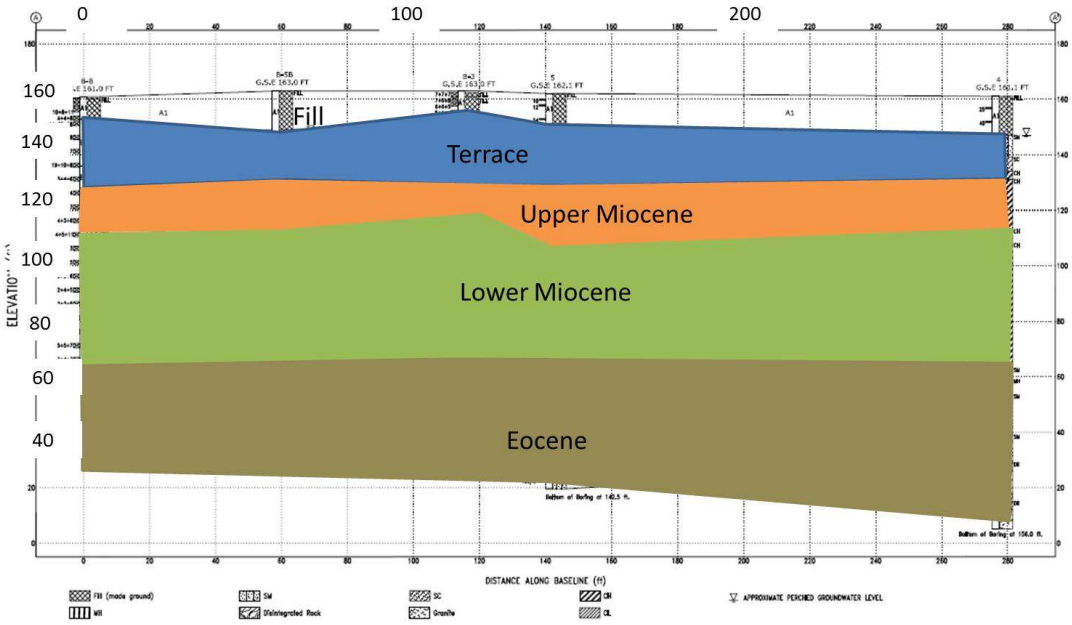


Figure 4. Site Stratigraphy

Table 1. Cohesionless and Cohesive Soil Properties

Name	γ_{unsat} kN/m^3[pcf]	γ_{sat} kN/m^3 [pcf]	v' [-]	E' MPa [psf]	c' [psf]	ϕ' [°]	K_o [-]
Stratum A1 - Coarse-Grained Fill	18.8 [120]	19.3 [123]	0.35	9.6 [200,000]	0	32	0.5
Stratum B1 - Coarse-Grained Terrace	18.8 [120]	19.3 [123]	0.35	19.2 [400,000]	0	35	0.5
Stratum E - Eocene	20.4 [130]	20.9 [133]	0.35	23.9 [500,000]	0	40	0.5
Stratum F- Cretaceous	21.2 [135]	21.7 [138]	0.35	35.9 [750,000]	0	42	0.5
Stratum G - Disintegrated Rock	22 [140]	22.5 [143]	0.35	47.9 [1,000,000]	0	45	0.5

Name	γ_{unsat} kN/m^3[pcf]	γ_{sat} kN/m^3 [pcf]	Cc [-]	Cs [-]	c' kPa [psf]	ϕ' [°]	Su kPa [psf]
Stratum B2 - Fine-Grained Terrace	18.1 [115]	18.5 [118]	0.39	0.015	4.8 [100]	30	96 [2,000]
Stratum C2 - Fine-Grained Upper Miocene	18.1 [115]	18.5 [118]	0.39	0.015	4.8 [100]	30	120 [2,500]
Stratum D - Fine-Grained Lower Miocene	15.7 [100]	16.2 [103]	0.525	0.020	12 [250]	31	239 [5,000]

STABILIZATION OPTIONS AND LOAD PATH

The existing structure that would remain in place was modeled using Autodesk Revit and REM FEM analysis software. Multiple stability options were considered, including new internal concrete shear walls, new steel braced frames, exterior steel trusses on the north face, new exterior cast-in-place augercast piles integral to a new retaining wall on the north face, and combinations of each of these solutions. The best option was not solely cost-driven. The owner's desired use of part of the structure during construction, encroachment limits due to easements on the northern exterior of the structure, and minimizing disruptions to the surrounding structures were all taken into account. It was determined that the best option to support lateral loads on the existing building during the partial demolition and adjacent excavation would be seven new 2.7 m by 2 m (9 ft by 6.75 ft) full height concrete columns along the cut plane, each with an integral 0.6 m (2 ft) thick concrete shear wall perpendicular to the line of demolition. These large columns, referred to as buttresses, would be supported on a continuous grade beam the entire length of the existing structure at the face of the cut plane on Column Line D. Support of the grade beam and buttresses during the adjacent excavation required a pile system designed jointly by the geotechnical and structural engineers (Figure 5).

The structural engineer determined the lateral loads that needed to be resisted at each level and distributed the loading to the seven new concrete buttresses located along the cut plane and their adjacent concrete shear walls. The new buttresses were spaced 7.3 m (24 ft) on center to match the existing grids and columns. Connections to the new concrete elements were designed and detailed. Finally, a continuous grade beam along the cut plane was initially modeled to support the loads. If an adjacent excavation were not required, the grade beam would be sized for the allowable soil bearing capacity. Additionally, soil friction between the grade beam and soil was not sufficient to resist the lateral loads imparted by seismic and wind load and the unbalanced soil load on the existing structure. In order to support the grade beam below the bottom of the excavation as well as provide resistance to lateral loading, micropiles were utilized. Micropiles also met the restrictions for tight access and low headroom with a clear span of less than 2.8 m (9.2 ft) on the existing lowest level.

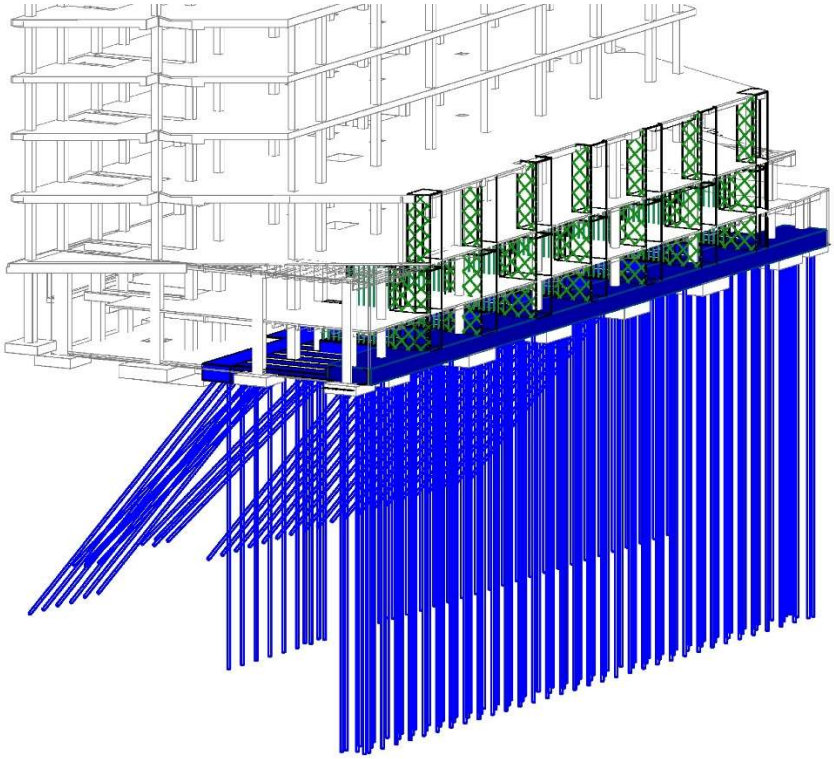


Figure 5. Selected Stabilization Option

FOUNDATION LAYOUT AND STIFFNESS

The maximum service loads were 3560 kN (800 kips) vertical and 1780 kN (400 kips) lateral at each new buttress. An initial approach was formulated between the geotechnical and structural engineers to install micropiles at 1.8 m (6 ft) on center along the length of the building cut plane to support the vertical services loads. This spacing was driven by the spacing of the soldier piles and tiebacks for the SOE. The micropiles along Column Line D were centered between the tiebacks to avoid a conflict.

A range of micropile diameters, with maximum capacities and spring constants, were provided to the structural engineer. This data was used to model the size of grade beam necessary to support the new lateral stability elements. The grade beam's stiffness, along with the micropile's spring constant, were used to determine both the vertical load distribution to the micropiles and the building settlement at the cut plane once the pit was installed. It was an iterative process. As the new grade beam got stiffer, the vertical loads were redistributed to the micropiles and the building settlement was altered. This change would adjust the length of micropiles required and their respective spring constant. After four iterations, it was determined that the grade beam's vertical loads would be supported on 95 vertical micropiles with a 427 kN (96 kip) capacity and a spring constant of 505 kips/in. A 178 mm (7 in) diameter casing with an 552 MPa (80 ksi) yield strength was used with a #14 epoxy coated center bar with a yield strength of 517 MPa (75 ksi). The casing extended for the full unbonded length (see Figure 6).

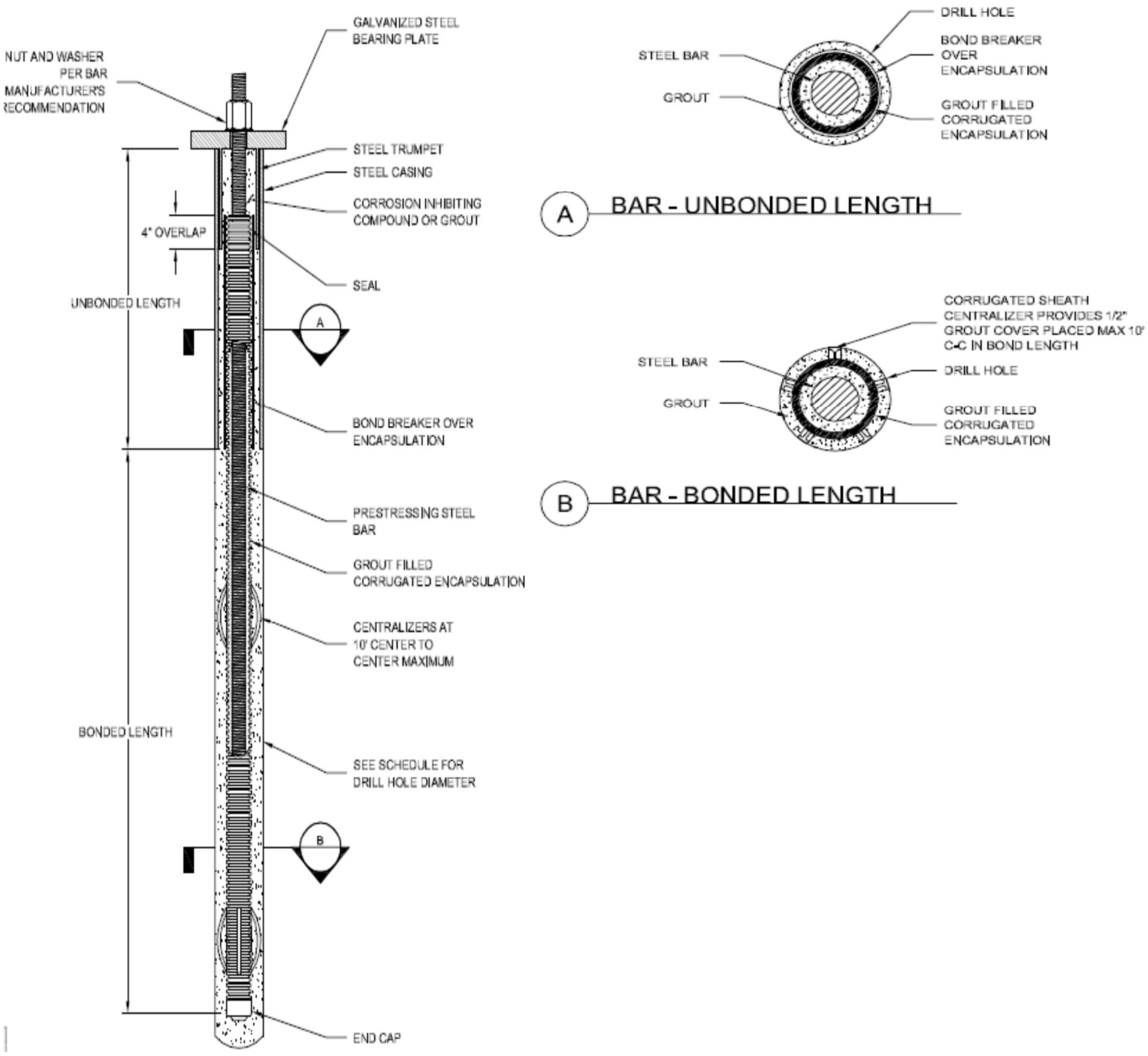


Figure 6. Micropile Details

This solution supported the vertical loads at Column Line D below the SOE, but did not address the lateral loading requirement. Ideally, battered micropiles would be installed through the new grade beam; however, the proximity of the SOE tiebacks precluded this option. Additionally, the battered piles would need to extend beyond the passive wedge formed by the 16.7 m (55 ft) deep bottom of excavation, making the battered piles much longer than would be needed for bonding into competent soils.

Installation of a post-tensioned battered pile coupled with a vertical micropile was determined to be the ideal solution. This A-frame system was located approximately

9.1 m (30 ft) away from the building cut plane and in line with the vertical micropiles along the front grade beam. A horizontal tie beam consisting of two post-tensioned tierods was used to transfer the lateral loads from the cut plane back to the line of A-frame micropiles (Figures 7 and 8).

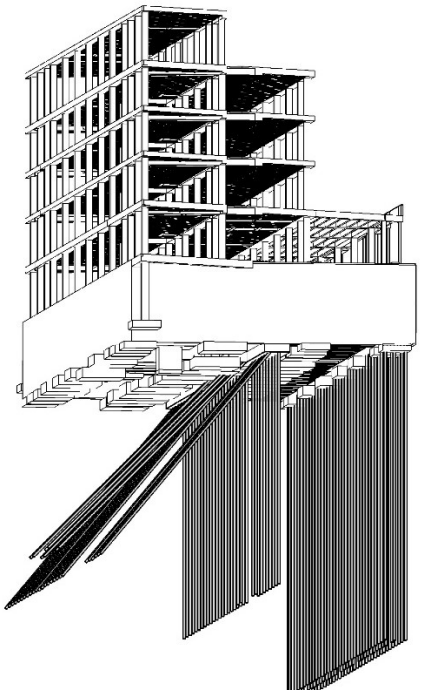


Figure 7. 3D View of Foundation Layout

In a similar fashion to the vertical load distribution, the stiffness of the new tie beam housing the A-frame piles was analyzed iteratively to determine how the lateral loads would be distributed to the coupled micropiles. As the grade beam size was adjusted for ideal load distribution, the coupled micropile capacities and spring constants were updated to reflect actual loads along each frame. Eventually, the ideal solution based on the coupled micropile lengths, battered pile installation angle for lateral load resistance, and stiffness of the front grade beam were determined. The final design included 34 coupled battered pile assemblies connected to 30 horizontal tie beams containing a total of 60 horizontal post-tensioned tierods.

The maximum horizontal load for most areas was 298 kN (67 kips) per 1.8 m (6 ft) width. Due to the inability to access and install micropiles around the existing elevator pit, the adjacent horizontal loads in those areas were 1014 kN (228 kips) per 1.8 m (6 ft) width. The design load of the vertical micropiles was 578 kN (130 kips) in compression, and the design load of the battered micropiles was 578 kN (130 kips) in tension (pre-stressed). The vertical piles consisted of a 178 mm (7 in) diameter, 552 MPa (80 ksi) steel casing with a #18 epoxy coated center bar with a yield strength of 517 MPa (75 ksi). The battered micropiles were designed as 44 mm (1.75) in All-Thread bar with a 1034 MPa (150 ksi) yield strength and Class I corrosion protection according to the Post-Tensioning Institute (PTI). Nicholson elected to use a four strand anchor rather than a solid bar for ease of tensioning.

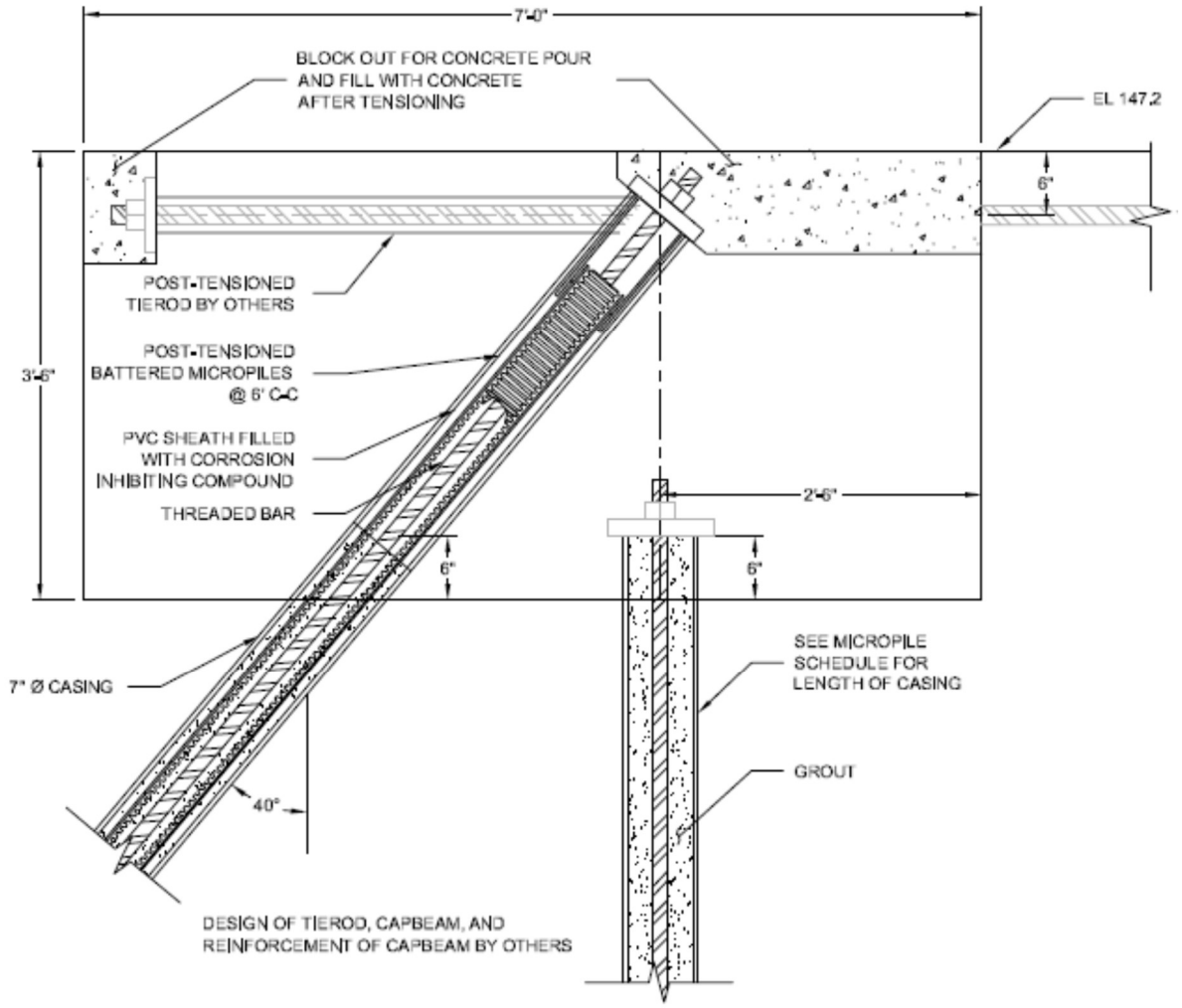


Figure 8. Battered and vertical micropile A-frame

INSTALLATION SEQUENCE

In order for the system to work as intended, an installation sequence was specified. All vertical and battered micropiles were installed before any new construction progressed. Once the micropiles were installed (see Figure 9), the new grade beams, shear walls, and buttresses were constructed. In addition, the horizontal post-tensioned ties were cast into the new tie beam and tensioned after the concrete had achieved the specified strength. This was done prior to advancement of the adjacent excavation in order to reduce movements. Lastly, the structural connections between the buttresses and shear walls were installed. Once this was complete the battered piles in the A-frame systems were tensioned and the portion of the structure to be demolished was removed.



Figure 9. Micropile Installation

MICROPILE BOND LENGTHS

The micropile bonds lengths and load transfer ratios were designed based on the results of tension load tests performed on four tiedowns installed from the Pavilion parking lot. The tiedowns were cased through the overburden soils and bonded 3 m (10 ft) into the desired stratum, whether terrace deposits, upper Miocene, lower Miocene, or a combination of upper and lower Miocene. A 140 mm (5.5 in) drag bit was used and the tiedowns were first gravity-grouted and then globally post-grouted in two stages using a sleeved-port pipe system. The test load was increased incrementally until geotechnical failure of the tiedown or until the maximum safe test load was reached.

Prior to installation of production piles, two sacrificial verification load tests were performed (TP39 and TP 58). Table 2 shows the mobilized load transfer ratio and bond strength in each bond stratum. An ultimate bond strength of 137 kPa (20 psi) was used for the design.

Table 2. Summary of Load Testing Results

Test Pile	Bond Stratum	Post Grouting Stages	Bond Length	Mobilized Load Transfer Ratio	Mobilized Bond Strength
1 (bar)	Terrace	2	3 m (10 ft)	267.1 kN/m (18.3 kip/ft)	552 kPa (80 psi)
2 (strand)	Upper Miocene	2	3 m (10 ft)	132.8 kN/m (9.1 kip/ft)	276 kPa (40 psi)
3 (bar)	Lower Miocene	2	3 m (10 ft)	105.1 kN/m (7.2 kip/ft)	220 kPa (32 psi)
4 (bar)	Lower Miocene	3	3 m (10 ft)	166.4 kN/m (11.4 kip/ft)	345 kPa (50 psi)
TP39 (bar)	Upper and Lower Miocene	2	11.9 m (39 ft)	109.5 kN/m (7.5 kip/ft)	228 kPa (33 psi)
TP58 (bar)	Upper and Lower Miocene	none	17.7 m (58 ft)	80.3 kN/m (5.5 kip/ft)	165 kPa (24 psi)

CONNECTION TO EXISTING FOOTINGS

Vertical micropiles installed along Column Line D were cored through the existing footings using a 228 mm (9 in) diameter hole that provided a 25.4 mm (1 in) annular space for the steel casing. The existing footings were 609 mm (24 in) deep and had a compressive strength of 28 MPa (4,000 psi). Using Figure 10 and an annular width of 25.4 mm (1 in), an ultimate bond stress of 3 MPa (430 psi) was conservatively used. Grout with an unconfined compressive strength of 34 MPa (5,000 psi) was specified.

CONCLUSIONS

This project was highly successful in multiple ways. Daily operations were maintained safely at the existing pavilion during construction. Instrumentation and monitoring data indicated that total horizontal movement of the existing building following construction of the SOE was approximately 10 mm (3/8 in).

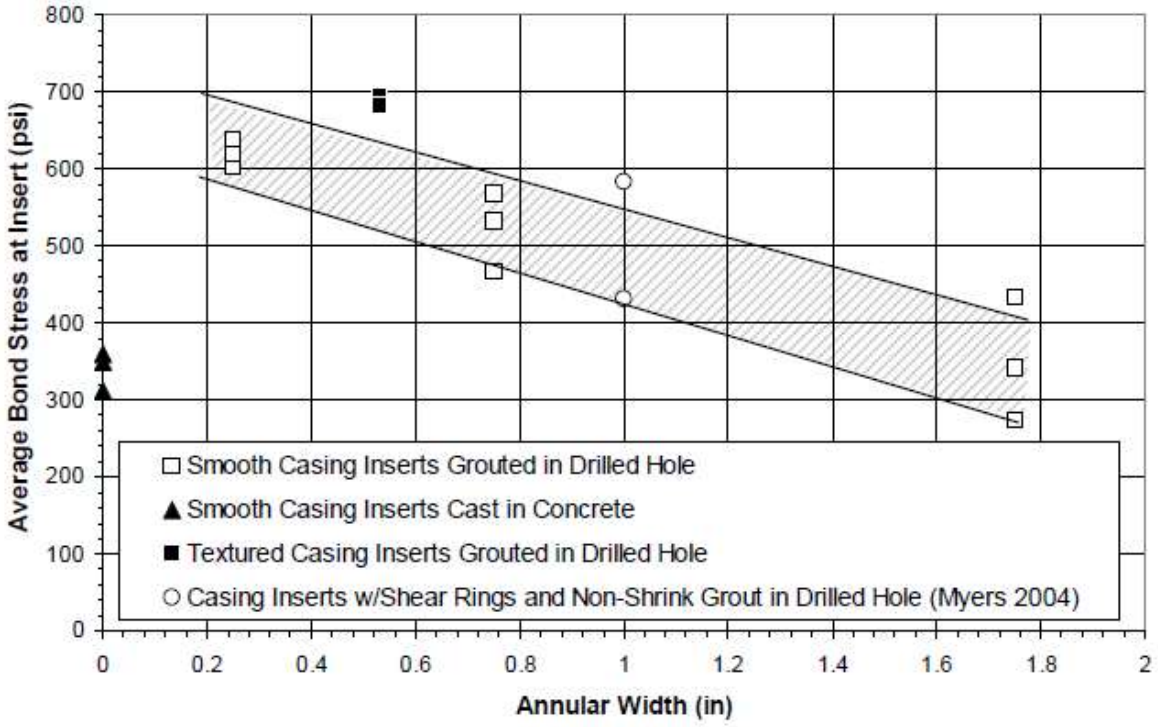


Figure 10. Bond Stress of Existing Concrete (From Gomez et al, 2005)

The project successfully consolidated many pediatric services into one building to provide comprehensive outpatient care under a single roof. This $200 million investment by VCU Health also improved the historic and vital Broad Street corridor of Downtown Richmond. Sustainability in construction and design was a focus of the project. The creative engineering solutions by Schnabel and DMWPV allowed effective redevelopment of an existing brownfield site rather than building on a Greenfield site. VCU Health is seeking LEED Silver certification from the U.S. Green Building Council.

REFERENCES

Gómez, J., Englert, C., Robinson, H. (2013) “Design of A-Walls for Stabilization of Slopes and Embankments in Soft Soils”. 7th International Case Histories Conference, Chicago, IL, May 2013.

Gómez, J., Robinson, H., Cadden, A., “Nonlinear Analysis of Lateral Stability of Micropiles Subject to Axial Load”. ISM’s 11th International Workshop on Micropiles, Milan, Italy, October 2012.

Gómez, J., Cadden, A., Traylor, R., and Bruce, D., (2005) “Connection Capacity Between Micropiles and Concrete Footings: Interpretation of Test Results and Design Recommendations.” Proceedings of the ADSC GEO3 QA/QC Conference, Dallas, TX, November 2005.

RECENT ADVANCES IN OVERBURDEN AND DOWN-THE-HOLE DRILLING TECHNIQUES

Donald A. Bruce[1] and Rudy Lyon[2]

ABSTRACT

The safe and efficient drilling of overburden (fills and natural soils) and rock is integral to many specialty geotechnical construction techniques. The state of practice for overburden drilling techniques was most recently described by Bruce in 2012, and the history of Down-the-Hole (DTH) drilling for rock was provided by the authors in 2013 (Bruce et al., 2013). Thereafter, development and innovation have continued, principally to satisfy specialty contractors' goals for systems providing faster production, lower costs, more consistent and reliable performances, and easier operation and maintenance. This paper describes more recent developments in overburden drilling, and reviews innovations in DTH methods operated by air, and by water.

1. BACKGROUND

In specialty geotechnical construction techniques such as grouting, ground anchors, micropiles and ground freezing, overburden is regarded as those materials overlying top of geological rock. Hence, overburden can comprise fill materials (for example the materials constituting an embankment dam or levee), or it can be solely natural, unlithified deposits such as alluvium, colluvium or glacial outwash and till deposits. Often, as in the case of a reclaimed urban site, or for an embankment dam, both fills and natural soils will, together, constitute the overburden that must be penetrated to reach the bedrock which is to be the ultimate host of the process.

Because overburden is so variable in terms of variations in grain size, density, stiffness or degree of saturation, there are many different types of overburden drilling systems, as recently described by Bruce (2012). In certain applications, such as the drilling of embankment dams, there are governing Federal regulations (e.g., USACE 1997) which have driven the popularity of a certain overburden drilling system, such as rotosonic (Bruce and Davis, 2005). This relative newcomer to a field which was opened almost 50 years ago has been well described by various authors, such as Stare et al. (2012), and is now not just the chosen method, but the specified method for drilling through existing embankment dams to place standpipes for rock grouting, and for installing instrumentation.

With regards to rock drilling, the generic drilling methods are somewhat fewer – rotary drilling, or rotary percussive drilling, either by top hammer, or by DTH hammer. As described by Bruce et al. (2013), air-flushed drilling with top hammers began in Swedish mines in 1873, while DTH drilling, again with air flush (and activation) became operational first in 1950. Early industry debates about the relative merits of rotary vs.

[1] President, Geosystems, L.P., P.O. Box 237, Venetia, PA 15367; Phone: 724-942-0570; Fax: 724-9421911; e-mail: dabruce@geosystemsbruce.com

[2] R&D Manager, Center Rock Inc., 1 W. 4th Street, Salem, VA 24153; Phone: 540.389.7033; Fax: 540-389-7044; e-mail: rlyon@centerrock.com

rotary percussive drilling for grout holes should really have been about the benefits of water flush over air flush since, in our opinion, air flush will clog fissures in competent rock masses, and will create extreme levels of ground disturbance in the variable conditions present in karstic carbonate terrains. However, for fast, reliable and straight drilling in rock where grouting is not the purpose of the drill hole, then air flushed DTH is still a very popular and sensible choice, and it is not the case that development and innovation in air DTH technology has stalled – quite the contrary.

In this paper, recent developments in overburden drilling and in DTH drilling are presented, in order to update the state of practice review of 2012.

2. OVERBURDEN DRILLING

The overburden drilling systems in use in North America as of 2012 (and, coincidentally, 2003), are as summarized in Figure 1, and are as described by Stare et al. (2012). Most recently, research has focused on producing for specialty geotechnical construction contractors overburden drilling systems which are robust, reliable, user friendly, and compatible with standard sizes of commercially available drill casing (e.g., 5½ inches, 7 inches, and 9⅝ inches). Two typical examples are the SuperJaws® system provided by Numa, and the Elemex system of Atlas Copco.

SuperJaws® features "wings" that extend out beyond the end of the casing while in the drilling position. It is the direct descendent of the venerable Acker Anchor Underreaming System. When drilling is completed, "the bit is simply lifted off bottom, causing the wings to retract back into the guide body. This allows all tooling to be extracted while leaving the casing in place. There is no forward or reverse rotation required, nor any expensive rings left in the hole" (Numa Website, 2012). It is promoted in two versions. One uses an inexpensive drive shoe, welded to the front of the casing. As the bit advances through the formation, the casing is advanced at the same rate due to the drive shoulder on the guide body engaging the drive shoe welded to the casing. The second version — "SuperJaws® ND" — uses thick wall welded casing or thick wall threaded casing. The guide body has no drive shoulder and the casing is advanced via a casing hammer, duplex diverter, or dual rotary system. This version is often used in micropile and tieback work where the casing is to be recovered, or in deep overburden areas where high amounts of friction can develop around the casing. Both systems are used for drilling holes 5½ to 42 inches in diameter, and are provided in 2-, 3- and 4-wing configurations, depending on diameter.

Atlas Copco claims their Elemex system was designed to meet the environmental challenges of using compressed air in urban locations, as well as optimizing drill bit performance. It minimizes air escape to the surrounding ground as the high pressure air (used in the hammer) never touches the ground directly, but is redirected. The air is blown from the bit face against an extended ring bit (mounted on the casing), causing the redirection, but still maintaining the cleaning action. The ring bit encloses the drilling area and keeps the air in the flushing grooves. This ring bit also prolongs the life of the pilot bit. This is a simple and reliable system to operate (hence the name) and is claimed to drill faster and straighter holes than when "drilling with an old type of underreaming system" (Atlas Copco Website, 2012).

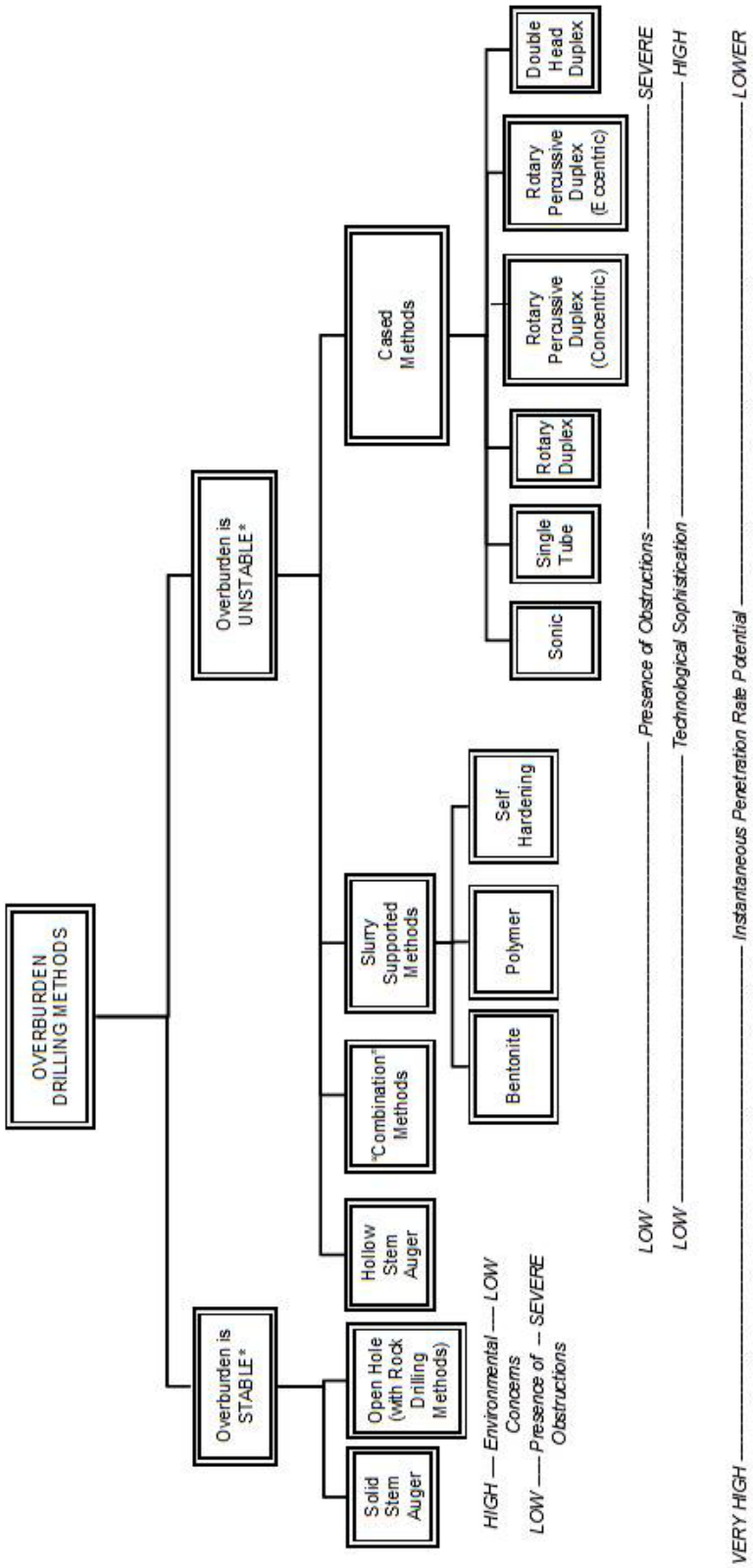


Figure 1. Basic drill method selection guide for overburden (Bruce, 2012).

A new type of casing underreaming and advancing system has recently been developed by Center Rock Inc. This features a patented method of extending and retracting cutting wings on the central pilot bit in a very simple and reliable fashion. Unlike other underreamed systems, the wings, when extended, are locked out mechanically, and so do not rely on downward pressure on the bit. They therefore prevent the outer casing from accidentally slipping off if a very soft or voided horizon is suddenly encountered. The system, named Roto Loc, leaves no sacrificial component in the ground, and fits casings of standard sizes 5½ to 24-inch diameter.

Roto Loc consists of three major parts, as shown in Figure 2. A SHANK adapts the system to a DTH hammer. The shank also includes a threaded section which screws into and out of the pilot. In addition, the shank also includes a conical end which engages the wings to force them outward when the shank is screwed clockwise into the pilot. A set of WINGS are contained within the pilot. The wings cut the kerf from the borehole needed to make clearance for the advancing casing. The wings are then allowed to retract when the shank is unscrewed and the assembly is pulled back through the casing. The PILOT holds all the components together with a retaining wire (not shown) which prevents the shank from fully unscrewing. The pilot contains a female thread which the shank engages. It also contains pockets which house and guide the wings. The front face of the pilot contains the cutting structure which advances the hole. Since the pilot leads the cutting structure of the wings it also provides radial stability and so the ability to drill straighter through pinnacled karstic terrains. This reduces bending stresses on the casing which, in extreme cases, may cause it to rupture, so leading to loss of casing at depth.

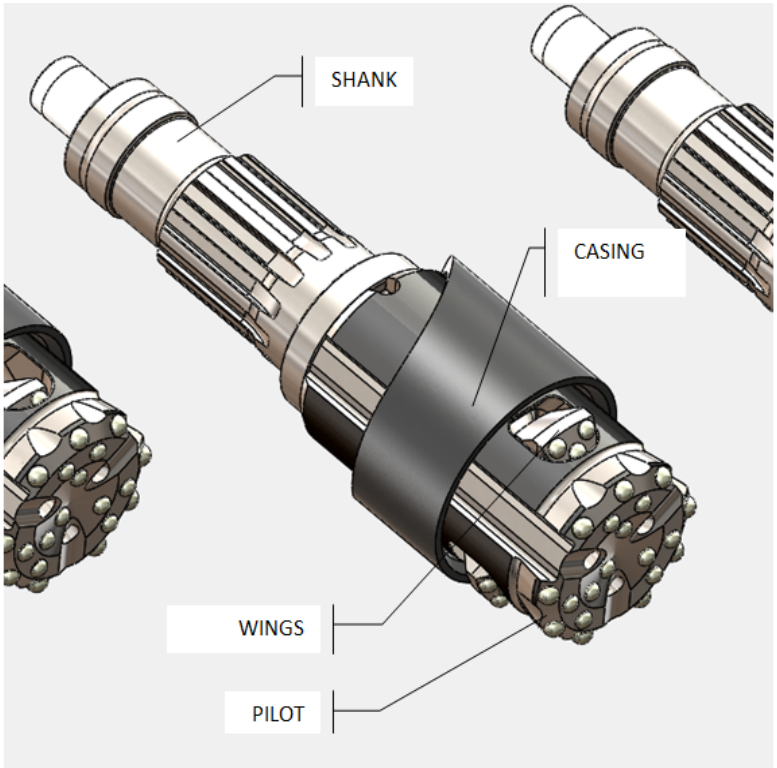


Figure 2. Roto Loc components (7" (178 mm) casing system) with the wings extended below the casing.

An exploded view of the Roto Loc system and parts is shown in Figure 3. In this view the retaining wire is clearly visible.

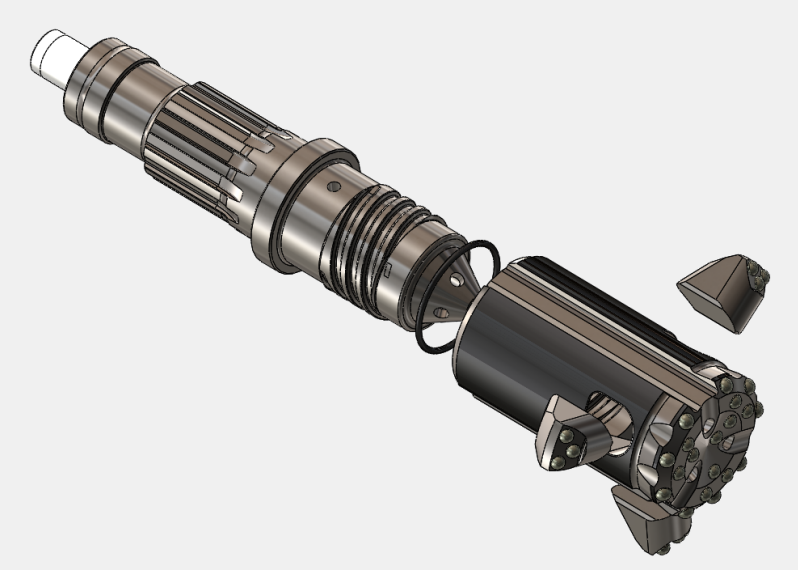


Figure 3. Exploded view of Roto Loc.

Practical consideration for setup and operation include the following:

1. It is suggested that operating air pressures do not exceed 250 psi. With consideration for the compressor to be used, adjustments to jet subs or internal chokes should be made.
2. Due to the fact that a short period of reverse rotation and rattling (short burst of percussion without rotation) are required, the hammer joints (backhead and chuck) should be Baker-Locked and torqued to reduce the chances of accidental loosening.
3. Hammer, drill rod, and casing string are lifted onto drill and torqued. The flushing bell is added.
4. Advance Roto Loc through casing until wings are exposed.
5. Flush system with blowing air to ensure any debris that may be in the Roto Loc are blown free.
6. While blowing and rotating, advance assembly into soil and begin drilling. It is common to inject substantial volumes of water if drilling through clays or sticky soils.
7. Depending on the distance between end of casing and the wings, it may be possible to add drill rods and casings without retracting the wings.
8. The process for extracting the Roto Loc from the casing is to stop rotating, rattle system to loosen the Roto Loc thread following by roughly ¾-1 full rotation in reverse with Roto Loc on the bottom of the hole. Then retract wings into the pilot and extract the hammer and Roto Loc through the casing.

Table 1 summarizes the various sizes of Roto Loc systems. Note that when an "S" follows the diameter, the system contains a casing drive ring attached to the pilot bit.

Table 1. Scope of Roto Loc Systems.

System	Diameter				Applicable Casing					
	Expanded	Expanded (mm)	Retracted	Retracted (mm)	Outside Dia	OD (mm)	Inside Dia	ID (mm)	Wall	W (mm)
RL-0513-B34	5.54	141	4.07	103	5.125	130.2	4.250	108.0	0.438	11.1
RL-0513-C40	5.54	141	4.07	103	5.125	130.2	4.250	108.0	0.438	11.1
RL-0550-B34	5.87	149	4.40	112	5.500	139.7	4.670	118.6	0.415	10.5
RL-0550-C40	5.87	149	4.40	112	5.500	139.7	4.670	118.6	0.415	10.5
RL-0600-C40	6.40	163	4.98	127	6.000	152.4	5.118	130.0	0.441	11.2
RL-0600-Q5	6.40	163	4.98	127	6.000	152.4	5.118	130.0	0.441	11.2
RL-0663-Q5	7.28	185	5.58	142	6.625	168.3	5.625	142.9	0.500	12.7
RL-0663S-Q6	7.28	185	5.58	142	6.625	168.3	6.050	153.7	0.288	7.3
RL-0663S-B35W	7.28	185	5.58	142	6.625	168.3	5.625	142.9	0.500	12.7
RL-0663S-Q5	7.28	185	5.58	142	6.625	168.3	5.625	142.9	0.500	12.7
RL-0700-Q6	7.75	197	5.90	150	7.000	177.8	6.000	152.4	0.500	12.7
RL-0700-B35W	7.75	197	5.90	150	7.000	177.8	6.000	152.4	0.500	12.7
RL-0763-Q6	8.35	212	6.50	165	7.625	193.7	6.625	168.3	0.500	12.7
RL-0763-B35W	8.35	212	6.50	165	7.625	193.7	6.625	168.3	0.500	12.7
RL-0863-Q6	9.33	237	7.54	192	8.625	219.1	7.625	193.7	0.500	12.7
RL-0963-Q8	10.38	264	8.39	213	9.625	244.5	8.565	217.6	0.530	13.5
RL-0963-B38W	10.38	264	8.39	213	9.625	244.5	8.565	217.6	0.530	13.5
RL-0963S-Q8	10.38	264	8.39	213	9.625	244.5	8.835	224.4	0.395	10.0
RL-0963S-Q8-HW	10.10	256	8.13	206	9.625	244.5	8.535	216.8	0.545	13.8
RL-1075-Q8	11.42	290	9.45	240	10.750	273.1	9.560	242.8	0.595	15.1
RL-1188-N10	12.40	315	10.43	265	11.875	301.6	10.715	272.2	0.580	14.7
RL-1275S-N10	13.41	341	10.90	277	12.750	323.9	11.750	298.5	0.500	12.7
RL-1338S-N10	14.00	356	11.47	291	13.380	339.9	12.350	313.7	0.515	13.1
RL-1600S-Q12	16.93	430	14.37	365	16.000	406.4	15.250	387.4	0.375	9.5
RL-1800S-Q20	18.82	478	16.10	409	18.000	457.2	17.000	431.8	0.500	12.7
RL-2000S-Q20	20.87	530	17.63	448	20.000	508.0	19.000	482.6	0.625	15.9
RL-2400S-Q20	24.88	632	21.89	556	24.000	609.6	23.000	584.2	0.500	12.7

3. DOWN-THE-HOLE (DTH) HAMMERS

3.1 Air-Powered DTH Hammers

Ongoing advancements to the Air-Powered DTH state of technology over the past decade can be divided into the following categories:

- Air cycle improvements which address the manner in which air is delivered to and exhausted from the working chambers of the DTH hammer.
- Air bypass systems which provide alternative means for consuming air.
- Piston and bit geometry improvements which have contributed to smoother running, higher frequency hammers, as well as reduced costs.
- Accessories are now offered to make DTH hammers perform better and work more reliably in a broad range of applications.

DTH hammers are very simple machines in operation. High pressure air comes in one end (connection) and low pressure air goes out the other (bit). The exhausting air cleans cuttings from the bit face and carries them up and out of the hole. The hammer consists of two working volumes that are alternately filled with and exhausted of compressed air. The challenge to creating an efficient design for conventional valved

hammers is to optimize timing points for the four valved ports along with appropriate volumes.

In contrast, Figure 4 shows a broken-away section of a typical, contemporary, valveless DTH hammer showing the two working air volumes that exert force on the piston. Figure 5 shows a detail of the drive and return working areas on a piston.

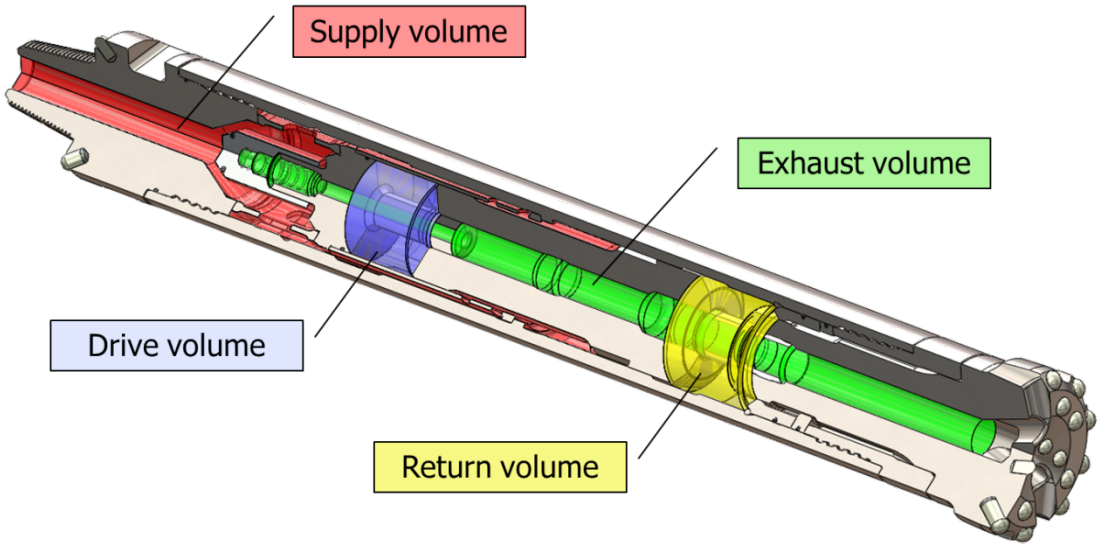


Figure 4. Typical valveless DTH hammer.

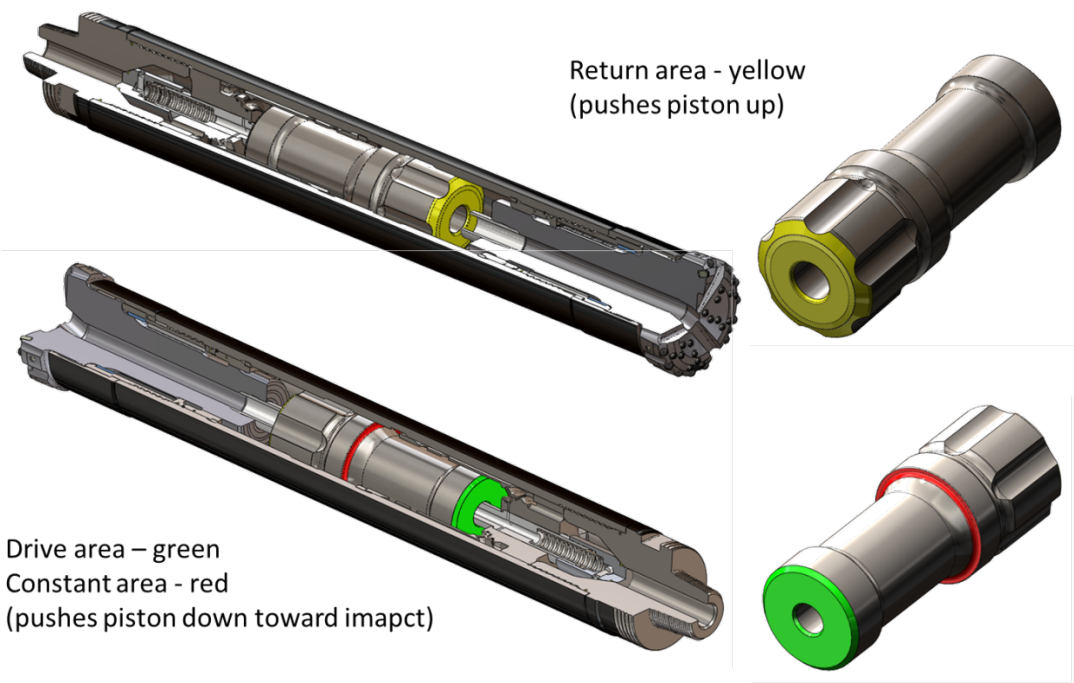


Figure 5. Piston working areas.

A long standing limitation to optimizing porting was that most DTH hammers have what is referred to as fixed port air cycles. The term fixed port means the supply and exhaust ports open and close at the same location regardless of piston direction. In 1990 Ingersoll-Rand developed a new hammer cycle that was a hybrid between valved and valveless. In this new design, the major working chamber (the drive volume) was supplied through a poppet valve that would open near the top of the stroke and then close near the bottom at impact. This enabled high pressure air to accelerate the piston over a longer portion of the piston stroke and thus develop more power, and so at the time, this improved DTH hammer efficiency by about 15-20% in terms of power developed per flow rate. Ingersoll-Rand and later Atlas Copco enjoyed the benefits of this patented product for years until the patent expired. At that time, Center Rock further developed the technology using heat resistant steel components to improve reliability over the plastic parts previously used by the original manufacturers.

Figure 6 shows a cross section of a Center Rock RX70 hammer containing a variant of a hybrid valve (shown in red). Air supply is to the left of the valve and drive air is on the right. As the valve is lifted off the angled seat, supply air is able to rapidly fill the drive volume. It is common for these new steel valves and seals to outlast other parts within the hammer. Other manufacturers, such as Rockmore International, have made efficiency gains through improved air passages granting reduced losses and restrictions.

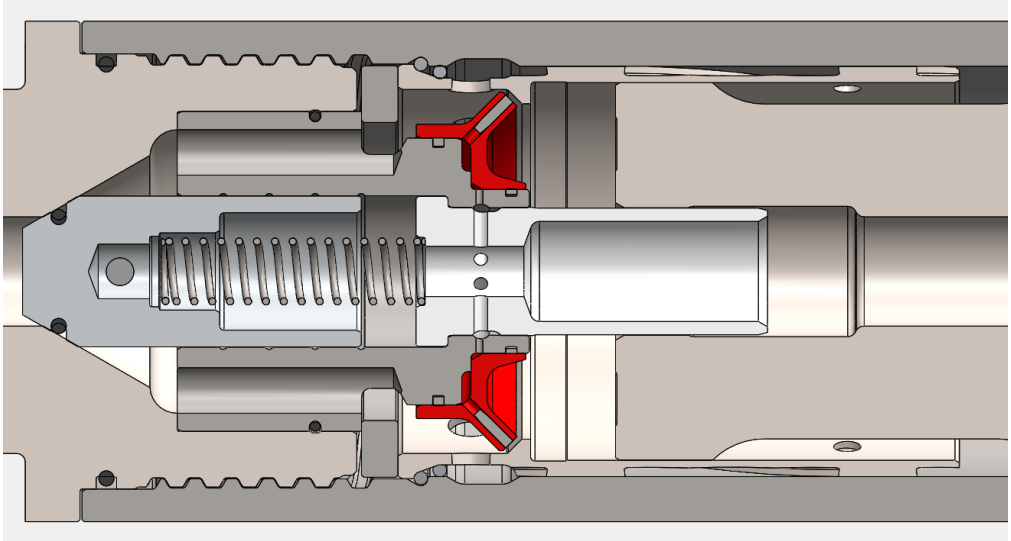


Figure 6. Steel hybrid valve and seals (RX70 Hammer).

For many applications that require high volumes of air, such as large diameter or deep holes, a means for bypassing air is required. This is simply because it would require too much pressure to push supplemental air through the hammer. Excess pressure would either overload the compressor or develop too much hammer power, or both. Either phenomenon will lead to excessive and accelerated wear, or sudden breakdown. Up until a few years ago, the only way to accomplish air bypass was to open an internal plug, called a choke, that would short circuit air from supply to exhaust. The problem with a choke system is that all the bypass air flowing through the hammer creates excessive backpressure on the piston which in turn generates a substantial loss

in performance. This limitation has been addressed with the creation of a down-hole jetsub which bypasses air above the hammer rather than inside it.

Another element of hammer design that has seen substantial improvement relates to the matching of piston and bit geometry. Newton's cradle (Figure 7) provides a good analogy to the goal of matching piston and bit mass and geometry. Mission-Sandvik took a major step forward with their introduction of the "Mission" series hammers in the late '90's. This new series of hammer touted mirror technology in which the bit and piston were mirror images of each other. Center Rock took this concept a step further by more closely matching bit and piston mass and substantially lightening both. This became the core technology in a new hammer type (RX series), that features high frequency and smoother operation to reduce vibration-induced wear on the hammer and the drill head. High frequency is caused by the light piston and smooth operation from the bit recoil being absorbed by the piston rather than the housing, as is common in conventional hammers.

Other accessories provide additional flexibility for air adjustment such as including check valves with pressure relief systems for oil and gas operations as well as down-hole water separators called Hydrocylones for extracting power-robbing injected water from the compressed air.

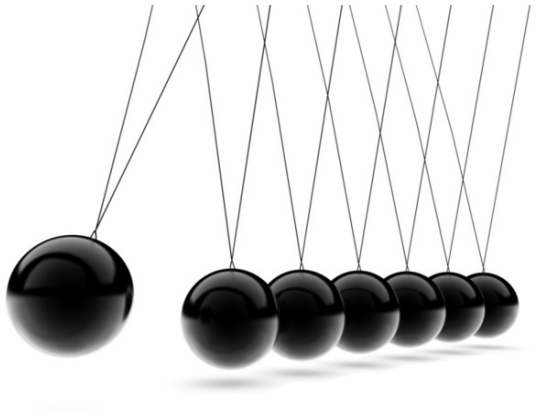


Figure 7. Newton's Cradle.

3.2 Water-Powered DTH Hammers (WDTH)

The concept of a water-powered Down-the-Hole hammer (WDTH) had been explored prior to G. Drill acquiring the original patent from Atlas Copco in 1988. LKAB, a huge underground mining company owned by the Swedish Government and providing about 90% of the European Union's iron ore, purchased G. Drill in 1991 and encouraged the commercial development of the WDTH for mining-related operations. The first full-scale WDTH production works were carried out for LKAB in 1995. Since then over 30 million lineal meters of drilling have been recorded in both underground and surface applications. The most commonly used WDTH's are produced by Wassara, also based in Sweden, although cheaper equivalents are manufactured in certain Asian countries without regard to patent right or protection.

Water, delivered at up to 180 bar, is used to activate the impact mechanism of the hammer at high frequency and with high efficiency. When the water leaves the hammer, it has a low pressure and low up-hole flush velocity (100-500 ft/min) which is still adequate to bring the cuttings to the surface and to clean the borehole. This "gentle" drilling mechanism simply reflects the fact that water is an incompressible medium, unlike compressed air, the volume of which expands as pressure reduces (such as occurs when air flush passes out of the hammer and begins to move up the drill hole annulus). The hydrostatic column created above the hammer helps to keep the hole stable and prevents collapse. In strata with high water tables it prevents ground water being sucked into the hole, as would be the case with air flush, giving rise to hole stability problems and potentially environmental implications.

Typical dimensions and operating parameters for WDTH hammers are shown in Table 2.

Table 2. Water-Powered Down-the-Hole hammer, bit dimensions and operating parameters.

HAMMER	Ø DRILL BIT	WATER CONSUMPTION	MAX OPERATING PRESSURE
W50 (2")	60mm, 64mm (2⅜", 2½")	80-130 l/min (20-35 USgpm)	170 bar (2500 psi)
W70 (3")	82mm, 89m (3¼", 3½")	130-260 l/min (35-70 USgpm)	180 bar (2600 psi)
W80 (3.5")	95mm (3¾")	130-260 l/min (35-70 USgpm)	180 bar (2600 psi)
W100 (4")	115mm, 120mm (4½", 4¾")	225-350 l/min (60-95 USgpm)	180 bar (2600 psi)
W120 (5")	130mm, 140mm (5⅛", 5½")	300-450 l/min (80-120 USgpm)	180 bar (2600 psi)
W150 (6")	165mm (6½")	350-500 l/min (95-130 USgpm)	150 bar (2200 psi)
W200 (8")	216, 254mm (8½", 10")	470-670 l/min (125-180 USgpm)	150 bar (2200 psi)

There are numerous other advantages to using WDTH. There is reduced component wear since the velocity of the flushing water is relatively low, resulting in low rates of wear on the surface of the hammer and drill rods. It is not unusual for the service life of the W100 hammer body to be up to 30,000 lft. even in very abrasive conditions, while the limitation on rod usage is typically thread wear at over 100,000 lft. Hammers are serviced every 5,000-10,000 lft. of drilling, depending on water quality.

Less harm is caused to the ground since the flushing water exits the hammer under low pressure and, given the fact that the rate of flow is moderate, the up-hole velocity is correspondingly low. Further, the hydrostatic pressure created by the flushing water helps stabilize the hole wall and therefore promotes straightness in soft formations or overburden by reducing "overbreak." Likewise, such low up-hole velocities permit the use of tight tolerance hammer and rod stabilizing devices further enhancing straightness, and deviations in the range of up to 1 degree can be anticipated, and values less than 0.2 degree can be achieved.

WDTH permits very fast and straight drilling for grout holes and has already been used throughout North America for over 15 years on major dam remediation projects. WDTH can also be used with the Roto Loc overburden drilling system to install casings from 4½ to 8½ inches in diameter.

A potential disadvantage of WDTH is that water requirements are not insubstantial, although this may not in reality be a problem when drilling adjacent to a reservoir. Further, the initial capital investment in the basic components (hammers,

rods, and pumps especially) will be higher than for air DTH, and this may deter contractors with meager resources. However, the main technological concern is that, if the hole becomes blocked, then the formation will "see" the full delivery pressure of the pump and so may hydrofracture. The authors would comment as follows.

Firstly, unlike air, water is an incompressible fluid and so, upon exiting the WDTH, by Boyle's Law, it will immediately suffer a pressure drop (P x V = K). Secondly, the authors have never seen a situation develop where either a) loss of flush return at the surface has not met with immediate response by the driller, and/or b) a total annulus blockage has actually occurred. The authors have often observed transient pressure "spikes" on nearby piezometers when drilling in karstic formations with the WDTH, but have never seen any long-lasting effect. No dam safety incidents have been recorded to the authors' knowledge, resulting from the use of WDTH technology.

4. FINAL REMARKS

It is clear that very significant and important developments continue to be made in both overburden drilling and down-the-hole drilling techniques. These are partly driven by contractors' needs (e.g., the development of Roto Loc for micropile drilling in karst), and partly by intense market competition among the hammer manufacturers (e.g., the hybrid valve innovation in the RX series hammers). In both cases, these developments have been greatly facilitated by highly sophisticated computer-aided design capabilities. The authors believe that there still remains wide scope for similar advances to be made by equipment manufacturers for the foreseeable future.

REFERENCES

Atlas Copco Website (2012).

Bruce, D.A. (2012). "The Evolution of Small Hole Drilling Methods for Geotechnical Construction Techniques," ADSC EXPO, ADSC: The International Association of Foundation Drilling, March 14-17, San Antonio, TX, 18 pp.

Bruce, D.A. (2012). "Specialty Construction Techniques for Dam and Levee Remediation," Spon Press, an imprint of Taylor and Francis, 304 pp.

Bruce, D.A., R. Lyon, and S. Swartling (2013). "The History of Down-the-Hole Drilling and the Use of Water-Powered Hammers," Association of State Dam Safety Officials Annual Conference, Providence, RI, September 8-12, 11 pp.

Bruce, D.A., and J.P. Davis. (2005). "Drilling through Embankments: The State of Practice," USSD 2005 Conference, Salt Lake City, UT, June 6-10, 12 p.

Stare, D.P., T.L. Dreese and D.A. Bruce (2012). "Specialty Construction Techniques for Dam and Levee Remediation," Chapter 2, Spon Press, an imprint of Taylor and Francis, 304 pp.

U.S. Army Corps of Engineers (USACE) (1997). "Engineering and Design Procedures for Drilling in Earth Embankments," CECW-EG, Report No. 1110-1-1807, September 30.

Deep Resonant Micro Piling for Netherlands Grade Separation

AUTHORS: Mathew Janes, M.E.Sc., P.Eng., Resonance Technology International Inc.

Abstract:

The Resonator RD 260 Resonant Pile Driver delivers ground disturbance free, high production micro pile installation. The Resonator was recently used at the site of a major grade separation south of Amsterdam, at Den Haag, to install 34 m long micro piles. The micro piles are used as both compression and tension elements for the support of the structure walls and roof and to hold down the roadway base due to hydraulic uplift forces.

A test program involving several installation methods proved the Resonant driver would install the 168 mm dia 34 m length test pile to full depth in just 11 to 15 minutes. The Resonator was crane mounted and drove a single length 34 m tube through mixed sands and silts with CPT Qc of over 300 Bar. The single pass pipe was installed with a loss bit and no flushing. Thus, the micro pile was installed with zero ground vibration, no spoil and no flushing fluids to contend with. Competing methods included sonic drilling (which could only penetrate to 19 m depth) and conventional water flush drilling which took over 90 minutes to reach a depth of 28 m.

The micro piles were pressure grouted during casing removal at intervals of 3 m and at grout pressures of 20 Bar. Load testing confirmed the micro pile capacity to be 1125 kN to 2160 kN, depending upon the grouting procedures.

Rotterdamsebaan Tunnel Grade Separation Project

The city of Den Haag is constructing an underground thoroughfare between the perimeter highway system and the downtown core. The project is called the Rotterdamsebaan and features the "Victory Boogie-Woogie Twin Tunnels". The construction involves extensive connection road reconstruction, tunnel approaches and a section of twin tunnels.



Figure 1. The future South Tunnel Approach at the Rotterdamsebaan

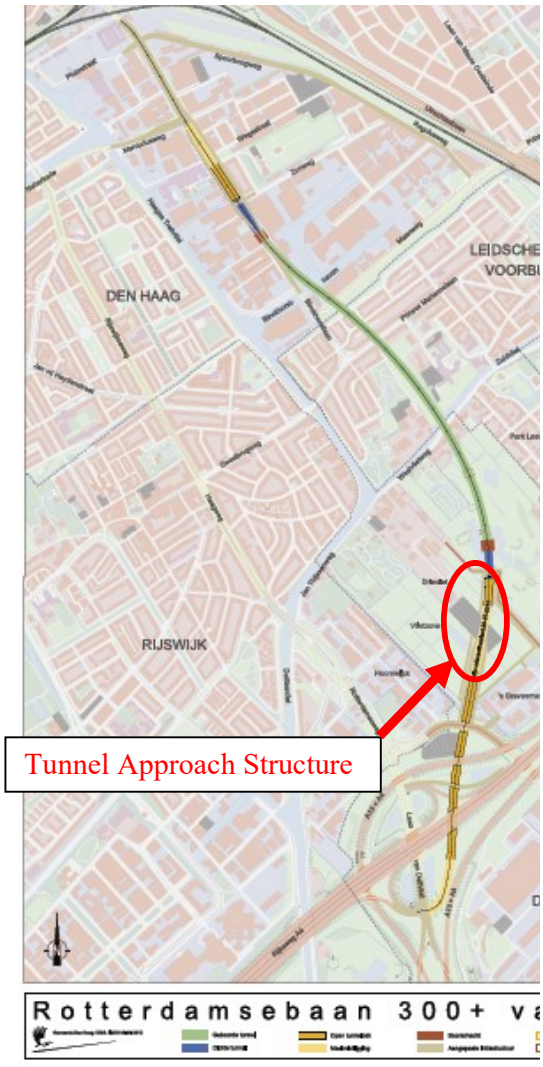


Figure 2. Rotterdamsebaan Site plan.

The tunnel approaches are being constructed to depths of 8-10 m within water bearing sands and silts. The alluvial formation remains compact to dense to depths of over 50 m. The tunnel approaches will be constructed in the wet with steel sheet piling cofferdams at the approach and exit shafts. The base of the cofferdams will be susceptible to hydrostatic upheave forces and piping due to the high water table and weak soils.

A tremmied base slab will be used to support and hold down the road surface. The tremmie base slab will consist of a 1-1.3 m thick reinforced concrete slab integrated with 26 m long tension micropiles. The micropiles are to be constructed from existing grade to depths of 34 m. The micropiles are constructed using high tension reinforcing bars and high strength grout placed in 'Resonated' holes or conventional drilled holes.

A test program was conducted to verify both installation method and micropile tension capacity. 6 months prior to construction a test program was conducted using 3 methods to construct the micropiles followed by tension load tests.

How Does Resonance Work?

The Resonant Pile Driving method is gaining acceptance around the world as a new method to rapidly drive piles free of ground borne vibrations. The high frequency vibrator resonates the pile, essentially turning the pile into a spring, to excite the toe of the pile with high accelerations and low amplitude. High acceleration with low amplitude generates high penetration rates, but the high frequency stress waves are quickly dissipated in the soil. Typically Resonator ground borne vibrations are measured at below 1 mm/sec within 1 to 5 m of the pile. The Resonant method can drive a pile next to a glass of wine, without causing ripples, as has been demonstrated on numerous piling sites.

The Resonant method uses a hydraulic piston - cylinder geometry to generate high magnitude, high frequency oscillating forces. This is a very different mechanism than the eccentric mass technology used in conventional and variable moment vibrators.

A unique valve geometry achieves the high frequency flow switching necessary to oscillate the hydraulic piston at up to 180 Hz (10800 VPM). The valve is controlled electronically for maximum accuracy of the desired frequency using an in dependent hydraulic circuit. The separate, main hydraulic circuit controls force and amplitude. The volume of hydraulic oil delivered to the piston (flow rate) determines the vibration amplitude while the hydraulic pressure determines the peak force.

The main advantage of the Resonant piston-cylinder method is that it allows the vibration frequency to be tuned to the natural frequency of the pile, which excites the pile like a spring. Exciting the pile like an axial spring allows the storage (build up) and release of vast amounts of energy. In this way the pile is brought to a high acceleration state that penetrates through the soil quickly. The challenge is to continuously tune the vibration frequency to the natural frequency of the pile and soil as it is advances into the ground. A computer algorithm has been developed for the Resonant Driver which automatically performs this tuning function. Through tuning to the Resonant frequency of the pile the maximum driving efficiency and maximum force at the pile tip is achieved.

Test Program and Tension Load Test Results

BAM Contractors NV was awarded the foundation aspects of the project as part of a joint venture contract. The contractor undertook an extensive test program to prove the construction methodology, productions and anchor capacity. The test program was conducted as a separate contract 6 months prior to commencement of the project.

Three methods of micropile construction were used for the test program: conventional drilling double rotary top rotary drives and water flushing, the sonic drill method and Resonant pile driving. Conventional rotary drilling using a casing and drill string with separate top drive (with reverse rotation) and water flushing was used. The 163 mm dia segmental casings were advanced to a depth of 28 m and a 63 mm dia high strength bar inserted. Grout was tremmied into the hole with incremental pressure grouting to 20 Bar conducted as each 1.5 m section of drill string was removed. Grout volumes were monitored during each test pile to ensure consistency between micropiles and prevent a false test result due to over grouting.

The second micropile construction method used the Mid-sonic drill mounted on a 163 mm dia drill casing made up of two sections: the first 19 m long and the second 15 m long. The casing was advanced using a loss bit with no flush. The sonic method vibrates the pipe axially at very high frequency (150Hz or 9000 VPM) in order to advance the tip. The BAM had used this method successfully on a previous anchor program and

achieved very high productions for anchors driven to a depth of 22 m. However, at this site a dense layer at a depth of 16 m proved to be too tough for the sonic drill heads. The sonic drill heads were the Midsonic SonicSamp product by Eijkelkamp (NL). The midsonic drill advanced the 19 m casing to a depth of about 17.5 m and could not advance it further or remove the casing.

The third micropile construction method used the Resonator pile driver on the same 19 m and 15 m long casings. In this case the Resonator was used to remove the 19 m stuck casing from the sonic drill test. The casing was driven to 19 m depth and the 15 m section added. The casing was driven with the loss bit in place and no flushing to the target depth of 28 m where soils with Qc on the order of 30+ MPa were encountered. The casing was driven with the Resonant driver in only 14 minutes, so an attempt was made to drive the casing to the full length of 34 m. The casing was driven to full depth in another 3 to 4 minutes. Despite the ease of achieving additional micropile length, all test anchors were installed to a 28 m depth.

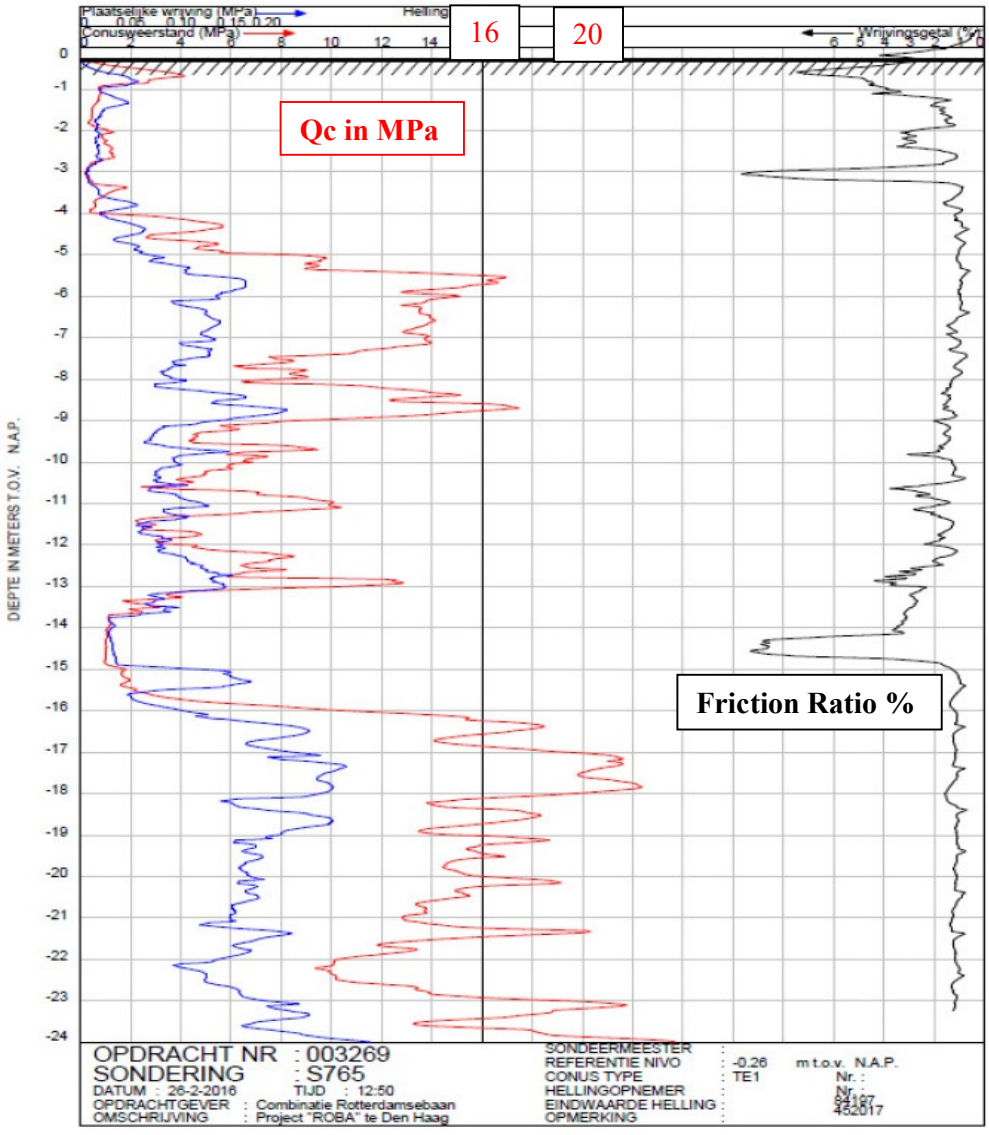


Figure 3a. Typical CPT at Rotterdamsebaan site, Den Haag, page 1.

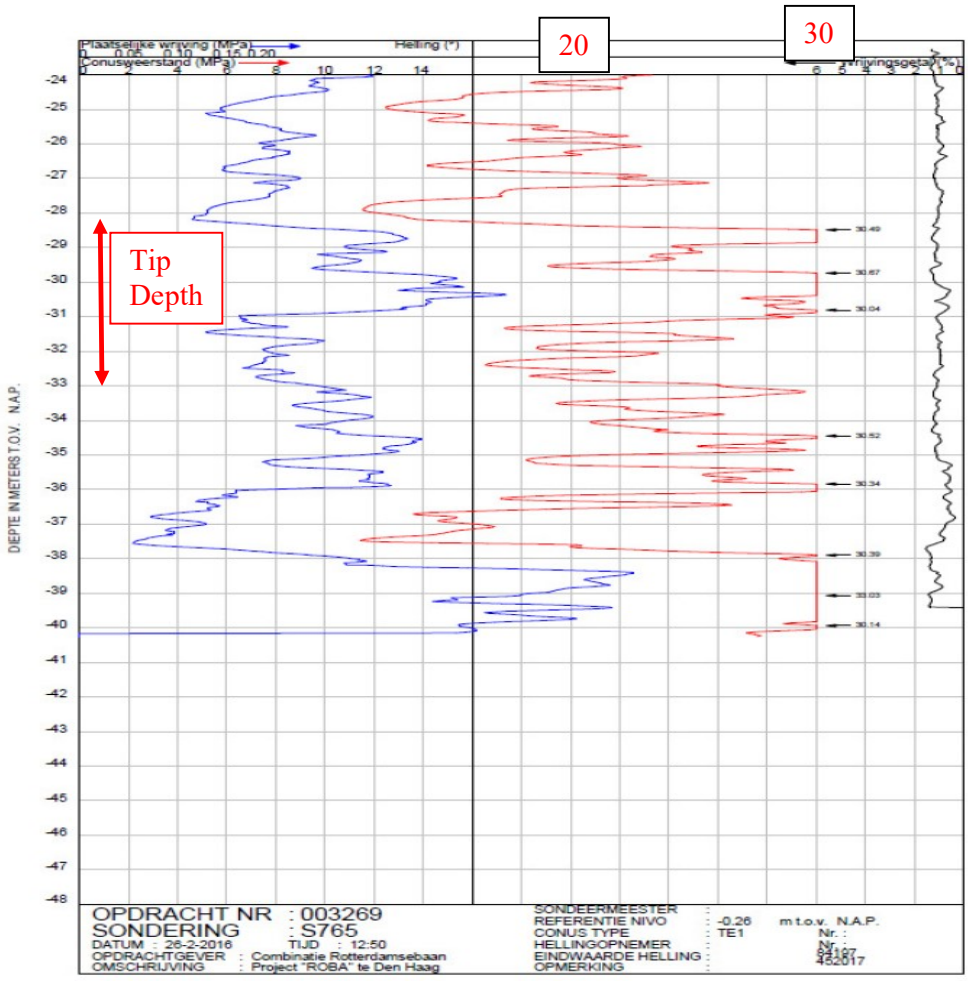


Figure 3b. Typical CPT at Rotterdamsebaan site, Den Haag, page 2.

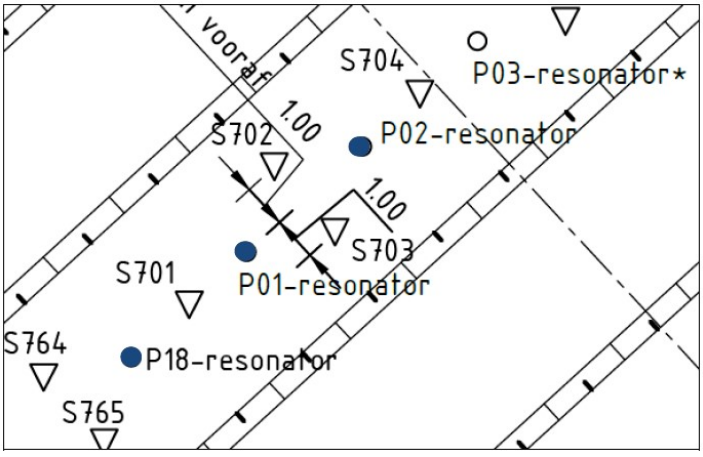


Figure 4 South approach site plan showing Resonator Test Anchors

The loss bit was fitted with an O-ring seal to prevent groundwater from entering the casing during driving. As a result the bar could be inserted into the casing in the dry and grout placed into the casing without the need for a tremmie, which improved production. The grout line was connected to the top of the casing and the Resonator clamp was fabricated with a seal to permit constant pressure grouting to 20 Bar during casing extraction.

The test program was continued using the conventional drill method and Resonator driver for over 30 anchors to explore alternative methods and establish optimum production. On several occasions grout takes were deemed too large and the anchors abandoned. In the end a selection of 6 anchors were tension load tested.

Anchor testing was conducted on selected, representative anchors. Selection was based upon optimum production methods and what were deemed to be representative grout takes for both initial grouting and during pressure grouting. Despite the care taken during installation tension load test capacity varied greatly between micropiles.

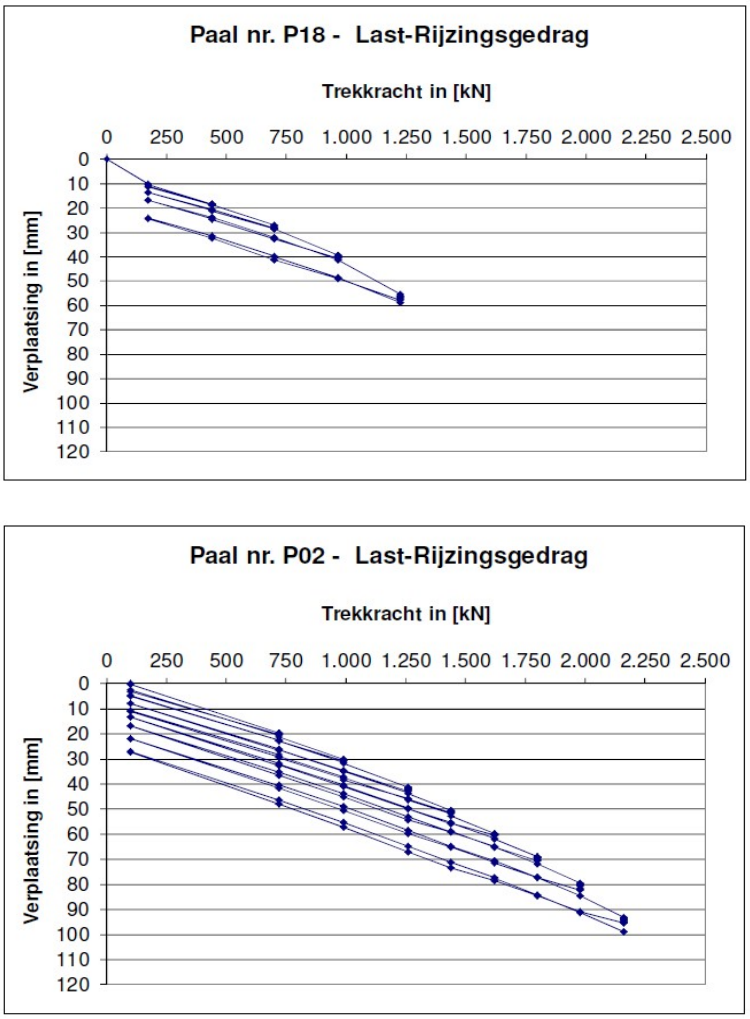


Figure 5 Test Anchor load results

Three Resonator installed micropiles were tested with anchor bond zones of 6.5 m, 7.5 m and 8.5 m for piles P01, P02 and P18 respectively. All anchor bond zones were developed to 28 m tip elevation. Thus the anchor zones started at 21.5 m, 20.5 m and 19.5 m respectively. The load test results indicated peak loads for the Resonator driven micropiles varied between 1250 kN and 2200 kN (failure was by creep at 2 mm per log cycle). Pile P02, with the 7.5 m bond zone provided the highest capacity at 2200 kN, or 442 kPa bond stress while micropiles P01 and P18 provided 228 kPa and 238 kPa bond stress respectively. The wide range may have been due to variance in grout takes during pressure grouting. Micropile P02 took 200% of the pressure grout volume of micropiles P01 and P18. The P01 and P18 anchor capacities fell below the expected bond stress

(approximately 300 kPa). Though the higher capacity bond stress was achieved with the higher grout takes under pressure grouting, it was not assumed that this could be achieved for all production micropiles. Thus, the lower grout takes and lower bond stress was assumed for design purposes.

Production Micropiles

A total of over 4000 tension micropiles were required for the two tunnel approaches to the Victory Boogie-Woogie Twin Tunnels. The micropiles were spaced at 1.8 to 2.4 m centre centre on a rectangular grid. Low cut offs, at between 2 and 9 m below grade, meant that bars were not proud of the working surface. However, micropile 'holes' were abundant and treacherous for equipment and workers. Given the large number of micropiles two spreads of equipment were commissioned for the project. A conventional drilling spread was used which included 2 Klemm drills, 2 support excavators outfitted with drill casing and drill string handling arms, an excavator for spoil removal, a 150 tonne service crane and a grout plant. The drills and accompanying equipment comprised a crew of 11, including a foreman. The crews worked an 11 hour day and produced up to 4 micropiles per drill per day.



Figure 6. The South Tunnel Approach during foundation construction

Figure 6 shows the conditions on site during micropile installation. The drills and service machines are seen in the foreground within the future cofferdam footprint. The 150 tonne crane handling the Resonator is located beyond the drills. The drilling area of the site proved problematic due to the introduction of copious amounts of water for drilling and casing cleaning. Spoil removal proved particularly problematic with large amounts of wet sands and grout to be handled on a crowded site with poor access.

For production work the Resonator was installed on a 40 m vertical lead mounted on a 150 tonne base crane. The Resonator power pack (400 Hp) was mounted on a frame attached to the back of the crane. The leader was mounted with a sliding casing gate to support the 163 mm dia, 34 m long casing at its midpoint and avoid buickling. The grouting system used a 32 mm dia grout line which doubled as a water line for washing down equipment and cleaning the connection between the Resonator and the casing. A permanent grout nipple was integrated into the top of the casing for introduction of pressurized grout during extraction. Figure 7 shows the Resonator with clamp and sealing spigot and the top of the casing. A large diameter top casing was fabricated to accommodate the Resonator clamp. A machined and polished centre spigot was attached to the clamp base which located and centered the clamp into the casing, but also offered a high pressure seal during pressure grouting. The clamp was connected and removed hydraulically, moved away from the centre opening of the casing during bar insertion and initial grouting and then re-introduced to form a grout seal and clamp attachment during extraction.



Figure 7. Resonator showing the drive casing and connection detail

The Resonator equipment consisted of a single 150 tonne crane with 40 m vertical leader, the RD 260 Resonator and power pack and a grout plant. The crew of 3 consisted of a crane operator, a front end man and the grout plant operator. The crane operator had a Resonator controller in the cab along with grouting and crane loading readouts. Frequent site visits and support were provided by PVE staff for training and

equipment support. The Resonator production averaged 14 to 17 minutes for installation of the micropile casing, 12 to 17 minutes to flush the grout lines and fill the casing with grout and 17 to 20 minutes to extract the casing during pressure grouting. As a result typical production consisted of 1 micropile per hour or 7 to 9 micropiles per day. Micropile driving as rapid as 4 minutes for the full 34 m length was achieved. Higher productions are achieved with accurate tuning of the driving frequency to resonance and the correct blend of vibration amplitude and downward force. A common mistake is to over crowd or push on the pile while driving. This tends to dampen the vibration and alter the natural frequency of the system. Application of low downward push and allowing the Resonant vibration to do the work achieves the highest productions. Similarly on extraction, the use of too much pull can slow removal of the casing. While push and pull are required during install and extraction, the use of limited assistance results in the highest production rates.

Reliability of the RD 260 Resonator system proved to be poor at first with repeated electronic problems and fuse issues integrating the power pack to the control system for the Resonator. This was followed by mechanical issues which included isolator failures, and frequency motor stability problems. Over a period of weeks these issues were resolved and the Resonator provided more reliable service.

A major accident and safety issue occurred when the pile gate was left open during driving of the casing. The long, small dia pipe, despite a heavy wall, buckled under the crowd load in the absence of a midpoint lateral support. This caused the pipe to buckle, failing the clamp bolts and brought the casing pipe and clamp head to the ground. Fortunately there were no injuries. The Resonator operation was halted during the investigation. The Resonator program was renewed, but a change was made in the geometry of the frame applying the push and pull force. The Resonator is provided with an isolated yoke for pushing and pulling, however, the contractor had chosen to mount the leader guide directly to the backing mass of the Resonator by-passing the yoke isolation. This applied all loads directly through the internal biasing spring of the Resonator. Following this change and an upgrade to the power pack spool (frequency) circuit the mechanical issues with the Resonator dissipated and the project was completed with average productions of 40 micropiles per week.

This paper would not be possible without the co-operation and efforts provided by the staff of the BAM Contractors at the Rotterdamsebaan project and PVE – Dieseko Staff of Sliedrecht, Netherlands.

KIT FOR HOLLOW-BAR DRILLED AND GROUTED MICROPILES AND SOIL NAILING - MEANING AND MISUSE OF THE CE-MARK

Björn Ischebeck, Friedr. Ischebeck GmbH, Ennepetal, GERMANY

Alice Y. Kayser, Friedr. Ischebeck GmbH, Ennepetal, GERMANY

ABSTRACT

The construction product market is one of the largest markets in Europe. To ensure a reasonable safety level in regards to health, durability, energy economy and protection of the environment it requires harmonized legislation.

In 1989, the construction Product Directive is launched which was binding only to the member states. The harmonization of all requirements for every application seemed impossible.

European technical standards for Execution of special geotechnical works: Micropiles (EN 14199:2015) and Execution of special geotechnical works: Soil nailing (EN 14490:2010) define the requirements for the execution and the product itself.

2011/ 2013 the Construction Product Regulation is introduced binding directly each citizen. This Regulation harmonized the assessment of essential product characteristics.

A construction product means any product or kit, which is produced and introduced into the market for incorporation in a permanent manner in construction works or parts thereof.

If a construction product is covered by a Harmonized Standard or conforms to a European Technical Assessment (ETA) the manufacturer shall draw up a Declaration of Performance.

The ETA is based on a European Assessment Document (EAD), which consists of the harmonized technical specification. This technical data sheet shows the definition of the essential characteristics and the method of verification.

The characteristics are related to the system as well as to the single components (such as steel load bearing element and coupling nut) and include:

- Load bearing capacity
- Resistance against fatigue
- Resistance against alternating loads (tension and compression)
- Transfer of the impact energy produced by roto-percussion
- Protection against corrosion

The declaration of performance must express the performance of the construction product in relation to the essential characteristics. The declaration of performance shall bear a CE Marking.

The declaration of performance gives transparency about the characteristics of the offered product. There is a national approval or the engineer has to decide if the product fulfills the requirements and is fit for purpose.

This paper shall give an overview about the actual legislation in Europe in regards to Micropiles and Soil Nails and technical requirements resulting thereof.

KEYWORDS

Construction Product Regulation EU 305/2011, CE Mark, European Assessment Document (EAD), European Technical Assessment (ETA), Declaration of Performance (DoP), EN 14199 Micropile, EN 14490 Soil Nailing

1. BACKGROUND OF CONSTRUCTION PRODUCT REGULATION

Construction products[1], which belong to one of the largest markets in Europe, are assigned to be included into final constructions or involved to support the construction process. Building sites (design and execution phase) always need special attention and therefore rules for Member States on health and safety, protection of animals, properties and environment, but also durability and energy economical aspects are important goals.

Construction product Council Directive 89/106/EEC[2] was the first step in 1989 to harmonize all product classifications and applications within European Union to achieve above mentioned goals. Any product that has been introduced into the market under the Directive needed to follow national laws like national product standards, national technical approvals / specifications and provisions that had been prepared by each Member State based on their own needs. Due to the quantities of documents and individual focuses it is confusing, therefore technical documentation needs to be simplified and unified for the EU.

Since 1st July 2013 the harmonization has been completed with the construction product Regulation (CPR) No. EU/305/2011and for new products entering the market no further national laws are allowed anymore to fulfil requirements according to this regulation. The CPR directly repeals the former Directive (valid from 21st Dec. 1988 to 30th June 2013) and is a binding legislative act to be applied instantly for all European countries. Content of the CPR covers everything concerning any construction product or kit[3] and it shall simplify the assessment of product performance.

One goal described in the CPR is the elimination of technical barriers for products within the EU. To achieve this goal, products have to be according to harmonized technical specifications. These technical specifications shall assess the performance of products. Essential characteristics of products' performances have to be verified by tests, calculation methods and other instruments that are explained in harmonized standards and/or European Assessment Documents (EAD[4]). If a product is not covered or not completely covered in a harmonized standard, an EAD is needed for this product. The EAD describes the type of product it applies to.

The EAD is basis for a European Technical Assessment (ETA). The EOTA defines ETA as "…a document providing information about the performance of a construction product, to be declared in relation to its essential characteristics."[5] As soon as an ETA is published it has to be adopted in the market.

European Technical Approvals, also abbreviated as ETA, were issued until 30th June 2013. These type of ETAs have a valid period by end of 2018. No ETApprovals will be published anymore after 1st July 2013.

EAD and ETAssessment are basis of a product to receive a CE marking (CE mark). The CE mark shall show and express, that this marked product has been checked for essential characteristics according to harmonized standards.

---

[1] Construction products will be simplified to products

[2] EEC = European Economic Community

[3] Definition 305/2011: "'kit' means a construction product placed on the market by a single manufacturer as a set of at least two separate components that need to be put together to be incorporated in the construction works"

[4] The European Organization for Technical Assessment (EOTA) is responsible for developing and publishing EADs.

[5] www.eota.eu

Details on above mentioned documents and procedures mainly needed for the CE mark will be described in this paper. Due to changes of directives into regulations as explained above and confusion in regards to meaning of expressions like ETA (ETAssessment or ETApproval) clarifying is needed. This paper finishes with a summary and outlook.

2. OVERVIEW EUROCODES AND EU STANDARDS IN REGARDS TO HOLLOW BARS

European standards and Eurocodes are an outcome of lowering trade barriers with uniform level of safety within the EU. There are 10 Eurocodes for the construction industry distinguished between the following:

- Eurocode 0 (EN 1990) : Basis of structural design
- Eurocode 1 (EN 1991) : Actions on structures
- Eurocode 2 (EN 1992) : Design of concrete structures
- Eurocode 3 (EN 1993) : Design of steel structures
- Eurocode 4 (EN 1994) : Design of composite steel and concrete structures
- Eurocode 5 (EN 1995) : Design of timer structures
- Eurocode 6 (EN 1996) : Design of masonry structures
- Eurocode 7 (EN 1997) : Geotechnical design
- Eurocode 8 (EN 1998) : Design of structures of earthquake resistance
- Eurocode 9 (EN 1999) : Design of aluminum structures

Micropiles or Soil Nails belong to the geotechnical field and thus EC 7 shall be used for micropile designs. In regards to standards, product regulations are differentiated between the descriptions of characteristics and application fields with the product. Because of that, application standards for micropiles are regulated in EN 14199 and EN 14490, which include references to product material requirements like for example EN 10210[6].

The main component to create a micropile is the hollow bar, in addition to the main are accessories like drill bit, coupling nut, washer plate and spherical collar nut that belong to the whole kit for installing micropiles.

Looking at the product kit hollow bar precisely, it is not only EC 7, which is relevant to be fulfilled. The kit also needs to comply with further requirements according to EC 0, EC 2 and EC 3 (s. Figure 1). The EC 0 defines among other topics different design working life periods dependent on construction types, e.g. 100 years for bridges. The EC 2 requires various grout cover thicknesses in different constellations to meet crack width limitations and corrosion protection. The EC 3 governs steel structures, which includes slip between steel components.

Eurocodes regulate everything concerning structural design. Products however used for construction are covered either by harmonized standards (hEN)[7] or EADs. European standards in general are developed to support harmonization of Europe.

---

[6] EN 10210 “Hot finished structural steel hollow sections” is a harmonized standard for products made of fine-grain steel and can be found on the European commissions’ website.

[7] hEN can be labeled as such, if i) the European commission and the EFTA instruct CEN, CENELEC or ETSI by a standardization request to develop the standard and ii) the European commission published the standard in an EU Official Journal (OJ). EFTA = European Trade Association; CEN = Comité Européen de Normalisation = European Committee for Standardization; CENELEC = Européen de Normalisation Électrotechnique = European Committee for Electrotechnical Standardization; ETSI = European Telecommunications Standards Institute

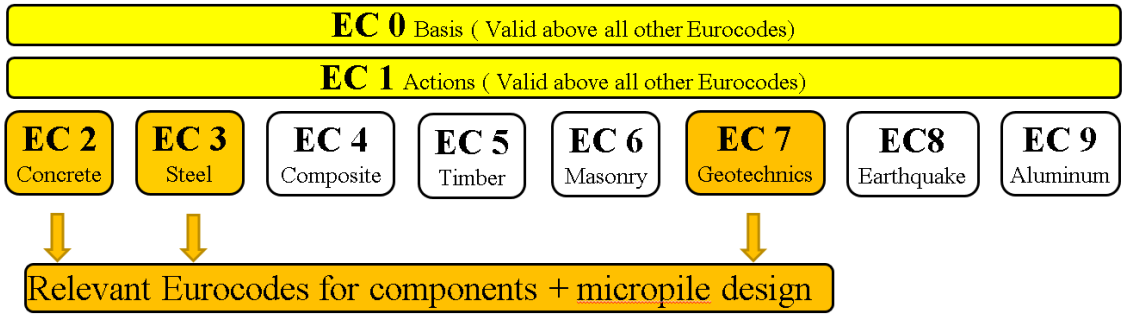


Figure 1: Overview Eurocodes – relevance for geotechnical design

3. BACKGROUND AND MEANING OF CE MARK

CE[8] mark means colloquially "Conformity with Europe". This mark, attached to a product, shall simplify and in the end represent all test procedures that had been done with the product which received the mark for these reasons. Furthermore it shall be easy for users to recognize and therefore trust in its safe use, but what is behind the CE mark? The mark shall express that the manufacturer takes responsibility for the conformity in regards to the main characteristics published in the DoP.

Where can one find the specification? How does the process of receiving the CE mark look like?

If a product is covered by a harmonized European standard (hEN) or European Assessment Document (EAD), specifications and test methods to evaluate the characteristics are described in that hEN respectively EAD. As soon as hEN or EAD exist for a certain product, all products of this kind from a manufacturer need to carry the mark when entering the European market without barriers. A product shall automatically simply specified as checked for its main characteristics according to the related hEN or EAD solely by carrying the mark. If there is no hEN or EAD for a product, the product needs to be specified in a European Technical Assessment (ETA). The ETA can be applied with special application forms (manufacturer's technical files / technical documents) from the manufacturer to the Technical Assessment Body (TAB). The TAB checks after incoming application for a certain product, if a hEN or EAD exist for that product. If so, the application will be declined. If not, an EAD has to be developed in order to work as basis for the ETA. (s. Figure 2)

3.1 European Assessment Document (EAD)

The EAD is a harmonized technical specification and includes all information to characterize a product. A general description and the intended use is first part of an EAD, followed by essential characteristics that are relevant for the intended use of the product. The EAD is completed with methods and criteria for assessing the performance of the product, but also principles for the applicable factory production control.[9] All together the EAD gives all necessary descriptions and tools to verify the characteristics of a product.

[8] CE = Communautés Européennes = European Communities

[9] www.eota.eu: "What is an EAD?"

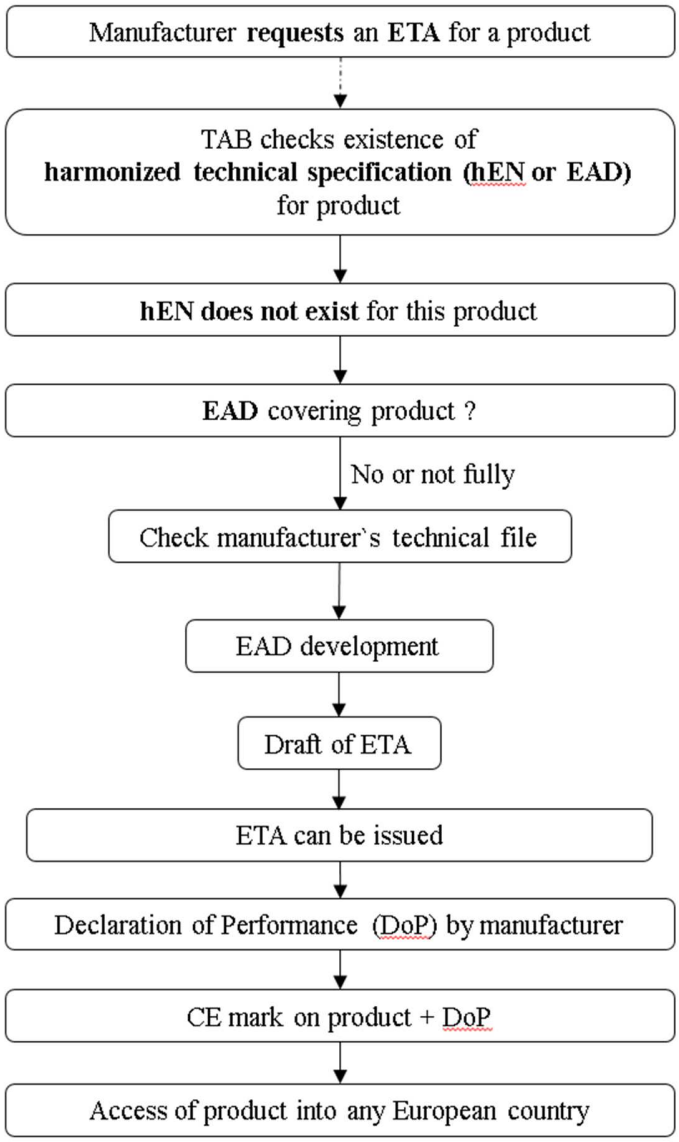


Figure 2: ETA development, if product is not or not fully covered by an EAD
(Own research based on www.eota.eu „How an EAD is developed? " and Regulation No. 305)

Based on technical documents the organization of TABs is able to proceed with the application for an ETA and inform the Commission of the work program (Regulation No. 305/2011 – Annex II).

3.2 European Technical Assessment (ETA)

"The … ETA is a document providing information about the performance of a construction product, to be declared in relation to its essential characteristics."[10] With an existing ETA a manufacturer can CE mark a product. An ETA consist of "…general information on the manufacturer and product type, name and

[10] Source: www.eota.eu - "What is an ETA?"

manufacturing plant. Performances of the product to be declared and references to the methods used for its assessment. Technical details necessary for the implementation of the AVCP[11] system."[12]

3.3 Declaration of Performance (DoP)

A product, that is characterized by a hEN or ETA and therefore carrying a CE mark, needs to be accompanied by a DoP. The DoP shall be drawn up by the manufacturer and provide information on the product performance based on the hEN or ETA.

Based on above explained processes and documents for a product, which had been applied for a CE mark, this product type from a manufacturer must carry a CE mark when entering the European market. The CE mark therefore enables the product a complete free entrance to the end user within Europe without any further tests but only accompanied with the DoP.

4. CRITERIA EXAMPLE OF HOLLOW BAR KIT IN AN EAD

The essential characterization of a product in an EAD is beside other contents described in section 3.1 mandatory for an ETA application. Therefore this section gives a closer look into some examples of essential characteristics of the hollow bar kit.

4.1 Load bearing capacity

A hollow bar kit, which is made of steel, shall secure constructions and transfer loads into the ground after correct and successful installation. Therefore the load bearing capacity is a key essential characteristic during the life cycle of the hollow bar kit. Load bearing capacity depends on material composition and amount of material. Steel types and their characteristics varies tremendously with incremental changes of the steel composition. Depending on the requirements for specific applications steel brings suitable individual characteristics along.
Considering the hollow bar precisely, the steel type and dimension (wall thickness respectively effective area of cross section) are both important to be capable of transferring the loads from a construction into soil in general. Tolerances of wall thicknesses are further an issue of quality control, as more or less material amount influences the load carrying capacity.
In addition to material composition, the system, especially the coupling nut, has to be able to carry the loads into ground. The hollow bar has to be the weakest point, if it comes to any failure at all, but not the coupling nut. The coupling nut is connecting each hollow bar to each other as a rigid joint and in case of overloading the system, the hollow bar (steel) shall deform and elongate visibly as much as necessary for one can react and do something against e.g. a moving tie-back wall, etc. before any accident or collapse arise.

4.2 Resistance against fatigue

Fatigue occurs with time and diverse environmental influences can accelerate the material aging process.
Steel quality and the joints are important characteristics in respect of resistance against fatigue. Following characteristics have significant effects on steel quality. Notched impact strength evaluates the material resistance against fracture due to sudden impacts. The higher the resulting test value the more energy can be taken by the material, which means the resistance against higher impacts is better (absorption of energy). Carbon content of steel composition has a huge influence on the steel character brittleness, which shall be

[11] AVCP = Assessment and Verification of Constancy of Performance
[12] Source: www.eota.eu - "What I s an ETA?"

low to resist impact energies. Ductility, ability of plastic deformation, is another important variable considering overloading effects.
There are many characteristics that a system has to bring along in able to withstand alternating loads, which are not going into negative, without resulting in a fatigue fracture or loosening of any joints.

4.3 Resistance against alternating loads (tension and compression)

Alternating loads changing from positive to negative more specifically changing from compression to tension require above (section 4.2) mentioned characteristics, but special attention on joints in specific. These have stricter requirements and therefore i.e. a steel ring as central stop in a coupling nut is supportive as tight steel to steel connection to transfer loads, but also reduce work on site (no additional counter nuts necessary).

4.4 Transfer of the impact energy produced by roto-percussion

Depending on the soil type the installation process is accompanied by roto-percussive impact energy. Such impact energies have an effect on the whole hollow bar system, which is used as drilling tool, and therefore the steel material needs to fit these conditions (while and after installation). Notched impact strength is another characteristic to point out in this context, as ductile material last longer, either while drilling process or afterwards during working life.

4.5 Protection against corrosion

Corrosion is a tremendously important issue. There are different understandings and ways to realize the corrosion protection. The most favorable way in realizing corrosion protection will definitely be a cost efficient, easy, but also reliable way. Reinforced concrete is used in the whole world for centuries and it is a common understanding that concrete is perfect material to protect steel. Requirements on steel quality, thread shapes and other characteristics are described in standards. Yield strength of steel has to be limited to concrete strain in order to function as a composite material. Uniform elongation is necessary to have an even development of cracks in regards to corrosion protection and predictable development. Slip within coupling has to be limited as well to prevent unnecessary development of cracks in the area of joints.
In total cracks are needed in reinforced concrete, but in general need to be kept as small as possible. Cracks smaller than 0.1 mm (grout cover thickness in an economical and required manner and in combination with limited yield strength and suitable thread shape) are seen as self-healing therefore it is a goal to achieve.

5. TRANSPARENCY CONCERNING NATIONAL TECHNICAL APPROVAL AND DOP

Due to an overwhelming offer and variety of products for clients, contractors and design engineers, they are challenged with identifying and assessing the main characteristics of a chosen system or technique, thus this audience needs to be informed and trained properly. The suitability of a product for a certain job site solution needs to be checked. It is recommended that above mentioned audience should have knowledge and awareness about the product differences and suitabilities they choose.

National technical approvals for products, if differ from harmonized technical specifications, will be replaced by DoP and CE marking bit by bit as soon as the latter exists for a product. The change will take a certain period of time (s. background of construction product regulation in section 1). The DoP is therefore one document for an applicant to use and extract the necessary information. Independently from the CE mark on the product, the corresponding application with the product will be described and approved separately. Some applications need more and others less criteria, therefore beside product criteria described in the DoP the appropriate application standards, like EN 14199 and EN 14490, are also necessary to have a complete information package.

Applications differ from construction site to construction site and there are various solutions as well. Guidelines and manuals are generally always supportive, but under certain circumstances engineers still have a specific scope for decision-making. This condition leads to importance of experience and information level of applicants.

6. SUMMARY AND OUTLOOK

CE mark and DoP together are important for the European Union to keep barriers away respectively customs clearances low and therefore speed up goods traffic. This information package also represents the result from a long way of development, where many parties of countries are involved to ensure the correctness of product definition and prevent misuse. Nevertheless misuse or misinterpretation is easily created, if a product carries a CE mark and the user does not know the background or meaning of this mark. A CE marked product always have to be accompanied by the DoP to be complete. The DoP however is not a grading document pointing out the suitability for a certain application. It is an accompanying document in combination with the CE mark to give transparency about essential characteristics, but only to show that it conforms the minimum requirements according to the harmonized technical specifications.

Regulation No. 305 gives another push in the construction product market and shall guide all parties with clearer handling of products. Such big changes need time and clarification to have real understanding of transparency and benefit.

7. REFERENCES

European Standards (EN)

EN 10210:	Hot finished structural steel hollow sections
EN 14199:	Execution of special geotechnical works - Micropiles
EN 14490:	Execution of special geotechnical works - Soil nailing
EN 1990:	Eurocode 0: Basis of structural design
EN 1991:	Eurocode 1: Actions on structures
EN 1992:	Eurocode 2: Design of concrete structures
EN 1993:	Eurocode 3: Design of steel structures
EN 1994:	Eurocode 4: Design of composite steel and concrete structures
EN 1995:	Eurocode 5: Design of timer structures
EN 1996:	Eurocode 6: Design of masonry structures
EN 1997:	Eurocode 7: Geotechnical design
EN 1998:	Eurocode 8: Design of structures of earthquake resistance
EN 1999:	Eurocode 9: Design of aluminum structures

Regulation and Council directive

Regulation No 305/2011
Directive 89/106/EEC

Webpages

https://www.eota.eu/en-GB/content/what-is-an-eta/18/
https://www.eota.eu/en-GB/content/elements-of-the-eta-process/19/
https://www.eota.eu/en-GB/content/what-is-an-ead/30/

https://www.eota.eu/en-GB/content/how-an-ead-is-developed/40/
https://www.eota.eu/en-GB/content/what-is-ce-marking/48/
https://europa.eu/european-union/law_en
http://eurocodes.jrc.ec.europa.eu/

33 CONGRESS SQUARE - A CASE STUDY
BOSTON, MA

Anthony C. Barila, P.E. and John R. McKinnon

INTRODUCTION

The interior of four structures that were annexed to form the original headquarters of the Fidelity Investment Company at 82 Devonshire Street in Boston, MA will be selectively demolished to allow for the internal addition of a 14 story structure. The foundations of the new office building will be supported on high capacity drilled micropiles. There will be 51 micropiles to support the new super columns, 67 micropiles to support the core of the new structure plus 19 micropiles to support the tower crane foundation. In addition, 8 micropiles were required to underpin two columns immediately next to a support of excavation (SOE) system that will allow access to the core mat foundation. The critical component of the SOE is 15 micropiles that will act as soldier piles.

Two pile load tests were performed, one in compression to a maximum test load of 1010 tons (8.9 MN) and one in tension to a maximum test load of 458 tons (4.1 MN). The test results were excellent. Based on these results, the geotechnical engineers agreed to reduce the rock socket length by 50% from the original design.

Hub was contracted jointly to the Consigli Construction Company (project construction manager) and RelatedBeal (the project developer). The structural engineer was MacNamara Salvia. Haley & Aldrich was the geotechnical engineer.

FOCUS OF THIS PAPER

This paper will focus solely on the core piles and the results of the pile load tests. Also, the results of these tests along with others that hub has performed over the past five years has led us to recommend that the industry revisit the design of high capacity rock socketed micropiles.

The main points of emphasis for future discussions will be the following:

- reevaluate strain compatibility within a confined section such that higher allowable stresses in high strength steel can be utilized;

- utilize a higher allowable stress in grout;

- evaluate the load distribution at and below the casing tip to develop an alternative approach to determine the rock socket length that is now solely based on friction and 100% of the design load; and

- evaluate the steel design within the rock socket using the load distribution data from these tests.

SITE CONDITIONS AND SCHEDULE

Two pile load tests were performed from March 28 to April 6, 2016 prior to the completion of the overall structural design. The tests were performed in a very tight open area adjacent to the project structures.

The core piles were installed from January 6 to February 11, 2017. The piles were installed from a level about 25 ft. (7.62 m) below street level. The piles were installed with two different drill rigs. Eight of the piles were installed with the Davey-Kent DK-525 drill rig at an area with only 10 ft. (3.1 m) of headroom. This drill rig was lowered to the drill locations via a hoist hatch next to an alley. Photo 1 shows the DK (without the mast) being lowered. After significant demolition of the existing structures was completed up to the roof level, a Casagrande C-8 drill rig was utilized for the remaining 59 piles. This drill rig entered the building from one of the main streets that surround the buildings. The rig walked inside a portion of the building and down a ramp (cut at the SOE) to access the drill level for the remaining piles. Photo 2 shows the C-8 crawling thru the opening and down the ramp down to the work level.



Photo 1: The DK-525 low headroom drill rig hoisted into the building though a small hole in the street.

The majority of the micropiles were installed while heavy demolition of the existing structures was in full swing. The work areas resembled a “war zone” during this process. Photo 3 shows the “scars” of the demolition process as the core area is redeveloped up to roof level.



Photo 2: The Casagrande C-8 entering the building off Quaker Lane. A hole was created in the outer wall just big enough for the C-8 to enter. The length of the mast had to be factored into the required clearance when walking down the ramp to 25 feet (7.3 meters) below street level.



Photo 3: Drilling support of excavation piles in the demolished center of the structure which will be the future location of the core.

ORIGINAL DESIGN

The original design loads for the micropiles was 325 tons (2.9 MN) in compression, 150 tons (1.3 MN) in tension and 11 tons (97.9 KN) lateral. The micropile design consists of the following:

- a 10 ¾ in. (273 mm) OD; 0.545 in. (13.8 mm) wall casing drilled down into stable rock;

- a core pipe [8.625 in. (219 mm) OD; 0.719 in.(19.8 mm) wall] to reinforce the rock socket plus 15 ft. (4.6 m) above the casing tip;

- a core pipe [7.0 in. (179 mm) OD; 0.50 in. (12.7 mm) wall] in the upper 25 ft. (7.6 m) of the micropile to sustain the bending moment due to the lateral load at the top of the pile;

- a 2.5 in. (63.5 mm) Grade 150 bar to support the tension load; and

- 5000 psi (34.4 MPa) grout.

The length of the rock socket was specified by the Engineers to be 34 ft. (10.2 m) long. Refer to Figure 1 which shows the above details. Refer to the section of the coring log that describes the coring of the rock. In Figure 2

PILE LOAD TESTS

Two pile load tests were performed - one in compression to 1010 tons (8.9 MN) and one in tension to 458 tons (4.1 MN). The pile load tests were performed about three months before a wind tunnel study was performed which reduced all the design load components. The final micropile design is provided in a separate section below.

Compression Test

Figure 3 shows a cross-section of the test pile arrangement which consisted of four (4) reaction piles and the test pile in the middle. Photos 4 thru 9 show drilling of the test pile and the reaction piles, setting up the test beams and the final test pile setup. Note that the test pile was drilled with a low headroom drill rig (DK-525) to provide drill rates for the casing to simulate the low headroom conditions anticipated for the production piles inside the buildings. The reaction piles were drilled with a Casagrande C-8 drill rig.

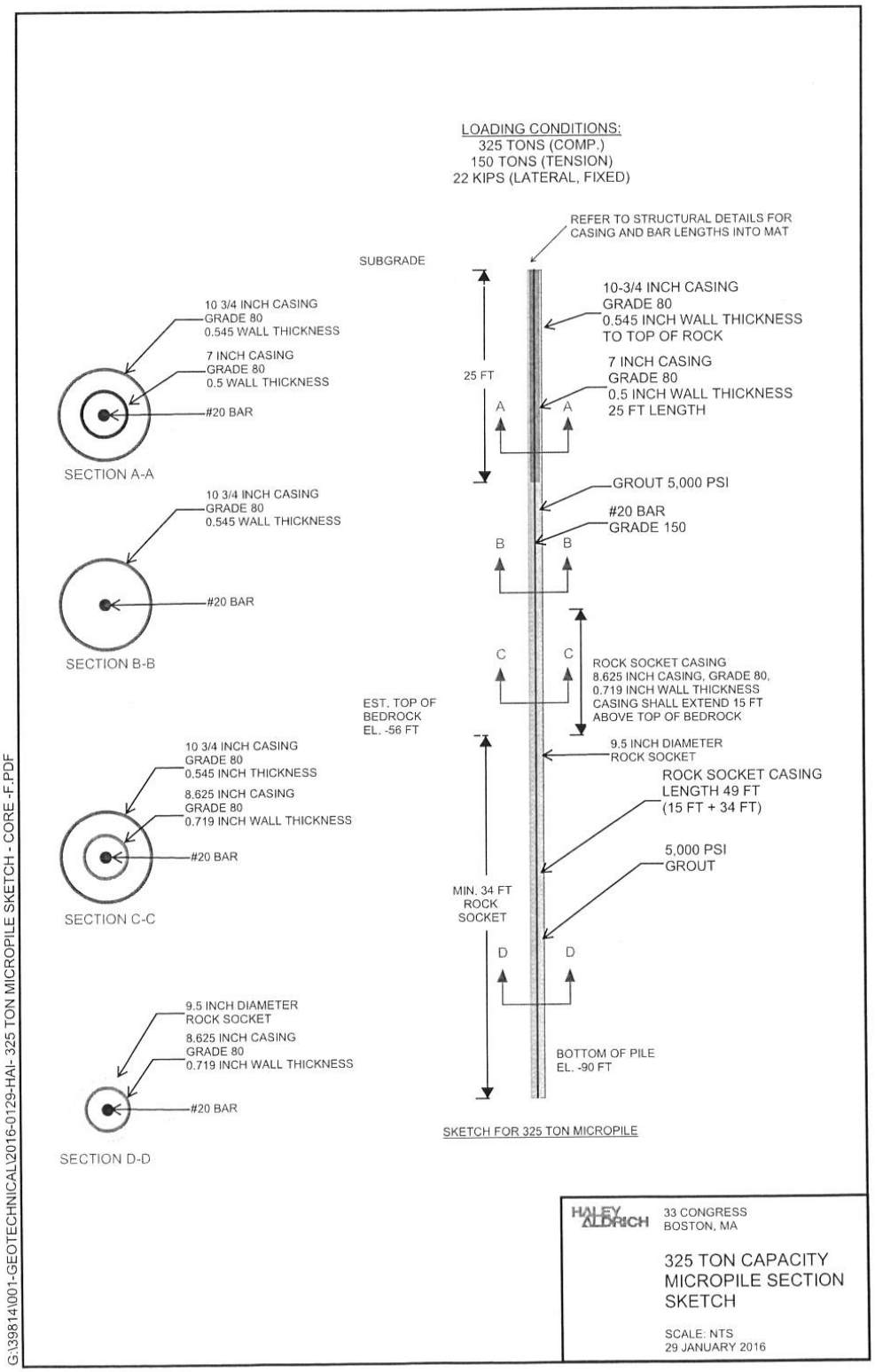


Figure 1: Original core pile design which was the basis for the pile load tests.

HALEY ALDRICH

CORE BORING REPORT

Boring No. HA-B1

Project	CONGRESS SQUARE, 33 CONGRESS STREET, BOSTON, MA
Client	RELATED BEAL
Contractor	CRAWFORD DRILLING SERVICES, LLC

File No. 39814-002
Sheet No. 1 of 5
Start February 24, 2016
Finish February 29, 2016
Driller Daryl Green
H&A Rep. C. Sullivan
Elevation 25.0 (est.)
Datum Boston City Base
Location See Plan

	Casing	Sampler	Barrel	Drilling Equipment and Procedures
Type	HW / NW	S	NX	Rig Make & Model: Deitrich D120
Inside Diameter (in.)	4 / 3	1 3/8	2.6	Bit Type: Roller Bit
Hammer Weight (lb)	Auto/Auto	140	-	Drill Mud: None
Hammer Fall (in.)	Auto/Auto	30	-	Casing: Drive & wash HW 14', NW spin 85'
				Hoist/Hammer: Cat-Head, Automatic Hammer

Depth (ft)	Drilling Rate (min./ft)	Run No.	Run Depth (ft)	Recovery/RQD in.	Recovery/RQD %	Weathering	Elev./ Depth (ft)	Visual Description and Remarks
		S11	74.0 75.3					Note: Roller bit from 75.25 to 79.0 ft below ground surface through WEATHERED BEDROCK.
	3	C1	79.0 80.3	15 0	96 0	Moderate		C1: Hard, moderately weathered, gray to blue gray, fine grained to aphanitic DIABASE. Extremely fractured with clay infilling.
80	5							
	7	C2	80.3 81.3	12 0	100 0	Moderate		C2: Similar to above
	3.5	C3	81.3 84.0	32 0	100 0	Moderate		C3: Hard, moderately weathered, gray to blue gray, fine grained to aphanitic DIABASE. Joints moderate to high, dipping, close to extremely close, moderate, rough, planar to undulating, discolored weathering on joints with occasional clay/calcite, open. Note: Borehole caved due to rock falling in. Advanced NW casing to 84 ft.
	4							
	4	C4	84.0 85.0	11 5	92 42	Slight		C4: Hard, slightly weathered, gray to blue gray, fine grained to aphanitic DIABASE. Joints moderate to indiscernible due to amount of fracturing, rough, planar to undulating, discolored weathering, occasional clay/calcite deposit, open.
85	3	C5	85.0 88.3	40 8	100 20	Slight-Moderate		C5: Hard, slightly to moderately weathered, gray to blue gray, fine grained to aphanitic DIABASE. Joints extremely fractured, set orientation indiscernible, rough, planar to stepped, discolored weathering, clay, infilled, open.
	2							
	2							
	3							
	3.5	C6	88.3 89.4	12 0	97 0	Slight-Moderate		C6: Similar to above
	3	C7	89.4 92.4	36 0	100 0	Slight-Moderate		C7: Similar to above
90	3.5							-BEDROCK-
	3.5							
	2.5	C8	92.4 97.4	60 12	100 20	Slight-Fresh		C8: Hard, slightly weathered to fresh, gray to blue gray, fine grained to aphanitic DIABASE. Joints moderately dipping to high angle, moderate to extremely close, rough, planar to undulating, discolored weathering with occasional quartz/calcite deposits, open.
	2.5							
95	3							

Water Level Data

Date	Time	Elapsed Time (hr.)	Depth (ft.) to: Bottom of Casing	Bottom of Hole	Water
2/25/16	0715	15	64	56	25.0
2/26/16	0700	16	84	85	25.8
2/29 /16 Tooling in hole; unable to measure					

Sample Identification

O - Open End Rod
T - Thin Wall Tube
U - Undisturbed Sample
S - Split Spoon
G - Geoprobe

Well Diagram

Riser Pipe
Screen
Filter Sand
Cuttings
Grout
Concrete
Bentonite Seal

Summary

Overburden (lin. ft.) 75.25
Rock Cored (lin. ft.) 41.5
Samples 11S, 17C

Boring No. HA-B1

Note: Soil identification based on visual-manual methods of the USCS as practiced by Haley & Aldrich, Inc.

H+A CORE LOG PG1-07-1 HA-UB09-BOS.GLB HA-TB+CORE+WELL-07-1.GDT \\BOS\GINT\39814-002-TBC.GPJ Mar 11, 16

Figure 2: Coring log taken describing the coring of the rock

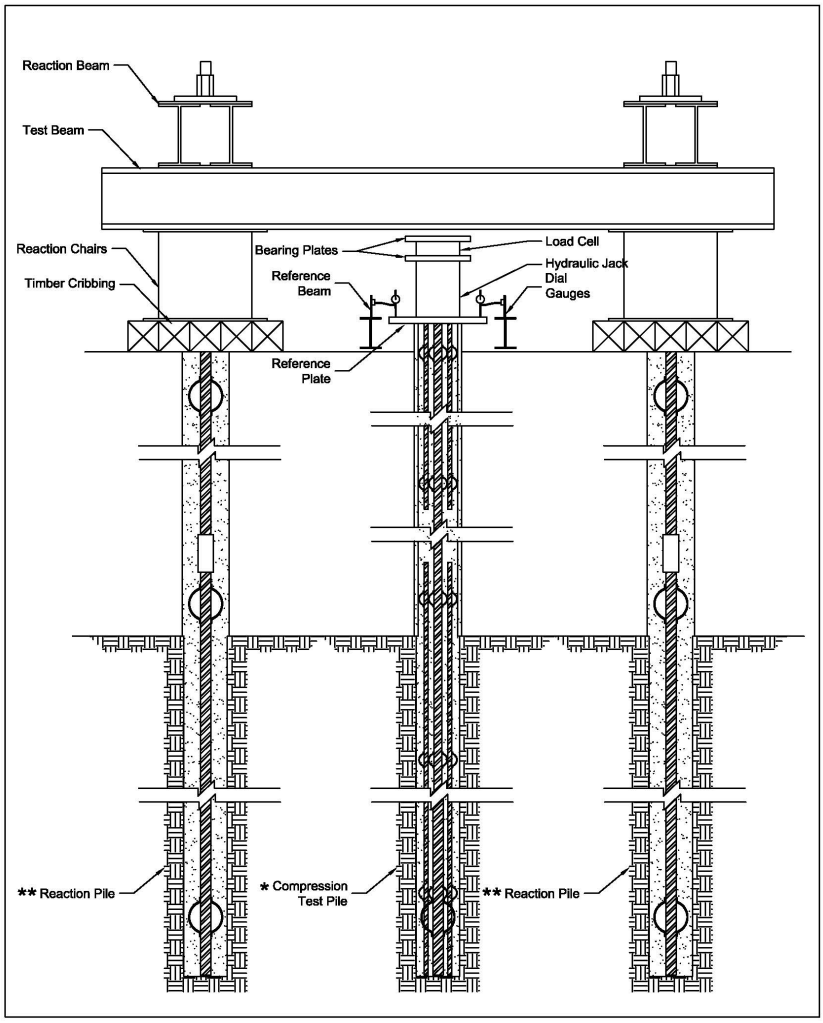


Figure 3: Section of the compression test layout



Photo 4: DK-525 drilling the compression test pile

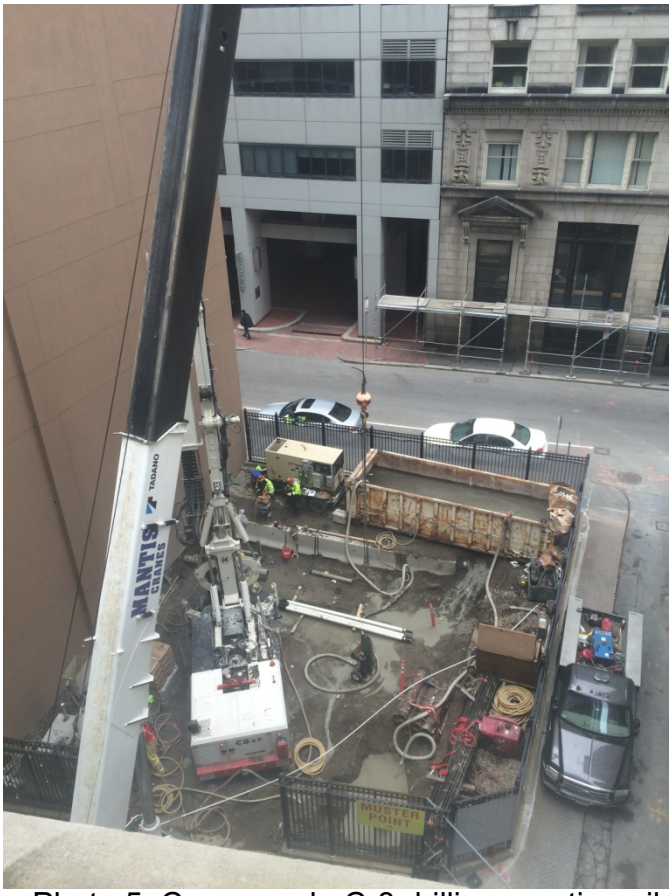


Photo 5: Casagrande C-8 drilling reaction piles.


Photo 6: Setting up the test frame



Photo 7: Test frame setup complete


Photo 8: Recording pile movement during the pile load test

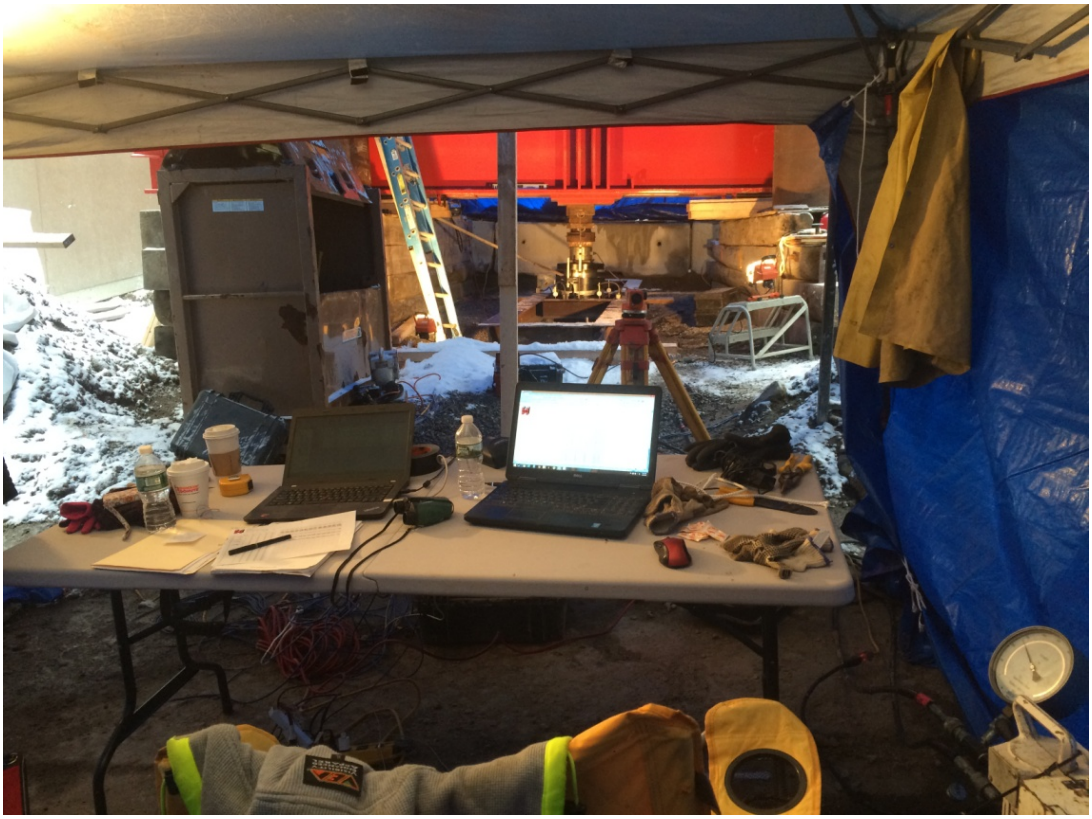


Photo 9: Test frame covered during the test to protect the instrumentation from the elements during the test. A data logger and laptops were utilized to monitor and record the instrumentation installed within the test pile.

Figure 4 shows the plot of pile settlement versus load for the test pile. The "curve" is essentially linear for the entire loading schedule. The total settlement of the pile was 1.471 in. (34.36 mm) at 650 tons (5.8 MN) and 2.656 in.(67.46 mm) at 1010 tons (8.9 MN). The net settlement after unloading from 1010 tons (8.9 MN) was only 0.372" (9.5 mm). The total creep movement at 1010 tons (8.9 MN) from 1 minute to 90 minutes was only 0.032 in. (0.813 mm).

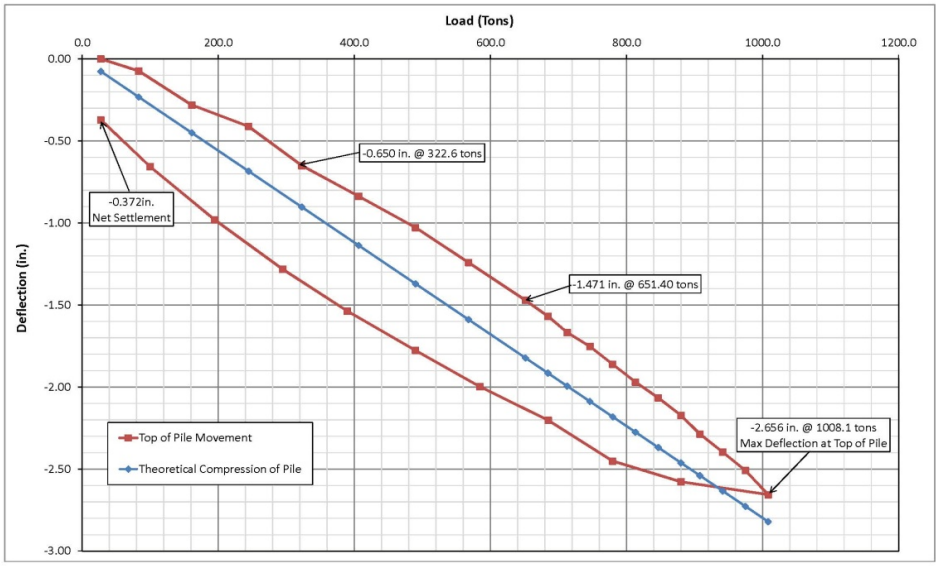


Figure 4: Compression test settlement versus load graph

Figure 5 shows the distribution of the test load throughout the full depth of the test pile. A total of 13 strain gauges were attached to the 2.5 in. (63.50 mm) Grade 150 bar. Geokon 4911 “sister bars” were utilized. Nine of the strain gauges were placed within the 25 ft. (7.6 m) rock socket.

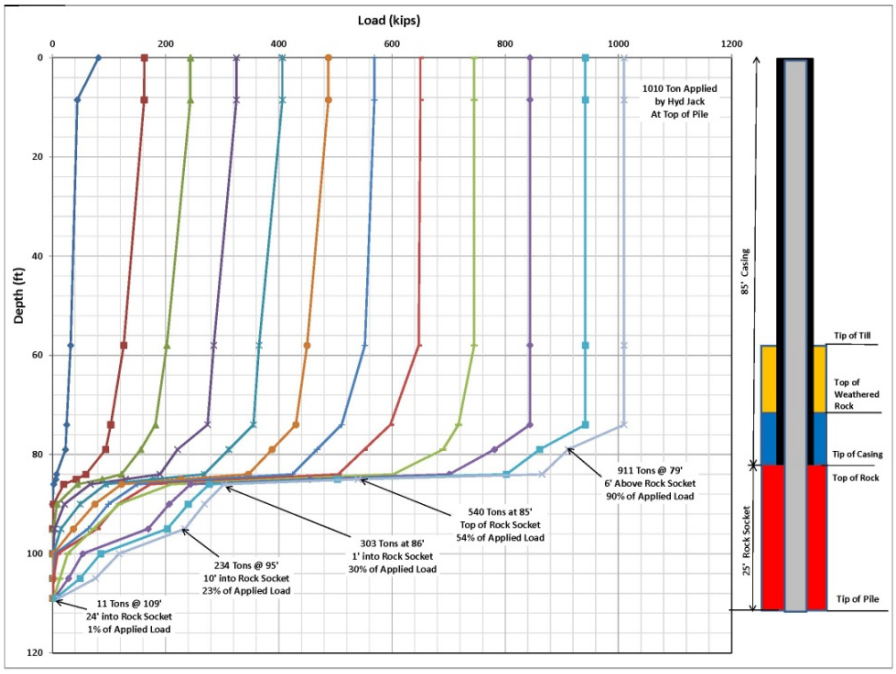


Figure 5: Compression test load distribution graph

The large number of strain gauges within the socket were utilized to confirm that a significant amount of the test load would be “shed” at or just below the casing tip. Note that 145 tons of the maximum test load was transferred above the casing tip within the weathered rock. There was 540 tons (4.8 MN) at the casing tip (54% of the test load) and only 303 tons (2.7 MN) at a depth of 1.0 ft. (0.3 m) below the casing. This is only 30% of the applied test load. Hence, 263 tons (2.3 MN) was “shed” in one foot below the casing tip and 562 ton from one foot above the casing to one foot below the casing. At 10 ft. (3.04 m) below the casing tip, 234 tons (2.1 MN) remained, or 23% of the max. test load.

Tension Test

One of the four reaction piles for the compression test was utilized to perform a pile load test in tension. Figure 6 shows the test pile consisting of:

- a 3 in. (76.2 mm) Grade 150 bar;

- a rock socket length of 25 ft. (7.6 m);

- location of three strain gauges and two tell-tales within the rock socket.

Note that the bar was debonded with a PVC pipe close to the top of the rock socket. The depth to stable rock was 79 ft. (24 m).

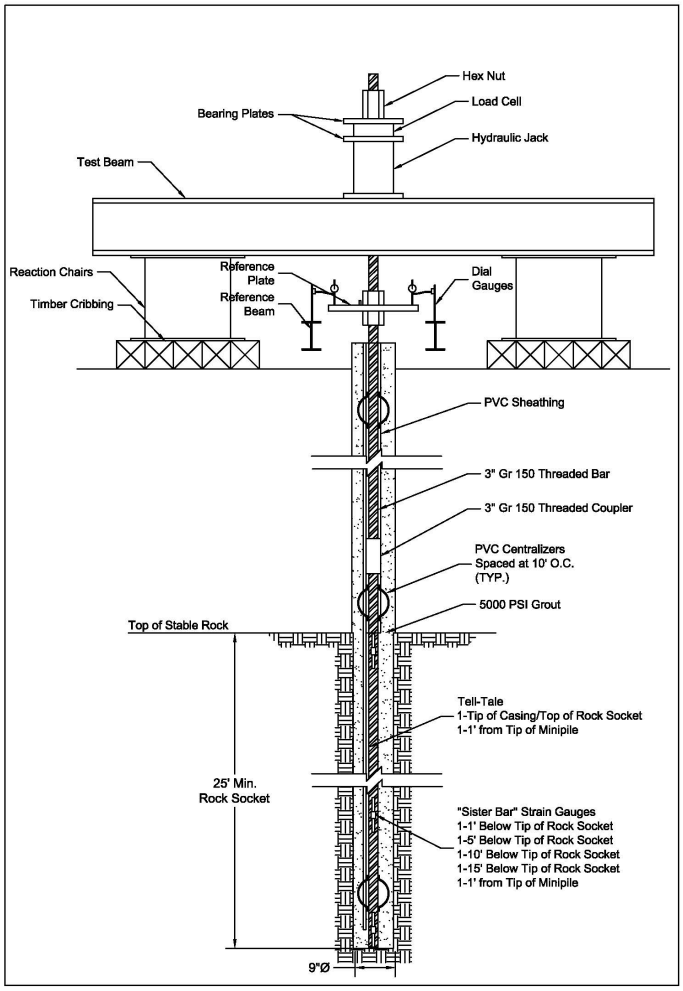


Figure 6: Tension test pile detail

Figure 7 presents the plot of test load vs elongation. The “curve” is essentially linear up to about 400 tons (3.6 MN) which is close to the minimum yield strength of the bar [~ 420 tons (3.7 MN)]. The bar begins to show plastic deformation beyond this point which accelerates between 450 tons (4.01 MN) and 458 tons (4.08 MN). The net “settlement” after unloading is 1.006 in. (25.55 mm) which is very close to the actual total movement at 458 tons (4.07 MN) less the theoretical elongation of the bar, if it were fully elastic at that load. The recorded elongation during the test was strictly due to the elongation of the bar, as evidenced by the recorded small movement [only 0.026 in. (0.661 mm)] at the tip of the pile.

Figure 8 presents the test load distribution thru the test pile. Note that all the drill casing had been extracted after the bar was installed and grouted. Also, the PVC sheathing that was utilized to debond the bar was installed to a depth of about 5 ft. (1.5 m) above the top of rock (we wanted to be 100% certain that the sheathing did not extend into the rock socket). The combination of both items explains why some of the test load was transferred above the top of rock. This resulted in 344 tons (3.1 MN) or 75% of the max. test load being transferred to the top of rock which is still significant. Approximately 115 tons (1 MN) were transferred one foot into the rock socket. Only 10 tons (89 KN) was recorded at a depth of 1.5 M (5 ft.) into the rock socket. Hence, a total of 334 tons (3.1 MN) was transferred in the upper 5 ft. (1.5 m) of the rock socket. This is

73% of the maximum test load. Note that the creep at the maximum test load was only 0.022 in. (0.558 mm) from 1 to 10 minutes.

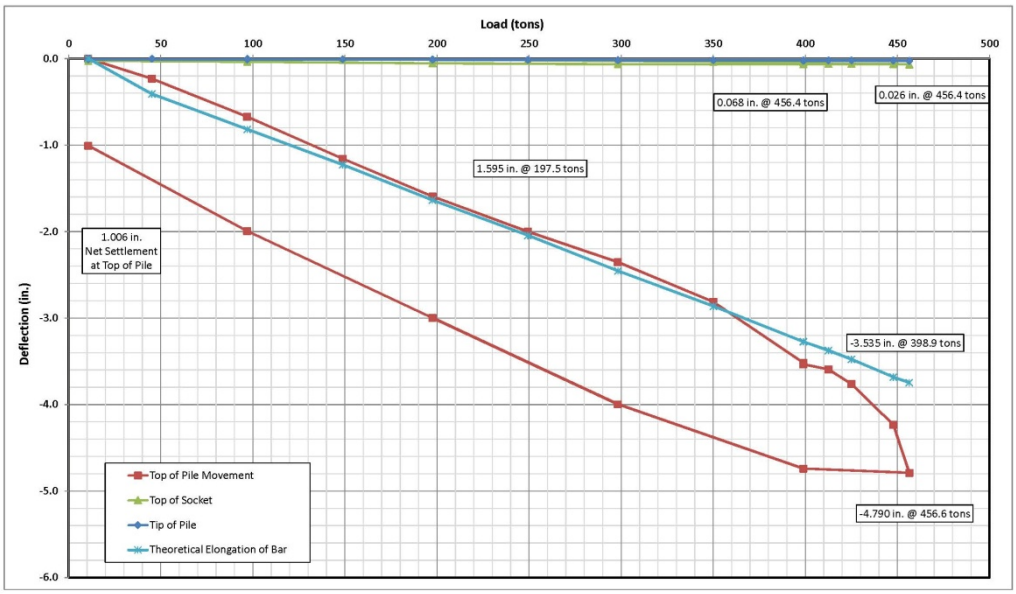


Figure 7: Tension test elongation versus load graph

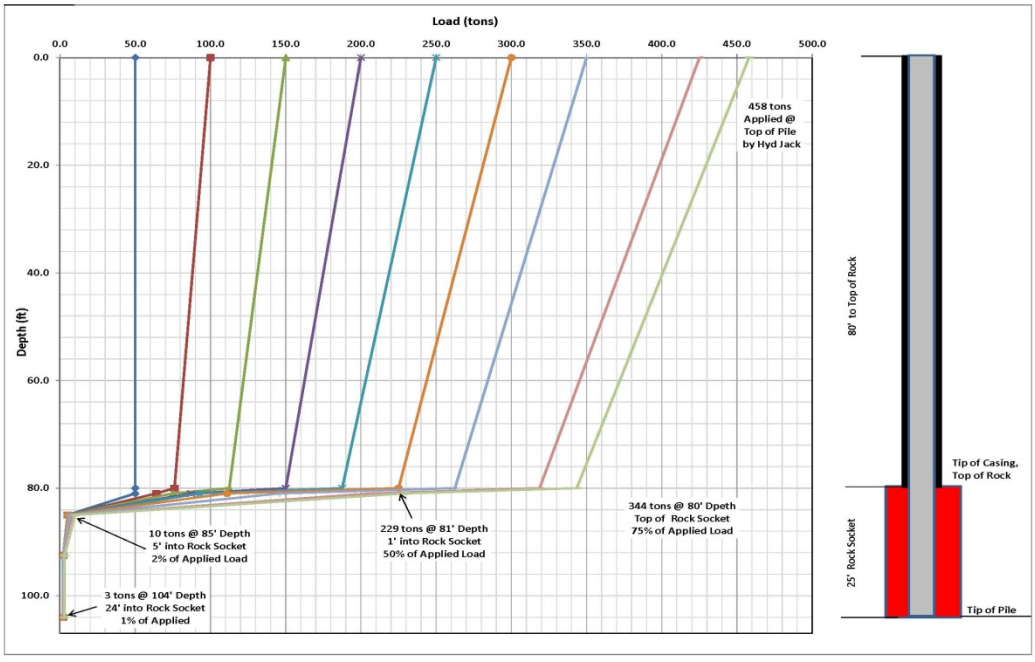


Figure 8: Tension test load distribution graph

Evaluation of Test Results

The significance of the test results is as follows:

1) The plot of settlement v test load and the creep results at maximum test load for the compression test clearly indicate that this test pile could have been subjected to a significantly higher load. If the reaction piles and the test beams had a higher overall capacity, this pile could have seen tested to 2000 tons (17 MN) without any significant increase in total movement and creep.
2) The compression test pile and many others that Hub Foundation has performed to high loads show that a significant portion of the test load is transferred to the tip of the casing and is supported in compression by the combination of the rock and grout column directly below the casing. In addition, the majority of the balance of the test load is transferred within the upper 5 ft. (1.5 m) of the rock socket.
3) The plot of elongation v test load of the tension test was essentially elastic within 267% of the design load or 400 tons (3.6 MN). The recorded elongation was solely that of the bar with only a minor movement within the rock socket.

The above evaluation and test results plus other similar tests can be utilized to develop the basis for changes to the overall design of high-capacity rock-socketed micropiles.

FINAL DESIGN

After the pile load test was completed, the project performed wind tunnel modeling of the structure to attempt to reduce the lateral loadings on the core of the new structure. The results of these model studies were extremely beneficial, thereby, reducing the loadings on the core piles, such that, a smaller diameter pile could be utilized.

The final design capacity of the core piles was 280 tons (2.5 MN) in compression, 120 tons (1.1 MN) in tension and 8.1 tons (72 KN) lateral. Internal core pipes were utilized to provide the structural requirements within the rock sockets and at the upper portion of the piles to take care of the bending moments from the lateral loads. Refer to Figure 9 which provides a sketch of the micropile design.

The micropiles for the core consist of the following:

- 9.625 in. (244 mm) OD; 0.545 in. (13.8 mm) wall casing drilled down into stable rock;

- a core pipe [6.302 in. (160 mm) OD; 0.85 in. (21.6 mm) wall] to reinforce the rock socket plus 15 ft. (4.6 m) above the casing tip;

- a core pipe [6.625 in. (168 mm) OD; 0.475 in. (12.1 mm) wall] in the upper 15 ft. (4.6 m) of the micropile to sustain the bending moment due to the lateral load at the top of the pile.

- a 1.75 in. (44 mm) Grade 150 bar to support the tension load; and

- 5000 psi (34.5 MPa) grout.

The length of the rock socket was evaluated from the pile load tests and was reduced to 17 ft. (5.2 m) long.

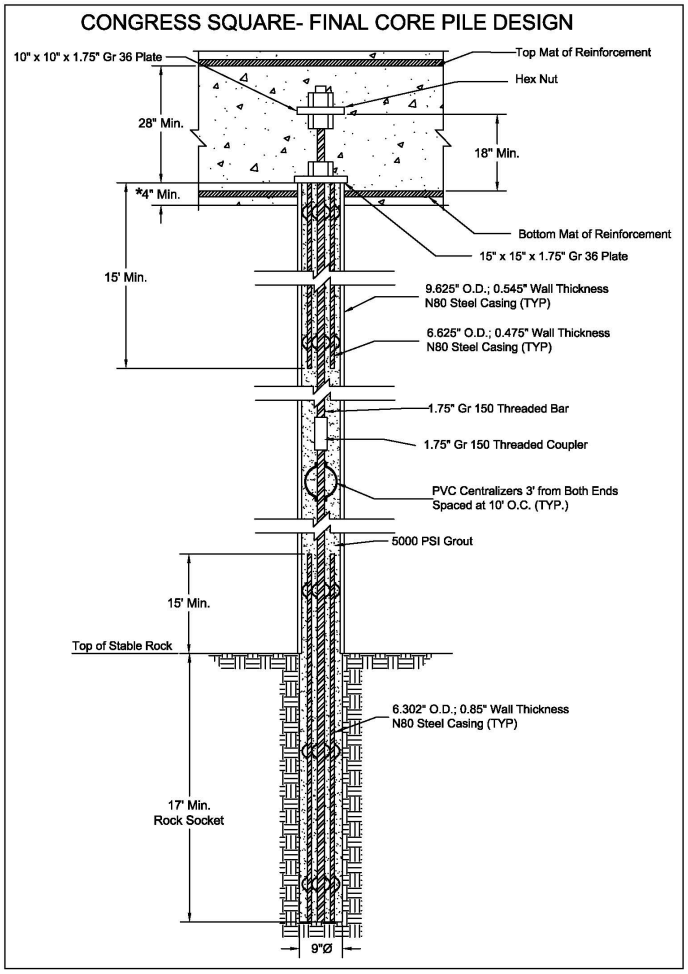


Figure 9: Final micropile design for the core piles

PILE INSTALLATION

The micropiles for the core of the structure were installed with two different drill rigs. Due to physical restraints and the omnipresent demolition process, Hub could only drill with one rig at a time.

Photos 10 thru 12 provide a view of the extreme difficulty of installing the low headroom micropiles within confined surroundings. Although about 25 ft. (7.6 m) below street level and in an “hostile” environment, the installation of the micropiles with unlimited headroom proved to be a much smaller challenge. Photos 13 thru 15 provide views of this process.



Photo 10: Casagrande C-8 drilling core piles within the central core while a snow storm hammered Boston outside.



Photo 11: Drilling in tight places with minimal access



Photo 12: Drilling in a narrow corridor



Photo 13: Installing pile reinforcing with a fork truck while piles are drilled elsewhere

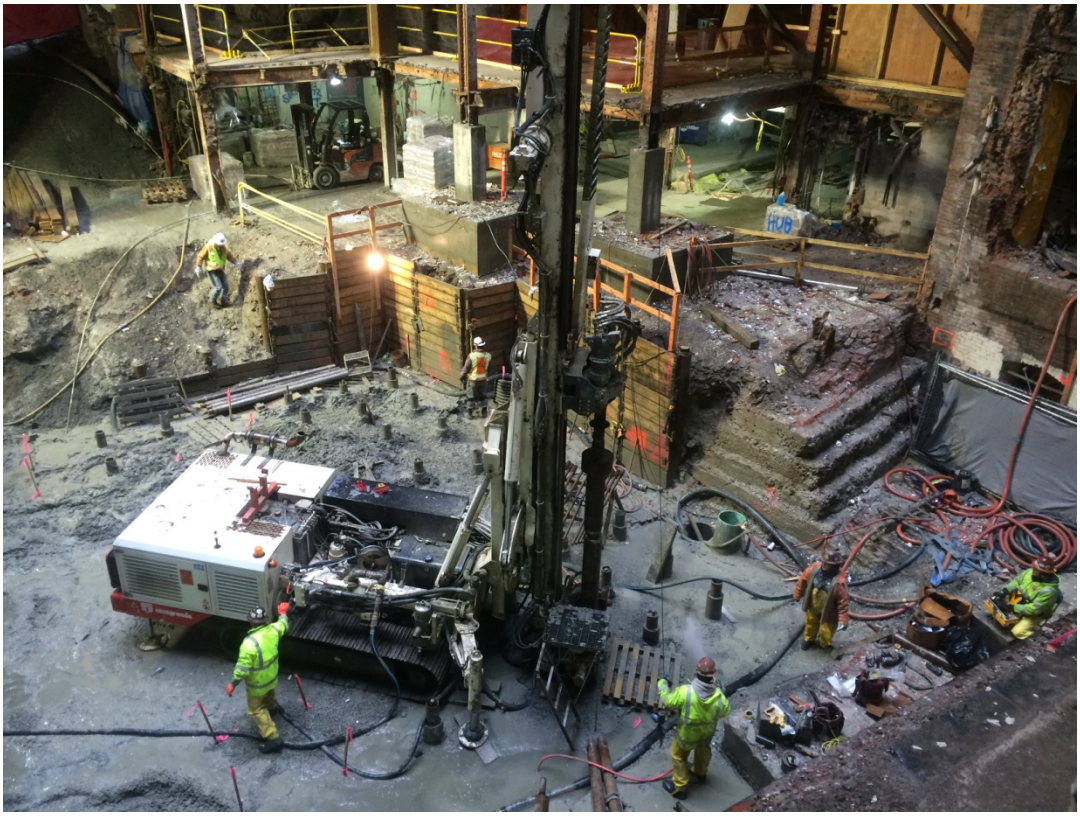


Photo 14: Casagrande C-8 drilling core piles

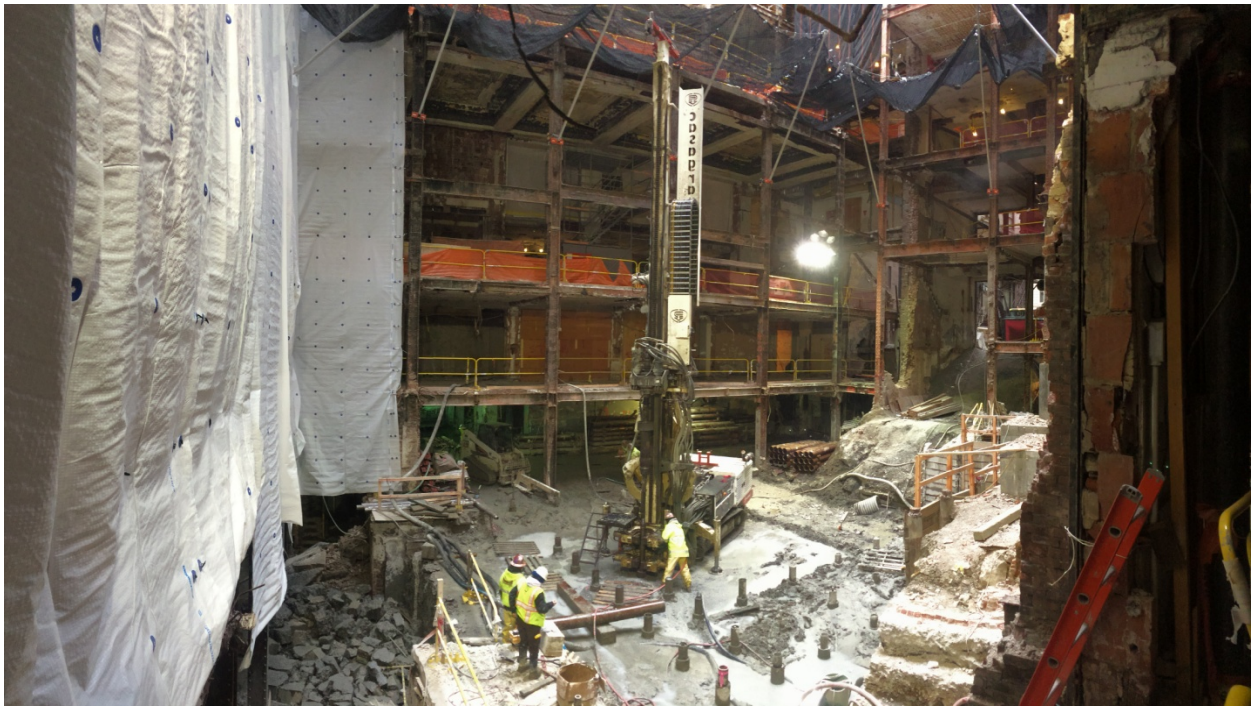


Photo 15: Casagrande C-8 working its way out of the core

CONCLUSION

The structural components that are utilized in the current micropile market consist of relatively low cost but high strength pipe manufactured for the oil drilling industry. The yield stress of the pipe ranges from 80 ksi (551.8 MPa) to 140 ksi (965.3 MPa). This pipe is used for both the permanent drill casing seated into stable rock and, as in this project, for the core pipe to increase the overall capacity thru portions of the pile length. In addition, continuously threaded bars with yield stress of 75 ksi (517 MPa) to 150 ksi (1034 MPa) are included to provide additional compression and tension capacity. The current codes (IBC and/or local codes) only allow a fraction of the yield stress of the steel components, up to 32 ksi (220 MPa). Consideration should be given to form a committee to review this and make recommendations to increase this value to a higher allowable stress for the different steel components.

The above point was the emphasis of an excellent technical paper, “Design with High-Strength Steel Reinforcement in Micropiles - Clearing up the Misconception in Strain Compatibility”, by Terence P. Holman, John R. Wolosick and Thomas D. Richards. This paper was published in the ADSC Foundation Drilling magazine in August/September of 2016. The current strain compatibility models ($F_y = 0.003\ E_{steel}$) is based upon unconfined sections in axial compression or combined compression and flexure. Studies reported in this paper cite results that indicate that ultimate strain levels can be up to 10 times higher in confined columns. Based upon these results and the recommendations made by Holman, et al, allowable stresses in steel can be safely increased from $0.4F_y$ to $0.5\ F_y$, up to 60 ksi (413 MPa). Note that the industry designs tension elements with allowable stresses of 60% of ultimate stress. This is 90 ksi (621 MPa) for 150 ksi (1,035 MPa) bars and 162 ksi (1,035 MPa) for 270 ksi (1,863 MPa) strands. Tension elements face a much more challenging environment than steel in compression in a confined environment within grout and rock. Also, the allowable stress in the grout should be increased from $0.33f'_c$ [up to 1600 psi (11 MPa)] to $0.4f'_c$. Note that the grout mixes that are now utilized in micropile installations have 28 day compression strengths of at least 6000 psi (41.3 MPa) and up to 8000 ps (55.1 MPa). The maximum allowable stress for grout in a confined condition should be increased to a minimum of 2000 psi (13.8 MPa). Note that these recommendations will only apply to permanently cased micropiles into dense tills and rock.

The current evaluation of determining the length of rock sockets should be modified to account for the path of the load distribution that has been demonstrated by numerous pile load tests in rock. The concept that load transfer within the bond length of micropiles is solely in friction needs to be revisited. The test data that Hub Foundation has developed over the past 5 years for high capacity micropiles show that a significant percentage (55% to 90%) of the applied test load is supported by the steel casing (the stiffest member of the pile) and tra nsferred to the tip of the casing. This load is supported in compression by the rock and the confined grout column below the casing. The majority of the balance of the test load is, typically, transferred within the upper 5 ft. (1.5 m) of the rock socket. The industry continues to ignore this critical factor and continues to design these high capacity micropiles with the only transfer being friction or bond between the grout and the rock socket. Depending upon the level of conservatism

that is utilized in determining the bond value of the rock (based upon rock type and quality), this, typically, results in excessive rock socket lengths.

Another possible modification to high capacity rock-socketed micropiles is the structural design within the rock sockets. If only 10% to 45% of the maximum test load is transferred into the socket, why do we design these long rock sockets for 100% of the design load? This is a very critical question, especially for low headroom micropiles where the size of couplers and the acceptable level of grout cover have the greatest impact on the design capacity.

In conclusion, the biggest impediment to the growth of the micropile industry is the design of the rock sockets for high capacity micropiles. It is Hub's goal to continue with the application of high and higher capacity micropiles to be utilized to solve critical constructability issues with deep foundations. Hub Foundation is planning for 400 tons (3.6 MN) to 500 tons (4.5 MN) micropiles on future projects. We strongly recommend that ISM along with DFI and ADSC review our recommendations and that of Holman, et al, to modify the design of high capacity rock-socketed micropiles.

STATNAMIC LOAD TESTING ON A 406 MM (16 IN) DIAMETER MICROPILE

Paul J. Axtell[1], P.E., D.GE, David S. Graham[2], P.E., Joseph D. Bailey[3], P.E.

ABSTRACT

The Highway 53 relocation project in Virginia, MN involves construction of a very tall bridge across a currently inactive iron ore mine pit. This pit is partially flooded and serves as the community's drinking water source. The new bridge is 345 m (1,132 ft) long with a three-span, plate girder superstructure. Two intermediate 60 m (200 ft) tall piers are located within the pit. The foundations for the intermediate piers consist of bored pile groups installed using techniques common to micropile construction. Extremely challenging and highly variable subsurface conditions exist at the site, which range from uncontrolled iron ore mine waste fill to very hard rock that can also be highly fractured and abrasive. Despite the conditions, foundations up to 53 m (175 ft) deep were successfully installed using down-the-hole hammer methods and full-length permanent casing. An extremely aggressive construction schedule added to the difficulties. Full-scale foundation load testing using the Statnamic rapid loading method was conducted in support of the design and construction with a separate pre-design phase contract. This paper describes the Statnamic testing and associated unique behavior of a 406 mm (16 in) diameter test micropile.

INTRODUCTION

The new alignment of Trunk Highway 53 (TH 53), which is just southeast of Virginia, Minnesota and shown in Figure 1, is being relocated to allow for future iron ore mining operations. The new section of highway will include a three-span bridge (MnDOT bridge number 69129). The new bridge will cross the currently inactive and flooded Rouchleau Mine Pit. The proposed structure is approximately 345 m (1,132 ft) long with two abutments and two intermediate piers. The superstructure will be a steel plate girder bridge with eight girder lines. The abutments will be founded on spread footings and the two piers will be founded on groups of 762 mm (30 in) diameter bored piles. The term "bored pile" is used herein to describe drilled piles that are constructed using similar methods and equipment for micropiles, yet are larger diameter than typical micropiles. Although arbitrary, micropiles are generally considered to have a diameter of 305 mm (12 in) or less.

Due to the extremely heterogeneous subsurface conditions and the formidable foundation construction difficulties that were anticipated, a design-phase load test program was conducted prior to the construction contract. The primary intent of the test program was to verify the feasibility of constructing deep foundations with sufficient size and strength to support a 60 m (200 ft) tall bridge. The design must also accommodate dynamic demands, both geotechnical and structural, resulting from anticipated future mine blasting operations, in addition to the more typical force effects.

[1] Principal Engineer, Dan Brown and Associates, Overland Park, Kansas, paxtell@dba.world
[2] Project Engineer, Dan Brown and Associates, Chattanooga, Tennessee, dgraham@dba.world
[3] Geotechnical Engineer, Applied Foundation Testing, Green Cove Springs, Florida , jbailey@testpile.com

The secondary intent of the test program was to perform axial compressive load tests on the test foundations. The potential benefits of design-phase load test programs are well established and generally include mobilization of nominal resistance values in excess of those estimated by design computations and increased reliability as manifested through increased resistance factors at the strength limit state. Accordingly, three axial compressive load tests were conducted on three separate test foundations using the rapid test method and associated Statnamic testing device. Note that other testing methods were considered, including traditional top-down tests and bi-directional cell tests, but, given the anticipated subsurface conditions, required loading magnitude, and pile type, the Statnamic device was determined to be the only plausible option.



Figure 1: Site location; Virginia, MN 288 km (180 miles) north of Minneapolis, MN.

The three foundations successfully constructed and tested included two, 610 mm (24in) diameter elements and one 406 mm (16 in) diameter element. The focus of this paper will be on the construction and load test behavior of the 406 mm (16 in) diameter foundation, which most closely represents the size typically associated with micropiles.

SUBSURFACE CONDITIONS

The test program area was located on Mine Waste Fill (MWF) material placed during past mining operations to create a haul road. The ground surface at the site was relatively flat with existing surface elevations between approximately 400 m (1,312 ft) and 402 m (1,318 ft). The MWF is approximately 37 to 40 m (120 ft to 130 ft) thick, extending to around Elevation 363 m (1,190 ft).

There is significant uncertainty regarding both the composition and placement of the mine waste fill. Historical records describing its composition or placement methods do not exist or are not available, but historic photographs providing general knowledge do exist. A historic photograph with the test program location super-imposed is provided in Figure 2. A similar view at the time of the load test program is presented in Figure 3.

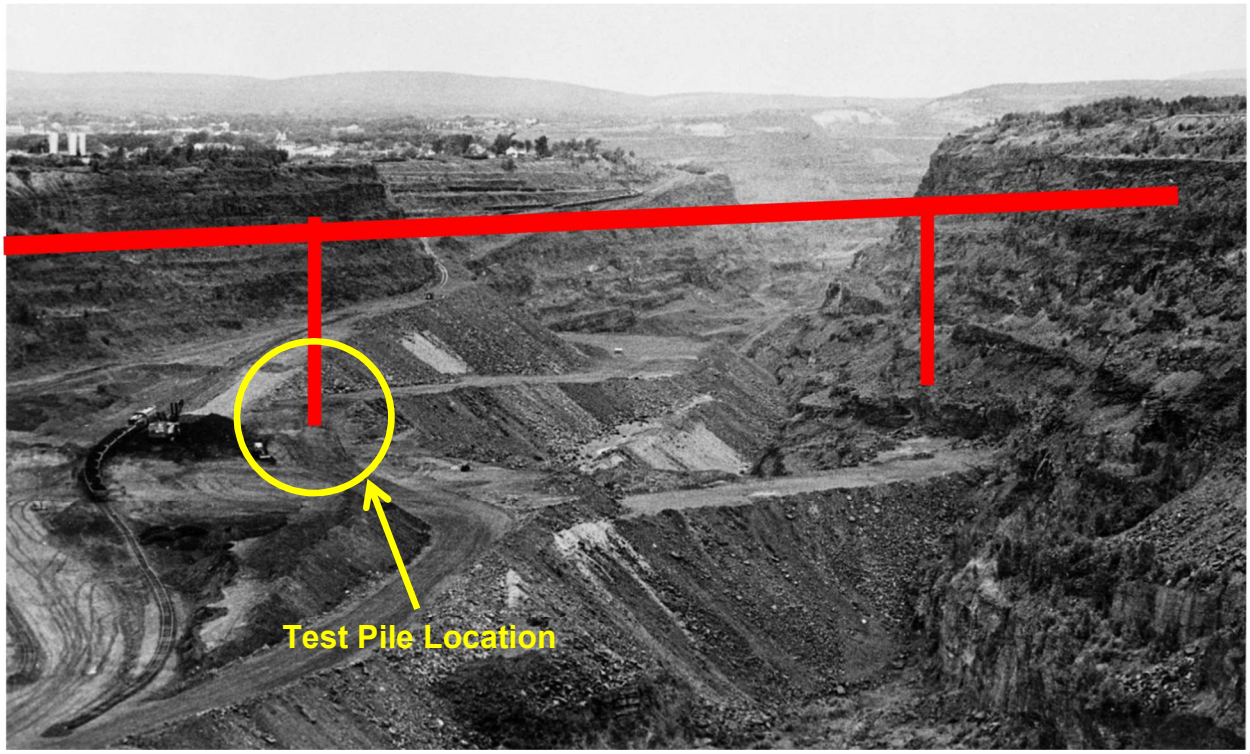


Figure 2: Site photograph circa 1940's during active mining and prior to flooding the pit; The red lines indicate the approximate location of the proposed bridge structure.

Borings in the MWF provided visual evidence of its general characteristics. Coring yielded recovery of rock of the nature illustrated by the photo in Figure 4-a. Rotosonic drilling recovered predominately soil-like materials with rock fragments as shown in Figure 4-b. Each of the two sampling methods effectively recovered a biased sampling of different material sizes. It is probable the fill consists of a wide range of particle sizes, from fine granular soil to rock particles that extend into the cobble and boulder size ranges. A reasonable conclusion is the MWF is highly variable but consists mostly of Biwabik Iron Formation rock fragments that may have been crushed, blasted, and/or weathered to produce a rock fill with interstitial granular soil.



Figure 3: Site photograph in March 2015 (load test site on left near the crane).

The particles comprising the MWF have higher density than typical soil particles due to the high iron mineral content. Specific gravity tests on three laboratory samples range from 3.404 to 3.827 (soil particle specific gravity for soils derived primarily from quartz is typically between 2.6 and 2.7). Based on the 3.685 average specific gravity for the three laboratory tests and an estimated range of void ratios between 0.3 and 0.8, the dry unit weight ranges from 20.4 kN/m^3 to 27.5 kN/m^3 (130 pcf to 175 pcf) and the saturated unit weight ranges from 24.3 kN/m^3 to 29.8 kN/m^3 (155 pcf to 190 pcf).

Below the MWF is bedrock of the Lower Cherty member of the Biwabik Iron Formation. The upper 12 m (40 ft) of bedrock was weathered and highly fractured based on borings, geophysical survey, and foundation construction observations. Core recovery in the weathered zone ranged from 23% to 100%, and rock quality designation (RQD) ranged from 0% to 87%. There is a particularly weathered zone between Elevations 360 m and 352 m (1,180 ft and 1,155 ft) that includes zones of no recovery and material described as residual soil. Bedrock below Elevation 351 m (1,150 ft), as shown in Figure 5, is more competent and is described as being thin to medium bedded with weak to medium oxidation. Joint descriptions varied from close to wide. Core recovery in the competent bedrock below Elevation 351 m (1,150 ft) is between 85% and 100% with most runs yielding 100% recovery. RQD in this zone ranges from 50% to 100%. Unconfined compression strength tests conducted on specimens taken from intact bedrock cores between Elevations 343 m and 352 m (1,126 ft and 1,155 ft) range from 45.7 MPa to 213.3 MPa (6,628 psi to 30,922 psi) with an average of 116.1 MPa (16,832 psi). Across the project site, nearly 200 unconfined compression tests were performed on recovered bedrock core samples. Uniaxial strengths up to 482.8 MPa (70,000 psi) have been measured with average compressive strengths well above 137.9 MPa (20,000 psi). This provides insight into the strengths that some particles may have in the MWF above bedrock.



(a)



(b)

Figure 4: MWF material recovered (a) by coring and (b) by Rotosonic drilling.



Figure 5: Biwabik Iron Formation rock core near the tip of the test pile.

Groundwater at the time of the test program construction and testing was at Elevation 399 m (1,310 ft), commensurate with the level of the adjacent reservoir in the flooded pit.

TEST PILE CONSTRUCTION

Veit was the specialty subcontractor that installed the test piles and the subsequent larger diameter production piles. The 406 mm (16 in) diameter test pile was cased over its entire 52.9 m (173.6 ft) length with 12.7 mm (0.5 in) wall steel casing. A Bermingham BHD40 drill head on a Bermingham lead system was attached to a Manitowak 888 crawler crane, as shown in Figure 6.



Figure 6: Test pile installation.

An Atlas Copco QL120 down-the-hole hammer was initially used in conjunction with a 406 mm (16 in) diameter Atlas Copco Elemex pilot and ring bit. However, that ring bit system proved ineffective and failed on two attempts during construction and was subsequently replaced with a Symmetrix pilot and ring bit, also manufactured by Atlas Copco. The Symmetrix system proved successful on the first attempt. Photographs of the damaged Elemex ring bit and collar upon extraction of the pile casing are provided in Figures 7 and 8.



Figure 7: Casing and damaged ring bit after extraction.


Figure 8: Damaged Elemex ring collar upon removal from casing.

As stated earlier, installation of the 406 mm (16 in) diameter casing began using an Elemex pilot and ring bit. At an embedment depth of 32.6 m (107 ft), the ring bit became detached. The casing was removed from the hole which subsequently collapsed. The average penetration rate was on the order of about 66 seconds per meter and entirely in the MWF. The penetration rate is only provided as an indicator and is a function of many variables including the volume of compressed air, discharge effluent flow rate, bit wear, and soil conditions, to name a few.

Upon extraction of the casing, the Elemex ring bit was replaced and the casing was installed in the same hole location as the previous attempt. At an embedment depth of 26.5 m (87 ft), the ring bit again became detached. The casing was again removed from the hole which subsequently collapsed. The average penetration rate was on the order of about 39 seconds per meter, again entirely in the MWF.

At this point, a 406 mm (16 in) diameter Symmetrix pilot and ring bit was attached and the casing was installed in the same location as the previous two attempts. The average penetration rate over depths commensurate with use of the Elemex system was on the order of about 46 seconds per meter in the MWF. Upon encountering fractured bedrock, the average penetration rate decreased to about 236 seconds per meter on average. The casing was advanced to a depth of 49.9 m (163.7 ft) or Elevation 351.6 m (1,153.3 ft), which placed the tip of the pile in weathered and highly fractured bedrock. Grouting was attempted after placement of a full-length reinforcing cage. Approximately 11.5 m^3 (15 yd^3) of neat cement grout was placed in the pile by tremie, but the entire volume of grout left the pile. Note the theoretical volume inside the casing was 6.5 m^3 (8.5 yd^3). At that point, the cage was removed to ensure it was not resting in fluid grout.

One week later, casing advancement continued and the casing was advanced another 3.8 m (12.6 ft) to a depth of 53.8 m (176.3 ft) or Elevation 347.8 m (1,140.7 ft) and tipped in relatively sound and less fractured bedrock. Over the final 30 cm (1 ft) of casing embedment, the penetration rate decreased substantially to about 43 minutes per meter. The cage was placed again and grouting was conducted to finalize construction of the test pile. Again, neat cement grout was placed from the bottom-up using a 38 mm (1.5 in) diameter tremie. The theoretical volume was about 6.9 m^3 (9.0 yd^3) and matched well with the volume placed.

The reinforcement cage consisted of four number 18 (57 mm diameter), grade 75 (517 MPa yield stress) all-thread longitudinal bars with number 4 (12.7 mm diameter) grade 60 (414 MPa yield stress) hoops on a 30 cm (1 ft) vertical spacing, as shown going into the casing in Figure 9. Threaded couplers were used to splice 12.2 m (40 ft) sections of longitudinal reinforcing together. Applied Foundation Testing (AFT) attached sisterbar strain gages to the longitudinal bars as the cage was hung in the vertical position.

Neat Portland cement grout was tremie placed using a Schwing BPA-450 grout pump from the bottom-up in the fully-cased excavation after placement of the reinforcement cage and verification of a clean bottom with a weighted tape, as shown in Figure 10. The grout was mixed offsite and delivered to the site in ready mix trucks.

A conceptual schematic of the completed test pile is provided in Figure 11 relative to the subsurface conditions.

The 28-day design strength of the neat cement grout was 34.5 MPa (5,000 psi) although compression test results conducted on test specimens cast in the field resulted in an average 28-day strength of 48.3 MPa (7,000 psi). However, the 406 mm (16 in) test pile was tested 44 days after grout placement and the compressive strength at the time of testing was extrapolated and estimated to be just under 55.2 MPa (8,000 psi) at that time. The extrapolated strength of the grout commensurate with the time of the test was used to analyze the results.



Figure 9: Installation of reinforcing cage.



Figure 10: Completion of grout placement.

STATNAMIC LOAD TESTING

The rapid load test method using the Statnamic device was performed by AFT using their 18.7 MN (4,200 k) mechanical catch device in general accordance with ASTM D7383-10 "*Axial Compressive Force Pulse {Rapid} Testing of Deep Foundations*". Multiple levels of embedded strain instrumentation were installed in the test pile and monitored during the single cycle load application. Additional instrumentation included a calibrated load cell, multiple pile top accelerometers to attain pile top displacement via double integration, and optical survey of the pile top before and after testing as redundant measure of permanent displacement.

Pairs of strain gages were installed at 180° separations at seven locations along the test pile. The strain gage locations are provided in Table 1.

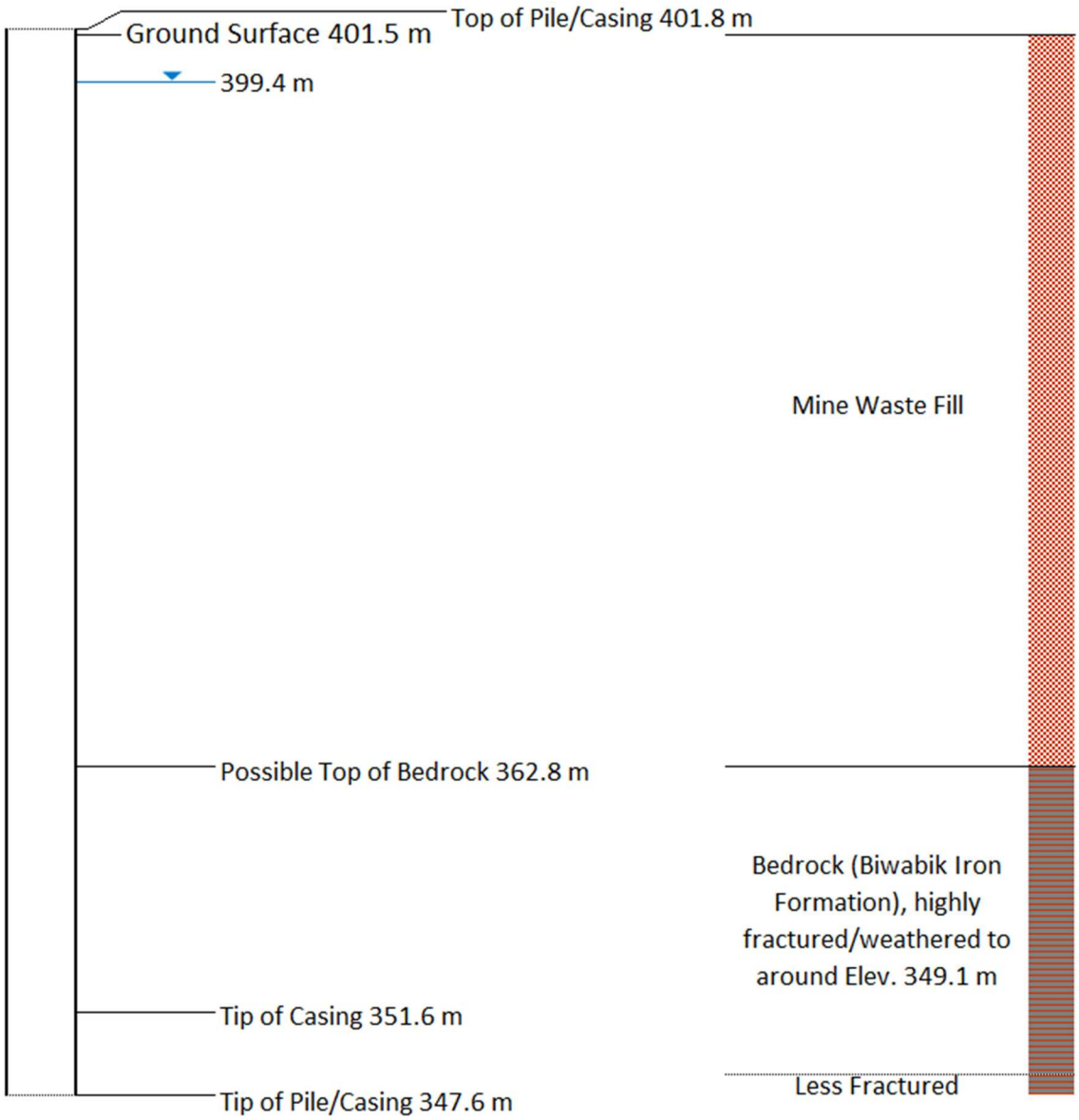


Figure 11: As-built schematic of 406 mm (16 in) diameter test pile.

Table 1: Test pile strain gage location summary.

Location	Depth Below Pile Top (m)	Elevation (m)	Adjacent Soil or Rock Material
Pile Top	0	401.8 (1,318 ft)	--
Surface	0.3 (1 ft)	401.5 m (1,317 ft)	MWF
Level 1	0.9 (3 ft)	400.9 m (1,315 ft)	MWF
Level 2	14.3 (47 ft)	387.5 (1,271 ft)	MWF
Level 3	28.0 (92 ft)	373.8 (1,226 ft)	MWF
Level 4	40.9 (134 ft)	361.0 (1,184 ft)	Weathered & Fractured Biwabik
Level 5	44.8 (147 ft)	357.0 (1,171 ft)	Weathered & Fractured Biwabik
Level 6	49.1 (161 ft)	352.7 (1,157 ft)	Weathered & Fractured Biwabik
Level 7	53.7 (176 ft)	348.2 (1,142 ft)	Relatively Competent Biwabik
Pile Tip	54.3 (178 ft)	347.6 (1,140 ft)	Relatively Competent Biwabik

Of particular interest is the observation that either of the ring and pilot bit systems produces a slight overcut necessary to advance the full-length casing. Theoretically, the annular void remaining around the external circumference of the casing is about 12.7 mm (0.5 in) if the walls of the excavation remain perfectly stable. During design of the test program, it was anticipated the MWF, and to some extent, the weathered and highly fractured Biwabik Iron Formation bedrock, would collapse the small annular void around the pile. Accordingly, some reduction in side resistance was expected although the precise magnitude was unknown. It was anticipated that an appreciable amount of side resistance would be mobilized during load testing along the 53.7 m (176 ft) long pile.

During construction of the test pile and following two separate failures of the Elemex bit system, the following important observations were made during removal of the casing from 32.6 m and 26.5 m (107 ft and 87 ft), respectively:

1. Upon removal of the casing, the hole did collapse as expected, providing some qualitative indication the small annular void would collapse; and
2. Despite the annular void collapse, insufficient side resistance existed to prevent extraction of the casing despite the depth of embedment.

Prior to load testing, these observations suggested the pile would be continuously supported in side resistance along its length but also the magnitude of side resistance would be relatively low. Therefore, it was estimated the majority of the load would be transferred to the tip of the pile and transferred to the very hard bedrock in base resistance.

Forty-four days after being cast, the pile was load tested. A maximum derived static load of 13.4 MN (3,017 k) was applied to the pile head, which equates to an average pressure of 103 MPa (15,000 psi); nearly twice the unconfined compressive strength of the grout. The total displacement of the pile head during testing was 138 mm (5.44 in).

Upon unloading, there was no permanent set but rather it was observed the pile had rebound and the final location of the pile top was approximately 13 mm (0.5 in) above the location prior to testing. In fact, Test Pile 1, which was a 610 mm (24 in) diameter pile, rebounded so dramatically that its pile top was approximately 51 mm (2.0

in) above the location prior to testing, as shown in Figure 12. This highly unusual behavior was a result of a combination of the following:

1. enormous base resistance;
2. minimal side resistance; and
3. large elastic pile deformations.

The enormous base resistance results from a very hard, competent bedrock at the tip along with a clean hole prior to grout placement. The minimal side resistance was discussed above and anticipated as a result of the construction method. The observed elastic pile deformations result from a relatively large magnitude of load applied to a long, relatively small diameter pile, which, in cross-section, contained 20% steel and 80% grout.

Upon dissipation of the rapid compressive load, the elastic shortening of the pile was not restrained by sufficient side resistance causing large pile rebound accelerations. This resulted in the pile rebounding upward out of the ground. After coming to rest, the available side resistance was sufficient to support the static weight of the test pile.

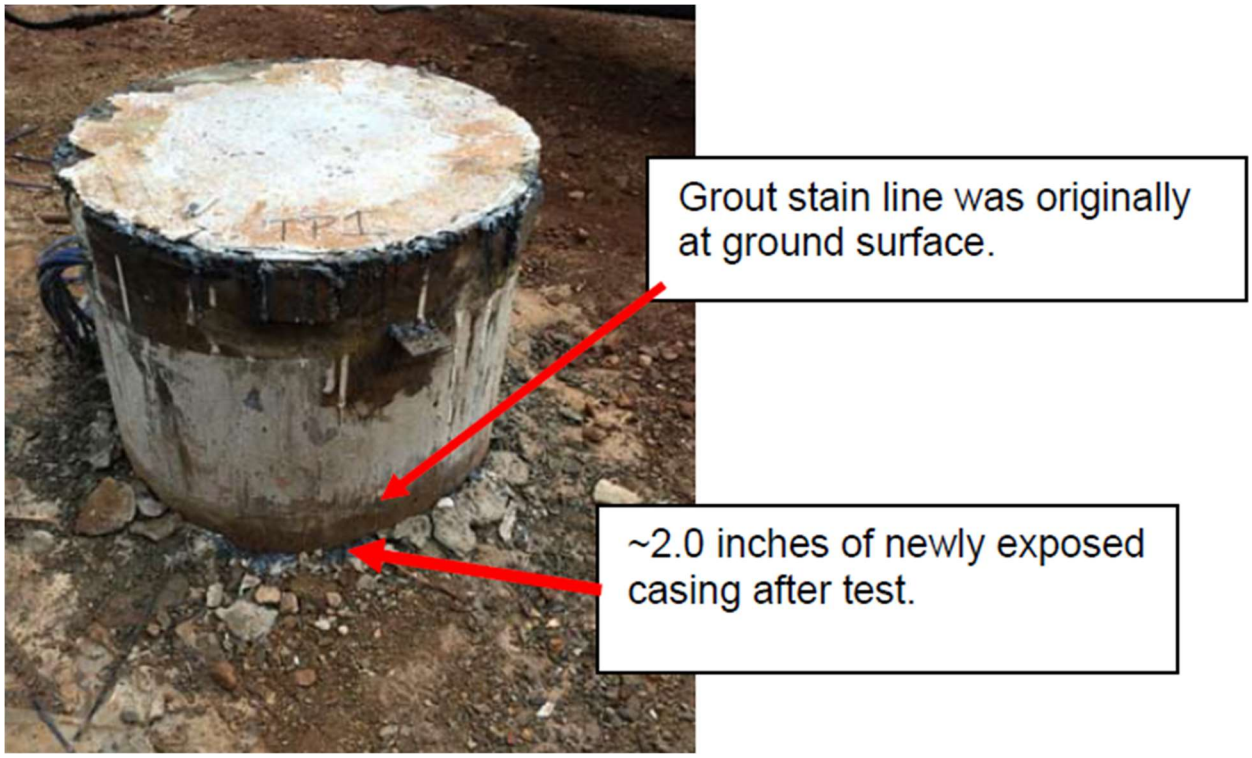


Figure 12: 610 mm (24 in) diameter test pile following Statnamic test.

Review of the strain gage data indicated the pile was structurally overstressed during testing, as manifested in prevalent cracking of the grout. However, because the grout was confined within a steel casing, full plastic yielding of the composite pile section did not occur. It can be concluded that under this substantial loading magnitude, the pile did not behave as a perfectly composite steel/concrete body.

While the strain gages did perform before, during, and after testing, the data was deemed unusable for the purposes of computing the side resistance because of the

cracking of the grout and the non-composite pile behavior. This unfortunate fact is estimated to be a result of applying such a large magnitude of load, which the pile could obviously handle with ease from a geotechnical perspective but which caused distress structurally.

CONCLUSIONS

The primary intent of the test program was to evaluate the constructability of the deep foundation elements using essentially large micropile installation techniques. It was determined the proposed foundation type was indeed constructible despite the formidable subsurface challenges. While initial attempts with the Elemex bit system proved unsuccessful, the Symmetrix system was capable of installing the casing in an economical manner.

Both bit systems produce a slightly oversized hole necessary to advance the casing. This oversized hole substantially reduces the magnitude of side resistance even after the small annular void collapses around the exterior circumference of the pile after installation.

The Statnamic test applied a derived static compressive load of 13.4 MN (3,017 k) with a corresponding total displacement of 138 mm (5.44 in). The combination of enormous base resistance, minimal side resistance, and huge elastic pile deformation under rapid compressive load produced a highly unusual behavior in which the pile rebounded upward out of the ground following load dissipation.

As hypothesized prior to, and demonstrated during, the axial design of the pile was controlled by structural considerations rather than geotechnical limitations. Even in the absence of appreciable side resistance, sufficient base resistance exists that exceeds the structural strength of the pile. Finally, the maximum value of base resistance was not fully mobilized, even under the enormous stress applied during the Statnamic test.

ACKNOWLEDGEMENTS

The authors wish to acknowledge the effort and expertise of Veit, who was up to the challenge of constructing these difficult foundations. The authors also wish to acknowledge MnDOT for their wisdom in seeing the value of load test programs.

MICROPILE QA/QC TESTING USING THERMAL PROFILING

William B. Wright, P.E.[1], Matthew, L. Silveston, P.E.[2],
Thomas C. Smoak, III, P.E.[3], William L. Snow, Jr., P.E.[4].

ABSTRACT

With increasing frequency, hollow bar micropiles are being used as a foundation solution along Coastal South Carolina. On a recent project, micropiles were installed using a size 40/20 and 52/26 continuously threaded, hollow core steel bars. The hollow space in the bar allowed an innovative application of Thermal Integrity Profiling (TIP) equipment, normally used for drilled shaft installation verification, to be applied to micropiles. We utilized a single strand of thermal wire sensors inserted into the hollow center bar after completion of micropile installation. A data logger recorded the concrete temperature over a 24 to 36 hour period as heat was generated during the exothermic hydration reaction. Processing software then used the temperatures recorded to generate a 3-dimensional model of the micropile.

The adopted building code in South Carolina is the 2015 IBC, which requires full time inspection of cast-in-place foundations and requires verification of element diameters. Using the known pile length and grout volume, the average pile diameter can be calculated. However, none of the required inspection methods allows direct verification of the pile diameter, which may vary with depth and soil strata.

TIP testing can also detect micropile defects including cave-in or clogged soil cuttings which prevent full grout cover and protection of the steel center bar from corrosion. Even load tests, which are the ultimate proof of capacity, cannot guarantee that defects are not present. While load tests are generally performed on 1% to 2% of the production piles, the ease of TIP testing allows for inspection coverage of 10% to 20%.

While this method of verification cannot replace full time inspection of a qualified inspector or load testing, it can be performed relatively easily, and is another valuable and innovative method to determine proper pile installation.

[1] *Senior Consultant, Terracon Consultants, Inc., 1450 5th Street West, North Charleston, SC 29405, 843-884-1234, Bill.Wright@terracon.com*

[2] *Senior Principal, Terracon Consultants, Inc., 1450 5th Street West, North Charleston, SC 29405, 843-884-1234,Matt.Silveston@terracon.com*

[3] *Project Engineer, Terracon Consultants, Inc., 1450 5th Street West, North Charleston, SC 29405, 843-884-1234,Thomas.Smoak@terracon.com*

[4] *Staff Geotechnical Engineer, Terracon Consultants, Inc., 2201 Rowland Avenue, Savannah, GA 31404, 912-629-4000,wlsnow@terracon.com*

INTRODUCTION

Due to the poor soil conditions along coastal South Carolina, hollow bar micropiles are being utilized more frequently. This is especially true in sensitive historical or residential areas where vibrations that are commonly generated during installation of other pile types can be problematic.

As an example, the College of Charleston which is located in the center of the historic district, has all but banned driven piles from being utilized during renovations or on new construction projects on its campus. This is primarily due to issues with vibrations and noise associated with a previous project which occurred in 2010. Another cause for increased micropile use in Charleston is the tight footprint of the increasingly congested city. In many renovations, the construction areas are limited to areas between or inside existing buildings where it is impossible to assemble cranes used to install driven or auger cast piles.

Since micropiles are not used as commonly as other pile types, one drawback to micropiles is the lack of familiarity among some engineers and building code officials. Due to this lack of familiarity, more stringent quality control requirements are sometimes added to the project specifications. It is common to have up to 10 percent of the production piles to have a form of integrity testing performed to verify the integrity of the pile. In auger cast piles, this is accomplished by performing Crosshole or Single Hole Sonic Logging (CSL/SSL) in accordance with ASTM D6760. CSL cannot be performed on most micropiles because the access tube that is used for the test will not have enough grout cover for the test to have accurate results. Thermal Integrity Profiling (TIP) is another technique that can be used to meet the requirements of the specifications which require integrity and dimension verification of production piles.

PROJECT INFORMATION

Terracon was involved in a project where a 3.0 meter (10 feet) tall MSE (Mechanically Stabilized Earth) wall between two split level buildings began showing signs of movement, loss of ground, and failure. This MSE wall was connected to the building foundation walls and would cause structural damage to the adjacent inhabited buildings during failure. A wall repair solution was needed which did not compromise the existing structures.

Complete demolition and rebuild was not practical due to the potential undermining of the adjacent buildings. More common repair techniques were initially explored, and a soil nail repair option was pursued and designed. The soil nail design was bid on by subcontractors. However, due to the arrangement of the buildings and MSE wall, access to the wall was limited and the bids returned from the subcontractors reflected the difficulty of the repair. Due to these higher than expected bids, Terracon was asked to evaluate

other more cost effective options, and developed a buttress-wall design. After evaluating the loading demands of the wall, it was determined that in addition to the buttresses, vertical deep foundations would be needed to reinforce the existing MSE wall. Since the adjacent buildings were occupied and due to the limited space available for equipment, micropiles were chosen as the deep foundation support option.

MICROPILE DESIGN

Structural Design

A hollow bar micropile was chosen for the project which is classified as a Type E micropile in Chapter 10, Section 10.9 of the 2014 LRFD Bridge Design Specifications by American Association of State Highway and Transportation Officials (AASHTO). Since vertical micropiles worked best with the configuration of the wall and existing building, lateral loading was significantly higher than most scenarios where micropiles would be used. Due to these high shear loads, the upper 3.0 meters (10 feet) of the micropiles used steel casing. A combined effort from the structural engineer and geotechnical engineer was needed to determine the required capacities. Ultimately, a micropile with a diameter of 254 millimeters (10 inches) was selected for the project.

Geotechnical Design

We utilized previously obtained Cone Penetration Test (CPT) data near the wall to generate the subsurface profile for geotechnical micropile design. The soil profile consisted of approximately 9.4 meters (31 feet) of interbedded sands and clays over the Cooper Marl Formation. The Cooper Marl Formation is a uniform, well-studied, over-consolidated calcareous clayey to sandy silt which is typically the bearing stratum for deep foundations in the Charleston, SC area. The axial and compressive analysis was performed using the LCPC method (Bustamante and Gianeselli, 1982). The soil layers overlying the Cooper Marl Formation were neglected due to the potential for liquefaction and down drag loads. The available pile capacity is developed from embedment in the Cooper Marl Formation. Due to the small amount of available room and the small number of piles, a factor of safety of 3 was used and a load test was omitted. This resulted in an embedment depth of 13.5 meters (45 feet) below existing grade. Lateral pile software was then used to verify that the lateral deflections of the cased 254 millimeter (10 inch) diameter micropile were within tolerable limits.

MICROPILE QUALITY ASSURANCE/QUALITY CONTROL

The adopted building code in South Carolina is the 2015 IBC, which requires full time inspection of cast-in-place foundations and requires verification of element diameters. Generally, the micropile diameter can be verified by measuring the size of the cutting head used. Since the pile length and cutting head diameter are known, and the grout volume is calculated by counting the number of pump strokes from a calibrated hopper, the average pile diameter can be determined. These methods are reliable and meet the requirements of the IBC, however, none of the required inspection methods allows direct verification of the pile diameter, which may vary with depth and soil strata.

Inspections alone may not entirely satisfy the requirements of the project specifications which may require up to 10% of the piles to be verified by integrity testing. While static load tests or proof tests may be performed, it can be cumbersome and expensive to run load tests on such a high percentage of production piles. Also, since production piles cannot be tested to failure, load tests may not be the most effective verification method. For this project, Terracon performed Thermal Integrity Profiling (TIP) to verify proper micropile installation, as an alternate verification method.

THERMAL INTEGRITY PROFILING (TIP) BACKGROUND

Thermal Integrity Profiling (TIP) is a technique commonly used to verify integrity of drilled shafts. The system uses digital thermocouples assembled on a wire and linked in a series. The thermocouples monitor the temperature of the shaft's concrete as it hydrates. By reviewing the temperature data, the heating and subsequent cooling of the micropile can be reviewed. Analysis of the data is generally performed prior to the peak heat of hydration. Using the known volume of concrete and the shaft's geometry, analysis of the data can provide indications of bulges and necks based on thermal mass of the concrete section. Using software developed by Pile Dynamics, Inc. (PDI), concrete cover and pile radius can be calculated, as well as a 3-dimensional image of the pile can be generated.

A modification of this was used for evaluating micropiles. A single thermal wire was lowered down the annulus of the hollow center bar. The annulus space was water filled to provide a conductive medium for the heat generated by the hydrating grout of the micropile. Since centralizers are attached to the bar at a vertical spacing of 3.0 meters (10 feet), the hollow center bar is assumed to be centered and only one thermal wire is needed for testing. Review of the temperatures will reveal zones of increased heat as well as relatively cooler areas. When combined with grout volumes, the design length and diameter of the pile, the hotter zones can be correlated to bulges. Assuming that the center bar is truly centered, the cooler zones would be interpreted as necks within the pile. However, this assumption of centering is a potential flaw in the approach and if the center bar drifts to one side, the temperatures would appear cooler as it moves away from

the center of the pile. While the pile is assumed to be adequate, a misaligned center bar may be evaluated as a problematic pile. To help overcome this, careful review of the installation logs and monitoring of the pile are crucial.

MICROPILE QA/QC TESTING USING THERMAL PROFILING

We utilized a single strand of sensors inserted into the water filled hollow bar after completion of micropile installation. Since the hollow center of the bar is used to inject grout into the bottom of the micropile, the grout first had to be removed to allow the thermal sensors to be inserted. This was accomplished by inserting a spherical sponge into the top of the hollow bar, and attaching a pump to the top of the rod. The known volume of grout within the hollow core of the rod was exchanged with water by pumping. This allowed the hollow core to be cleared without diluting the structural grout at the bottom of the micropile with water. Of the 12 micropiles tested, we had difficulty clearing the core of 3 micropiles. Figures 1, 2 and 3 are from the installation of one of the micropiles. Once the thermal sensors were inserted, a data logger recorded the grout temperature over a 24 to 36 hour period as heat was generated during the exothermic hydration reaction. Processing software then used the temperatures recorded to generate a plot of temperature versus depth (see Figures 5 & 8), a plot of radius vs. depth (see Figures 6 & 9) and a 3-dimensional model of the micropile (see Figures 7 & 10). These models allow the viewing of variation of the micropile diameter with depth, which could not be accomplished using typical methods discussed in the 2015 IBC.



Figure 1. Viewing down from the top of the adjacent retaining wall, the installation of one of the micro-piles can be seen.



Figure 2. After drilling, the grout is pumped from the center of the bar.



Figure 3. Pumping grout from the center bar of the installed pile.



Figure 4. A cased section is lowered into the drilled and grouted hole. The casing is aligned along the center bar with a series of collars within the casing.

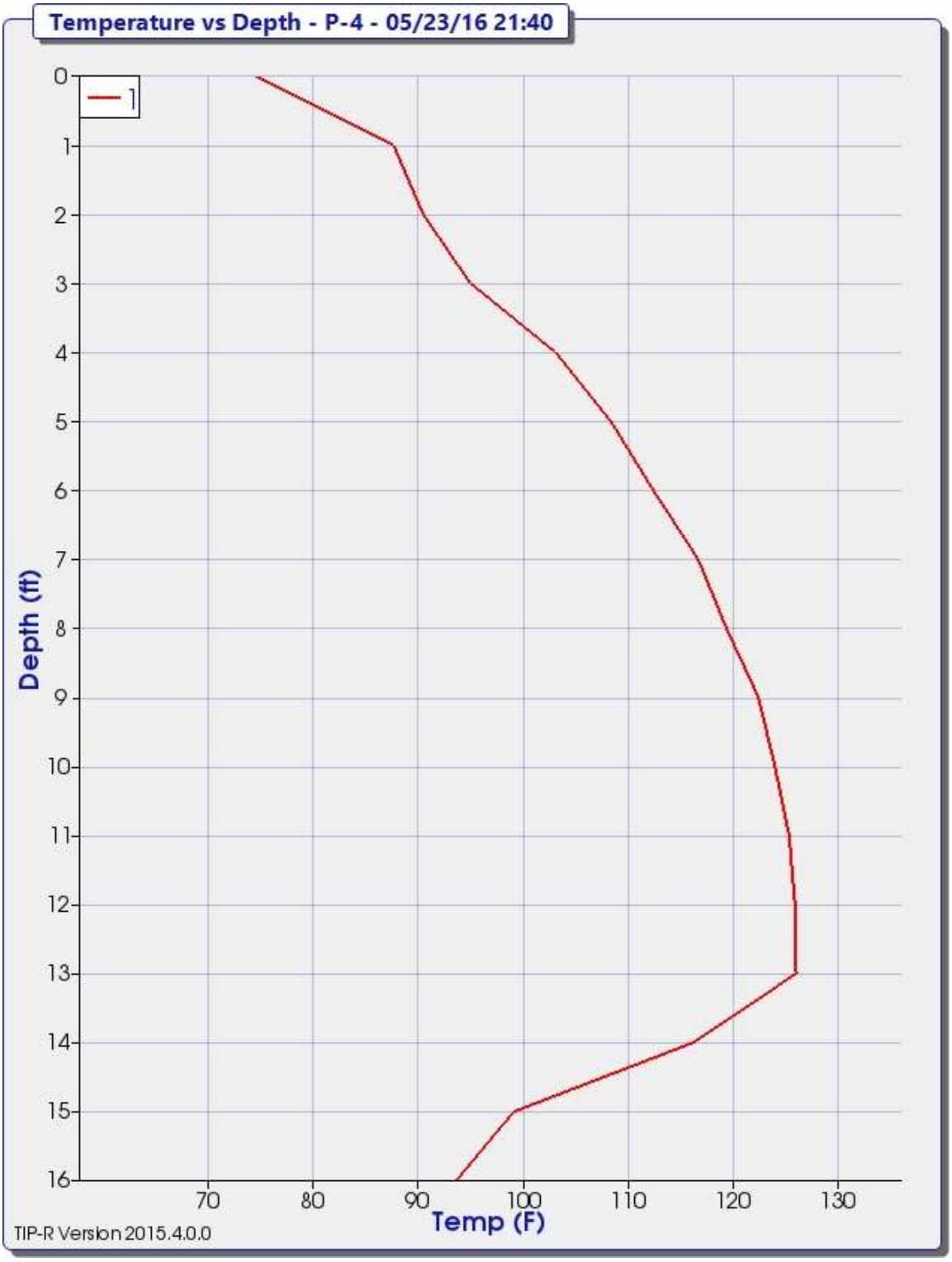


Figure 5. Temperature vs Depth plot for Pile #4.

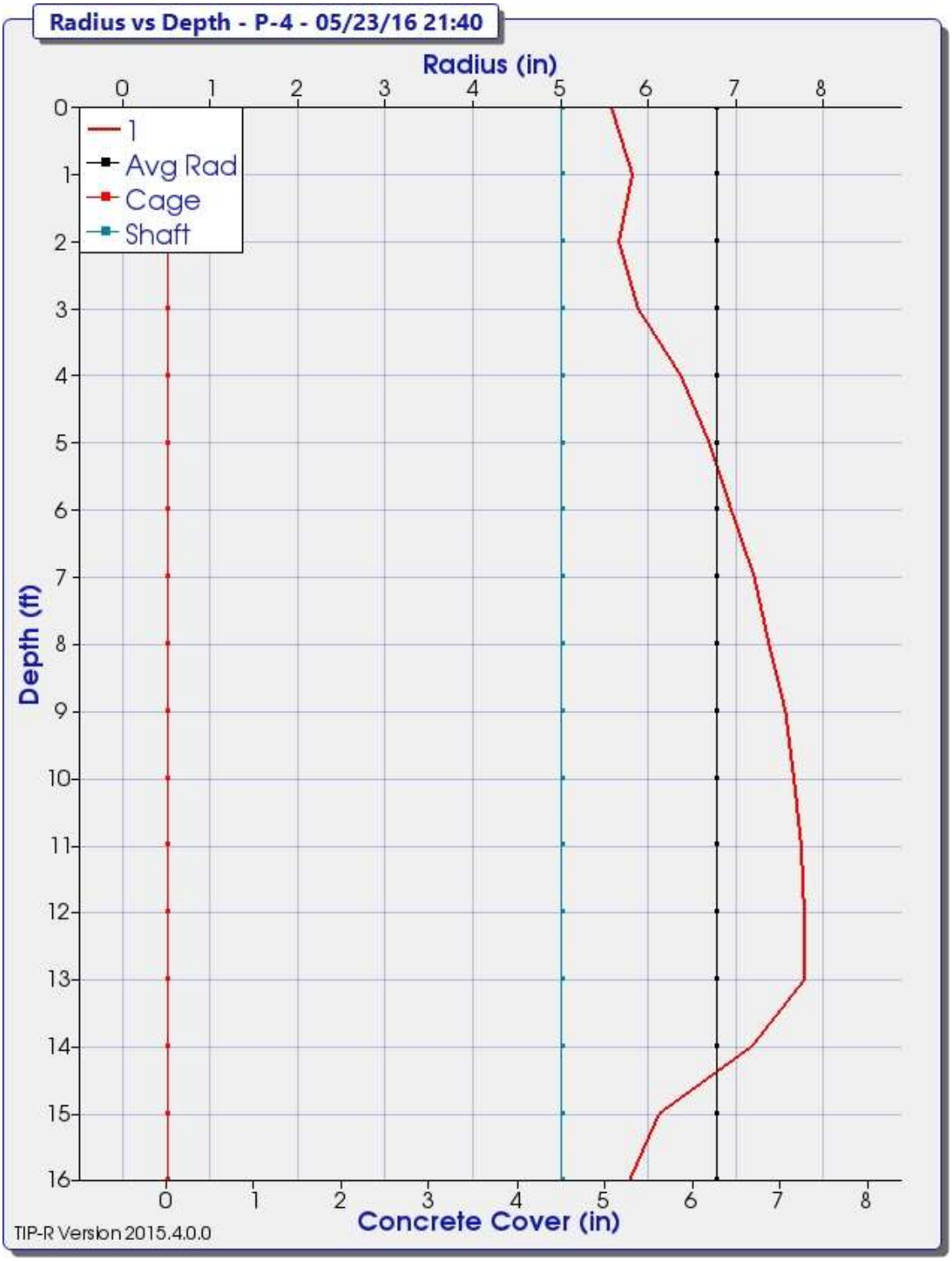


Figure 6. Using the temperature data and measured grout volumes from Pile #4, calculations of the pile's radius can be made. The dashed red vertical line is the center bar, the dashed purple line is the design radius of the pile. The dashed vertical black line is the average radius of the pile. The red line is the calculated radius base on the temperature data.

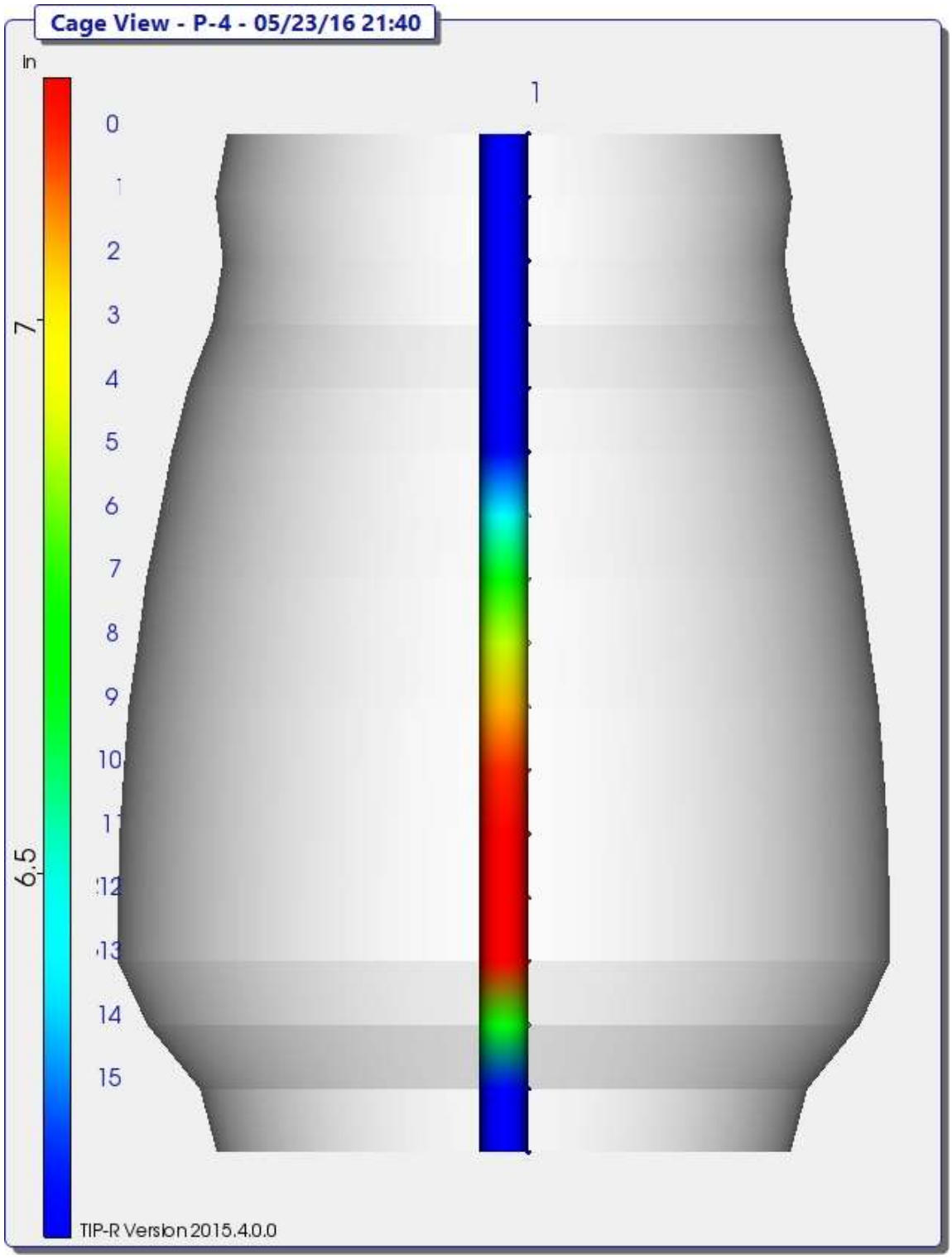


Figure 7. Using the analysis software, a 3D model of Pile #4 can be developed. The center colors correspond to the radius of the pile.

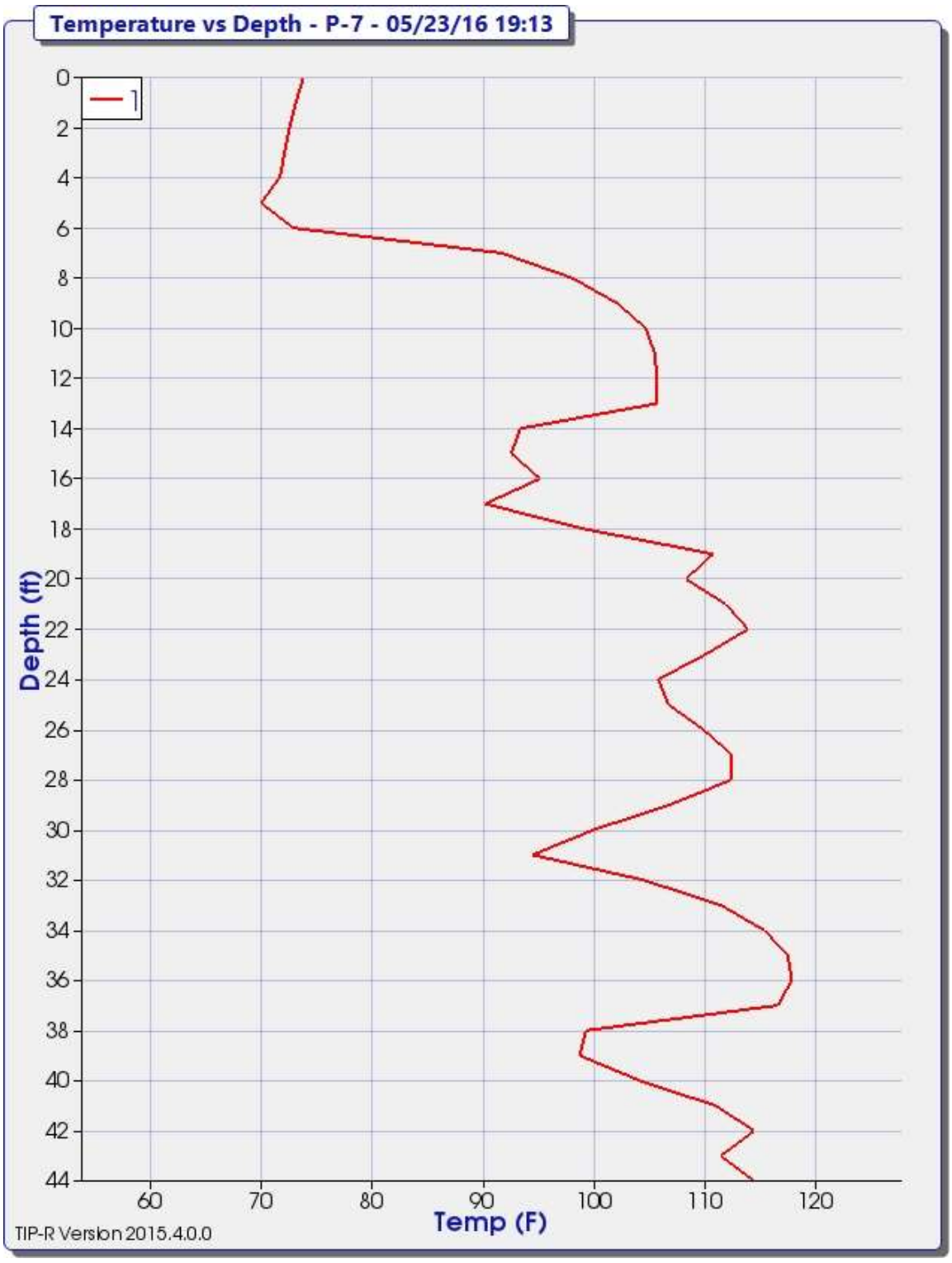


Figure 8. Temperature vs Depth plot for Pile #7.

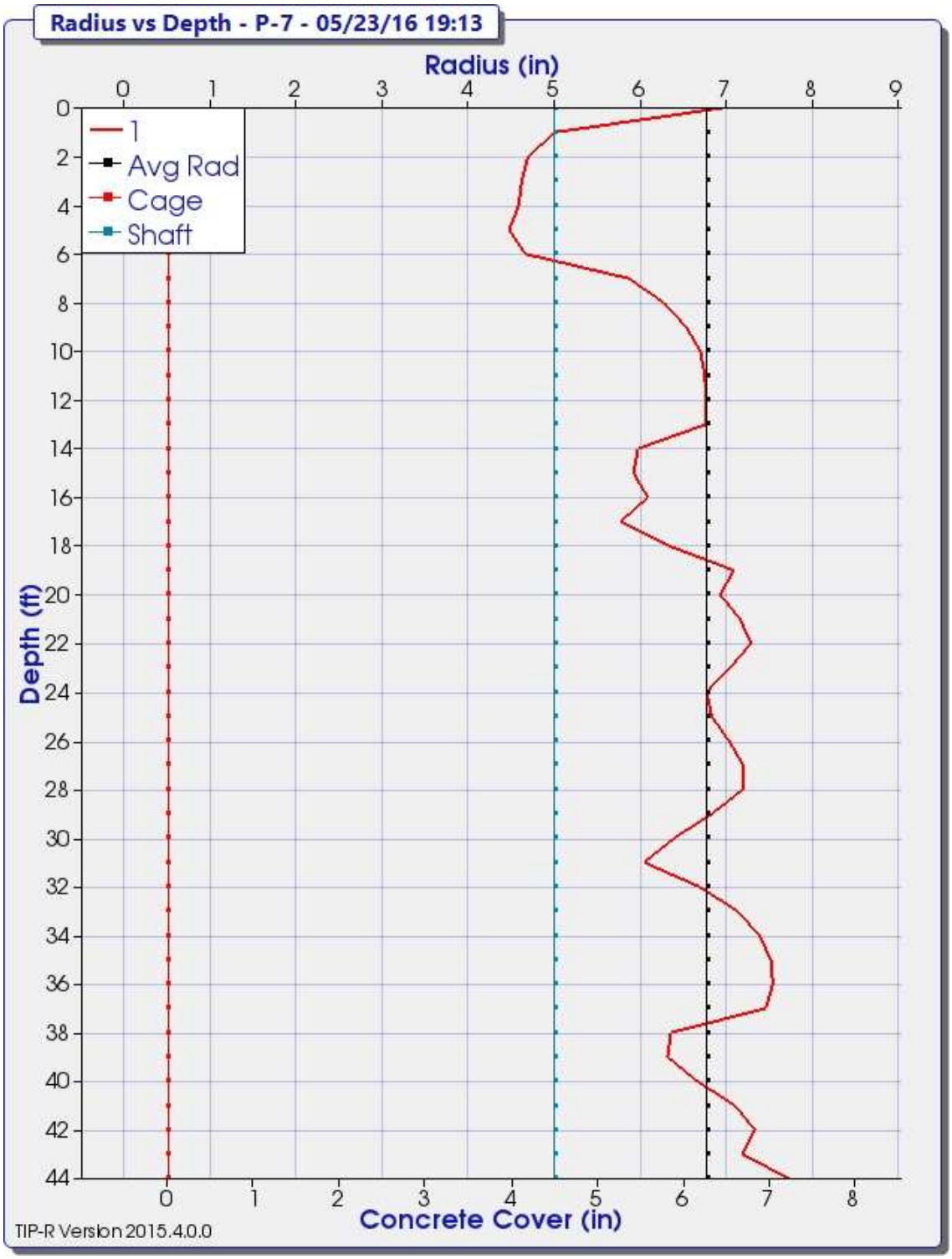


Figure 9. Using the temperature data and measured grout volumes from Pile #7, calculations of the pile's radius can be made. The dashed red vertical line is the center bar, the dashed purple line is the design radius of the pile. The dashed vertical black line is the average radius of the pile. The red line is the calculated radius base on the temperature data.

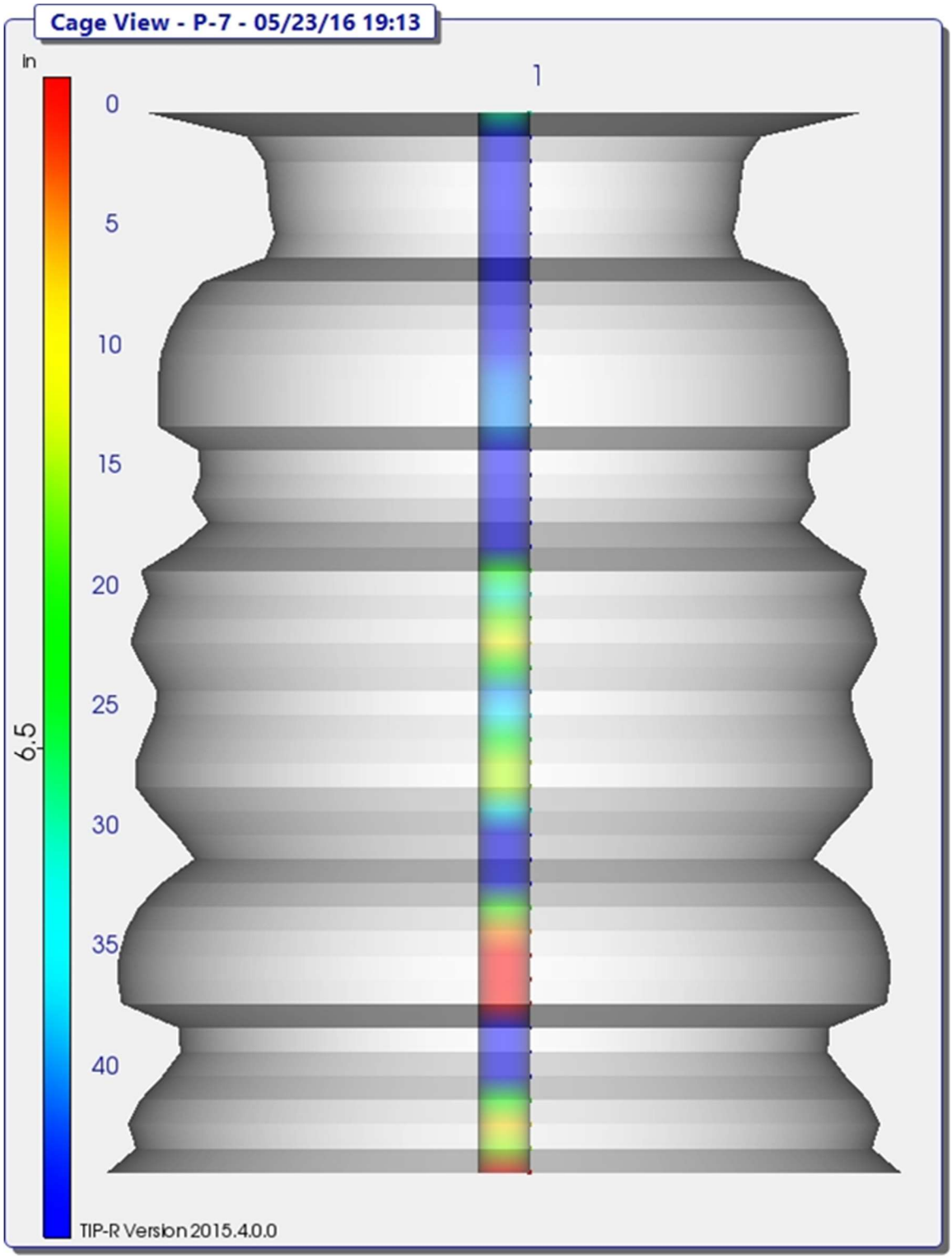


Figure 10. Using the analysis software, a 3D model of Pile #7 can be developed. The center colors correspond to the radius of the pile.

TIP testing can also detect micropile defects including cave-in or clogged soil cuttings which prevent full grout cover and protection of the steel center bar from corrosion. Even load tests, which are the ultimate proof of proper installation, cannot guarantee that defects are not present. While load tests are generally performed on 1% to 2% of the production piles, the TIP inspection method allows for 10% to 20% inspection coverage.

CONCLUSIONS

Table 1 presents the calculated average micropile diameter determined from full-time quality control inspections as compared to the Average micropile diameter determined by TIP testing.

Table 1: Comparison of calculated average micropile diameter vs. average micropile diameter from TIP testing.

Pile No.	Design Diameter mm. (in.)	Embedment Depth m. (ft.)	Grout Volume m^3 (ft^3)	Calculated Average Diameter mm. (in.)	Average Pile Diameter from TIP Testing mm. (in.)
#1	254 (10)	13.5 (45)	1.1 (40)	325 (12.8)	371 (14.6)
#2	254 (10)	13.5 (45)	1.3 (45)	343 (13.5)	345 (13.6)
#3	254 (10)	13.5 (45)	1.3 (45)	343 (13.5)	345 (13.6)
#4	254 (10)	13.5 (45)	1.3 (45)	343 (13.5)	345 (13.6)
#5	254 (10)	13.5 (45)	1.3 (45)	343 (13.5)	Not Performed[1]
#6	254 (10)	13.5 (45)	1.3 (45)	343 (13.5)	345 (13.6)
#7	254 (10)	13.5 (45)	1.3 (45)	343 (13.5)	345 (13.6)
#8	254 (10)	13.5 (45)	1.3 (45)	343 (13.5)	345 (13.6)
#9	254 (10)	13.5 (45)	1.2 (42.5)	335 (13.2)	Not Performed[1]
#10	254 (10)	13.5 (45)	1.3 (45)	343 (13.5)	Not Performed[1]
#11	254 (10)	13.5 (45)	1.3 (45)	343 (13.5)	345 (13.6)
#12	254 (10)	13.5 (45)	1.3 (45)	343 (13.5)	345 (13.6)

1. Since the annular space of the rod could not be cleared, the thermal sensors could not be installed and TIP testing was not performed.

As seen in Table 1, the TIP testing results agree with the expected micropile diameters. While the average diameter is useful information, it does not guarantee that necking or narrower portions of the pile are not present. As seen in Figure 7 and Figure 10, the diameter determined by TIP testing can vary with depth. TIP testing allows for a more detailed view of the pile profile and can alert the project team to potential issues

with installation methods or the in-situ soil profile. The figures displaying the results of TIP testing for each of the tested micropiles are included in the Appendix.

While this method of verification cannot replace full time inspection by a qualified inspector or load testing, it can be performed relatively easily, and is another valuable and innovative method to determine proper pile installation.

Since this was a relatively small project, we did not physically pull any of the piles to verify the results of the TIP testing with the actual micropile diameters. To further evaluate TIP testing methods with micropiles, Terracon is planning on working in the future to install test piles at a coastal Charleston site and then performing TIP testing, static load tests, and actually pulling the test piles to compare TIP results to the actual pile.

REFERENCES

2015 International Building Code. Country Club Hills, Ill: ICC, 2014. Print.

AASHTO LRFD Bridge Design Specifications. Washington, D.C: American Association of State Highway and Transportation Officials, 2014. Print.

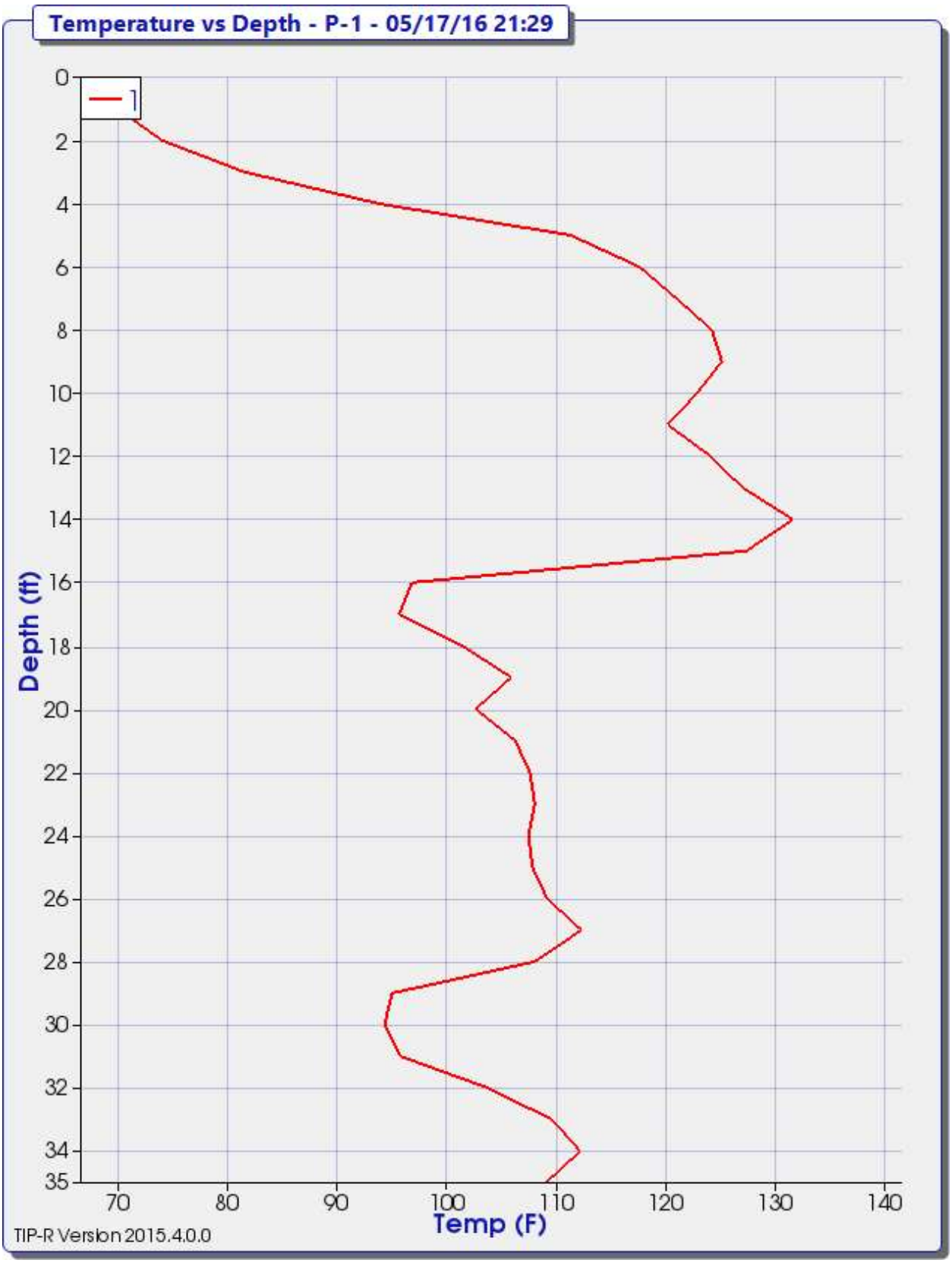
ASTM D 6760-08, “Standard Test Method for Integrity Testing of Concrete Deep Foundations by Ultrasonic Crosshole Testing”, American Society for Testing and Materials, Philadelphia, PA, Construction Vol 4:08

ASTM D 7949-14, “Standard Test Methods for Thermal Integrity Profiling of Concrete Deep Foundations”, American Society for Testing and Materials, Philadelphia, PA, Construction Vol 4:09

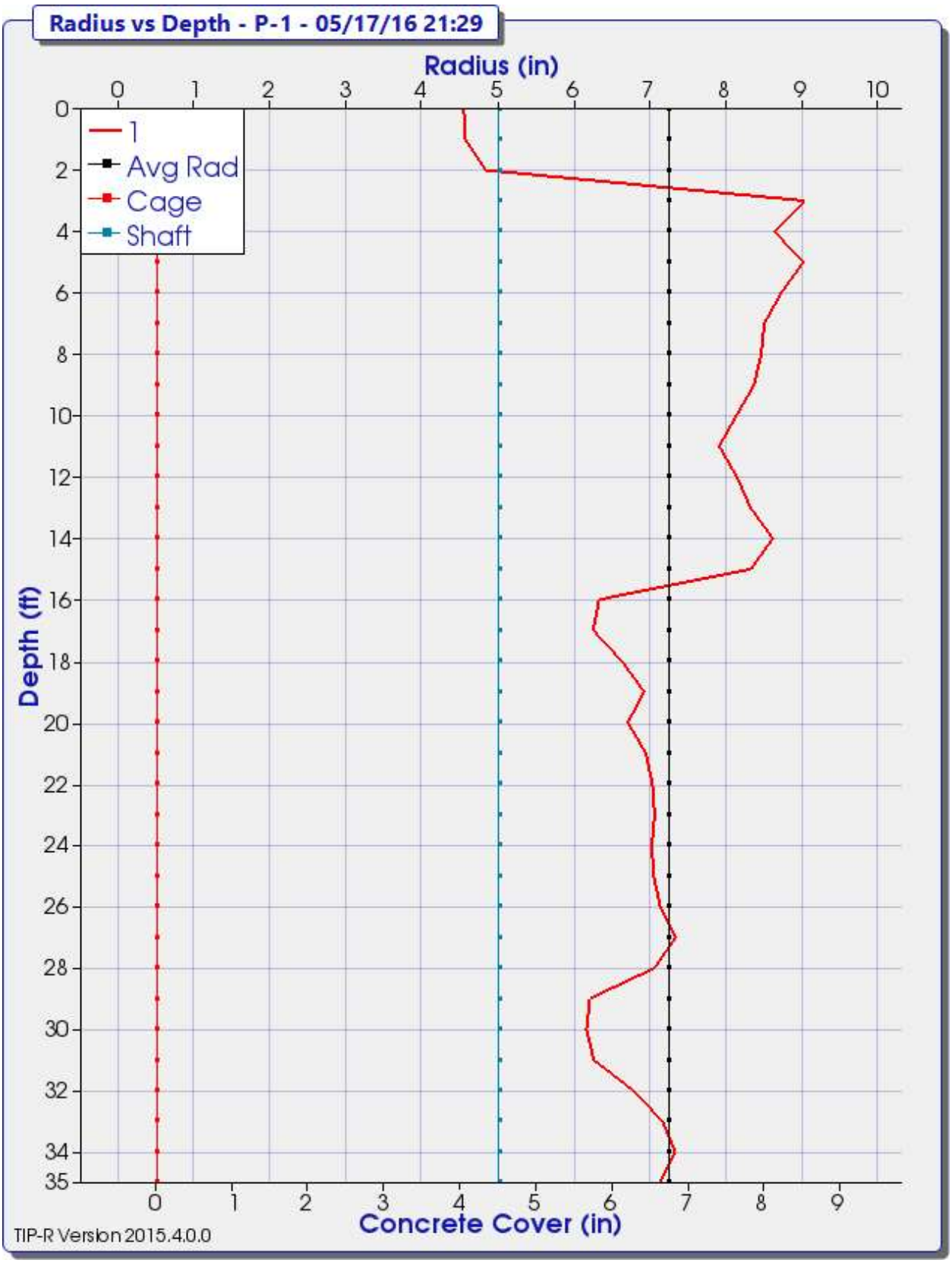
Piscsalko, P.E., George, “Thermal Integrity Profiler (TIP)”, Pile Dynamics, Inc., May, 2016. Print.

Appendix

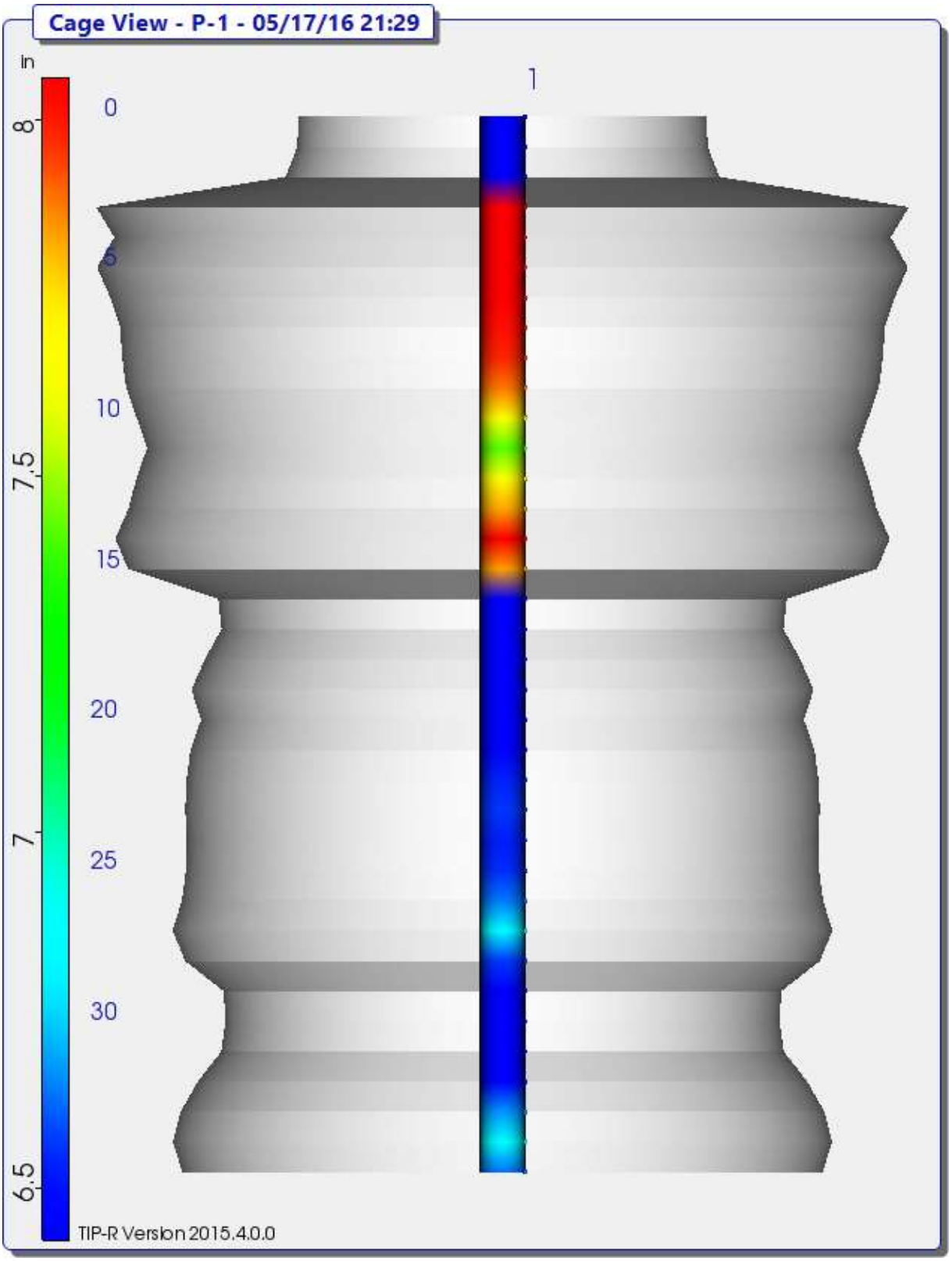
Pile 1 - Temperature vs. Depth



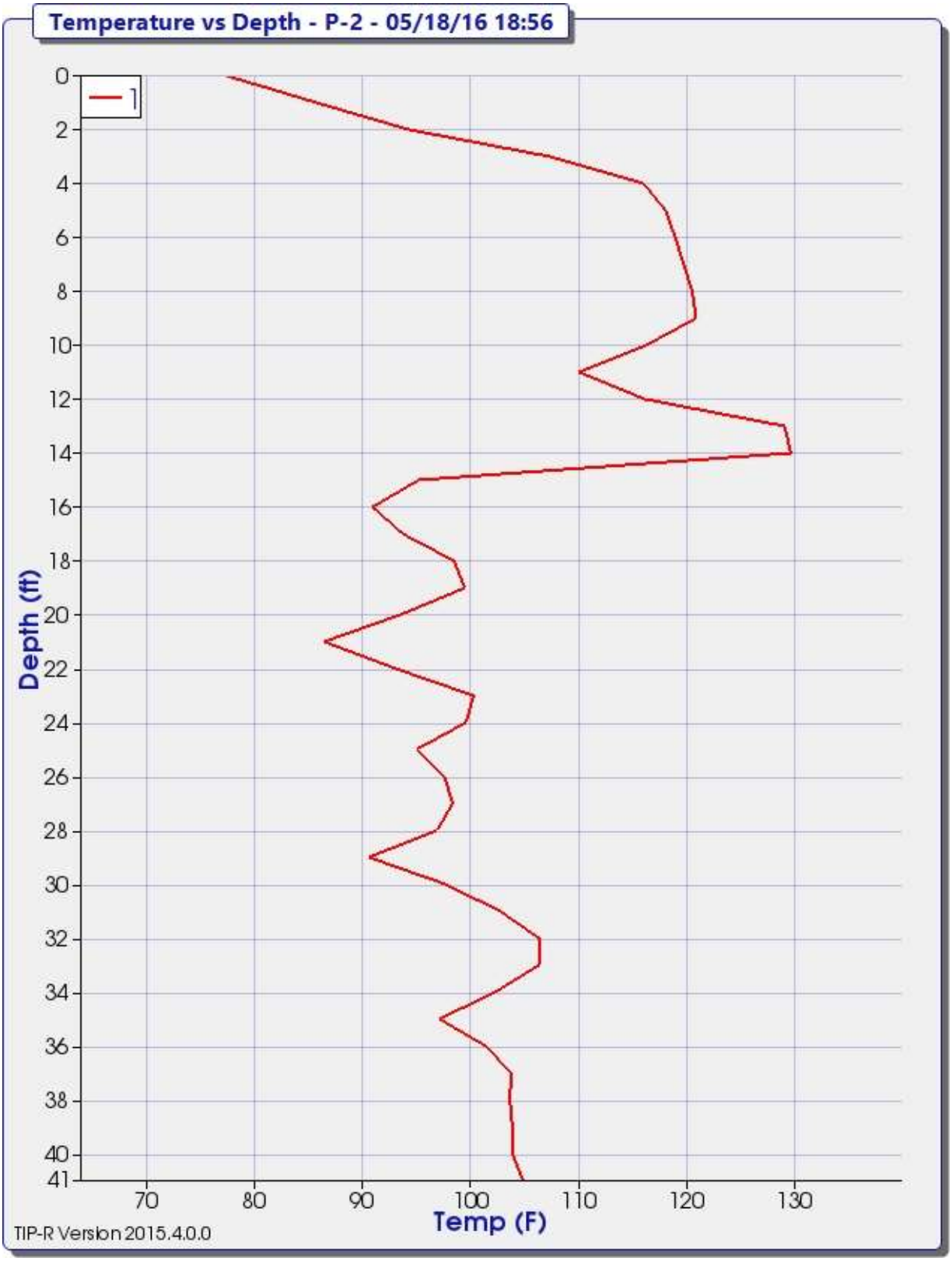
Pile 1 – Radius vs. Depth



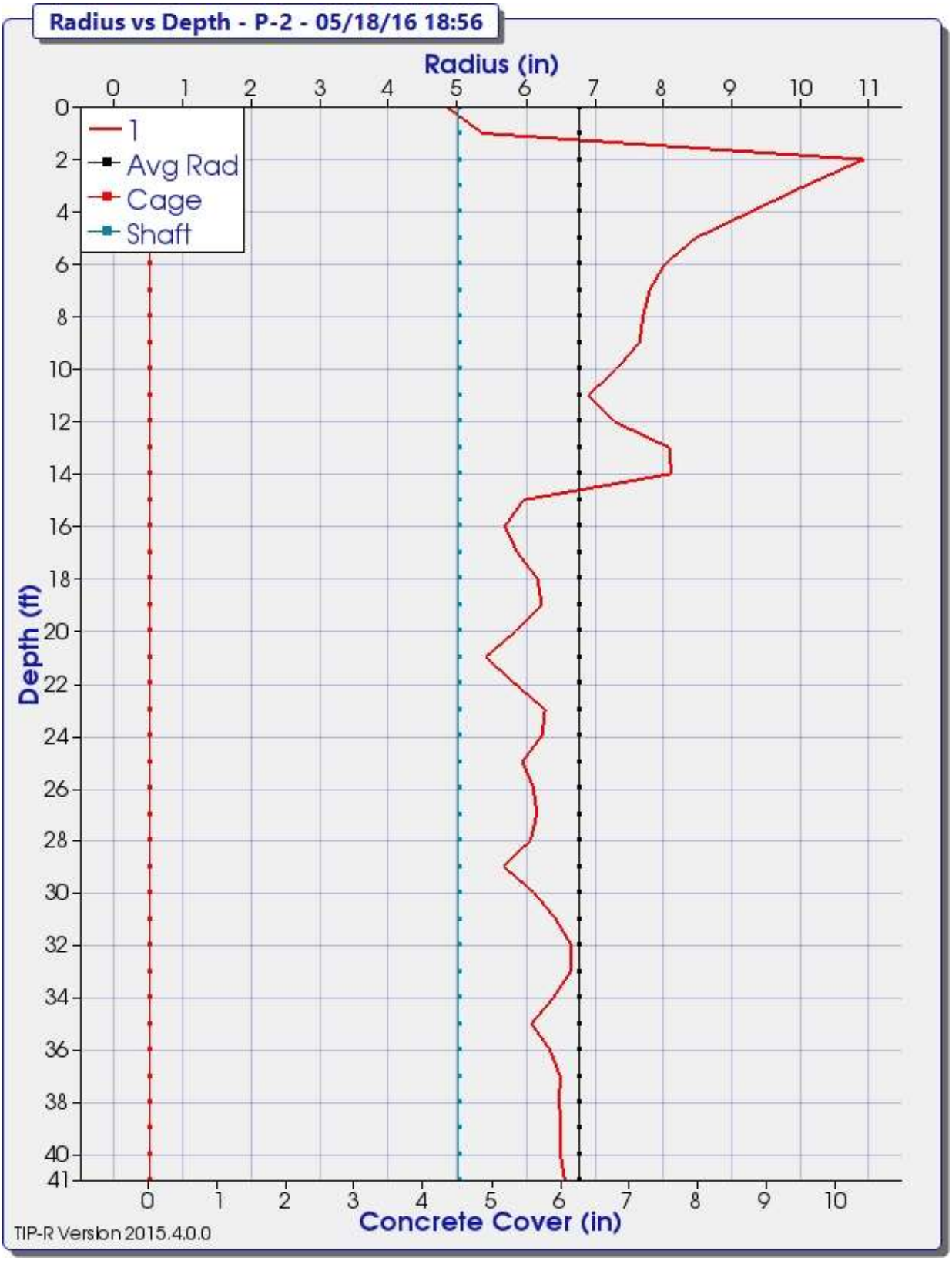
Pile 1 – 3D Cage View



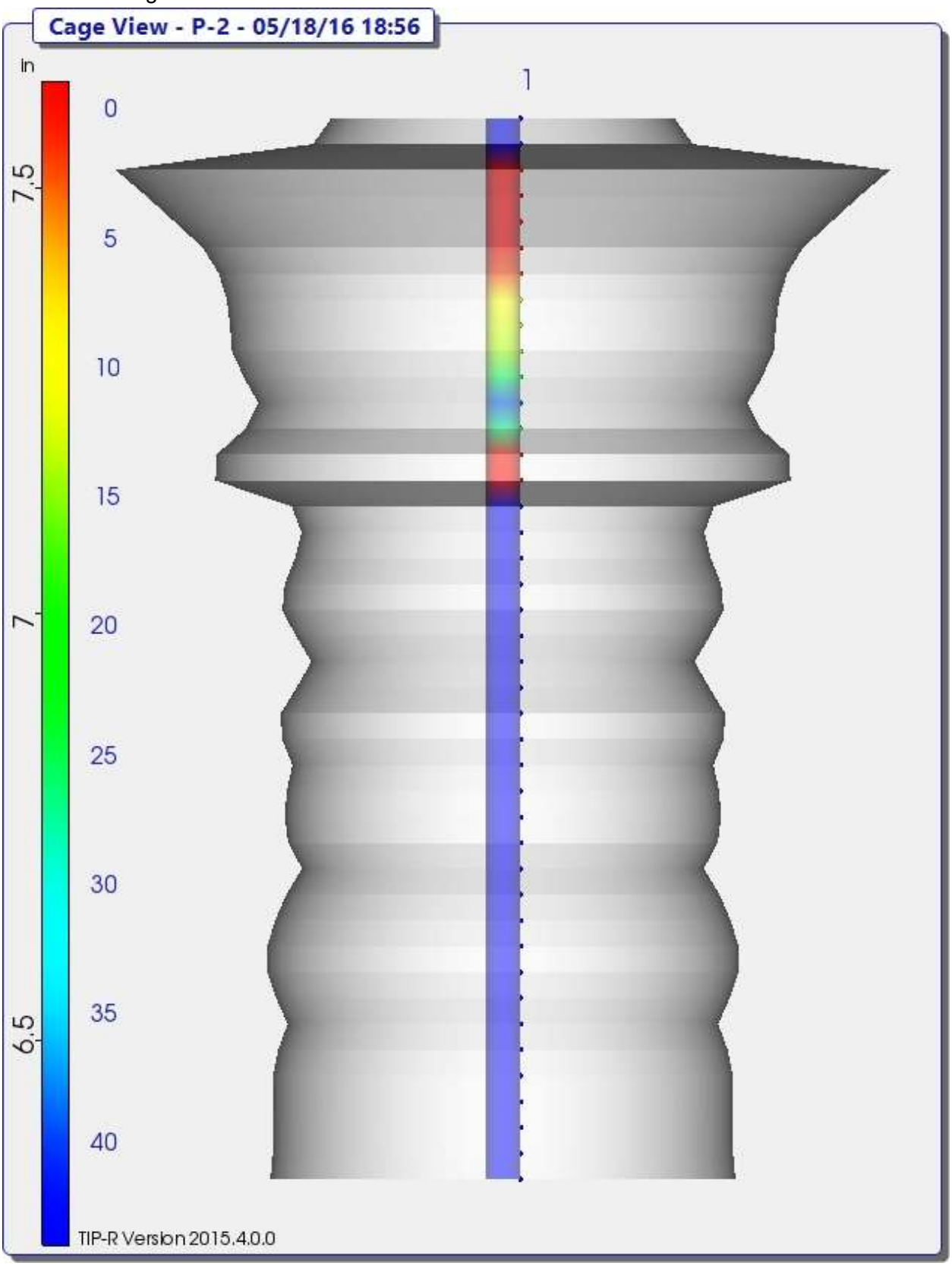
Pile 2 – Temperature vs. Depth



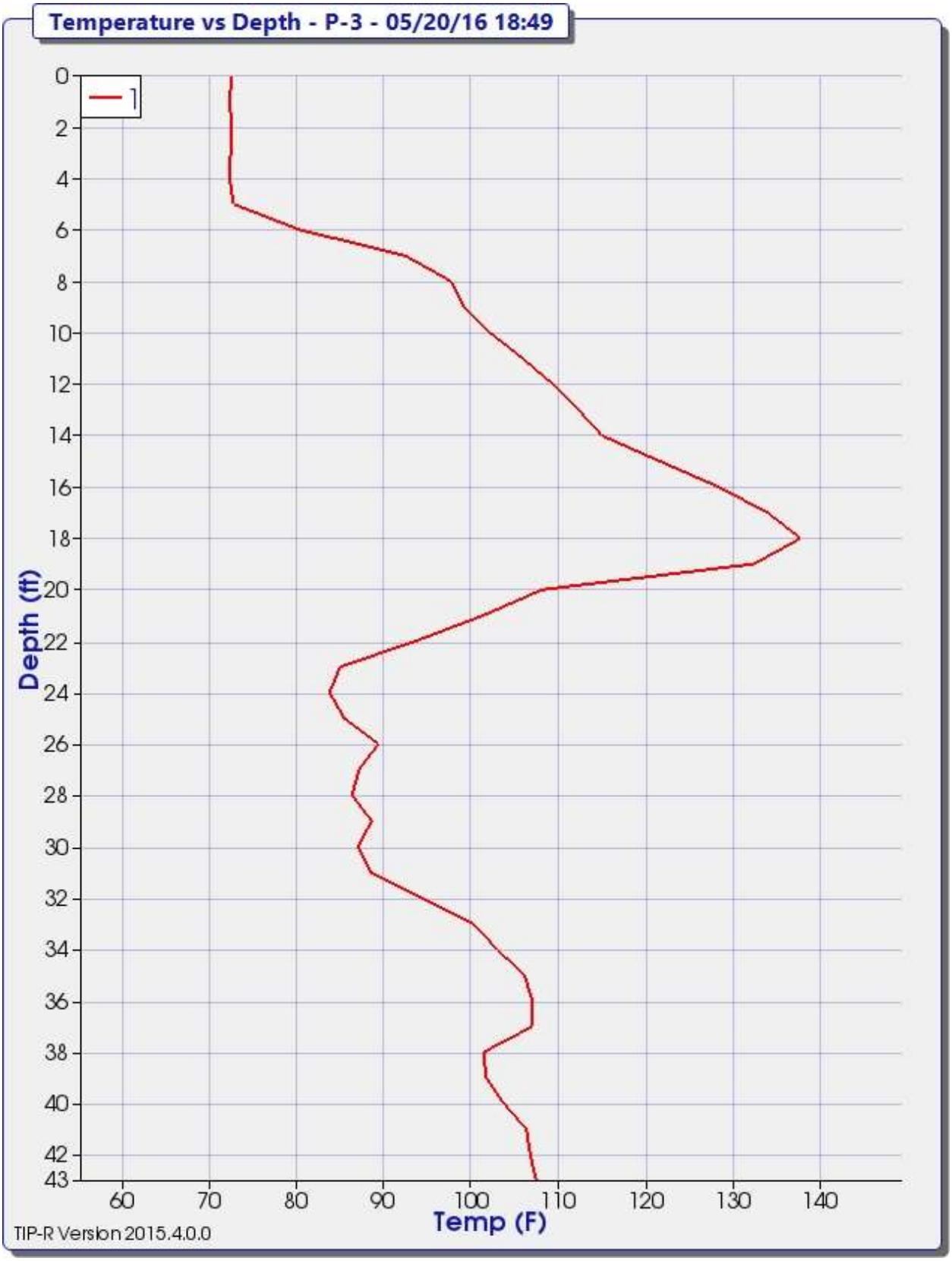
Pile 2 – Radius vs. Depth



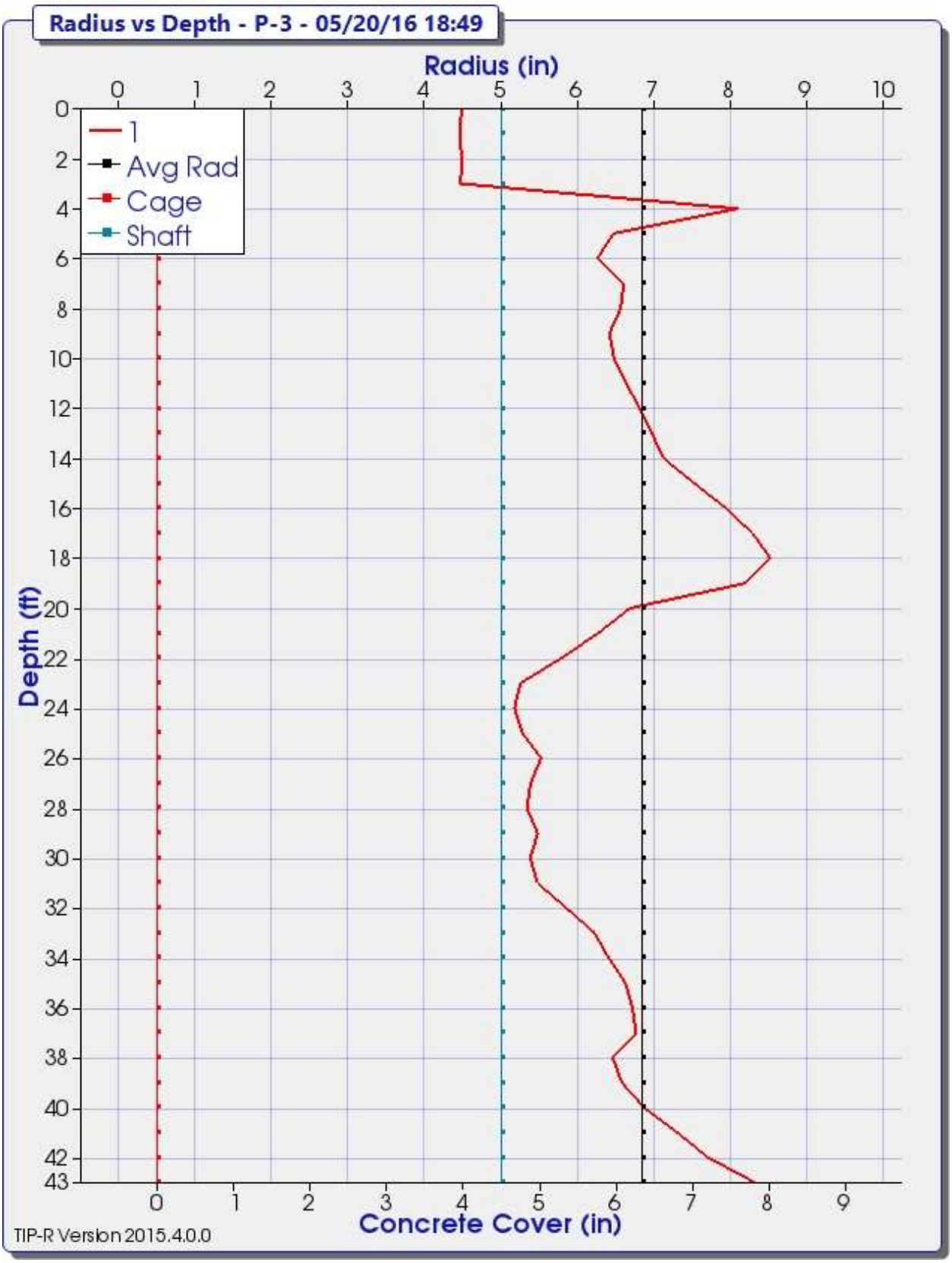
Pile 2 – 3D Cage View



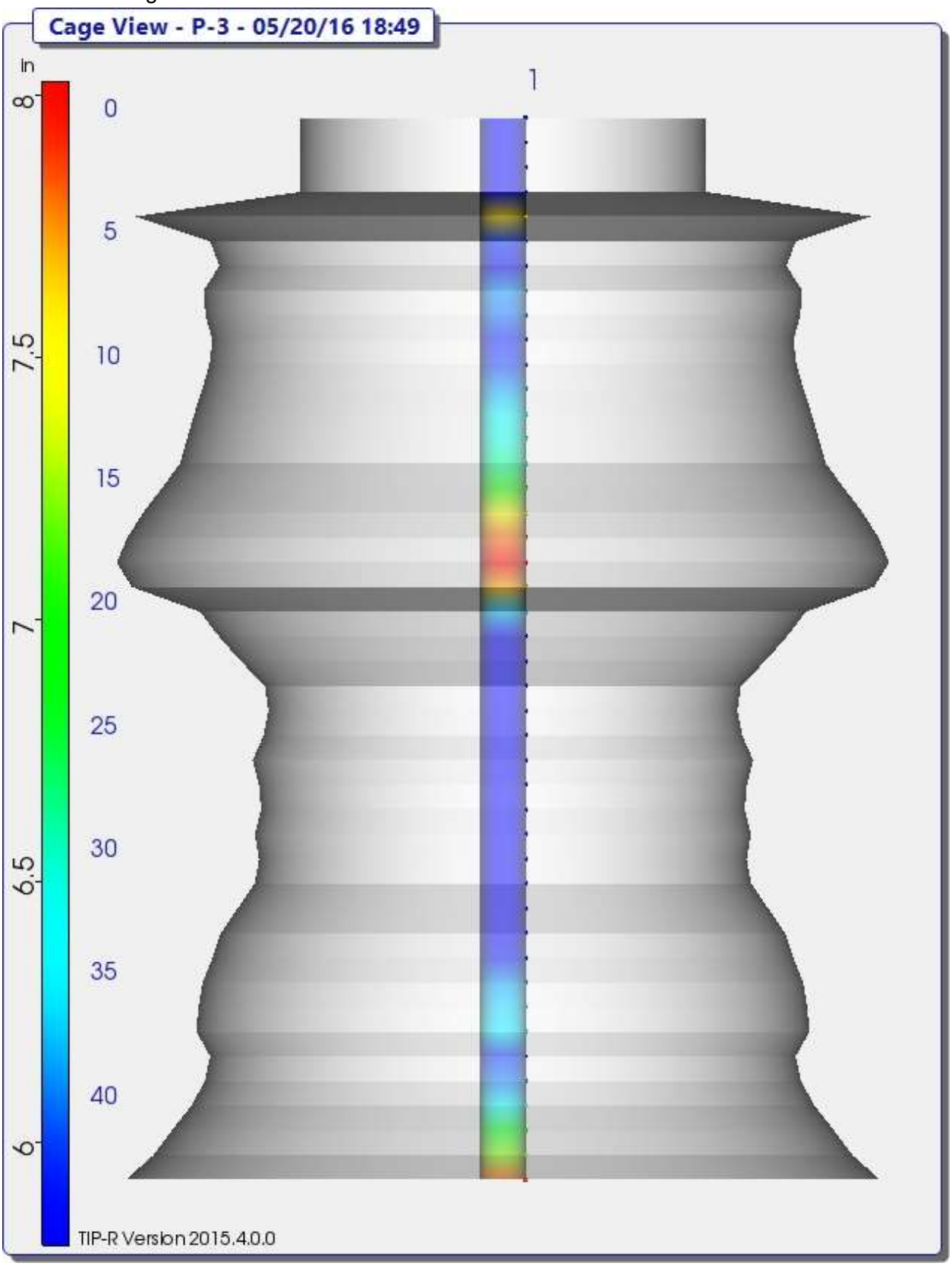
Pile 3 – Temperature vs. Depth



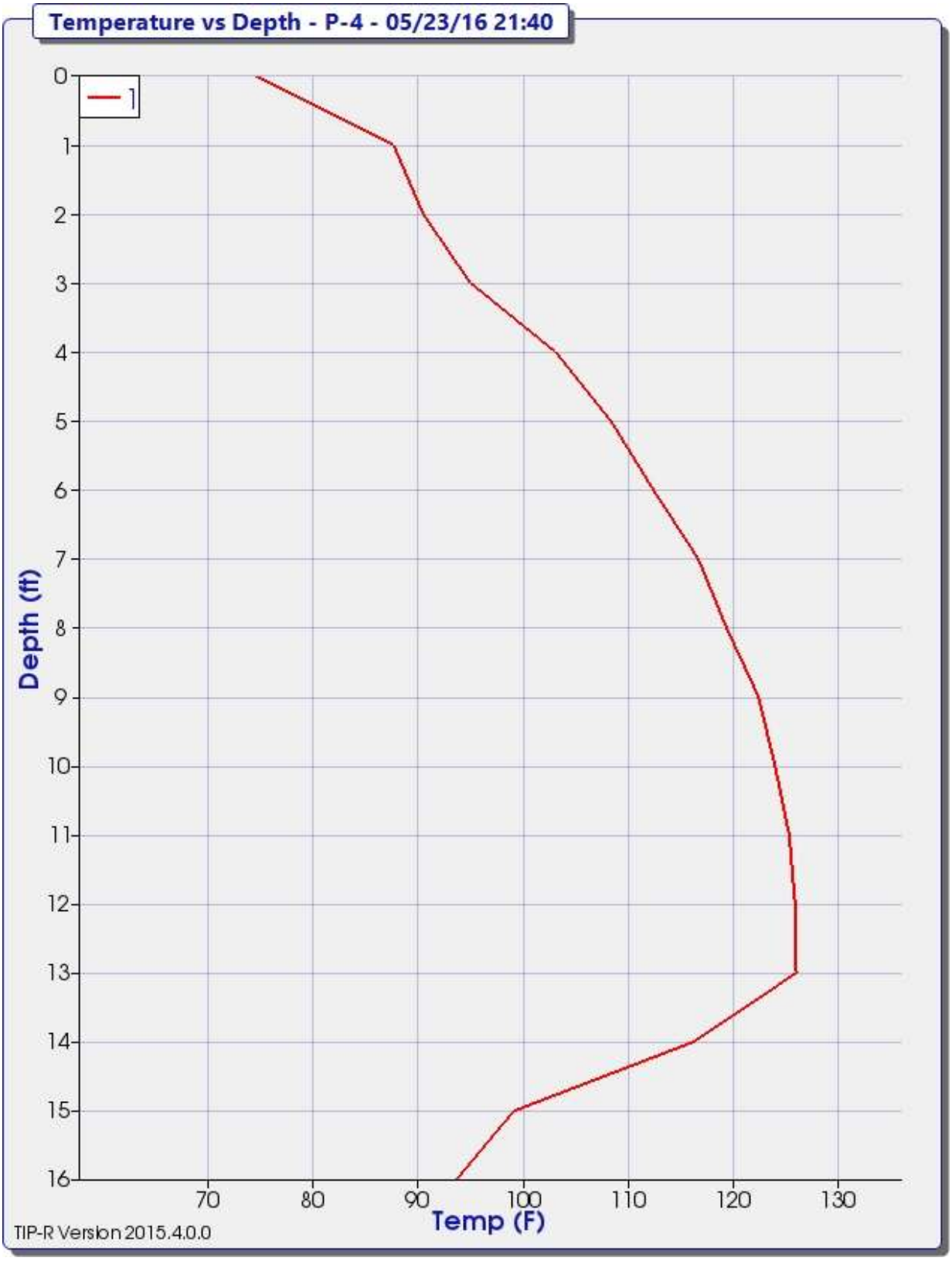
Pile 3 – Radius vs. Depth



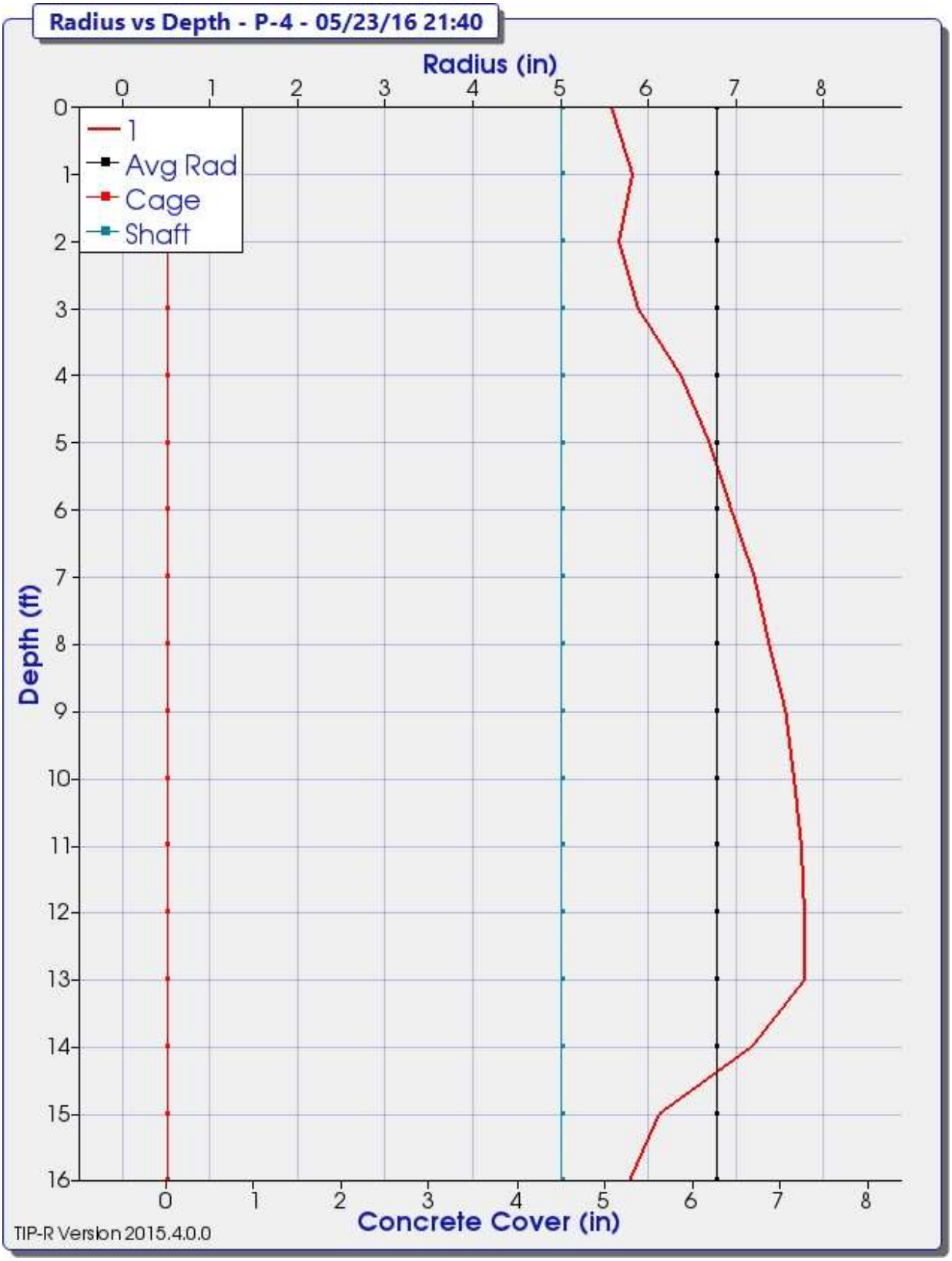
Pile 3 – 3D Cage View



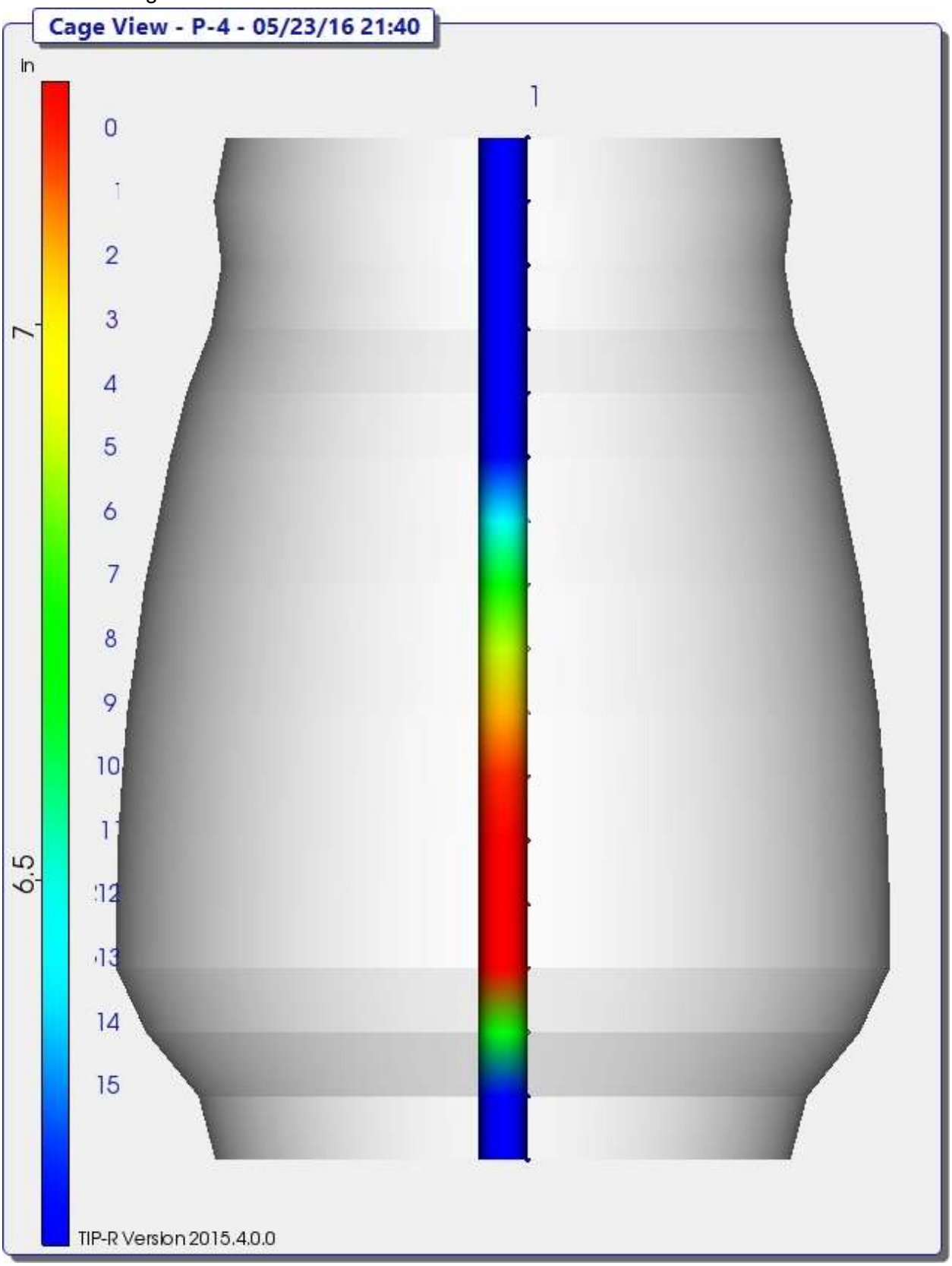
Pile 4 – Temperature vs. Depth



Pile 4 – Radius vs. Depth



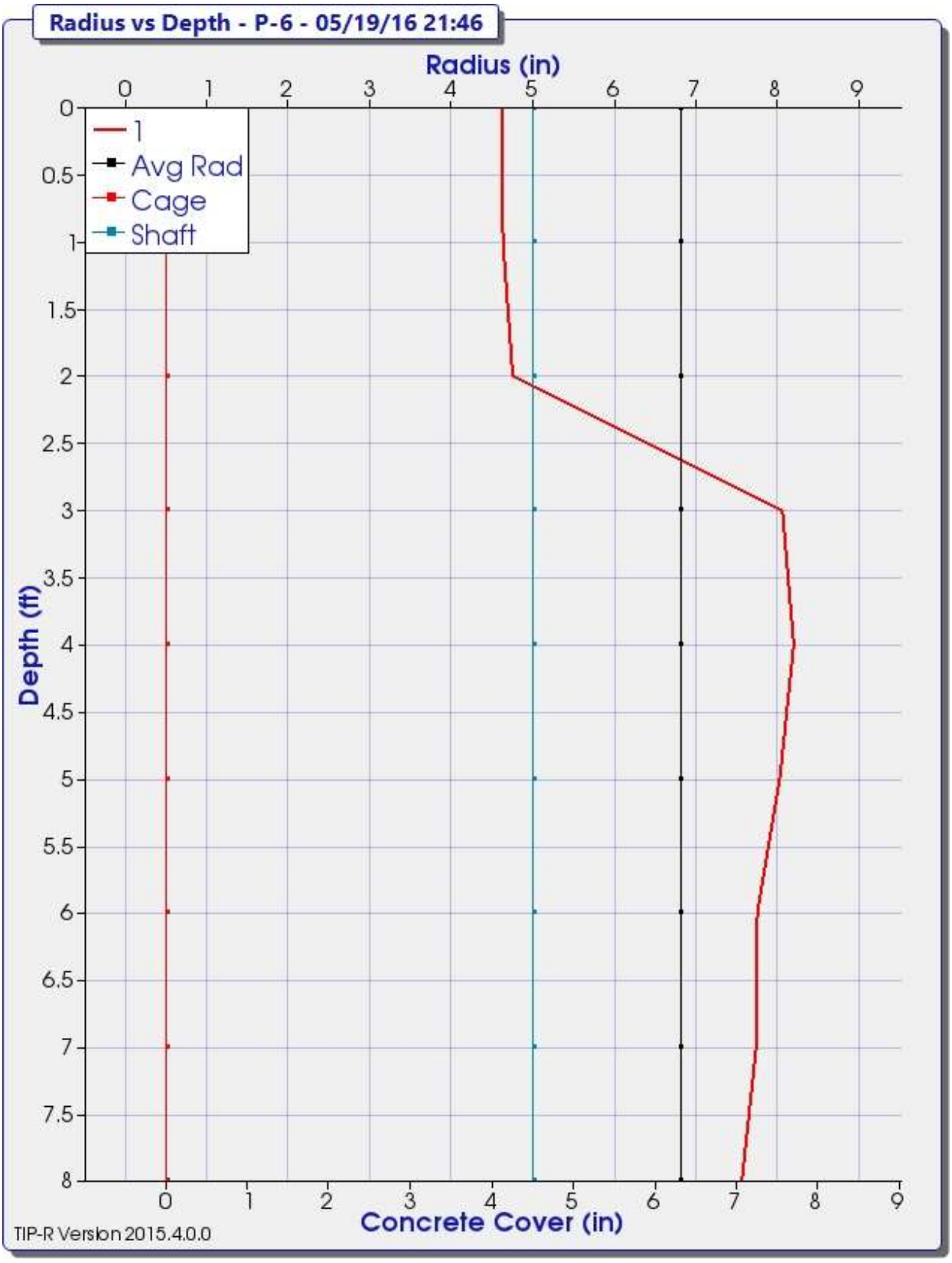
Pile 4 – 3D Cage View



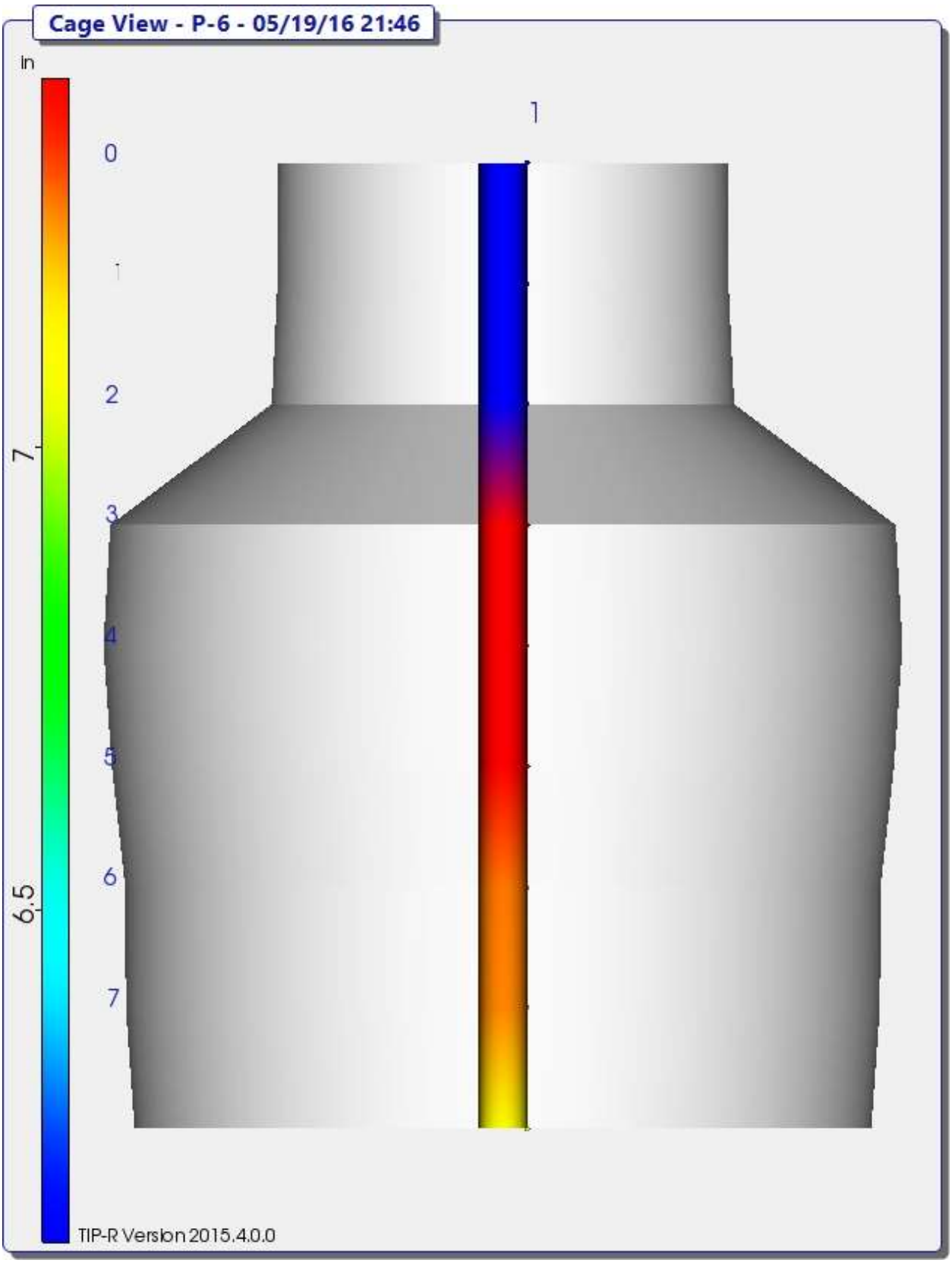
Pile 6 – Temperature vs. Depth



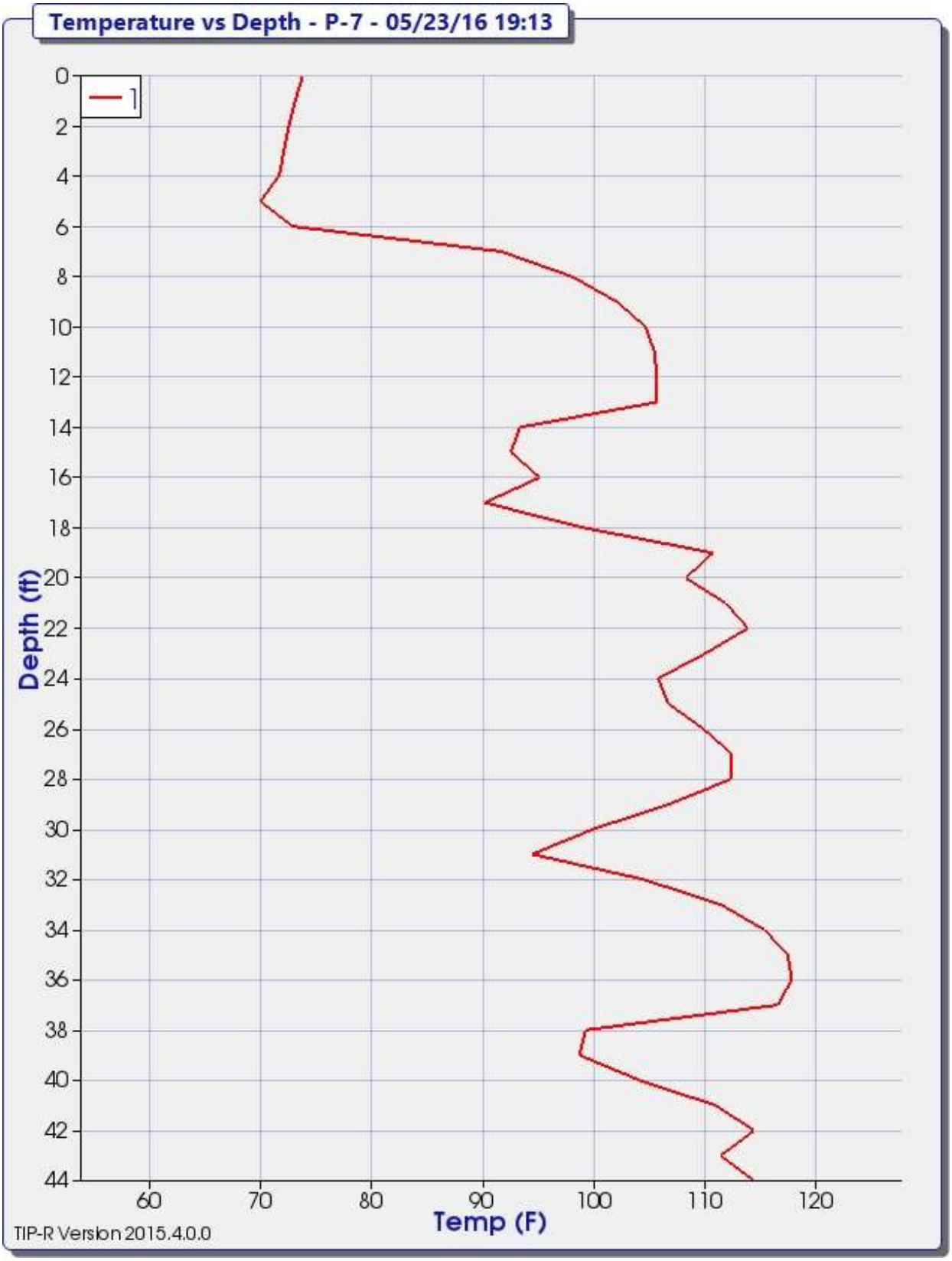
Pile 6 – Radius vs. Depth



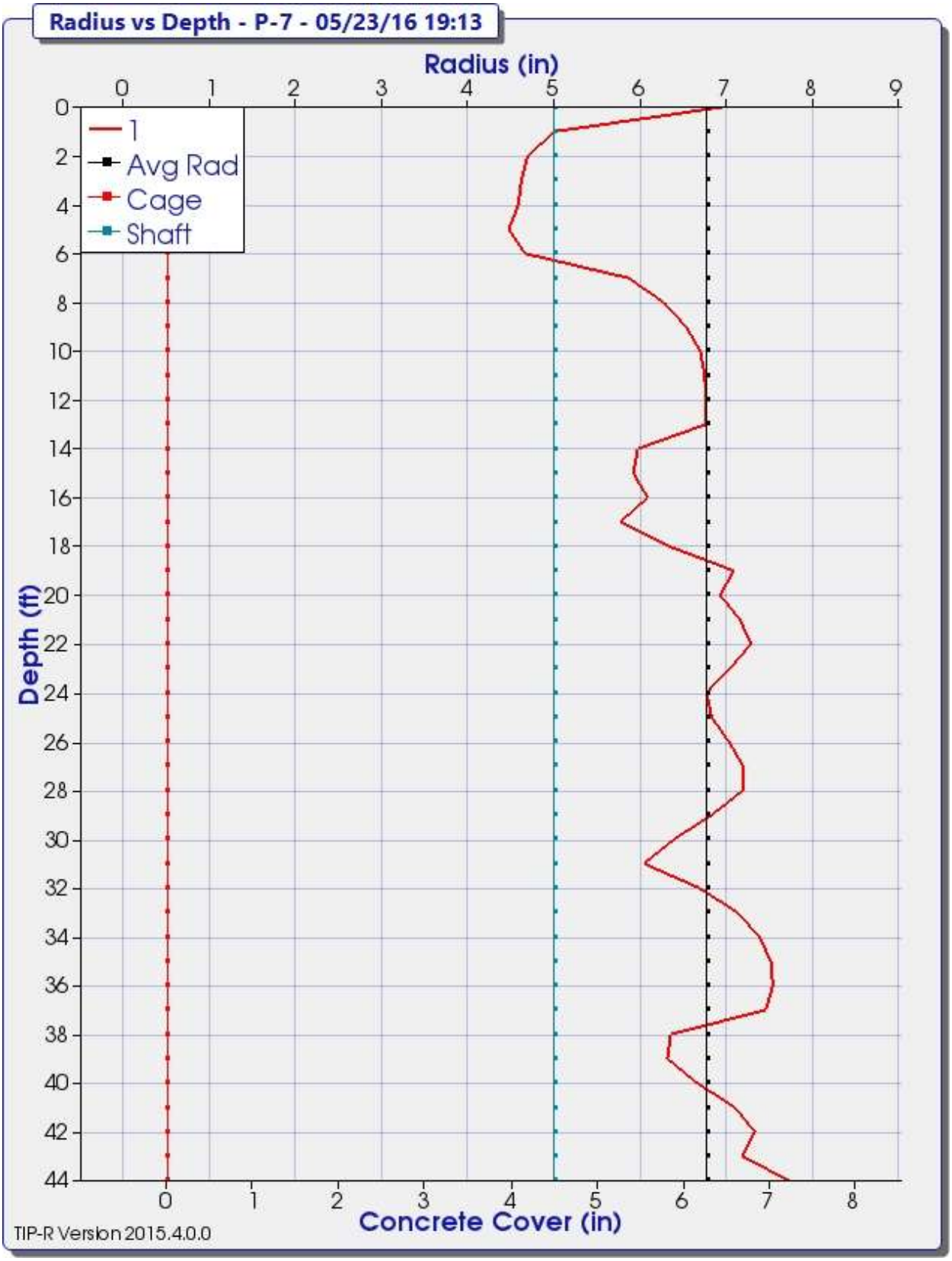
Pile 6 – 3D Cage View



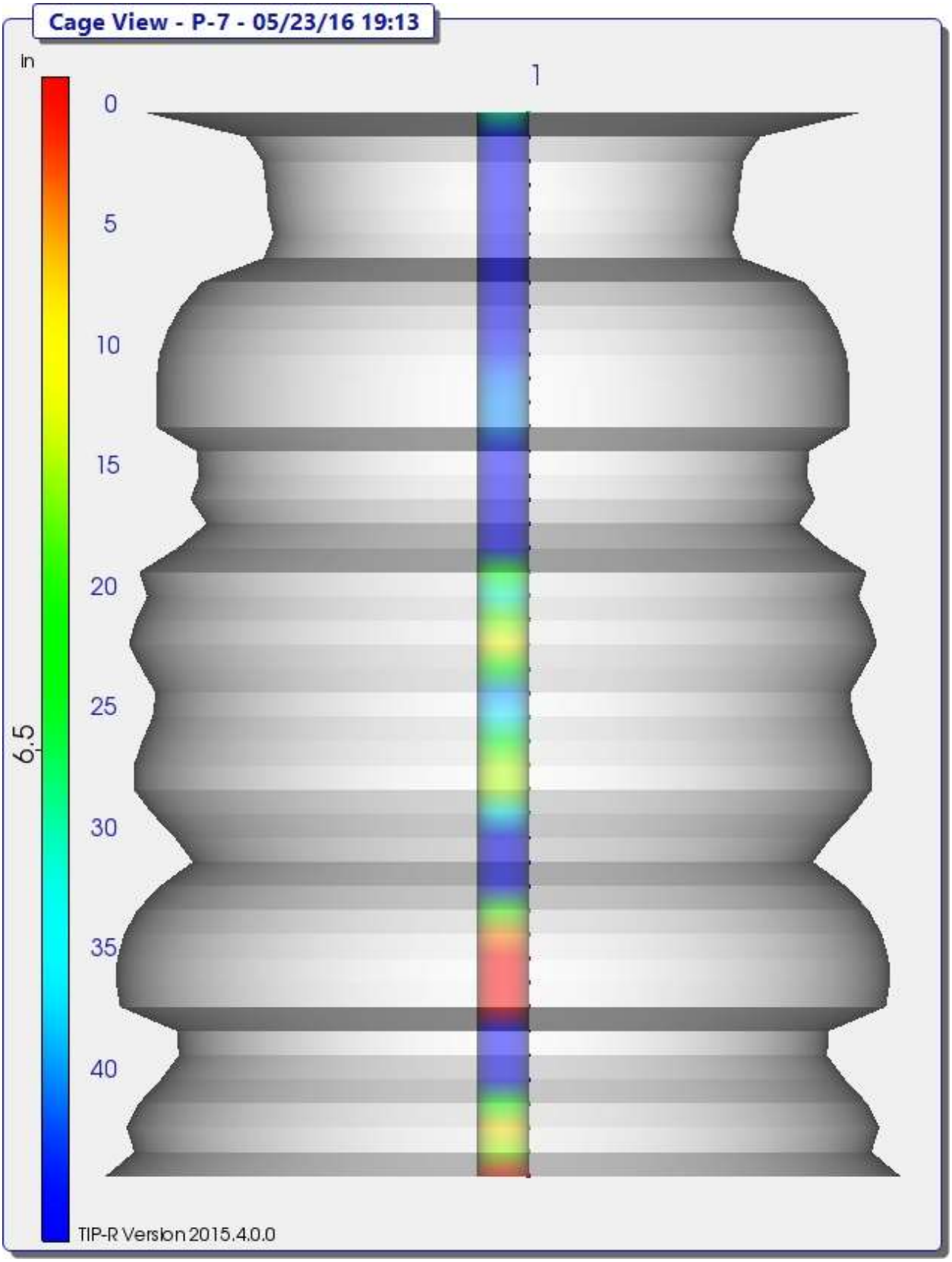
Pile 7 – Temperature vs. Depth



Pile 7 – Radius vs. Depth



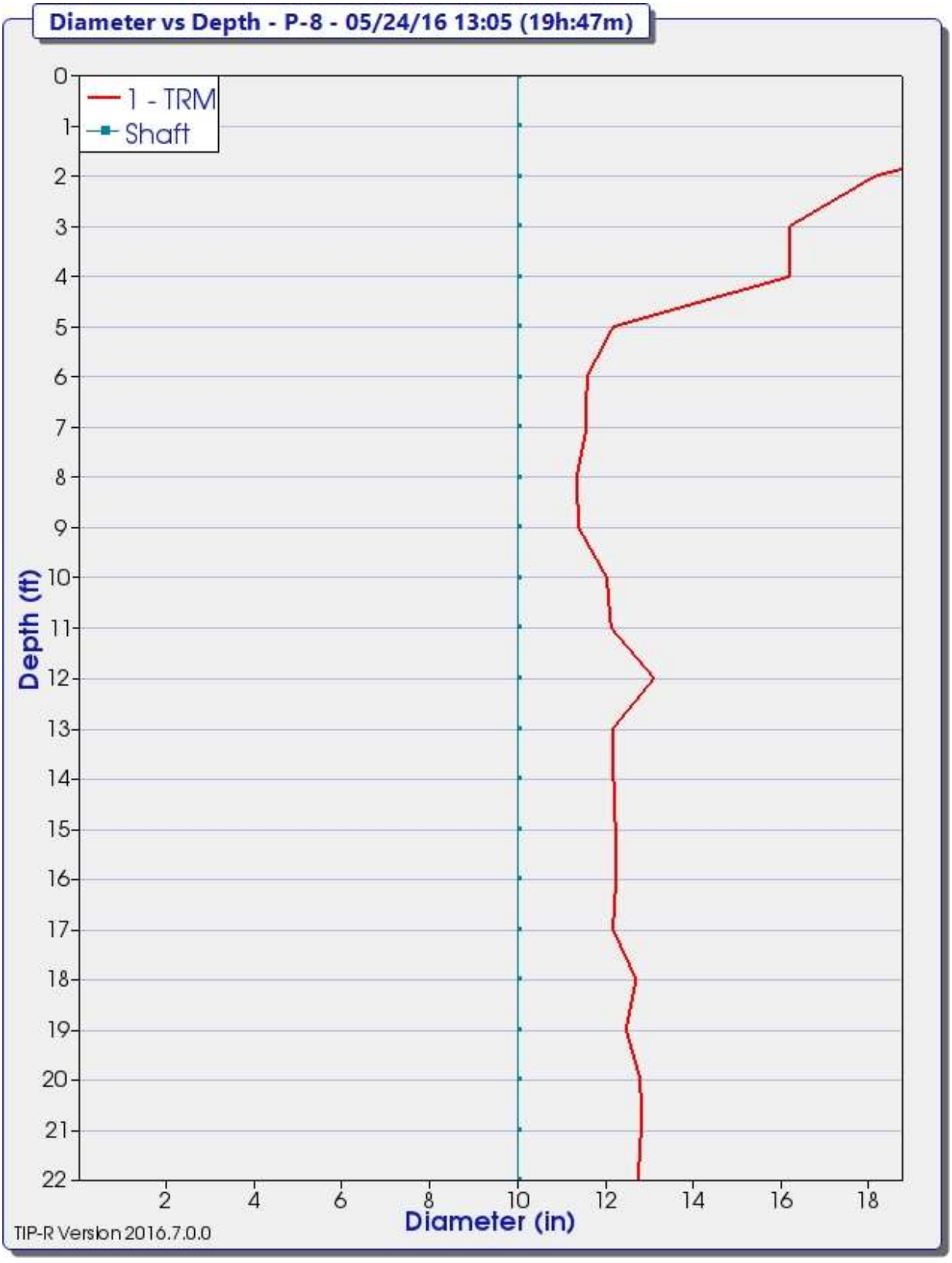
Pile 7 – 3D Cage View


Cage View - P-7 - 05/23/16 19:13
in
6.5
0
5
10
15
20
25
30
35
40
1
TIP-R Version 2015.4.0.0

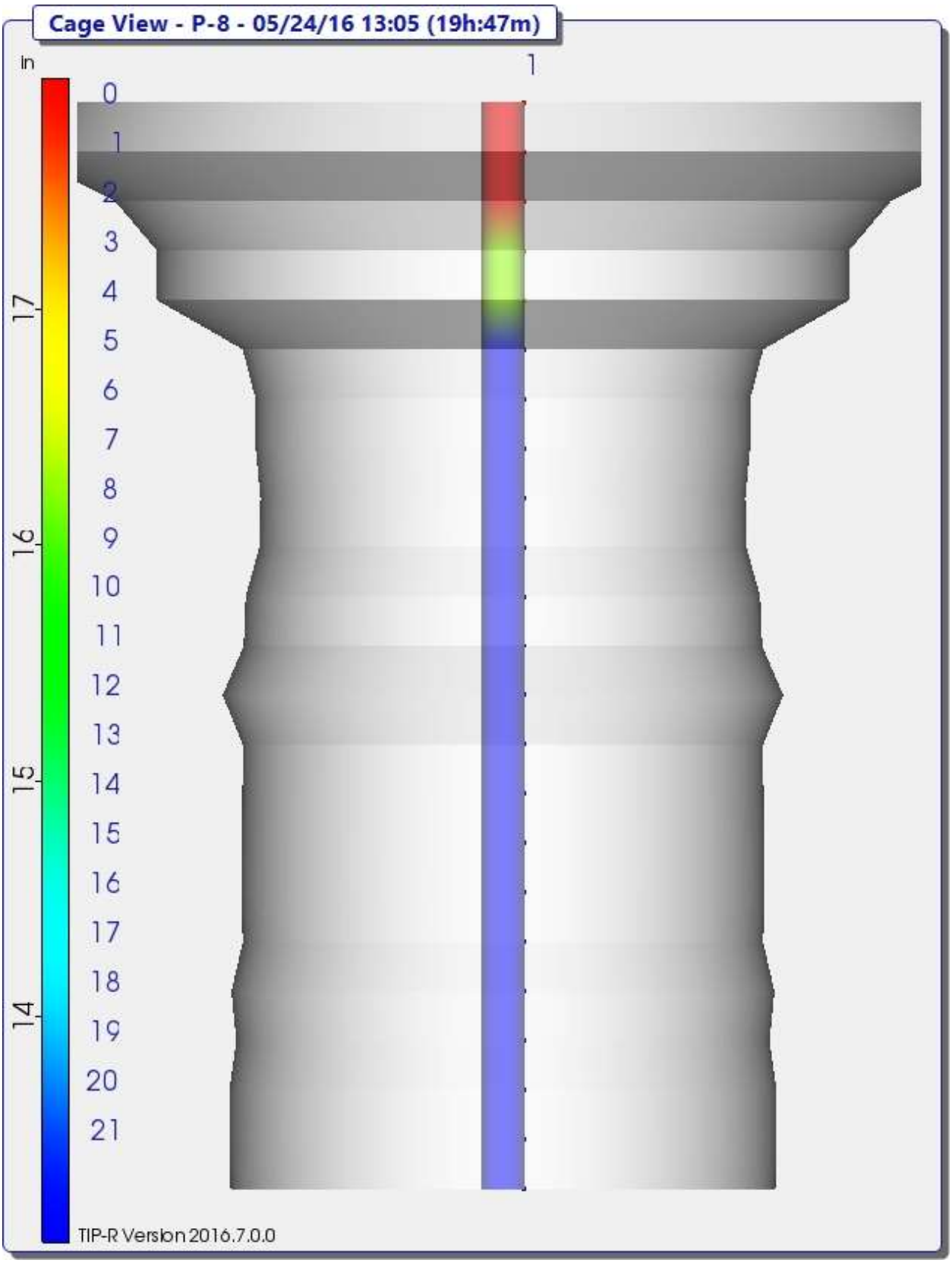
Pile 8 – Temperature vs. Depth



Pile 8 – Radius vs. Depth



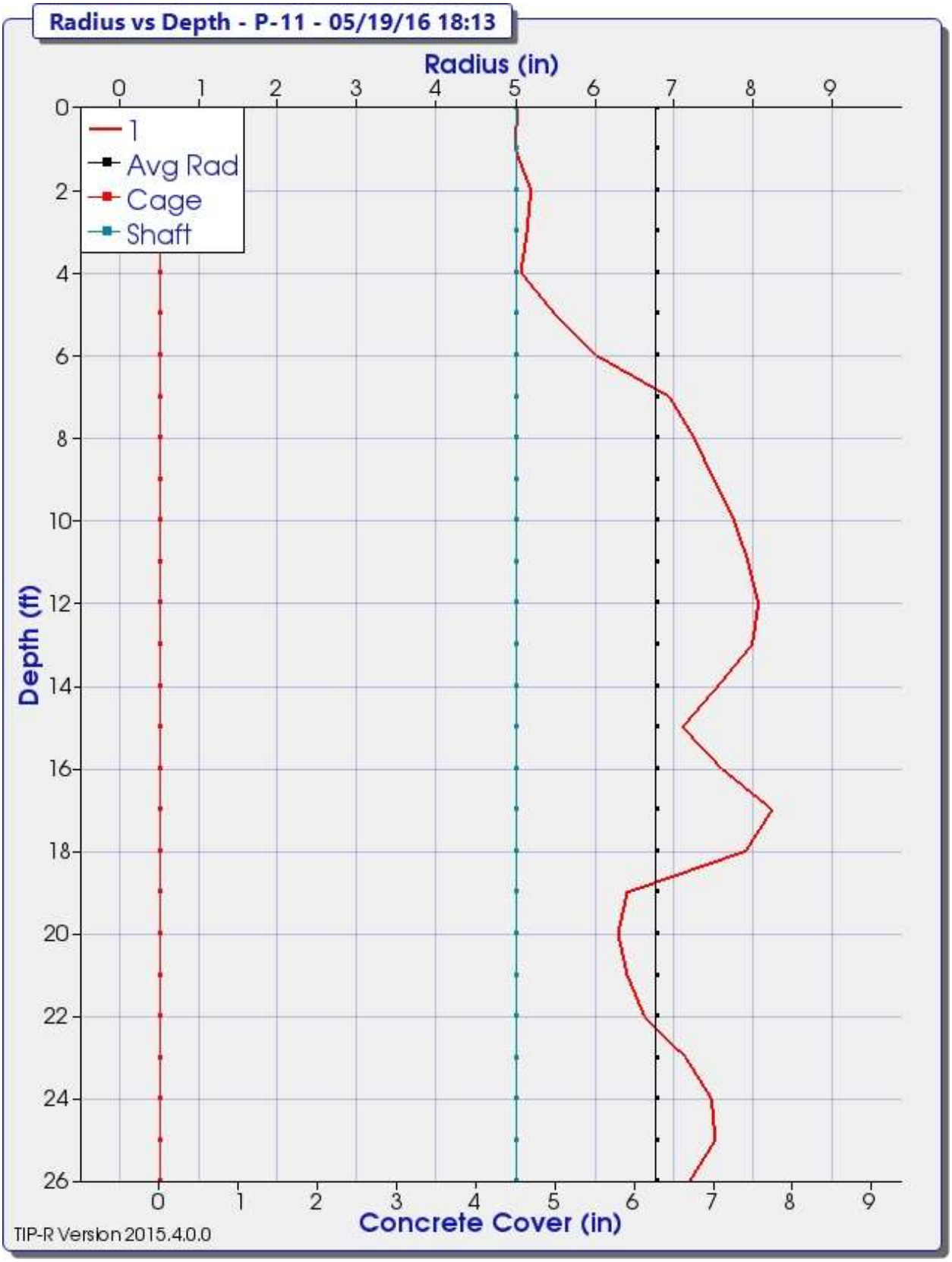
Pile 8 – 3D Cage View



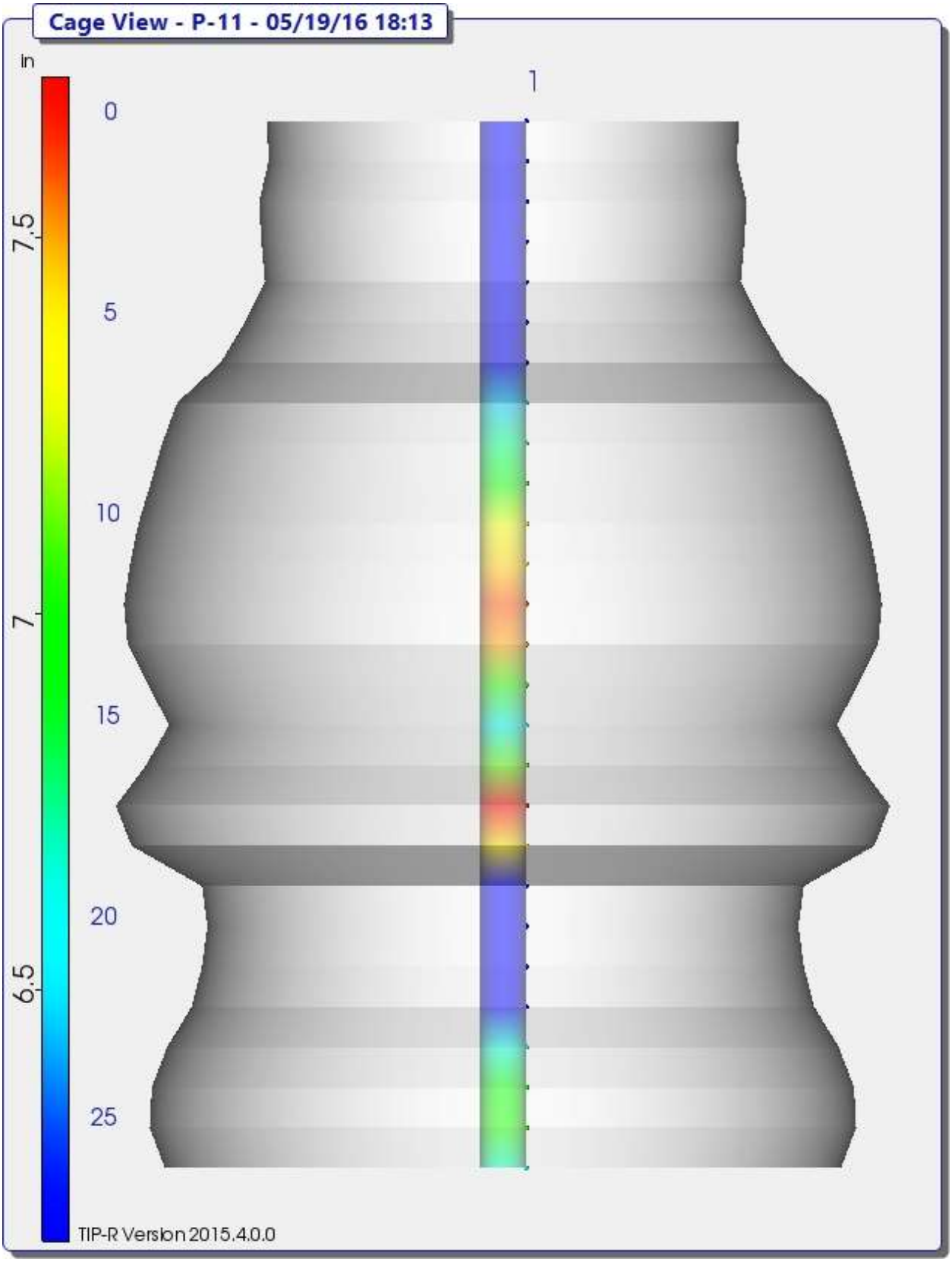
Pile 11 – Temperature vs. Depth



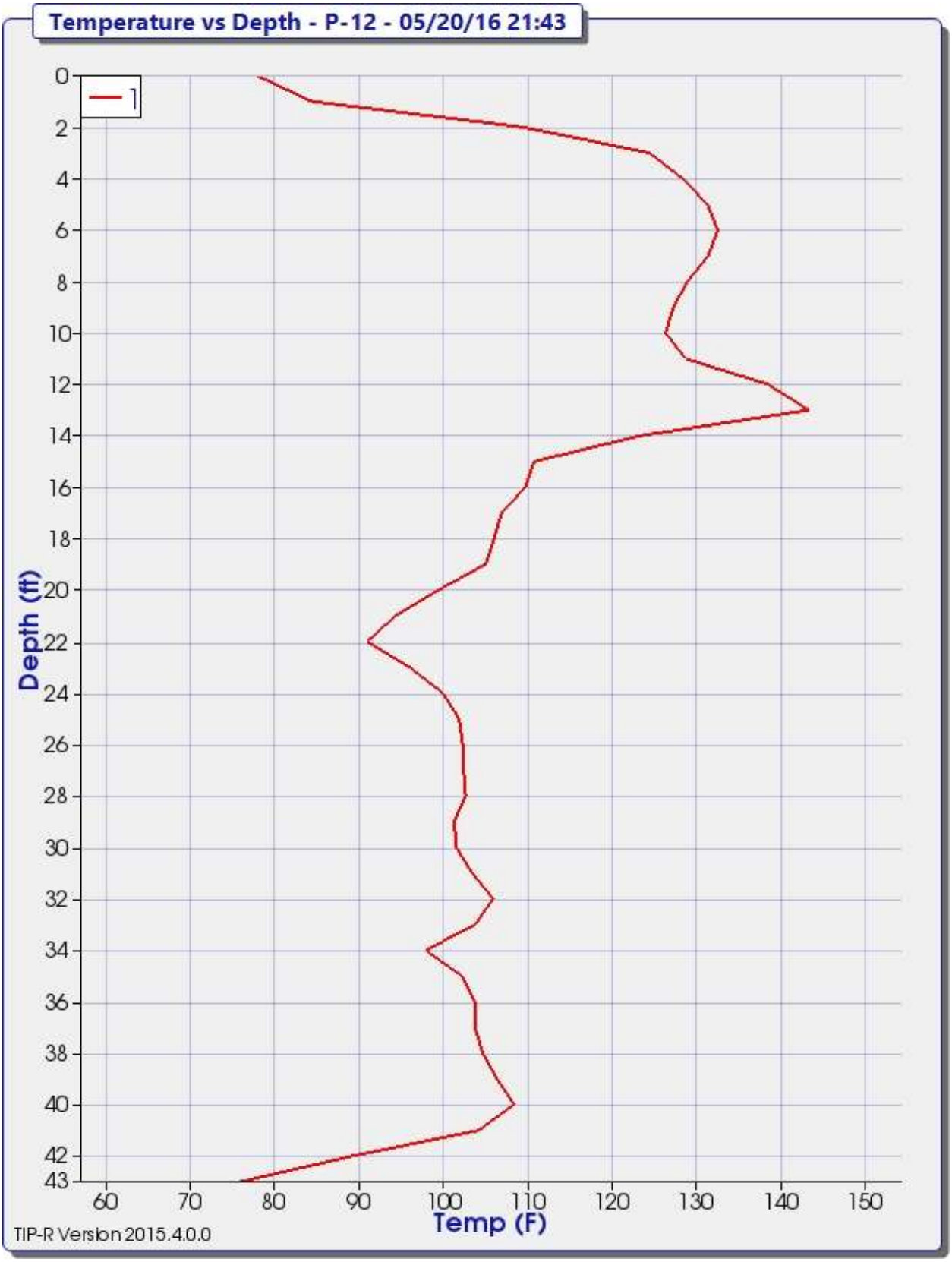
Pile 11 – Radius vs. Depth



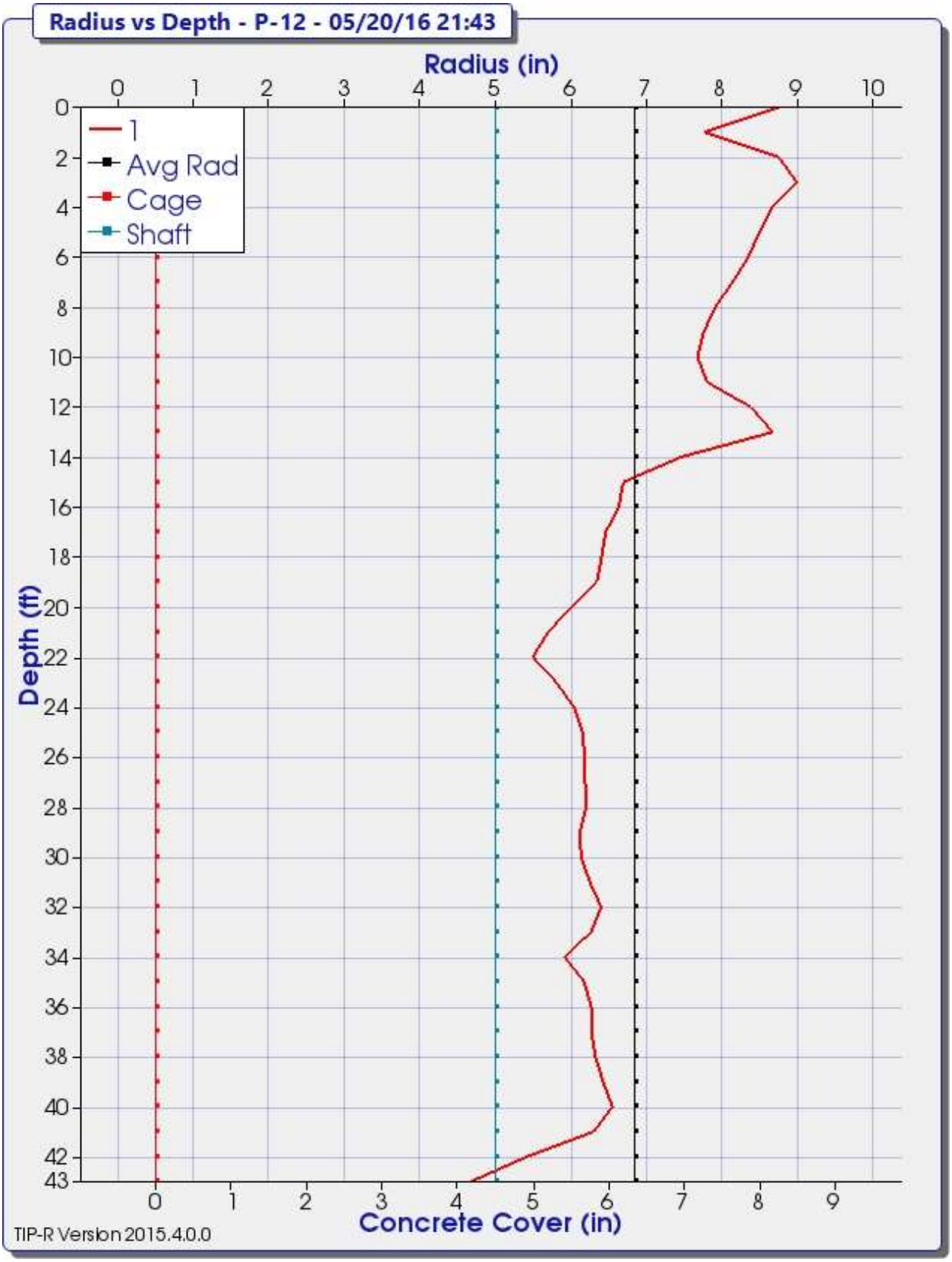
Pile 11 – 3D Cage View



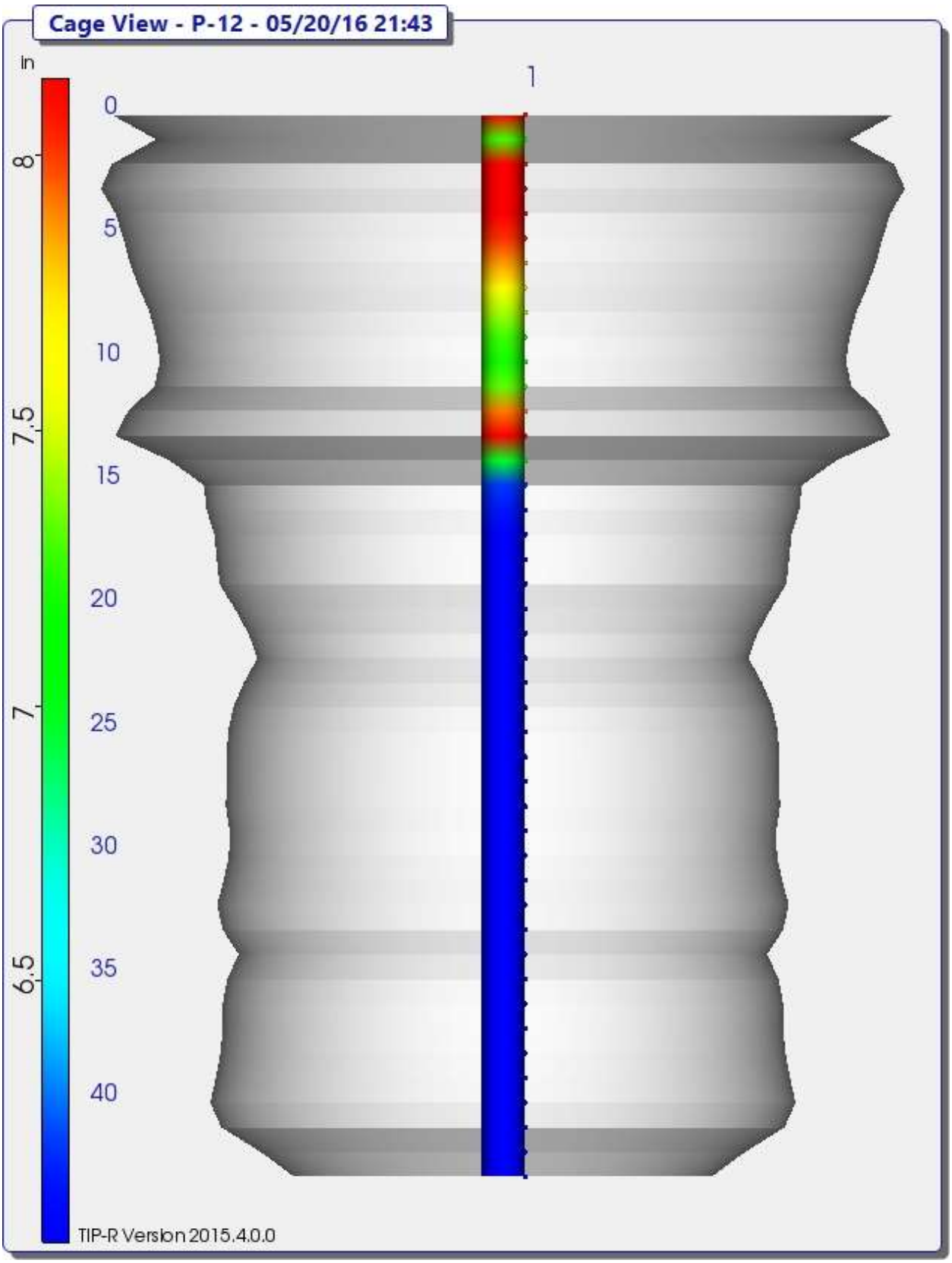
Pile 12 – Temperature vs. Depth



Pile 12 – Radius vs. Depth



Pile 12 – 3D Cage View


Cage View - P-12 - 05/20/16 21:43
in
8
7,5
7
6,5
0
5
10
15
20
25
30
35
40
1
TIP-R Version 2015.4.0.0

MICROPILE DESIGN AND CONSTRUCTION IN LIMITED ACCESS WETLAND HABITAT

Steve Davidow, P.E., S.E., P.Eng., Quanta Subsurface, LLC
Nick Salisbury, Crux Subsurface, Inc.

ABSTRACT

This paper will discuss the use of micropiles as a specialty deep foundation solution to limited construction access challenges within the Troy Meadows wetland portion of PSE&G's 500 kV Susquehanna to Roseland Electric Reliability Project. Micropile foundations were constructed utilizing primarily helicopter access for seven 500 kV double-circuit tubular steel pole structures within the protected habitat. The successful implementation of a design-build strategy between the overhead design team and the contractor led to significant refinements in the foundation design. Value engineering efforts focused on refinement of tower loading geometry and load cases, assessment of geotechnical conditions, and reduction of foundation footprint within the wetlands environment. The paper will detail design and routing of the overhead alignment, as well as permitting restrictions and area of impact limitations. It will then provide an in-depth analysis of micropile foundation design utilizing concrete pile caps, and a detailed overview of construction methodologies.

PROJECT OVERVIEW

The Susquehanna to Roseland Electric Reliability Project (SRERP) is a new 500 kV transmission line spanning from the Susquehanna power plant in Berwick, Pennsylvania, to the Roseland switching station in Roseland, New Jersey. A portion of the alignment crosses Troy Meadows, a 3,100-acre freshwater marsh located in Morris County, New Jersey. The area has been designated as a Priority Wetland by the U.S. Environmental Protection Agency as well as a National Natural Landmark by the National Park Service. Within the protected area, the project scope included replacement of seven 230 kV lattice towers with seven new double-circuit 500 kV monopoles.

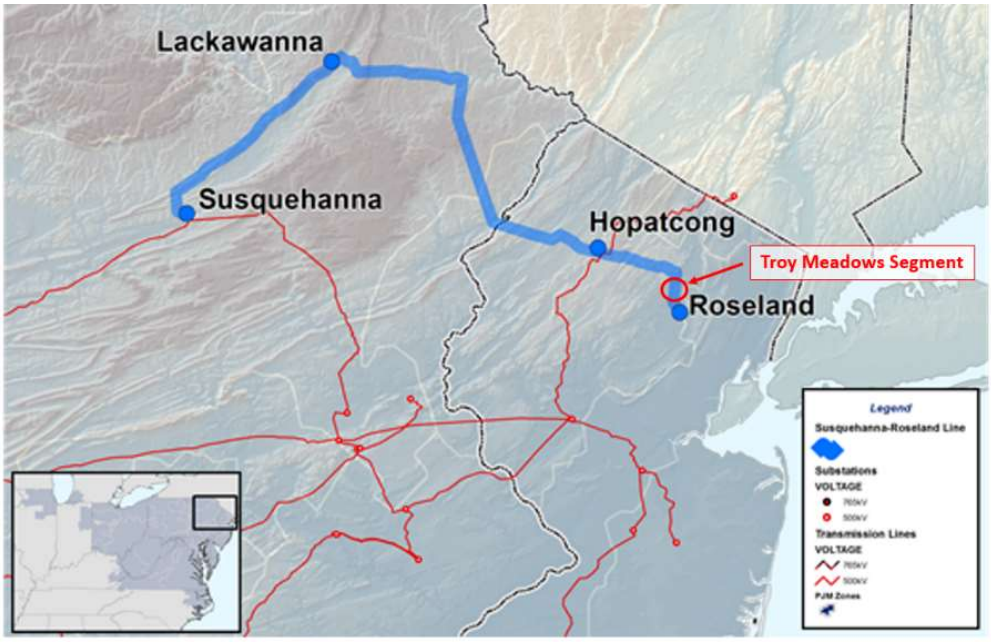


Figure 1: SRERP Alignment Map

ACCESS RESTRICTIONS

As a portion of the project siting application, detailed routing studies were completed for three potential alignment routes. The New Jersey Board of Public Utilities concurred with the owner that utilization of the existing Right-of-Way, which traversed the Troy Meadows wetland, was the preferred route for the new 500 kV SRERP.

Initial designs considered the use of a variety of conventional foundations, such as drilled shafts and driven piles. However, road construction for transportation of the necessary equipment and materials would have required extensive temporary access construction comprised predominantly of timber matting. Timber mat roads were determined to pose significant risk on two fronts; variability with changing environmental conditions, and opposition from conservation groups. Ultimately, the decision to utilize helicopter construction methods was selected to control project costs.



Figure 2: Completed Line Construction through Troy Meadows

Selecting a foundation type to meet the needs of the project was a challenging process which involved extensive input from the project designers and contractors. A comparative study was conducted to determine the foundation type that would impose the least environmental impact, and which could also be constructed entirely by helicopter. Micropile foundations were ultimately selected and the design team worked with the overhead line contractor to select a design-build micropile foundation contractor.

Micropile foundations have been employed for numerous transmission line projects requiring helicopter construction techniques. They can be installed with lighter weight equipment and materials making them conducive to light and medium lift helicopter transportation. The compact nature of the equipment also allows for a minimized area of temporary and permanent disturbance. The project team opted to employ a design-build delivery method, which they believed created the highest level of risk management and assurance of on-time completion. These were crucial elements to a project with an aggressive schedule governed by electrical outage schedules.

MICROPILE FOUNDATIONS

Micropiles have been used internationally since their development in Italy in 1952 (FHWA, 1997). In North America, the use is somewhat more recent, and is widely considered a specialty geo-construction technique, with most of the technical knowledge residing with the contractor. The industry standard for design and construction utilizing micropiles remains the FHWA State of Practice review in 1997 and updated in 2005. There have been major efforts made in the quest for a “unified” design approach, which includes publications by AASHTO and the IBC in recent years. The FHWA manual remains the most comprehensive resource available to designers to-date.

Micropiles are a small diameter (typically less than 12 inches), high-capacity drilled and grouted replacement pile. In contrast to a displacement pile, a replacement pile involves the removal of subsurface material, creating a void in which foundation elements are installed. In the transmission industry, most foundation designs employ composite micropiles reinforced with a solid threaded bar and steel casing. They are constructed by drilling a borehole through overburden material and into a bearing stratum, placing reinforcement, and grouting. They are capable of resisting axial tension and compression with applied lateral load. Micropiles have a cased upper section, composed of steel tubes, and an uncased lower bond section, which develops friction with the surrounding bearing stratum. The cased section interacts with the surrounding soil or rock to provide lateral capacity to the foundation. The piles are also reinforced with a high-capacity threaded steel bar, which extends from the top of the pile through the lower bond section, transferring axial force through friction with the grout and ground. The pile group works in tension and compression to resist overturning as shown in Figure 3.

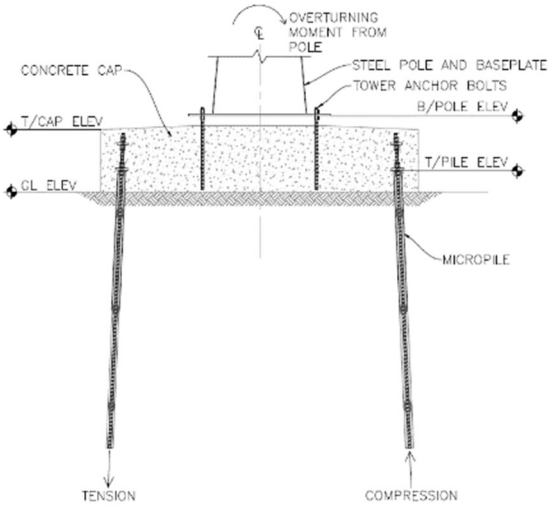


Figure 3: Micropile Tension and Compression

Micropiles are particularly advantageous to projects with one or more significant geological, structural, logistical, environmental, access or performance challenge. They are an especially favorable option where:

- The subsurface conditions are “difficult”, e.g., hard rock, soils with boulders, or debris, existing foundations, high groundwater.
- There is restricted access and/or limited overhead clearance.
- There are subsurface voids (e.g., karstic limestone).
- Vibrations and noise must be limited.
- Structural settlement must be minimized.
- Relatively high unit loads (e.g., up to 450 K axial for a single pile) are required.

The various micropile types (A, B, C, and D) are defined by the drilling and grouting methods employed during installation (FHWA, 1997). The selection of the micropile type

will typically be left to the discretion of the contractor and dictated by subsurface conditions.

MICROPILE DESIGN

Micropile foundations designed for this project consisted of a varying number of grouped micropiles arranged in circular arrays. The piles are angled away from center and derive their capacity through interaction with the native soils/bedrock. A patented Foundation Schedule was developed for each foundation location, defining the range of probable geotechnical overburden and bond units. Highly trained field personnel employed this data to allow for real-time foundation optimization. Standard Penetration Test (SPT) samples were collected during the drilling of the first pile at a given location. These samples effectively characterized the geotechnical conditions in the overburden material for lateral resistance at various depths, and continued characterization into the bond unit. In combination with the Foundation Schedule, these SPT values and field observation of geotechnical material enabled the piles to be site-specifically optimized, determining both the quantity of piles, as well as the lengths of cased and uncased sections.

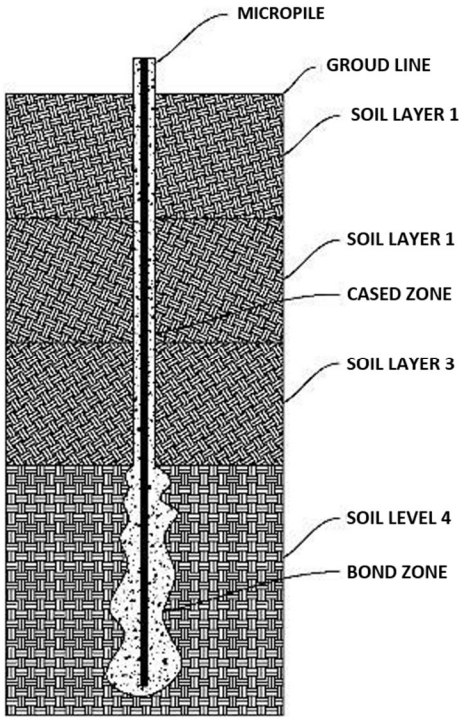


Figure 4: Micropile Installation Schematic

The initial geotechnical report for the alignment did not provide boring data at every structure site, leaving some uncertainty on the depth to bedrock as design commenced. The anticipated geotechnical conditions are summarized in Table 1, and consisted of weak cohesive soils over bedrock at variable depths of approximately 50 feet to 110 feet below ground surface.

Table 1: Expected Geotechnical Conditions

				Recommended Soil Properties					
Layer	Depth	Soil Type	Average N-Value	Effective Friction Angle (ϕ')	Effective Cohesion (c')	Undrained Shear Strength (S_u)	Total Unit Weight (γ_t)	Material Stiffness €	Strength Reduction Factor (α)
	(ft)			(degrees)	(psf)	(psf)	(pcf)	(ksi)	
1	0-5.5	Soft peat and organic silt	0	0	0	250	100	NA	1.10
2	5.5-40	Stiff silty clay	14	0	0	940*	125	0.6**	0.75
3	40-51	Very stiff to hard clayey silt	30	30	100***	0	130	2.1**	1.00
4	51-65	Very dense gravel and silty sand	100+	36	0	0	135	10+**	1.00

** Soils generally vary from stiff to very stiff. Cohesion values for unconfined compression tests in the Troy Meadows area varied from about 750 psf to 1190 psf, for an average value of approximately 940 psf.*

*** Based on blow count and/or unconfined compression test correlations with published data.*

**** Recommended soil parameters assume these glacial soils behave as granular materials.*

VALUE ENGINEERING AND DESIGN

Prior to foundation construction, two rounds of value engineering were completed, effectively decreasing the number of micropiles and total disturbance area of the concrete caps. The first round of value engineering investigated altering the original conceptual foundation design supplied by the contractor, which included larger diameter micropiles utilizing a bolted steel pile cap. The original steel cap was segmented and intended to be field-assembled on the micropile array into a larger cap. While steel pile caps can provide many benefits to project cost and schedule, the magnitude of tower loads and challenging geotechnical conditions within Troy Meadows were not conducive to an economical steel cap design. Changing the cap material from steel to concrete improved the fixity between the piles and cap, and eliminated the field fit-up associated with the bolted steel cap. The revision to the cap design led to a reduction in micropile casing diameter and a more efficient layout of individual micropiles.

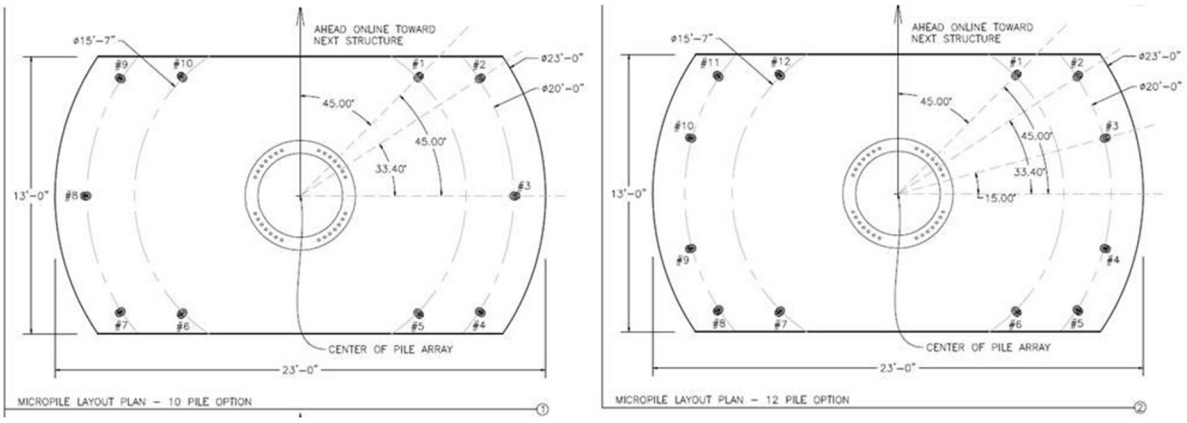


Figure 5: Value Engineered Concrete Cap Design

The second round of value engineering analyzed the use of site-specific directional structure loading. The use of directional loading components and individual load combinations allowed the foundation design team to reduce the size of the concrete pile cap, decreasing the total permanent disturbance area. The revised concrete cap design is shown in Figure 3.

Micropiles and pile caps were designed to satisfy strength requirements by utilizing the maximum bi-directional structure reactions applied longitudinally and transversally to the foundations. The reactions were provided by the pole manufacturer and listed as a group of individual load combinations. All load combinations were individually considered to ensure an economical design could be achieved. Representative tower loads are shown in Table 2.

Table 2: Tower Reactions with Overload Factor

				Design Loads				
Structure Number	Tower Type	Load Case	GROUP Design Load Case	Trans Shear (kip)	Long Shear (kip)	Axial (kip)	Trans Moment (kip-ft)	Long Moment (kip-ft)
82/3	160'	NESC Extreme Wind	Transverse	147.725	0	198.84	14381.675	8.15
		Bound Cond TR	Longitudinal	32.6625	56.6125	379.21	3208.275	9185.75
81/6, 82/4	175'	NESC Extreme Wind	Transverse	150.0375	0	203.55	15969.0875	8.775
		Bound Cond TL	Longitudinal	33.0125	56.75	387.81	3589.0125	9882.5125
81/5	190'	NESC Extreme Wind	Transverse	154.4375	0	214.75	18412.0625	11.325
		Bound Cond TL	Longitudinal	33.55	56.7875	407.71	4169.475	10940.975
81/4, 82/1, 82/2	195'	NESC Extreme Wind	Transverse	155.925	0	218.13	19250.9875	12.0375
		Bound Cond TL	Longitudinal	33.7375	56.7875	413.68	4370.5875	11307.2625

The micropile analysis subjects pile groups to vertical, lateral, and overturning loads in a three-dimensional model for the proposed pile group geometry. The pile head condition can be modeled as fixed, pinned, or elastically restrained by the pile cap, depending upon the type of connection detail utilized between the piles and the cap. The designer defines the nonlinear response of the soil in the form of t-z and q-w curves for axial loading, t-θ curves for torsional loading, and p-y curves for lateral loading in flat ground conditions. The final solution requires several iterations to accommodate the nonlinear response of each of the piles, resulting in load re-distribution amongst the pile group. Following numerous design iterations, a final micropile solution for each soil or rock unit is chosen. This analysis identifies the individual pile loads (axial, shear, and moment) and the maximum internal stress in each pile. By analyzing this data along the length of each pile, the depth-to-fixity of the pile casing (the depth below which the casing is no longer needed to resist lateral loading) is determined. Vertical, lateral, and rotational foundation deflections must also be reviewed and compared to structure performance requirements. The number of micropiles, casing size, and minimum casing embedment were selected for each foundation option to efficiently satisfy loading and deflection criteria, and were summarized in the Foundation Schedule for each structure.

The geotechnical report included soil corrosivity tests at several micropile foundation locations, which indicated that aggressive soils would be encountered. The designer conservatively chose to follow a corrosion resistance method which used a sacrificial steel thickness of 4 millimeters applied to the radius of the casing for a 75 year design life in accordance with recommendations in FHWA SA-97-070.

The structural concrete pile cap was designed in accordance with American Concrete Institute (ACI) standards using Load and Resistance Factor Design (LRFD) methodology. Embedded steel elements in the concrete pile cap were designed in accordance with the current edition of the Steel Construction Manual published by the American Institute of Steel Construction, Inc. (AISC), using LRFD. The Micropiles were designed using the methods of FHWA Micropile Design and Construction Guidelines (FHWA 2000), in combination with LRFD methodology per AISC and ACI. Figure 3 illustrates the bi-directional layout of the micropile groups for varying pile quantities determined by the field characterization method. The anchor bolts for the transmission pole were developed in the concrete cap through the use of termination plates and additional shear, as shown in Figure 5.

FOUNDATION CONSTRUCTION

Once it was determined that helicopter support and micropile foundations would be employed, individual activities needed to be scheduled within a condensed project time frame. The construction schedule for this section of the project was restricted by an electrical outage schedule governed by numerous factors. An active bald eagle nest located in close proximity to the ROW further limited construction within the wetland habitat to a 106 day window, with just 60 days allotted for foundation work.

Lightweight, componentized drill rigs were utilized, providing for efficient helicopter transport. In addition to the aforementioned access constraints, foundation challenges included limited geotechnical data; drilling spoils containment with the presence of standing surface water; concrete placement within a protected habitat; and installing heavily loaded structures in deep, soft soils. Geotechnical reports suggested rock at depths ranging from 80 to 120 feet, but exact depths were unknown.



Figure 6: Minimized Drill Site Footprint

The ambiguity in depth to rock and rock quality prior to installation necessitated designs be developed for both Type A and Type B micropiles. Type A micropiles are gravity-grouted piles installed in rock or other consolidated material. Type B refers to low-

pressure-grouted micropiles installed in unconsolidated materials. Pressures for a Type B micropile typically range between 20-200 psi, and neat cement grout is injected into the drilled hole as temporary steel drill casing or auger is withdrawn. The developed Foundation Schedule was employed to determine the grouting method and adapt the pile design to actual geotechnical conditions at the time of installation. Geological characterization was completed during the drilling of the first pile at each foundation location, effectively determining the pile type, quantity and depth for each structure. The accelerated project schedule did not allow for delays associated with redesign, and the ability to employ predetermined solutions removed much of the risk associated with limited geotechnical data.

A unique closed cell cofferdam setup was employed at each site to reduce construction impacts to the wetland. The setup, illustrated in Figure 7, consisted of curved steel sheets, weighing approximately 2,000 pounds. The sheets were driven into the ground to provide a stable platform for equipment in soft soils and groundwater, contain drill cuttings and fluids from entering the wetland, and act as a form for concrete placement during micropile cap construction. Cofferdams were constructed utilizing helicopter portable cranes and small excavators set onto local areas of crane matting. The use of this equipment significantly reduced helicopter hours, contributing toward schedule compliance and control of overall project costs. A rotating drill carriage and micropile drill were set on the cofferdam and used to install micropiles in an array of vertical and battered piles.



Figure 7: Drill Site Setup

During drilling operations, the portable cranes were used to handle casing and drill rods, which were staged on temporary crane mats. The cranes fed the drill as piles were installed to depths ranging from 90 to 150 feet. The cranes also served to place micropile testing equipment during the proof test program at each foundation.

Following micropile installation, the drill and drill carriage were removed from the site to allow for cuttings removal, tying of rebar and form construction. A pre-constructed anchor bolt cage was flown to the site and supported by the cofferdam, and concrete was cast

from crane-type concrete buckets. A high early concrete design was chosen to accelerate sufficient strength for form removal, allowing poles to be set less than one week following placement.



Figure 8: Completed Concrete Cap

CONCLUSION

The use of micropile foundations and helicopter portable tubular steel poles allowed the project team to meet an aggressive construction schedule within the Troy Meadows wetland. Foundation work was completed ahead of schedule and all seven monopoles were erected in just three days.

Innovative design and construction methods allowed for work to be completed with minimal impacts to the protected habitat. Accessing foundation sites by helicopter eliminated the significant risk associated with installing and managing matted access roads and matted work areas. This also reduced the total impact to the wetland. The use of the closed cell cofferdams allowed foundation crews to contain drill cuttings and fluids, and created a minimal area of impact from drilling activities.

The 500 kV Troy Meadows segment went into service on April 1, 2014.

REFERENCES

American Concrete Institute (ACI). (2008). “Building Code Requirements for Structural Concrete” (ACI 318-08) and Commentary, *American Concrete Institute (ACI) Committee 318*, publication no. 318-08.

American Institute of Steel Construction (AISC). (2008). *Steel Construction Manual. 13th edition.*

Armour, T, Groneck, P, Keeley, J & Sharma, S (2000). “Micropile Design and Construction Guidelines Implementation Manual.” *Report no. FHWA-SA-97-070*.

Armour, T, Groneck, P, Keeley, J, Sabatini, PJ, Tanyu, B (2005). “Micropile Design and Construction Reference Manual.” *Report no. FHWA-NHI-05-039.*

GROUP. Computer software. *http://www.ensoftinc.com/*. Vers. 2013. Ensoft, Inc.

Reese, L. C., and Van Impe, W. F. (2001). “Single Piles and Pile Groups Under Lateral Loading.” A. A, Balkema, Rotterdam, Netherlands.

SUPPORT OF THE MORRIS ISLAND LIGHTHOUSE USING MICROPILES

William L. Snow, Sr.[1], William B. Wright, PE[2], & Will Snow, Jr., PE[3]

HISTORY OF THE MORRIS ISLAND LIGHTHOUSE (MIL)

The Morris Island Lighthouse is located between the Jetties leading to the Charleston, South Carolina harbor and Folly Beach, South Carolina. The present structure is the third lighthouse to occupy this location. The first navigational aid was erected in 1673 and consisted of a raised pan filled with pitch, which was set afire at night to guide early ships. The next structure was built in 1767 and constituted the first real lighthouse, standing 42 feet in height.

In 1838 a second lighthouse was built on the site. It measured 102 feet tall and featured a revolving light. This structure lasted until 1862 when Confederate troops destroyed it to deny its use to Union troops as a lookout during the War of Northern aggression. Navigators steered these waters without a lighthouse for nearly a decade until 1876, when the current structure was built under the direction of the U.S. Army Corp of Engineers. A review of documents authored by Peter C. Hains, Major of Engineers, U.S. Army indicate the foundation of the new lighthouse consisted of 264 wooden piles (15" yellow pine, of unknown length, but possibly as much as 56 feet long). On top of these piles a "grillage" was constructed and a concrete cap, approximately 11 feet in height was built to transfer the weight of the lighthouse to the piles and ultimately to the bearing soil strata below. In 1886, the Charleston area suffered a major earthquake (7.6 magnitude). Major damage was done throughout much of the area including a slight "list" of the lighthouse to the northeast. It is said that the cast of the beacon was reduced from 18 miles to approximately 6 miles, causing much distress to navigators until the beacon platform was re-leveled. This list of the tower structure is evident to the present day.

The current lighthouse structure was originally built approximately 1200 feet from the shoreline of the Atlantic Ocean. Over the years the Corp of Engineers have undertaken several programs to aid navigation and to keep the Charleston harbor open to increased shipping demands. Significantly, around the turn of the last century a pair of Jetties were constructed, drastically changing the approach direction for ships entering the Charleston harbor. In subsequent years the harbor began to experience accelerated siltation. In an effort to prompt a natural flushing mechanism for the harbor, an opening of several hundred yards across was accomplished near the shore intersection with the South Jetty. This breach, known locally as "Dynamite Hole" partially met its intended purpose, however the new flow of water began to rapidly scour the ocean face of Morris Island, located directly South of the "hole". Within a few short years, the beach of Morris Island was eroded to such an extent that the MIL now sits surrounded by the sea.

The original lighthouse was designed so that the wooden piles would always be below the existing water table of Morris Island. The theory being that the piles would not rot or deteriorate as long as they were continually submerged. The scouring of the soil

[1]President, Palmetto Gunite Construction Co, Inc., PO Box 388, Ravenel, SC 29470, 843-889-2227, snowwl@aol.com
[2]Terracon Consultants, Inc., 1450 5th St. W., North Charleston, SC 29405, 843-514-0016, wbwright@terracon.com
[3]Terracon Consultants, Inc., 2201 Rowland Ave., Savannah, GA 31404, 912-200-9120, will.snow@terracon.com

surrounding the structure resulted in the piles being exposed to salt water, but more importantly, to water born parasites such as ship worms or tereda worms, as they are locally known. The introduction of these organisms led to severe deterioration of the original support piles. The deterioration of the lighthouse structure and foundation led to the current effort to save the lighthouse from the harsh Atlantic environment. An organization known as “Save the Light” bought the structure in 1999, and is spearheading the effort to “Save the Light”.

SAVE THE LIGHT, INC. (STL)

Save the Light, Inc. was formed in 1996. Its sole purpose is to facilitate the saving of the Morris Island Lighthouse structure. The lighthouse function was discontinued in 1962 by the U.S. government. The structure was sold to a private owner and in subsequent years it began to show the results of decades and neglect as the harsh environment of the ocean took its toll. Although the light has long been extinguished, the lighthouse itself represents an intricate and permanent place in the history and culture of the local area. This particular lighthouse has survived the ravages of nature, the torment of war and the follies of man as it has stood sentry for the community that is James Island and the Charleston area. It is more than a symbol, it is a major part of the local heritage and maritime culture.

In the months and years after it acquired the light, STL, Inc. has worked to raise the funds needed to restore this structure both structurally and in time, aesthetically. The repairs completed through 2008 represented Phase I of those repairs. Phase I basically cleaned up decades of early efforts and repairs aimed at delaying the inevitable deterioration around the structure. In the fall of 2009, STL, Inc. requested proposals from pre-qualified firms to develop a design/build concept to preserve and strengthen the existing foundation. After several months of receiving and reviewing these proposals, a design/build team was selected and a contract of approximately $2 million was executed.

DESIGN ANALYSIS

The design of the project was begun with several unknown properties. Key answers needed before a final design could be completed included: determining the weight of the structure; understanding the design intent of the original foundation; the condition of the original foundation components and the strength of the existing materials; the condition of the tower structure and its impact on the intended repairs, and other conditions that may become evident as the project continued.

The initial exploration of the structure yielded much information. Key among these findings were the weight of the structure (4400 tons), the average strength of the concrete foundation (3000 psi ave), the strength of the bricks (2300 psi ave), and a general understanding of the original design intent as well as the general condition of the original support structure.

Although many of the properties of the existing foundation remain a mystery, enough became known to lead the design/build team to the conclusion that the existing foundation piles were deteriorated to the point that they could not be counted on to support the structure into the future. It was therefore decided that Micropiles would be

installed with the intent that they carry 100% of the weight of the structure, thus discounting any residual contribution of the original foundation piles. Another key element investigated was the soil profile immediately adjacent to the structure. Although the original designer did accumulate some knowledge of this profile, the team lacked enough modern technical information and/or description to confidently proceed with the final design. Current and modern soil boring information was a critical element for this project.

The final design assumptions were accumulated based on information obtained from the site by the design/build team. Due to the complexity and logistics of the site, every member of the team was involved in gathering this critical information.

FINAL FOUNDATION DESIGN

As outlined above, several key design elements became clear after modern soil borings were obtained and as the site was investigated. This information led the designers to conclude that the structure could be supported on Micropiles and the load of the structure could be transferred to those piles. A theoretical pile length was calculated based on soil data collected and a test pile program was developed to confirm these assumptions.

An inspection and testing program was developed to monitor the work as it progressed. Key elements of this program included the test pile program, installation of monitors on the existing tower and existing foundation system, and the installation of tilt meters around the structure. These instruments enabled the geotechnical and construction services engineer to monitor and understand what was going on within and without the structure, long before such information would normally be readily apparent.

A key concern of everyone involved with the project was the tower structure's ability to withstand the installation of the new support system. Much attention was given to the condition of the existing tower as well as the forces that would be placed on it during construction. The Micropile system used on this project produced virtually no adverse loads or impact to the existing structure.

The final design of the project included the installation of 68 micropiles with an allowable compressive design capacity of 75 tons per pile. The piles were to be placed on a predetermined spacing which would allow the load of the existing structure to be transferred and supported by the new piles. In addition to the new pile support system, filter fabric and subsequently sand was to be placed in the space between the existing structure and the sheet pile wall constructed under Phase I of the restoration process.

CONSTRUCTION

The significance of saving time was crucial to the ultimate success of the project as crews were in a race with the calendar with anticipation of the fall hurricane season. Early in the procurement process everyone involved recognized the very real possibility that the lighthouse structure may not have the ability to survive another major storm. At the very least, it was known that construction would be difficult or impossible during the fall storm season. For this reason, every effort was made to maximize the time spent at the site. Crews were set up working 3, 13-hour days per week, per crew. With two separate crews operating on a rotating schedule, there was work going on six days a

week with Sundays off. This held true throughout the project and was instrumental in completing the project ahead of the projected schedule and “beating the clock” to the storm season.

The gathering of core samples and the coring in anticipation of the Micropiles continued until a jack-up barge could be mobilized to the site. On June 7, 2010, the marine contractor mobilized and lifted the barge on the site and immediately began to place sand into the cell. The buildup of sand enabled the placement of Micropile equipment into the cell and the test pile program was begun by placing 2 test piles and appropriate reaction piles. After sufficient curing of the test piles was completed, a load test was conducted by the geotechnical engineer and the final pile design was confirmed.

The Micropile system selected for this project was the TITAN system, manufactured by Ischebeck. Titan Micropiles consist of a continuously threaded, hollow reinforcing rod as the load carrying steel member, together with a grout body of Portland cement grout with a minimum compressive strength of 5000 psi. This system allows for the transfer of tensile and compressive forces from the friction between the threaded rod via the grout body and the soil. The grout body functions as a conduit of the radial friction with the soil, provides stiffness against buckling, and corrosion protection for the steel.

After the pile length and diameters were determined and verified, the placement of production piles began. Production rates varied somewhat due to several reasons. Chief among the limiting factors was the weather and the ability to re-supply the construction supplies. Everything had to be transported from land by barge and/or tug boat, usually on a daily basis. Wind, weather and the resulting wave action greatly affected and hindered this operation. Items needing transport included fuel, several tons of steel rods, hundreds of tons of cement and surprisingly enough, thousands of gallons of fresh water. One of the most frustrating occurrences on the project was when, although surrounded by the Atlantic Ocean, work came to an abrupt halt when crews ran out of fresh water used in the Micropile installation.

The Micropiles were installed on two concentric rows around the base of the lighthouse structure. They were placed in a staggered fashion to insure that no eccentric loads were placed on the lighthouse during construction that would destabilize the existing support. The installation of Micropiles actually became one of the least problematic efforts on the project.

The procedure for installing Micropiles is in fact the system’s greatest advantage. The process utilizes equipment that can be mobilized and placed on sites where normal driven pile equipment is not practical. While driven piles are certainly possible over water, on projects such as the Morris Island Lighthouse, mobilization of the equipment needed would have been prohibitive. A second and equally important advantage of the Micropile system is the total lack of vibration which would have been present had driven piles been attempted. Micropiles in general are not considered as a method to replace driven piles, but instead are traditionally used where mobilization, vibration, accessibility and even noise are major limiting concerns for the given project.

Micropiles are however being used on larger and more complex projects. The strengths being achieved are becoming more and more predictable and are far more substantial than in the past. Verifiable and repeatable tests have yielded compressive loads of well over 150 tons in compression, 50 tons in tension and lateral loads of 9 to 11 kips in the Charleston area. As with any deep foundation system, these load

characteristics are site specific and should only be relied on with respect to the soil characteristics of a given site.

The procedure for placing Micropiles is fairly straight-forward. A threaded, hollow rod with a drill head is rotated into the ground. As the rod is extended down, a drilling grout mixture is pumped through the hollow rod thus removing the coil cuttings from the hole. When the rods have been drilled to the design depth, a structural grout is pumped through the rod. This grout enters the hole at the bottom and lists the lighter drilling grout up and out of the hole. When all of the drilling grout is gone, the Micropile is basically complete with a steel rod in the center of a structural grout column.

After the final Micropile was placed, the entire cell was filled with sand to a point approximately 18 inches below the top of the existing sheet pile wall. The sand was completely surrounded by filter fabric to ensure the sand would not be eroded by the surrounding waters. The filter fabric was then capped with excess grout castings, left over from the Micropile installation. Future work on the restoration effort will include placement of additional rip-rap around the structure as funds become available.

The final component of Phase II was the construction of a permanent dock platform to be utilized in the future. After the dock was completed, the jack-up barge was lowered and demobilized on Friday, July 30th, thus ending construction of Phase II of the restoration of the Morris Island Lighthouse.

Utilization of Micropiles at the Expansion of BMO Field, Toronto, Canada

Jim Bruce, P.Eng., Geo-Foundations Contractors Inc., jbruce@geo-foundations.com,
Naresh Gurpersaud, M.A.Sc., P. Eng., Geo-Foundations Contractors Inc., (519) 853-3216, ngurpersaud@geo-foundations.com
Anojan Sivaloganathan, Geo-Foundations Contractors Inc., (519) 853-3216, asiva@geo-foundations.com
Daniel R. MacLean, P.Eng., Geo-Foundations Contractors Inc., (519) 853-3216, dmaclean@geo-foundations.com

ABSTRACT

BMO Field is an outdoor stadium located on the shores of Lake Ontario in Toronto, Canada. It was opened in 2007. The venue was originally constructed for the Major League Soccer franchise, *Toronto FC*, but was expanded starting in 2014 to accommodate the Canadian Football League's *Toronto Argonauts* in time for the kickoff to the 2016 season. From 2014 to 2016, a $120 million (CAD) renovation project was completed that included an 8,400-seat expansion, significant upgrades to the hospitality zones, and twin canopies that will keep most of the spectators under cover. The west canopy is founded on micropiles.

The micropiling portion of the project consisted of the installation of 46 piles, with factored tension/compression loading as high as 3000 kN /4000 kN per micropile, all for support of new pile cap and grade beam foundations for the west canopy. Alignments range from vertical to 1:4 batters. Sizing and selection of micropile central reinforcement at this project was governed by EA as stipulated by the structural engineer, EA_{min}. This aspect, combined with the particularly deep rock sockets driven by the high magnitude uplift forces, led to a unique opportunity to forego full scale load testing.

Micropiles were selected for this project due to severely restricted access at the west canopy column bases' locations. The stadium's existing infrastructure includes a state of the art *SubAir* system consisting of boilers and piping previously installed at the cost of several millions of dollars. The system heats (and, when necessary, drains) the soil below the playing surface, keeping the natural grass field healthy and happy regardless of the season or the weather. Selected portions of this system would have had to be demolished to accommodate conventional deep foundations, whereas the micropiles were able to be constructed from inside an existing utility closet with no modification to any aspect of the existing *SubAir* system infrastructure.

This paper provides a detailed case history of this project, looking at the design of the micropiles, their installation and the QA/QC measures utilized.

1.0 INTRODUCTION

For a six week period at the end of 2016, the national and international professional sports spotlight shone very brightly on Toronto's newly refurbished BMO Field, beginning with the Grey Cup Championship game (Canada's equivalent to the SuperBowl) in November, then the Major League Soccer MLS Cup final (broadcast in 70 countries), and finally the NHL Centennial Classic outdoor ice hockey game on New Year's Day 2017. For those of us involved in designing and constructing the refurbishments, the stadium could not have looked better. The centerpiece of the 120 million dollar (CAD) project was the new twin canopy set that provides cover to the east and west grandstands at the 36,000 capacity stadium. While construction of foundations for the east

grandstand was straightforward – large-diameter drilled shafts bearing on rock approximately 6 metres below existing grade – design and construction of foundations for the west canopy was considerably more involved, primarily due to the presence of an existing, multi-million dollar *SubAir* system crowding the footprint of the new foundations. Incorporation of highly loaded (in both tension and compression) micropiles into the foundation design for the west canopy made foundation construction not only possible, but also both safe and efficient.

Also known as the Canadian National Soccer Stadium, BMO Field is located at Exhibition Place on the north shore of Lake Ontario in downtown Toronto, Canada. The stadium is home to Canada's National Soccer Team, as well as MLS franchise, Toronto FC and most recently the Canadian Football League's Toronto Argonauts. In 2014, a major renovation project was undertaken at BMO Field to increase the seating capacity by 8,400 seats and construct canopies to cover the grandstands. The expansion also included changes to allow for the use of the facility by a CFL team.

A key feature of the improvements at BMO Field was the construction of twin canopies that will span the entirety of each of the east and west grandstands. Each of the new canopies is supported by "super columns". While the east canopy super columns are supported on large diameter drilled shafts (typically referred to in Toronto as caissons) the west canopy super columns are supported by foundations comprised of micropile-supported pile caps and grade beams constructed within existing indoor spaces. The west canopy micropiles are capable of resisting substantial uplift, compressive and lateral forces, and are socketed several metres into shale bedrock. Figure 1 shows the BMO field renovations in progress looking north.

The micropiling scope at BMO Field consisted of installation of 46 piles, with factored loading ranging from 3000 kN in tension to 4000 kN in compression per micropile. Alignments range from vertical to 1:4 batters. The configuration of each pile is comprised of a permanent casing embedded 0.300 m into bedrock, and bundled bar central reinforcing that extends the full depth of pile into a 4 metre to 9 metre long rock socket. The micropile design on this project was governed by EA_{min}, as stipulated on a pile by pile basis by the structural engineer. This aspect of the design, combined with the fact that the rock socket depths were designed to be particularly deep in consideration of ensuring adequate embedment to mobilize sufficient bedrock mass during factored uplift loading, enabled the micropile designer to offer considerable savings to the owner by foregoing full scale load testing.

Micropiles were selected for this project due to access restrictions at the locations of the west canopy foundations and the presence of a state of the art *SubAir* system that heats and/or drains the soil below the playing surface. Selected portions of this multi-million dollar system would have had to be demolished to accommodate conventional piling rigs, whereas micropiling drill rigs could access the pile locations via utility closets with no alterations required to any component of the existing system.



FIGURE 1: BMO FIELD RENOVATIONS IN PROGRESS, LOOKING NORTH

2.0 PROJECT SETTING

Access restrictions from existing floor plans, low headroom and multiple buried services (Fig. 2) resulted in major foundation constructability challenges. In order to avoid the buried services, the pile cap excavations were completed prior to micropile installation, using an engineered excavation support system consisting of micropile soldier piles and hardwood lagging. The shoring allowed seamless relocation of underground utility services away from the trajectory of micropiles and expedited the construction of pile caps and grade beams, an important step in achieving the schedule goals of the general contractor, PCL Constructors Canada Inc. The shoring system in the mechanical room [Area A] and the delivery/storage room [Area C] comprised of 140 mm diameter drilled pipe soldier piles, welded tee sections, 75 mm thick lagging boards, walers and struts. At the hallway [Area B], the shoring system consisted of a trench box which was created by interlocking 150 mm thick timbers and steel angles as corner supports.

The piles were installed in three main work areas, designated Areas A, B and C (Fig. 2), each with its own unique combination of lateral and headroom restrictions. An excavation support system was installed at Areas A & C prior to pile installation to allow for relocation of existing buried services (Fig. 5) prior to drilling. Installation of a steel piling template and suspended steel plate platforms was carried out to facilitate high precision construction of the piles and enable the safe construction of the pile caps. All piles in Areas A and C were installed from temporary suspended platforms with top-of-plate elevation coincident with finished floor grade, covering the supported temporary excavation footprint and steel pipe templates with robust steel plating capable of safely supporting the load of the electric-over-hydraulic crawler drill rig.

In order to address the requirement for high precision layout (i.e., exacting tolerances with respect to pile locations in plan and pile batter), steel pipe templates were installed inside the excavation support system. After the steel templates were installed 2.13 metres below grade, a mudslab was

poured to secure the assembly in place during drilling. Road plates were used to cover the excavation and provide a working platform for the drill rig. All micropiles were constructed with the aid of the templates.

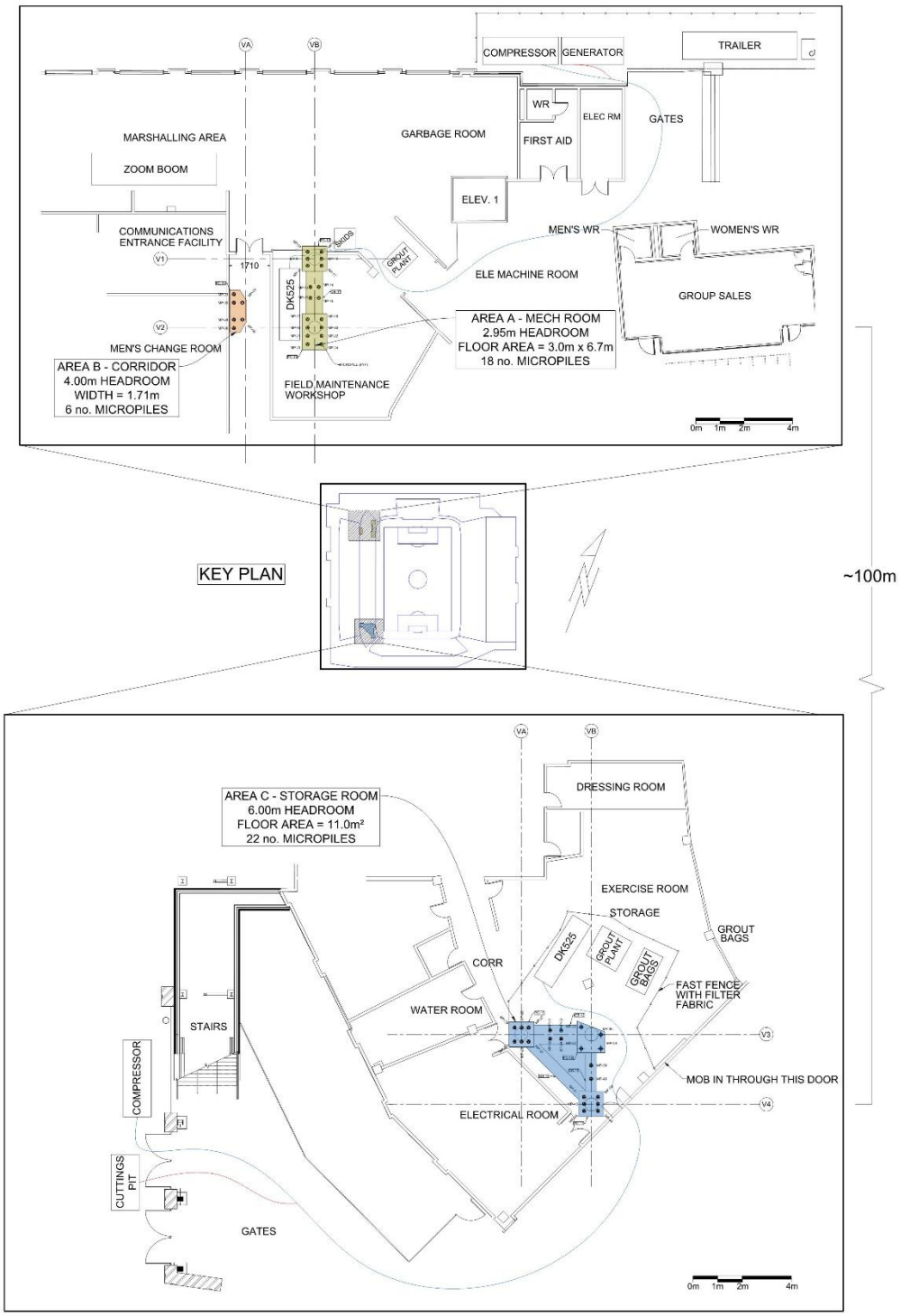


FIGURE 2: MICROPILE WORK AREAS

The mechanical room [Area A] presented the most challenging combination of above-grade working conditions, where the available headroom was only 2.95 metres. Setting up over each pile location was challenging due to crowding from highly sensitive mechanical equipment and piping. A total of 18 no. micropiles were constructed in Area A. Extra emphasis was placed on safety since only one access route was available to the small footprint (3.0 m x 6.7 m) work zone. This also created restrictions in terms of maneuverability.

In total, 6 micropiles were constructed in a 1.7-metre-wide hallway [Area B], which was only accessible via a 2.0 m high x 1.5 m wide doorway. This narrow hallway required extra consideration during drilling as it was within close proximity to a shallow-founded shear wall – the lateral offset was only 400 mm. The working grade was sloped at 6% with available headroom of just 4 metres. The maximum load carrying micropile in Area B was designed to resist 3000 kN (ULS) axial tension, 2690 kN (ULS) axial compression with a minimum stipulated EA, EA_{min} of 1080 MN.

In Area C, 22 no. micropiles were constructed in headroom of 6.0 metres. These micropiles were the largest load carrying piles installed, with 1925 kN (ULS) axial tension, 3975 kN (ULS) axial compression and requiring an EA exceeding 1420 MN. Workers had to avoid making excessive noise, as offices were located near this area. MLS games were also in session every other weekend, so cleanliness of the working area and clear delineation of the hoarded area and its hazards was especially important in order to adequately protect both the public from the construction hazards and the micropiling equipment from the public.

3.0 SUBSURFACE CONDITIONS

The proposed micropile locations were covered by existing concrete slabs-on-grade overlying fill soils as thick as 1.5 metres. Fill at this site is comprised of cohesionless sand and gravel, or crushed stone aggregate in some areas.

Clayey silt till is present below the fill layer. The clayey silt till found at the site is predominantly of very stiff to hard consistency with SPT ‘N’ values ranging from 25 to 90. There are lenses of wet sand and gravel present in deeper levels of the till deposits.

Glacial till is underlain by bedrock of the Georgian Bay Formation comprising of laminated to thinly bedded grey shale. The depth to bedrock ranges from 4.6 to 7.6 metres below existing grade. The bedding of the Georgian Bay Formation is typically flat lying with the upper 1 to 2 metres comprised of weathered shale. All micropiles were socketed in sound rock.

The approximate depth to the groundwater table is 1.5 metres below existing grade but the clayey silt till generally prevents the migration of water. Figure 3 shows a typical profile of the subsurface conditions at the BMO Field site.

No particularly corrosive soils were identified in the project geotechnical investigation.

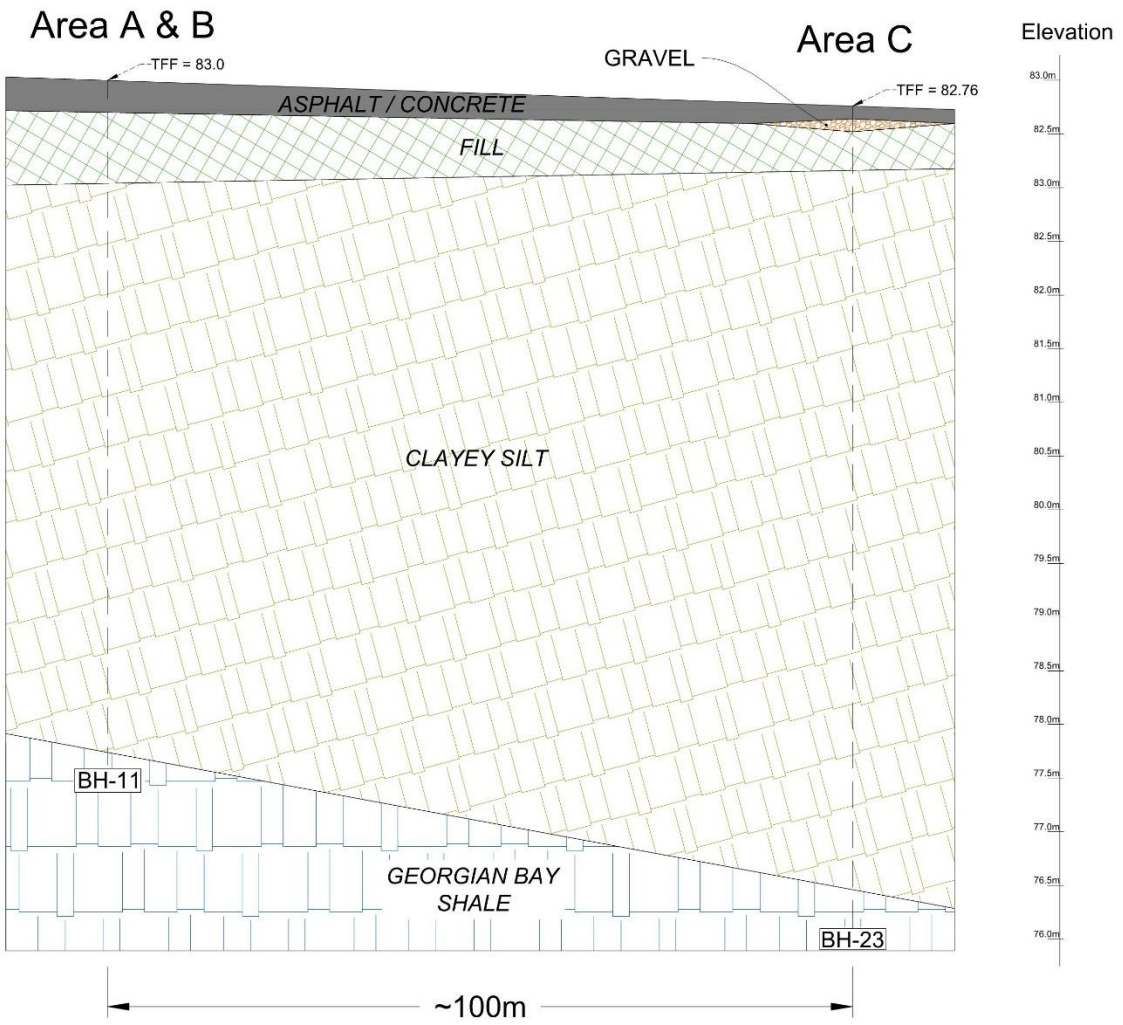


FIGURE 3: SUBSURFACE PROFILE

4.0 MICROPILE DESIGN CONSIDERATIONS

Detailed micropile design was completed in accordance with the USFHWA Micropile Design and Construction Guideline (Publication no. FHWA SA 97-070), June 2000, using Load Resistance Factored Design (LRFD) Method. Each micropile features a permanent casing embedded a minimum of 0.3 m into bedrock to stabilize the drilled hole, and bundled-bar central reinforcing that extends the full depth of pile into a rock socket 4 to 9 metres deep in sound shale bedrock. The small footprint of Areas A, B, and C (Fig. 2) imposed strict limitations on the space available for the footprints of the new pile caps and grade beams, which in turn limited the quantity of micropiles, driving the need for micropiles capable of individually resisting particularly significant loads. Consequently, high capacity micropiles with the ability to withstand factored loads per micropile as high as 3000 kN in axial tension and 4000 kN in axial compression were required. In light of this particularly high loading, the structural engineer stipulated, on a pile by pile basis, an EA_{min} for each micropile, ranging from 780 MN to 1420 MN.

4.1 Micropile Structural Design

The stipulated minimum individual pile EA necessitated (relative to what would be required if strength alone governed) a relatively large cross sectional area of steel per micropile, and this aspect motivated the selection of a multiple-bar central reinforcement arrangement to enable ease of installation within the close quarters of the mechanical closet in which the micropile construction was staged. As a conservative measure the EA of the casing and grout was ignored in the calculation. As can be seen in Table 1, three different bundled bar arrangements were employed to meet or exceed, on a pile type by pile type basis, the stipulated loads and minimum EA. Pile Type 1 reinforcement consists of a 2 - #18 bar bundle; Pile Type 2 reinforcement consists of a 3 - #18 bar bundle. Pile Type 3 reinforcement consists of a 3 - #20 bar bundle.

In conformance with ASTM A615, the minimum cross sectional area of each #18 bar is reported by the manufacturer, Williams Form Hardware, as 2581mm^2; similarly, the cross-sectional area of steel of a single #20 bar is 3168mm^2. As can be seen in Table 1, stipulated minimum EA ranged from 770 MN to 1420 MN. For the lightest loaded and least stiff pile type (Type 1 @ P_t = 2000kN; EA_{min} = 770 MN) , a 2 - #18 bar bundle was used. For the highest loaded and most stiff pile type (Type 3 @ P_c = 3995kN; EA_{min} = 1480 MN) a 3 - #20 bar bundle was used.

Employing the calculation for stipulated EA: cross sectional area, **A** multiplied by Young's modulus, **E**, the actual stipulated EA of the most lightly reinforced micropile Type (designated BMO Type 1) is 2 x 2581mm^2 x 200000 MPa =1032 MN. The majority of the micropiles on the project are comprised of 3 - #18 bar bundles, for which a minimum EA of 1080 MN per pile was required and an EA_0 of 1548 MN per pile was constructed. The most demanding EA requirement at four micropile locations in Area C required a EA_{min} of 1420 MN, and for this case, a 3 - #20 bundle was used to deliver a constructed pile EA_0 of 3 x 3168mm^2 x 200000 MPa =1900 MN. In order to house the 3 - #20 bars, a larger diameter casing was warranted; the casing at these piles was upsized from 245 mm to 273 mm diameter. After upsizing the bar sizes sufficiently to satisfy the stipulated minimum EA requirements, the axial strength requirements were already easily satisfied, including the governing (with respect to strength) section immediately below the tip of the casing. A 100 year assumed service life was used for the design of the micropiles at this site by incorporating corrosion "protection" via consideration of a 1.6 mm sacrificial outer shell (per USFHWA Chapter 5 / Table 5.14.3.3 prescription) at each of the bundled bars that make up the central reinforcement over the full depth of pile. All central threaded bars extend from the bottom of the rock socket, through the casing, into the pile cap, and project above the top bearing plates a sufficient distance (Fig. 7) to enable positioning and engagement of the top plates by a set of upper hex nuts (1 upper nut per bar).

Consideration of sacrificial steel as a means of providing corrosion "protection" is the authors' career-long preference for the mandatory designing against losses resulting from corrosion of the principal micropile reinforcement. In stark contrast to corrosion protection via encapsulation, the area of steel reinforcement is significantly greater for sacrificial steel-based designs on an

equivalent strength basis and, consequently, sacrificial steel based designs should outperform equivalently strong encapsulated designs for the first 100 years after their respective installations.

Sacrificial steel was the method used for the BMO Field micropiles, and it was imperative that the stipulated minimum EA must be satisfied for the 100-year condition because, presumably, if the performance of the super columns relies on micropile EA as stipulated at time = 0, performance of the super column foundations at time = 100 years must surely also rely on pile EA at time = 100 years. Table 1 lists the EA_0 and EA_{100} for each pile type. Note that EA_{100} exceeds EA_{min} for all pile types.

The micropile design called for 30 MPa neat cement grout using Type GU (USA Type 1) cement mixed in a high-shear colloidal mixer at maximum 0.45 water-to-cement and a minimum specific gravity of 1.85 g/cm^3.

Drilling of individual micropile holes was completed in two stages: advancement of the thick-walled permanent casing to sound rock using concentric, percussive duplex drilling technique, followed by drilling of the rock socket using down-the-hole percussion with air-and-water flush. The casing acted as a protective conduit from surface to bedrock and helped stabilize the borehole and was left in place to make a more robust compression-resisting and bending-resisting installation.

TABLE 1: SUMMARY OF MICROPILE DESIGN CHARACTERISTICS

Bundle	Area of Steel, A_0 (catalogue) (mm^2)	100 Year Area of Steel, A_{100} (mm^2)	EA_0 (MN)	EA_{100} (MN)	EA_{min} as Stipulated by Structural Engineer (MN)	Factored Compression Load as Stipulated by Structural Engineer (kN)	Factored Tension Load as Stipulated by Structural Engineer (kN)
3 - #20 bars	9504	8709	1900	1741	1420	3995	1925
3 - #18 bars	7743	6819	1548	1363	1080	2690	3000
2 - #18 bars	5162	4546	1032	909	770	980	1190

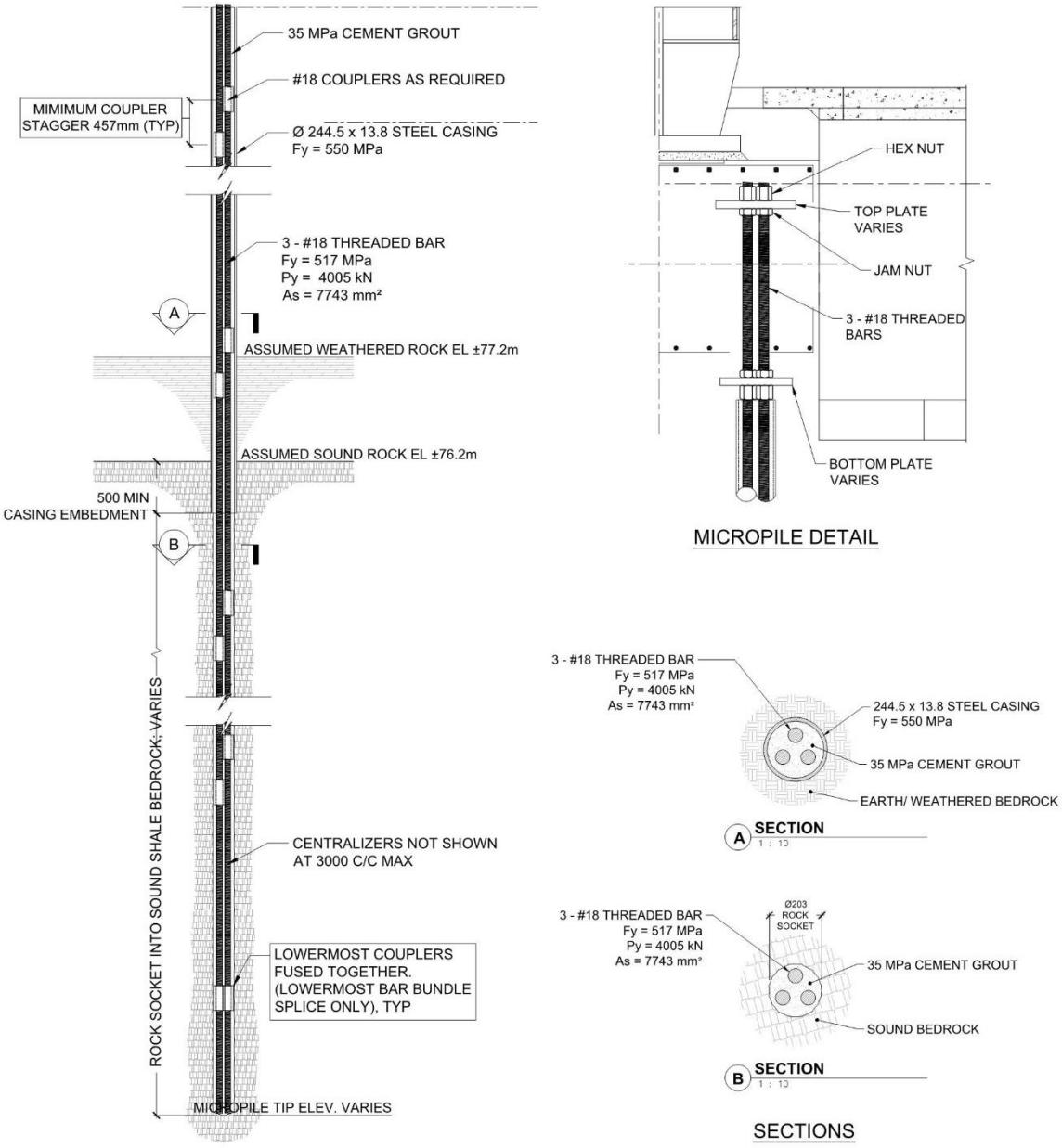


FIGURE 4: TYPICAL MICROPILE FOR A MINIMUM EA OF 1080 MN

4.2 Micropile Geotechnical Design

Recognizing the potential value to the project in terms of significant cost savings, schedule optimization and health and safety risk mitigation, the micropile designer/constructor, Geo-Foundations, tabled a proposal whereby the dozens of past high-magnitude static compressive load tests performed at other, representatively constructed micropiles socketed in the Georgian Bay shale and constructed by Geo-Foundations (Bruce & Gurpersaud, 2012),could be taken as proxy for the present project, thereby eliminating costly, potentially hazardous pile load testing. This approach was accepted by the structural and geotechnical consultants based on their

collective knowledge of micropile utilization in Ontario and their careful study of the detailed past test results.

Without even considering the strength of the medium into which it is bonded, the geotechnical capacity of any micropile depends as much on the workmanship employed as on the drilling and grouting methods selected for its construction. In other words, a micropile's capacity is, much more so than other, large diameter drilled foundation technologies, very process-sensitive. This sensitivity extends to the actual geotechnical properties of the ground into which load is transferred via grout-to-ground bond stress. Before any micropile designer can possibly consider foregoing load testing to verify design assumptions, he/she must be assured that the assumed design properties are certain to be realized at all constructed micropiles. This was a reasonable supposition applicable to the BMO Field project. Numerous load tests have been performed at various past projects constructed by Geo-Foundations, on micropiles socketed in Georgian Bay shale, and every one of these tests has proved, unequivocally, that micropiles socketed in Georgian Bay shale using percussive drilling with air and water flush and grouted using 35 MPa grout delivered via Type A grouting can safely and reasonably be designed using an assumed ultimate grout-to-rock bond stress value of 1750 kPa. This value was used for the BMO Field micropile design without confirmation via load testing.

As one last concession to foregoing load testing at this project, the grouting procedure was upgraded to Type B (per USFHWA designation) with the certain knowledge that Type B grouting should perform as well as, and likely better than, the Type A grouting that was employed at the load tested piles taken as proxy for BMO Field pile load testing. All piles were pressure grouted through the top of the casing following successful completion of tremie grouting.

With the permanent casing being terminated 0.3 metres into sound rock, all potential load transfer over the length of cased pile embedded in the overburden and weathered rock above the top of the rock socket was, appropriately, ignored. This approach was adopted despite all piles being grouted via Type B grouting.

5.0 MICROPILE CONSTRUCTION

The super columns for the east canopy were installed in open areas (and on grade) which allowed for the relatively simple and straightforward installation of large diameter caissons. However, micropile construction was the only viable option for the west canopy given the need to locate its pile cap/ grade beam inside the restricted access and low headroom of an existing mechanical closet. The added benefits of utilizing micropiles included a relatively quiet installation and small footprint operation, allowing all nearby amenities to perform uninterrupted.

Permanent casing was installed from grade into sound rock using a rotary percussive concentric duplex drilling system. Subsequently, the rock socket was installed and the drill string was extracted once the casing wall and rock socket were cleaned with jets of compressed air and water.

Each micropile had a unique bar arrangement, predicated on its unique frequency of bar splices resulting from its combination of available overhead clearance and load resisting requirements. The central reinforcement at every pile consisted of a bundled threaded bar arrangement, extending from the bottom of the rock socket, through the casing, into the pile cap, and above its

eventual cutoff elevation. These bars were installed using a staggered layering of splice locations as follows: (a) the starting assembly included equal bar lengths, (b) the second layer consisted of 2.1, 2.6 and 3.0 metre long bars to create a staggered effect, (c) all subsequent layers included bars of equal lengths, which continued the staggered layering effect, and (d) the last layer included the same length bars as the second layer so that all bars ended at the same elevation. The staggered layering approach was implemented as a means of avoiding weak (with respect to bending) cross-sections.



FIGURE 5: RELOCATED UNDERGROUND SERVICES & DRILLING TEMPLATE

In order to improve the micropile detailing (a.k.a. finishing) operation, a “finder” type spacer was placed above the last coupler and the portions of bars extending into the pile cap were greased. The spacer guaranteed the correct centre-to-centre distance of the portions of the threaded bars projecting above the underside of pile cap so that the nuts could be placed without interference from one another; the grease prevented adhesion between the central threaded bars and grout body so that the nuts could be affixed without great effort (such as what is experienced when attempting to turn a hex nut onto grout-fouled threaded bar). Each micropile was then tremie grouted, and once the casing was full, the grout was pressurized by injecting additional grout under pressure through the top of the casing (USFHWA Type B grouting). The micropile detailing work included removing the casing and grout above the cut-off elevation, and installation of the top and bottom bearing plates (Fig. 7).

An electric-hydraulic drill rig on a crawler base, using a remotely located generator and compressor, was used in Areas A and B due to limited available space. The pneumatic-powered grout plant, featuring a high-shear colloidal mixer with a mechanical agitator hopper, was placed

adjacent to both of these work areas. A diesel-powered drill rig with a telescopic drill mast was used in Area C.



FIGURE 6: MICROPILE DRILLING IN AREA A

6.0 QUALITY CONTROL / QUALITY ASSURANCE

Specific gravity testing of the grout was conducted at least once for each micropile. Testing was completed in accordance with the method described in API Recommended Practice 13B-1 with a calibrated *Baroid* Mud Balance. Also, two sets of cubes were taken per micropile for unconfined compressive strength (UCS) testing. Actual cube test break results ranged from 41 to 92 MPa.

Comprehensive real time quality control was performed by a full time designate of the micropile engineer of record using a 64-point *Inspection and Testing Protocol* (ITP), which consisted of multiple *Hold, Measure & Record, Witness, Verify and Review* points (see attached Appendix). A record of piling summarizing construction dates, rock socket lengths, grout quantities consumed, casing and threaded bar schedules including casing and threadbar splice locations, cut-off elevations, along with remarks, was completed for each micropile. This comprehensive approach to inspection and testing resulted in the filing of 12 non-conformance reports, each of which was deemed minor and was reviewed in detail before ultimately being accepted and signed off by the micropile engineer. At the conclusion of the project, the micropile engineer penned a letter to the

structural engineer testifying to the completeness of the micropile scope of work and the fitness of the micropiles to perform as intended.

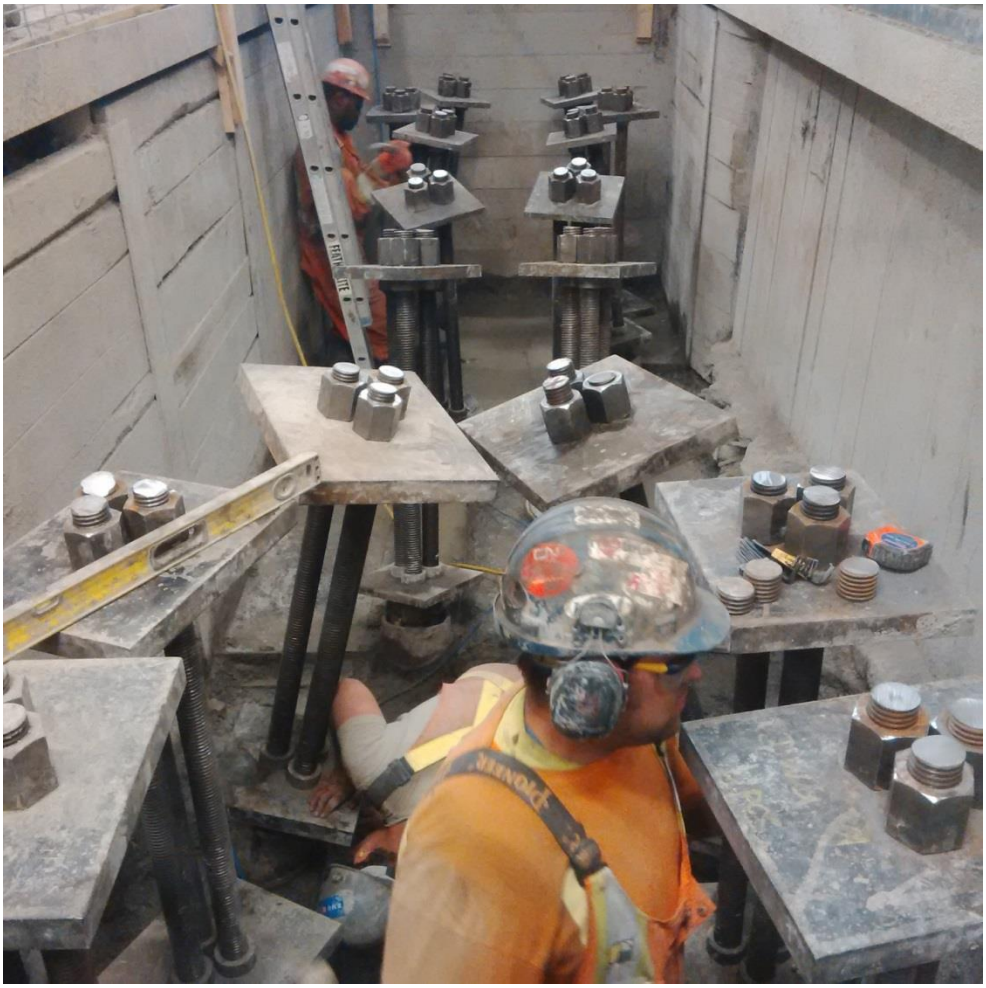


FIGURE 7: DETAILED MICROPILES IN AREA A

7.0 DISCUSSION

No micropile load tests were conducted at BMO Field. The authors wish to make very clear that this paper does not advocate for the elimination of load testing from micropile projects. Micropile performance will always be, much more so than in the case of conventional foundation technologies, closely aligned to the drilling and grouting methodology and workmanship employed in their construction, and load testing of representatively constructed, sacrificial, pre-production micropiles ought to be an integral component of every micropile design. It is most important, in the case of BMO Field, to recognize that, in a sense, load testing WAS conducted, because the load tests considered from other sites and taken as proxy for BMO Field load testing, were representative of the proposed BMO Field design in every aspect: magnitude of loading, drilling method, key construction personnel involved, and rock socket geology. The micropiles constructed at BMO Field represent a rare case where engineering judgement (closely aligned

with the specific experience) of a seasoned designer/practitioner stood as a reasonable alternative to full scale load testing, especially when considering the health and safety risks avoided. The decision to forego micropile load testing at BMO Field was both well informed, and not taken lightly.

The early involvement of the specialty design-build micropile contractor on this project provided significant cost savings to the Owner. In the past, Geo-Foundations has conducted numerous load tests on micropiles rock-socketed into Georgian Bay Formation shale (Bruce & Gurpersaud, 2011 & 2012). The value-engineering proposal to forego load testing was based on the contractor's extensive applicable local experience, and acceptance of this proposed approach by the owner's principal consultants enabled the reasonable elimination of a costly pre-production static compression load test on a sacrificial micropile.

Design of the micropiles was well coordinated with the project design team which included the owner's Structural and Geotechnical consultants. The EA_{100} of the piles was the governing structural requirement, and close communication between the structural engineer and micropile engineer identified, early in the collaborative process, the importance of stipulated, EA_{min} to foundation performance. The close interaction with the Owner's team also allowed for pile arrangement design optimization within tight quarters.

Time was of the essence on this project, with important project milestones predicated on micropile scope completion in a timely matter. Optimization was achieved by incorporating the design and installation of the excavation support system within the speciality micropile contractor's scope of work.

The geotechnical reports indicated the presence of numerous historic, abandoned foundations potentially present in the subsurface profile at this site. Micropiles constructed using percussive duplex drilling method significantly enhanced the contractor's ability to construct the micropiles at this site through any and all buried obstructions encountered.

An electric powered drill rig was used in Areas A and B to maintain the air quality in that work space. The drill rig was selected for this project based on the available clearances, environmental and safety concerns. The drilling operation was carried out using a low-energy process in order to avoid any impact on existing adjacent services, as well as preserving harmony with respect to the ongoing operations at the facility.

8.0 CONCLUSIONS

Micropiles were successfully installed under restricted access conditions to support significant loads from canopy-supporting super columns at BMO Field in Toronto. A significant amount of planning and input by a specialty foundation trade contractor accelerated the construction schedule, satisfied the design requirements and mitigated potential risks associated with existing buried and above-grade infrastructure. The design-build approach to the micropile scope, including early contractor involvement and including the support of excavation required to enable construction of new pile caps, provided numerous benefits and cost savings to the owner, as well as ensuring that all important and possibly obscure performance requirements were addressed

prior to construction. This collaborative approach significantly improved the project's chances of avoiding surprises/setbacks during the construction phase.

All micropiles were installed in a safe manner with a high level of quality control at the BMO Field site. The design bases, construction sequence and installation methods employed were integral to the successful execution of the micropile scope of work.

9.0 ACKNOWLEDGEMENTS

Jim Bruce, P. Eng., of Geo-Foundations was the designer for the micropiles. Entuitive, Inc. were the owner's structural engineer; Terraprobe Inc. were the owner's geotechnical engineer.

The authors wish to thank PCL Constructors Canada Inc. for their usual excellent job of procurement and delivery, in all respects, of this special project. Thanks also are due the micropile construction superintendent, drill rig operators, grout plant operators, labourers, field engineers and CAD technicians from Geo-Foundations Contractors Inc. who contributed to the safe and successful delivery of the BMO Field Micropile Project.

10.0 REFERENCES

Bruce, J. and Gurpersaud, N., (2011). *Micropiles at the Transformation AGO Project*. Proceedings of the 36th Annual Conference on Deep Foundations, October 18-21, 2011, Boston, MA.

Bruce J., and Gurpersaud, N. (2012). *Evolution of high capacity micropiles in the Toronto Metropolitan Area*. Proceedings of the 65th Canadian Geotechnical Conference, Winnipeg, Manitoba, September 30 to October 3, 2012

Geotechnical Report (2014). *BMO Stadium Additions, Exhibition Place, Toronto, Ontario*. Report prepared by Terraprobe Inc., File No. 11-14-4035.

USFHWA (1997). *Micropile Design and Construction Guidelines – Implementation Manual.* Publication No. FHWA-SA-97-070.

APPENDIX

Inspection and Testing Protocol

220115 BMO FIELD EXPANSION - MICROPILES

MICROPILE INSTALLATION - INSPECTION AND TEST PLAN

Structure: Super column to support a Canopy		**Task:** Permanent Micropile Installation	
Micropile No. (Mark): MP02	**Date:** Mar 25, 2015 & 26	**Reference Drawings:** MP1, MP2, MP3, MP4	
Prepared by: Anojan Sivaloganathan		**Reference Specification:**	

No.	Quality Control Attributes	QC Point	QC Initial/Date	Comments
1	Ensure all drawings are the latest revision and stamped for Construction.	R	JY 3/25	construction drawings received on 24 Mar 2015
2	Verify material has been received and checked	V	JY 3/25	
3	Verify layout and location for drilling	H	JY 3/25.	using template, setup in place before drilling
4	Verify drill mast is plumb for vertical piles prior to drilling	V	JY 3/25	
5	Verify azimuth and batter of the drill mast for batter piles prior to drilling	V	N/A.	
6	Check casing assembly schedule for this micropile prior to casing installation	V	JY 3/25.	total casing length 27'
6a	Verify permanent casing joints are in full contact shoulder-to-shoulder at splice #1	V	JY 3/25.	
6b	Verify permanent casing joints are in full contact shoulder-to-shoulder at splice #2	V	JY 3/25.	
6c	Verify permanent casing joints are in full contact shoulder-to-shoulder at splice #3	V	JY 3/25.	
6d	Verify permanent casing joints are in full contact shoulder-to-shoulder at splice #4	V	JY 3/25	
6e	Verify permanent casing joints are in full contact shoulder-to-shoulder at splice #5	V	JY 3/25.	
6f	Verify permanent casing joints are in full contact shoulder-to-shoulder at splice #6	V	JY 3/25.	
7	Verify permanent casing is embedded in sound rock to minimum specified depth of 0.5m.	H	JY 3/25.	
9	Record date of casing installation, total casing length and geodetic elevation of casing tip.	M	JY 3/25.	total casing length 27' = 8.23 m plate RL = 83.60 top casing = 83.78 (no thread) TIP casing = 83.78 - 8.23 = 75.55
8	Verify rock socket length is greater than specified minimum length.	H	JY 3/26	measured depth = 17.15 (from plate RL) PILE bottom = 66.45
10	Confirm casing wall and rock socket are cleaned with jets of compressed air and water	V	JY 3/26	socket length = 75.55 - 66.45 = 9.1m > 9m
11	Verify tremie grout tube is secured to bottom of bar	V	JY 3/26.	
12	Check bar assembly schedule for this micropile prior to central bar bundle installation	V	JY 3/26	9.5' + 7' + 3x9' + 10' 9.5' + 8.5' + 3x9' + 8.5' 9.5' + 10' + 3x9' + 7'
12a(i)	Confirm full penetration of bottom bar into splice #1a	V	JY 3/26	
12a(ii)	Confirm full penetration of bottom bar into splice #1b	V	JY 3/26	

220115 BMO FIELD EXPANSION - MICROPILES

MICROPILE INSTALLATION - INSPECTION AND TEST PLAN

Structure: Super column to support a Canopy		**Task:** Permanent Micropile Installation
Micropile No. (Mark): MP 02.	**Date:** Mar 25, 26, 2015	**Reference Drawings:** MP1, MP2, MP3, MP4
Prepared by: Anojan Sivaloganathan		**Reference Specification:**

No.	Quality Control Attributes	QC Point	QC Initial/Date	Comments
12a(iii)	Confirm full penetration of bottom bar into splice #1c	V	JY 3/26	
12a(iv)	Confirm full penetration of top bar into splice #1a	V	JY 3/26	
12a(v)	Confirm full penetration of top bar into splice #1b	V	JY 3/26	
12a(vi)	Confirm full penetration of top bar into splice #1c	V	JY 3/26.	
12b(i)	Confirm full penetration of bottom bar into splice #2a	V	JY 3/26	
12b(ii)	Confirm full penetration of bottom bar into splice #2b	V	JY 3/26	
12b(iii)	Confirm full penetration of bottom bar into splice #2c	V	JY 3/26	
12b(iv)	Confirm full penetration of top bar into splice #2a	V	JY 3/26	
12b(v)	Confirm full penetration of top bar into splice #2b	V	JY 3/26	
12b(vi)	Confirm full penetration of top bar into splice #2c	V	JY 3/26	
12c(i)	Confirm full penetration of bottom bar into splice #3a	V	JY 3/26	
12c(ii)	Confirm full penetration of bottom bar into splice #3b	V	JY 3/26	
12c(iii)	Confirm full penetration of bottom bar into splice #3c	V	JY 3/26.	
12c(iv)	Confirm full penetration of top bar into splice #3a	V	JY 3/26	
12c(v)	Confirm full penetration of top bar into splice #3b	V	JY 3/26	
12c(vi)	Confirm full penetration of top bar into splice #3c	V	JY 3/26.	
12d(i)	Confirm full penetration of bottom bar into splice #4a	V	JY 3/26	
12d(ii)	Confirm full penetration of bottom bar into splice #4b	V	JY 3/26	
12d(iii)	Confirm full penetration of bottom bar into splice #4c	V	JY 3/26	
12d(iv)	Confirm full penetration of top bar into splice #4a	V	JY 3/26	
12d(v)	Confirm full penetration of top bar into splice #4b	V	JY 3/26	
12d(vi)	Confirm full penetration of top bar into splice #4c	V	JY 3/26	
12e(i)	Confirm full penetration of bottom bar into splice #5a	V	JY 3/26	
12e(ii)	Confirm full penetration of bottom bar into splice #5b	V	JY 3/26	

220115 BMO FIELD EXPANSION - MICROPILES

MICROPILE INSTALLATION - INSPECTION AND TEST PLAN

Structure: Super column to support a Canopy	**Task:** Permanent Micropile Installation	
Micropile No. (Mark): MP02	**Date:** Mar 25, 26, 2015	**Reference Drawings:** MP1, MP2, MP3, MP4
Prepared by: Anojan Sivaloganathan		**Reference Specification:**

No.	Quality Control Attributes	QC Point	QC Initial/Date	Comments
12e(iii)	Confirm full penetration of bottom bar into splice #5c	V	JY 3/26	
12e(iv)	Confirm full penetration of top bar into splice #5a	V	JY 3/26	
12e(v)	Confirm full penetration of top bar into splice #5b	V	JY 3/26	
12e(vi)	Confirm full penetration of top bar into splice #5c	V	JY 3/26.	
13	Ensure there are no couplers in the red zone	V	JY 3/26.	pile cutoff level = 83.6 − 0.45 − 1.6 + 0.1 = 81.65 top of 7' coupler = 80.82 < 81.65.
14	Confirm the finder is at the appropriate elevation	V	JY 3/26.	
15	Verify central bar bundle extends to bottom of the hole	H	JY 3/26.	top of bar about 0.8m below plate hole.
16	Verify central reinforcement extends above eventual cutoff elevation	H	JY 3/26	top of bar: 66.45 + 16.31 = 82.76. suggested bar cutoff 83.00 ∴ needs to be extended
17	Record total length of central reinforcement.	M	JY 3/26.	total length of bars = 53.5' = 16.31 m.
18	Confirm maximum centralizer spacing along threadbar does not exceed 10' c/c.	V	JY 3/26.	A.S
18a	Verify PVC centralizers are used for vertical piles	V	JY 3/26.	
18b	Verify steel centralizers are used for battered piles.	V	N/A	
19	Verify cement used for grouting is free of lumps	W	JY 3/26.	
20	Ensure grout has minimum s.g at grout plant of 1.85 g/cm^3	H	JY 3/26	SG = 1.91
21	Record specific gravity of sampled grout	M	JY 3/26.	
22	Ensure grout injection continues until efflux at top of casing has specific gravity ≥ 1.85 g/cm^3	H	[redacted] 3/26.	measured by Anojan.
23	Record date of grouting and total tremie grout take	M	JY 3/26.	26 × 40 kg/bag = 1040 kg
24	Record volume of grout & pressure during type B grouting	M	JY 3/26.	2 × 40 kg/bag = 80 kg. 80 psi and top of casing lifted.
25	Verify six sample cubes are cast per micropile	V	JY 3/26	cubes done by consultant.
26	Verify micropiles left undisturbed a minimum 72 hours	V	JY 3/29	

Date of Work Complete: _____

S. [redacted]
Performer or Work Supervisor

Date of Record Complete: 3/29/2015

JY.
QC Inspector Initials

JUN YIN.
QC Inspector Name

Legend: **H** – Hold Point **W** – Witness Point **M** - Measure & Record **V** – Verification **R** – Review Documents

MICROPILES FOR COMBINED DEEP SLIP AND STRUCTURAL LOADING

Allan Herse CPEng, MIEAust, RPEQ, Lambert Ezaejugh PhD, CPEng, MIEAust, RPEQ
and
Kenneth Wilson BE Civil, MIEAust

ABSTRACT

The use of grouted injected micropiles in an A-Frame configuration as a solution to slope stability problems has been well documented in case studies around the globe. Typically, they consist of a series of downslope and upslope micropiles installed through the failure plane with the pile heads terminating in a concrete capping beam. Despite its wide usage across the world, its use in Queensland, Australia is limited. The Queensland Department of Transport and Main Roads (TMR), with over 33,353 kilometres of road network under its jurisdiction, has traditionally continued to use established methods such as soil nails and soldier piles in managing slip repairs on their network. However, following severe weather events in 2011 to 2013which resulted in multiple slip failures, micropiles were first introduced as temporal stabilising measure.

Since their introduction in 2011, TMR has subsequently allowed the use of micropiles as a permanent stabilising measure on a trial basis for the Gatton Clifton Road and Kin Kin Road slip repairs. The approval for their use followed a rigorous design / design review processes. It was intended that the performance of the remediated sites, which were instrumented and are currently being monitored by TMR, will form the basis for the acceptance or otherwise of the method as permanent stabilising measure on TMR road network.

This paper examines the use of hollow bar micropiles which have been used in an A-Frame arrangement to permanently remediate two deep slip failures at Gatton Clifton Road and Kin Kin Road in Queensland, Australia. At the Kin Kin Road slip, the micopile structure in addition to providing the stabilising action for a deep slip failure, also catered for the applied forces from a 1.5m retaining wall which facilitated a widening of the road.

1.0 BACKGROUND

Several seasons of severe wet weather in South East Queensland, Australia between 2011 and 2013 resulted in a large number of slope stability issues to various degrees within the Queensland road network (Hinds, 2015; Ezeajugh et al 2016). Much of the instability was found in the rural network on dual lane roads vital for the local communities for both their economic and social importance.

A range of measures within TMR's tool box for stabilising such slips include re-grading the failed slope to a stable batter geometry, the use of rockfill stabilising berms, gabion wall retention, soil nailing, geosynthetic reinforcement and the use of large diameter bored/ CFA piles. The bored piles are often installed on the road shoulder with a series of 750mm to 900mm diameter reinforced concrete bored shafts at centres of up to three pile diameters with the pile heads

[1] *Engineering Manager, Piling & Civil Australia aherse@pcacontracting.com.au*
[2] *Principal Geotechnical Engineer, Queensland Department of Transport and Main Roads Emeka.L.Ezaejugh@tmr.qld.gov.au*
[3] *Design Engineer, Piling & Civil Australia kwilson@pcacontracting.com.au*

terminating in a continuous concrete capping beam. Installation of these types of structures usually requires piling rigs weighing over 40 tonnes along with other associated machinery and equipment that requires a full road closure during construction.

The full closure of these roads in rural areas is often controversial and extremely inconvenient for the local community. Quite often, there is also the significant expense of carrying out temporary works to support the large piling rigs and supporting equipment.

In 2011, several slips were identified in the hinterland areas of Peachester and Maleny in South East Queensland. Temporary emergency works were required to support a number of slips with TMR seeking new and innovative solutions that were quick to install with minimal impact on the local communities. As a result, several sites were stabilised using micropile A-Frame structures with equipment that could work within the confines of a single lane of traffic such that the road could remain open.

Since 2011, several other sites have been stabilised using micropile A-Frame structures for both permanent and temporary solutions following the design method published in the *FHWA NHI-05-039 Micropile Design and Construction* manual (FHWA NHI-05-039 December 2005). Where the micropile A-Frame arrangements were used as permanent stabilising measures, their approval for use were on the basis of a trial. As such they were instrumented and are currently being monitored by TMR. The two candidate sites where permanent A-Frame micropile stabilising structures were installed were the Gatton Clifton Road and Kin Kin Road slips. At the Kin Kin Road slip, in addition to stabilising the deep slip failure, the A-Frame micropiles were required to support the loads from a 1.5m high insitu concrete retaining wall cast directly onto the A-Frame capping beam.

The retaining wall on top of the capping beam introduced additional axial, shear and bending loads which are not covered by the FHWA design method. These applied forces required additional analysis highlighting some limitations in the assumptions made within the FHWA method particularly in relation to the function and geometry of the capping beam.

This paper will compare the design of two permanent A-Frame micropile structures and discuss various limitations of the FHWA design method. Particular focus will be on the design of the Kin Kin Road A-Frame structure and the additional steps and assumptions that had to be addressed due to the applied forces from the retaining wall stem above the capping beam.

2.0 DISCUSSION OF CURRENT A-FRAME DESIGN PRACTICES

The design approach for micropile A-Frame structures is well documented by the FHWA in chapter 6 of their micropile design guide released in December 2005. The design process follows twelve steps which involve modelling the slope, determining the additional shear resistance required to achieve an acceptable factor of safety, configuring the A Frame to provide this resistance e and determining the axial loads within the piles.

The resulting micropile A-Frame structure generally consists of two or more rows of downslope and upslope raking micropiles extending for a sufficient depth below the slip plane and terminating at ground level within a reinforced concrete capping beam. Figure 1 is an illustration from the FHWA design manual depicting the general cross section of a micropile A-Frame structure.

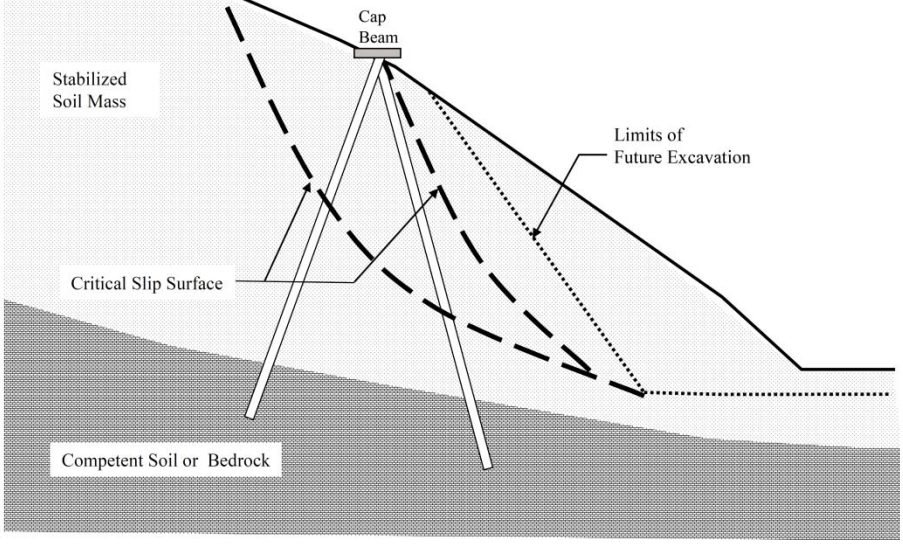


Figure # 1 FHWA depiction of general cross section of an A Frame micropile structure

The FHWA design procedure focuses on solving the geotechnical aspects of the slope stability problem. Although it gives some guidance on the potential size of the capping beam, its scope is limited to determining the required shear resistance to achieve a suitable factor of safety for a deep slip and leaves the structural design of the capping beam mostly up to the structural designer.

The assumption is that the maximum axial load is at the critical slip interface and the “axial loads transferred to the ground surface should be small” (FHWA NHI-05-039 December 2005). As such, the FHWA approach for the design of the capping beam only addresses differential settlements along the length of the capping beam from variations in the soil and for any anchor forces in the event that ground anchors are required.

As a consequence, once a solution for slope stability has been determined using the steps in the FHWA process, additional steps are required for any external applied forces to the structure.

It is interesting to note that section 6.7.10 of *FHWA NHI-05-039 December 2005* suggests a typical capping beam is in the order of 2m wide and 1m deep. However, the document is silent on the requirement for the A-Frame structure to consider either the self-weight of the capping beam to prevent surcharging the slope nor is there mention of potential lateral earth forces acting on the

capping beam. The function of the capping beam in the FHWA method is one of pile head fixity only.

As such, it may be prudent on some slopes, for the designer to check for the load case during construction when the concrete has not yet cured and is unsupported by the micropiles to ensure it does not cause localised instability. Particularly when using a capping beam in the order of magnitude suggested by FHWA.

A secondary check for completeness may also include the potential shear and overturning moment induced into the piles from the earth pressure acting on the upslope vertical edge particularly on relatively steep slopes or when external surcharge load from sources such as vehicles are relatively close to the capping beam.

For the majority of structures, the effects of earth pressure forces on the capping beam or the self-weight of the capping beam itself are small and insignificant, however, the designer should be mindful of the limitations of the FHWA design method and use their engineering judgement as to when external forces interacting with the capping beam or induced by the capping beam require additional design steps to be considered.

3.0 DESIGN CONSIDERATIONS FOR APPLIED FORCES TO THE CAPPING BEAM

The addition of external applied loads to the capping beam requires consideration of the geometry of the micropile to pile cap connection and pile layout to determine how the external forces are transferred into the micropiles and how these forces impact on the maximum load within each of the rows of micropiles.

3.1 Gatton Clifton Road

In late 2013 a site near the town of Gatton in the Darling Downs region west of Brisbane was rectified with an A-Frame positioned on the edge of the road near the crest of the slope. Figure 2 illustrates the location of the Gatton A-Frame directly beneath the metal crash barrier.



Figure 2 – Completed A Frame at Gatton

The FHWA design method was used for the design of the Gatton Clifton Road project. Due to the potential for localised erosion and minor downslope slips below the A-Frame, PLAXIS 2D was used to check for deflections for load cases involving the temporary loss of passive resistance below the structure resulting from future erosion or shallow slips within the downslope. Limits were set by the Queensland Transport and Main Roads Department (TMR) on the maximum allowable deflection for the structure for serviceability.

The PLAXIS 2D modelling introduced an additional step in the design process. The A-Frame was divided up into six different design sections with varying micropile layouts to adjust the stiffness of the structure in order to meet the deflection limits set by TMR. Figure 3 below illustrates the PLAXIS 2D model used on one of the critical design sections with a maximum calculated deflection of 132mm.

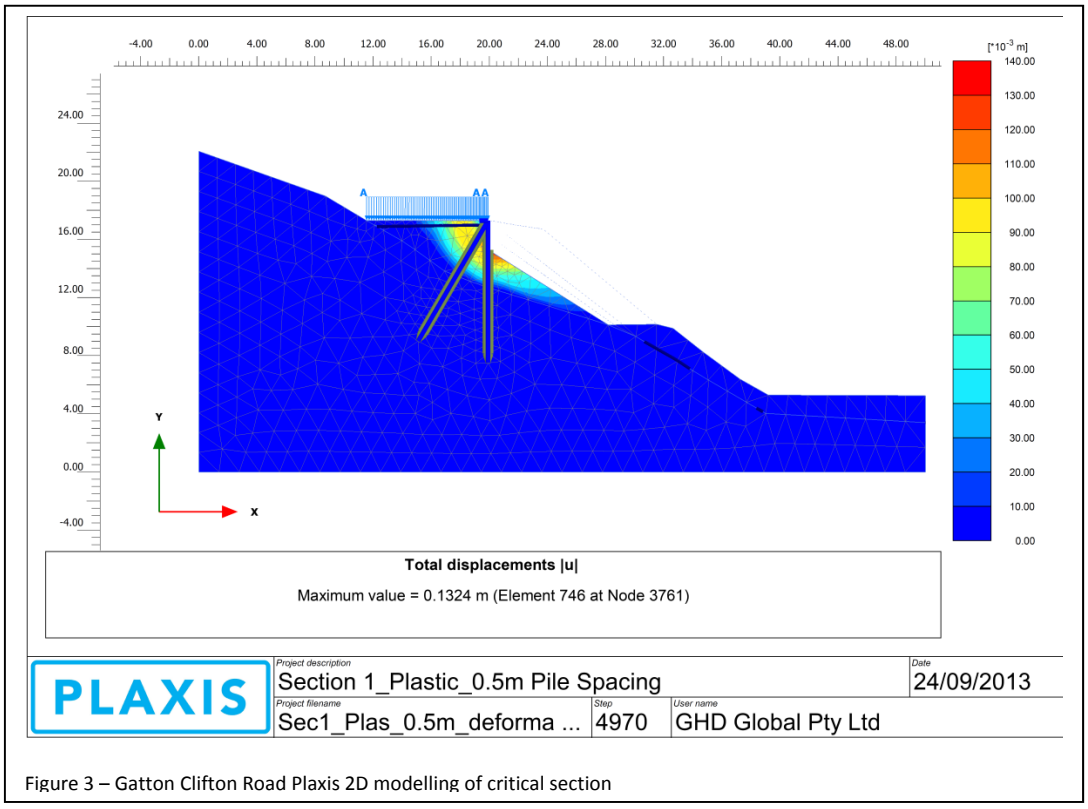


Figure 3 – Gatton Clifton Road Plaxis 2D modelling of critical section

The PLAXIS 2D modelling raised some interesting questions during the design process in relation to the geometry of the micropiles and their interaction with the capping beam which are not addressed in the FHWA design process.

The FHWA design process simply considers the capping beam as a way of pinning the pile heads together to form the A-Frame structure. Although this is a suitable assumption for the basis of the overall A-Frame design, by ignoring the contribution of the capping beam connection, the calculated deflections in the PLAXIS 2D modelling resulted in a much higher maximum deflection of 159mm as compared to the 132mm at the ultimate limit state in the final model which included some stiffness from the capping beam.

This difference in deflection for the two models was not critical for the Gatton Clifton Road project. The A-Frame structure was in place to solve the deep slip condition with the potential calculated deflections only being possible in the temporary condition caused by potential future erosion or slips in the downslope prior to remediation works being undertaken. However, it did highlight the importance of correctly modelling the capping beam and micropile connection on projects where load transference into the micropiles from applied loads on the capping beam is a permanent structural requirement. This will be discussed further in the following section relating to the A-Frame structure on Kin Kin Road.

3.2 Kin Kin Road

In early 2015, a site on Kin Kin Road in the Sunshine Coast Hinterland north of Brisbane, Australia received funding from the Queensland Government to rectify a potential deep slip which had developed tension cracks near the centreline of Kin Kin Road adjacent a local creek.

To reduce the risk of future downslope slips, the Kin Kin A-Frame was positioned beyond the crest of the slope at a level 2.5m below Kin Kin Road. As a means of widening the road corridor, a 1.5m high cast insitu reinforced concrete retaining wall was integrated into the capping beam. Figure 4 illustrates a typical cross section through the Kin Kin structure detailing the position of the A-Frame structure with the integrated concrete retaining wall.

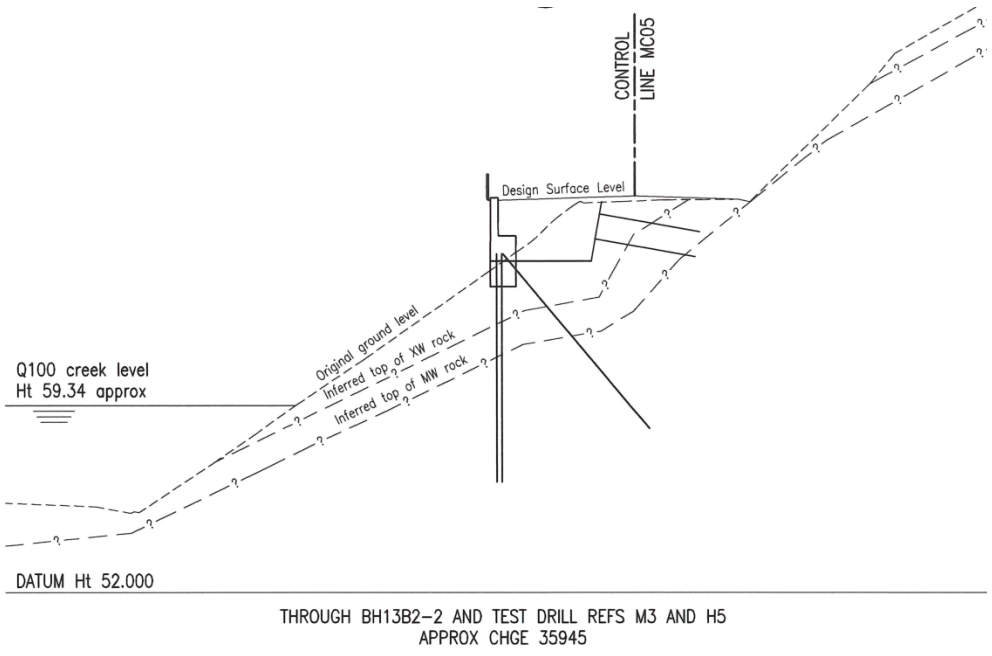


Figure 3 – Location of downslope Kin Kin A-Frame

The addition of the retaining wall to the capping beam required a unique design approach involving the following procedures;

1. **Step # 1 – Designing the A-Frame for Slope Stability**. This step involved the design of the A-Frame structure to stabilise the deep slip in accordance with the FHWA design method.
2. **Step # 2 – Designing the A-Frame piles to carry the applied load from the 1.5m high retaining wall.** This involved taking the horizontal shear at the base of the wall due to lateral earth pressure and the resulting overturning moment about the toe and including these forces in the A Frame micropile design.
3. **Step # 3 – Overall deflection check.** Using PLAXIS 2D to ensure the serviceability deflections were within required design limits.
4. **Step # 4 – Check pile forces for combined axial and bending.** Using PLAXIS 2D, pile forces were determined to enable a check for combined axial and bending for the serviceability load case.

Each of these steps are discussed in further detail below.

Step # 1 – Designing the A-Frame for Slope Stability

Following the procedures in the FHWA design procedure, it was determined that the slip circle failure plane was at a depth of 3.5m. This soil consisted of a layer of medium dense gravelly sand fill with lenses of firm to stiff sandy silt overlaying residual soil consisting of medium dense to dense sandy gravelly silt.

Ischebeck Titan 40/20 hollow bar micropiles with 90mm drill bits were selected for use in the project. Using proprietary effective skin friction values for the material above the slip, an ultimate pile load (P_{ult}) was calculated to be 164kN.

Slope W modelling was undertaken to determine the required shear resistance per lineal metre run of capping beam to provide an acceptable factor of safety, for both the extreme ground water condition and the normal ground water condition (1.3 and 1.5 respectively). It was determined that a shear contribution per pile of 105kN/lin.m of capping beam was required.

The battered pile group was modelled with the rear (upslope) micropiles raking back into the slope at 40 degrees from vertical while the front (downslope) row of micropiles remained vertical due to the fairly steep downslope batter. The micropile group was analysed for its shear capacity ($H_{ult\ pair}$ = 125kN) which resulted in a spacing of 600mm per pile group with a factor of safety for soil flow of 3.2.

Step # 2 – Designing the A-Frame piles to carry the applied load from the 1.5m high retaining wall.

The applied loads on the capping beam of the A-Frame from the 1.5m high retaining wall were calculated to produce the following design actions;

M^*_{ot} = 59kNm/m

$V^*_{sliding}$ = 71kN/m

To resolve these forces into the micropiles, the distance between point of entry of the hollow bar micropiles into the underside of the capping beam was deemed to be the moment arm for the purposes of calculating the reactions required to resist the applied moment.

As such, a distance of 500mm between the front and rear rows of micropiles resulted in pile forces of 71kN per pile of compression for the front row of micropiles and 137kN per pile of tension for the rear row of micropiles.

To determine the maximum pile force, an approach was taken which assumed the full structural load is transferred through the 3.5m deep slip plane to be developed within the bonded length below the slip plane. As such, a maximum pile force was calculated as 301kN per micropile by adding the maximum applied tensile force (137kN) to the P_{ult} value of 164kN per pile from the FHWA modelling.

It could be argued that since the micropiles were not de-bonded through the upper 3.5m of soil that some pile load would be distributed above the slip plane. However, an assumption was made in the event of an active slip, the full applied load from the retaining wall above the capping beam would need to be developed within the bond zone below the slip plane.

The combination of load for both geotechnical and structural forces within the pile group using static analysis is believed to be much more complex than simply adding the two maximum forces together. This is because at the point of maximum geotechnical load, the ultimate geotechnical force in the pile requires the soil to move along the length of the pile. As it does so, the forces acting on the retaining wall are changing as the structure begins to deflect.

As such, further modelling was conducted to check how the structure would deflect through finite element modelling (FEM) using PLAXIS 2D. FEM was also used to check the pile forces during the serviceability load condition.

Step # 3 – Overall deflection check

The first of two FEM checks was to determine serviceability and ultimate deflections of the A-Frame and retaining wall. Similar to the Gatton Clifton Road project, the A-Frame structure was required to meet deflection criteria for the ultimate load case which included temporary loss of passive pressure on the downslope from erosion or future downslope slip.

Initially, the structure was modelled assuming;

a) A Mohr-Coulomb model for soil and rocks
b) The micropiles and capping beam were modelled as plate elements
c) The micropile intercept was coincident at a node centred on the underside of the capping beam ignoring the transverse spacing of the front and rear rows of micropiles within the capping beam.
d) Median strength values for soil parameters were used
e) Surcharge loads were applied directly behind the retaining wall assuming no road shoulder

The PLAXIS 2D model is illustrated in Figure 4 below.

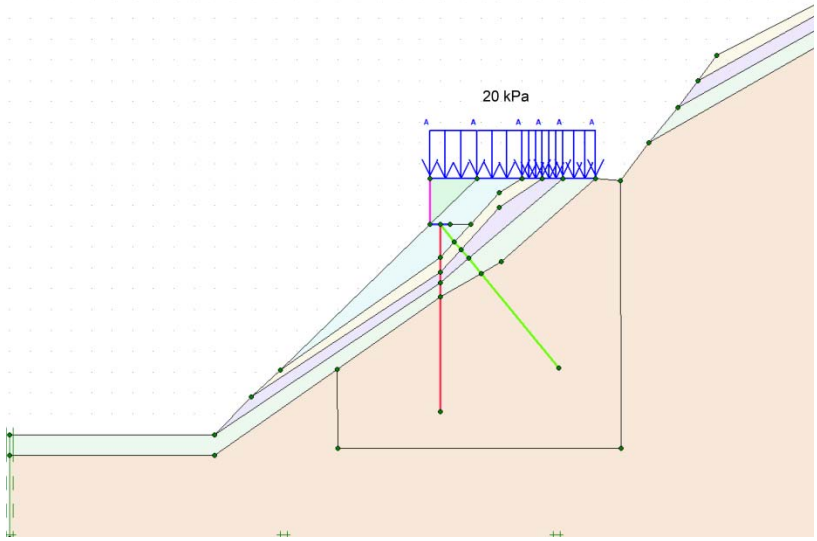


Figure 4 : Initial PLAXIS 2D model

The results of this initial model are summarised in Table 1 below.

Loading Stage	Displacements (mm)
Place new fill and construct pavement (Serviceability condition)	17
Remove partial soil (Fill and Residual) on the passive side of the micropile wall	21
Apply traffic loading equivalent to 20kPa surcharge without removing passive support	34
Apply traffic loading equivalent to 20kPa surcharge after removing passive support	52
Apply Q100 flood level and groundwater on ground surface (Ultimate condition)	55

Table 1 : Initial PLAXIS 2D results for overall deflection of the A-Frame structure

Analysis of the results of the initial modelling led to a refined approach being undertaken which took into account the transverse spacing of the front and rear rows of micropiles within the capping beam. This lead to a much stiffer structure and the deflections reduced accordingly.

The refined model can be seen in Figure 5 below.

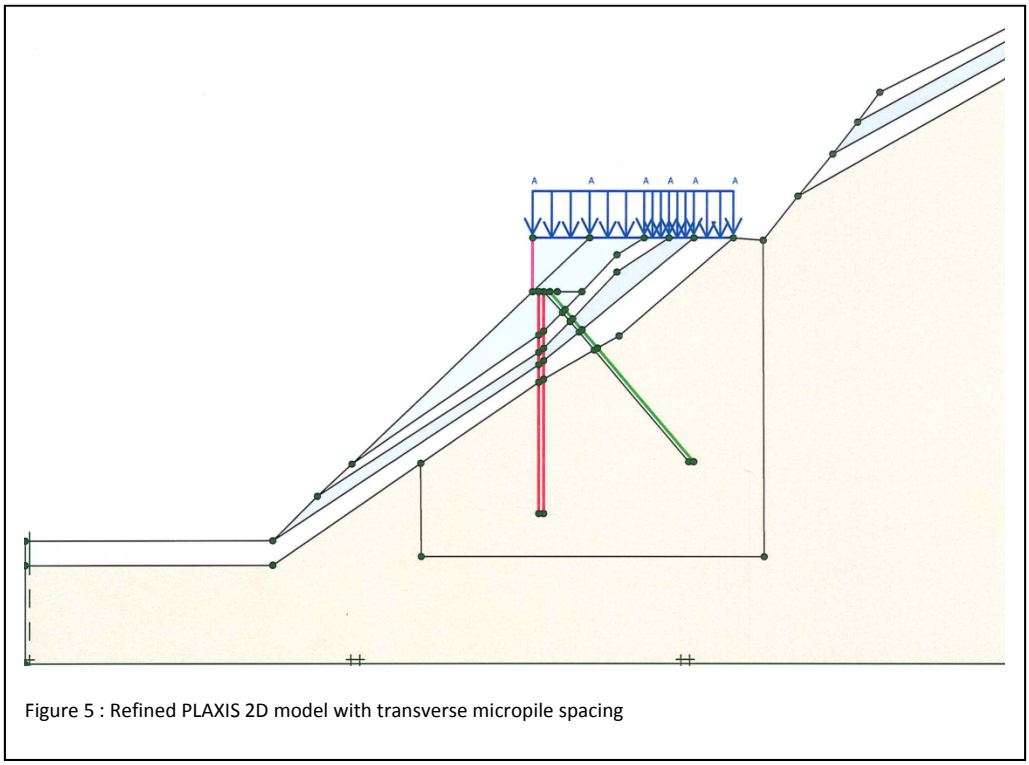


Figure 5 : Refined PLAXIS 2D model with transverse micropile spacing

With the transverse micropile spacing included in the model, the ultimate condition under full Q100 flood level and high water table reduced from 55mm in the initial model to 3.5mm in the refined model.

The deformed PLAXIS 2D model is contained in Figure 6 and demonstrates the nature of the deflection of the structure in the ultimate load case where passive resistance is potentially lost directly in front of the wall.

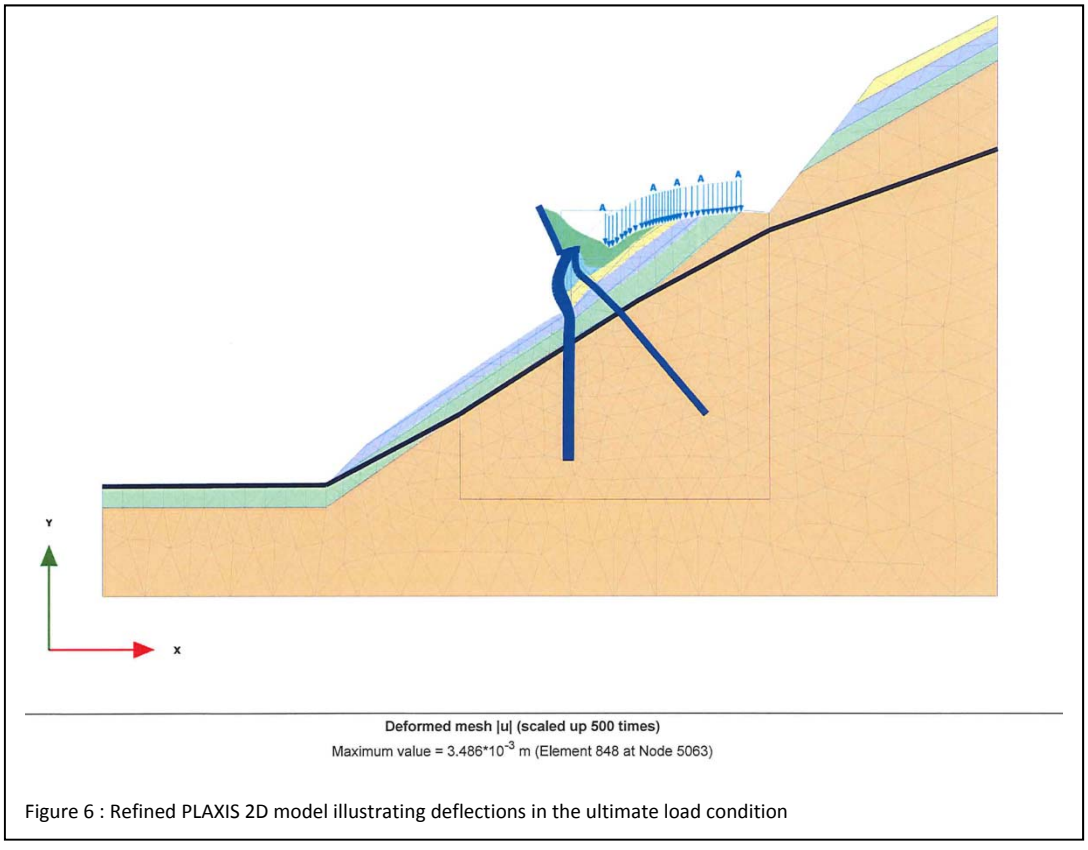


Figure 6 : Refined PLAXIS 2D model illustrating deflections in the ultimate load condition

Step # 4 – Check pile forces for combined axial and bending.

The model in Figure 6 indicated that some deflection would occur in the front vertical row of micropiles between the underside of the capping beam and the entry point into the ground.

Although the deflection of the structure was well within limits required by the Department of Transport and Main Roads Queensland, the designers were interested in checking the micropiles for combined axial and bending capacity due to the relative slender nature of the micropile elements.

Although the micropiles had been designed for the maximum combined load of P_{ult} from the FHWA geotechnical analysis along with the ultimate applied load from the retaining wall, this was a maximum tensile force calculated from the upslope raking pile applied for simplicity to all of the micropiles.

For the combined axial and bending check , the refined PLAXIS 2D model was used to determine the axial and bending forces within the individual micropiles. Due to the nature of the PLAXIS 2D being a geotechnical modelling tool, the model was limited to providing serviceability forces only due to the inability to include the ULS applied structural loads combined with the un-factored soil properties. A global factor of 2 was applied to relate ULS to SLS forces

To provide the stiffness required for limiting deflection of the A-Frame, a micropile layout including a single upslope row of raking micropiles combined with a double downslope row of vertical micropiles was selected. Figure 7 below demonstrates the micropile layout selected in the final design with the raked piles being on the upslope and the vertical piles being downslope.

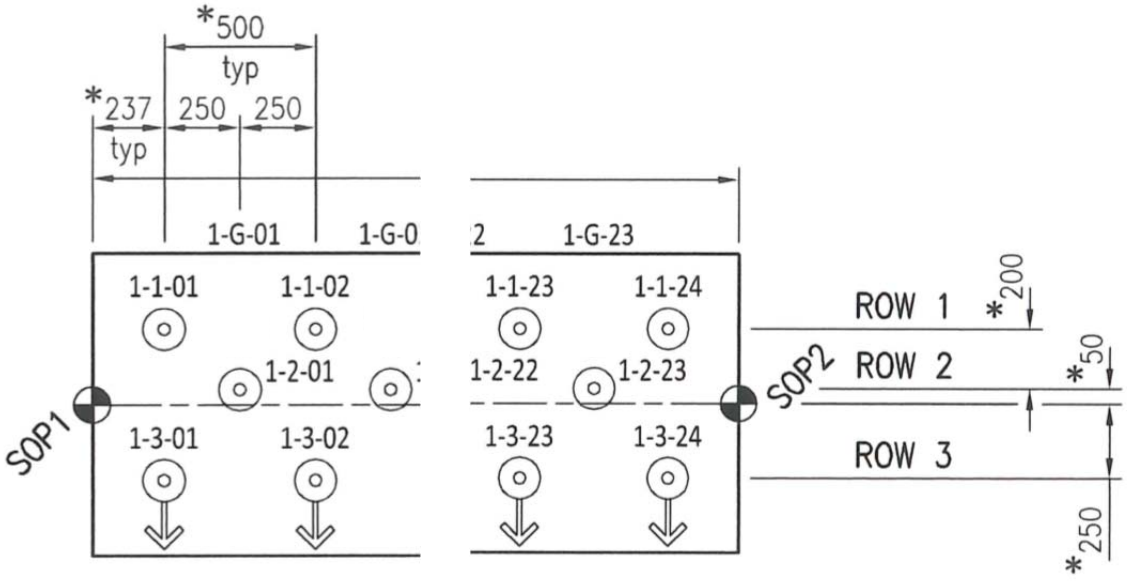


Figure 7 : Final micropile layout

Due to the capping beam having a high relative stiffness compared to the micropiles with fixity of the micropiles potentially being neither fully pinned or fully fixed, the fixity of the micropiles was modelled for both a pinned and fixed head condition to compare the effect on pile forces. The results are illustrated graphically below in Figures 8 and 9.

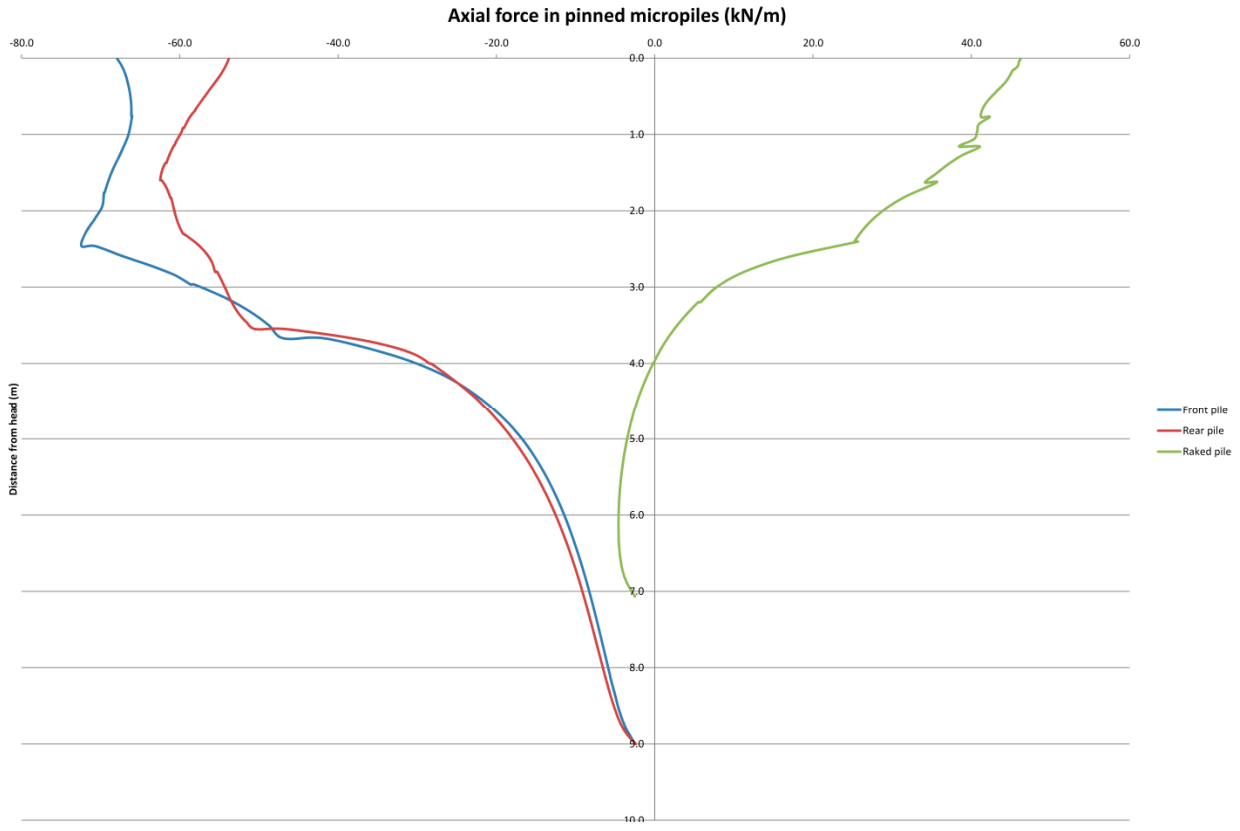


Figure 8 : Axial force for pinned head condition

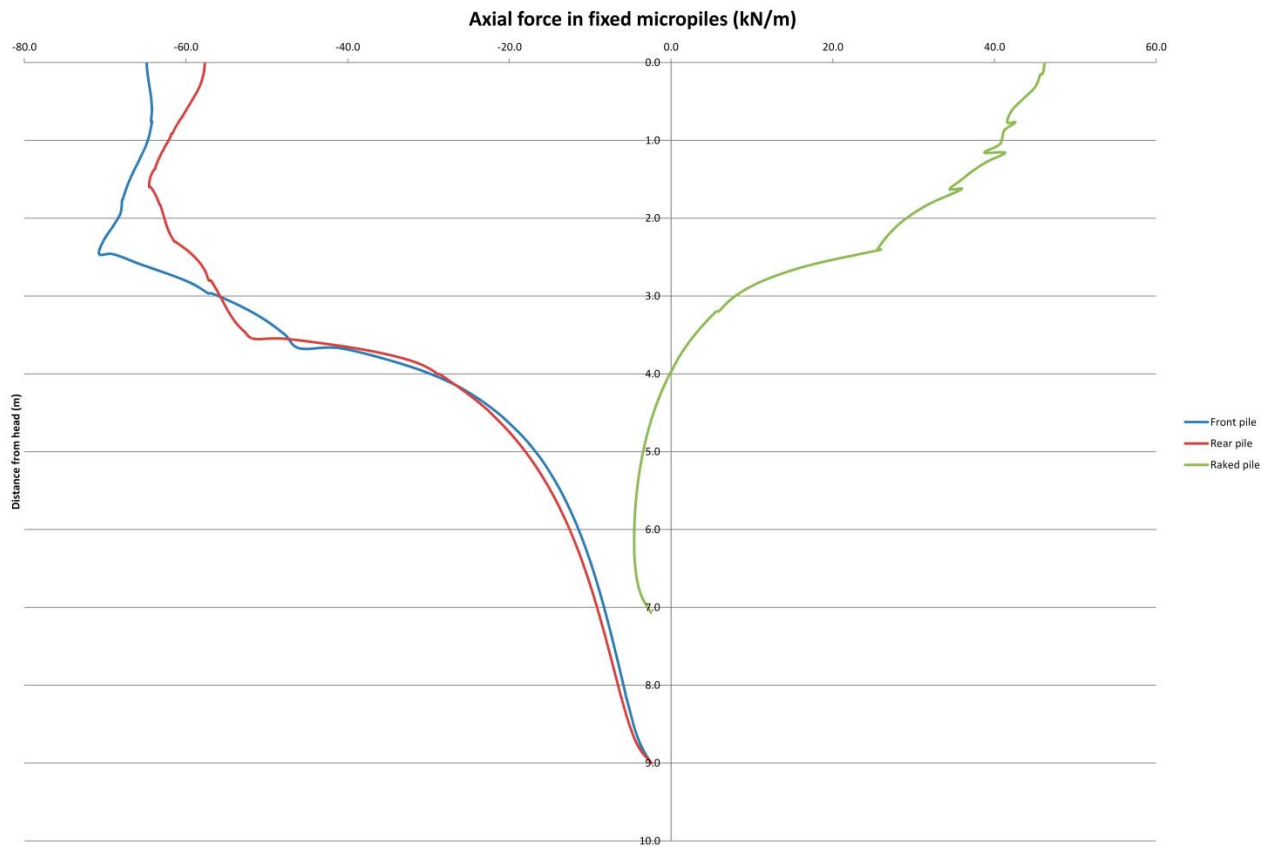


Figure 9 : Axial force for fixed head condition

From the analysis, the unfactored axial force in the micropiles was similar for both fixed and pinned head conditions with the pinned head condition producing a slightly higher force per micropile.

A factor of 2 was then used to factor the force up for the limit state condition used in the combined axial and bending check in accordance with Australian Standard "*AS4100 – 1998 Steel Structures".*

The results of the combined axial and bending checks for both the tension and compression piles are contained in Tables 2 and 3. It should be noted that a reduction factor of 0.5 was used on the bending capacity from the LPILE analysis for the semi-exposed outer vertical downslope pile. This is due to the potential loss of restraint for the outer piles during the worst case scenario for potential future downslope slip or erosion of soils providing passive resistance.

Raked Pile (Tension)	M* (kNm)	N* (kN)	ϕMs (kNm)	ϕNs (kN)	ϕMrx [1] (kNm)	Result
40 / 20 bar	0.49	47	2.9	382	2.5	OK

Table 2 : Combined axial and bending results of the micropile in tension

Vertical Pile	M* (kNm)	N* (kN)	ϕMs (kNm)	eff length (mm- limit)	ϕNc (kN)	ϕMi [1] (kNm)	
40 / 20 bar	0.32	72.5	2.9 [2]	1385	81	0.32	OK
40 / 20 + grout col	0.32	72.5	3.0 [3]	2770	81	0.32	OK

Table 3 : Combined axial and bending results for the micropile in compression

1 Combined axial compression and bending AS4100 cl 8.4.2
2 METHOD 2 as section 11.4.1
3 0.5 x LPILE value

The micropiles were found to be OK for combined axial and bending forces. This was the final check in the design process.

4.0 FINAL REMARKS

Although providing a solution for the Kin Kin Road slip remediation, the process of designing the A-Frame micropile structure with an integral concrete retaining wall proved to be challenging due to the interaction between the structural and geotechnical components.

The FHWA design method for the A-Frame considers the shear resistance required by the structure and does not require the capping beam to do any more than simply fix the pile heads together. The potential for applied forces to act upon the capping beam and be resisted by the micropiles is not covered as they are not required for a simple slope stability solution.

The PLAXIS 2D design checks were also beneficial for checking the potential serviceability deflections of the structure but there were limitations in the benefits of PLAXIS 2D when it came to the structural design when incorporating the applied static loads. The two processes didn't quite work together as well as they could due to complexities when comparing the static calculations of the structural design to the PLAXIS 2D geotechnical model which allows the structure to deflect.

The PLAXIS 2D design checks were also beneficial for checking the potential serviceability deflections of the structure but there are inherent limitations using a geotechnical package to determine structural forces.

The combination of the static structural analysis and the forces obtained from the geotechnical model proved to be more complex than originally thought which may have resulted in the final design being somewhat conservative. That said, inclinometers within the structure will be used for further analysis and refinement which should result in a more refined approach for similar structures in the future.

REFERENCES

Ezeajugh, Berends and Lester (2016). "Design and remediation of the Mt Morgan Range section of the Burnett Highway following Cyclone Oswald". 27th ARRB Conference, Melbourne, Victoria.

Hinds (2015). "Risk management in action. Transport network reconstruction program. Reconstruction following multiple natural disasters". IP0021-Hinds-E.doc. Department of Transport and Main Roads, Queensland, Australia.

Micropile Design and Construction (2005). Federal Highways Administration Publication, US Department of Transportation, FHWA NHI-05-039

AS4100-1998 Steel Structures, Standards Australia

CASE HISTORY: ROCKEFELLER UNIVERSITY RIVER CAMPUS BUILDING MINI-CAISSONS

Andrew Burns, PE (Posillico, College Point, NY)
Michael Quasarano, PE (Posillico, College Point, NY)

ABSTRACT

In 2015, Rockefeller University, a historic, cloistered medical research campus on the Upper East Side of Manhattan along the East River, embarked on the construction of a new building. The building would be squeezed into a tight slot between adjacent buildings and over the top of the busy six-lane FDR Drive. The foundations on either side of the FDR Drive presented different challenges to the design and construction of mini-caisson piles.

On the upland side west of the FDR Drive, drilling contractor Posillico offered the owner a value-engineered alternate to replace a proposed deep pier/wall on rock and rock anchors with a pile cap supported by 16 battered mini-caissons. An unconventional pile design featuring a steel pipe installed within the drill casing allowed the piles to develop the required lateral stiffness and isolate load transfer below the adjacent existing building foundation. The alternate solution eliminated the rock anchors and reduced the costly rock excavation by almost 2,700 tonnes (3000 tons) from the original plan. The owner also requested that the contractor accelerate the schedule in order to allow for steel erection to begin 2 months earlier than planned. On the riverside east of the FDR Drive, Posillico redesigned the 340-mm (13-3/8-inch) diameter 5,425-kN (600-ton) mini-caissons to 457-mm (18-inch) diameter for 10,850-kN (1200-tons). This led to a reduction in pile quantity and accelerated an important schedule milestone. The lateral requirements for both foundations required drilling the casing through the bedrock and partially extracting it to achieve the load transfer through friction in the rock socket.

This paper reviews the unconventional pile design details. It also explains how a proprietary under-reaming drilling system allowed the contractor to meet the compressive and lateral design requirements while also allowing for the use of smaller rigs than would otherwise be needed. Additionally, the paper reviews some of the difficult urban construction conditions within limited access environments including overhead and underground utilities, heavily planned material and equipment logistics and tight coordination of protection of traffic on the extremely busy FDR Drive.

BACKGROUND

Manhattan's Upper East Side is densely developed with primarily residential high rise buildings and street level retail shops. It is situated between Central Park and the East River. The FDR Drive – a six lane limited access highway – runs north-south along the river. Between the FDR Drive and the river is the John Finley Walk – a popular esplanade used by joggers, dog walkers, and anyone else from the neighborhood seeking a brief respite from the urban experience. The Upper East Side is also home to Rockefeller University – a world renowned

medical research facility founded in 1901. The existing tree-lined campus sits atop a 40-foot high, hundred-year-old schist rock retaining wall. It features cloistered gardens amongst notably neoclassical architecture. Figure 1 shows a Google Earth view of the Rockefeller University Campus.



Figure 1. Google Earth view of Rockefeller University's tree-lined campus, the FDR Drive, and the John Finley Walk esplanade along the East River on Manhattan's densely populated Upper East Side (looking west).

New York City is currently undergoing a development boom for medical research institutions. In an effort to maintain its prestigious position and continue to attract talented researchers, Rockefeller University engaged Turner Construction Co. as construction manager in a campus expansion program known as the Stavros Niarchos River Campus. The program is built around construction of a 2-story building designed to span 24 meters (80 feet), east-west, over the top of the FDR Drive for 290 meters (950 feet), north-south, along the river. The new facility will feature state-of-the-art laboratories, administrative space, and a cafeteria. Atop the building, the cherished outdoor spaces and gardens of the existing campus will extend eastward to overlook the East River. Figure 2 shows a rendering of the project after completion.



Figure 2. Artist's rendering of the Rockefeller University campus following completion of the Stavros Niarchos River Campus construction (looking west).

The overarching structural design concept was based on installing piles in a narrow gap between the FDR Drive and the esplanade on the east side as the bedrock drops off below the deep East River. The western foundations consisted of piles along the southbound shoulder of the FDR Drive. Together, these pile foundations would support the new building which would be prefabricated in 19 modules and set during highway closures at night. Additionally, mechanical and electrical rooms (MERs) would be built between existing campus buildings on shallow foundations with rock anchors on higher elevation bedrock.

This paper focuses on issues related to the deep foundations required to support the new River Campus building. In particular, it focuses on two alternate pile designs proposed by the contractor – one pre-bid and the other post-award. The pre-bid alternate involved adding mini-caissons in lieu of piers and footings on rock within the existing campus for the MERs. The post-award alternate involved increasing the capacity of the individual caissons in the original design, east of the FDR Drive, to reduce the number of piles and, thus, accelerate the schedule.

PRE-BID VALUE ENGINEERED ALTERNATE: MINI-CAISSONS IN LEIU OF ROCK EXCAVATION

The base bid design for the MER shear wall foundations did not call for piles. Instead, rock excavation would be required in order to construct the new foundations beyond the influence depth of the adjacent buildings. The bedrock formation was known ahead of time to be hard and would require a great deal of line and channel drilling in order to make excavation possible without negatively impacting the adjacent structures. Additionally, due to the limited access to the area, loading out excavated rock was difficult and expensive. The original design also called for rock anchor tie downs due to tension loads on the shear wall foundations.

During the bid process, in an effort to reduce the duration and cost of construction, the contractor, Posillico, proposed installing mini-caissons that would provide the required compressive, tensile, and lateral capacities and would be designed so as to isolate the loads below the depth of the adjacent buildings. The cost for these mini-caissons was more than offset by saving almost 2700 tonnes (3000 tons) of rock excavation (and associated line and channel drilling as well as loading out, trucking and disposal) along with elimination of the shear wall on column line A1 (figure 4B) and associated rock anchors. Figure 3 shows the type of space and logistical constraints that drove up the excavation costs. Figures 4A and 4B contain the original designs as well as key components of the proposed alternate. Figure 5 is a geologic section through MER A showing the dramatic difference in bedrock elevations.

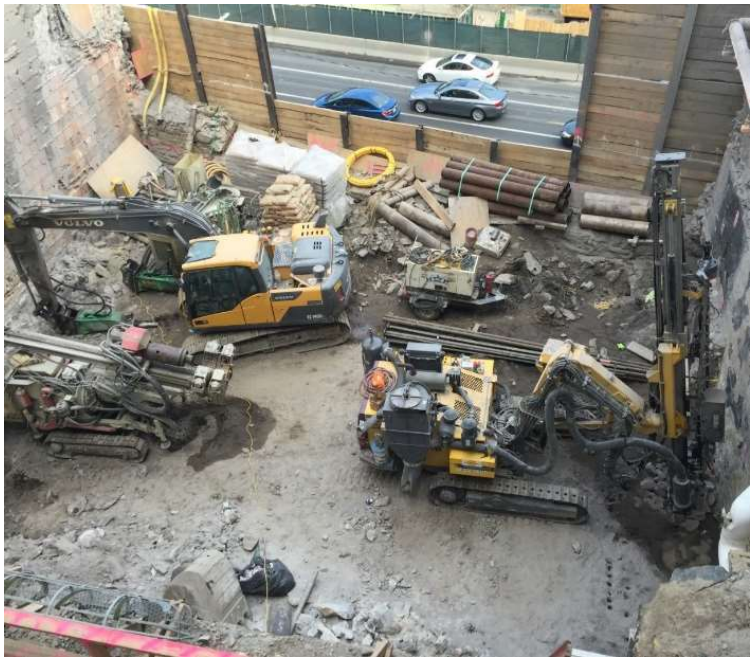


Figure 3. Construction of MER B foundation was performed with small rigs within tight constraints. At right is a small drill rig line drilling for rock excavation. The idle drill rig at left was used to install the alternate mini-caissons. Also shown is a small excavator used to break, excavate, and load out the rock, during night shifts, onto the FDR Drive, in the background.

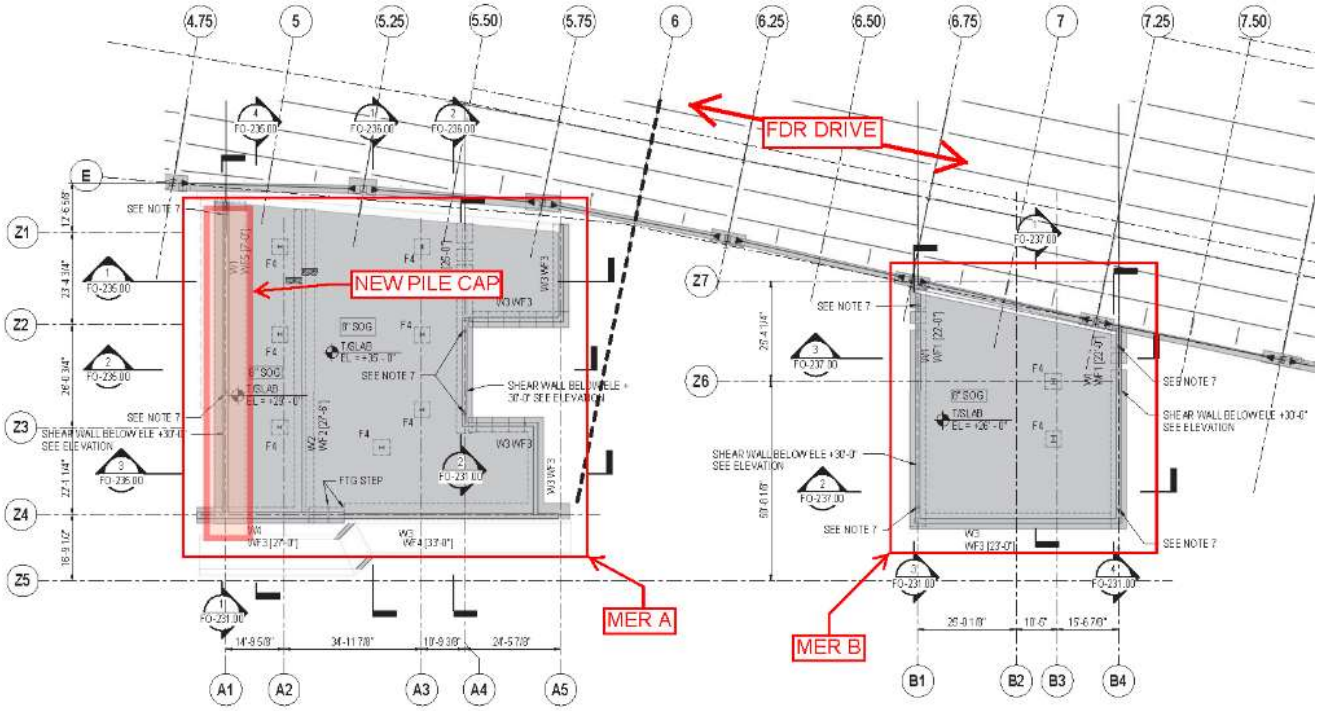


Figure 4A. Original foundation plan of MER A and B and the outline of the proposed pile cap.

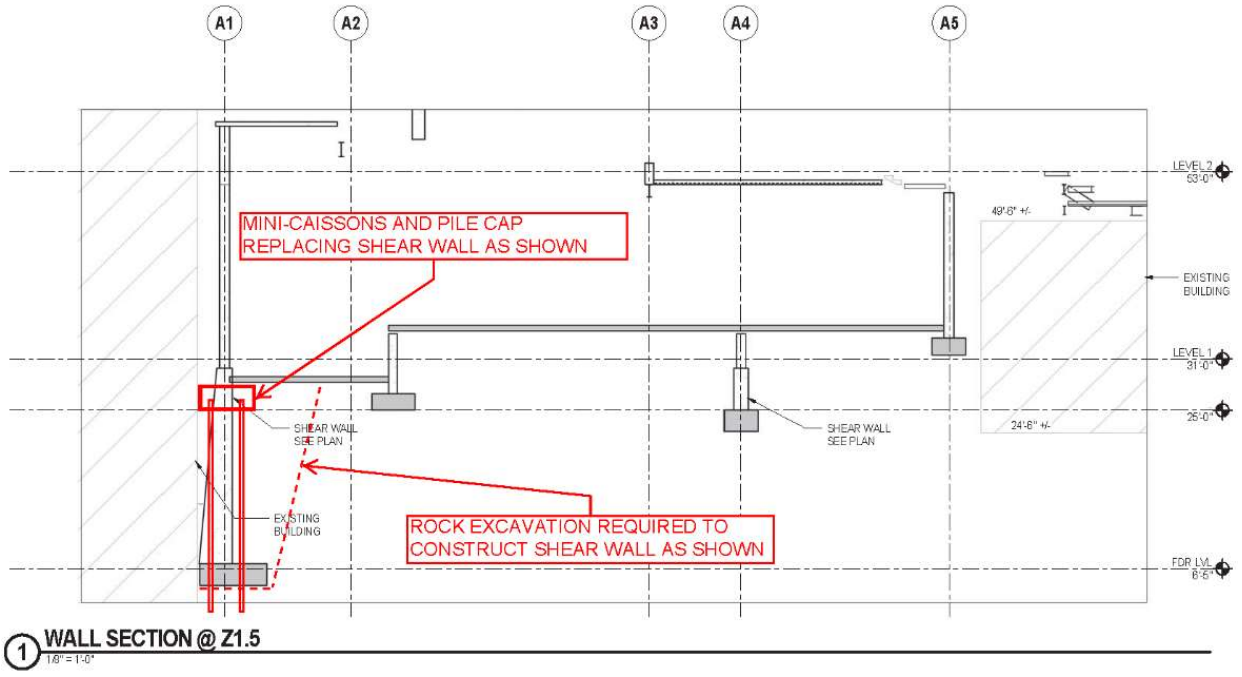


Figure 4B. Section through the MER A foundation per base bid (Section 1 from figure 4A).

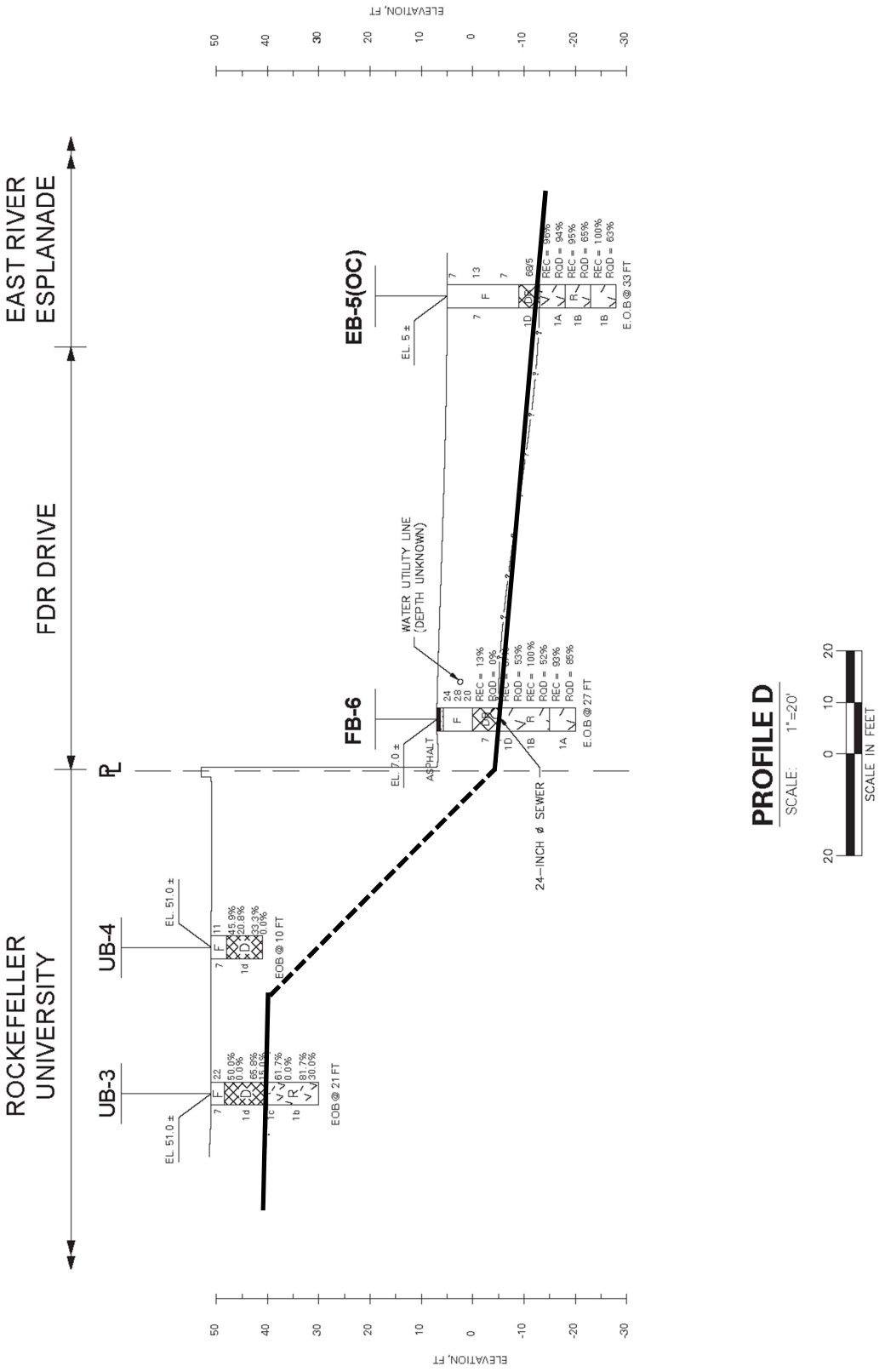


Figure 5. Geologic Section taken through MER A (labeled “ROCKEFELLER UNIVERSITY”), the FDR Drive, and the East River Esplanade (John Finley Walk).

In order to meet the allowable load and isolation requirements, the contractor proposed installing a 340-mm (13-3/8-inch) diameter casing down through the bedrock. Once the full drill depth was achieved, the casing was extracted to create a rock socket for transferring compressive and tensile loads via grout-to-ground bond. In order to isolate the load down past the adjacent foundations, an inner 273-mm (10-3/4-inch) diameter casing was inserted inside the 340-mm (13-3/8-inch) casing. The inner casing was wrapped in polyethylene sheeting as a bond breaker. Lateral load requirements were met by battering the piles as shown in figure 5.

.

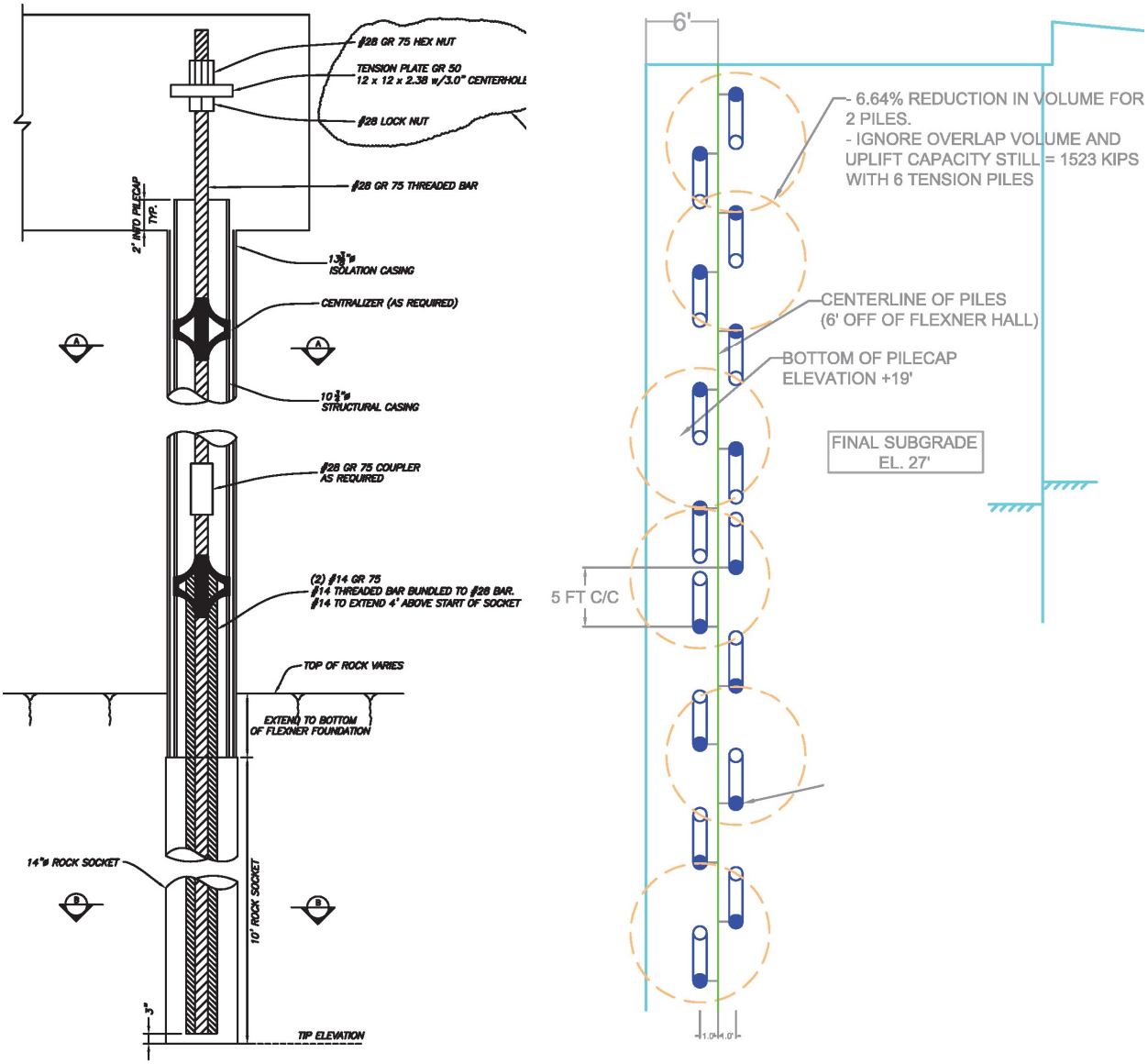


Figure 6. Pile layout and details for proposed alternate mini-caissons in lieu of the MER A shear wall shown in figure 4B.

Alternate mini-caisson allowable axial loads were 3620 kN (400 tons) in compression and 1810 kN (200 tons) in tension. Tension design was based on rock cone failure analysis shown by dashed circles and associated call outs in figure 5. The pile details in figure 5 show 273-mm (10-3/4-inch) inner load bearing casing and the 340-mm (13-3/8-inch) outer isolation casing. What is not made clear in figure 5 is the actual vertical dimension between the top of bedrock and the top of the rock socket. This ranged from 6 ot 8 meters (20 to 25 feet). The casing was typically drilled 9 to 11 meters (30 to 35 feet) into bedrock and extracted 3 meters (10 feet). It was only possible to drill the casing through the rock by using an under-reaming system. For this project, Posillico chose to use the Roto Loc system by Center Rock, Inc.



Figure 7. Construction of MER A foundation was performed with small rigs within tight constraints. The photo shows the installation of mini-caissons battered 1 on 4 (horizontal to vertical). Also shown, upper right, are the active electrical ducts just above the drill rig mast. The headroom restrictions required the use of 5-foot long casing and drill rods.

POST-AWARD VALUE ENGINEERED ALTERNATE: 457-MILLIMETER (18-INCH) DIAMETER 10,850 KILONEWTON (1200-TON) "MINI"-CAISSONS

Working in and around existing active facilities involved many logistical challenges. These included coordination of traffic patterns with the NYC Department of Transportation (DOT), the

location/protection/maintenance/relocation of active utilities, as well as existing structural conditions – many of which were not understood fully or even discovered in some cases until the demolition and construction in an area began. These “verify-in-field” situations lead to many changed conditions and redesigns throughout this project. The net result of these changes was an increase in scope of the foundation construction work. As a result of this increased scope, the owner authorized compensation for acceleration of the schedule (i.e. working overtime). In addition to the acceleration to make up for changed conditions and redesigns, the owner simultaneously sought to reduce the overall duration of the base contract. The contractor was repeatedly requested to present additional ideas to expedite the foundation construction.

The support for the new River Campus building required the installation of deep foundations between the FDR Drive and the esplanade. According to the Geotechnical Report, the FDR Drive and the esplanade are constructed on a pile supported relieving platform while a granite block faced concrete gravity retaining wall serves as the bulkhead along the river shoreline. Contract requirements included maintenance and protection of all 6 travel lanes on the FDR Drive. It also required maintaining a 2.4-meter (8-foot) wide portion of the esplanande between the work zone and the river (left side of figure 7) open to pedestrian traffic. Any required shutdowns would have to be done during night shifts. To further complicate matters, there were several other major construction projects being performed simultaneously along other sections of the FDR Drive. This lead to weekly coordination between the DOT and all of the general contractors to “hash out” competing logistical concerns.

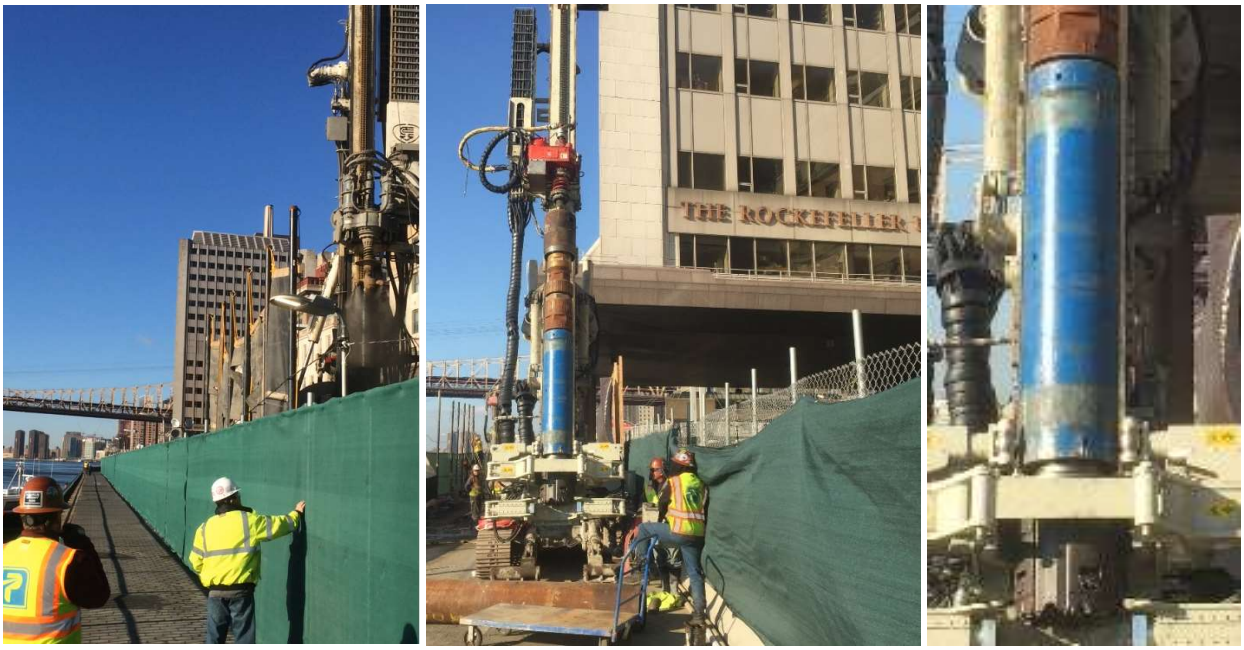


Figure 7. Maintaining vehicular traffic on the FDR Drive and pedestrian traffic on the esplanade, shown at left, while rock drilling with air-flush required planning and constant vigilance to prevent property damage and injury to the public. The Roto Loc under-reaming system can be seen in the photo on the right.

Maintaining vehicular and pedestrian traffic limited the width of the work zone for the foundation construction to between 2.4 and 5.5 meters (8 and 18 feet) with very limited access. Equipment and materials were brought to the site during evening lane closures. Compressors and grout plants were situated on service barges off shore. The limited width of the work zone, in turn, also limited the size of the drill rigs that could be safely utilized. When the owner asked the contractor for any and all ideas to reduce the duration of foundation construction (in addition to adding second and third drill rigs), the approach was simple: what are the largest drill rigs we can utilize and what is the greatest pile capacity that can be installed with such rigs?

The original base bid design called for 60 each 5,425-kN (600-ton) 340-mm (13-3/8-inch) diameter mini-caissons. Posillico proposed replacing 48 of these with 28 each 10,850-kN (1200-ton) 457-mm (18-inch) diameter caissons. Twelve caissons would remain unchanged. Thus, the total quantity of piles was reduced from 60 to 40. This is estimated to have saved approximately 2 weeks off a 6-week critical path schedule item. Every week was critical in the eyes of the owner. The intent was to begin steel erection as soon as the prefabricated modules were available.

Due to the age, design and construction, and condition of the existing seawall, the piles would be required to handle the lateral loads imposed on the new structure under seismic code considerations. The original contract drawings called for casing embedded 1.5 meters (5 feet) into bedrock with a socket diameter larger than the casing outside diameter, lower right in figure 8. This embedment was required in order to provide enough base shear resistance – especially for piles where bedrock was shallow, say, on the order of 6 to 9 meters (20 to 30 feet) below pile cut off elevation. Figure 8 also shows the final shop drawing for the alternate 10,850-kN (1200-ton) caisson.

Additionally, static lateral load tests were performed on both size piles to confirm that lateral soil/pile responses were within acceptable limits. One-third of the piles were battered at a slope of 1 on 6 (horizontal to vertical) in the east-west direction, perpendicular to the seawall, in order to provide required resistance to lateral movement towards the river and prevent side-loading the seawall. This lateral capacity was achieved through the tensile capacity of the caissons. Additionally, one-third of the piles were battered 1 on 5 north-south.

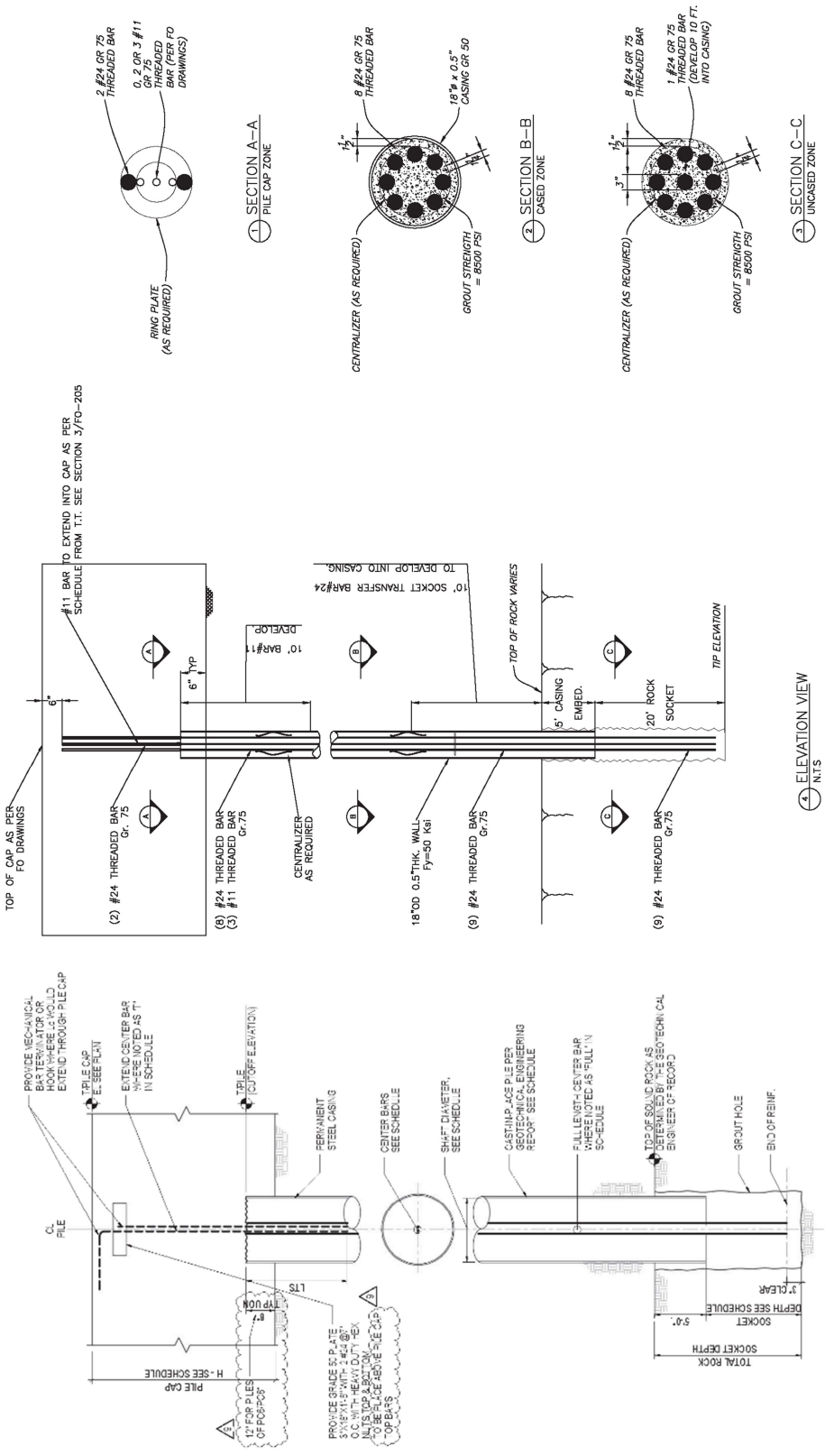


Figure 8. Pile details for the base bid 340-mm (13-3/8-inch) diameter mini-caisson and the alternate 457-mm (18-inch) diameter caissons.

In order to provide this casing embedment into bedrock, Posillico again chose to use Center Rock's Roto Loc under-reamer. In this case, Center Rock custom-built their system to 457-mm (18-inch) diameter to accommodate the contractor's requirements. As was the case in the MER A foundations, using an under-reamer reduces the torque requirements on the drilling equipment which, in turn, makes it possible to drill relatively larger diameter piles to greater depths with relatively smaller drill rigs. This torque reduction was even more critical as the casing diameter was increased to 457 mm (18 inches). Figure 9 shows a detail of the Roto Loc operating principle. It is noteworthy that the increased rock socket diameter turned out to be critical in meeting the 2014 New York City Building Code's requirements for clear grout cover of reinforcement in the rock socket.



Figure 9. Expanded detail view demonstrating the operating principle of the Roto Loc under-reaming system manufactured by Center Rock, Inc.

CLOSING REMARKS

In closing, this case history provides an example of a contractor with specialty knowledge in the area of pile design and construction collaborating with an owner, their design engineers, and their construction manager to reduce construction costs and durations. Although the two alternate caisson designs were only part of the overall project, they represented a disproportionate safety, quality, schedule, and cost risk exposure for all stakeholders. These alternates contributed toward meeting the owner's goal of commencing steel erection per the originally anticipated schedule milestone despite a 2-month late start and numerous redesigns and scope increases. Figure 10 shows one of the pre-fabricated 2-story steel frame building modules, 24 meters by 15 meters (80 feet by 50 feet) in plan, being set at night over a closed FDR Drive with one of North America's highest capacity crane barges.

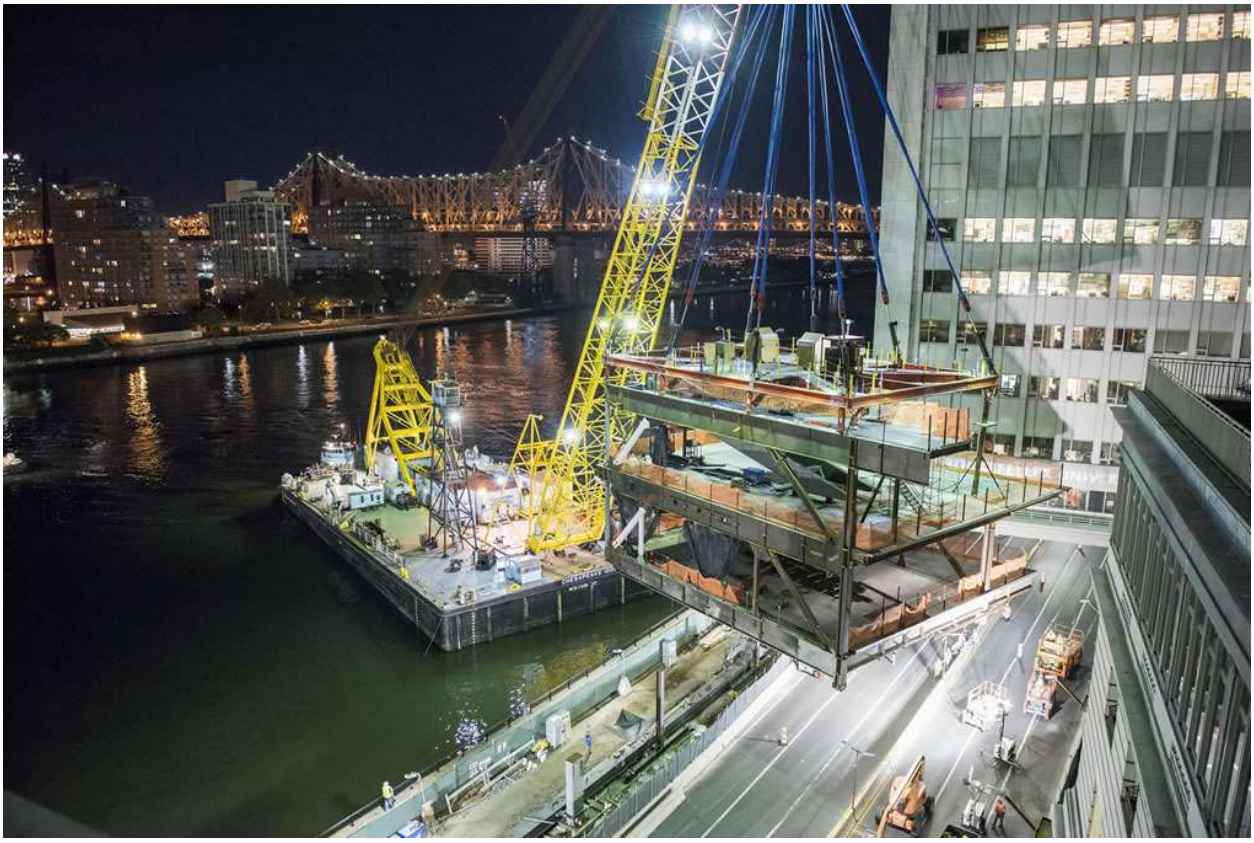


Figure 10. Foundations installed east and west of the FDR Drive supported prefabricated building modules set during night time highway closures. In all, 19 such sections were set over a 2-month period.

MICROPILE INSTALLATION USING THE PREVENTER SYSTEM TO CONTROL THE INFLUX OF GROUNDWATER DUE TO A HIGH WATERTABLE

Sean Beirne-Lewis

General Manager, Ground Engineering – Ischebeck TITAN Group

ABSTRACT

An 8 storey building located in Dubai had undergone some form of movement within the basements leading to cracked columns, walls and slabs. Active water ingress penetrated through cracks in the basement slab and walls. Cracks to the columns were initially identified in 2012 and were repaired in mid 2014 and appear not to have re-cracked since.

A geotechnical and structural assessment of the building was carried out and concluded that structurally the building was within the limits of acceptance. However, the consulting engineer carried out a detailed design to enhance the stability of the structure, which involved a combination of grouting and micropiling.

Some, 312No. 15.0m TITAN 40/20 micropiles (4670m) and over 580No.3.0m tube a manchette steel grouting tubes were both successfully installed using the preventer system.

This paper examines construction processes involved in installing the micropiles using the TITAN preventer system.

INTRODUCTION

PROJECT BACKGROUND

The building is located in Deira, Dubai, approximately 500m from the Creek. The structure was built in 2007 and consisted of 8 stories and two basements. In 2012 cracks to the walls, columns and slab were identified and led to partial water ingress. As a result, the building was completed closed and has been for over 3 years. In mid 2014 the consulting engineer instructed repairs to be carried out on the building which seems to have worked, as they appear not to have re-cracked since.

A review of the geotechnical data suggested two potential mechanisms may have initiated the building movement. These were a variation in the rock head quality and elevation and disturbance of the rock quality close to the perimeter diaphragm wall.

Subsequently building movement and crack monitoring programmes were implemented, with data suggesting that movements were stable. However additional measures to further enhance stability were proposed. The design included grouting

to enhance the strength and stiffness of the underlying soils and reduce the permeability. In addition to this, the design included underpinning, using micropiles.

The geotechnical report identified a water table at -1.46m, with the micropile installation level at -4.45m. This posed a significant risk of water influx during the micropile installation, once the water proof membrane under the slab was penetrated. The use of the preventer system successfully allowed the installation of the micropiles and TAM grouting tubes whilst controlling and restraining the water influx.

GROUND CONDITIONS

The geology of the United Arab Emirates has been substantially influenced by the deposition of marine sediments caused by numerous sea level changes during recent geological time. To the north-east the country is mountainous, but in the main the country is relatively low-lying, with near surface geology being dominated by Quaternary to late Pleistocene deposits made up of Aeolian dune sands and sabkha/evaporates.

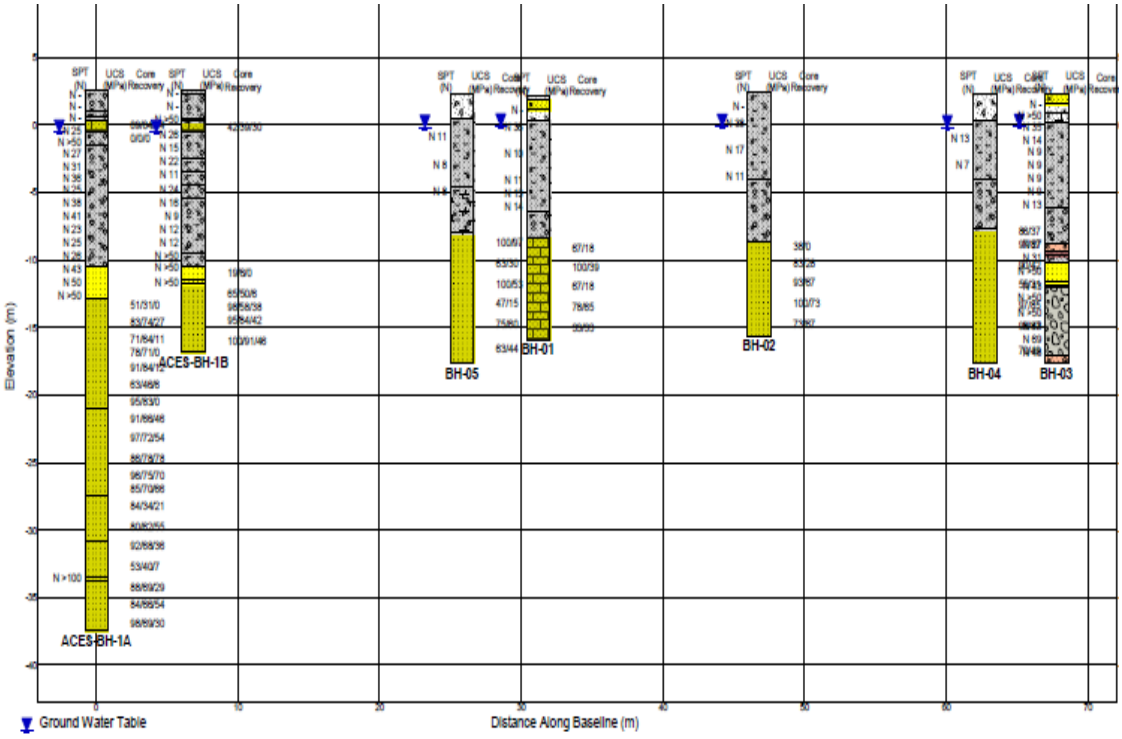


Figure 1 - Typical Boreholes

In Dubai the ground conditions essentially consist of superficial deposits of beach dune sands together with marine sands and silts. These superficial deposits are underlain by alternating beds of calcarenite, carbonate sandstone, sands and cemented sands.

The ground conditions on site in Dierra are typical and consisted of approximately 9.0m of sand overlying 1.5m thick bed of Calcarenite, which in turn overlaid the calcareous sandstone. At basement 2, the installation involved drilling through 2.0 – 3.0m of sand before the calcarenite/calcareous sandstone was encountered.

DESIGN

The micropile design was carried out by the Piling Contractor, however at the time of writing this paper the detailed design was unavailable as a reference.

The working load of the micropile was T_w = 256kN and to accommodate the load for a permanent design case the 40/20 was adopted (Yield Load = 425kN Ultimate Load = 540kN). The overall length of the micropile was 15.0m (allowing for the 400mm slab) and was installed using a 115mm cross cut drill bit. This allowed for an approximate 12.0m bond within the calcarenite and calcareous sandstone.

Due to the groundwater containing sulphate, corrosion protection of the micropile tendon was provided by an epoxy/galvanised coating, which met the permanent design life required.

INSTALLATION

Prior to commencement of the installation of the micropiles all drilling positions where marked on the basement concrete slab. Once this was completed the micropile positions where diamond core drilled using a 150mm diameter barrel, by rotation, using a water lubricant. The 400mm thick concrete slab was core drilled to a depth of 350mm, passing through the last row of steel reinforcement. As a precaution a mechanical packer was positioned close to the core hole to control any groundwater as a result of over coring.



Figure 2 – Mechanical Packer



Figure 3 – Diamond Core Drilling Set Up

Once the core drilling was completed, the walls of the core hole were roughened up using an electric hammer. This was carried out to improve the friction/bond capacity

between the existing concrete slab and the new head detail. Once this was completed the core hole was cleaned of any resultant concrete debris.

The next procedure involved the set up of the preventer. First, four mechanical anchor bolts were installed into the concrete basement slab. A rubber gasket was then positioned over the four bolts, sitting directly on to the concrete slab. With this in position, the flange head plate and gate valve were installed directly over the core hole and bolted to the slab with the anchor bolts. The gate valve acted as a secondly preventer, sealing the core hole after installation. This allowed the preventer to be removed at an earlier stage, freeing it up for another micropile installation.



Figure 4 – Flange Head Plate & Gate Valve

Once the gate valve was successfully installed, the preventer was then fixed and secured to the flange plate using four M12 bolts.

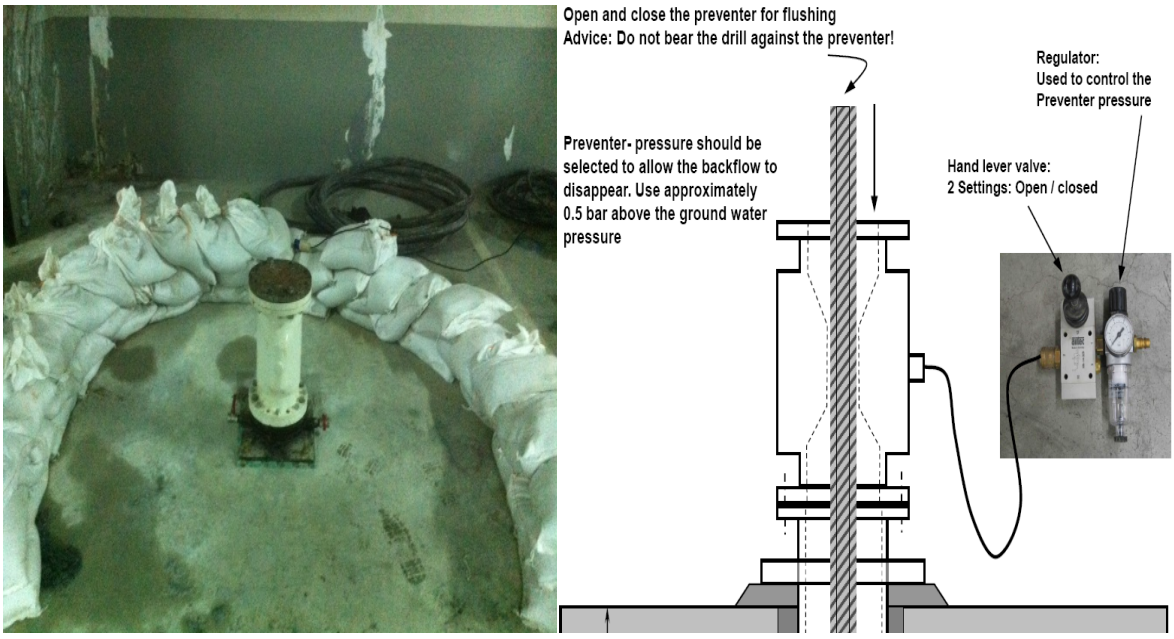


Figure 5 - Installed Preventer

The preventer is essentially a valve system, fitted with a 19mm thick rubber tube insert, which is connected to a compressor via an air line. The system is operated by opening and closing the rubber insert, by applying air pressure to inflate (close) or deflate (open) the rubber insert. The air line supplies an air pressure of between 3 to 6 bar.

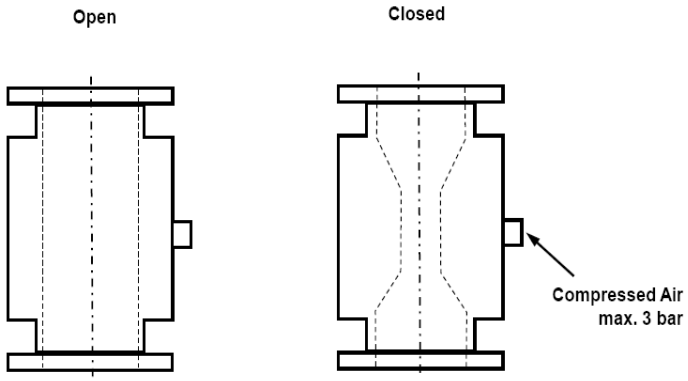


Figure 6 - Preventer Positions

Micropile installation

Installation through the preventer involved adjusting the pressure to allow a “gentle” backflow, which is essentially employed to lubricate the rubber insert. It is the responsibility of the preventer engineer to determine the required pressure during the installation process. During this project the pressures required were typically 1.5 bar during drilling and 3 to 4 bar when closed.

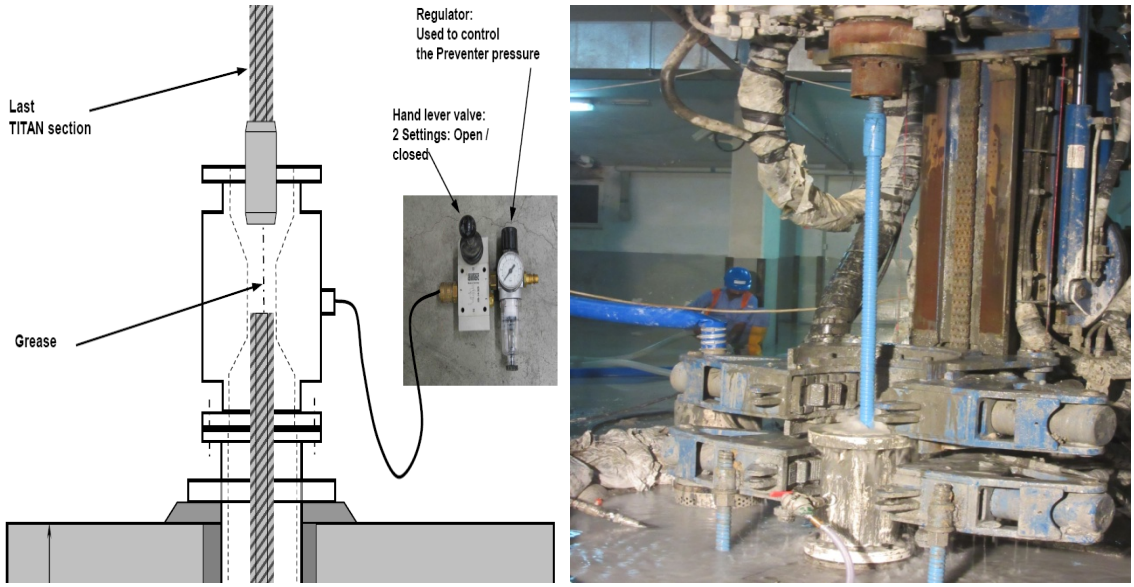


Figure 7 - Micropile Installation

The micropile installation used a water flush, due to the proximity of the rock head, however on occasions a cement grout, with a water cement ratio of 1 (by weight) was used as a flushing fluid.

The quality of the cement grout body and bond were improved by adopting a slower drilling rate and frequently cleaning out the drill hole. This process known as reaming, involved repeatedly extracting and reinserting the drilling rod/micropile, while continuing to rotate the rod and flushing out the drill hole. This procedure allowed the debris to be flushed from the drill hole to the surface and was continually monitored by the drilling operative.

Grouting

Once the micropile had reached the 15.0m design depth, dynamic pressure grouting was carried out. Dynamic pressure grouting is the term given to the simultaneous process of injecting grout, whilst rotating the micropile tendon, resulting in a dense grout body encapsulating the tendon. The cement grout used for the micropile had a water/cement ratio of 0.35 to 0.4, with a strength = 35N/mm^2 after 28 days. Due to the proximity of the Creek, the cement grout used was a high sulphate resistant cement. In addition Epsilone was added to improve the pumping of the cement grout.

The stiff grout mix displaces the thinner flushing medium used to support the drill hole, encouraging it to return to the surface.

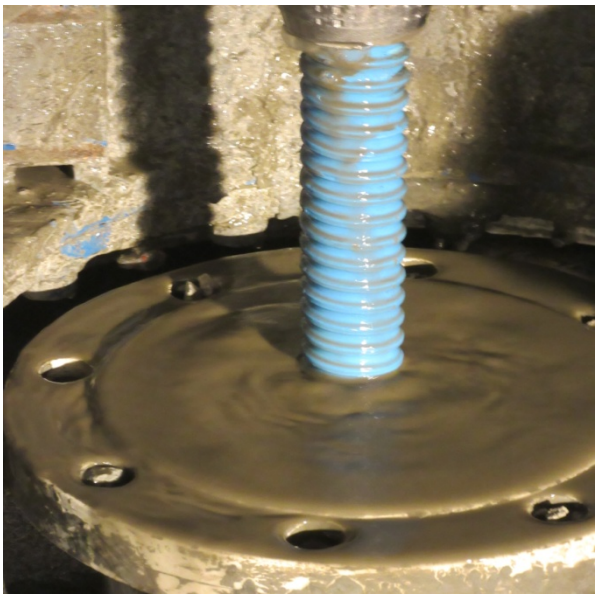


Figure 8 - Grout Return

The drilling operator monitored the consistency of the grout mix and was responsible for determining when the dynamic grouting process should be stopped. Typically 12 bags (50kg each) of cement grout were used per micropile and injected at about 20 bar pressure.

The micropile was installed to its final design depth by using a recoverable extension bar and coupling nut. The assembly was loosened and flushed with water, inside the preventer to clean it. The last section of the micropile was then pushed 5cm below the top of the basement slab.

On completion of this operation, the gate valve was closed and the injection of the non-shrink grout began, in order to fill the micropile head, providing contact to the existing concrete slab. A minimum of 20 litres of grout was pumped, with a water cement ratio of 0.35. In order to obtain a compressive strength of 45Mpa at 28 days, high range water reducers and expansive admixtures where used. To increase the curing time of the grout, 5 litres of Sodium Silicate Liquid was simultaneously pumped with the grout, through the gate valve.

Once the grouting procedure was completed a blank flange plate and gasket was bolted to the top of the preventer to close the unit completely. The compressed air was set to allow the disassembly and cleaning process. Between 6 – 12 hours after the installation the preventer was removed, leaving the flange and gate valve in place. With the grout cured, the flange/gate valve assembly was removed. The local slab area was cleaned and non-shrink grout was injected into the core hole up to the slab surface.

The head detail arrangement consisted of a 100mm pipe with a welded helix on the outside, a spherical collar nut and washer plate.

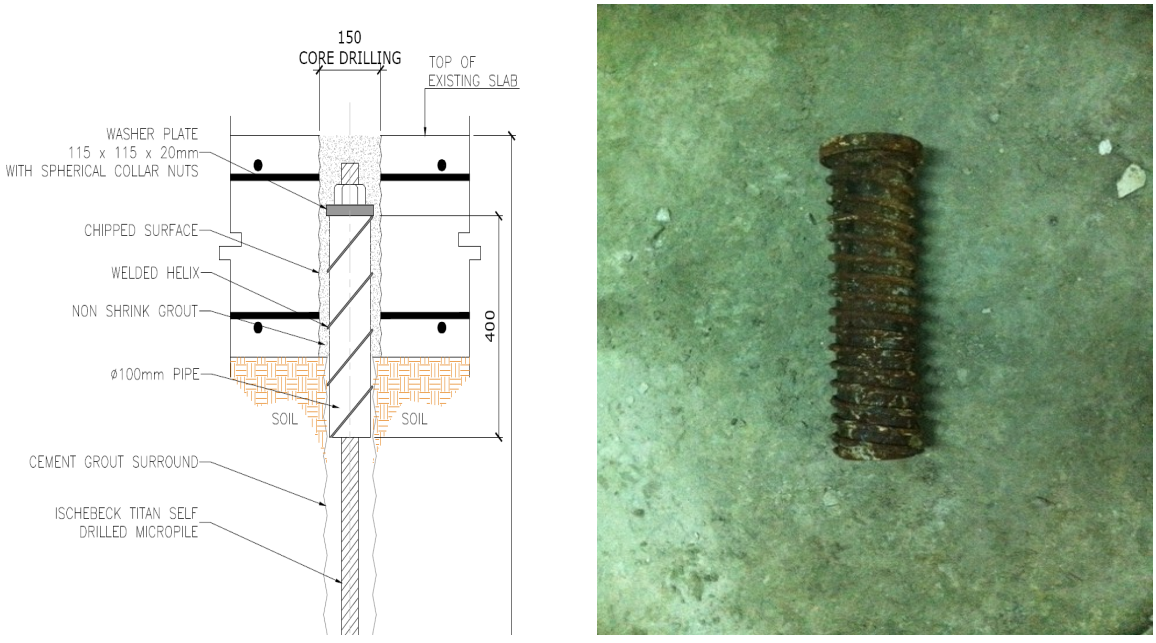


Figure 9 - Micropile Head Detail

SITE CONSTRAINTS

The installation of the micropiles was carried out in basement 2 and presented a number of constraints to the drilling contractor. Firstly the headroom was limited to 2.4m and resulted in the micropile tendons being cut and coupled in 1.0m sections. In addition the restricted headroom, only allowed the use of one preventer due to their height measuring 450mm. Additional security was offered by the gate valve, which measured only 100mm in height.



Figure 10 – Electric Drilling Rig

The confined space also led to the drilling contractor using an electric drilling rig to eliminate any fumes. The drilling rig worked almost continuously for 3.5months, amassing a total of more 1700 drilling hours in an incredibly humid environment..



Figure 11 - Ground Water Back Flow

An issue that needed to be addressed was the back pressure of water. Because the micropile tendon is hollow, the ground water found its way up the centre of tendon. A no return valve system was proposed and used on occasions to limit the return of ground water. The no return valve was fitted in to the hole of the hollow bar, at the drill bit end of the micropile. This allowed the flushing and grouting process to continue whilst stopping the flow of ground water up through the hollow micropile

TESTING

Grout Tests

The quality of the grout was tested for density, viscosity and bleeding. Cube samples were taken of the production grout, by the grout mixer operator. The samples were taken at a frequency of three cubes per shift and tested at 28 days. The grout cubes were cast, cured and tested to ASTM C109, in an independent accredited laboratory.

In addition the compressive strength of the micropile production grout was tested according to DIN EN 445.

Tension Test

Preliminary micropile tension tests were carried out as per the project specification, in order to verify the design of the micropile system and construction methods. The preliminary tests were performed outside of the project area to avoid any risk to working micropiles or damage to the slab.

In total 16 proof tension tests were carried out, in line with the consulting engineer's specifications, which included the following test load schedule.

Table 1 – Testing Regime

Stage	Load	Hold Time
1	AL	1 minute
2	0.25 DL	1 minute
3	0.50 DL	1 minute
4	0.75 DL	1 minute
5	1.00 DL	1 minute
6	1.33 DL	60 minute Creep Test
7	1.67 DL (Max. Test Load)	1 minute
8	AL	1 minute

All the tests followed the project specifications, with all 16No. tension tests passing the design criteria



Figure 12 – Test Set Up

Push out tests were also carried out on the micropile head arrangement to test the connection at the grout/concrete slab and grout/steel bond interfaces.

CONCLUSIONS

In total 312No. 15.0m 40/20 micropiles and over 580No.3.0m tube a manchette steel grouting tubes were successfully installed using the preventer system. The system eliminated the need to temporarily dewater the site, which was an advantage to the client, considering the close proximity of a major underground metro station. It is estimated that the use of the preventer saved the project nearly AED 2,000,000 in temporary dewatering costs. The preventer provided a safe, economical and fast method of micropile installation for a confined, complex project that had a high water table.



REFERENCES

EN14199 – 2005 –Execution of Special geotechnical works - Micropiles

FHWA (SA-97-070 June 2000) Micropile Design & Construction Guidelines

DIBt (German Institute of Building Technology) – National Technical Approval – Z - 34.14.209 – December 2014

Engineering Geology of Dubai – UAE – Emad Sharif & Mohd. J. Ahmed – January 2010

ACKNOWLEDGEMENTS

A special thanks to Omar Boughannam (Project Manager) and Paulo Lopes (Technical Manager) of NSCC International.

A CASE STUDY ON THE CONSTRUCTION AND FIELD LOADING TEST OF WAVEFORM MICROPILE

Young-Eun Jang[1], Jin-Tae Han[2], Ki Won Park[3], Myung Cheol Pyun[4]

ABSTRACT

For improving the behavior of the conventional micropile, a new-concept waveform micropile was suggested. The waveform micropile has a modified construction process, and the waveform shape on the pile shaft is formed through jet grouting. The waveform micropile provides additional shaft resistance due to the shape of the waveform grout body, which was confirmed through a series of experiments and numerical analysis. In this study, 96 waveform micropiles were applied to a bridge abutment construction site, and their field applicability was evaluated based on the construction process and loading test. The paper discusses the details of the design and installation of the waveform micropile, including the loading test results.

INTRODUCTION

Even if the micropile has a small diameter (less than 300 mm), it brings relatively high frictional resistance provided through the high-strength steel bar and the surrounding grout. Micropiles have been widely used to support different types of static and seismic loadings. They are also known as a solution for construction sites located in congested areas. The use of micropiles, however, leads to higher construction costs compared to the use of the other existing foundation types as it requires the use of steel reinforcement. Also, micropiles provide much less tip resistance than skin friction due to their small diameter. Han et al. (2013) suggested the use of a modified conventional micropile named “waveform micropile” for improving not only the cost efficiency but also for extending its application to other areas. As the name implies, the construction process of waveform micropile requires the formation of a grout body with a waveform

[1] Ph.D. candidate, UST (University of Science & Technology), South Korea, 82319100237, 82319100561, yejang@kict.re.kr

[2] Senior researcher (associate professor, UST), Korea Institute of Civil Engineering and Building Technology, South Korea, 82319100259, 82319100561, jimmyhan@kict.re.kr

[3] Executive vice president, DAERYUN Construction Co., Ltd, South Korea, 8229063010, 8229063020, pkw4961@naver.com

[4] President, DAERYUN Construction Co., Ltd, South Korea. 8229063010, 8229063020, mcpyun@daeryeon.com

shape through jet grouting. Figure 1 shows a comparison of the conventional micropile and the waveform micropile. The configuration of the waveform micropile can be described with the pile shaft (D_2) and the shear key (D_1) diameters. As grouting instead of the conventional casing is employed in the installation of the waveform micropile, better contact between the waveform grout and the ground was expected to be achieved, and the overall bearing capacity was ultimately expected to increase. Jang & Han (2015) and Jang & Han (2016) examined the constructability and behavior of the waveform micropile through experimental studies. The field and laboratory test results showed that the waveform micropile can be installed under in-situ conditions, and that its bearing capacity significant increases compared to the conventional micropile. The waveform micropile system was applied to a bridge construction site as an abutment foundation. This paper introduces the construction project, from its overview to the detailed issue in the geotechnical aspect related to the construction of the waveform micropile.

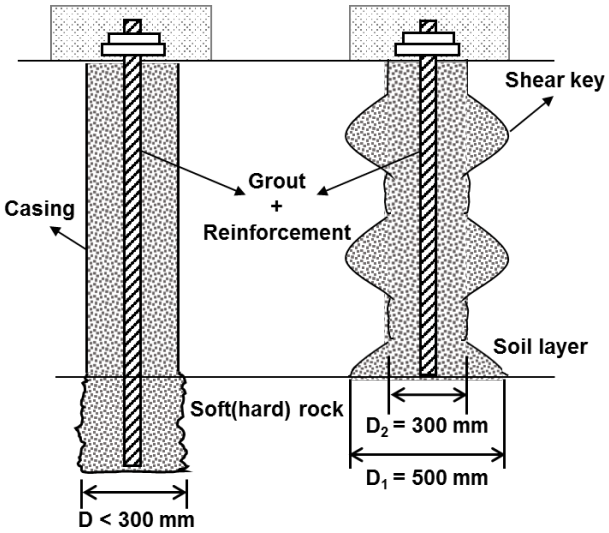


Figure 1. Comparison of micropile configurations

SITE INVESTIGATION AND PILE DESIGN

The waveform micropile system was constructed for the abutment foundation located at the highway expansion site in the City of Gyeonggi, South Korea. The steel pipe pile was originally assigned for use at the site, but it was changed to waveform micropile to obtain constructability at a limited working space near the abutment. A total of 96 waveform micropiles were planned to be installed at location groups A and

B based on the SPT values and loading conditions as shown in Table 1 and Figure 2. To ensure stability against lateral loads such as the live load, and the earth pressure, the upper 2 m of the pile was installed with a steel casing. First, the vertical bearing capacity of the waveform micropiles were calculated using Eq. 1 suggested by the FHWA (Federal Highway Administration) Micropile Reference Manual (FHWA, 2005).

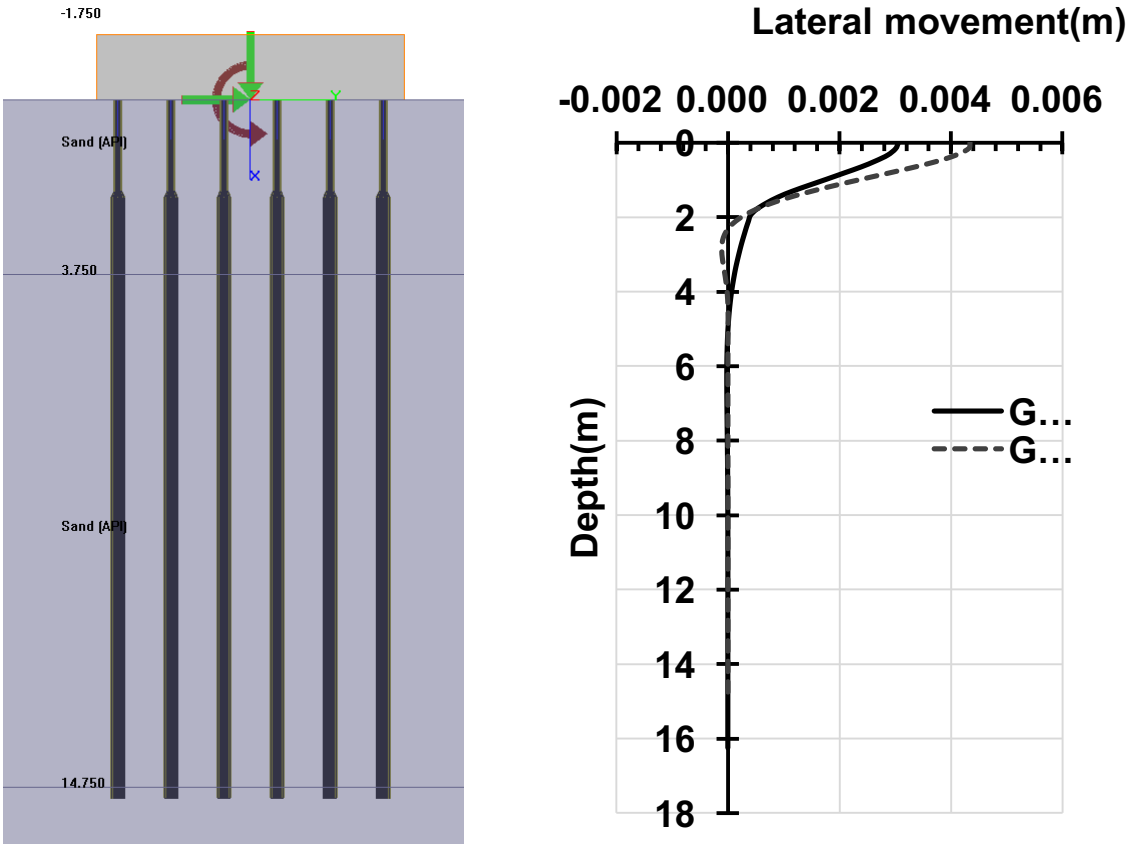
$$Q_a = \alpha_{bond} \cdot D \cdot L/\mathrm{F.S.} \quad (1)$$

Where, α_{bond} is the grout-to-ground ultimate bond strength (kPa), *D* is the diameter of the pile, *L* is the bond length of the pile, and *F.S.* is the factor of safety. The diameters D_1 and D_2 of the waveform micropiles were 500 and 300 mm, respectively. However, for bearing capacity calculation, we assumed a waveform micropile diameter of 300 mm (D_2) in order to obtain a conservative value. The α_{bond} values were selected from the FHWA manual considering the grouting method and the ground characteristics. The allowable design capacity Q_a of the waveform micropiles was determined using an F.S. of 2.5, as shown in Table 1. The results showed that the waveform micropile system was enough to resist the vertical force (P) of 400 kN with the allowable design capacity of about 800.2 kN for group A and 733.2 kN for group B. Then the lateral stability of the pile was evaluated using the software Group v7.0. The analysis result showed that the lateral displacement of piles in groups A and B was very small as shown in Figure 2, which indicated that the waveform micropiles were capable of supporting the lateral force 60 kN for the project site. For the numerical analysis, we also assumed a simplified geometry with a single diameter of 300 mm which corresponds to D_2 of the waveform micropile as shown in Figure 2(a).

Table 1. Design bearing capacity calculation results

Location	**Depth (m)**	**Soil type**	**α_{bond} (kN/m^2)**	**Q_a (kN)**
Group A	2.00	Silty sand with gravel	Casing	
	1.70	Silty sand with gravel	240.0	153.7
	11.0	Silty sand	130.0	539.1
	1.50	Silty sand	190.0	107.4
	Design bearing capacity Q_a/pile			800.2
Group B	2.00	Silty sand with gravel	Casing	
	1.50	Silty sand with	240.0	135.7

		gravel		
	10.0	Silty sand	130.0	490.1
	1.50	Silty sand	190.0	107.4
	Design bearing capacity Q_a/pile			733.2



(a) Pile group modeling (b) Lateral movement-depth response

Figure 2. Lateral movement analysis of waveform micropiles

Figure 3 shows the construction details of the micropiles. A total of 96 piles were installed and 48 piles (24 piles x two locations) at each location for groups A and B, respectively. The layout for each location was 4 x 6, and the minimum center-to-center pile spacing was 2.5 times the shaft diameter D_2 (300 mm) of waveform micropile.

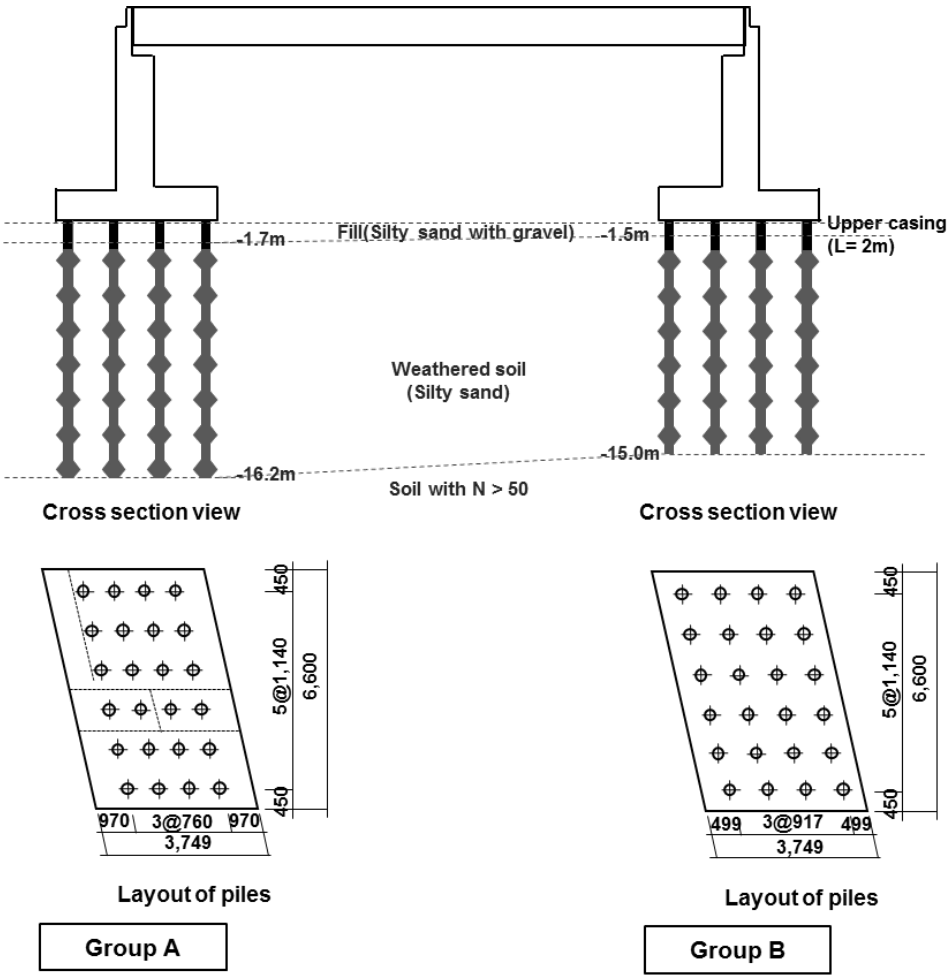


Figure 3. Description of the pile arrangement and layout for the construction

INSTALLATION OF THE WAVEFORM MICROPILE

The general construction process of the waveform micropile consists of the following four steps, as presented in Figure 4.

Step (a) - Drilling the pile shaft up to the required depth using a waterjet

Step (b) - Forming a waveform grout body by enlarging the pile shaft using the jet grouting method

Step (c) - Placing steel reinforcement in the waveform grouting

Step (d) - Completion of construction

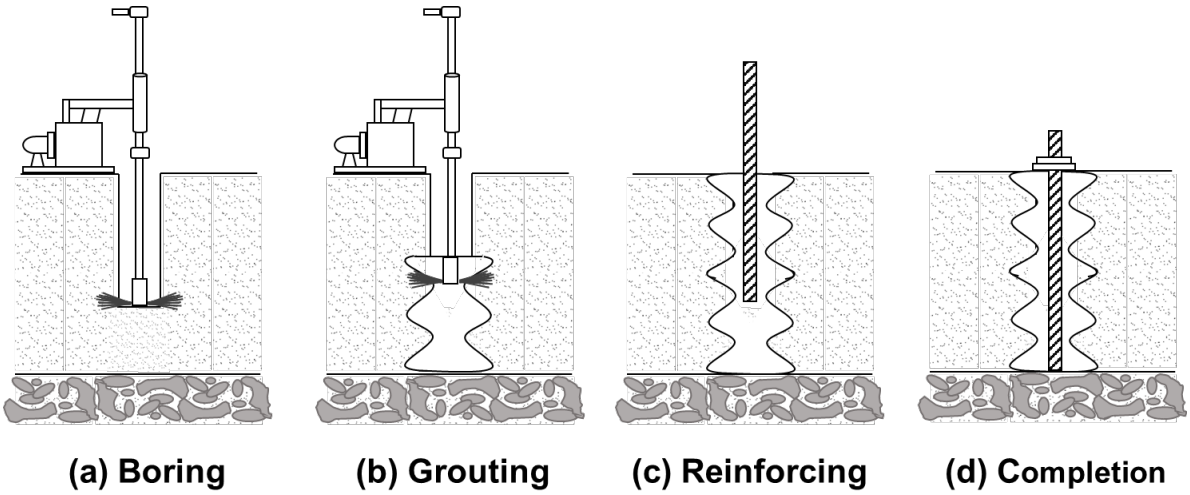


Figure 4. Construction process of the waveform micropile

The installation works of the 96 waveform micropiles in this study were performed with the construction steps. For the shear key formation of waveform grouting, the grouting injection time was controlled for enlarging the pile shaft to 300 and 500 mm, while the grouting pressure was fixed at about 400 bar. Figure 5 shows the construction steps of the waveform micropile: site preparation, pre-installation of the upper casing, drilling, and jet grouting work.



(a) Site preparation



(b) Inserting the casing (L=2 m)



(c) Boring the ground with a waterjet



(d) Jet grouting



(e) Reinforcing with a steel bar



(f) Completion

Figure 5. View of the field construction of the waveform micropile

LOADING TESTS AND RESULTS

The loading tests were conducted to evaluate the stability of the waveform micropiles under the vertical and lateral forces. Figure 6 presents the test facilities for the pull-out and lateral loading tests. Two pull-out loading tests and two lateral loading tests were carried out on a single waveform micropile, which was randomly selected from groups A and B. According to the FHWA manual, the maximum load that can be applied for the proof test for evaluating the vertical pile's stability is about 160% of the design bearing capacity. Therefore, the pull-out loading tests were conducted until the test load reached about 640 kN, following the loading test standards of ASTM D1143-81 (2007). The lateral loading tests were also performed by loading the pile with a 60 kN

increasing force. Both tests were very carefully continued while monitoring the movement of the pile head to prevent unexpected disturbance to the piles and the adjacent ground. During the tests, the load-movement response of the pile was measured using displacement transducers (LVDTs).



(a) Pull-out loading test (b) Lateral loading test

Figure 6. Pictures of the loading test of the waveform micropile

Figure 7 and 8 present the test results of the load-displacement curves determined through the pull-out and lateral loading tests, respectively. As the tests were carried out to prove that the piles were properly installed and stabilized, the ultimate bearing capacity could not be estimated. Thus, only the displacement at the design load was verified according to the tolerable movement criteria of abutment foundation as summarized in Table 2. As shown in Figure 7, the pull-out loading test was finished at about 160% (640 kN) of the design load 400 kN. The vertical displacement at the design load was 4.3 mm for group A and 2.2 mm for group B, and therefore it was considered relatively small compared with the allowable vertical movement of 40 mm and 50 mm as presented in Table 2. This indicates that the bearing capacity of the piles are sufficient to resist the loading conditions of abutment. The verification test results for the laterally loaded pile are shown in Figure 8. As explained above, the test load was applied with a step-by-step increasing rate while monitoring the displacement of the pile head to prevent any effect on the pile stability. The final loading step was 130% (76 kN) of the lateral force, and the displacements were 7.9 and 0.5 mm, corresponding to the 60 kN lateral force. The lateral displacements at both locations were small, but the reason why group A showed much smaller displacements seems to be related to the difference in N values between the two groups. Compared to the allowable lateral movement of 38 mm and 25 mm shown in Table 2, it was found that

the waveform micropile provides enough stability against lateral loadings (Bozozuk, 1978; Moulton et al., 1985).

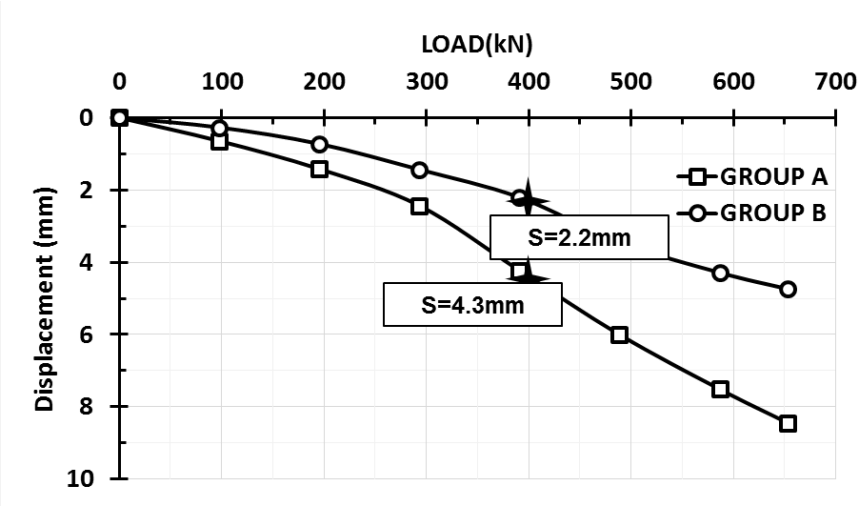


Figure 7. Pull-out loading-settlement relationship for the waveform micropiles

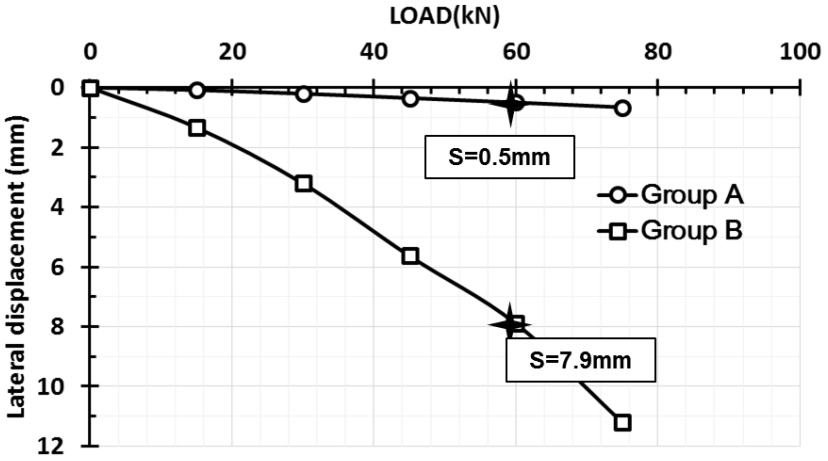


Figure 8. Lateral loading-settlement relationship for the waveform micropiles

Table 2. Tolerable movement ranges for abutment foundation

Criteria	Reference
Vertical movement 40mm Horizontal movement 38mm	Moulton et al., 1985
Vertical movement 50mm Horizontal movement 25mm	Bozozuk, 1978

CONCLUSION

This paper described the field application of the newly developed waveform micropile, which combined the concept of the conventional micropile with the jet grouting method to enhance the pile's performance. From the installation of 96 waveform micropiles for supporting the abutment structure, it was confirmed that the use of the waveform micropile system is an efficient construction method in terms of constructability and construction speed. Loading tests were carried out to verify the vertical and lateral behaviors of the waveform micropile, and the test results demonstrated that the field application was successfully performed.

ACKNOWLEDGEMENT

This research was supported by a grant from "Design and construction of artificial ground with the vertical spaces above existing urban infrastructure" which is funded by the Korea Institute of Civil Engineering and Building Technology (KICT).

REFERENCES

ASTM D 1143-81 (2007), *Standard test method for piles deep foundations under static axial compressive load*, Annual book of ASTM Standards.

Bozozuk, M. (1978), *Bridge Foundation Move*, Transportation Research Record No. 678, Transportation Research Board, Washington, DC, pp. 17-21.

FHWA (2005), *Micropile Design and Construction: Reference Manual*, FHWA-NHI-05-039, Federal Highway Administration, Vol. 1, No. 1, pp. 7-28.

Han, J. T., Kim, S. R., Jang, Y. E., and Lee, S. H. (2013), "Evaluation of bearing capacity of waveform micropile by numerical analyses", *Journal of the Korea Academia-Industrial cooperation Society*, Vol. 14, No. 11, pp. 5906-5914.

Jang, Y. E., and Han, J. T. (2015), "Study of load capacity of waveform micropile by centrifuge test", *Proc. Of the 25th International Offshore and Polar Engineering Conference*, International Society of Offshore and Polar Engineers, pp. 700-706.

Jang, Y. E., and Han, J. T. (2016), "A study on the constructability and load bearing characteristics of the waveform micropile by field tests", *Proc. Of the 69th Canadian*

Geotechnical Conference, Canadian Geotechnical Society, pp. 1-6.

Moulton, L. (1985), *Tolerable Movement Criteria for Highway Bridges*, Federal Highway Administration Publication Report No. FHWA-TS-85-228, pp. 99.

MICROPILE FOUNDATION – THE EASY WAY

Dipl.-Ing, Andreas Brandner, IB-Brandner, Karl-Schoenherr-Strasse 8, A-6020 Innsbruck – Austria, Phone +43 512 563 3320, Fax +43 512 563 3324, Email office@ib-brandner.com

ABSTRACT

Micropiles are an upcoming foundation element and many colleagues – designers as well as contractors - are surprised about the possibilities.

But Micropiles are not something new – they have been used already for a very long time as foundation elements. What´s new are the materials used. Very simple and easy to use are Ductile Iron Cast Piles, which are in use in Europe since the beginning of the 90-ties – especially in Austria. Admissible bearing capacity varies between 300 kN up to 1100 kN depending on diameter and wall thickness. The main part of the pile system is the coupling, which enables an "unlimited" length and besides that no wasted piece of ductile iron cast pile. Combined with a reinforcement bar the piles can also be used for tension piles.

1. SHORT GLIMPSE ON HISTORY

In historic times, micropiles were widely used as foundations for prehistoric buildings to protect them against flooding, wild animals and neighbours. These piles were timber logs – diameter around 15 cm and lengths between 3-5 meters, depending on the needs and water level. To protect the piles against wave impacts blocs of stone were placed around the foundation.

Buildings on pile foundations can be traced back to the Neolithic age and are in use up to present.

World famous examples of pile foundation made of timber logs are Venice in northern Italy, Amsterdam or Hamburg.

At the beginning of the past century micropiles made of steel – pipes or steel girders -, reinforced concrete – precast or made in place – replaced the wooden piles.

After a technology transfer – licence agreement – in 1986 between Gustavsberg AB and TRM Ductile Iron Cast Piles were developed in Austria, where the story of success began.

2. SYSTEM DESCRIPTION

Basic material developed in early 1960 provided everything a rugged pile system needed – ductility, corrosion resistance, impact strength and easy handling were part of the story of success. Within 30 years more than 7 million m of pile pipes were produced and installed all over the world.

Core element is the patented coupling, which enables a varying length without limitation. The Ductile Iron Pile has a coupling, which is bending resistant and friction locked. Assembling can be done without tools or welding. Piles can be driven by hydraulic blow hammers mounted on excavators and filled with mortar working as end bearing piles or in addition the ring gap was injected with mortar and the piles working as friction piles. In addition, the Ductile Iron Piles are corrosion resistant and environmentally compatible and due to recyclability sustainable in a high aspect.



Figure 1 – coupling of DIP after 30 years

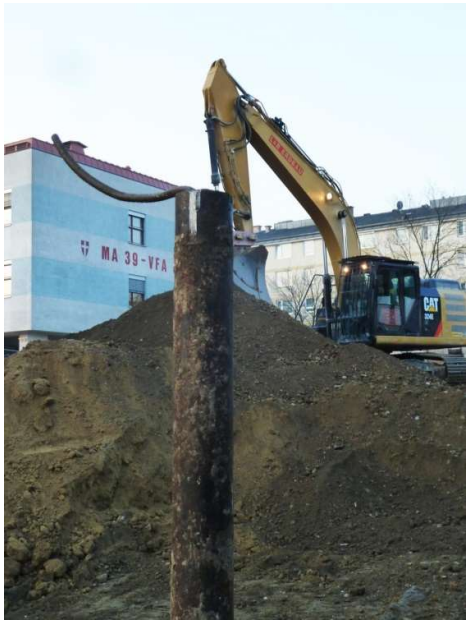


Figure 2 – excavated pile after 30 years of use

Admissible bearing capacity varies between 300 kN to 1100 kN depending on diameter and wall thickness.
Specially designed driving shoes for different types of soil depending whether the pile will be injected or noninjected provide ideal adaption to the needs on site.
Parts such as coupling sleeves, pile-caps, pipe support shoes are available for the system.



Figure 6 – special parts

Depending on ground properties ductile piles can be prepared as grouted and concrete filled friction piles or nongrouted either filled with concrete or not end bearing piles.
The pile shoe is the base for the pile tubes which are inserted into the conical socket of the element before pile driving. The full displacement pile is driven to the final depth, which can be fixed on site during execution - based on pile testing parameters. Excess length is cut off and can be reused so no debris and disposal costs, no reworking of pile heads, no trimming losses and no unusable sections. Besides that, groundwater balance is not changed while driving from above.
Another advantage is the short construction time – 200-400 m per day can be installed.

3. STRUCTURAL AND GEOTECHNICAL DESIGN

Design can be done per Eurocodes – EN 1990, EN 1991-2, EN 1992-2, EN 1993-2, EN 1997-1, EN 1537, EN 14199, national regulations concerning bridges released by FSV and approvals – or other national codes and standards. European codes allow the design following the semi probabilistic safety concept using partial safety coefficients. Due to class of importance and

complexity EN 1990 demands for geotechnical design and execution at least an independent check of both. Following this 4-eye principle – design independently checked and released - and special site supervision provides required safety of foundation system. Driving criteria can be fixed based on test results either for end bearing piles – no further movement of pile while hammering or max 10 mm movement within 20 second in dense non-cohesive and stiff cohesive soils.

In medium dense or loose non-cohesive soils a friction pile is the choice. In medium dense soils the bearing capacity of ductile piles varies between 90 kN/m for a 118-mm pile with 190 mm shoe and 118 kN/m for a 170-mm pile with 250 mm shoe.

Due to minor stiffness micropiles may only be charged by axial loads – horizontal loads can be taken by installing battered piles.

4. EXAMPLES OF DUCTILE IRON PILES FOUNDATIONS

Some examples will show the versatile use of the ductile iron pile system.

4.1 Bridge foundation

To meet the safety demands of the aviation authority the runway of Innsbruck Airport had to be elongated and therefore the riverbed of nearby river Inn had to be moved. To meet the logistic challenges of the huge excavation transport necessary for the move of the riverbed a temporary bridge suitable for a maximum capacity of 50-ton dump truck had to be erected. With a total length of 63 m and two spans of 30 and 33 meters the two abutments and one bridge pier had to be built. The contractor awarded with the earthworks for the airport chose the proposition of IB-Brandner to use the ductile iron cast system as foundation for the abutments and the pier. As the site was at the border of the water protection and conservation area for the City of Innsbruck water supply the use of concrete and injection was not allowed. Ground conditions showed a layer system of river deposits of silty sand, sand, sandy gravel with a medium density.

Design and burdens had to be coordinated with the waterways authority. During construction period the foundation had to meet the demand of a 25-year flooding and ice impact. To protect the piles from washout and wave impact, boulders of 2 tons per piece were grouped round the pilecap of the pier and the pilecaps for the abutments.



Figure 7 – Pile driving for pier foundation



Figure 8 – driven piles – straight and battered

To manage the horizontal loads battered piles were provided and for tension piles a reinforcement bar was inserted after piledriving was finished and grouting was executed.

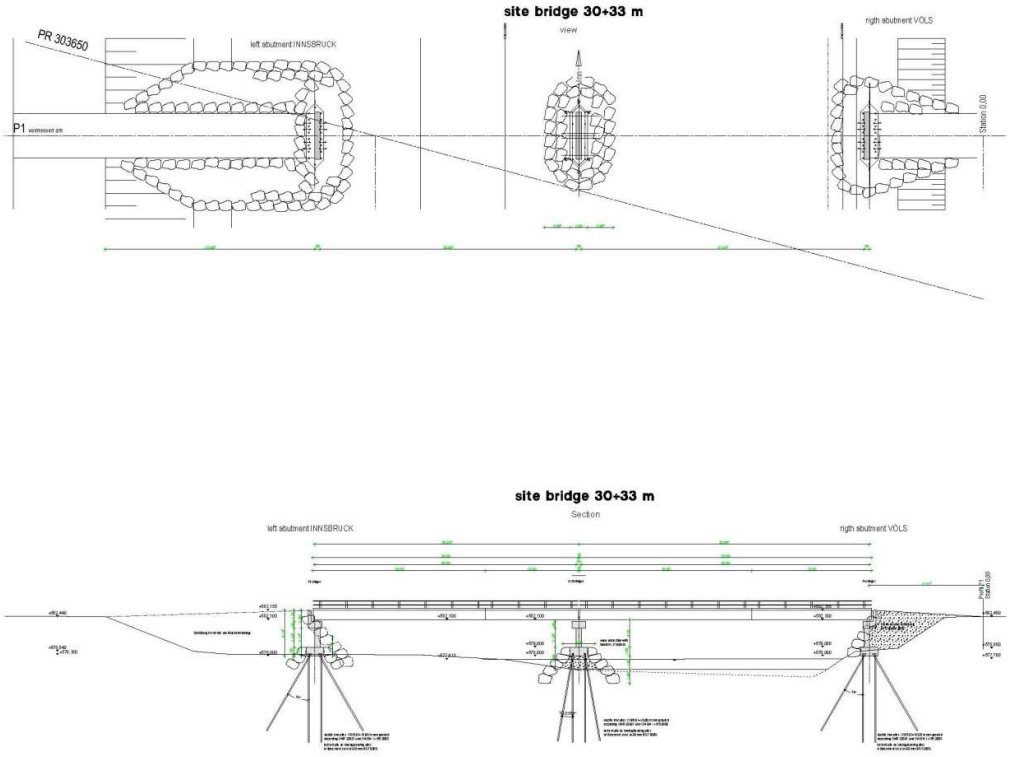


Figure 9 – Bridge foundation – view and section

Pile driving works for the pier was done from the left abutment side, where only little backfill had to be done for enabling the excavator to reach the piling platform. All foundation work was executed during low water season – autumns and early winter – and the bridge could be opened after a short construction period of 2 months due to a prefabricated steel superstructure.

After the move of the riverbed was finished the bridge including foundation had to be dismantled, the piles were cut by an excavator mounted hydraulic cutter at the bottom of riverbed.

4.2 Slope Stabilization

Near Vienna at the S1 highway around the city a slope slide occurred after completion of earthworks and recultivation. Access to the site was restricted as the highway could not be closed completely but traffic was deviated.

To stabilize the slide a dowel system was chosen using ductile iron piles instead of GEWI-piles. Piledriving was done in a few days with an excavator mounted hydraulic hammer on a slope with 30° inclination.



Figure 11 a+b – Slope stabilization on S1 highway Austria

4.3 Noise protection Wall Foundation

Along a railway line in France a noise protection wall had to be erected. As foundation system, ductile iron piles were chosen to meet the needs of design to carry the loads and the time schedule. Two piles for each foundation had to be driven close to the railway line and the electric supply lines. Due to the flexible installation, the challenges could be managed in a technically outstanding and commercially competitive way. As there occurred also tension in the piles a reinforcement bar was provided to take up this impact.



Figure 12 a+b – noise protection wall foundation France

Piles were grouted friction piles of 5 m length.

4.4 Foundation of a residential building

At a slope above Innsbruck a residential building was to be erected. Ground conditions were rather complex – beneath a manmade backfill of 1,50 m a 2,50-m layer of peat covered the final dense sand layer. Below the peat permanent surface water flow lead to saturated sand, which became soft and tricky while disturbing it. In an alternative design IB-Brandner changed the proposed foundation with drilled micropiles to the ductile iron pile system. Pipes with 170 mm diameter and 9 mm thickness were used to take the foundation loads of the building and

leading these loads to a stable ground. Space was restricted on site, so work was done with one excavator for the earthworks as well as for piling.



Figure 12 a+b – piling works residential building



Figure 13 – preparation of foundation level

Piles were grouted friction piles of up to 15 m length depending on depth of stable ground. The choice of this pile system saved in total € 65.000 , of which the contractor got 50% and made a good deal.

4.5 Foundation of electric power line

To strengthen the reliability of the electric power supply in Austria a new HT power line had to be erected. As an alternative proposal for the foundation of the towers, the contractor suggested to use ductile iron piles. As the piles were alternating load piles tension had to be considered. The solution was to insert reinforcement bars into the grouted pile.



Figure 14 a+b – piling works electric power line HT

Piles were grouted friction piles of up to 15 m length depending on depth of stable ground. Executed lengths were fixed on site per driving progress. Advantage was the simple and cheap installation and flexibility on site.

4.6 Pit lining for a residential building

General Contractor BODNER awarded IB-Brandner just 3 weeks ago, with the design of a pit lining for a residential building in Innsbruck. As neighbors, did not agree to anchoring into their property and stiffening would hinder the contractor from effective excavation and concrete works, a slender and rigid solution had to be designed. Space available was just 35 cm for the whole pit lining system. For the first time the ductile iron pile system was used not as a foundation system but was used for pit lining in combination with shot concrete.

Ground conditions showed beneath a layer of backfill 1 m, a layer of dense silty sand covering the final ground consisting of medium dense sandy gravel.



Figure15 – ground conditions

After the first 2 piles, it came out that the provided shoes did not work for this kind of work – the necessary rigid clamping length of the pile to work as a cantilever beam could not be reached. So, it was decided to leave the shoe off and the piles were driven without a shoe into the ground. With this method, we could meet the design requirements and could excavate the pit without a stiffening beam construction. The space between the piles was filled with a reinforced concrete arch.



Figure 16 a+b – pit lining piles and shot concrete arches

To meet these requirements for pit linings as well and to create a new field IB-Brandner works together with the pipe producer on the design of a new driving shoe, which enables the pile driving to greater depth.

5. SUMMARY

The development of ductile iron cast piles as an additional market for pipes, starting in the 80s, was the right decision. A “simple to use” system showing advantages against other pipe type piles - technically as well as commercially was born. The system is ideal for sites anywhere on the globe and suitable for any project size – from small to big.
The examples shown demonstrate the versatility of the ductile iron pile system and the advantages compared to other driven steel piles:

- Corrosion resistant pile material (better than regular steel pipe)
- Impact resistant
- Simple and reliable rigid connection in the coupling
- No waste pipe on site – flexible length
- Recyclability of pipe material
- Environmentally non hazardous
- High capacity for a micropile
- Easy to work with – hydraulic hammer, excavator, grouting pump

- Low noise production
- Low vibrations
- Commercially competitive – 200-400 m/day

References:

30 Years of Ductile Iron Piles – *EADIPS European Association for Ductile Iron Pipe Systems, FRG Fachgemeinschaft Guss-Rohrsysteme (FGR) e.V.*

TRM – *Ductile cast-iron piles Technical report*

EN 1990 Eurocode – *Basis of structural design*

EN 1991-*2 Eurocode 1: Actions on structures – Part 2: Traffic loads on bridges*

EN 1992-2 *Eurocode 2: Design of concrete structures — Part 2: Concrete bridges — Design and detailing rules (consolidated version)*

EN 1993-2 *Eurocode 3 — Design of steel structures — Part 2: Steel Bridges (consolidated version)*

EN 1997-1 *Eurocode 7: Geotechnical design — Part 1: General rules (consolidated version)*

EN 14199 *Execution of special geotechnical works — Micropiles*

ON B 2567 *Piles of Ductile Iron – Dimensions, installation and quality assurance*

DIBt Z-34.25-*230 Allgemeine Bauaufsichtliche ZulassungTRM DUKTILRAMMPFAHL 04.11.2013*

STUDY OF DIFFERENT APPLICATION EFFICIENCIES AND SIMULATION MODELS FOR MICROPILES ON SLOPES

Ching-Jiang Jeng[1] Chih-Chang Lin[2]

ABSTRACT

This paper discusses the application of micropiles on slopes along constructions and castle walls in historical site maintenance. Using the PLAXIS finite element method to perform simulations. The attainable results include that underpinning and strengthening with inverted L-shaped micropiles in coordination with low-pressure grouting reinforcement can increase the safety factor of slopes along the castle wall of historical sites, improve the foundations of the castle walls to substantially reduce the total amount of displacement, significantly inhibit the settlement, and alleviate the subsidence trend of the foundation structure of castle walls. Likewise, gantry-style micropile reinforcement methods can enhance the safety factor, reduce the total amount of displacement, as well as inhibit and alleviate the soil settlement. In summary, micropiles can indeed be used to provide useful stability to the foundation and inhibit the displacement in order to strengthen the slope state along the castle walls of historical sites, where the working space is relatively narrow. It is anticipated that the analytical results of this paper can be used as a reference for similar projects.

Keywords: micropiles, PLAXIS numerical analysis, application efficiencies, slope stability.

1. INTRODUCTION

In this paper, the finite element program of PLAXIS was used to conduct an in-depth analytical study on the effectiveness of micropiles when applied to slopes for the maintenance and strengthening of historical sites. PLAXIS, the finite element program, was adopted to conduct stability analysis on the retaining wall structure of micropiles.

The derivation method of the PLAXIS program for safety factors adopts the stress behavior of micropiles during the sliding displacement on stratum. When doing a safety analysis using the ϕ/c reduction method, that is conducting repeated reductions on the soil strength parameters (c values of soil cohesion and tanψ of

[1] Associate professor, Huafan University, Department of Environmental and Hazards-Resistant Design, New Taipei City, Taiwan, 886-2-26632102, 886-2-26639003, jcjhf@cc.hfu.edu.tw
[2] Master, Huafan University, Department of Environmental and Hazards-Resistant Design, New Taipei City, Taiwan, 886-2-26632102, 886-2-26639003, jcjhf@cc.hfu.edu.tw

friction angles within soil). The strength reduction factor (RF) during the moment of destruction is defined as the safety factor (Fan & Chien, 2004).

In this study, the analysis cases for maintenance applications of micropiles on slopes along constructions and castle walls of historical sites are discussed. Currently, there are many engineering disaster remediation methods commonly used, yet the micropile method has special applicability in situations where the relatively narrower areas along the boundary lines require the use of small equipment. In this paper, the effects of actual cases with and without a micropile retaining structure are discussed and the effect of rainfall on the analysis results.

2. DISCUSSIONS OF ACTUAL CASE STUDIES

2.1 Case (1): Basic data survey of Ershawan Fort (Haimen Tianxian)

The site of this case is located on the uphill area of Zhongzheng Road in Keelung City. The historical site of Ershawan Fort, also known as Haimen Tianxian, (Refer to Figure 1 for detail). The strata of this site consist of mainly sandstone and siltstone, intercalated with shales. The rock quality is generally good. The ground surface has a layer of weathered overburden; the partial platform area may contain backfill. The slope surface is generally stable and has no potential slippage going down to the bedrock, thus only the backfill and overburden may have problems of local subsidence deformation. Being judged by the terrain contour lines that are outwardly steep convex, the foundation of the castle walls may be partially located in the backfill. In addition, owing to rainwater infiltration within the plaza of the fort, cracks appeared in the cement-mortar pointing between the rock blocks at a corner of the fort walls. Furthermore, slightly differential settlement also occurred in the wall foundation at the same site.

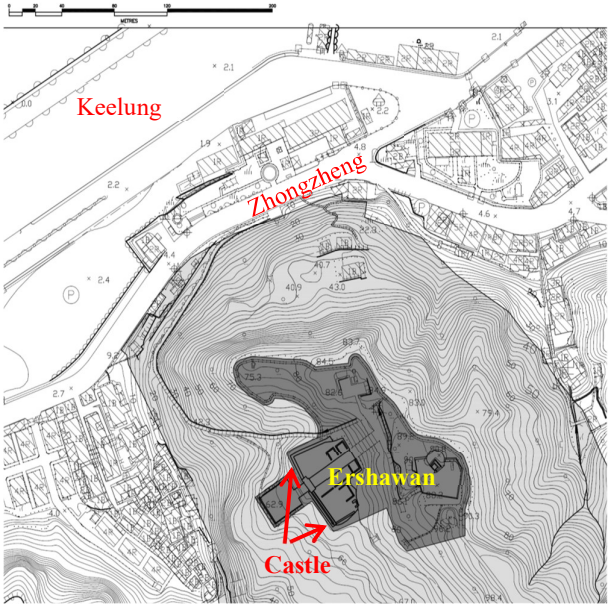


Figure 1: Map of historical site Ershawan Fort (Jeng & Yu, 2015)

Two holes, each with a depth of 15 meters, were drilled in the barrack area within the plaza of the fort; the positions of holes are shown in detail in Figure 2. In addition to the sampling test, an inclinometer is buried for subsequent monitoring purposes of slope displacement and groundwater level observation. According to the drilling results, the overburden layer beneath the ground surface of this site (3.6m ~ 4.1m depth) consists of yellow-brown and gray silty sand with rock fragments. The N-value of a standard penetration test ranges between about 7 to 12, which is classified as a loose to medium dense sandy soil layer. Whereby for the ground surface close to the BH-1 region (i.e. castle wall's corner), the overburden layer is about 2 ~ 2.5m and classified as backfill layer.

According to the test results, the unit weights of soil ranged between 19.0kN/m^3 ~ 19.3kN/m^3; the shear strength parameters C values ranged between 7.8kPa ~ 38.3kPa; ϕ angle ranged between 25.8° ~ 28.3°. Beneath the overburden layer is the rock formation. The rock formation mainly consists of sandstone to siltstone, where BH-1 showed more obvious weathering at first 1.7m thickness; its rock quality designation (RQD) index falls at about 16% to 33%, classified as poor to extremely poor. The indices of rock quality designation for the remaining soil layers can reach more than 75%, classified as good grades.

Inclinometers are also buried inside the drilled holes at this site in order to facilitate subsequent long-term observations on slope stability. After the drilling was completed and the initial values of inclinometers were observed, subsequent measurements were conducted on 27th November 2014. The results showed that there is downward slope surface displacement change at about 2 m depth below the ground surface of the BH-1 hole, the maximum displacement of the hole opening is about 2.7mm.

2.1.1 *Numerical analysis on the current state of the site*

The main slope stability analysis of the site focused on the cross-section stability of the slope in the backfill area at the northwest corner of the castle wall. Hereby in accordance with the drilling and test results, the slope stability analysis is conducted by analyzing the cross-sectional detail in Figure 3. The contents of analysis include the safety factor of the potential sliding surface, and settlement deformation analysis. The parameters obtained through the relevant tests are compiled in Table 1 and Table 2. The PLAXIS program is used to analyze the cross section of the current state (without remediation). The analysis results are shown in Figure 4 and Figure 5.

For the resulting safety factors under normal conditions and rainstorm conditions as well as the subsidence deformation analysis results, it is generally recommended that the safety factor of normal conditions is required to reach at least 1.5; whereas under rainstorm conditions, the safety factor is required reach 1.2. According to the results, regardless of slope conditions, both safety factors can reach above the generally recommended value, thus the slope stability is

generally regarded as safe. Moreover, according to the subsidence deformation profile results, the PLAXIS program analysis shows that a larger amount of subsidence will be distributed in the body of castle wall itself and the soil layer beneath it, thus there is the possibility of tension crack occurrence. The maximum displacement under rainstorm conditions is evaluated to be about 22mm (Figure 4); the vertical subsidence deformation of the foundation surface is about 4.5mm (Figure 5). The areas enclosed by subsidence profile as shown in Figure 5 is defined as subsidence sink area. The analysis results above more or less coincide with the changes in depth from the second inclinometer observations.

2.1.2 Analysis and comparison of the reinforcement options for the foundations of the castle wall

According to the concepts of reinforcement design, the reinforcement of this Case (1) is divided into four options for analyses and comparisons. Option 1 is a proposal of underpinning and strengthening the retaining wall by first imposing the micropiles and then adding low-pressure grouting. Option 2 is underpinning and strengthening the retaining wall reinforcement with micropiles using different types of volumetric grouting. Option 3 is a single-row of micropiles. Option 4 is a single-row of micropiles with grouting.

(1) **Option 1: Underpinning and strengthening – Micropiles and low pressure grouting** (as shown in Figures 2-3)

The existing castle wall is at the northwest corner of the barracks area. Obvious cracks have appeared in the cement-mortar pointing between the rock blocks at a corner of the castle walls. According to the stratigraphic drilling data and the foundation test results, it is determined that the cracks and subsidence of the castle wall should be related to its partially located in the backfill area. Thus, micropiles are used to penetrate the rock around the peripheral platform of the castle wall as measures for underpinning and strengthening the foundations of the castle wall as well as confining the slope displacement. One row of micropiles is drilled vertically in connection with another row of inclined micropiles to be laid with a horizontal angle of depression of 15 degrees toward the inside plaza (Fig. 3). The diameters of the holes are about 11cm to 15 cm; the length of the vertical pile is about 10m and the length of the inclined pile is about 15m. Steel pipes with a diameter of 76mm and thickness of 4mm were placed into the holes; mortar with 1:1 proportion of cement and sand was poured into the pile holes. The tops of the two rows of micropiles are joined with a reinforced concrete (RC) collar beam, wherein the inclined micropiles with the depression angle of 15° is additionally locked into steel plate by threading the endpoint of the micropile; while one end of the 75° edge-bend rebar was inserted into the steel pipe of the inclined micropiles, the other end is hooked to the collar beam as a joint. To prevent the micropiles from staggered influences between each other during the process of construction,

it is recommended that all the planar angles of construction of inclined micropiles are set to be parallel to the corner of castle wall at 45°(as shown in Fig. 2). Furthermore, to ensure that the contacting stress of the castle walls on the foundation is more balanced, an inclined grout hole is drilled inside the castle wall, local grouting reinforcement was carried out within the overburden layer of the castle wall's base bottom.

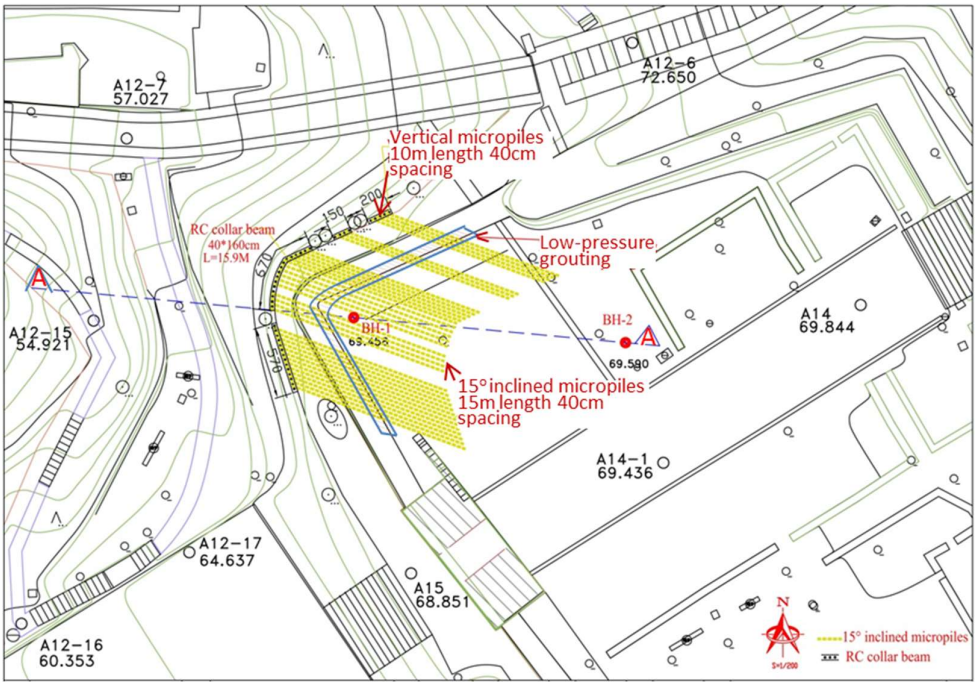


Figure 2: Plane diagram of the micropile configuration scenario for the underpinning strengthening and reinforcement of castle walls

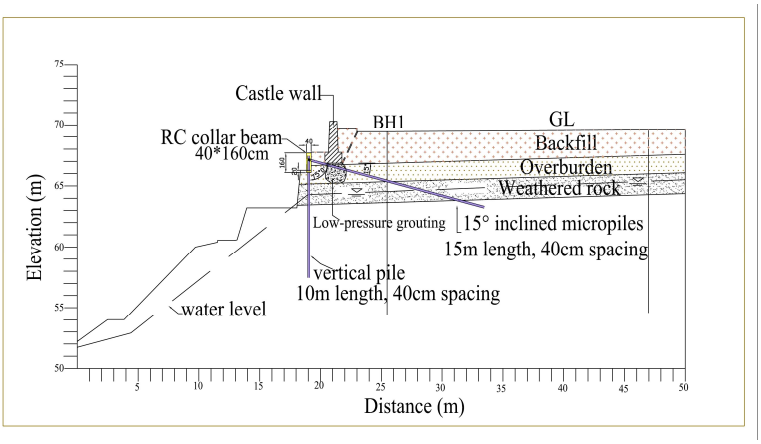


Figure **3**: Details of Cross-Section A where underpinning strengthening and reinforcement are imposed for Castle Wall

Table 1: Parameters of soil, rock formation, and grouting

Parameter / Soil layer	Cohesion **C** KPa	ø (degree)	**E** KPa	γ_t KN/m³	Poisson's ratio ν
Backfill	5	25	$2x10^3$	19.5	0.3
Rock formations	45	30	$9x10^6$	23	0.3
Weathered rock	40	30	$4x10^6$	22	0.3
Overburden	6	25	$4x10^3$	21	0.3
Castle wall	30	25	$2x10^6$	23	0.3
Grouting	40	30	$6x10^6$	23	0.3

Table 2: Parameters of micropile

Axial stiffness	EA	1.42×10^6	kN/m
Flexural rigidity	EI	$1.65x10^3$	kN˙m²/m
Equivalent thickness	d	0.4	M
Bulk Density	w	2	kN/m³/m
Poisson's ratio	ν	0.15	

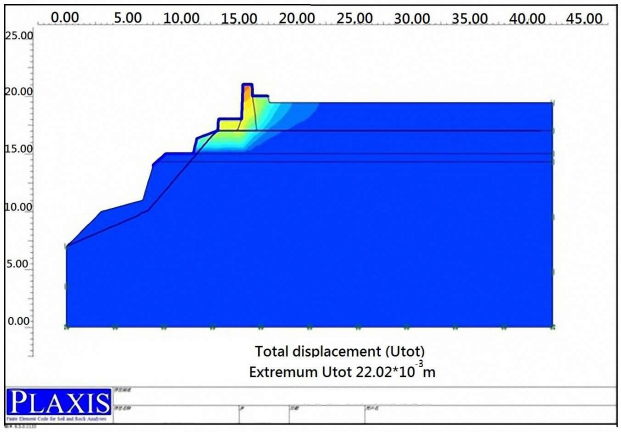


Figure 4: Current state - Rainstorm - Total displacement distribution(Maximum value of 22.02mm)

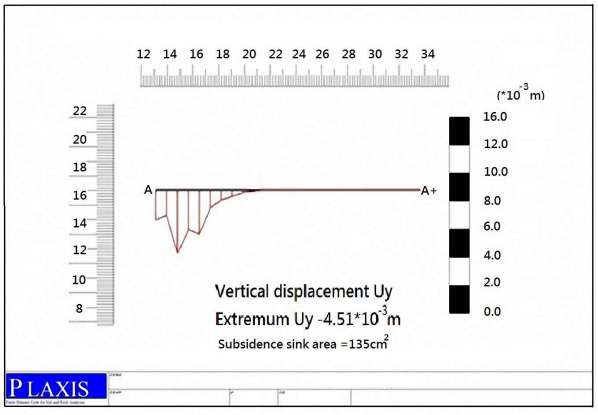


Figure 5: Current state - Rainstorm - Foundation subsidence profile (Maximum value of 4.5mm)

The results of the foundation reinforcement analysis by underpinning and strengthening the retaining walls of castle are shown in detail in Figure 6.
As indicated, after conducting reinforcement with micropiles and grouting (Volume of 2.0m x 1.6m/m length), the maximum displacement under rainstorm conditions can be reduced from 22mm to 7mm; while the vertical subsidence of the foundation of the castle walls can be reduced from 4.5mm to 1.25mm, that is to one-quarter that of the current state.

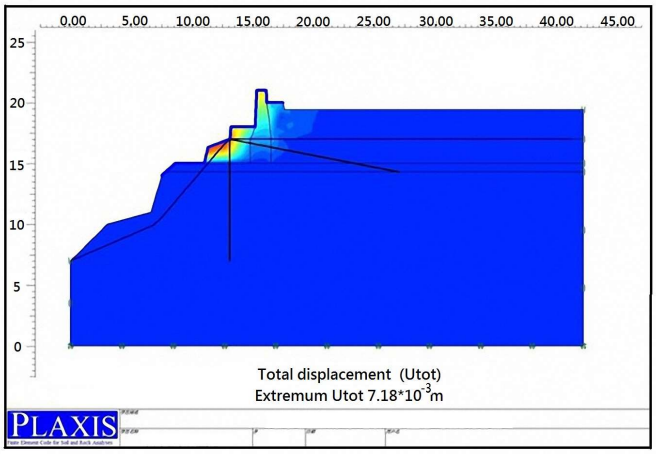


Figure 6: Total displacement after micropiling and grouting (Maximum value of 7.18mm)

(2) **Option 2: Underpinning reinforcement with Micro piles and different type/volumetric grouting**

Using micropiles as the underpinning reinforcement for the foundation of this confined space has advantages due to the particular applicability of the method in narrow spaces. The micropile with its horizontal angle of depression provides underpinning action to the foundation of the castle wall, but due to its small cross-section, there is a possibility of insufficient EI rigidity, thus low-pressure grouting is added to the foundation of the castle wall.

2.1.3 Comprehensive comparisons of the effectiveness of four options for Case (1)

After compiling the four options, the comparisons between each type of reinforcement are shown in Table 3. The comprehensive descriptions are as follows:
From Table 3, installing single-row vertical micropiles in the initial slope of the castle wall in its current state forms the retaining wall in the ground that directly enhances the safety factor by 5.6%. The maximum displacement is significantly decreased by 53.1%; the single-row vertical micropiles have improved the displacement resistance significantly. The amount of vertical subsidence of castle

wall's foundation has reduced by 37.6%. If further reduction of the soil deformation behind the retaining wall in the ground is required, it is necessary to add additional reinforcement measures. Below are the comparative discussions on the effectiveness of each reinforcement type as shown in Table 3.

Comparing Type 1 with Type 2, inserting single-row vertical micropiles with additional grouting will enhance the safety factor from 5.6% to 6.3%; controlling the maximum displacement amount, causes a progressive decrease from -53.1% to -58.4%; while the amount of vertical subsidence of the foundation of the castle wall decreases by 82.6% progressively from the initial slope condition. Thus, the single-row micropiles with grouting reinforcement can significantly improve the soil subsidence trend around the piles as well as reduce the amount of soil deformation after forming the retaining wall in the ground. Comparing the vertical subsidence sink areas of Type 1 and Type 2, Type 1 is 98cm^2; Type 2 is 15.6cm^2, thus a difference of 84% between the two is found.

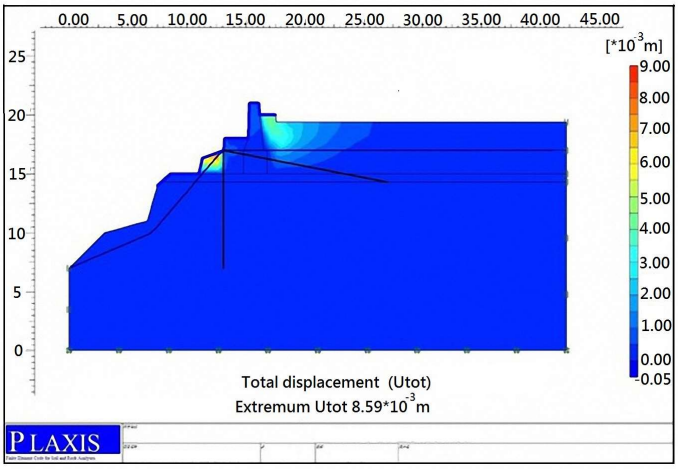


Figure 7: Micropiles + 1 times volume of grout – Rainstorm – (Total maximum displacement of 8.59mm)

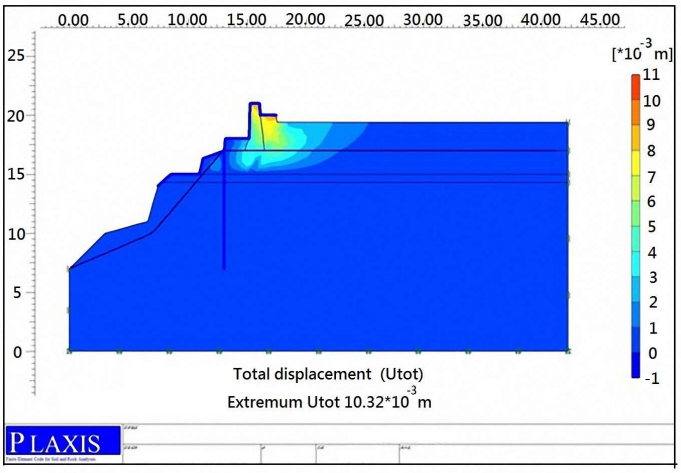


Figure 8: Single-row micropiles - Rainstorm – (Total Maximum displacement of 10.32mm)

Table 3: Comprehensive comparisons on the effectiveness of each option for Case (1)

Reinforcement Type / Comparative Item	(0). Initial condition	(1). Single-row vertical piles	(2). Single-row vertical piles with grouting	(3). Vertical and inclined piles with grouting	(4). Type (3) with 1.5 times the grouting in convex shape	(5). Type (4) with grouting in L-shape	(6). Type (3) with 2 times of the grouting
Factor of safety (FS)	1.723	1.820(+5.6%)	1.831(+6.3%)	1.919(+11.4%)	1.926(+11.8%)	1.902(+10.4%)	1.924(+11.7%)
Total displacement (mm)	22.02	10.32(-53.1%)	9.16(-58.4%)	8.59(-61.0%)	8.44(-61.7%)	8.70(-60.5%)	8.55(-61.2%)
Foundation Subsidence (mm)	4.49	2.80(-37.7%)	0.78(-82.6%)	0.77(-82.8%)	0.76(-83.1%)	0.33(-92.6%)	0.19(-95.8%)
Subsidence sink area (cm^2)	135	98(-27.4%)	15.6(-88.4%)	15.4(-88.6%)	15.9(-88.2%)	10.9(-91.9%)	6.2(-95.4%)

Note: the percentage in brackets means the effectiveness percentage compare to initial condition.

Comparing Type 3 with Type 1 and Type 2, the addition of inclined micropiles significantly improves the safety factor by 11.4%; the maximum displacement decreases significantly by 61% compared with the maximum value at the initial condition. Compared with Type 1 and Type 2, the displacement amount is decreased from 53.1% to 61%, with respect to Type 0; the value of declining magnitude has increased. Comparing Type 2 and Type 3 with Type 1, after using micropiles to form the retaining wall in the ground beneath the castle wall's foundation, the only differences are with or without grouting. The subsidence amount is directly affected so that it decreases significantly 82.9%. This proves that grouting can significantly improve the subsidence.

Comparing Type 3 with Type 6, when the volume of low-pressure grouting injected beneath the castle wall's foundation is increased by 2, the safety factor is increased from 11.4% to 11.7%; the maximum displacement can be decreased from the - 61% trend to - 61.2%; the magnitude has been slightly enhanced by 0.2%. While the maximum benefit is that the vertical subsidence amount of castle wall's foundation can be reduced from - 82.9% to - 95.8%, a decrease of 13%. Considering the vertical subsidence sink area, Type 3 has an area of 15.4 cm^2 and Type 6 has an area of 6.2 cm^2; the difference in the vertical subsidence sink area between the two decreases by 60%. Therefore, a larger grouting volume reduces vertical subsidence and also has the benefit of directly inhibiting the soil's vertical subsidence behind the retaining wall in the ground.

Comparing Type 4 with Type 5 that use different volumetric shapes of low-pressure grouting under the foundation of the castle wall, a comparison of the convex shape and the L shape at 1.5 times of the volume, shows that the benefits to the safety factor and the maximum displacement are only slightly different. While for the vertical subsidence amount of castle wall, the L shape can reduce

the -83% trend to -92.7%; for the vertical subsidence sink area, Type 4 has an area of 15.9 cm^2 and Type 5 has an area of 10.9 cm^2. The difference in the sink area of vertical subsidence for the two decreases by 31%. Thus, comparisons of the configuration type and the position show that the vertical subsidence sink position of the L shape closer to the castle wall's foundation has a more significant improvement on controlling the amount of soil vertical subsidence behind the retaining wall in the ground.

2.2 Case (2): Samantabhadra Temple (pu-shian shih) in Sanxia District

The site of this case is located along the slope of Samantabhadra Temple (pu-shian shih) on Touliaokeng Road, Sanxia District, New Taipei City. Due to erosion by typhoons and heavy rains in recent years, many places near the hall appear differential settlement, affecting the safety of access and surrounding buildings. The location of the site is shown in Figure 9.

2.2.1 Determination on the Cause of Destruction

The position of the disaster is located in the plaza next to the hall. Cracks and deformations have appeared on the square floor and boundary walls. According to the contour map and the field survey results, it has been determined that the main causes are because the plaza occupies a larger flat space, part of the boundary walls' foundation could be in the backfill zone, and the adjacent private land is in the steeper sloping surface. The current state is supported by a simple retaining wall and a short intersegment buttress, the disaster caused by differential settlement was triggered by heavy rains.

2.2.2 Planning Concept of Reinforcement Options

Adopting the gantry reinforcement option, micropiles are installed between the inside of the retaining wall and the square floor to penetrate into the rock. With a double-row pile configuration with an interval of 1.5 m between rows, a spacing of 40 cm in between piles, hole diameter of about 20 cm, and vertical pile length of 10m, the 37kg rail piles are inserted into the holes and mortar with 1:1 proportion of cement and sand poured into the holes. In between the double-row micropiles, the tops of the piles are connected with RC collar beam to form the gantry model to strengthen the micropiles and confine the slope displacement. The planar and cross-sectional details are illustrated in Figure 9 and Figure 10.

2.2.3 Stratigraphic Parameters of the Base

According to the on-site construction drilling survey results for the site of this case, the parameters of stratigraphic soil are compiled in Table 4; the micropile

parameters are listed in Table 5.

2.2.4 Analysis and comparisons of reinforcement options

For the analysis using the PLAXIS program, the result is shown in Figure 11. The following analytical method is a progressive step-by-step option analysis: Option1 is single-row piles; Option 2 is double-row piles; and Option 3 is double-row piles with RC collar beam. After the analysis, the results and the current state were compared.

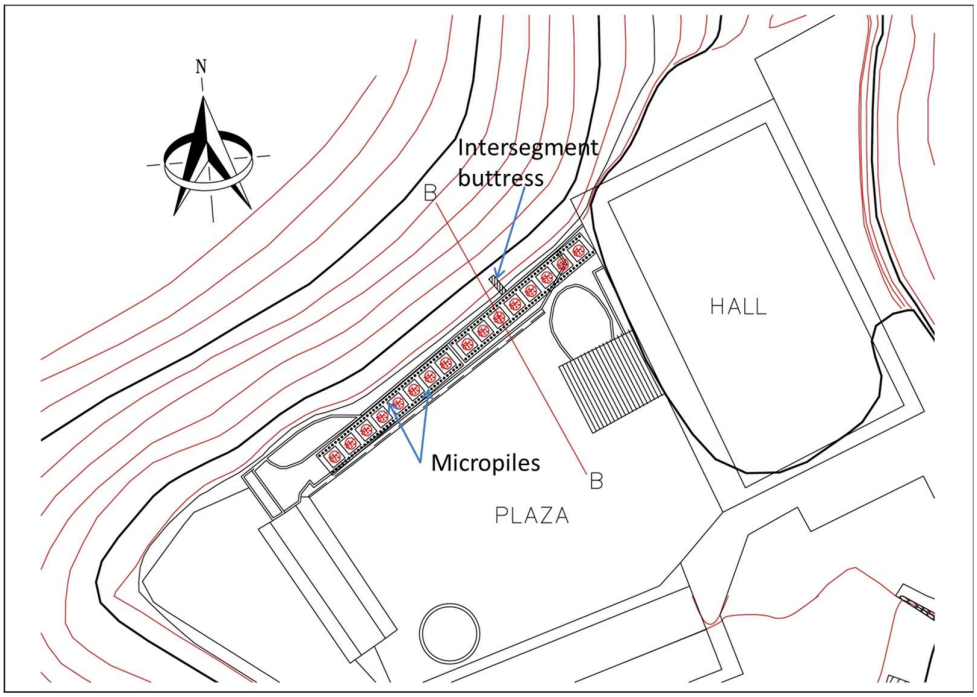


Figure 9: Micropile configuration state for gantry reinforcement option in Case (2)

Table 4: Parameters of soils in Case (2)

Parameter / Soil	Cohesion **C**	**ø**	**E**	γ_t	Poisson's ratio **ν**
	KPa	(Degree)	KPa	KN/m³	
Backfill	5	30	$2x10^3$	19.5	0.3
Rock formation layer	50	32	$9x10^6$	23	0.3
Weathered rock	40	30	$4x10^6$	22	0.3
Overburden	10	30	$4x10^3$	21	0.3

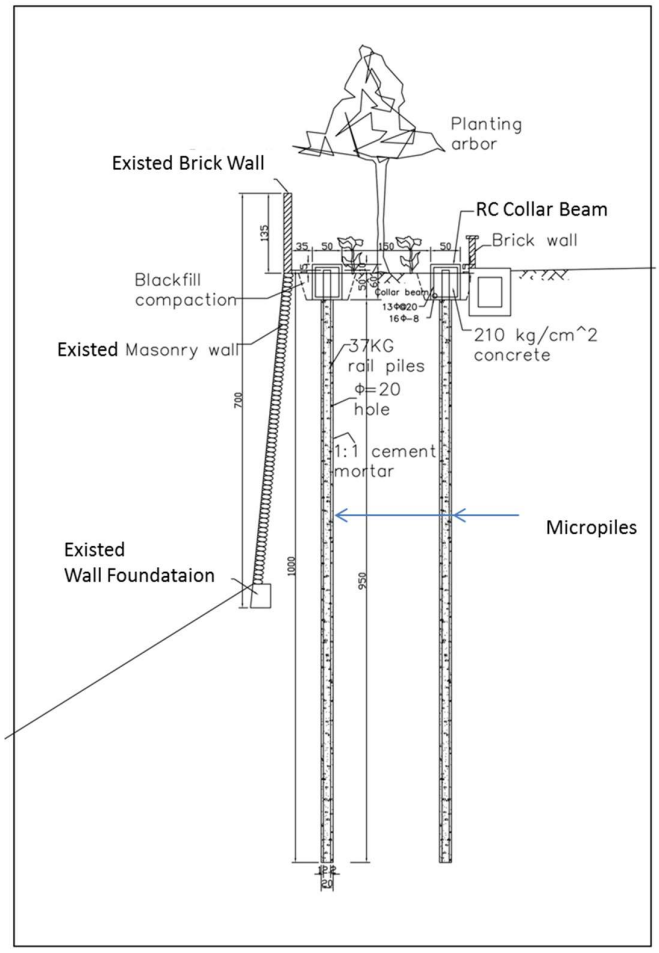


Figure 10: Cross-section B-B view of micropiles in Case (2)

Table 5: Parameters of micropile

EA	kN/m	4.11×10^6
EI	$kN \cdot m^2/m$	9.1×10^3
d	m	0.4
w	$kN/m^2/m$	2
ν	0.15	

Option 2: Double-row micropiles are installed to penetrate the rock. The interval between the two rows of piles is 1.5m, the spacing between each pile is 40 cm. The analysis result of the PLAXIS program shows that under rainstorm conditions, the maximum displacement in the condition of double-row micropiles can be reduced from 24mm to 7.58mm; while the amount of vertical subsidence of the retaining wall and floor can be reduced approximately from 6mm to 0.78mm (one-seventh). These results show that the double-row micropiles have a significant improvement on both the displacement and amount of vertical subsidence of the original retaining wall, flower bed, and plaza.

Option 3: In between the two rows of micropiles, the tops of the piles are connected with a RC collar beam to a gantry to strengthen between the rows of

piles and confine the slope displacement. The analysis results is shown in Figure 12. Under the rainstorm conditions, the maximum displacement can be reduced from 24mm to 6.4mm; while the amount of vertical subsidence of the retaining wall and floor can be approximately reduced from 6mm to 0.9mm (one-sixth). Thus, the option of double-row micropiles with RC collar beams is the most effective for improving the safety factor and maximum displacement.

2.2.5 Case (2): Comprehensive comparisons of the effectiveness of reinforcement next to the Samantabhadra Temple

From Table 6, as the direct benefit of installing single-row micropiles to form the retaining wall in the ground is an increase in the safety factor by 40.9%; the maximum displacement decreases significantly by 67.4%; while the amount of vertical subsidence decreases significantly by 66.6%. Thus, the single-row vertical micropiles can alleviate and improve the subsiding soil surrounding the piles; and after the retaining wall in the ground is formed, the soil deformation has decreased. Its direct contribution is its significant improvement in resisting the displacement and inhibiting the amount of vertical subsidence. A comparison of the total displacement sink area (i.e. areas enclosed by retaining wall displacement) shows that it can be reduced from 840cm^2 to 273cm^2; the improvement to the total displacement sink area is a reduction of 67%. The subsidence sink area can be reduced from 218.6 cm^2 to 45 cm^2, that is, the improvement of the vertical subsidence sink area is a reduction of 79%. Thus, the contributions of single-row vertical micropiles have significantly enhanced the resistance of the displacement sink area; and the improvement of inhibiting the vertical subsidence sink area has also been enhanced. Overall, the direct benefit of single-row vertical micropiles is an increase in the safety factor from 1.1 to 1.55, which is more than the generally recommended safety factor of 1.5. In terms of security, Option 1 has met the stability requirements.

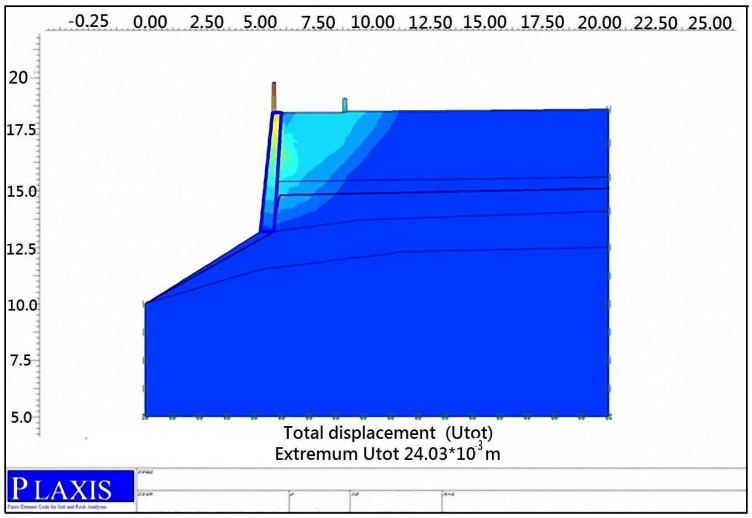


Figure 11: (B-B current - rainstorm) total displacement (Maximum value of 24.03mm)

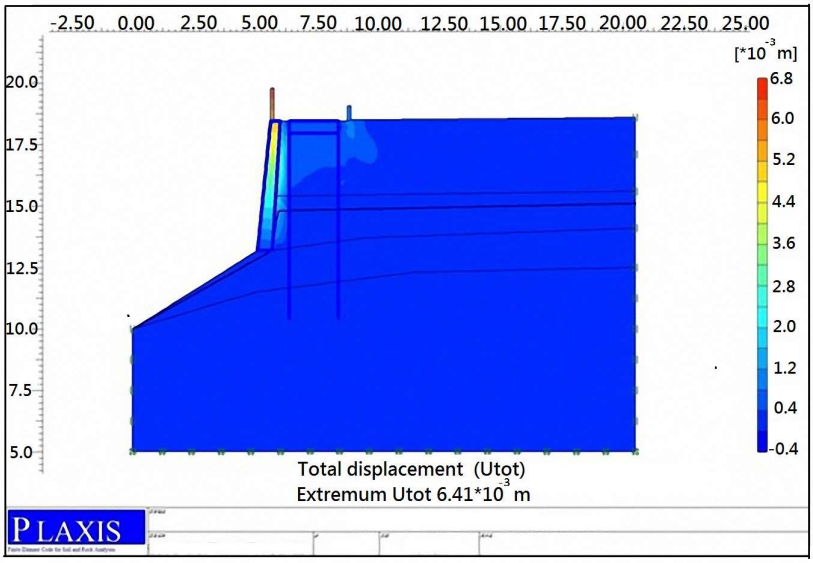


Figure 12: Double-row micropiles with collar beam under rainstorm conditions – (Maximum total displacement of 6.41mm)

Table 6: Comprehensive comparison of reinforcement effectiveness under rainstorm conditions for Samantabhadra Temple in Case (2)

Reinforcement type / Comparative item	(0). Initial condition	(1). Single-row micropiles	(2). Double-row micropiles	(3). Option (2) + Collar beam
Safety factor	1.10	1.55	1.61	1.75
Displacement (mm)	24.03	7.84	7.58	6.41
Subsidence (mm)	5.99	2.00	0.78	0.95
Displacement sink (cm^2)	840	273	262.5	224
Subsidence sink (cm^2)	218.6	45	13.1	9.0

By comparing Type 2 with Type 3, the difference in the benefit of double-row micropiles and gantry-style micropiles is that the safety factor is further enhanced from 46.4% to 59.1%; the safety factor has been slightly increased by about 12.7%; the maximum displacement can be reduced from -68.5% to -73.3%, a decline in magnitude of about -4.8%, while subsidence amount in the retaining wall and plaza floor increases by about 2.9%. The total displacement sink area can be reduced from 262.5cm^2 to 224cm^2, an improvement of about 14.6 %. The vertical subsidence sink area can be reduced from 13.1cm^2 to 9.0cm^2 (31%). Thus, when the effectiveness of Type 3 gantry-style micropiles is compared with that of Type 2 double-row micropiles, a direct improvement is achieved in the safety factor, total displacement, and vertical subsidence. Taking the loss of earth of the soil body of the plaza due to the total displacement sink and the vertical subsidence sink into consideration, it is recommended to adopt the Type 3 gantry-style micropile reinforcement for improvement. This option forms a frame-type structure on the planar architecture. Within the frame, the space can

still provide gridiron for planting in configuration with grafting, which can give the functional benefits of taking both the ecological environment and protecting the soil from erosion loss into consideration.

3. CONCLUSIONS AND RECOMMENDATIONS

According to the analysis results, micropile application can provide several benefits; these benefits are summarized below as a reference for similar projects.

(1) In both cases, the direct benefit of installing single-row vertical micropiles to form a retaining wall in the ground is an enhanced safety factor of about 6% to 40%; and the maximum displacement is significantly reduced from about 53% to 67%. Moreover, if the single-row vertical micropiles are coupled with grouting, the soil subsidence trend near the pile bodies can be improved significantly, so that after forming the retaining wall in the ground, the amount of soil deformation can be further reduced; the amount of reduction is about 82%.

(2) In Case (1), the micropiles are underpinned in an inverted L-shaped manner in order to increase strength. Additionally installing an inclined pile can further enhance the safety factor by about 11%; and after forming the retaining wall in the ground, the total displacement and amount of soil subsidence are further reduced by 8% and 45% (comparing the percentage difference between Type 3 and Type 1 list in Table 3) respectively.

(3) For micropiles coupled with low pressure grouting of different volumes and configurations, only slight differences were apparent in the safety factor and the maximum displacement. The major contribution is to reduce the subsidence amount and this has direct relationship with the position of the grouting. As the improvement position is closer to the vertical subsidence sink, its improvement on the amount of vertical subsidence of soil after installing the retaining wall in the ground is more significant.

(4) Among the reinforcement methods for the vertical subsidence of the foundation of a castle wall at a historical site in this paper, taking consideration of the narrow and confined space of construction, equipment, manpower, and other conditions from the perspectives of engineering design, it is recommended to use the method of installing the micropiles in inverted L-shaped manner with low-pressure grouting for strength and reinforcement. The effectiveness of Option 1 in the improvement of safety factor, total displacement, and amount of vertical subsidence is the best. After reinforcement, under rainstorm conditions, the maximum displacement can be reduced from 22mm to 7mm; while the vertical subsidence of the castle wall's foundation can be reduced approximately from 4.5mm to 1.25mm (one-quarter).

(5) In Case (2), the micropiles with gantry configuration can enhance the safety factor with a maximum enhancement of up to about 59%; the total displacement and soil subsidence amount can be drastically reduced by about 73% and 84%.

Furthermore, this construction method provides alternative function by forming a frame-type structure on the planar architecture to provide scope for planting in the frame, which can take consideration of both the ecological environment and protection of the soil from erosion loss.

REFERENCES

Fan Chia-Cheng, Chien Chin-Lung, (2004), Study on the Mechanical Behavior and Restoration Technology of Embankment Construction Ecology Method for Collapsed Road in Mountain Area, *2004 Cross-Straits Proceedings for Sino-Geotechnics/Geotechnical Engineering Seminar*, Taipei, Thesis No. 69.

Jeng, Ching-Jiang, Yu, Yu-Yu (2015), *Report on the Damage Cause Investigation and Restoration Planning Design for the Historical Sites of Urshawan Fort* (*Geotechnical Division*), Keelung City Cultural Affairs Bureau.

PRELOADING AND HEAD CONNECTION METHOD FOR MICROPILE

Je-Yong Park[1], Changho Choi[2], Hyun-Sik Yu[3], Hee-Jeong Yang[4], Ki-Hwan Lee[5]

ABSTRACT

Micropiles are used extensively for underpinning or retrofit of existing foundations. In some cases, micropiles must be preloaded to reduce excessive settlements and to prevent overloading of the existing foundations when the new or additional load is applied. In this aspect, the preload must be properly and permanently locked in the head of micropiles. This paper describes a newly developed preloading and head connection method for micropile, provides a means of more efficiently enhancing the micropile-to-footing connection capacity and increasing the load carried by micropiles. An experimental study was conducted to investigate the total capacity of the micropile-to-footing connection. The results of tests showed that the developed micropile preloading systems (*i.e.*, steel cone and split-threaded wedges) could provide cost-effective engineering solution for strengthening existing foundations and increase the structural capacity of the micropile-to-footing connection.

1. INTRODUCTION

Micropiles were originally developed for underpinning existing structures. The underpinning of existing structures may be performed for preventing structural movement and upgrading load-bearing capacity of existing structures (Sabatini et al., 2005). In many cases, micropiles are installed through the existing footing such as spread footing or pile cap to resist additional loads caused by the vertical expansion of structures. With this application, the additional loads from the superstructure will be shared between the micropiles and the existing foundations, and soil-structure interaction analyses need to be performed to estimate the amount of load that will be shared by each individual foundation element.

Load transfer from the existing foundation to the micropiles is an important mechanism to consider when designing an existing foundation underpinned by micropiles. This mechanism has not been well investigated or understood (El Kamash et al., 2016). Although the complicated load-transfer mechanism of composite foundation systems makes an accurate prediction of individual loads difficult, it is important to estimate the load-sharing ratios between the foundation's components for the optimized design of micropile, depending upon the design concept employed.

---

[1] Executive Director, Golden Engineering Co.,Ltd., 11, Beobwon-ro 11-gil, Songpa-gu, Seoul, 05836, Korea. +82-70-4449-8326, +82-2-456-1614, pjycon@empas.com

[2] Research Fellow, Korea Institute of Construction Technology, Geotechnical Engineering Research Division, 283, Goyang-daero, Ilsanseo-gu, Goyang-si, Gyeonggi-do, 10223, Korea. +82-31-910-0785, +82-31-910-0221, chchoi@kict.re.kr

[3] Manager, R&D Institute, Lotte E&C, 3, Naruteo-ro 10-gil, Seocho-gu, Seoul, 06527, Korea. +82-2-3483-7844, +82-2-3483-7899, yux2hnsk@lottenc.com

[4] Senior Manager, R&D Institute, Lotte E&C, 3, Naruteo-ro 10-gil, Seocho-gu, Seoul, 06527, Korea. +82-2-3483-7843, +82-2-3483-7899, hjyang@lottenc.com

[5] President, Golden Engineering Co.,Ltd., 11, Beobwon-ro 11-gil, Songpa-gu, Seoul, 05836, Korea. +82-70-4449-8323, +82-2-456-1614, lkhjin@hanmail.net

In some cases, preloading the micropiles prior to the connection to the existing foundations is necessary to transfer the part of the load from the existing foundations to the new micropiles. The purpose of preloading is to generate the displacement of micropile by jacking against the existing foundations during the installation phase, thereby preventing overloading of the existing foundations when additional load is applied.

This paper describes the developed micropile preloading systems and presents an experimental study on micropile-to-footing connection capacity. The results of tests showed that the developed method could provide cost-effective engineering solution for strengthening existing foundations and increase the structural capacity of the micropile-to-footing connection.

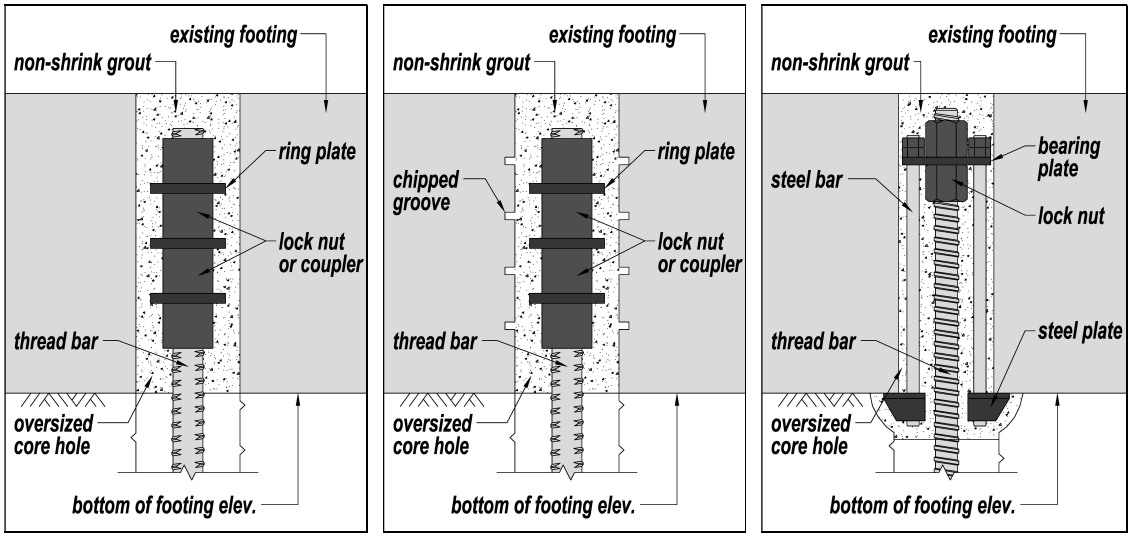
2. PRELOADING AND CONNECTION METHOD

The preloading and connection method, which may be used for applications where micropiles are installed through the existing foundations, was developed to increase the load-sharing ratio of micropile and enhance the micropile-to-footing connection capacity. The conventional connection method, typically used in South Korea, is shown in Figure 1 (Type A is normally used). Steel ring plates are attached to the top section of thread bar prior to pile installation. After the pile is installed, the annulus between the core hole and the micropile is cleaned and filled with non-shrink cement grout. Figure 2 shows the developed preloading and connection method. The construction sequence of the developed method are as follows (see Figure 3):

- Step 1: After the pile is installed, thread four reaction rods into the steel cone, and locate this steel cone above the centralizer through the core hole (typically 200mm diameter).
- Step 2: Place four split-threaded wedges around the cone.
- Step 3: Place bearing plate over four reaction rods. Thus, the bearing plate with five holes is seated on the thread bar (typically 65mm diameter).
- Step 4: Install four hex nuts and four temporary reaction rods. Set the hydraulic jack assembly on the existing footing. Gradually increase the pump pressure to the desired set point for interlocking between the wedges and the existing concrete (the cylinder moves upward). After that, remove the hydraulic jack assembly.
- Step 5: Place expandable steel bar (seated on the thread bar) and four nut holders. The compression preload is transferred to the thread bar via this expandable steel bar.
- Step 6: Set the hydraulic jack assembly on the existing footing, and gradually increase the pump pressure to the desired set point for preloading the micropile (the cylinder moves downward). Tighten the four hex nuts to fasten the bearing plate firmly using the nut holders. Therefore, the preload is locked in the micropile. The preload value determined by the design engineer is based on project-specific requirements.
- Step 7: Remove the hydraulic jack assembly, four nut holders and four

temporary reaction rods.

·Step 8: Fill the core hole completely with non-shrink cement grout.



(a) Type A (b) Type B (c) Type C

Figure 1. Micropile to footing connection detail (Conventional method)

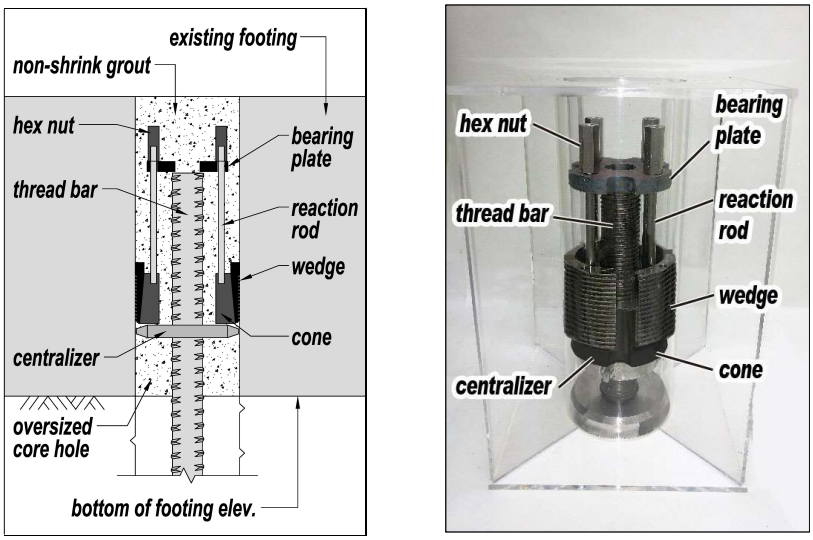


Figure 2. Micropile to footing connection detail (Developed method)

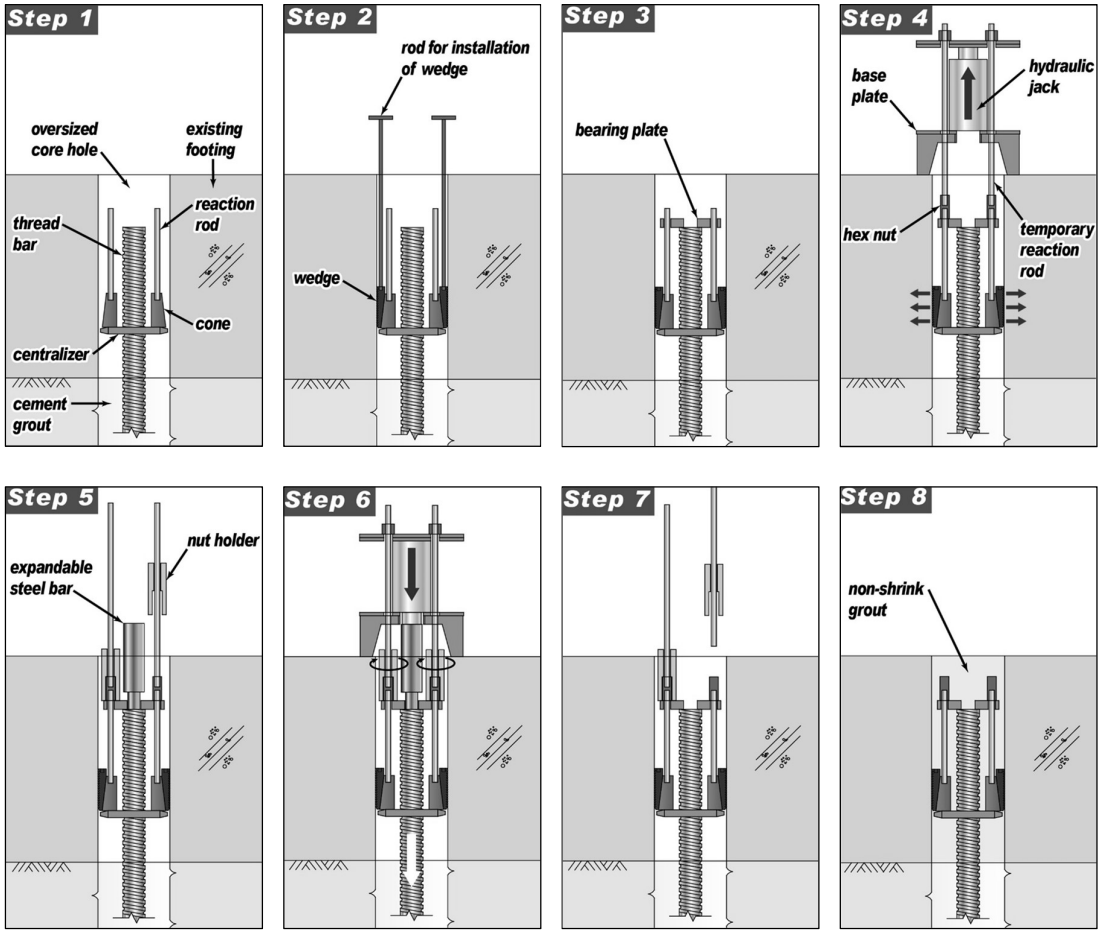


Figure 3. Construction sequence of the developed preloading and connection method

The advantages of the developed method are ease of installation, reduced construction time and cost reduction due to eliminating the need for typical preloading equipment which includes the reaction beam, tie-down anchors, etc.

3. CONNECTION LOAD TEST

The displacement-controlled compression load tests were performed on the micropiles connected to Reinforced Concrete (RC) footings to compare the two connection methods. Table 1 shows the reinforcement, RC footing and grout properties assumed for the specimens. For installation of the micropiles, 200mm diameter core holes were drilled through the RC footings (see Figure 4(a)). The prefabricated micropiles were installed in the core holes, and the core holes were filled with grout. The full-scale prototype three wedges were installed for the developed connection. The test set-up is shown in Figure 4(c), and the tests were performed until yield.

As shown in Figure 5, the total structural capacity of the developed connection is enhanced due to interlocking between the split-threaded wedges and the existing concrete.

Table 1. Reinforcement, RC footing and grout properties

Connection method	Reinforcement	RC footing			Grout
		Dimensions B×L×H mm (in)	Compressive strength MPa (ksi)	Core hole diameter mm (in)	Compressive strength MPa (ksi)
Conventional Method (Type A)	• Thread bar - D=65mm • Ring plate (3 pcs) - OD=170mm - T=25mm	1,000 (39.37) × 1,000 (39.37) × 600 (23.62)	27 (4.0)	200 (7.87)	30 (4.5)
Developed method	• Thread bar - D=65mm • Cone (1 pc) - Hc=100mm • Wedge (3 pcs) - Hw=100mm	1,000 (39.37) × 1,000 (39.37) × 600 (23.62)	27 (4.0)	200 (7.87)	30 (4.5)

Note: D=thread bar diameter; OD=ring plate outside diameter; T= ring plate thickness; Hc=cone height; Hw=wedge height; B=RC footing width; L=RC footing length; H=RC footing height



(a) RC footing coring (b) Ring plates attached to thread bar (c) Test set-up

Figure 4. Preparation of specimens and test set-up

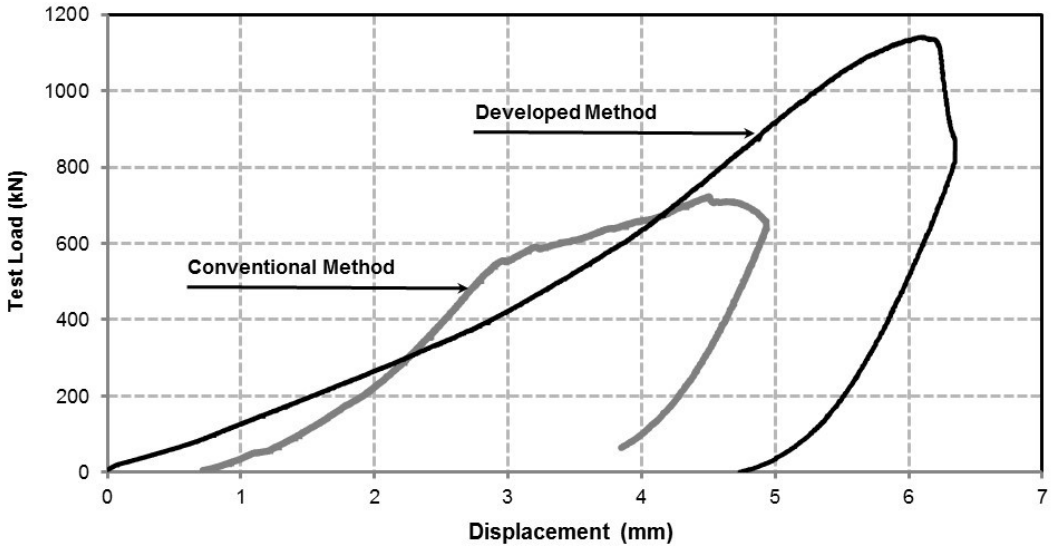


Figure 5. Results of connection load tests

4. CONCLUSIONS

Due to eliminating the need for typical preloading equipment which includes the reaction beam, tie-down anchors, etc., the developed micropile preloading and connection method is both efficient and economical. Thus, this method can provide competitive and useful engineering solution for strengthening existing foundations, depending on the specific application.

However, additional research on the structural behaviors, including time-dependent prestress loss and wedge-concrete interlocking under different preloading conditions, is certainly required for further development of this method.

ACKNOWLEDGEMENT

This study was supported by a grant (code 16TBIP-C092759-02) from Support for Infrastructure and Transportation Technology Commercialization Program funded by Ministry of Land, Infrastructure and Transport of Korean government.

REFERENCE

Sabatini, P., Tanyu, B., Armour, T., Groneck, P., and Keeley, J. (2005). *Micropile Design and Construction-Reference Manual*, Report No. FHWA-NHI-05-039, Federal Highway Administration, 3-9p.

El Kamash, W. and Han, J. (2016). *Numerical Analysis of Existing Foundations Underpinned by Micropiles*, Int. J. Geomech., 10.1061/(ASCE)GM.1943-5622.0000833, 1p.